COORDINATION BETWEEN CENTRAL AND LOCAL CONTROL OF PHOTOVOLTAIC GENERATION SYSTEM FOR CONTROLLING VOLTAGE VIOLATION AND UNBALANCE IN DISTRIBUTION SYSTEMS

Mr. Anuwat Chanhome

A Dissertation Submitted in Partial Fulfillment of the Requirements
for the Degree of Doctor of Philosophy in Electrical Engineering
Department of Electrical Engineering
Faculty of Engineering
Chulalongkorn University
Academic Year 2018

การทำงานประสานระหว่างการควบคุมส่วนกลางและการควบคุมส่วนท้องถิ่นของการผลิตไฟฟ้าจากพลังงานแสงอาทิตย์ เพื่อควบคุมแรงดันเกินและแรงดันไม่สมดุลในระบบจำหน่ายไฟฟ้า

นายอนุวัฒน์ จันทร์โฮม

วิทยานิพนธ์นี้เป็นส่วนหนึ่งของการศึกษาตามหลักสูตรปริญญาวิศวกรรมศาสตรดุษฎีบัณฑิต
สาขาวิชาวิศวกรรมไฟฟ้า ภาควิชาวิศวกรรมไฟฟ้า
คณะวิศวกรรมศาสตร์ จุฬาลงกรณ์มหาวิทยาลัย
ปีการศึกษา 2561

Thesis Title	COORDINATION BETWEEN CENTRAL AND LOCAL CONTROL OF PHOTOVOLTAIC GENERATION SYSTEM FOR CONTROLLING VOLTAGE VIOLATION AND UNBALANCE IN DISTRIBUTION SYSTEMS
By	Mr. Anuwat Chanhome
Field of Study	Electrical Engineering
Thesis Advisor	Assistant Professor SURACHAI CHAITUSANEY, Ph.D.

Accepted by the Faculty of Engineering, Chulalongkorn University in Partial Fulfillment of the Requirement for the Doctor of Philosophy

..... Dean of the Faculty of Engineering
(Professor SUPOT TEACHAVORASINSKUN, Ph.D.)

DISSERTATION COMMITTEE

..... Chairman
(Associate Professor NAEBBOON HOONCHAREON, Ph.D.)

..... Thesis Advisor
(Assistant Professor SURACHAI CHAITUSANEY, Ph.D.)

..... Examiner
(Associate Professor KULYOS AUDOMVONGSEREE, Ph.D.)

..... Examiner
(Assistant Professor SURAPONG SUWANKAWIN, Ph.D.)

..... External Examiner
(Pradit Fuangfoo, Ph.D.)

อนุวัฒน์ จันทร์โฮม : การทำงานประสานระหว่างการควบคุมส่วนกลางและการควบคุมส่วนท้องถิ่นของการผลิตไฟฟ้าจากพลังงานแสงอาทิตย์ เพื่อควบคุมแรงดันเกินและแรงดันไม่สมดุลในระบบจำหน่ายไฟฟ้า. (COORDINATION BETWEEN CENTRAL AND LOCAL CONTROL OF PHOTOVOLTAIC GENERATION SYSTEM FOR CONTROLLING VOLTAGE VIOLATION AND UNBALANCE IN DISTRIBUTION SYSTEMS) อ.ที่ปรึกษาหลัก : ผศ. ดร.สุรชัย ชัยทัศนีย์

พลังงานแสงอาทิตย์เป็นพลังงานที่สะอาดและไม่ก่อมลพิษให้กับสิ่งแวดล้อม ประกอบกับในหลายๆ ประเทศมีการขยายตัวทางเศรษฐกิจ ทำให้ประเทศเหล่านั้นมีความต้องการใช้ไฟฟ้าเพิ่มมากขึ้น และมีการสนับสนุนให้มีการติดตั้งระบบผลิตไฟฟ้าจากพลังงานแสงอาทิตย์เพิ่มขึ้น โดยเฉพาะอย่างยิ่งในระบบแรงดันต่ำเนื่องจากภาคครัวเรือนมีศักยภาพเพียงพอที่จะติดตั้งระบบผลิตไฟฟ้าจากพลังงานแสงอาทิตย์ได้ ประกอบกับค่าบำรุงรักษาและค่าการติดตั้งในปัจจุบันมีราคาต่ำลง อย่างไรก็ตามเมื่อมีระบบผลิตไฟฟ้าจากพลังงานแสงอาทิตย์เพิ่มขึ้นในระบบแรงดันต่ำย่อมเกิดผลเสียต่อระบบแรงดันต่ำได้ อันประกอบด้วย (1) การสูญเสียกำลังการผลิต เนื่องจากระบบป้องกันแรงดันไฟฟ้าเกินของระบบผลิตไฟฟ้าจากพลังงานแสงอาทิตย์ทำงาน โดยเฉพาะระบบผลิตไฟฟ้าจากพลังงานแสงอาทิตย์ที่อยู่ปลายสาย และ (2) ความไม่สมดุลของแรงดันไฟฟ้าในแต่ละเฟส เนื่องจากการติดตั้งระบบผลิตไฟฟ้าจากพลังงานแสงอาทิตย์แบบเฟสเดียว

ระบบผลิตไฟฟ้าจากพลังงานแสงอาทิตย์ในงานวิจัยฉบับนี้จะพิจารณาเฉพาะระบบผลิตไฟฟ้าจากเซลล์แสงอาทิตย์ (PV System) เท่านั้นและเพื่อแก้ไขปัญหาที่เกิดขึ้นต่อระบบแรงดันต่ำดังกล่าวข้างต้น จึงจะได้ประยุกต์ใช้การควบคุมระบบผลิตไฟฟ้าจากเซลล์แสงอาทิตย์ เพื่อให้สามารถรองรับการเพิ่มการเชื่อมต่อกับระบบแรงดันต่ำได้ โดยการควบคุมดังกล่าวจะอาศัยการทำงานประสานกันระหว่างศูนย์ควบคุมกลาง (Central Control) และศูนย์ควบคุมส่วนท้องถิ่น (Local Control) ของระบบผลิตไฟฟ้าจากเซลล์แสงอาทิตย์ ศูนย์ควบคุมกลางทำหน้าที่หาค่าพารามิเตอร์ให้กับศูนย์ควบคุมส่วนท้องถิ่น โดยพิจารณาจาก (1) ระบบผลิตไฟฟ้าจากเซลล์แสงอาทิตย์จะต้องจ่ายกำลังไฟฟ้าจริงที่ค่าสูงสุด และ (2) ภายใต้สภาวะความไม่แน่นอนในระบบแรงต่ำจะต้องไม่ทำให้เกิดแรงดันเกิน โดยอาศัยวิธีการหาค่าเหมาะสมด้วยการเคลื่อนที่ของอนุภาคแบบ 2 ชั้น (2-stage Particle Swarm Optimization (PSO)) ส่วนศูนย์ควบคุมส่วนท้องถิ่นจะรับค่าพารามิเตอร์เพื่อนำมาใช้กับสมการ P(U) และ Q(U) Function โดยสมการ P(U) Function ใช้ในการปรับกำลังไฟฟ้าจริงและ Q(U) Function ใช้ในการปรับกำลังไฟฟ้าเสมือนที่ได้จากระบบผลิตไฟฟ้าจากเซลล์แสงอาทิตย์เมื่อแรงดันที่จุดติดตั้งเปลี่ยนแปลงไป ในวิทยานิพนธ์ฉบับนี้ การแก้ปัญหาการไหลของกำลังไฟฟ้าควบคู่กับสมการ P(U) และ Q(U) Function จะอาศัยวิธีนิวตันราฟสัน (Newton-Raphson Method) โดยพิจารณาควบคู่กับการปรับระยะการก้าวของวิธีนิวตันราฟสัน (Step-length Adjustment) ระบบทดสอบที่ใช้จะเป็นระบบแรงต่ำที่มี 19 และ 29 จุดโหลด และผลลัพธ์ที่ได้สามารถแสดงให้เห็นว่า ค่าพารามิเตอร์ที่ได้จากศูนย์ควบคุมกลางสามารถทำให้ศูนย์ควบคุมส่วนท้องถิ่นทำงานได้อย่างมีประสิทธิภาพภายใต้สภาวะความไม่แน่นอนในระบบแรงต่ำ

สาขาวิชา	วิศวกรรมไฟฟ้า	ลายมือชื่อนิสิต .....
ปีการศึกษา	2561	ลายมือชื่อ อ.ที่ปรึกษาหลัก .....

5671437221 : MAJOR ELECTRICAL ENGINEERING
KEYWORD: LV distribution system, Loss of real power generation, Voltage unbalance, PV system, Central control, Local control, PSO

Anuwat Chanhome : COORDINATION BETWEEN CENTRAL AND LOCAL CONTROL OF PHOTOVOLTAIC GENERATION SYSTEM FOR CONTROLLING VOLTAGE VIOLATION AND UNBALANCE IN DISTRIBUTION SYSTEMS. Advisor: Asst. Prof. SURACHAI CHAITUSANEY, Ph.D.

Solar energy is a clean and pollution-free energy. Economic growth has led to increased demand for electricity in many countries, which has encouraged the installation of solar power generation systems, especially in LV distribution system. Households have the potential to install solar power generation systems because the costs of installation and maintenance have been continuously decreased. However, when there are many connected solar power generation systems in LV distribution system, the following problems may occur: (1) Loss of real power generation due to the operation of overvoltage protection of solar power generation systems, especially the ones on downstream nodes and (2) Voltage unbalance due to the connection of single-phase solar power generation system.

In this dissertation, solar power generation system is determined as only Photovoltaic (PV) system. To cope with the above mentioned problem in LV distribution systems, this dissertation applies a control strategy to support high PV penetration which is the coordination between central and local controls. Central control is used to assess parameter setting for local control by considering the following principles: (1) the total connected PV system must inject real power output at the maximum value and (2) the parameter setting result must not cause voltage violation under uncertainty condition in LV distribution system. 2-stage Particle Swarm Optimization (PSO) is applied in central control for the parameter assessment of local control. The parameter setting will be sent to local control which consists of P(U) and Q(U) functions. P(U) and Q(U) functions are used for real and reactive power output adjustment from connected PV system respectively. The operation of P(U) and Q(U) functions will be regulated when the voltage at the connection point of PV system changes. In this dissertation, the power flow algorithm with using local control P(U) and Q(U) functions applies Newton-Raphson Method with step-length adjustment. The test systems are modified 19 and 29 node distribution systems. The power flow results show that the parameter setting obtained from central control enables the local control operate effectively under uncertain conditions in LV distribution systems.

Field of Study: Electrical Engineering Student's Signature .....
Academic Year: 2018 Advisor's Signature .....

ACKNOWLEDGEMENTS

Firstly, I would like to express my deep sense of gratitude to my advisor, Assistant Professor Dr. Surachai Chaitusaney for providing invaluable guidance, comments and suggestions throughout my PhD course. I am really glad to his dedication and keen interest above all his overwhelming attitude to help his students that had been solely and mainly responsible for completing my work. He helped me to a very great extent to accomplish this dissertation.

I would like to offer my sincere thanks to my thesis examination committee: Associate Professor Dr. Naebboon Hoonchareon, Associate Professor Dr. Kulyos Audomvongseree, Assistant Professor Dr. Surapong Suwankawin and Dr. Pradit Fuangfoo.

Finally, I am thankful to my parents who support, encourage and pray for my great success. Their kind blessings and good wishes for me and my future turn everything into easier.

Anuwat Chanhome

TABLE OF CONTENTS

Page

LIST OF TABLES

Page

LIST OF FIGURES

Page

LIST OF ABBREVIATIONS

Abbreviations

AEDP	Alternative Energy Development Plan
c-Si	Crystalline Silicon
DSOs	Distribution System Operators
ESS	Energy Storage System
FIT	Feed-In-Tariff
ICs	Integrated Circuits
LV	Low Voltage
MEA	Metropolitan Electricity Authority
MPP	Maximum Power Point
MV	Medium Voltage
OLTC	On-Load Tap Changer
pc-Si	Poly Crystalline Silicon
PEA	Provincial Electricity Authority
PSO	Particle Swarm Optimization
PV	Photovoltaic
SCADA	Supervisory Control and Data Acquisition

Constant Parameters

$D^{\sigma\sigma'}$	Distance between conductor phase σ and σ' (feet)
f	Frequency (Hz)
I_{MPP}^{0}	MPP current at nominal cell operating temperature (A)
I_{sc}^{0}	Short-circuit current at nominal cell operating temperature (A)
K_i	Current temperature coefficient (A/°C)
K_v	Voltage temperature coefficient (V/°C)
n	Number of overall nodes in LV distribution system
N_{OT}	Nominal cell operation temperature (°C)
N_s	Number of PV module
p_g	Earth resistivity (Ω-m)

r^{σ}	Resistance of conductor phase σ (Ω)
r_c^{σ}	Radius of conductor of any phase σ (feet)
V_{MPP}^{0}	MPP voltage at nominal cell operating temperature (V)
V_{oc}^{0}	Open-circuit voltage at nominal cell operating temperature (V)

Indices

i	Index of nodes or connection point in distribution system
j	Index of nodes in distribution system that connect to node i
k	Notation indicates at k^{th} iteration of power flow algorithm
h	Notation indicates at h^{th} iteration of power flow algorithm
m	Notation indicates real-part value
max	Notation indicates maximum value
min	Notation indicates minimum value
ne	Notation indicates negative sequence
npv	Notation indicates the total number of connected PV systems
po	Notation indicates positive sequence
r	Notation indicates imaginary-part value
$rated$	Notation indicates rated value
sch	Notation indicates scheduled value
ze	Notation indicates zero sequence
σ	Notation indicates any phase A, B or C

Variables

GMR^{σ}	Geometric Mean Radius of conductor phase σ (feet)
I_{i-j}^{σ}	Line current at any phase σ between nodes i and j (A)
K_1	Parameter setting of both continuous and piecewise linear Q(U) local control functions
K_2	Parameter setting of both continuous and piecewise linear Q(U) local control functions
P_{MPP}	MPP power from PV array (W)

s_{irr}	Solar irradiance (kW/m^2)
T_{amb}	Ambient temperature (°C)
T_{cell}	Cell temperature (°C)
V_{cri}	Parameter setting of continuous P(U) local control function
V_{p1}	Parameter setting of piecewise linear P(U) local control function
V_{p2}	Parameter setting of piecewise linear P(U) local control function
V_q	Parameter setting of continuous Q(U) local control function
V_{q1}	Parameter setting of piecewise linear Q(U) local control function
V_{q1}	Parameter setting of piecewise linear Q(U) local control function
VUF_i	Voltage unbalance factor at node i
w	Step-length value
Y_{ij}	Admittance matrix between nodes i and j (pu.)
$z^{\sigma\sigma}$	Self impedance of conductor phase σ (Ω/mile)
$z^{\sigma\sigma'}$	Mutual impedance between conductor phase σ and σ' (Ω/mile)
θ_{ij}	Phase angle of admittance matrix between nodes i and j (radians)
δ_i^{σ}	The phase angle at node i, phase σ (radians)
δ_p	Parameter setting of continuous P(U) local control function
δ_q	Parameter setting of continuous Q(U) local control function
ρ	Standard deviation value of normal distribution probability
μ	Mean value of normal distribution probability

CHAPTER 1
INTRODUCTION

The introduction begins with the problem statement which specifies the problem to be solved in this dissertation. After that, objective, scope, steps of study, and expected benefits are described. Finally, the dissertation structure is presented.

1.1 Problem Statement

Solar energy is a clean energy and does not cause pollution to environment. Therefore, the technology for generating electricity from solar energy has been developed such as Photovoltaic (PV). In many countries, the renewable energy, especially solar energy, is emphasized for replacing the electricity generation from fossil fuel. In Germany, their policy supporting the PV installation into the grid such as high Feed-In-Tariff (FIT) and Distribution System Operators (DSOs) are obliged to respond grid reinforcement cost to support PV installation according to §14 EEG [1]. Then, there are total PV installations around 41.3 Gigawatts peak (GWp) in Germany in 2016. In Thailand, there is Alternative Energy Development Plan (AEDP) [2] that total PV installations in 2035 should be around 11% of global electricity production. For total PV installation, the ministry of energy and the related agencies in Thailand have set the additional guidelines for covering in the household level to drive AEDP to meet the goal. The additional guideline relates PV installation at the house rooftop for supporting electricity in Low Voltage (LV) distribution system. However, more PV installations in LV distribution system can bring about such the following problems:

- Loss of real power generation because the overvoltage protection of the PV inverter is operated, whereby most PV inverters in the downstream nodes are disconnected.
- Voltage unbalance due to the connection of a single-phase PV inverter.

Generally, the aforementioned problems can be resolved by the followings [3-6]:

- Installing an MV/LV transformer with an On-Load Tap Changer (OLTC).
- Installing an energy storage system.

- Changing conductor size of LV feeder.

However, installing an OLTC has the limitation that it increases significantly the cost of the MV/LV distribution transformer and is unable to change tap positions frequently when voltage variation occurs on the LV feeder due to intermittent sunlight. Energy storage systems, which have been proved as flexible tools for peak-shaving, power shifting, and electrical backup, are still very expensive. Finally, changing into larger conductor size have to invest for new line conductor.

To support more PV installation or high PV penetration in LV distribution system, many previous researches [7-13] have studied in controlling PV system instead because it is cheaper than installing OLTC, installing energy storage system, or changing into new larger conductor. In addition, PV system is an electronic device that can adjust power output frequently. The previous researches [7-13] have been studied with different three aspects as follows.

1. **Central control regulates each PV system directly**: In the research [7], central control or Distribution System Operator (DSO) regulates only reactive power output from each PV system every 10 second in 3-phase balanced LV grid. In the researches [8, 10], central control regulates maximum allowable real power output and reactive power output from each PV system every 1 hour. The research [8] considers on 3-phase balanced LV distribution system but the research [10] considers on 3-phase unbalanced LV distribution system. The researches [7, 8] consider only 3-phase PV system and the research [10] considers only single-phase PV system.
2. **Each PV system is controlled by self-local control**: Each PV system have self-local control to adjust real or reactive power output automatically. The research [11] considers only local control Q(U) function which reactive power output will be changed when voltage at the connection of PV system is changed. The research [12] considers only local control P(U) function which real power output will be changed when voltage at the connection of PV system is changed. Finally, the research [9] considers both P(U) and Q(U) function. All researches [9, 11, 12] consider on 3-phase balanced LV distribution system and only 3-phase PV system.

3. **The coordination between central and local control**: In this case, central control can adjust parameter setting of local control of each PV system. The research [13] considers the adjustment of local control once per day. The local control includes Q(P) function, which reactive power output will be changed when real power output is changed, and real power limitation which PV system will not generate real power output more than specified real power limitation. The research [13] considers on 3-phase unbalanced LV distribution system and only single-phase PV system.

All researches [7-13] determine the control of PV system by central or local control for controlling voltage, current and transformer capacity in LV distribution system within the limit. The researches [7-9, 11, 12] consider on 3-phase balanced LV distribution system but the actual LV distribution system is normally a 3-phase unbalanced grid. All researches [7-13] determine PV system as only 3-phase or 1-phase connection that conflict the actual situation. The actual LV distribution system will be connected by both 3-phase and 1-phase PV system. The research [7] needs very reliable communication system because central control communicate each PV system every 10 seconds. If the communication system fails, PV system cannot adjust reactive power according to the command of central control and, then system voltage may be risen and exceed the limit if the system load is decreased. Consequently, some PV system will be disconnected from LV distribution system by its overvoltage protection of each PV system. The researches [8] and [10] predict load and solar irradiance one hour ahead and find optimal maximum allowable real power output and reactive power output from each PV system. The researches [8] and [10] do not consider the uncertainty of load and solar irradiance during one hour and, then the disadvantage is that if the system load during one hour ahead such as 30 minutes ahead decreases from the predicted system load, it can cause voltage rise that may exceed the limit and some PV system will be disconnected from LV distribution system. The researches [11] and [12] consider fixed parameter setting of local control P(U) or Q(U) function from the load and solar irradiance profile which are assumed as the same in every day. The disadvantage is as load and solar irradiance profile actually are not the same in every day and, then the result of fixed parameter setting of local control is not reliable for applying in real LV distribution system. The research [9] determines the same

parameter setting of local control of each PV system which the system voltage results can be within the limit. However, the research [9] does not determine the maximum utilization of real power output from each PV system. Finally, the research [13] find the parameter setting from predicted load and solar irradiance profile one day ahead. The disadvantage is that if the actual load is less than the predicted load, it can cause voltage rise that may exceed the limit and some PV system will be disconnected from LV distribution system.

In this research, the coordination between central and local control is chosen for the applied control strategy because communication system does not need for very reliable system and the parameter setting of local control can be adjusted to suit each specific time period. Some researches [7-9, 11, 12] consider LV distribution system as a 3-phase balanced distribution system that conflict with the actual LV distribution system. Then, this research considers LV distribution system as 3-phase unbalanced distribution system. All researches [7-13] consider PV system as only 3-phase or 1-phase connection. Then, this research considers PV system as both 3-phase and 1-phase connection according to actual situation in LV distribution system. All researches [7-13] does not consider the uncertainty of load and solar irradiance. Then, this research considers the uncertainty of load and solar irradiance carefully for finding optimal parameter setting of local control. Moreover, All researches [7-13] does not consider the voltage unbalance due to the connection of 1-phase PV system. Then, the voltage unbalance is considered in this research. Local control scheme function is determined both continuous and piecewise linear functions. The power flow algorithm with using local control function will apply Newton-Raphson method with step-length adjustment. 2-stage Particle Swarm Optimization (PSO) will be applied for finding optimal parameter setting of local control in this research. The optimization problem is maximization of real power output from overall PV systems. The modified 19-node and 29-node will be demonstrated to show the effectiveness of the result of the optimal parameter setting of local control.

The main contribution of this dissertation can be concluded that the uncertainty of load and solar irradiance are considered carefully for finding optimal parameter setting of local control. The power flow results from the optimal parameter setting can

be shown in Chapter 7 and they are regulated within the limit effectively under the uncertainty of load and solar irradiance.

1.2 Objective

- Determine the coordination between central and local control strategy to support high PV penetration in LV distribution system.
- Determine the solution for assessing the optimal parameter setting of local control of PV system by considering the uncertainty of load and solar irradiance..

1.3 Scope of Research Work and Limitations

1. Only LV distribution system is considered.
2. LV distribution system is considered as only radial system.
3. 3-phase PV system is considered as generating only positive sequence current.
4. PV system of any one household has only one PV inverter.
5. PV system is assumingly lossless.
6. PV system can be embed both two types of local control function such as continuous and piecewise linear functions but only one type can be selected to operate at specific time.
7. LV distribution system is considered as 3-phases 4-wires system with multi-grounded.
8. LV distribution system is considered in normal condition and fault condition is not considered.
9. The constraints of line flow limit, transformer capacity limit, voltage limit, voltage unbalance factor limit in LV distribution system are considered.

1.4 Steps of Study

1. Studying the principles of LV distribution system.
2. Studying 3-phases power flow.
3. Studying grid connected PV system standards.

4. Reviewing the literatures related to the voltage control in LV distribution system.
5. Reviewing the literatures related to PSO optimization technique.
6. Formulating and developing the optimization problem in order to determine the optimal parameters setting of local control.
7. Determining the relevant data in simulation.
8. Simulating the test system.
9. Concluding the research and writing the dissertation and academic papers.

1.5 Dissertation Structure

The rest of this dissertation is organized as follows. In the next chapter, the current situation of PV system in LV distribution system in many countries is presented. Chapter 3 clarifies interconnection system requirements for PV system in LV distribution system in many standards. In Chapter 4, the applied control strategy is presented in coordination between central and local control. In Chapter 5, 2-stage PSO and the power flow algorithm with using local control function will be explained in optimization process. Chapter 6 presents 2 test systems and 1 week collected data in test system details. After that, the simulations are demonstrated in 2 test systems and 1 week collected data and the results are discussed. Finally, the conclusion of this research is drawn.

CHAPTER 2

THE CURRENT SITUATION OF PV SYSTEM IN LV DISTRIBUTION SYSTEMS

PV system is a renewable energy source that has grown steadily in many countries, because solar energy is a clean energy source that is never used up and is environmentally friendly. Plus, the prices of equipment related to the PV system are on the downward trend. It is the cause for many country to expand the electrical generation by promoting rooftop PV system installation at residence or at LV distribution system. In this chapter, it will be divided into 3 topics.

2.1 Components of PV System

There are two components of PV system that are consisted of PV array and PV inverter as shown in Figure 2.1.

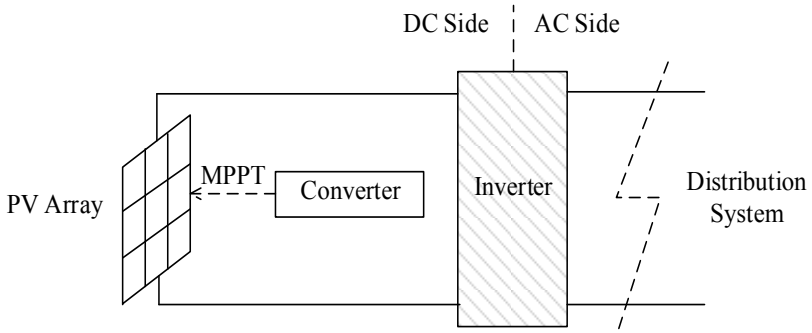

Figure 2.1 PV System

2.1.1 PV Array

Photovoltaic (PV) cell is an electronic invention made of semiconductor and it is responsible for turning light energy into electricity. The light may be from the sun or lamp. Many PV cells are combined together into PV module to produce higher voltages, current and power levels. A PV array is the complete DC current generating unit, consisting of any number of PV modules. The most popular substance that is used to produce PV cell can be divided into 2 type [14-16].

2.1.1.1 Silicon

At the present, PV cell is mostly produced from silicon substance and it can be divided into two types according to the crystal characteristic.

1. Crystalline silicon can be divided into mono and poly crystalline silicon. Silicon is one of the most abundant elements in the world from the smelting and sanding processes and, then, silicon is the cheapest semiconductor material. Silicon is commonly used as a substance for electronic industry such as transistors and Integrated Circuits (ICs). For mono crystalline silicon or c-Si, it is popular and widely used, such as in remote rural areas, or in places where access to electricity utilities is difficult, such as in the northern part of Thailand. For poly crystalline silicon or pc-Si, it is a result of the efforts to reduce the cost of c-Si solar cells. pc-Si solar cells production have lower cost than c-Si solar cells around 10% and, then, pc-Si solar cells are popular in Thailand too.
2. Amorphous silicon is the product of silicon substance too but not in the form of crystals. Amorphous silicon cause a thin layer of silicon only 300 nano metre thin. It is lightweight, easy to manufacture, has the advantage of not polluting the environment. The application of amorphous silicon are such as small calculator and watch.

2.1.1.2 Non-Silicon

Non-silicon solar cells are made of other substance that is not silicon. The highlight of this type of solar cell is the efficiency of up to 25 percent, but the price is very high. It is rarely used on the earth. Often used in space, such as satellites and concentrated solar power plant. Currently, only 7% of this type of solar cells is used.

2.1.1.3 Maximum Power Point Calculation of PV Array

PV array can produce DC current when sunlight fall onto the PV cell and PV inverter will track DC current at Maximum Power Point (MPP) which can be calculated regarding to the solar irradiance, ambient temperature, and the characteristic of module as shown in equations (2.1)-(2.5) [17].

$$T_{cell} = T_{amb} + s_{irr}\left(\frac{N_{OT} - 20}{0.8}\right) \quad (2.1)$$

$$I_{sc} = \frac{s_{irr}}{0.8}(I_{sc}^{0} + K_i[T_{cell} - N_{OT}]) \quad (2.2)$$

$$V_{oc} = V_{oc}^{0} + K_v[T_{cell} - N_{OT}] \quad (2.3)$$

$$FF = \frac{V_{MPP}^{0} \cdot I_{MPP}^{0}}{V_{oc}^{0} \cdot I_{sc}^{0}} \quad (2.4)$$

$$P_{MPP} = N_s \cdot FF \cdot V_{oc} \cdot I_{sc} \quad (2.5)$$

where T_{cell}, T_{amb} and N_{OT} are temperature (°C) of cell, ambience and nominal cell operation respectively. s_{irr} is solar irradiance (kW/m^2); V_{oc}^{0} is open-circuit voltage at normal cell operating temperature (V); I_{sc}^{0} is short-circuit current at normal cell operating temperature (A); V_{MPP}^{0} is MPP voltage at normal cell operating temperature (V); I_{MPP}^{0} is MPP current at normal cell operating temperature (A); K_v and K_i are voltage and current temperature coefficient (V/°C and A/°C) respectively; N_s is number of PV module; P_{MPP} is MPP power from PV array (W).

2.1.2 PV Inverter

PV inverter is a device that converts DC current into AC current to connect to electrical system properly and PV inverter must meet the requirement from grid code [18, 19] such as PV inverter must not generate harmonic current exceeding the limit and must be able to adjust Power Factor (PF). Most of PV inverter will initiate to generate real power output when solar irradiance is more than 0.05 kW/m^2 [20].

In this research, a single-phase PV system is defined as a PV system that consists of only one single-phase inverter which apparent power output at any connected phase can be calculated from P(U) and Q(U) local control functions. A three-phase PV system is defined as a PV system that consists of only one three-phase inverter. For a three-phase PV inverter, it is considered as positive-sequence current generation source [21]. Then, positive-sequence current ($I_i^{po} = I_i^{po,r} + j \cdot I_i^{po,m}$) can be calculated, when total generation $P_{i,pv}$ and $Q_{i,pv}$ are known from P(U) and Q(U) local control functions, in equation (2.6). The derivation of equation (2.6) is shown in Appendix A. After I_i^{po} is obtained, each phase current injection can be calculated from equation (2.7) where zero and negative sequence currents (I_i^{ze} and I_i^{ne}) are defined as

zero because this inverter generates only positive-sequence current. Finally, apparent power output of each phase can be calculated from equation (2.8) where δ is phase angle. The P(U) and Q(U) local control functions will be addressed later in Chapter 4.

$$\begin{bmatrix} I_i^{po,r} \\ I_i^{po,m} \end{bmatrix} = \frac{1}{3} \times \begin{bmatrix} V_i^{po,r} & V_i^{po,m} \\ V_i^{po,m} & -V_i^{po,r} \end{bmatrix}^{-1} \times \begin{bmatrix} P_{i,pv} \\ Q_{i,pv} \end{bmatrix} \tag{2.6}$$

$$\begin{bmatrix} I_i^A \\ I_i^B \\ I_i^C \end{bmatrix} = \begin{bmatrix} 1 & 1 & 1 \\ 1 & a^2 & a \\ 1 & a & a^2 \end{bmatrix} \times \begin{bmatrix} I_i^{ze} \\ I_i^{po} \\ I_i^{ne} \end{bmatrix} = \begin{bmatrix} I_i^{po} \\ a^2 \cdot I_i^{po} \\ a \cdot I_i^{po} \end{bmatrix} \quad ; a = 1\angle 120° \tag{2.7}$$

$$\begin{aligned} \begin{bmatrix} P_{i,pv}^A + j \cdot Q_{i,pv}^A \\ P_{i,pv}^B + j \cdot Q_{i,pv}^B \\ P_{i,pv}^C + j \cdot Q_{i,pv}^C \end{bmatrix} &= \begin{bmatrix} V_i^A \angle \delta_i^A & 0 & 0 \\ 0 & V_i^B \angle \delta_i^B & 0 \\ 0 & 0 & V_i^C \angle \delta_i^B \end{bmatrix} \times \begin{bmatrix} I_i^A \\ I_i^B \\ I_i^C \end{bmatrix}^* \\ &= \begin{bmatrix} V_i^A \angle \delta_i^A \cdot \left(I_i^{po,r} - j \cdot I_i^{po,m}\right) \\ V_i^B \angle (\delta_i^B + 120°) \cdot \left(I_i^{po,r} - j \cdot I_i^{po,m}\right) \\ V_i^C \angle (\delta_i^C - 120°) \cdot \left(I_i^{po,r} - j \cdot I_i^{po,m}\right) \end{bmatrix} \end{aligned} \tag{2.8}$$

For example, there is three-phase PV inverter connected with node i that phase A, B and C voltages are $220\angle 0°$, $225\angle -127°$ and $221\angle 121°$ V respectively. Total power output $P_{i,pv} + jQ_{i,pv}$ is $5{,}000 - j2{,}000$ VA. Then, power output of each phase can be calculated in 4 steps as follows.

STEP 1: Find positive sequence voltage from equation (2.9).

$$\begin{bmatrix} V_i^{ze} \\ V_i^{po} \\ V_i^{ne} \end{bmatrix} = \begin{bmatrix} 1 & 1 & 1 \\ 1 & a^2 & a \\ 1 & a & a^2 \end{bmatrix}^{-1} \times \begin{bmatrix} V_i^A \\ V_i^B \\ V_i^C \end{bmatrix} \tag{2.9}$$

Then,

$$V_i^{po,r} + jV_i^{po,m} = 221.4297 - j7.85454\ V \tag{2.10}$$

STEP 2: Find positive sequence current from equation (2.6).

$$I_i^{po,r} + jI_i^{po,m} = 7.62 + j2.74\ A \tag{2.11}$$

STEP 3: Find current of each phase from equation (2.7).

$$\begin{bmatrix} I_i^A \\ I_i^B \\ I_i^C \end{bmatrix} = \begin{bmatrix} 7.62 + j2.74 \\ -1.44 - j7.97 \\ -6.19 + j5.23 \end{bmatrix} \text{A} \tag{2.12}$$

STEP 4: Find power output of each phase from equation (2.8).

$$\begin{bmatrix} S_i^A \\ S_i^B \\ S_i^C \end{bmatrix} = \begin{bmatrix} 1{,}677.29 - j602.87 \\ 1{,}627.48 - j821.03 \\ 1{,}695.23 - j576.11 \end{bmatrix} \text{VA} \tag{2.13}$$

2.2 The Current Situation of PV System in Thailand

Thailand is near the equator and can absorb sunlight throughout the year. Most areas get solar irradiance around 5 kWh/m^2. Therefore, Thailand is a high potential country for installing PV system. Thai government support under the AEDP plan [2] requires the use of renewable energy to replace fossil fuels by at least 30% or 6,000 MW within 10 years.

Currently, the purchase of electricity from PV system is fixed Feed-In-Tariff (FIT). FIT is the policy tool, designed to accelerate investment in installation of PV system by offering long-term contracts. FIT comes from the calculation of plant construction costs, operating and maintenance costs over a 25 year life span. In addition, a special FIT purchase rate has been set in addition to the normal FIT purchase rate for projects in the southern border provinces of Thailand that include Yala, Pattani, Narathiwat and 4 districts in Songkhla such as Jana, Tepa, Sabayoi and Natawee to strengthen the electrical stability in the area. FIT in Thailand can be shown in Table 2.1.

Table 2.1 FIT rate for PV system in Thailand

Type	**Installed Capacity**	**FIT rate (Bath/kWh)**	**Supported period (year)**	**Special FIT (Bath/kWh)**
House	Less than 10 kWp	6.85	25	+0.5
Small Business Buildings	More than 10 to 250 kWp	6.40	25	+0.5
Medium or large-sized business building / factory	More than 250 to 1,000 kWp	6.01	25	+0.5

Type	Installed Capacity	FIT rate (Bath/kWh)	Supported period (year)	Special FIT (Bath/kWh)
Government agencies and agricultural cooperatives.	More than 1 to 5 MWp	5.66	25	-

From data in 2015 as shown in Figure 2.2 [22], the installed solar PV system volume was lower than the AEDP 2012-2021 target (the target is 3,800 MW). Then, Thai government should increase incentives to increase the installation of PV system as planned or as close to the plan as possible.

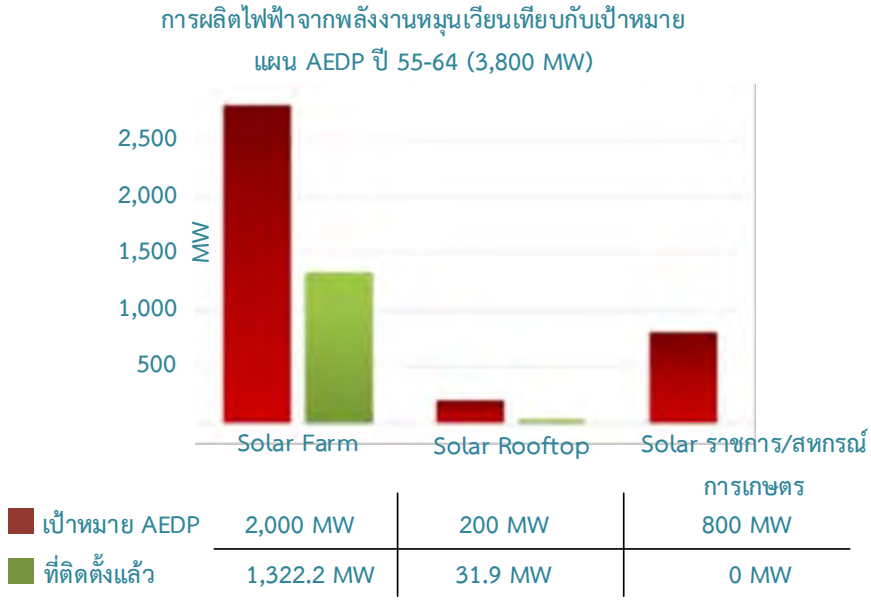

Figure 2.2 The bar chart between the installed PV capacity and the AEDP 2012-2021 target[22]

2.3 The Current Situation of PV System in Other Countries

PV system is a widely used electricity generation system in foreign countries. In this section, the countries with the highest proportion of installed PV capacity are presented such as Germany, Japan and USA.

2.3.1 Germany

Germany or the Federal Republic of Germany located at latitude 51° 30' 0" and longitude 10° 30' 0". Figure 2.3 compares the intensity of sunlight in Germany compared to Thailand. Thailand has an average solar intensity of 1,800 kWh/m^2, which is higher than Germany with an average solar intensity of 950 kWh/m^2. It is found that Germany has a lower average solar intensity per square meter than Thailand but Germany is currently the top proportion of PV system in the world. Electricity generated from renewable energy as shown in Figure 2.4, it is showed that Germany can generate 217,857 GWh from renewable energy source in 2017. Considering only solar power, Germany can generate 39,895 GWh from solar power generation in 2017 and electricity generated from solar power generation is on the rise every year.

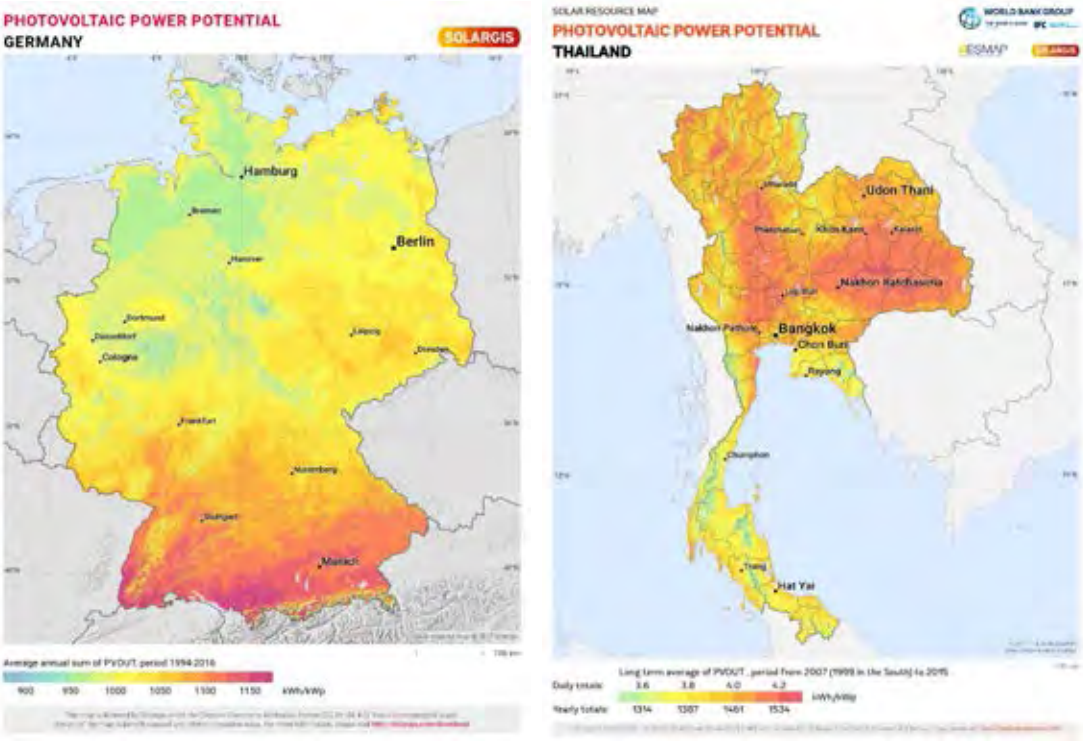

Figure 2.3 The intensity of solar radiation in Germany and Thailand [23]

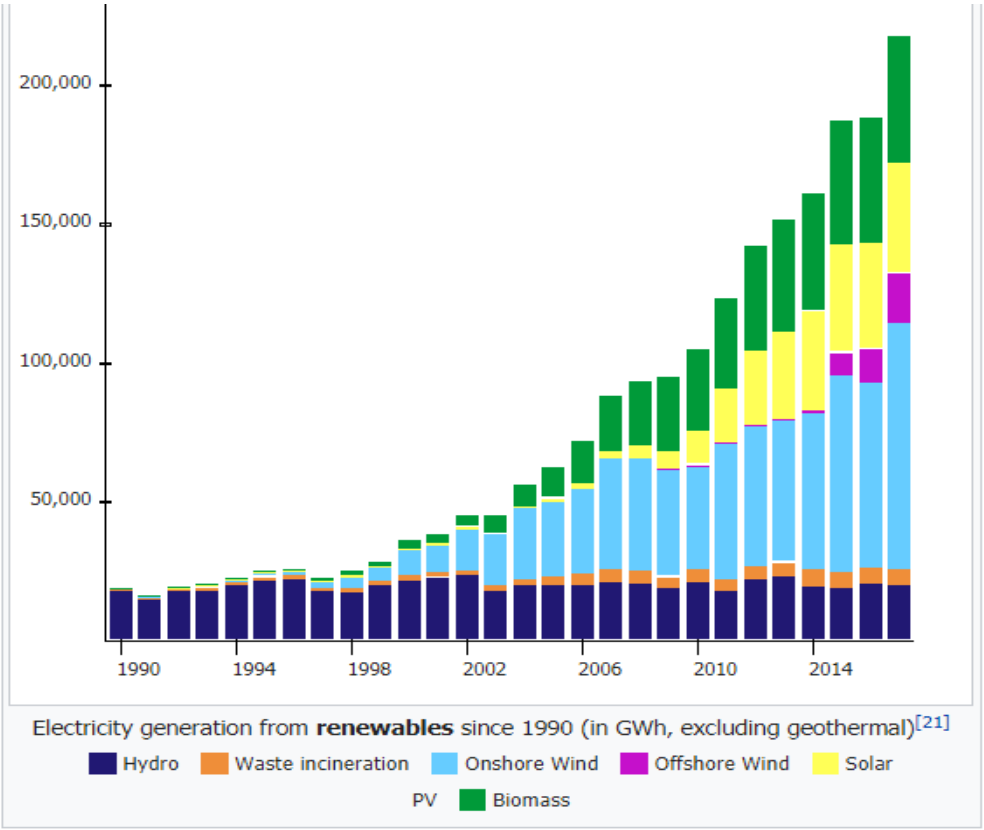

Figure 2.4 Electricity generated from renewable energy [24]

The cost of electricity produced by PV system is comparable to other fuels as shown Figure 2.5 that the tariff of consumed electricity in Germany was cheap at the beginning but the prices are rising every year (shown in Line 5). The FIT of PV system was previously very expensive and is likely to decline rapidly (shown in Line 1). The tariff of consumed electricity and the FIT of PV system are the same in 2012 (as shown in the chart) and the FIT of PV system is a tendency to decrease continuously in the future.

The rate of electricity purchased from Germany's solar PV systems is Fix Feed-in-Tariff as shown in Table 2.2.

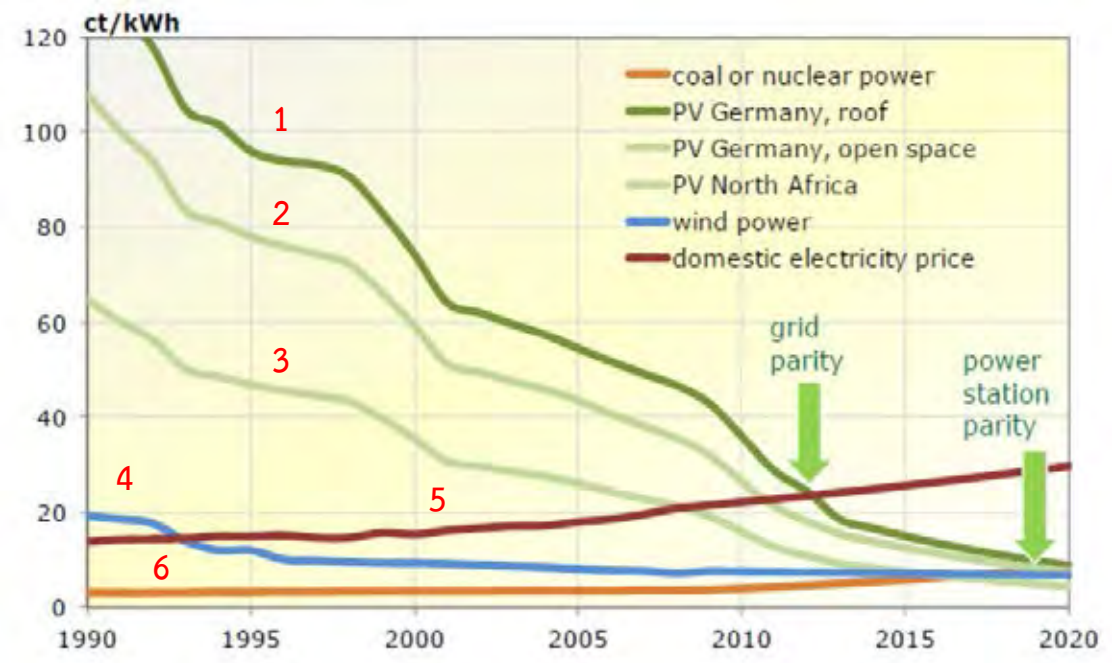

Figure 2.5 Price of electricity from various power generation systems [25]

Table 2.2 FIT rate for PV system in Germany [26]

Installed PV Capacity	**FIT rate (ct/kWh)**
< 10 kWp	19.5
< 40 kWp	18.5
< 1,000 kWp	16.5
< 10 MWp	13.5

2.3.2 Japan

Japan is another successful country in installing PV system. In Japan, the installed PV capacity of 2010 was 990 MW, 95% of which was installed on the roof of the house. But after the earthquake and the explosion of the Fukushima nuclear power plant in 2011, Japan has turned its attention to more renewable electricity generation. In 2011, total PV capacity was installed at 1,296 MW which PV system on the roof are 80%. In 2012, total PV capacity has been installed 1,718 MW, up 33% from the previous year.

Japan aims to install PV systems by 2030 as shown the target plan in Figure 2.6, expectedly with a 36.4 GW share of installed PV systems at residence, a 34.6 GW share of installed PV systems for a plant of PV system is less than 1 MW and a 29.1 GW share of installed PV systems for a plant of PV system is more than 1 MW. The total installed PV systems will be 100 GW in 2030 or 11% of the electricity demand in Japan.

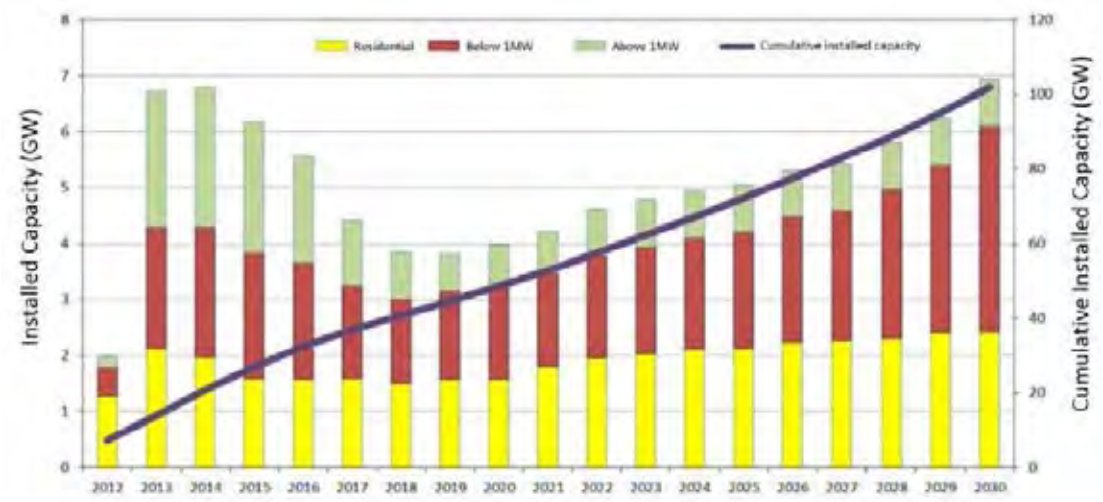

Figure 2.6 The target of installed PV capacities [27]

For the electricity price trend per kWh produced from PV systems, Figure 2.7 shows that in 2010, the cost of electricity generated from solar PV systems was 40 JPY/kWh. It is twice as expensive as consumed electricity price, but the price per kWh of electricity produced by solar PV systems is on the downward trend. In 2014, the price of electricity generated by PV systems is expected to decrease to 26 JPY/kWh which is lower than the consumed electricity price of the same year at 26.3 JPY/kWh.

Figure 2.7 Electricity price per kWh from residential PV generation system [28]

2.3.3 USA

The United States is another country with more installed PV systems. Even though the electricity generated by PV systems is only 0.4% of the country's capacity, it has grown significantly. Figure 2.8 shows the size of the installation of a PV system. The overall size of the installation is likely to increase every year, especially on residence side.

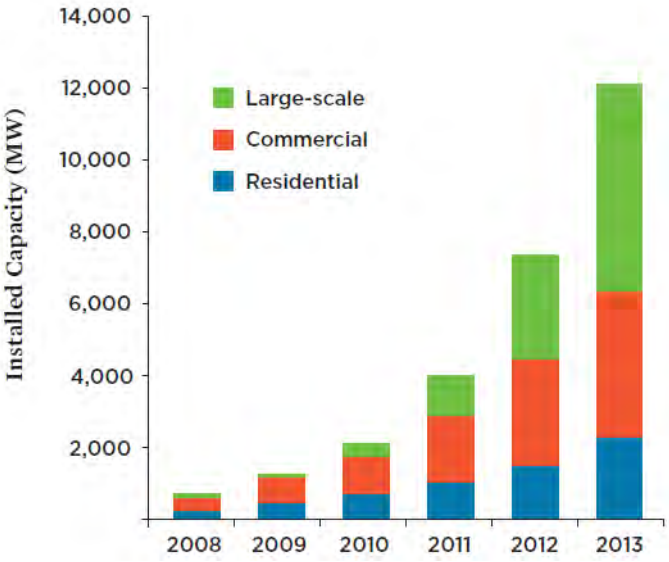

Figure 2.8 The installed PV capacity [29]

The price of solar panels per panel and the cost of installing PV system in the United States is shown in Figure 2.9. Looking back in 2008, the cost of installing PV system are $ 8 per watt, while the cost is decreased into the half in 2017. The cost of PV system installation is on the downward trend during the year 2008-2012 that the price of solar panels dropped by 86% and the total PV system installation cost dropped by 39%. In 2013-2017, the price of solar panels decrease by 6% while the price of whole installation decreased by 33%.

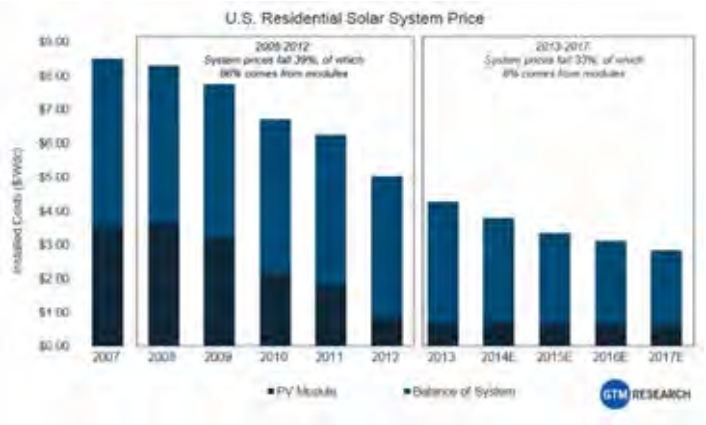

Figure 2.9 Cost of installing solar PV system in the United States [30]

CHAPTER 3

INTERTCONNECTION SYSTEM REQUIREMENTS FOR PV SYSTEM IN LV DISTRIBUTION SYSTEM

To respond the increase in household PV system or PV system connected to LV distribution system, it should have a standard to support connected PV system to prevent problems in LV distribution system. In this research, there are 4 standards to be considered as follows.

3.1 VDE-AR-N 4105:2011-08, Power Generation Systems Connected to the Low-Voltage Distribution Network – Technical Minimum Requirements for the Connection to and Parallel Operation with Low-Voltage Distribution Networks (2011) [31]

This standard is used in Germany. It applies to the planning, construction, operation and modification of PV systems that are connected to a network operator's LV system and operated in parallel with LV system. The details of this standard can be clarified into:

3.1.1 Capacity of PV System

If several single phase PV inverters are connected to the same connection point, then uniform distribution of the power supplied to the three line conductors shall be aimed for, where a maximum power difference of 4.6 kVA shall not be exceeded. For the maximum allowable capacity of PV systems in LV system, it will be determined by system operator.

3.1.2 Power quality at the connection point of PV system

Connecting a PV inverter to LV system, it requires the following feature:

3.1.2.1 Voltage and PF Control

PV inverter must disconnect from LV system when voltage is out of limit as follows where V_N is normal operating voltage.

Table 3.1 The duration of PV inverter for disconnecting from LV system

Protective Function		Protection Relay Setting Values	
Voltage drop protection	$V <$	$0.8 \cdot V_N$	< 100 ms
Rise-in-voltage protection	$V >$	$1.1 \cdot V_N$	< 100 ms
Rise-in-voltage protection	$V \gg$	$1.15 \cdot V_N$	< 100 ms

Irrespective of the number of feed-in phase, PV inverter shall allow for operation under normal stationary operating conditions in the voltage tolerance band $V_N \pm 10\%$ and in their permissible operation points starting with an active power output of more than 20% of the rated active power with the following displacement factors $cos\ \varphi$ or PF. Figure 3.1 shows the standard characteristic curve for $cos\ \varphi$(P) or PF(P) where P_{out} is real power output from PV inverter and P_{rates} is rated real power of PV inverter.

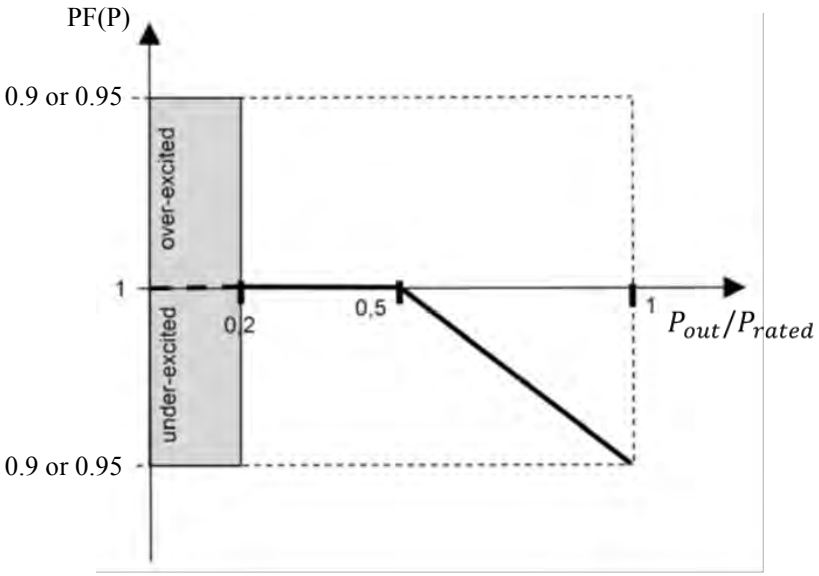

Figure 3.1 Standard characteristic curve for cos φ(P) or PF(P) [31]

- PV inverter size ≤ 3.68 kVA:
  PF = $0.95_{\text{under-excited}}$ to $0.95_{\text{over-excited}}$ which can be adjusted in fixed PF.
- PV inverter size ≤ 13.8 kVA but > 3.68 kVA:
  Characteristic curve provided by network operator within PF = $0.95_{\text{under-excited}}$ to $0.95_{\text{over-excited}}$ (see Figure 3.2).

- PV inverter size > 13.8 kVA:

  Characteristic curve provided by network operator within PF = $0.90_{\text{under-excited}}$ to $0.90_{\text{over-excited}}$ (see Figure 3.2).

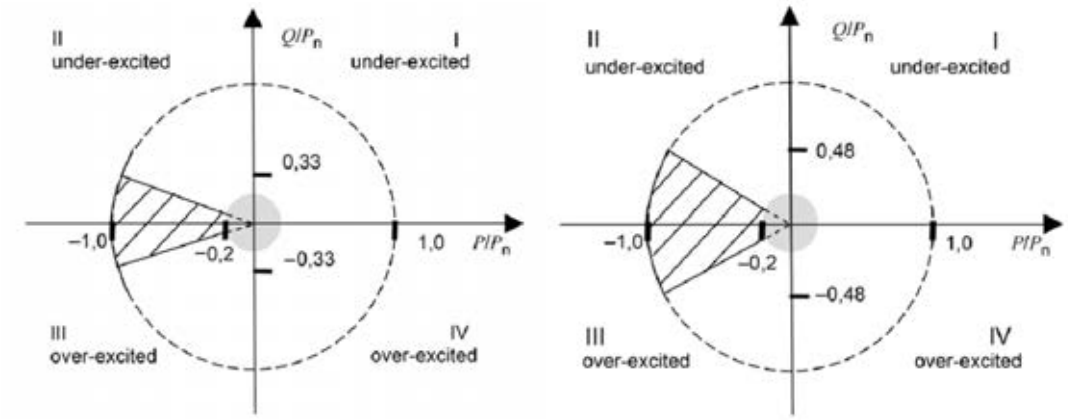

(a) PV inverter size ≤ 13.8 kVA but > 3.68 kVA

(b) PV inverter size >13.8 kVA

Figure 3.2 Limit power range for the reactive power of PV inverter [31]

3.1.2.2 Frequency Control

PV inverter must disconnect from LV system when voltage is out of limit between 47.5 to 51.5 Hz as follows.

Table 3.2 The duration of PV inverter for disconnecting from LV system

Protective Function	**Protection Relay Setting Values**	
Frequency decrease protection $f <$	47.5 Hz	< 100 ms
Frequency increase protection $f >$	51.5 Hz	< 100 ms

At frequencies between 50.2 Hz and 51.5 Hz, all adjustable PV inverter shall reduce (for frequency increase) or increase (for frequency decrease) the active power P_M generated instantaneously (at the time of exceeding the mains frequency 50.2 Hz; freezing the value on the current level) with a gradient of 40% of P_M per Hertz (see Figure 3.3, where P_M is the power generated at the time of exceeding 50.2 Hz; P is the power reduction; f_{mains} is the mains frequency). From this, it follows that PV inverter will continuously move up and down the frequency characteristic curve in the

frequency range of 50.2 Hz to 51.5 Hz with regard to its active power feed-in ("running along the characteristic curve").

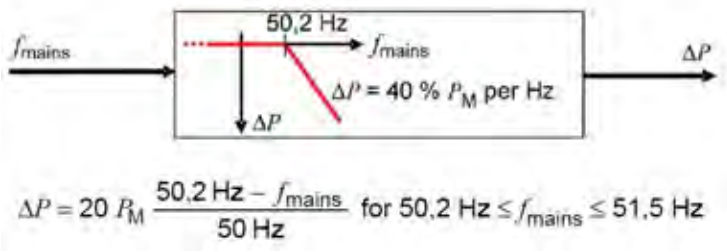

Figure 3.3 Active power reduction at over-frequency [31]

3.1.2.3 Flicker Control

Flicker describes a phenomenon which is characterized by voltage fluctuations whose frequency and amplitude are of a magnitude that causes lamps supplied with this voltage to show disturbing brightness fluctuations. PV inverter shall not exceed long-term severity values (P_{lt}) at 0.5.

3.1.2.4 Harmonic Control

According VDE-AR-N:4015-2011 [31], permissible harmonic currents related to the network short-circuit power S_{kv} that may be supplied in a network connection point can be shown in Table 3.3.

3.1.2.5 DC Current Control

In this standard, the limit of DC current generation from PV inverter does not specify.

3.1.3 The Need for Communication System

In Germany, audio-frequency centralized ripple-control, which are usually operated at frequencies between approximately 100 Hz and 1,500 Hz, use to broadcast control action, such as limiting real power output, to connected PV inverter. Broadcasting levels of audio-frequency impulses are normally about 1% V_N to 4% V_N.

Table 3.3 Permissible harmonic currents [31]

Ordinal number ν, μ	Permissible related harmonic current i_{vzul} in A/MVA
3	3
5	1,5
7	1
9	0,7
11	0,5
13	0,4
17	0,3
19	0,25
23	0,2
25	0,15
$25 < \nu < 40$[a]	$0,15 - 25/\nu$
Even	$1,5/\nu$
$\mu < 40$	$1,5/\nu$
$42 < \nu,\mu < 178$[b]	$4,5/\nu$

[a] Odd.

[b] Integral and non-integral within a range of 200 Hz with the mid-band frequency ν. Measurement in accordance with DIN EN 61000-4-7 (0847-4-7.)

3.2 Standard for Interconnecting Distributed Resources with Electric Power Systems, PEA Grid Code, Thailand (2016) [19]

This standard is used in 74 provinces of Thailand, except Bangkok, Nonthaburi and Samutprakarn. The details of this standard can be clarified into:

3.2.1 Capacity of PV System

In LV distribution system with voltage level 380/220 V, PV system can connect to LV system with single phase connection if the capacity of single phase PV inverter is not more than 5 kW. In case of more than one single phase PV inverter need to connect to LV system, the owner must distribute into each phase connection and the summation of single phase PV inverter at any phases must not be more than 5 kW. Moreover, total connection of PV inverter behind distribution MV/LV transformer must not be more than 15% of the capacity of that MV/LV transformer.

3.2.2 Power quality at the connection point of PV system

The owner must control the PV inverter to comply the followings:

3.2.2.1 Voltage and PF Control

PV inverter must disconnect from LV system if voltage, line to neutral, exceed the limit according to Table 3.4. For PF control, PV inverter must be able to adjust Power Factor (PF) 0.95 lagging to 0.95 leading with only fixed PF method.

Table 3.4 The duration of PV inverter for disconnecting from LV system

Voltage Level	Duration (sec)
$V_{i,l-n} < 50\%$	0.3
$50\% \leq V_{i,l-n} < 90\%$	2.0
$90\% \leq V_{i,l-n} < 110\%$	Still Connect
$110\% \leq V_{i,l-n} < 120\%$	1.0
$V_{i,l-n} \geq 120\%$	0.16

3.2.2.2 Frequency Control

PV inverter must synchronize with LV system all time. If frequency is out of limit 47 to 52 Hz, PV inverter must disconnect from LV system within 0.1 sec.

3.2.2.3 Flicker Control

PV inverter must have short-term and long-term severity values (P_{st} and P_{lt}) within the limit: $P_{st} \leq 1.0$ and $P_{lt} \leq 0.8$.

3.2.2.4 Harmonic Control

For harmonic voltage, total harmonic distortion must be less than 5%, Moreover, odd and even harmonic voltages must be less than 4% and 2% respectively. For harmonic current, the limit can be shown in Table 3.5.

3.2.2.5 DC Current Control

PV inverter must not generate DC current more than 0.5% of rated current of PV inverter into LV system.

3.2.3 The Need for Communication System

PV system connected with LV system does not need the communication system connected with Supervisory Control And Data Acquisition (SCADA) of PEA.

Table 3.5 Harmonic order and current limit

Harmonic Order	Current Limit (A rms)	Harmonic Order	Current Limit (A rms)
2	48	11	19
3	34	12	6
4	22	13	16
5	56	14	5
6	11	15	5
7	40	16	5
8	9	17	6
9	8	18	4
10	7	19	6

3.3 Standard for Interconnecting Distributed Resources with Electric Power Systems, MEA Grid Code, Thailand (2016) [18]

This standard is used in 3 provinces of Thailand, include Bangkok, Nonthaburi and Samutprakarn. The details of this standard can be will clarified into:

3.3.1 Capacity of PV System

In LV distribution system with voltage level 380/220 V, PV system can connect to LV system with single phase connection if the capacity of single phase PV inverter is not more than 5 kW. In case of more than one single phase PV inverter need to connect to LV system, the owner must distribute into each phase connection and the summation of single phase PV inverter at any phases must not be more than 5 kW. Moreover, total connection of PV inverter behind distribution MV/LV transformer must not be more than 15% of the capacity of that MV/LV transformer.

3.3.2 Power quality at the connection point of PV system

The owner must control the PV inverter to comply the following:

3.3.2.1 Voltage and PF Control

PV inverter must disconnect from LV system if voltage exceeds the limit according to Table 3.3. For PF control, PV inverter must be able to adjust Power Factor (PF) 0.95 lagging to 0.95 leading with only fixed PF method.

Table 3.6 The duration of PV inverter for disconnecting from LV system

Voltage Level (Volt)		**Duration (sec)**
Line to Line	**Line to Neutral**	
$V_{i,l-l} < 199$	$V_{i,l-n} < 115$	0.1
$199 \leq V_{i,l-l} < 346$	$115 \leq V_{i,l-n} < 200$	2.0
$346 \leq V_{i,l-l} < 416$	$200 \leq V_{i,l-n} < 240$	Still Connect
$416 \leq V_{i,l-l} < 539$	$240 \leq V_{i,l-n} < 311$	2.0
$V_{i,l-l} \geq 539$	$V_{i,l-n} \geq 311$	0.05

3.3.2.2 Frequency Control

PV inverter must synchronize with LV system all time. If frequency is out of limit 47 to 52 Hz, PV inverter must disconnect from LV system within 0.1 sec.

3.3.2.3 Flicker Control

PV inverter must comply as follows: IEC 61000-3-3 if rated current of PV inverter is less than 16 A; IEC 61000-3-5 if rated current of PV inverter is more than 75 A; IEC 61000-3-11 if rated current of PV inverter is less than 75 A.

3.3.2.4 Harmonic Control

MEA defines only harmonic current limit as shown in Table 3.7.

3.3.2.5 DC Current Control

PV inverter must not generate DC current more than 0.5% of rated current of PV inverter into LV system.

3.3.3 The Need for Communication System

PV system connected with LV system does not need the communication system connected with SCADA of MEA.

Table 3.7 Harmonic order and current limit

Odd-Harmonic Order	Current Limit (%)	Even-Harmonic Order	Current Limit (%)
3-9	4.0	2-10	1.0
11-15	2.0	12-16	0.5
17-21	1.5	18-22	0.375
23-33	0.6	24-34	0.15
≥35	0.3	≥36	0.075
Total Harmonic Distortion			5

3.4 IEC/TR 61850-90-7: Communication networks and systems for power utility automation – Part 90-7: Object models for power converters in distributed energy resources (DER) systems (2013)

PV systems tend to increase the connection in LV distribution system because of the policies of many countries and the reduction cost of related devices in PV system. The increment of PV installation in LV distribution system will cause high PV penetration problem in LV distribution system. National Research Energy Laboratory (NREL) recommends in supporting high PV penetration in LV distribution system that PV inverter should develop into advanced or smart one whose include non-autonomous and autonomous functions in PV inverter and the details can be shown in Table 3.8.

The above 3 standards (VDE-AR-N:4105-2011, PEA and MEA grid code) do not recommend smart PV inverter to support high PV penetration in LV distribution system. PEA and MEA grid code specify high PV penetration level at 15% of the size of MV/LV distribution transformer. For VDE-AR-N:4105-2011, the high PV penetration level depends on the assessment from grid operator. However, this IEC/TR 61850-90-7 standard [32] talks about the control function in smart PV inverter that the

main functions can be described such as immediate control, volt-var management, watt-triggered behavior and voltage-watt management function.

Table 3.8 Autonomous versus non-autonomous inverter functions [33]

Description		Functions	Associated Proceedings and Standards	
Autonomous	– No communications architecture needed – Behavior controlled by inverter operating parameters – Parameters defined at system commissioning or later – Parameters can be adjusted, behavior activated or deactivated at later date via remote or on-site changes	Low- / High-voltage ride-through	SIWG Phase 1	IEEE 1547a-2014
		Low- / High-frequency ride-through		
		Volt-var control (via dynamic reactive power injection)		
		Anti-islanding		
		Ramp-rate controls (for default/emergency conditions)		
		Provide reactive power (via fixed power factor)		
		Reconnect via "soft-start"		
		Frequency-watt	SIWG Phase 3	
		Voltage-watt		
		Dynamic current support		
		Smooth frequency deviations		
Non-Autonomous	– Communications and control infrastructure required – Direct control of inverter behavior – Control from remote operator commands or feedback, based on conditions at point of common coupling	Command DER to connect/disconnect	SIWG Phase 3	
		Limit real power		
		Set real power		
		Provide black-start capability		
		Respond to real power pricing signals		
		Participate in automatic generator control (AGC)		
		Provide spinning reserves or bid into market		
		Update static set points for autonomous functions (fixed power factor, volt-var curves, voltage ride-through, frequency ride-through)		

3.4.1 Immediate Control Functions

Immediate control functions assume a tightly coupled interaction between PV systems and a controlling entity (utility, energy service provider or grid operator). This implies that the controlling entity has knowledge about the capabilities of the PV systems, can request updates on their current status, can expect the PV systems to

follow the command to the best of their capabilities, and will receive a direct response from the PV systems on the results from following the command.

3.4.1.1 Connect/Disconnect from Grid Function

This function causes the PV system to immediately physically connect or disconnect from LV system at the connection point to LV system.

3.4.1.2 Adjust Maximum Generation Level up/down Function

This function sets the maximum generation level at the connection point to LV system as percentage. This limitation could be met by limiting PV output.

3.4.1.3 Adjust Power Factor Function

Fixed power factor will be managed through issuing a power factor value and corresponding excitation.

3.4.2 Volt-Var Management Functions

Since utilities (and/or grid operator) will be requesting var support from many different PV systems with different capabilities, different ranges, and different local condition, it would be very demanding of the communications systems, unnecessary, and ultimately impossible for the utilities to issue explicit settings to each PV system every time a change is desired. Therefore, volt-var behaviors can be configured in to a PV inverter using arrays that establish a volt-var relationship or curve for use during normal operating system.

3.4.2.1 Available Var Support Mode With No Impact On Watts Function

As one example of volt-var modes, the available vars mode reflects the calculation of the most efficient and reliable var levels for PV systems at specific connection point to LV system without impacting the watts output. This mode could also help compensate for local high voltage due to real power output back flow in LV system. In this mode, PV systems will be provided with a double array of setpoints: a set of voltage levels and their corresponding var levels as % of available vars ($VArAval$). The voltage levels will range between $V1$ and $V4$ in increasing voltage values. Values between these setpoints will be interpolated to create a piecewise linear volt-var function. Figure 3.4 provides one example of volt-var settings for this mode.

For $VArAval$, it can be calculated in equation (3.1) where S_{spec} is the apparent power limit of PV inverter and P_{out} is real power output from PV inverter.

$$VArAval = \sqrt{S_{spec}^2 - P_{out}^2} \tag{3.1}$$

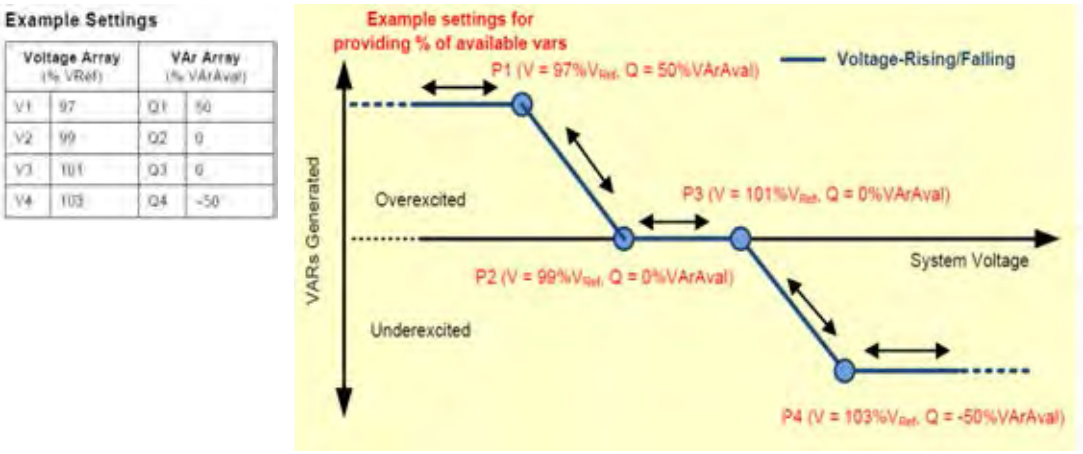

Figure 3.4 Available var support mode with no impact on watts function [32]

3.4.2.2 Static Mode Based on Setting or Fixed PF

Another example mode establishes fixed var settings for PV inverter as illustrated in Figure 3.5. This mode does not use curves but only settings.

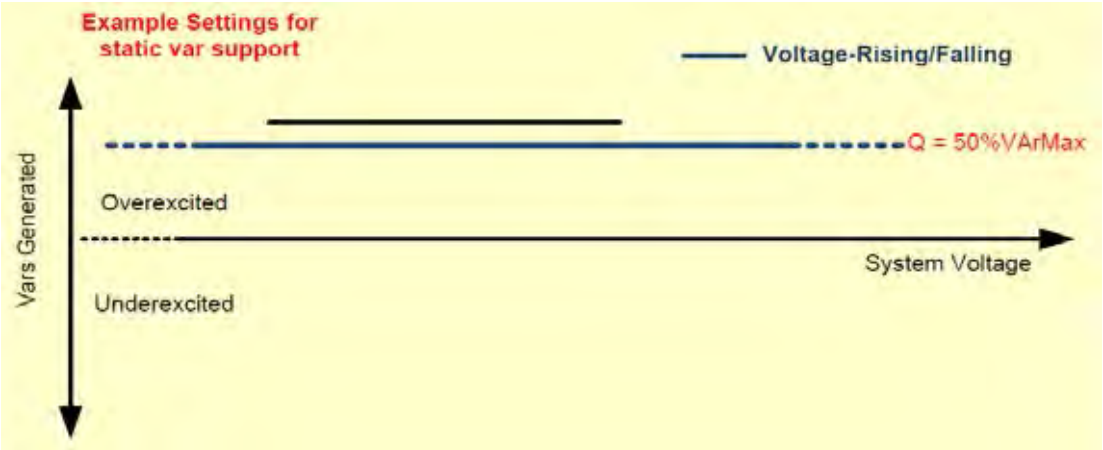

Figure 3.5 Static var support mode based on maximum reactive power ($VArMax$) [32]

3.4.2.3 Passive Mode With No Var Support

This example mode is the same as the mode in Subsection 3.4.2.2, except that the var levels are zero.

3.4.3 Watt-Triggered Behavior Functions

The amount of watts provided at the connection point to LV system can be set to gradually modify the power factor. This watt-power factor mode is shown in Figure 3.6. The power factor will be set in relation to the feed-in power, in this example ranging from 0.85 underexcited to 0.90 overexcited. These settings are not expected to be updated very often over the life time of the PV system.

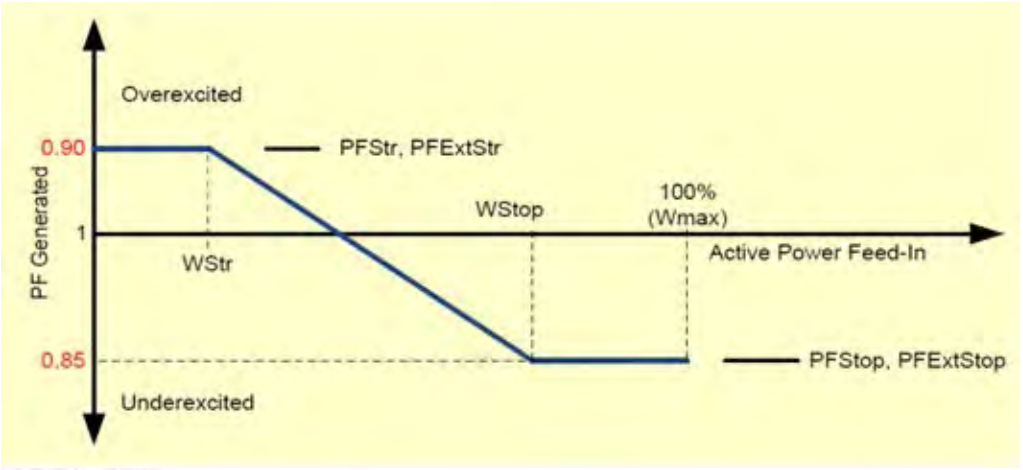

Example Settings

Power (% WMax)		Power Factor		Power Factor with convention defined by PFsign and PFExt	
WStr	20	PFStr	0.9	PFExtStr	Overexcited= False
WStop	40	PFStop	0.85	PFExtStop	Underexcited= True

Figure 3.6 Power factor controlled by feed-in power [32]

3.4.4 Voltage-Watt Management Functions

A voltage-watt management can be used for smoothing voltage deviation. From Figure 3.7, PV real power output will be constant if voltage increase from V1 to V2 but PV real power output will be decreasing if voltage is increasing from V2 to V3. It is because of prevention from overvoltage at V3 due to real power generation from PV inverter.

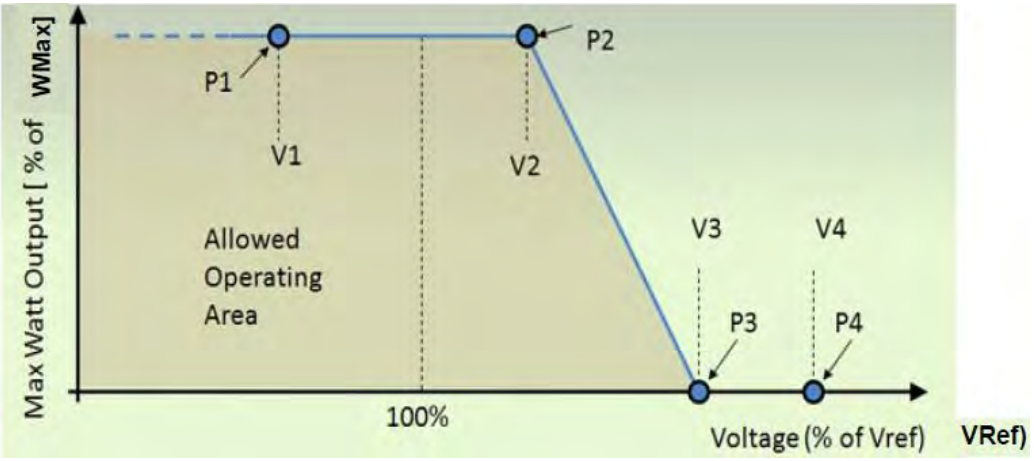

Figure 3.7 Configuration curve for maximum watts vs. voltage [32]

CHAPTER 4

COORDINATION BETWEEN CENTRAL AND LOCAL CONTROL

This chapter will address the problem in high PV penetration in LV system, which is aimed to be solved by applying only central or local control and coordination between central and local control.

4.1 Impact of the Installation of PV system in LV System

The connection of PV systems is currently increasing in LV distribution system, especially at households, due to the support of government and the decrease of solar PV system installation cost. However, more installation of solar PV systems in LV distribution system can cause the disadvantages as follows.

4.1.1 Voltage Unbalance

In the situation where there is too many solar PV systems installed in LV distribution system, especially single-phase PV inverter and the installation in each phase is not the same size. Consequently, the voltage in each phase is not equal which is the problem with unbalanced voltage in the LV system. For example, Figure 4.1 shows a connected single-phase PV inverter with only 2 phases (A and B) and also different size, so it will cause a voltage unbalance. From the IEC 61000-2-2 [33], it specifies voltage unbalance factor in LV distribution system that should not exceed 3% of The voltage unbalance factor can be calculated from equation (2.6) where VUF_i is voltage unbalance factor at node i; $V_{i,ne}$ is negative-sequence voltage at node i (V); $V_{i,po}$ is positive-sequence voltage at node i (V).

$$VUF_i = \frac{|V_{i,ne}|}{|V_{i,po}|} \times 100\% \tag{4.1}$$

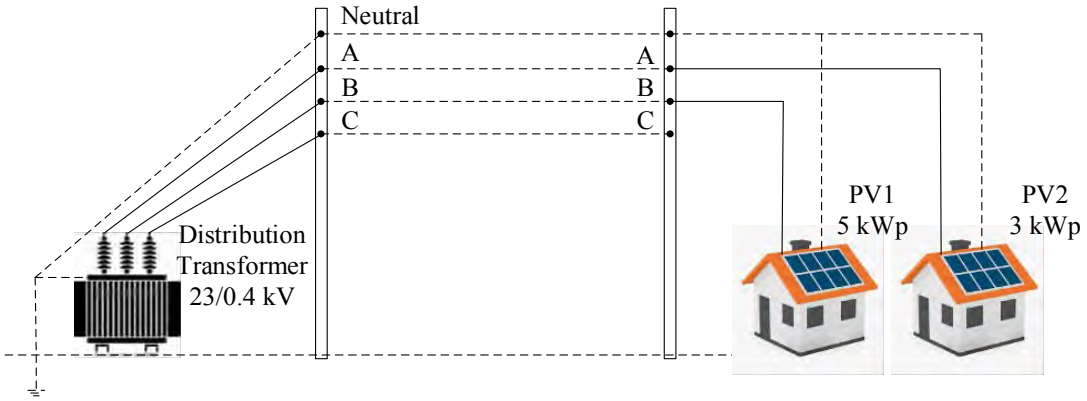

Figure 4.1 The example of installed single-phase PV inverter which causes voltage unbalance

4.1.2 Loss of PV generation

In the situation where there is solar PV system installed in LV system, especially on downstream nodes, voltage can be risen at the end of system as shown in Figure 4.2 (a). However, voltage can be ramped up over the overvoltage limit when system load is decreased as shown in Figure 4.2 (b) and, then the overvoltage protection of the PV inverter will operate, whereby the PV inverters in the downstream nodes are disconnected. Consequently, loss of PV generation is occurred.

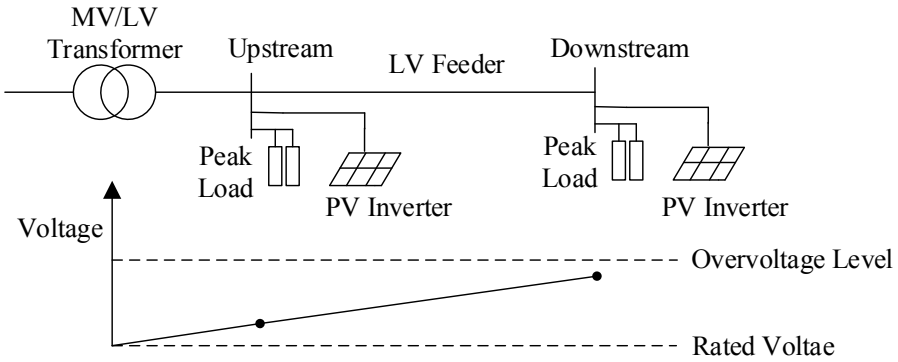

(a) At peak load

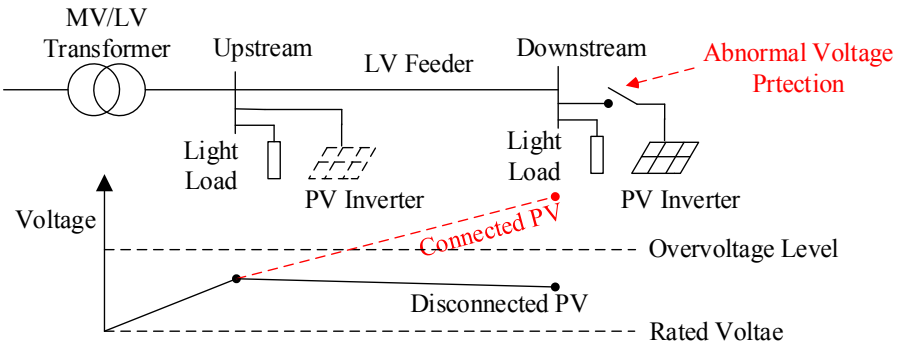

(b) At light load

Figure 4.2 Voltage profile example in LV distribution system

4.2 Central Control

The concept of central control is that there is a central computer unit which controls each connected PV system following the command of central unit such as adjusting power factor, real power output and reactive power. The diagram for the concept of central control can be shown in Figure 4.3. The advantage is fast response in voltage control in LV system through communication system. The disadvantage is the need of very reliable communication system because some PV system will be disconnected from LV system in some situations if the command in communication medium is lost or that PV system is uncontrolled as shown in Figure 4.4 which is modified from Figure 4.2 in light load situation.

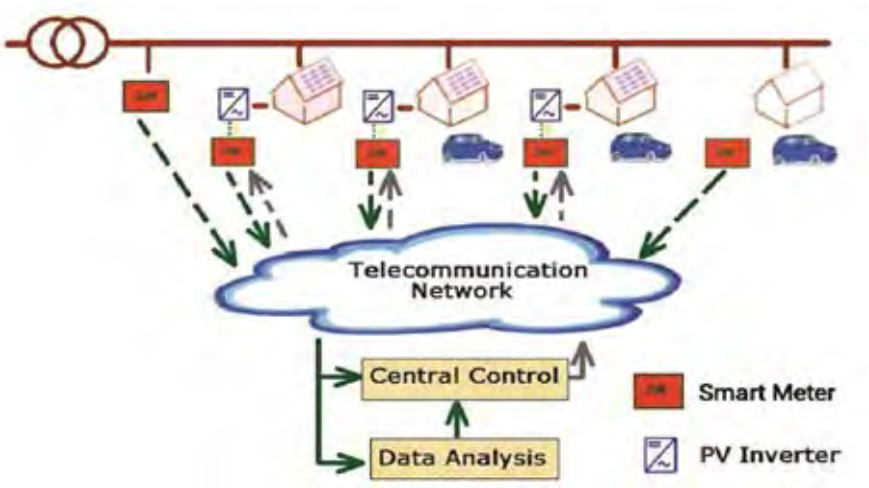

Figure 4.3 The diagram of central control and connected PV system [7]

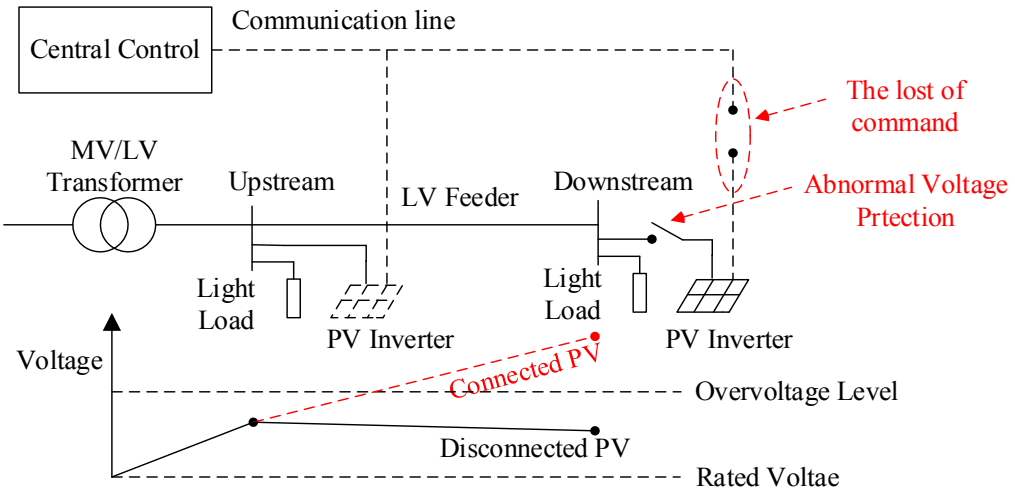

Figure 4.4 The communication lost which can cause the disconnected PV system

4.3 Local Control

Local control or autonomous control can operate at PV inverter autonomously. For example, they can be shown in previous Subsections 3.4.2 to 3.4.4. In Figure 3.4, volt-var function, when voltage at the connection point of PV system is changed, reactive power output from PV system is also changed. In Figure 3.6, watt triggered behavior function, when real power output from PV system is changed, reactive power from PV system is also changed. Finally Figure 3.7, voltage-watt management function, uses for smoothing voltage deviation. When voltage at the connection point of PV system is changed, real power output from PV system is also changed. The advantage of local control is that there is no need for communication system with other units because PV system just uses local condition for adjusting following local control function. The disadvantage is the parameter setting of local control is fixed for all times that it is not optimal for any specified period, such as one-week period because load profile from each one-week period is likely to be different. Then, optimal parameter setting should be readjusted every one week.

4.4 Coordination between Central and Local Control

This research applies coordination setting between central and local control to support high PV penetration in LV distribution system. It is because of benefits as followings:

- The coordination setting between central and local control does not need for very reliable communication system because central control rarely contacts with each PV system to update parameter setting of local control.
- When the communication signals to the PV systems are loss. Those PV systems can still operate following the past parameter setting of local control.

The big picture of the coordination between central and local control can be shown in Figure 4.5 which LV distribution system must be based on smart grid. LV distribution system must integrate with smart meter or even ambient weather sensor to monitor or predict the condition that affects LV distribution system. PV system must be smart and can be embedded local control for controlling real and reactive power output. Moreover, PV system must be capable to receive or send signal to remote unit or central control.

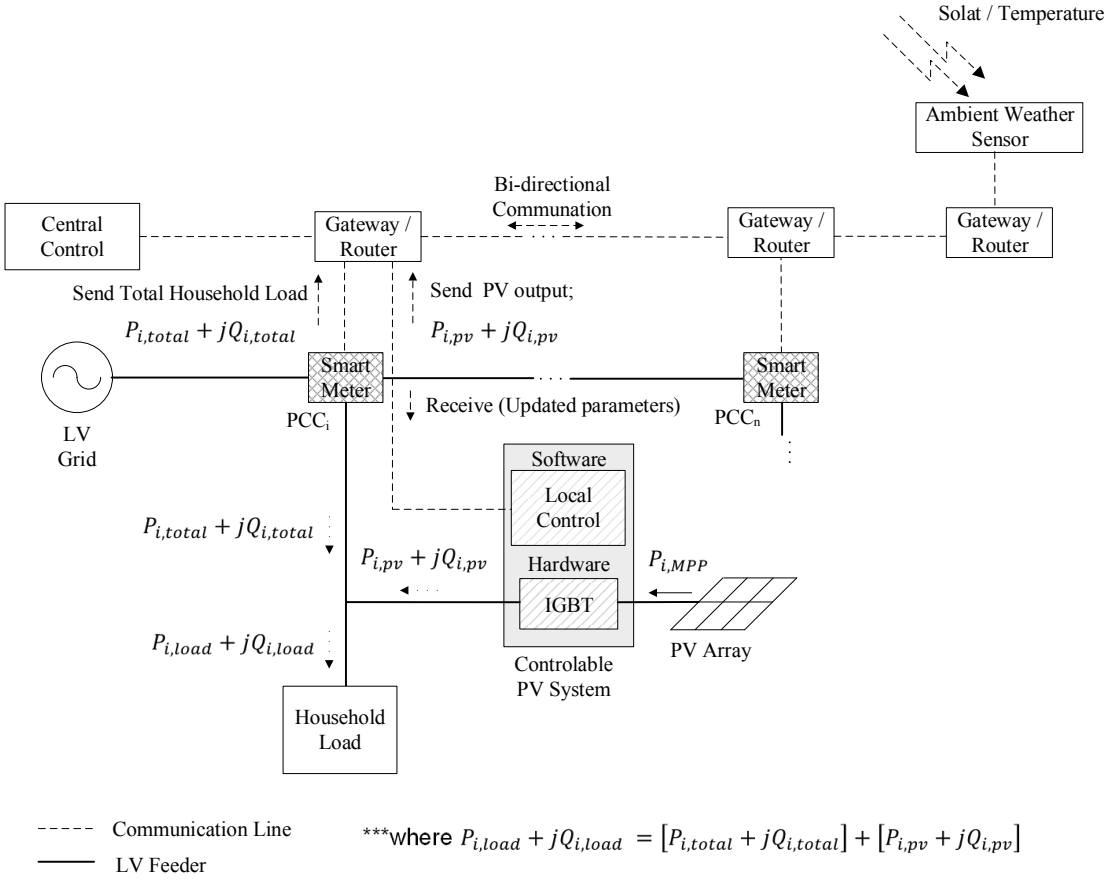

Figure 4.5 The coordination between central and local control

4.4.1 Local Control Application

In this dissertation, PV system is determined that it can be embed by both two types of local control function such as continuous and piecewise linear functions and, however, only one type can be selected to operate at specific time. The details of both two types of local control function can be explained as follows.

4.4.1.1 Continuous Local Control Function

Research [12] uses local control that can be shown in equation (4.2) where Q_i is reactive power output from PV inverter at connection point i (Var); Q_i^{max} is maximum reactive power capability of PV system at connection point i (VAr); δ_i is slop of $Q_i(Q_i^{max}, \delta_i, V_i)$ function at connection point i; V_i is voltage at the connection point i of PV system (pu.).

$$Q_i(q_i^{max}, \delta_i, V_i) = Q_i^{max}\left(1 - \frac{2}{1 + exp[-4\,(V_i - 1)/\delta_i]}\right) \quad (4.2)$$

Voltage-watt function or P(U) function in equations (4.3) and (4.4) that are used in this research. They can be modified from equation (4.2). Q_i^{max} in equation (4.2) is replaced by P_i^{max} or maximum real power output that depend on specified rated real power output ($P_{i,rated}$) and MPP from PV array ($P_{i,MPP}$) and P_i^{max} determination can be shown in equation (4.5). For $P_{i,MPP}$, it can be calculated from Equations (2.1)-(2.5). The constant 1 which is in term of exp in equation (4.2) is replaced by $V_{i,cri}^{\sigma}$ or $V_{i,cri}$. The variable δ_i in equation (4.2) is replaced by $\delta_{i,p}^{\sigma}$ or $\delta_{i,p}$. The variable V_i in equation (4.2) is replaced by $|V_i^{\sigma}|$ or $(|V_i^A| + |V_i^B| + |V_i^C|)/3$. The equations (4.3) and (4.4) are for single and three phase PV inverter respectively. The adjustment of $V_{i,cri}$ (or $V_{i,cri}^{\sigma}$) will cause the change of the voltage which initiates limiting real power as shown in Figure 4.6 (a). The adjustment of $\delta_{i,p}$ (or $\delta_{i,p}^{\sigma}$) will cause the change of slope as shown in Figure 4.6 (b).

$$P_{i,pv}^{\sigma} = P_i^{max}\left(1 - \frac{1}{1 + exp\left[-4\left(|V_i^{\sigma}| - V_{i,cri}^{\sigma}\right)/\delta_{i,p}^{\sigma}\right]}\right) \quad (4.3)$$

$$P_{i,pv} = P_i^{max}\left(1 - \frac{1}{1 + exp\left[-4\left(\frac{\left|V_i^A\right| + \left|V_i^B\right| + \left|V_i^C\right|}{3} - V_{i,cri}\right)\Big/\delta_{i,p}\right]}\right) \quad (4.4)$$

$$P_i^{max} = \begin{cases} P_{i,MPP} & ; P_{i,MPP} \le P_{i,rated} \\ P_{i,rated} & ; P_{i,MPP} > P_{i,rated} \end{cases} \quad (4.5)$$

where σ is any phase (A, B or C); V_i^{σ} is voltage at the connection point i of PV system (pu.); $V_{i,cri}$ (or $V_{i,cri}^{\sigma}$) and $\delta_{i,p}$ (or $\delta_{i,p}^{\sigma}$) are adjustable parameters at the connection point i of PV system.

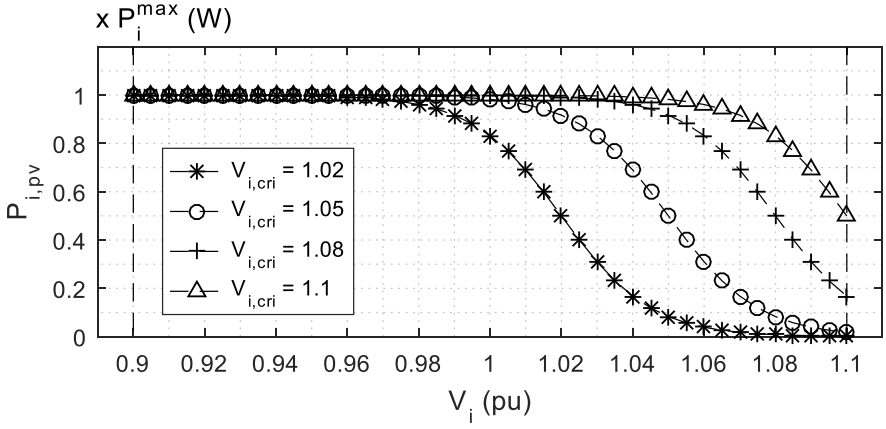

(a) Adjustment of $V_{i,cri}$ and fix of $\delta_{i,p}$ that equals 0.05

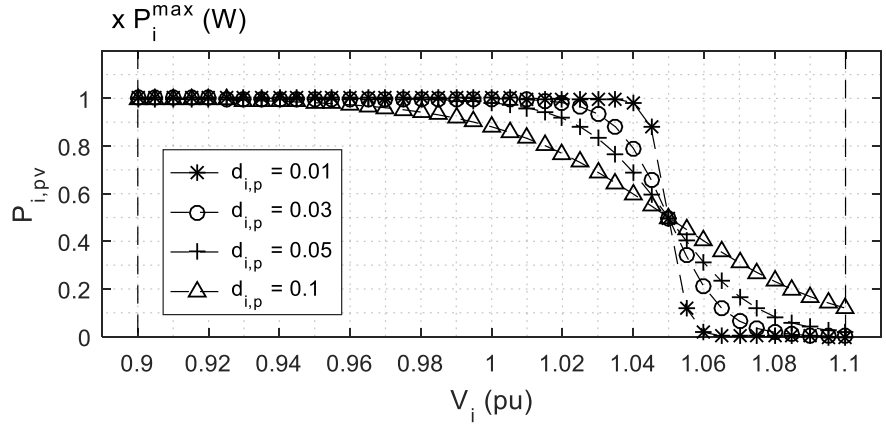

(b) Adjustment of $\delta_{i,p}$ and fix of $V_{i,cri}$ that equals 1.05

Figure 4.6 Characteristic curve of P(U) function when adjust $\delta_{i,p}$ or $V_{i,cri}$

For applying volt-var function or Q(U) function in equations (4.6) and (4.7), the constant 1 which is the first term of equation (4.2) is replaced by $K_{i,1}^{\sigma}$ or $K_{i,1}$. The

constant 2 in the second term of equation (4.2) is replaced by $K_{i,2}^{\sigma}$ or $K_{i,2}$. The variable V_i is replaced by V_i^{σ} or $(V_i^A + V_i^B + V_i^C)/3$. The other constant 1 which is in term of exp is replaced by $V_{i,q}^{\sigma}$ or $V_{i,q}$. The variable δ_i in equation (4.2) is replaced by $\delta_{i,q}^{\sigma}$ or $\delta_{i,q}$. The equation (4.6) and (4.7) are for single and three phase PV inverter respectively. The adjustment of $K_{i,1}$ (or $K_{i,1}^{\sigma}$) and $K_{i,2}$ (or $K_{i,2}^{\sigma}$) will cause the change of reactive power output as shown in Figure 4.7 (a). The adjustment of $V_{i,q}$ (or $V_{i,q}^{\sigma}$) will cause the change of the voltage which initiates to absorb or inject reactive power as shown in Figure 4.7 (b). Finally, The adjustment of $\delta_{i,q}$ (or $\delta_{i,q}^{\sigma}$) will affect the slope as shown in Figure 4.7 (c).

$$Q_{i,pv}^{\sigma} = Q_i^{max}\left(K_{i,1}^{\sigma} - \frac{K_{i,2}^{\sigma}}{1 + exp\left[-4\left(\left|V_i^{\sigma}\right| - V_{i,q}^{\sigma}\right)/\delta_{i,q}^{\sigma}\right]}\right) \tag{4.6}$$

$$Q_{i,pv} = Q_i^{max}\left(K_{i,1} - \frac{K_{i,2}}{1 + exp\left[-4\left(\frac{\left|V_i^A\right| + \left|V_i^B\right| + \left|V_i^C\right|}{3} - V_{i,q}\right)\Big/\delta_{i,q}\right]}\right) \tag{4.7}$$

where $K_{i,1}$ (or $K_{i,1}^{\sigma}$), $K_{i,2}$ (or $K_{i,2}^{\sigma}$), $V_{i,q}$ (or $V_{i,q}^{\sigma}$) and $\delta_{i,q}$ (or $\delta_{i,q}^{\sigma}$) are adjustable parameters at the connection point j of PV system.

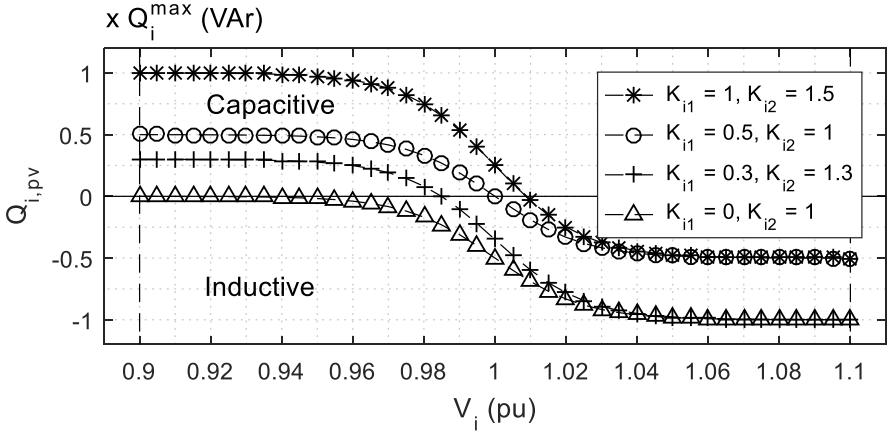

(a) Adjustment of $K_{i,1}$ and $K_{i,2}$ and fix of $V_{i,q}$ and $\delta_{i,q}$ which equal 1 and 0.05 respectively

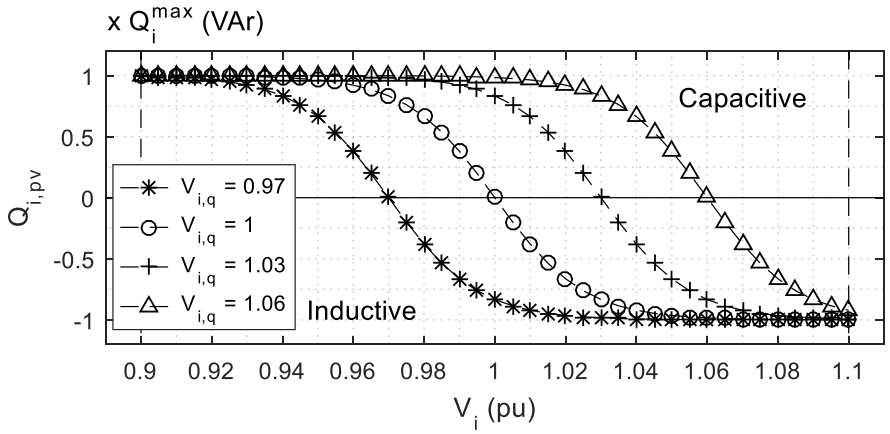

(b) Adjustment of $V_{i,q}$ and fix of $K_{i,1}$, $K_{i,2}$ and $\delta_{i,q}$ which equal 1, 2 and 0.05 respectively

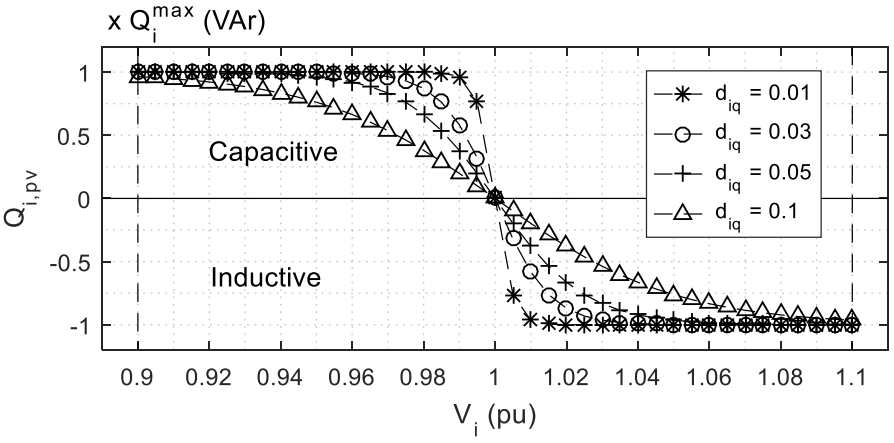

(c) Adjustment of $\delta_{i,q}$ and fix of $K_{i,1}$, $K_{i,2}$ and $V_{i,q}$ which equal 1, 2 and 1 respectively

Figure 4.7 Characteristic curve of Q(U) function when adjust $K_{i,1}$, $K_{i,2}$, $V_{i,q}$ or $\delta_{i,q}$

4.4.1.2 Piecewise Linear Local Control Function

Research [11] and many local control applications [34, 35] use piecewise linear local control function as shown in Figure 4.8.

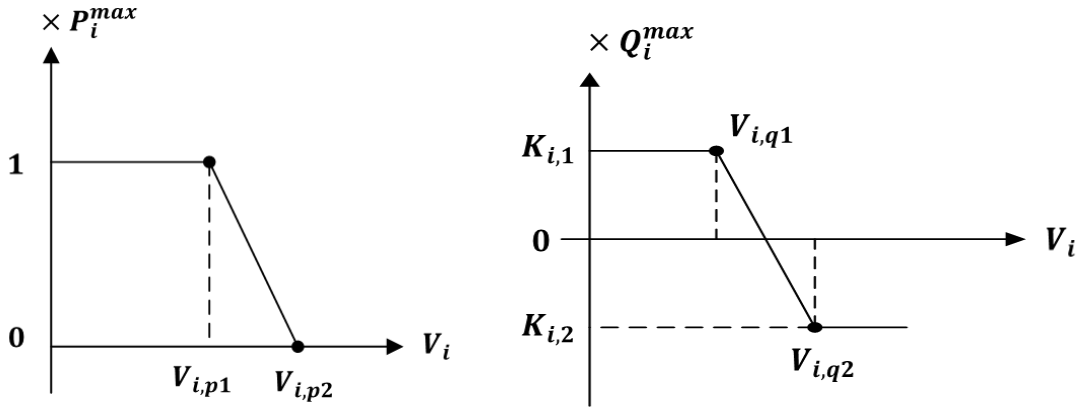

(a) P(U) function *(b) Q(U) function*

Figure 4.8 Piecewise linear local control function

For P(U) function at Figure 4.8 (a), $V_{i,p1}$ (or $V_{i,p1}^{\sigma}$) and $V_{i,p2}$ (or $V_{i,p2}^{\sigma}$) are adjustable parameters. The equations (4.8) and (4.9) are applied for 1-phase and 3-phase PV systems respectively.

$$P_{i,pv}^{\sigma} = P_i^{max} \cdot \begin{cases} 1 & ; |V_i^{\sigma}| < V_{i,p1}^{\sigma} \\ \dfrac{|V_i^{\sigma}| - V_{i,p2}^{\sigma}}{V_{i,p1}^{\sigma} - V_{i,p2}^{\sigma}} & ; V_{i,p1}^{\sigma} \le |V_i^{\sigma}| < V_{i,p2}^{\sigma} \\ 0 & ; V_{i,p2}^{\sigma} \le |V_i^{\sigma}| \end{cases} \tag{4.8}$$

$$P_{i,pv} = P_i^{max} \cdot \begin{cases} 1 & ; |V_i| < V_{i,p1} \\ \dfrac{|V_i| - V_{i,p2}}{V_{i,p1} - V_{i,p2}} & ; V_{i,p1} \le |V_i| < V_{i,p2} \\ 0 & ; V_{i,p2} \le |V_i| \end{cases} \tag{4.9}$$

$$P_i^{max} = \begin{cases} P_{i,MPP} & ; P_{i,MPP} \le P_{i,rated} \\ P_{i,rated} & ; P_{i,MPP} > P_{i,rated} \end{cases} \tag{4.10}$$

where $|V_i| = \frac{|V_i^A| + |V_i^B| + |V_i^C|}{3}$.

For Q(U) function at Figure 4.8 (a), $K_{i,1}$ (or $K_{i,1}^{\sigma}$), $K_{i,2}$ (or $K_{i,2}^{\sigma}$), $V_{i,q1}$ (or $V_{i,q1}^{\sigma}$) and $V_{i,q2}$ (or $V_{i,q2}^{\sigma}$) are adjustable parameters. The equations (4.11) and (4.12) are applied for 1-phase and 3-phase PV systems respectively.

$$Q_{i,pv}^{\sigma} = Q_i^{max} \cdot \begin{cases} K_{i,1}^{\sigma} & ; |V_i^{\sigma}| < V_{i,q1}^{\sigma} \\ f_i^{\sigma}(x) & ; V_{i,q1}^{\sigma} \le |V_i^{\sigma}| < V_{i,q2}^{\sigma} \\ K_{i,2}^{\sigma} & ; V_{i,q2}^{\sigma} \le |V_i^{\sigma}| \end{cases} \tag{4.11}$$

$$Q_{i,pv} = Q_i^{max} \cdot \begin{cases} K_{i,1} & ; |V_i| < V_{i,q1} \\ f_i(x) & ; V_{i,q1} \le |V_i| < V_{i,q2} \\ K_{i,2} & ; V_{i,q2} \le |V_i| \end{cases} \quad (4.12)$$

where $f_i^{\sigma}(x) = \frac{(K_{i,1}^{\sigma} - K_{i,2}^{\sigma})|V_i^{\sigma}| + K_{i,2}^{\sigma} \cdot V_{i,q1}^{\sigma} - K_{i,1}^{\sigma} \cdot V_{i,q2}^{\sigma}}{V_{i,q1}^{\sigma} - V_{i,q2}^{\sigma}}$; $f_i(x) = \frac{(K_{i,1} - K_{i,2})|V_i| + K_{i,2} \cdot V_{i,q1} - K_{i,1} \cdot V_{i,q2}}{V_{i,q1} - V_{i,q2}}$;

$|V_i| = \frac{|V_i^A| + |V_i^B| + |V_i^C|}{3}$.

4.4.1.3 Operational Region of Local Control

According to the manual [34], the operational region of local control of SMA PV inverter can be shown in Figure 4.9 which local control will operate on blue-shaded area at normal condition. $P_{i,rated}$ and $S_{i,rated}$ are the specified rated real and apparent power output of PV system at node i respectively. $Q_{i,max}$ is the maximum reactive power output that equals $0.5 \times P_{i,rated}$.

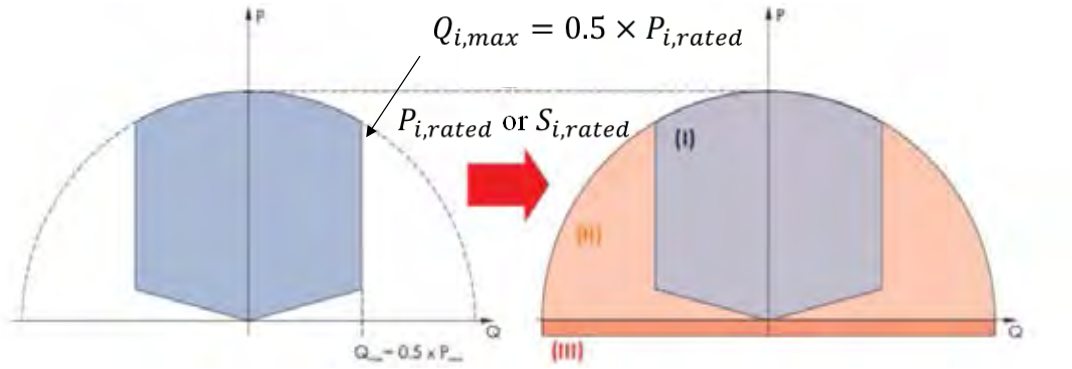

Figure 4.9 The operation region of local control of SMA PV inverter

To simplify the operational region in Figure 4.9, this dissertation determines the operational region as shown in Figure 4.10 that local control will operate on shaded area which real power output will be not more than $P_{i,rated}$ or the maximum allowable real power output which can be determined from equation (4.5) or equation (4.10).

Figure 4.10 The operational region of local control

4.4.2 Central Control Application

From research [36], it presents central control as shown in Figure 4.8 that contains 4 main parts such as (1) monitoring part of Advanced Metering Infrastructure (AMI) and ambient weather condition, (2) simulation part of distribution system model, (3) decision part to control PV system and (4) communication part to PV system.

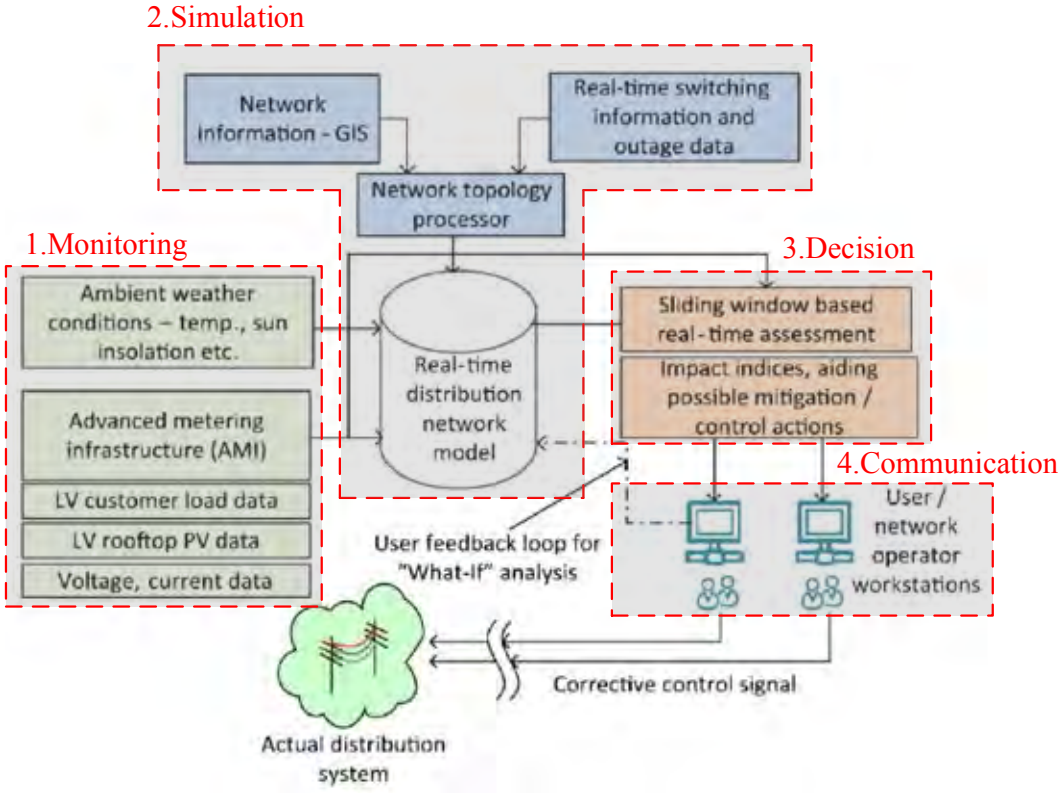

Figure 4.11 Central control diagram of research [36]

In this research, the modified central control is presented in Figure 4.9 that contains 5 main parts such as (1) communication part to PV system, (2) uncertainty analysis, (3) PV system model, (4) LV grid model and (5) decision or optimization part. For optimization part, it will be addressed later in Chapter 5.

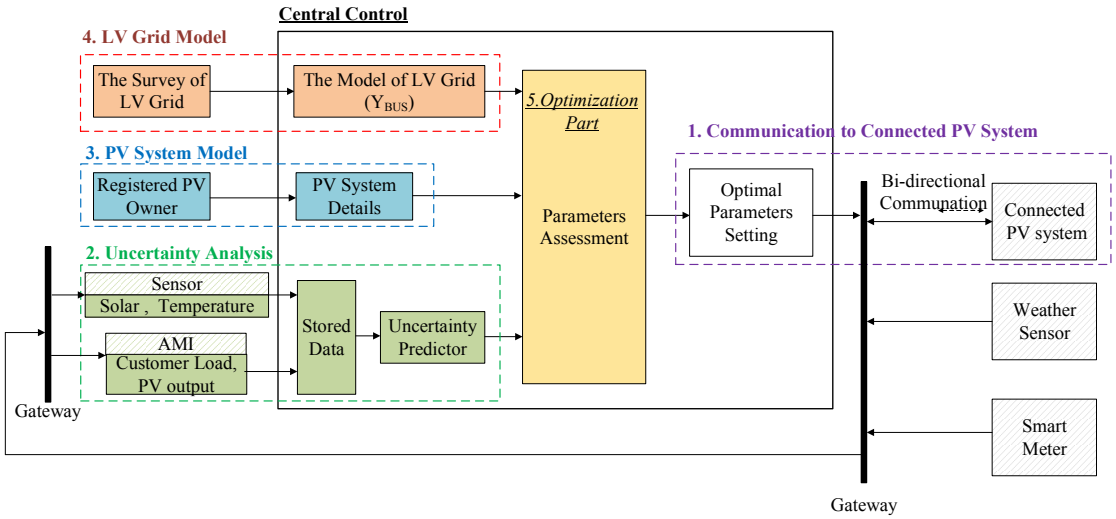

Figure 4.12 The modified central control

4.4.2.1 Communication Part to Connected PV System

This part is communication system between central control and connected PV system to send optimal parameter setting to local control of connected PV system. The optimal parameters setting will be obtained from optimization part which will be addressed later in Chapter 5. The parameters setting will depend on type of local control as shown in Tables 4.1 and 4.2 where npv is the total number of connected PV systems.

Table 4.1 The parameters setting of continuous local control function

PV	Local Control					
	P(U) Function		Q(U) Function			
1st	$V_{1,cri}$	$\delta_{1,p}$	$K_{1,1}$	$K_{1,2}$	$V_{1,q}$	$\delta_{1,q}$
2nd	$V_{2,cri}$	$\delta_{2,p}$	$K_{2,1}$	$K_{2,2}$	$V_{2,q}$	$\delta_{2,q}$
⋮	⋮	⋮	⋮	⋮	⋮	⋮
ith	$V_{i,cri}$	$\delta_{i,p}$	$K_{i,1}$	$K_{i,2}$	$V_{i,q}$	$\delta_{i,q}$
⋮	⋮	⋮	⋮	⋮	⋮	⋮
npv^{th}	$V_{npv,cri}$	$\delta_{npv,p}$	$K_{npv,1}$	$K_{npv,2}$	$V_{npv,q}$	$\delta_{npv,q}$

Table 4.2 The parameters setting of piecewise linear local control function

PV	Local Control					
	P(U) Function		Q(U) Function			
1st	$V_{1,p1}$	$V_{1,p2}$	$K_{1,1}$	$K_{1,2}$	$V_{1,q1}$	$V_{1,q2}$
2nd	$V_{2,p1}$	$V_{2,p2}$	$K_{2,1}$	$K_{2,2}$	$V_{2,q1}$	$V_{2,q2}$
⋮	⋮	⋮	⋮	⋮	⋮	⋮
ith	$V_{i,p1}$	$V_{i,p2}$	$K_{i,1}$	$K_{i,2}$	$V_{i,q1}$	$V_{i,q2}$
⋮	⋮	⋮	⋮	⋮	⋮	⋮
npv^{th}	$V_{npv,p1}$	$V_{npv,p2}$	$K_{npv,1}$	$K_{npv,2}$	$V_{npv,q1}$	$V_{npv,q2}$

4.4.2.2 Uncertainty Analysis Unit

This part collects data from AMI, which can monitor load of customer, and weather sensor, which can monitor ambient condition such as solar irradiance and ambient temperature to assess the operation of connected PV system. The uncertainty characteristic will be assessed or predicted in one day or one week ahead from the collected data in the previous period. The collected data will be assessed into uncertainty characteristic as shown in equation (4.13) which is normal distribution probability. Figure 4.14 (a) shows the example of collected data and Figure 4.14 (b) shows the transformed normal distribution curve with maximum, mean, and minimum data.

$$f(x) = \frac{1}{\sqrt{2p^2\pi}} e^{-\frac{(x-\mu)^2}{2p^2}} \quad ; x_{min} \leq x \leq x_{max} \tag{4.13}$$

where ρ is standard deviation value; μ is mean value; x is collected data value; x_{min} and x_{max} are minimum and maximum collected data value.

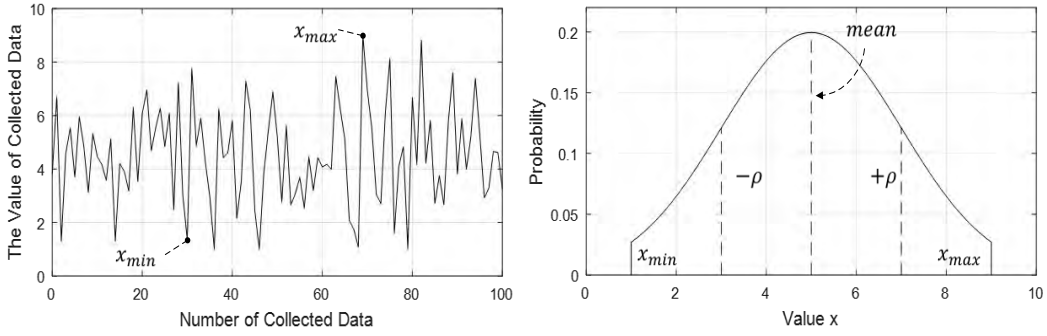

(a) The collected data *(b) Transformed normal distribution curve*

Figure 4.13 The example of normal distribution determination

This research determines 3-phase unbalance LV distribution system, connected with PV system. Then, 17 cases of the set of uncertainty will be determined to cover uncertainty problem as shown in Table 4.2. For minimum MPP of connected PV system, solar irradiance at 0.05 kW/m^2 [20] is considered because it is initial condition that PV system initiates to operate.

Table 4.3 Set of uncertainty for covering uncertainty problem

Case	**Load**			**MPP of connected PV system**
	Phase A	**Phase B**	**Phase C**	
z1	Mean	Mean	Mean	Mean
z2	Max	Max	Max	Max
z3	Max	Max	Max	Min
z4	Max	Max	Min	Max
z5	Max	Max	Min	Min
z6	Max	Min	Max	Max
z7	Max	Min	Max	Min
z8	Max	Min	Min	Max
z9	Max	Min	Min	Min

Case	Load			MPP of connected PV system
	Phase A	Phase B	Phase C	
z10	Min	Max	Max	Max
z11	Min	Max	Max	Min
z12	Min	Max	Min	Max
z13	Min	Max	Min	Min
z14	Min	Min	Max	Max
z15	Min	Min	Max	Min
z16	Min	Min	Min	Max
z17	Min	Min	Min	Min

4.4.2.3 PV System Model Determination

Central control needs to collect PV system details of customers for assessing the power generation from PV system. For example, Tables 4.4 and 4.5 show 2-kW and 10-kW PV system details respectively.

Table 4.4 2-kW PV system details

Parameters	Values	Parameters	Values
V_{oc}^{0} at Nominal Cell Operating Temperature (NOCT)	42.3 V	V_{MPP}^{0} at NOCT	33.7 V
I_{sc}^{0} at NOCT	7.16 A	I_{MPP}^{0} at NOCT	6.56 A
NOCT (N_{OT})	45 °C	Number of PV panel	12 panels
K_i	5.3 x 10^{-3} A/ °C	Rated real power of PV inverter	2,000 W
K_v	-1.404 x 10^{-1} V/ °C	Maximum reactive power of PV inverter	1,000 VAr

Table 4.5 10-kW PV system details

Parameters	Values	Parameters	Values
V_{oc}^{0} at NOCT	42.3 V	V_{MPP}^{0} at NOCT	33.7 V
I_{sc}^{0} at NOCT	7.16 A	I_{MPP}^{0} at NOCT	6.56 A
NOCT (N_{OT})	45 ^{o}C	Number of PV panel	58 panels
K_i	5.3 x 10^{-3} A/ ^{o}C	Rated real power of PV inverter	10,000 W
K_v	-1.404 x 10^{-1} V/ ^{o}C	Maximum reactive power of PV inverter	5,000 VAr

If 2-kW PV system connects to phase A and voltage at this connection point is 1.09∠0^{o} pu. Base system voltage is 230 V, line to neutral. The parameters setting of continuous local control function is follows: V_{cri}, δ_p, K_1, K_2, V_q and δ_q are 1.09, 0.02, 1, 2, 1 and 0.05 respectively. Solar irradiance and ambient temperature are 1 kW/m^2 and 30 ^{o}C respectively. Then, power output of this 2-kW PV system can be assessed in 3 steps as follows.

STEP 1: P_{rated} is 2,000 W. P_{MPP} will be 2,539.97 W according to the calculation in equations (2.1)-(2.5).

STEP 2: From equation (4.5), P^{max} will be 2,000 W.

STEP 3: According to P(U) function as shown in equation (4.3), P_{pv}^{A} is 1,000 W. According to Q(U) function as shown in equation (4.6), Q_{pv}^{A} is -998.51 VAr. Then, apparent power output from this 2-kW PV system is 1,000-j998.51 VA.

If 10-kW PV system connects to phases A, B and C under voltage 1.09∠0^{o}, 1.085∠-120^{o} and 1.095∠120^{o} pu. respectively. Base system voltage is 230 V, line to neutral. The parameters setting of V_{cri}, δ_p, K_1, K_2, V_q and δ_q equal 1.09, 0.02, 1, 2, 1 and 0.05 respectively. Then, power output of this 10-kW PV system can be assessed in 4 steps as follows.

STEP 1: P_{rated} is 10,000 W. P_{MPP} will be 12,276.51 W according to the calculation in equations (2.1)-(2.5).

STEP 2: From equation (4.5), P^{max} will be 10,000 W.

STEP 3: According to P(U) function as shown in equation (4.4), P_{pv} is 5,000 W. According to Q(U) function as shown in equation (4.7), Q_{pv} is -4,992.54 VAr. Then, total apparent power output from this 10-kW PV system is 5,000-j4,992.54 VA.

STEP 4: Since this is a three phase PV system, power output from each phase can be calculated from equations (2.6)-(2.8). $P_{pv}^{A} + jQ_{pv}^{A}$, $P_{pv}^{B} + jQ_{pv}^{B}$ and $P_{pv}^{C} + jQ_{pv}^{C}$ will be 1,666.67-j1,664.18, 1,659.02-j1,656.55 and 1,674.31-j1,671.81 VA respectively.

4.4.2.3 LV Grid Model Determination

As any wiring configuration, the calculation of self and mutual impedance can apply modified Carson's equations, as given in [37, 38], that are reprinted in equation (4.14) and (4.15).

$$z^{\sigma\sigma} = r^{\sigma} + 0.00158836 \cdot f + j0.00202237 \cdot f \cdot \left(ln\frac{1}{GMR^{\sigma}} + 7.6786 + \frac{1}{2} ln\frac{p_g}{f} \right) \quad (4.14)$$

$$z^{\sigma\sigma'} = 0.00158836 \cdot f + j0.00202237 \cdot f \cdot \left(ln\frac{1}{D^{\sigma\sigma'}} + 7.6786 + \frac{1}{2} ln\frac{p_g}{f} \right) \quad (4.15)$$

$$GMR^{\sigma} = r_c^{\sigma} \cdot \exp(-0.25) \quad (4.16)$$

where $z^{\sigma\sigma}$ is self impedance of conductor phase σ (Ω/mile); $z^{\sigma\sigma'}$ is mutual impedance between conductor phase σ and σ' (Ω/mile); r^{σ} is resistance of conductor phase σ (Ω); GMR^{σ} is Geometric Mean Radius of conductor phase σ (feet); $D^{\sigma\sigma'}$ is distance between conductor phase σ and σ' (feet); p_g is earth resistivity (Ω-m); f is frequency (Hz); r_c^{σ} is radius of conductor of any phase σ (feet).

For most applications, the primitive impedance matrix needs to be reduced to 3x3 matrix consisting of the self and mutual equivalent impedances for the three phases. LV branch is normally a four-wire grounded as shown in Figure 4.15 and branch impedance Z_{branch} can be shown in equation (4.17). However, the line have multi-

grounded or V^{NG} and $V^{NG'}$ equal to zero. Then, Kron reduction [38] can be applied to reduce to 3x3 matrix. For Y_{bus} formulation, it can be calculated from text book [39].

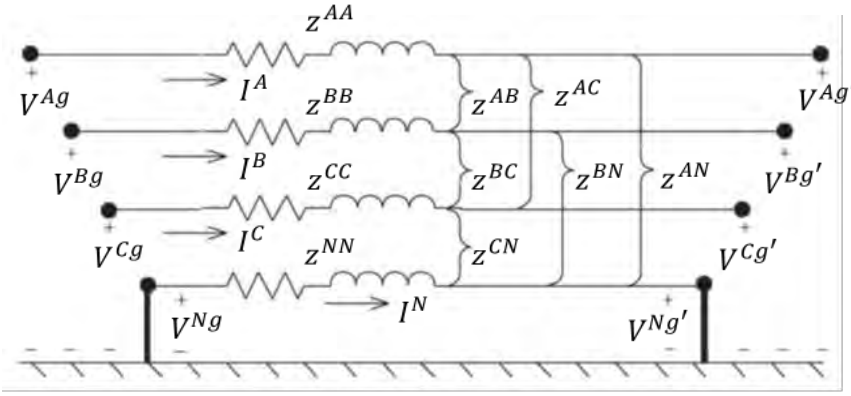

Figure 4.14 Four-wires grounded branch

$$Z_{branch} = \begin{bmatrix} z^{AA} & z^{AB} & z^{AC} & z^{AN} \\ z^{AB} & z^{BB} & z^{BC} & z^{BN} \\ z^{AC} & z^{BC} & z^{CC} & z^{CN} \\ z^{AN} & z^{BN} & z^{CN} & z^{NN} \end{bmatrix} \quad (4.17)$$

Assuming a LV line in Figure 4.16, the details is as follows.

- Line spacing between phase conductors is 20 cm that can be shown in Figure 4.16.
- Utilizing polyethylene insulated weatherproof aluminum conductors and the parameter can be shown in Table 4.8.
- Phase A, B, C and neutral use conductor size as 70, 70, 70 and 35 mm^2.

Table 4.6 The parameters of polyethylene insulated weatherproof aluminum conductors [40]

Conductor Size (mm^2)	**Conductor radius (mm)**	**Ampacities at 75℃ (A)**	**Resistance at 75℃ (Ω)**
35	3.30	190	1.0606
75	4.65	300	0.5414

From Figure 4.16, Z_{branch} calculation can be divided in 5 steps as follows.

STEP 1: Find GMR^A, GMR^B, GMR^C and GMR^N from equation (4.16) and they can be obtained as follows.

$$GMR^A = GMR^B = GMR^C = 0.0119 \text{ feet} \quad (4.18)$$

$$GMR^N = 0.0084 \text{ feet} \tag{4.19}$$

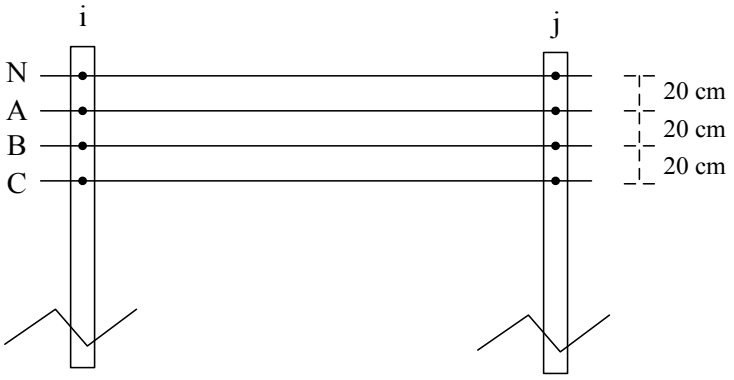

Figure 4.15 LV line configuration

STEP 2: Find self impedance from equation (4.14) and they can be obtained as follows.

$$z^{AA} = z^{BB} = z^{CC} = 0.6208 + j1.2597 \text{ ohms/mile} \tag{4.20}$$

$$z^{NN} = 1.1400 + j1.2944 \text{ ohms/mile} \tag{4.21}$$

STEP 3: Find mutual impedance from equation (4.15) and they can be obtained as follows.

$$z^{AN} = z^{AB} = z^{BC} = 0.0794 + j0.8541 \text{ ohms/mile} \tag{4.22}$$

$$z^{BN} = z^{AC} = 0.0794 + j0.7840 \text{ ohms/mile} \tag{4.23}$$

$$z^{CN} = 0.0794 + j0.7430 \text{ ohms/mile} \tag{4.24}$$

STEP 4: Z_{branch} can be formulated as follows.

$$Z_{branch} = \begin{bmatrix} 0.6208 + j1.2597 & 0.0794 + j0.8541 & 0.0794 + j0.7840 & 0.0794 + j0.8541 \\ 0.0794 + j0.8541 & 0.6208 + j1.2597 & 0.0794 + j0.8541 & 0.0794 + j0.7840 \\ 0.0794 + j0.7840 & 0.0794 + j0.8541 & 0.6208 + j1.2597 & 0.0794 + j0.7430 \\ 0.0794 + j0.8541 & 0.0794 + j0.7840 & 0.0794 + j0.7430 & 1.1400 + j1.2944 \end{bmatrix} \text{ ohms/mile} \tag{4.25}$$

STEP 5: Kron reduction is applied to reduce into 3x3 matrix due to neutral line is connected by multi-ground or neutral-ground voltage equal to zero.

$$Z_{branch} = \begin{bmatrix} 0.8389 + \text{j}0.8931 & 0.2770 + \text{j}0.5157\text{i} & 0.2650 + \text{j}0.4621 \\ 0.2770 + \text{j}0.5157 & 0.8000 + \text{j}0.9473 & 0.2475 + \text{j}0.5569 \\ 0.2650 + \text{j}0.4621 & 0.2475 + \text{j}0.5569 & 0.7786 + 0.9771\text{i} \end{bmatrix} \quad (4.26)$$

ohms/mile

CHAPTER 5

OPTIMIZATION PROCESS

This chapter will address the power flow algorithm with using local control function and 2-stage Particle Swarm Optimization (PSO) which is used for finding the optimal parameter setting of local control.

5.1 The Power Flow Algorithm with Using Local Control Function

Normally, equivalent real and reactive power equation of three-phase electrical system, where there is no PV system connection, can be written into equations (5.1)-(5.4) [41] as follows.

$$P_{i,load}^{\sigma} = \sum_{j=1}^{n} \sum_{\sigma' \in \{A,B,C\}} |V_i^{\sigma}||V_j^{\sigma'}||Y_{ij}^{\sigma\sigma'}|cos\left(\theta_{ij}^{\sigma\sigma'} - \delta_i^{\sigma} + \delta_j^{\sigma'}\right) \tag{5.1}$$

$$Q_{i,load}^{\sigma} = -\sum_{j=1}^{n} \sum_{\sigma' \in \{A,B,C\}} |V_i^{\sigma}||V_j^{\sigma'}||Y_{ij}^{\sigma\sigma'}|sin\left(\theta_{ij}^{\sigma\sigma'} - \delta_i^{\sigma} + \delta_j^{\sigma'}\right) \tag{5.2}$$

$$|Y_{ij}| = \begin{bmatrix} |Y_{ij}^{AA}| & |Y_{ij}^{AB}| & |Y_{ij}^{AC}| \\ |Y_{ij}^{AB}| & |Y_{ij}^{BB}| & |Y_{ij}^{BC}| \\ |Y_{ij}^{AC}| & |Y_{ij}^{BC}| & |Y_{ij}^{CC}| \end{bmatrix} \tag{5.3}$$

$$\theta_{ij} = \begin{bmatrix} \theta_{ij}^{AA} & \theta_{ij}^{AB} & \theta_{ij}^{AC} \\ \theta_{ij}^{AB} & \theta_{ij}^{BB} & \theta_{ij}^{BC} \\ \theta_{ij}^{AC} & \theta_{ij}^{BC} & \theta_{ij}^{CC} \end{bmatrix} \tag{5.4}$$

where $P_{i,load}^{\sigma}$ is real power load at node i, phase σ (pu.); $Q_{i,load}^{\sigma}$ is reactive power load at node i, phase σ(pu.); σ and σ' are any phase A or B or C; $|Y_{ij}|$ is the absolute value of admittance matrix between nodes i and j (pu.); θ_{ij} is phase angle of admittance matrix between nodes i and j (radians); n is number of overall nodes in LV distribution system; $|V_i^{\sigma}|$ is the magnitude of voltage at node i, phase σ (pu.); δ_i^{σ} is the phase angle at node i, phase σ (radians).

Equations (5.1) and (5.2) constitute a set of nonlinear algebraic equations in terms of the independent variables, voltage magnitude in per unit, and phase angle in

radians. Expanding equations (5.1) and (5.2) in Taylor's series about the initial estimate and neglecting all higher order terms results in the linear equations as shown in equation (5.5). Node 1 is assumed to be a slack node. Moreover, newton-raphson method need to solve equation (5.5) until ΔP_i^{ABC} and ΔQ_i^{ABC} nearly equal to zero.

$$\begin{bmatrix} \Delta P_2^{ABC} \\ \vdots \\ \Delta P_n^{ABC} \\ \hline \Delta Q_2^{ABC} \\ \vdots \\ \Delta Q_n^{ABC} \end{bmatrix} = \left[\begin{array}{ccc|ccc} \frac{\partial P_2^{ABC}}{\partial \delta_2^{ABC}} & \cdots & \frac{\partial P_2^{ABC}}{\partial \delta_n^{ABC}} & \frac{\partial P_2^{ABC}}{\partial |V_2^{ABC}|} & \cdots & \frac{\partial P_2^{ABC}}{\partial |V_n^{ABC}|} \\ \vdots & \ddots & \vdots & \vdots & \ddots & \vdots \\ \frac{\partial P_n^{ABC}}{\partial \delta_2^{ABC}} & \cdots & \frac{\partial P_n^{ABC}}{\partial \delta_n^{ABC}} & \frac{\partial P_n^{ABC}}{\partial |V_2^{ABC}|} & \cdots & \frac{\partial P_n^{ABC}}{\partial |V_n^{ABC}|} \\ \hline \frac{\partial Q_2^{ABC}}{\partial \delta_2^{ABC}} & \cdots & \frac{\partial Q_2^{ABC}}{\partial \delta_n^{ABC}} & \frac{\partial Q_2^{ABC}}{\partial |V_2^{ABC}|} & \cdots & \frac{\partial Q_2^{ABC}}{\partial |V_n^{ABC}|} \\ \vdots & \ddots & \vdots & \vdots & \ddots & \vdots \\ \frac{\partial Q_n^{ABC}}{\partial \delta_2^{ABC}} & \cdots & \frac{\partial Q_n^{ABC}}{\partial \delta_n^{ABC}} & \frac{\partial Q_n^{ABC}}{\partial |V_2^{ABC}|} & \cdots & \frac{\partial Q_n^{ABC}}{\partial |V_n^{ABC}|} \end{array}\right] \begin{bmatrix} \Delta \delta_2^{ABC} \\ \vdots \\ \Delta \delta_n^{ABC} \\ \hline \Delta |V_2^{ABC}| \\ \vdots \\ \Delta |V_n^{ABC}| \end{bmatrix} \tag{5.5}$$

$$\Delta P_2^{ABC} = \begin{bmatrix} \Delta P_2^A \\ \Delta P_2^B \\ \Delta P_2^C \end{bmatrix};\ \Delta Q_2^{ABC} = \begin{bmatrix} \Delta Q_2^A \\ \Delta Q_2^B \\ \Delta Q_2^C \end{bmatrix};\ \Delta \delta_2^{ABC} = \begin{bmatrix} \Delta \delta_2^A \\ \Delta \delta_2^B \\ \Delta \delta_2^C \end{bmatrix};\ \Delta |V_2^{ABC}| = \begin{bmatrix} \Delta |V_2^A| \\ \Delta |V_2^B| \\ \Delta |V_2^C| \end{bmatrix} \tag{5.6}$$

In equation (5.5), the Jacobian matrix gives the linearized relationship between small changes in voltage angle $\Delta \delta_i^{ABC}$ and voltage magnitude $\Delta |V_i^{ABC}|$ with the small changes in real and reactive power ΔP_i^{ABC} and ΔQ_i^{ABC}. Elements of the Jacobian matrix are the partial derivatives of equations (5.1) and (5.2), evaluated at $\Delta \delta_i^{ABC}$ and $\Delta |V_i^{ABC}|$. In short form, it can be written in equation (5.7).

$$\begin{bmatrix} \Delta P \\ \Delta Q \end{bmatrix} = \begin{bmatrix} J_1 & J_2 \\ J_3 & J_4 \end{bmatrix} \begin{bmatrix} \Delta \delta \\ \Delta |V| \end{bmatrix} \tag{5.7}$$

The diagonal and the off-diagonal elements of J_1 are the followings.

$$\frac{\partial P_{i,load}^{\sigma}}{\partial \delta_i^{\sigma}} = \sum_{j=1}^{n} \sum_{\sigma' \in \{A,B,C\}}^{\sigma \neq \sigma' \,\&\, i \neq j} |V_i^{\sigma}| |V_j^{\sigma'}| |Y_{ij}^{\sigma\sigma'}| sin\left(\theta_{ij}^{\sigma\sigma'} - \delta_i^{\sigma} + \delta_j^{\sigma'}\right) \tag{5.8}$$

$$\frac{\partial P_{i,load}^{\sigma}}{\partial \delta_j^{\sigma'}} = -|V_i^{\sigma}| |V_j^{\sigma'}| |Y_{ij}^{\sigma\sigma'}| sin\left(\theta_{ij}^{\sigma\sigma'} - \delta_i^{\sigma} + \delta_j^{\sigma'}\right);\ \sigma \neq \sigma' \,\&\, i \neq j \tag{5.9}$$

where j is any node in LV system.

The diagonal and the off-diagonal elements of J_2 are the followings.

$$\frac{\partial P_{i,load}^{\sigma}}{\partial |V_i^{\sigma}|} = 2|V_i^{\sigma}||Y_{ii}^{\sigma\sigma}|\cos(\theta_{ii}^{\sigma\sigma}) + \sum_{j=1}^{n}\sum_{\sigma'\in\{A,B,C\}}^{\sigma\neq\sigma' \,\&\, i\neq j} |V_j^{\sigma'}||Y_{ij}^{\sigma\sigma'}|cos\left(\theta_{ij}^{\sigma\sigma'} - \delta_i^{\sigma} + \delta_j^{\sigma'}\right) \tag{5.10}$$

$$\frac{\partial P_{i,load}^{\sigma}}{\partial |V_j^{\sigma'}|} = |V_i^{\sigma}||Y_{ij}^{\sigma\sigma'}|cos\left(\theta_{ij}^{\sigma\sigma'} - \delta_i^{\sigma} + \delta_j^{\sigma'}\right);\ \sigma \neq \sigma' \,\&\, i \neq j \tag{5.11}$$

The diagonal and the off-diagonal elements of J_3 are the followings.

$$\frac{\partial Q_{i,load}^{\sigma}}{\partial \delta_i^{\sigma}} = \sum_{j=1}^{n}\sum_{\sigma'\in\{A,B,C\}}^{\sigma\neq\sigma' \,\&\, i\neq j} |V_i^{\sigma}||V_j^{\sigma'}||Y_{ij}^{\sigma\sigma'}|cos\left(\theta_{ij}^{\sigma\sigma'} - \delta_i^{\sigma} + \delta_j^{\sigma'}\right) \tag{5.12}$$

$$\frac{\partial Q_{i,load}^{\sigma}}{\partial \delta_j^{\sigma'}} = -|V_i^{\sigma}||V_j^{\sigma'}||Y_{ij}^{\sigma\sigma'}|cos\left(\theta_{ij}^{\sigma\sigma'} - \delta_i^{\sigma} + \delta_j^{\sigma'}\right);\ \sigma \neq \sigma' \,\&\, i \neq j \tag{5.13}$$

The diagonal and the off-diagonal elements of J_4 are the followings.

$$\frac{\partial Q_{i,load}^{\sigma}}{\partial |V_i^{\sigma}|} = -2|V_i^{\sigma}||Y_{ii}^{\sigma\sigma}|\,sin(\theta_{ii}^{\sigma\sigma}) - \sum_{m=1}^{n}\sum_{\sigma'\in\{A,B,C\}}^{\sigma\neq\sigma' \,\&\, i\neq j} |V_j^{\sigma'}||Y_{ij}^{\sigma\sigma'}|sin\left(\theta_{ij}^{\sigma\sigma'} - \delta_i^{\sigma} + \delta_j^{\sigma'}\right) \tag{5.14}$$

$$\frac{\partial Q_{i,load}^{\sigma}}{\partial |V_j^{\sigma'}|} = -|V_i^{\sigma}||Y_{ij}^{\sigma\sigma'}|sin\left(\theta_{ij}^{\sigma\sigma'} - \delta_i^{\sigma} + \delta_j^{\sigma'}\right);\ \sigma \neq \sigma' \,\&\, i \neq j \tag{5.15}$$

In the case of having connected single phase PV inverters in the phase A, B or C at any node i, equivalent real and reactive power equation of three-phase electrical system can be written in equations (5.16)-(5.17).

$$P_{i,load}^{\sigma} = \sum_{j=1}^{n}\sum_{\sigma'\in\{A,B,C\}} |V_i^{\sigma}||V_j^{\sigma'}||Y_{ij}^{\sigma\sigma'}|cos\left(\theta_{ij}^{\sigma\sigma'} - \delta_i^{\sigma} + \delta_j^{\sigma'}\right) - P_{i,pv}^{\sigma} \tag{5.16}$$

$$Q_{i,load}^{\sigma} = -\sum_{j=1}^{n}\sum_{\sigma'\in\{A,B,C\}} |V_i^{\sigma}|\left|V_j^{\sigma'}\right|\left|Y_{ij}^{\sigma\sigma'}\right| sin\left(\theta_{ij}^{\sigma\sigma'} - \delta_i^{\sigma} + \delta_j^{\sigma'}\right) - Q_{i,pv}^{\sigma} \tag{5.17}$$

From equations (5.16)-(5.17), it can be transformed to the linear equations as shown in equation (5.7). The diagonal and the off-diagonal elements of J_1 are the followings.

$$\frac{\partial P_{i,load}^{\sigma}}{\partial \delta_i^{\sigma}} = \sum_{j=1}^{n} \sum_{\sigma' \in \{A,B,C\}}^{\sigma \neq \sigma' \,\&\, i \neq j} |V_i^{\sigma}||V_j^{\sigma'}||Y_{ij}^{\sigma\sigma'}| sin\left(\theta_{ij}^{\sigma\sigma'} - \delta_i^{\sigma} + \delta_j^{\sigma'}\right) \tag{5.18}$$

$$\frac{\partial P_{i,load}^{\sigma}}{\partial \delta_j^{\sigma'}} = -|V_i^{\sigma}||V_j^{\sigma'}||Y_{ij}^{\sigma\sigma'}| sin\left(\theta_{ij}^{\sigma\sigma'} - \delta_i^{\sigma} + \delta_j^{\sigma'}\right);\ \sigma \neq \sigma' \,\&\, i \neq j \tag{5.19}$$

The diagonal and the off-diagonal elements of J_2 are shown in equations (5.20) and (5.21) respectively where equations (5.22) and (5.23) are the differential equations of continuous and piecewise linear P(U) local control functions respectively.

$$\begin{aligned}\frac{\partial P_{i,load}^{\sigma}}{\partial |V_i^{\sigma}|} &= 2|V_i^{\sigma}||Y_{ii}^{\sigma\sigma}| \cos(\theta_{ii}^{\sigma\sigma}) \\ &\quad + \sum_{j=1}^{n} \sum_{\sigma' \in \{A,B,C\}}^{\sigma \neq \sigma' \,\&\, i \neq j} \left|V_j^{\sigma'}\right| \left|Y_{ij}^{\sigma\sigma'}\right| cos\left(\theta_{ij}^{\sigma\sigma'} - \delta_i^{\sigma} + \delta_j^{\sigma'}\right) - \frac{\partial P_{i,pv}^{\sigma}}{\partial |V_i^{\sigma}|}\end{aligned} \tag{5.20}$$

$$\frac{\partial P_{i,load}^{\sigma}}{\partial |V_j^{\sigma'}|} = |V_i^{\sigma}||Y_{ij}^{\sigma\sigma'}| cos\left(\theta_{ij}^{\sigma\sigma'} - \delta_i^{\sigma} + \delta_j^{\sigma'}\right);\ \sigma \neq \sigma' \,\&\, i \neq j \tag{5.21}$$

$$\frac{\partial P_{i,pv}^{\sigma}}{\partial |V_i^{\sigma}|} = \frac{-4 \cdot P_i^{max} \cdot exp\left[-4\left(|V_i^{\sigma}| - V_{i,cri}^{\sigma}\right)/\delta_{i,p}^{\sigma}\right]}{\delta_{i,p}^{\sigma} \cdot \left[1 + exp\left[-4\left(|V_i^{\sigma}| - V_{i,cri}^{\sigma}\right)/\delta_{i,p}^{\sigma}\right]\right]^2} \tag{5.22}$$

$$\frac{\partial P_{i,pv}^{\sigma}}{\partial |V_i^{\sigma}|} = P_i^{max} \cdot \begin{cases} \dfrac{1}{V_{i,p1}^{\sigma} - V_{i,p2}^{\sigma}} & ;\ V_{i,p1}^{\sigma} \leq |V_i^{\sigma}| < V_{i,p2}^{\sigma} \\ 0 & ;other \end{cases} \tag{5.23}$$

The diagonal and the off-diagonal elements of J_3 are the followings.

$$\frac{\partial Q_{i,load}^{\sigma}}{\partial \delta_i^{\sigma}} = \sum_{j=1}^{n} \sum_{\sigma' \in \{A,B,C\}}^{\sigma \neq \sigma' \,\&\, i \neq j} |V_i^{\sigma}||V_j^{\sigma'}||Y_{ij}^{\sigma\sigma'}| cos\left(\theta_{ij}^{\sigma\sigma'} - \delta_i^{\sigma} + \delta_j^{\sigma'}\right) \tag{5.24}$$

$$\frac{\partial Q_{i,load}^{\sigma}}{\partial \delta_j^{\sigma'}} = -|V_i^{\sigma}||V_j^{\sigma'}||Y_{ij}^{\sigma\sigma'}| cos\left(\theta_{ij}^{\sigma\sigma'} - \delta_i^{\sigma} + \delta_j^{\sigma'}\right);\ \sigma \neq \sigma' \,\&\, i \neq j \tag{5.25}$$

The diagonal and the off-diagonal elements of J_4 are shown in equations (5.26) and (5.27) respectively where equations (5.28) and (5.29) are the differential equations of continuous and piecewise linear Q(U) local control functions respectively.

$$\frac{\partial Q_{i,load}^{\sigma}}{\partial|V_i^{\sigma}|} = -2|V_i^{\sigma}||Y_{ii}^{\sigma\sigma}|\,sin(\theta_{ii}^{\sigma\sigma}) - \sum_{m=1}^{n}\sum_{\sigma'\in\{A,B,C\}}^{\sigma\neq\sigma'\ \&\ i\neq j}|V_j^{\sigma'}||Y_{ij}^{\sigma\sigma'}|sin\left(\theta_{ij}^{\sigma\sigma'} - \delta_i^{\sigma} + \delta_j^{\sigma'}\right) - \frac{\partial Q_{i,pv}^{\sigma}}{\partial|V_i^{\sigma}|} \tag{5.26}$$

$$\frac{\partial Q_{i,load}^{\sigma}}{\partial|V_j^{\sigma'}|} = -|V_i^{\sigma}||Y_{ij}^{\sigma\sigma'}|sin\left(\theta_{ij}^{\sigma\sigma'} - \delta_i^{\sigma} + \delta_j^{\sigma'}\right);\ \sigma\neq\sigma'\ \&\ i\neq j \tag{5.27}$$

$$\frac{\partial Q_{i,pv}^{\sigma}}{\partial|V_i^{\sigma}|} = \frac{-4\cdot K_{i,2}^{\sigma}\cdot Q_i^{max}\cdot exp\left[-4\left(|V_i^{\sigma}| - V_{i,q}^{\sigma}\right)/\delta_{i,q}^{\sigma}\right]}{\delta_{i,q}^{\sigma}\cdot\left[1+exp\left[-4\left(|V_i^{\sigma}| - V_{i,q}^{\sigma}\right)/\delta_{i,q}^{\sigma}\right]\right]^2} \tag{5.28}$$

$$\frac{\partial Q_{i,pv}^{\sigma}}{\partial|V_i^{\sigma}|} = Q_i^{max}\cdot\begin{cases}\dfrac{K_{i,1}^{\sigma} - V_{i,2}^{\sigma}}{V_{i,q1}^{\sigma} - V_{i,q2}^{\sigma}}\ ;\ V_{i,q1}^{\sigma}\le|V_i^{\sigma}|<V_{i,q2}^{\sigma} \\ 0 \qquad\qquad ;other\end{cases} \tag{5.29}$$

In the case of having connected three phase PV inverters in the phases A, B and C at any node i, equivalent real and reactive power equation of three-phase electrical system can be written in equations (5.30)-(5.31).

$$P_{i,load}^{\sigma} = \sum_{j=1}^{n}\sum_{\sigma'\in\{A,B,C\}}|V_i^{\sigma}||V_j^{\sigma'}||Y_{ij}^{\sigma\sigma'}|cos\left(\theta_{ij}^{\sigma\sigma'} - \delta_i^{\sigma} + \delta_j^{\sigma'}\right) - P_{i,pv}^{\sigma} \tag{5.30}$$

$$Q_{i,load}^{\sigma} = -\sum_{j=1}^{n}\sum_{\sigma'\in\{A,B,C\}}|V_i^{\sigma}||V_j^{\sigma'}||Y_{ij}^{\sigma\sigma'}|sin\left(\theta_{ij}^{\sigma\sigma'} - \delta_i^{\sigma} + \delta_j^{\sigma'}\right) - Q_{i,pv}^{\sigma} \tag{5.31}$$

From equation (5.30)-(5.31), it can be transformed to the linear equations as shown in equation (5.7). The diagonal and the off-diagonal elements of J_1 can be written into equations (5.32) and (5.33) respectively where $\frac{\partial P_{i,pv}^{\sigma}}{\partial\delta_i^{\sigma}}$ and $\frac{\partial P_{i,pv}^{\sigma}}{\partial\delta_j^{\sigma'}}$ can be clarified in Appendix B.1.

$$\frac{\partial P_{i,load}^{\sigma}}{\partial\delta_i^{\sigma}} = \sum_{j=1}^{n}\sum_{\sigma'\in\{A,B,C\}}^{\sigma\neq\sigma'\ \&\ i\neq j}|V_i^{\sigma}||V_j^{\sigma'}||Y_{ij}^{\sigma\sigma'}|sin\left(\theta_{ij}^{\sigma\sigma'} - \delta_i^{\sigma} + \delta_j^{\sigma'}\right) - \frac{\partial P_{i,pv}^{\sigma}}{\partial\delta_i^{\sigma}} \tag{5.32}$$

$$\frac{\partial P_{i,load}^{\sigma}}{\partial\delta_j^{\sigma'}} = -|V_i^{\sigma}||V_j^{\sigma'}||Y_{ij}^{\sigma\sigma'}|sin\left(\theta_{ij}^{\sigma\sigma'} - \delta_i^{\sigma} + \delta_j^{\sigma'}\right) - \frac{\partial P_{i,pv}^{\sigma}}{\partial\delta_j^{\sigma'}} \tag{5.33}$$

$$; \sigma \neq \sigma' \,\&\, i \neq j$$

The diagonal and the off-diagonal elements of J_2 can be written in equations (5.34) and (5.35) respectively where $\frac{\partial P_{i,pv}^{\sigma}}{\partial |V_i^{\sigma}|}$ and $\frac{\partial P_{i,pv}^{\sigma}}{\partial |V_j^{\sigma'}|}$ can be clarified in Appendix B.1.

$$\frac{\partial P_{i,load}^{\sigma}}{\partial |V_i^{\sigma}|} = 2|V_i^{\sigma}||Y_{ii}^{\sigma\sigma}|\cos(\theta_{ii}^{\sigma\sigma}) + \sum_{j=1}^{n}\sum_{\sigma'\in\{A,B,C\}}^{\sigma\neq\sigma'\,\&\,i\neq j} |V_j^{\sigma'}||Y_{ij}^{\sigma\sigma'}|cos\left(\theta_{ij}^{\sigma\sigma'} - \delta_i^{\sigma} + \delta_j^{\sigma'}\right) - \frac{\partial P_{i,pv}^{\sigma}}{\partial |V_i^{\sigma}|} \tag{5.34}$$

$$\frac{\partial P_{i,load}^{\sigma}}{\partial |V_j^{\sigma'}|} = |V_i^{\sigma}||Y_{ij}^{\sigma\sigma'}|cos\left(\theta_{ij}^{\sigma\sigma'} - \delta_i^{\sigma} + \delta_j^{\sigma'}\right) - \frac{\partial P_{i,pv}^{\sigma}}{\partial |V_j^{\sigma'}|};\ \sigma \neq \sigma' \,\&\, i \neq j \tag{5.35}$$

The diagonal and the off-diagonal elements of J_3 can be written into equation (5.36) and (5.37) respectively where $\frac{\partial Q_{i,pv}^{\sigma}}{\partial \delta_i^{\sigma}}$ and $\frac{\partial Q_{i,pv}^{\sigma}}{\partial \delta_j^{\sigma'}}$ can be clarified in Appendix B.1.

$$\frac{\partial Q_{i,load}^{\sigma}}{\partial \delta_i^{\sigma}} = \sum_{j=1}^{n}\sum_{\sigma'\in\{A,B,C\}}^{\sigma\neq\sigma'\,\&\,i\neq j} |V_i^{\sigma}||V_j^{\sigma'}||Y_{ij}^{\sigma\sigma'}|cos\left(\theta_{ij}^{\sigma\sigma'} - \delta_i^{\sigma} + \delta_j^{\sigma'}\right) - \frac{\partial Q_{i,pv}^{\sigma}}{\partial \delta_i^{\sigma}} \tag{5.36}$$

$$\frac{\partial Q_{i,load}^{\sigma}}{\partial \delta_j^{\sigma'}} = -|V_i^{\sigma}||V_j^{\sigma'}||Y_{ij}^{\sigma\sigma'}|cos\left(\theta_{ij}^{\sigma\sigma'} - \delta_i^{\sigma} + \delta_j^{\sigma'}\right) - \frac{\partial Q_{i,pv}^{\sigma}}{\partial \delta_j^{\sigma'}} \tag{5.37}$$

$$; \sigma \neq \sigma' \,\&\, i \neq j$$

The diagonal and the off-diagonal elements of J_4 can be written in equations (5.38) and (5.39) respectively where $\frac{\partial Q_{i,pv}^{\sigma}}{\partial |V_i^{\sigma}|}$ and $\frac{\partial Q_{i,pv}^{\sigma}}{\partial |V_j^{\sigma'}|}$ can be clarified in Appendix B.1.

$$\frac{\partial Q_{i,load}^{\sigma}}{\partial |V_i^{\sigma}|} = -2|V_i^{\sigma}||Y_{ii}^{\sigma\sigma}|\,sin(\theta_{ii}^{\sigma\sigma}) - \sum_{j=1}^{n}\sum_{\sigma'\in\{A,B,C\}}^{\sigma\neq\sigma'\,\&\,i\neq j} |V_j^{\sigma'}||Y_{ij}^{\sigma\sigma'}|sin\left(\theta_{ij}^{\sigma\sigma'} - \delta_i^{\sigma} + \delta_j^{\sigma'}\right) - \frac{\partial Q_{i,pv}^{\sigma}}{\partial |V_i^{\sigma}|} \tag{5.38}$$

$$\frac{\partial Q_{i,load}^{\sigma}}{\partial \left|V_j^{\sigma'}\right|} = -|V_i^{\sigma}|\left|Y_{ij}^{\sigma\sigma'}\right| sin\left(\theta_{ij}^{\sigma\sigma'} - \delta_i^{\sigma} + \delta_j^{\sigma'}\right) - \frac{\partial Q_{i,pv}^{\sigma}}{\partial \left|V_j^{\sigma'}\right|} \quad (5.39)$$

$$; \ \sigma \neq \sigma' \ \& \ i \neq m$$

The terms $\Delta P_i^{\sigma(k)}$ and $\Delta Q_i^{\sigma(k)}$ are the difference between the scheduled and calculated values, known as the power residuals, given by:

$$\Delta P_i^{\sigma(k)} = P_i^{\sigma sch} - P_i^{\sigma(k)} \quad (5.40)$$

$$\Delta Q_i^{\sigma(k)} = Q_i^{\sigma sch} - Q_i^{\sigma(k)} \quad (5.41)$$

The new estimates for bus voltages and phase angles are:

$$\delta_i^{\sigma(k+1)} = \delta_i^{\sigma(k)} + w_{\delta_i^{\sigma}}^{(h-1)\ or\ h} \cdot \Delta\delta_i^{\sigma(k)} \quad (5.42)$$

$$\left|V_i^{\sigma(k+1)}\right| = \left|V_i^{\sigma(k)}\right| + w_{V_i^{\sigma}}^{(h-1)\ or\ h} \cdot \Delta\left|V_i^{\sigma(k)}\right| \quad (5.43)$$

where w is step-length value.

Substituting equation (5.42) for δ_i^{σ} and δ_j^{σ} in equations (5.8) and (5.9) and substituting equation (5.43) for $|V_i^{\sigma}|$ and $\left|V_j^{\sigma}\right|$ in equations (5.8) and (5.9):

$$P_{i,load}^{\sigma} = \sum_{j=1}^{n} \sum_{\sigma' \in \{A,B,C\}} \left[|V_i^{\sigma}| + w_{V_i^{\sigma}} \cdot \Delta|V_i^{\sigma}|\right]\left[\left|V_j^{\sigma'}\right| + w_{V_j^{\sigma'}} \cdot \Delta\left|V_j^{\sigma'}\right|\right]\left|Y_{ij}^{\sigma\sigma'}\right| cos\left(\theta_{ij}^{\sigma\sigma'} - \delta_i^{\sigma} - w_{\delta_i^{\sigma}} \cdot \Delta\delta_i^{\sigma} + \delta_j^{\sigma'} + w_{\delta_j^{\sigma'}} \cdot \Delta\delta_j^{\sigma'}\right) \quad (5.44)$$

$$Q_{i,load}^{\sigma} = -\sum_{j=1}^{n} \sum_{\sigma' \in \{A,B,C\}} \left[|V_i^{\sigma}| + w_{V_i^{\sigma}} \cdot \Delta|V_i^{\sigma}|\right]\left[\left|V_j^{\sigma'}\right| + w_{V_j^{\sigma'}} \cdot \Delta\left|V_j^{\sigma'}\right|\right]\left|Y_{ij}^{\sigma\sigma'}\right| sin\left(\theta_{ij}^{\sigma\sigma'} - \delta_i^{\sigma} - w_{\delta_i^{\sigma}} \cdot \Delta\delta_i^{\sigma} + \delta_j^{\sigma'} + w_{\delta_j^{\sigma'}} \cdot \Delta\delta_j^{\sigma'}\right) \quad (5.45)$$

Expanding equations (5.44) and (5.45) in Taylor's series about the initial estimate and neglecting all higher order terms results in the linear equations leads to equation (5.46), The diagonal and the off-diagonal elements of J_1 are shown in equations (5.47) and (5.48) respectively.

$$\begin{bmatrix}\Delta P \\ \Delta Q\end{bmatrix} = \begin{bmatrix}J_1 & J_2 \\ J_3 & J_4\end{bmatrix}\begin{bmatrix}\Delta w_{\delta} \\ \Delta w_V\end{bmatrix} \quad (5.46)$$

$$\frac{\partial P_{i,load}^{\sigma}}{\partial w_{\delta_i^{\sigma}}} = \Delta\delta_i^{\sigma} \sum_{j=1}^{n} \sum_{\sigma' \in \{A,B,C\}}^{\sigma \neq \sigma' \,\&\, i \neq j} \left[|V_i^{\sigma}| + w_{V_i^{\sigma}} \cdot \Delta |V_i^{\sigma}| \right] \left[|V_j^{\sigma'}| + w_{V_j^{\sigma'}} \cdot \Delta |V_j^{\sigma'}| \right] |Y_{ij}^{\sigma\sigma'}| sin\left(\theta_{ij}^{\sigma\sigma'} - \delta_i^{\sigma} - w_{\delta_i^{\sigma}} \cdot \Delta\delta_i^{\sigma} + \delta_j^{\sigma'} + w_{\delta_j^{\sigma'}} \cdot \Delta\delta_j^{\sigma'} \right) \tag{5.47}$$

$$\frac{\partial P_{i,load}^{\sigma}}{\partial w_{\delta_j^{\sigma'}}} = -\Delta\delta_j^{\sigma'} \left[|V_i^{\sigma}| + w_{V_i^{\sigma}} \cdot \Delta |V_i^{\sigma}| \right] \left[|V_j^{\sigma'}| + w_{V_j^{\sigma'}} \cdot \Delta |V_j^{\sigma'}| \right] |Y_{ij}^{\sigma\sigma'}| sin\left(\theta_{ij}^{\sigma\sigma'} - \delta_i^{\sigma} - w_{\delta_i^{\sigma}} \cdot \Delta\delta_i^{\sigma} + \delta_j^{\sigma'} + w_{\delta_j^{\sigma'}} \cdot \Delta\delta_j^{\sigma'} \right); \; \sigma \neq \sigma' \,\&\, i \neq j \tag{5.48}$$

The diagonal and the off-diagonal elements of J_2 are the followings.

$$\frac{\partial P_{i,load}^{\sigma}}{\partial w_{V_i^{\sigma}}} = 2\Delta |V_i^{\sigma}| \left[|V_i^{\sigma}| + w_{V_i^{\sigma}} \cdot \Delta |V_i^{\sigma}| \right] |Y_{ii}^{\sigma\sigma}| \cos(\theta_{ii}^{\sigma\sigma}) + \Delta |V_i^{\sigma}| \sum_{j=1}^{n} \sum_{\sigma' \in \{A,B,C\}}^{\sigma \neq \sigma' \,\&\, i \neq j} \left[|V_j^{\sigma'}| + w_{V_j^{\sigma'}} \cdot \Delta |V_j^{\sigma'}| \right] |Y_{ij}^{\sigma\sigma'}| cos\left(\theta_{ij}^{\sigma\sigma'} - \delta_i^{\sigma} - w_{\delta_i^{\sigma}} \cdot \Delta\delta_i^{\sigma} + \delta_j^{\sigma'} + w_{\delta_j^{\sigma'}} \cdot \Delta\delta_j^{\sigma'} \right) \tag{5.49}$$

$$\frac{\partial P_{i,load}^{\sigma}}{\partial w_{V_j^{\sigma'}}} = \Delta |V_j^{\sigma'}| \left[|V_i^{\sigma}| + w_{V_i^{\sigma}} \cdot \Delta |V_i^{\sigma}| \right] |Y_{ij}^{\sigma\sigma'}| cos\left(\theta_{ij}^{\sigma\sigma'} - \delta_i^{\sigma} - w_{\delta_i^{\sigma}} \cdot \Delta\delta_i^{\sigma} + \delta_j^{\sigma'} + w_{\delta_j^{\sigma'}} \cdot \Delta\delta_j^{\sigma'} \right); \; \sigma \neq \sigma' \,\&\, i \neq j \tag{5.50}$$

The diagonal and the off-diagonal elements of J_3 are the followings.

$$\frac{\partial Q_{i,load}^{\sigma}}{\partial w_{\delta_i^{\sigma}}} = \Delta\delta_i^{\sigma} \sum_{j=1}^{n} \sum_{\sigma' \in \{A,B,C\}}^{\sigma \neq \sigma' \,\&\, i \neq j} \left[|V_i^{\sigma}| + w_{V_i^{\sigma}} \cdot \Delta |V_i^{\sigma}| \right] \left[|V_j^{\sigma'}| + w_{V_j^{\sigma'}} \cdot \Delta |V_j^{\sigma'}| \right] |Y_{ij}^{\sigma\sigma'}| cos\left(\theta_{ij}^{\sigma\sigma'} - \delta_i^{\sigma} - w_{\delta_i^{\sigma}} \cdot \Delta\delta_i^{\sigma} + \delta_j^{\sigma'} + w_{\delta_j^{\sigma'}} \cdot \Delta\delta_j^{\sigma'} \right) \tag{5.51}$$

$$\frac{\partial Q_{i,load}^{\sigma}}{\partial w_{\delta_j^{\sigma'}}} = -\Delta\delta_j^{\sigma'} \left[|V_i^{\sigma}| + w_{V_i^{\sigma}} \cdot \Delta |V_i^{\sigma}| \right] \left[|V_j^{\sigma'}| + w_{V_j^{\sigma'}} \cdot \Delta |V_j^{\sigma'}| \right] |Y_{ij}^{\sigma\sigma'}| cos\left(\theta_{ij}^{\sigma\sigma'} - \delta_i^{\sigma} - w_{\delta_i^{\sigma}} \cdot \Delta\delta_i^{\sigma} + \delta_j^{\sigma'} + w_{\delta_j^{\sigma'}} \cdot \Delta\delta_j^{\sigma'} \right); \; \sigma \neq \sigma' \,\&\, i \neq j \tag{5.52}$$

The diagonal and the off-diagonal elements of J_4 are the followings.

$$\frac{\partial Q_{i,load}^{\sigma}}{\partial w_{V_i^{\sigma}}} = -2\Delta|V_i^{\sigma}|\left[|V_i^{\sigma}| + w_{V_i^{\sigma}} \cdot \Delta|V_i^{\sigma}|\right]|Y_{ii}^{\sigma\sigma}|\sin(\theta_{ii}^{\sigma\sigma}) - \Delta|V_i^{\sigma}|\sum_{j=1}^{n}\sum_{\sigma'\in\{A,B,C\}}^{\sigma\neq\sigma' \,\&\, i\neq j}\left[\left|V_j^{\sigma'}\right| + w_{V_j^{\sigma'}} \cdot \Delta\left|V_j^{\sigma'}\right|\right]\left|Y_{ij}^{\sigma\sigma'}\right| sin\left(\theta_{ij}^{\sigma\sigma'} - \delta_i^{\sigma} - w_{\delta_i^{\sigma}} \cdot \Delta\delta_i^{\sigma} + \delta_j^{\sigma'} + w_{\delta_j^{\sigma'}} \cdot \Delta\delta_j^{\sigma'}\right) \tag{5.53}$$

$$\frac{\partial Q_{i,load}^{\sigma}}{\partial w_{V_j^{\sigma'}}} = -\Delta\left|V_j^{\sigma'}\right|\left[|V_i^{\sigma}| + w_{V_i^{\sigma}} \cdot \Delta|V_i^{\sigma}|\right]\left|Y_{ij}^{\sigma\sigma'}\right| sin\left(\theta_{ij}^{\sigma\sigma'} - \delta_i^{\sigma} - w_{\delta_i^{\sigma}} \cdot \Delta\delta_i^{\sigma} + \delta_j^{\sigma'} + w_{\delta_j^{\sigma'}} \cdot \Delta\delta_j^{\sigma'}\right);\ \sigma \neq \sigma' \,\&\, i \neq j \tag{5.54}$$

Substituting equation (5.42) for δ_i^{σ} and δ_j^{σ} in equations (5.16) and (5.17) and substituting equation (5.43) for $|V_i^{\sigma}|$ and $\left|V_j^{\sigma}\right|$ in equations (5.16) and (5.17) in the case of having connected single phase PV inverters in the phase A, B or C at any node i:

$$P_{i,load}^{\sigma} = \sum_{j=1}^{n}\sum_{\sigma'\in\{A,B,C\}}\left[|V_i^{\sigma}| + w_{V_i^{\sigma}} \cdot \Delta|V_i^{\sigma}|\right]\left[\left|V_j^{\sigma'}\right| + w_{V_j^{\sigma'}} \cdot \Delta\left|V_j^{\sigma'}\right|\right]\left|Y_{ij}^{\sigma\sigma'}\right| cos\left(\theta_{ij}^{\sigma\sigma'} - \delta_i^{\sigma} - w_{\delta_i^{\sigma}} \cdot \Delta\delta_i^{\sigma} + \delta_j^{\sigma'} + w_{\delta_j^{\sigma'}} \cdot \Delta\delta_j^{\sigma'}\right) - P_{i,pv}^{\sigma} \tag{5.55}$$

$$Q_{i,load}^{\sigma} = -\sum_{j=1}^{n}\sum_{\sigma'\in\{A,B,C\}}\left[|V_i^{\sigma}| + w_{V_i^{\sigma}} \cdot \Delta|V_i^{\sigma}|\right]\left[\left|V_j^{\sigma'}\right| + w_{V_j^{\sigma'}} \cdot \Delta\left|V_j^{\sigma'}\right|\right]\left|Y_{ij}^{\sigma\sigma'}\right| sin\left(\theta_{ij}^{\sigma\sigma'} - \delta_i^{\sigma} - w_{\delta_i^{\sigma}} \cdot \Delta\delta_i^{\sigma} + \delta_j^{\sigma'} + w_{\delta_j^{\sigma'}} \cdot \Delta\delta_j^{\sigma'}\right) - Q_{i,pv}^{\sigma} \tag{5.56}$$

From equations (5.55)-(5.56), it can be transformed to the linear equations as shown in equation (5.46). The diagonal and the off-diagonal elements of J_1 are the followings.

$$\frac{\partial P_{i,load}^{\sigma}}{\partial w_{\delta_i^{\sigma}}} = \Delta\delta_i^{\sigma}\sum_{j=1}^{n}\sum_{\sigma'\in\{A,B,C\}}^{\sigma\neq\sigma' \,\&\, i\neq j}\left[|V_i^{\sigma}| + w_{V_i^{\sigma}} \cdot \Delta|V_i^{\sigma}|\right]\left[\left|V_j^{\sigma'}\right| + w_{V_j^{\sigma'}} \cdot \Delta\left|V_j^{\sigma'}\right|\right]\left|Y_{ij}^{\sigma\sigma'}\right| sin\left(\theta_{ij}^{\sigma\sigma'} - \delta_i^{\sigma} - w_{\delta_i^{\sigma}} \cdot \Delta\delta_i^{\sigma} + \delta_j^{\sigma'} + w_{\delta_j^{\sigma'}} \cdot \Delta\delta_j^{\sigma'}\right) \tag{5.57}$$

$$\frac{\partial P_{i,load}^{\sigma}}{\partial w_{\delta_j^{\sigma'}}} = -\Delta\delta_j^{\sigma'}\left[|V_i^{\sigma}| + w_{V_i^{\sigma}} \cdot \Delta|V_i^{\sigma}|\right]\left[\left|V_j^{\sigma'}\right| + w_{V_j^{\sigma'}} \cdot \Delta\left|V_j^{\sigma'}\right|\right]|Y_{ij}^{\sigma\sigma'}| sin\left(\theta_{ij}^{\sigma\sigma'} - \delta_i^{\sigma} - w_{\delta_i^{\sigma}} \cdot \Delta\delta_i^{\sigma} + \delta_j^{\sigma'} + w_{\delta_j^{\sigma'}} \cdot \Delta\delta_j^{\sigma'}\right);\ \sigma \neq \sigma' \ \&\ i \neq j \tag{5.58}$$

The diagonal and the off-diagonal elements of J_2 are shown in equations (5.59) and (5.60) respectively where equations (5.61) and (5.62) are the differential equations of continuous and piecewise linear P(U) local control functions respectively.

$$\frac{\partial P_{i,load}^{\sigma}}{\partial w_{V_i^{\sigma}}} = 2\Delta|V_i^{\sigma}|\left[|V_i^{\sigma}| + w_{V_i^{\sigma}} \cdot \Delta|V_i^{\sigma}|\right]|Y_{ii}^{\sigma\sigma}|\cos(\theta_{ii}^{\sigma\sigma}) + \Delta|V_i^{\sigma}|\sum_{j=1}^{n}\sum_{\sigma'\in\{A,B,C\}}^{\sigma\neq\sigma'\ \&\ i\neq j}\left[\left|V_j^{\sigma'}\right| + w_{V_j^{\sigma'}} \cdot \Delta\left|V_j^{\sigma'}\right|\right]|Y_{ij}^{\sigma\sigma'}| cos\left(\theta_{ij}^{\sigma\sigma'} - \delta_i^{\sigma} - w_{\delta_i^{\sigma}} \cdot \Delta\delta_i^{\sigma} + \delta_j^{\sigma'} + w_{\delta_j^{\sigma'}} \cdot \Delta\delta_j^{\sigma'}\right) - \frac{\partial P_{i,pv}^{\sigma}}{\partial w_{V_i^{\sigma}}} \tag{5.59}$$

$$\frac{\partial P_{i,load}^{\sigma}}{\partial w_{V_j^{\sigma'}}} = \Delta\left|V_j^{\sigma'}\right|\left[|V_i^{\sigma}| + w_{V_i^{\sigma}} \cdot \Delta|V_i^{\sigma}|\right]|Y_{ij}^{\sigma\sigma'}| cos\left(\theta_{ij}^{\sigma\sigma'} - \delta_i^{\sigma} - w_{\delta_i^{\sigma}} \cdot \Delta\delta_i^{\sigma} + \delta_j^{\sigma'} + w_{\delta_j^{\sigma'}} \cdot \Delta\delta_j^{\sigma'}\right);\ \sigma \neq \sigma' \ \&\ i \neq j \tag{5.60}$$

$$\frac{\partial P_{i,pv}^{\sigma}}{\partial w_{V_i^{\sigma}}} = \frac{-4 \cdot \Delta|V_i^{\sigma}| \cdot P_i^{max} \cdot exp\left[-4\left(\left[|V_i^{\sigma}| + w_{V_i^{\sigma}} \cdot \Delta|V_i^{\sigma}|\right] - V_{i,cri}^{\sigma}\right)/\delta_{i,p}^{\sigma}\right]}{\delta_{i,p}^{\sigma} \cdot \left[1 + exp\left[-4\left(\left[|V_i^{\sigma}| + w_{V_i^{\sigma}} \cdot \Delta|V_i^{\sigma}|\right] - V_{i,cri}^{\sigma}\right)/\delta_{i,p}^{\sigma}\right]\right]^2} \tag{5.61}$$

$$\frac{\partial P_{i,pv}^{\sigma}}{\partial w_{V_i^{\sigma}}} = P_i^{max} \cdot \begin{cases} \dfrac{\Delta V_i^{\sigma}}{V_{i,p1}^{\sigma} - V_{i,p2}^{\sigma}} & ;\ V_{i,p1}^{\sigma} \leq |V_i^{\sigma}| + w_{V_i^{\sigma}} \cdot \Delta V_i^{\sigma} < V_{i,p2}^{\sigma} \\ 0 & ;other \end{cases} \tag{5.62}$$

The diagonal and the off-diagonal elements of J_3 are the followings.

$$\frac{\partial Q_{i,load}^{\sigma}}{\partial w_{\delta_i^{\sigma}}} = \Delta\delta_i^{\sigma}\sum_{j=1}^{n}\sum_{\sigma'\in\{A,B,C\}}^{\sigma\neq\sigma'\ \&\ i\neq j}\left[|V_i^{\sigma}| + w_{V_i^{\sigma}} \cdot \Delta|V_i^{\sigma}|\right]\left[\left|V_j^{\sigma'}\right| + w_{V_j^{\sigma'}} \cdot \Delta\left|V_j^{\sigma'}\right|\right]|Y_{ij}^{\sigma\sigma'}| cos\left(\theta_{ij}^{\sigma\sigma'} - \delta_i^{\sigma} - w_{\delta_i^{\sigma}} \cdot \Delta\delta_i^{\sigma} + \delta_j^{\sigma'} + w_{\delta_j^{\sigma'}} \cdot \Delta\delta_j^{\sigma'}\right) \tag{5.63}$$

$$\frac{\partial Q_{i,load}^{\sigma}}{\partial w_{\delta_j^{\sigma'}}} = -\Delta\delta_j^{\sigma'}\left[|V_i^{\sigma}| + w_{V_i^{\sigma}} \cdot \Delta|V_i^{\sigma}|\right]\left[\left|V_j^{\sigma'}\right| + w_{V_j^{\sigma'}} \cdot \Delta\left|V_j^{\sigma'}\right|\right]|Y_{ij}^{\sigma\sigma'}|cos\left(\theta_{ij}^{\sigma\sigma'} - \delta_i^{\sigma} - w_{\delta_i^{\sigma}} \cdot \Delta\delta_i^{\sigma} + \delta_j^{\sigma'} + w_{\delta_j^{\sigma'}} \cdot \Delta\delta_j^{\sigma'}\right);\ \sigma \neq \sigma' \ \&\ i \neq j \tag{5.64}$$

The diagonal and the off-diagonal elements of J_4 are shown in equations (5.65) and (5.66) respectively where equations (5.67) and (5.68) are the differential equations of continuous and piecewise linear Q(U) local control functions respectively.

$$\frac{\partial Q_{i,load}^{\sigma}}{\partial w_{V_i^{\sigma}}} = -2\Delta|V_i^{\sigma}|\left[|V_i^{\sigma}| + w_{V_i^{\sigma}} \cdot \Delta|V_i^{\sigma}|\right]|Y_{ii}^{\sigma\sigma}|\sin(\theta_{ii}^{\sigma\sigma}) - \Delta|V_i^{\sigma}|\sum_{j=1}^{n}\sum_{\sigma'\in\{A,B,C\}}^{\sigma\neq\sigma'\ \&\ i\neq j}\left[\left|V_j^{\sigma'}\right| + w_{V_j^{\sigma'}} \cdot \Delta\left|V_j^{\sigma'}\right|\right]|Y_{ij}^{\sigma\sigma'}|sin\left(\theta_{ij}^{\sigma\sigma'} - \delta_i^{\sigma} - w_{\delta_i^{\sigma}} \cdot \Delta\delta_i^{\sigma} + \delta_j^{\sigma'} + w_{\delta_j^{\sigma'}} \cdot \Delta\delta_j^{\sigma'}\right) - \frac{\partial Q_{i,pv}^{\sigma}}{\partial w_{V_i^{\sigma}}} \tag{5.65}$$

$$\frac{\partial Q_{i,load}^{\sigma}}{\partial w_{V_j^{\sigma'}}} = -\Delta\left|V_j^{\sigma'}\right|\left[|V_i^{\sigma}| + w_{V_i^{\sigma}} \cdot \Delta|V_i^{\sigma}|\right]|Y_{ij}^{\sigma\sigma'}|sin\left(\theta_{ij}^{\sigma\sigma'} - \delta_i^{\sigma} - w_{\delta_i^{\sigma}} \cdot \Delta\delta_i^{\sigma} + \delta_j^{\sigma'} + w_{\delta_j^{\sigma'}} \cdot \Delta\delta_j^{\sigma'}\right);\ \sigma \neq \sigma' \ \&\ i \neq j \tag{5.66}$$

$$\frac{\partial Q_{i,pv}^{\sigma}}{\partial w_{V_i^{\sigma}}} = \frac{-4 \cdot K_{i,2}^{\sigma} \cdot \Delta|V_i^{\sigma}| \cdot Q_i^{max} \cdot exp\left[-4\left(\left[|V_i^{\sigma}| + w_{V_i^{\sigma}} \cdot \Delta|V_i^{\sigma}|\right] - V_{i,q}^{\sigma}\right)/\delta_{i,q}^{\sigma}\right]}{\delta_{i,q}^{\sigma} \cdot \left[1 + exp\left[-4\left(\left[|V_i^{\sigma}| + w_{V_i^{\sigma}} \cdot \Delta|V_i^{\sigma}|\right] - V_{i,q}^{\sigma}\right)/\delta_{i,q}^{\sigma}\right]\right]^2} \tag{5.67}$$

$$\frac{\partial Q_{i,pv}^{\sigma}}{\partial w_{V_i^{\sigma}}} = Q_i^{max} \cdot \begin{cases} \dfrac{\Delta V_i^{\sigma}\left(K_{i,1}^{\sigma} - V_{i,2}^{\sigma}\right)}{V_{i,q1}^{\sigma} - V_{i,q2}^{\sigma}} & ;\ V_{i,q1}^{\sigma} \leq |V_i^{\sigma}| + w_{V_i^{\sigma}} \cdot \Delta V_i^{\sigma} < V_{i,q2}^{\sigma} \\ 0 & ;other \end{cases} \tag{5.68}$$

Substituting equation (5.42) for δ_i^{σ} and δ_j^{σ} in equations (5.30) and (5.31) and substituting equation (5.43) for $|V_i^{\sigma}|$ and $\left|V_j^{\sigma}\right|$ in equations (5.30) and (5.31) in the case of having connected three phase PV inverters in the phases A, B and C at any node i:

$$P_{i,load}^{\sigma} = \sum_{j=1}^{n} \sum_{\sigma' \in \{A,B,C\}} \left[|V_i^{\sigma}| + w_{V_i^{\sigma}} \cdot \Delta |V_i^{\sigma}| \right] \left[|V_j^{\sigma'}| + w_{V_j^{\sigma'}} \cdot \Delta |V_j^{\sigma'}| \right] |Y_{ij}^{\sigma\sigma'}| cos\left(\theta_{ij}^{\sigma\sigma'} - \delta_i^{\sigma} - w_{\delta_i^{\sigma}} \cdot \Delta\delta_i^{\sigma} + \delta_j^{\sigma'} + w_{\delta_j^{\sigma'}} \cdot \Delta\delta_j^{\sigma'} \right) - P_{i,pv}^{\sigma} \quad (5.69)$$

$$Q_{i,load}^{\sigma} = -\sum_{j=1}^{n} \sum_{\sigma' \in \{A,B,C\}} \left[|V_i^{\sigma}| + w_{V_i^{\sigma}} \cdot \Delta |V_i^{\sigma}| \right] \left[|V_j^{\sigma'}| + w_{V_j^{\sigma'}} \cdot \Delta |V_j^{\sigma'}| \right] |Y_{ij}^{\sigma\sigma'}| sin\left(\theta_{ij}^{\sigma\sigma'} - \delta_i^{\sigma} - w_{\delta_i^{\sigma}} \cdot \Delta\delta_i^{\sigma} + \delta_j^{\sigma'} + w_{\delta_j^{\sigma'}} \cdot \Delta\delta_j^{\sigma'} \right) - Q_{i,pv}^{\sigma} \quad (5.70)$$

From equations (5.69)-(5.70), it can be transformed to the linear equations as shown in equation (5.46). The diagonal and the off-diagonal elements of J_1 can be written into equations (5.71) and (5.72) respectively where $\frac{\partial P_{i,pv}^{\sigma}}{\partial w_{\delta_i^{\sigma}}}$ and $\frac{\partial P_{i,pv}^{\sigma}}{\partial w_{\delta_j^{\sigma'}}}$ can be clarified in Appendix B.2.

$$\frac{\partial P_{i,load}^{\sigma}}{\partial w_{\delta_i^{\sigma}}} = \Delta\delta_i^{\sigma} \sum_{j=1}^{n} \sum_{\sigma' \in \{A,B,C\}}^{\sigma \neq \sigma' \,\&\, i \neq j} \left[|V_i^{\sigma}| + w_{V_i^{\sigma}} \cdot \Delta |V_i^{\sigma}| \right] \left[|V_j^{\sigma'}| + w_{V_j^{\sigma'}} \cdot \Delta |V_j^{\sigma'}| \right] |Y_{ij}^{\sigma\sigma'}| sin\left(\theta_{ij}^{\sigma\sigma'} - \delta_i^{\sigma} - w_{\delta_i^{\sigma}} \cdot \Delta\delta_i^{\sigma} + \delta_j^{\sigma'} + w_{\delta_j^{\sigma'}} \cdot \Delta\delta_j^{\sigma'} \right) - \frac{\partial P_{i,pv}^{\sigma}}{\partial w_{\delta_i^{\sigma}}} \quad (5.71)$$

$$\frac{\partial P_{i,load}^{\sigma}}{\partial w_{\delta_j^{\sigma'}}} = -\Delta\delta_j^{\sigma'} \left[|V_i^{\sigma}| + w_{V_i^{\sigma}} \cdot \Delta |V_i^{\sigma}| \right] \left[|V_j^{\sigma'}| + w_{V_j^{\sigma'}} \cdot \Delta |V_j^{\sigma'}| \right] |Y_{ij}^{\sigma\sigma'}| sin\left(\theta_{ij}^{\sigma\sigma'} - \delta_i^{\sigma} - w_{\delta_i^{\sigma}} \cdot \Delta\delta_i^{\sigma} + \delta_j^{\sigma'} + w_{\delta_j^{\sigma'}} \cdot \Delta\delta_j^{\sigma'} \right) - \frac{\partial P_{i,pv}^{\sigma}}{\partial w_{\delta_j^{\sigma'}}} \; ; \; \sigma \neq \sigma' \,\&\, i \neq j \quad (5.72)$$

The diagonal and the off-diagonal elements of J_2 can be written in equations (5.73) and (5.74) respectively where $\frac{\partial P_{i,pv}^{\sigma}}{\partial w_{V_i^{\sigma}}}$ and $\frac{\partial P_{i,pv}^{\sigma}}{\partial w_{V_j^{\sigma'}}}$ can be clarified in Appendix B.2.

$$\frac{\partial P_{i,load}^{\sigma}}{\partial w_{V_i^{\sigma}}} = 2\Delta|V_i^{\sigma}|\left[|V_i^{\sigma}| + w_{V_i^{\sigma}} \cdot \Delta|V_i^{\sigma}|\right]|Y_{ii}^{\sigma\sigma}|\cos(\theta_{ii}^{\sigma\sigma}) + \Delta|V_i^{\sigma}|\sum_{j=1}^{n}\sum_{\sigma' \in \{A,B,C\}}^{\sigma \neq \sigma' \,\&\, i \neq j}\left[\left|V_j^{\sigma'}\right| + w_{V_j^{\sigma'}} \cdot \Delta\left|V_j^{\sigma'}\right|\right]\left|Y_{ij}^{\sigma\sigma'}\right|cos\left(\theta_{ij}^{\sigma\sigma'} - \delta_i^{\sigma} - w_{\delta_i^{\sigma}} \cdot \Delta\delta_i^{\sigma} + \delta_j^{\sigma'} + w_{\delta_j^{\sigma'}} \cdot \Delta\delta_j^{\sigma'}\right) - \frac{\partial P_{i,pv}^{\sigma}}{\partial w_{V_i^{\sigma}}} \tag{5.73}$$

$$\frac{\partial P_{i,load}^{\sigma}}{\partial w_{V_j^{\sigma'}}} = \Delta\left|V_j^{\sigma'}\right|\left[|V_i^{\sigma}| + w_{V_i^{\sigma}} \cdot \Delta|V_i^{\sigma}|\right]\left|Y_{ij}^{\sigma\sigma'}\right|cos\left(\theta_{ij}^{\sigma\sigma'} - \delta_i^{\sigma} - w_{\delta_i^{\sigma}} \cdot \Delta\delta_i^{\sigma} + \delta_j^{\sigma'} + w_{\delta_j^{\sigma'}} \cdot \Delta\delta_j^{\sigma'}\right) - \frac{\partial P_{i,pv}^{\sigma}}{\partial w_{V_j^{\sigma'}}};\ \sigma \neq \sigma' \,\&\, i \neq j \tag{5.74}$$

The diagonal and the off-diagonal elements of J_3 can be written into equation (5.75) and (5.76) respectively where $\frac{\partial Q_{i,pv}^{\sigma}}{\partial w_{\delta_i^{\sigma}}}$ and $\frac{\partial Q_{i,pv}^{\sigma}}{\partial \delta_j^{\sigma'}}$ can be clarified in Appendix B.2.

$$\frac{\partial Q_{i,load}^{\sigma}}{\partial w_{\delta_i^{\sigma}}} = \Delta\delta_i^{\sigma}\sum_{j=1}^{n}\sum_{\sigma' \in \{A,B,C\}}^{\sigma \neq \sigma' \,\&\, i \neq j}\left[|V_i^{\sigma}| + w_{V_i^{\sigma}} \cdot \Delta|V_i^{\sigma}|\right]\left[\left|V_j^{\sigma'}\right| + w_{V_j^{\sigma'}} \cdot \Delta\left|V_j^{\sigma'}\right|\right]\left|Y_{ij}^{\sigma\sigma'}\right|cos\left(\theta_{ij}^{\sigma\sigma'} - \delta_i^{\sigma} - w_{\delta_i^{\sigma}} \cdot \Delta\delta_i^{\sigma} + \delta_j^{\sigma'} + w_{\delta_j^{\sigma'}} \cdot \Delta\delta_j^{\sigma'}\right) \tag{5.75}$$

$$\frac{\partial Q_{i,load}^{\sigma}}{\partial w_{\delta_j^{\sigma'}}} = -\Delta\delta_j^{\sigma'}\left[|V_i^{\sigma}| + w_{V_i^{\sigma}} \cdot \Delta|V_i^{\sigma}|\right]\left[\left|V_j^{\sigma'}\right| + w_{V_j^{\sigma'}} \cdot \Delta\left|V_j^{\sigma'}\right|\right]\left|Y_{ij}^{\sigma\sigma'}\right|cos\left(\theta_{ij}^{\sigma\sigma'} - \delta_i^{\sigma} - w_{\delta_i^{\sigma}} \cdot \Delta\delta_i^{\sigma} + \delta_j^{\sigma'} + w_{\delta_j^{\sigma'}} \cdot \Delta\delta_j^{\sigma'}\right) - \frac{\partial Q_{i,pv}^{\sigma}}{\partial \delta_j^{\sigma'}};\ \sigma \neq \sigma' \,\&\, i \neq j \tag{5.76}$$

The diagonal and the off-diagonal elements of J_4 can be written in equations (5.77) and (5.78) respectively where $\frac{\partial Q_{i,pv}^{\sigma}}{\partial w_{V_i^{\sigma}}}$ and $\frac{\partial Q_{i,pv}^{\sigma}}{\partial w_{V_j^{\sigma'}}}$ can be clarified in Appendix B.2.

$$\frac{\partial Q_{i,load}^{\sigma}}{\partial w_{V_i^{\sigma}}} = -2\Delta|V_i^{\sigma}|\left[|V_i^{\sigma}| + w_{V_i^{\sigma}} \cdot \Delta|V_i^{\sigma}|\right]|Y_{ii}^{\sigma\sigma}|\sin(\theta_{ii}^{\sigma\sigma}) - \Delta|V_i^{\sigma}|\sum_{j=1}^{n}\sum_{\sigma'\in\{A,B,C\}}^{\sigma\neq\sigma'\ \&\ i\neq j}\left[|V_j^{\sigma'}| + w_{V_j^{\sigma'}} \cdot \Delta|V_j^{\sigma'}|\right]|Y_{ij}^{\sigma\sigma'}|sin\left(\theta_{ij}^{\sigma\sigma'} - \delta_i^{\sigma} - w_{\delta_i^{\sigma}} \cdot \Delta\delta_i^{\sigma} + \delta_j^{\sigma'} + w_{\delta_j^{\sigma'}} \cdot \Delta\delta_j^{\sigma'}\right) - \frac{\partial Q_{i,pv}^{\sigma}}{\partial w_{V_i^{\sigma}}} \tag{5.77}$$

$$\frac{\partial Q_{i,load}^{\sigma}}{\partial w_{V_j^{\sigma'}}} = -\Delta|V_j^{\sigma'}|\left[|V_i^{\sigma}| + w_{V_i^{\sigma}} \cdot \Delta|V_i^{\sigma}|\right]|Y_{ij}^{\sigma\sigma'}|sin\left(\theta_{ij}^{\sigma\sigma'} - \delta_i^{\sigma} - w_{\delta_i^{\sigma}} \cdot \Delta\delta_i^{\sigma} + \delta_j^{\sigma'} + w_{\delta_j^{\sigma'}} \cdot \Delta\delta_j^{\sigma'}\right) - \frac{\partial Q_{i,pv}^{\sigma}}{\partial w_{V_j^{\sigma'}}};\ \sigma \neq \sigma'\ \&\ i \neq j \tag{5.78}$$

The new estimates for step-change values are:

$$w_{V_i^{\sigma}}{}^{(h+1)} = w_{V_i^{\sigma}}{}^{(h)} + \Delta w_{V_i^{\sigma}}{}^{(h)} \tag{5.79}$$

$$w_{\delta_i^{\sigma}}{}^{(h+1)} = w_{\delta_i^{\sigma}}{}^{(h)} + \Delta w_{\delta_i^{\sigma}}{}^{(h)} \tag{5.80}$$

The procedure for power flow solution by the Newton-Raphson method is as follows. The related flow chart can be shown in Figure 5.1.

STEP 1: For load buses, where $P_i^{\sigma sch}$ and $Q_i^{\sigma sch}$ are specified, voltage magnitudes and phase angles are set equal to the slack bus values.

STEP 2: For step-change values, $w_{V_i^{\sigma}}{}^{(0)} = w_{\delta_i^{\sigma}}{}^{(0)} = 1$.

STEP 3: For load buses, $P_i^{\sigma(k)}$ and $Q_i^{\sigma(k)}$ are calculated from equations (5.1), (5.2), (5.16), (5.17), (5.30) and (5.31). $\Delta P_i^{\sigma(k)}$ and $\Delta Q_i^{\sigma(k)}$ are calculated from equations (5.40) and (5.41).

STEP 4: The elements of the Jacobian matrix (J_1, J_2, J_3 and J_4) are calculated from equations (5.8)-(5.15), (5.18)-(5.29) and (5.32)-(5.39).

STEP 5: The linear simultaneous equation (5.7) is solved directly by optimally ordered triangular factorization and Gaussian elimination. The $\Delta\delta_i^{\sigma(k)}$ and $\Delta\left|V_i^{\sigma(k)}\right|$ are obtained.

STEP 6: For load buses, $P_i^{\sigma(h)}$ and $Q_i^{\sigma(h)}$ are calculated from equations (5.44), (5.45), (5.55), (5.56), (5.69) and (5.70). $\Delta P_i^{\sigma(h)}$ and $\Delta Q_i^{\sigma(h)}$ are calculated from equations (5.40) and (5.41).

STEP 7: Determine:

$$max\left\{\left|\Delta P_i^{\sigma(h)}\right|, \left|\Delta Q_i^{\sigma(h)}\right|\right\} > max\left\{\left|\Delta P_i^{\sigma(h-1)}\right|, \left|\Delta Q_i^{\sigma(h-1)}\right|\right\}$$

- If the condition is correct, the new voltage magnitudes and phase angles are computed from equations (5.42) and (5.43) by $w_{V_i^{\sigma}}{}^{(h-1)}$ and $w_{\delta_i^{\sigma}}{}^{(h-1)}$. After that, $w_{V_i^{\sigma}}{}^{(h)} = w_{\delta_i^{\sigma}}{}^{(h)}$ are renewed that the value are accordingly reduced from {0.9, 0.8, …, 0.1}. Finally, go to ***STEP 3***.
- If the condition is vice versa, go to ***STEP 8***.
- If $max\left\{\left|\Delta P_i^{\sigma(h)}\right|, \left|\Delta Q_i^{\sigma(h)}\right|\right\} < \varepsilon$, the power flow algorithm is terminated and the new voltage magnitudes and phase angles are computed from equations (5.42) and (5.43) by $w_{V_i^{\sigma}}{}^{(h)}$ and $w_{\delta_i^{\sigma}}{}^{(h)}$.

STEP 8: The elements of the Jacobian matrix (J_1, J_2, J_3 and J_4) are calculated from equations (5.47)-(5.54), (5.57)-(5.68) and (5.71)-(5.78).

STEP 9: The linear simultaneous equation (5.46) is solved directly by optimally ordered triangular factorization and Gaussian elimination. The $\Delta w_{V_i^{\sigma}}{}^{(h)}$ and $\Delta w_{\delta_i^{\sigma}}{}^{(h)}$ are obtained.

STEP 10: The new step-length values are computed from equations (5.79) and (5.80). After that, go to ***STEP 6***.

For example, the calculation of ***The Power Flow Algorithm With Using Local Control Function*** can be shown in Appendix C.

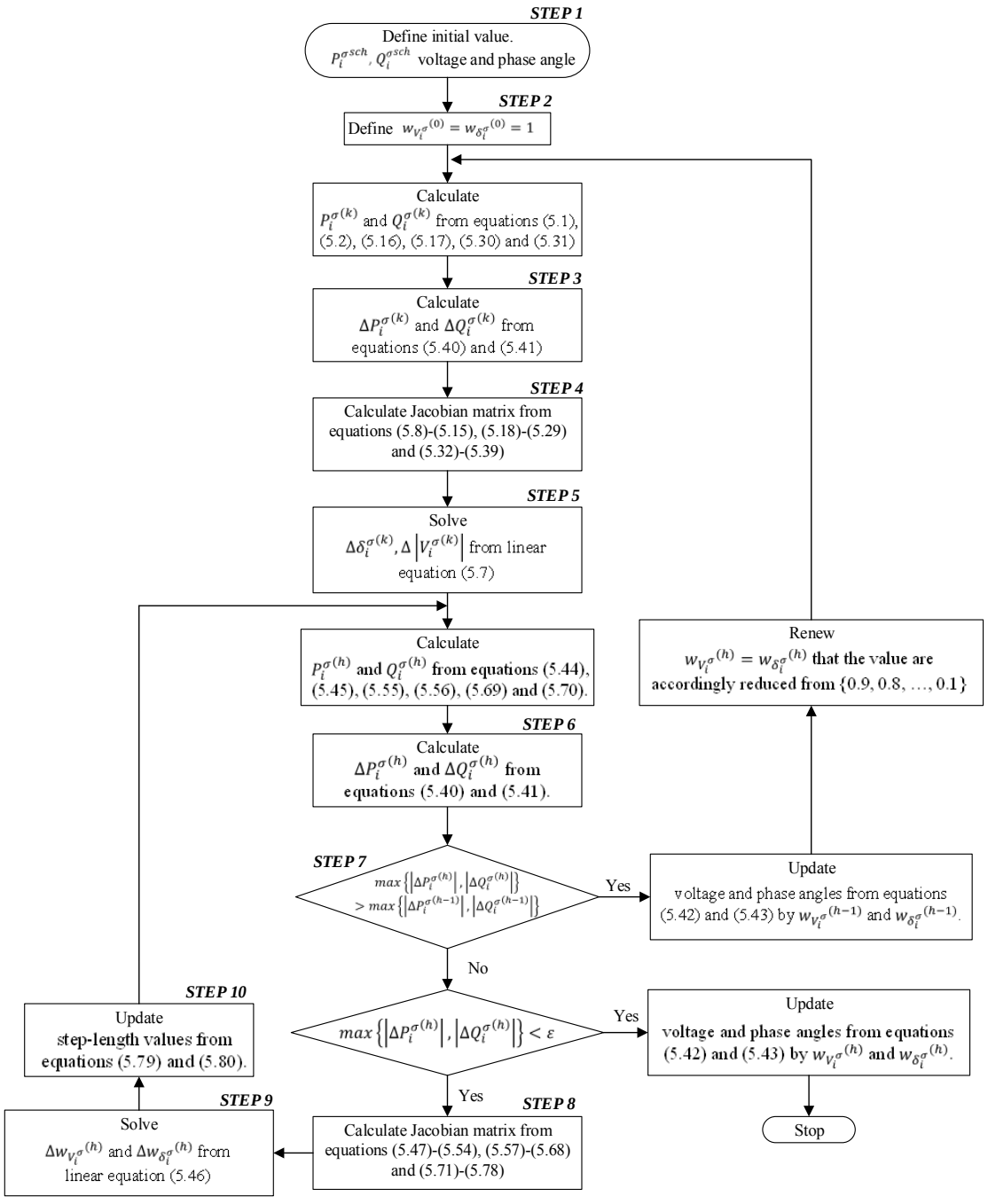

Figure 5.1 The flowchart of power flow algorithm with using local control function

5.2 2-stage PSO Process

This research determines the set of uncertainty in 17 cases as shown in Table 4.3 which is stated in Subsection 4.4.2.2 to cover uncertainty characteristics of load, solar irradiance and ambient temperature in one day or one week interval. Considering the benefit of PV owner, the main objective can be shown in equation (5.81) that total

real power output from overall connected PV system must be injected to LV distribution system at maximum value. The main objective (5.81) determines on the case z1 of the set of uncertainty as the representative condition because this case has the highest chance to occur according to normal uncertainty characteristic.

$$maximize\left[\sum_{i}^{n}\sum_{\sigma\in\{A,B,C\}}P_{i,pv,z1}^{\sigma}\right] \tag{5.81}$$

Subject to:

$$V_{min}^{\sigma} \le V_{i,z}^{\sigma} \le V_{max}^{\sigma} \tag{5.82}$$

$$\left|I_{i-j,z}^{\sigma}\right| \le I_{i-j,max}^{\sigma} \tag{5.83}$$

$$\left|S_{z}^{MV/LV}\right| \le S_{max}^{MV/LV} \tag{5.84}$$

$$VUF_{i,z} \le 3\%\,;\; VUF_{i} = \frac{|V_{i}^{ne}|}{|V_{i}^{po}|} \times 100\% \tag{5.85}$$

$$P_{loss,z} \le Loss_{max\,load,\,no\,PV} \tag{5.86}$$

where $z \in \{z1, z2, \dots, z17\}$; $P_{i,pv}^{\sigma}$ is real power output from each phase connection of PV system (W); V_{min}^{σ} and V_{max}^{σ} are minimum and maximum voltage limit (V) respectively; I_{i-j}^{σ} is line current at any phase σ between nodes i and j (A); $I_{i-j,max}^{\sigma}$ is maximum line current limit at any phase σ between nodes i and j (A); $S^{MV/LV}$ is the utilization capacity of distribution transformer (VA); $S_{max}^{MV/LV}$ is the capacity limit of distribution transformer (VA); P_{loss} is system loss (W); $Loss_{max\,load,\,no\,PV}$ is maximum loss in LV distribution system with no PV connection at maximum load (W).

Although objective function (5.81) determines only case z1, the constraints need to consider in overall 17 cases to qualify the correct solution under the uncertainty as shown in equations (5.82)-(5.86). At equation (5.82), voltage will not exceed voltage limit. Line current in equation (5.83) and the utilization capacity of distribution transformer in equation (5.84) will not exceed the limit. IEC 61000-2-2 standard defines that VUF limit in LV distribution system shall not exceed 3% in equation (5.81). At the view point of Distribution System Operator (DSO), high PV penetration can be permitted but PV connection must not cause higher loss than LV distribution system with no PV connection. Then, the constraint (5.86) is presented.

According to the optimization problem in equation (5.81), some readers may doubt that can this optimization problem determines on only severe case or case z16 (this case is considered on minimum load and maximum solar irradiance condition). Then, this question of doubt will be clarified in Appendix D. For the past proposal of this research, it presented the main objective as shown in equation (5.87) which maximizing the summation values along the total real power output from overall PV systems and the negative value of system loss. This concept is for maximizing the total real power output from overall PV systems as shown in equation (5.88) and minimizing system loss as shown in equation (5.89). The minimization of system loss equals the maximization of minus system loss as shown in equation (5.90).

$$maximize\left[\sum_{i}^{n}\sum_{\sigma\in\{A,B,C\}}P_{i,pv,z1}^{\sigma}\right]-P_{loss,z1} \tag{5.87}$$

$$maximize\left[\sum_{i}^{n}\sum_{\sigma\in\{A,B,C\}}P_{i,pv,z1}^{\sigma}\right] \tag{5.88}$$

$$minimize\left[P_{loss,z1}\right] \tag{5.89}$$

$$maximize\left[-P_{loss,z1}\right] \tag{5.90}$$

The summation of equation (5.88) and (5.89) is the equation (5.87). This past objective (5.87) seemed to solve maximization of total real power output from overall PV systems and minimization of system loss simultaneously. Thus, this past objective (5.87) was incorrect because the objective (5.88) of maximizing total real power output from overall PV systems is conflict with the other objective (5.89) of minimizing system loss. This conflict problem can be described in Appendix E.

To solve the optimization problem, there are many researches [42, 43] which apply PSO because PSO can solve optimization problem effectively. To solve the optimization problem as shown in equation (5.81), this research will apply PSO. Searching the optimal solution by PSO, the result will be at the optimal objective value. For objective value assessment according to the objective (5.81), there are 6 steps as follows and the related flow chart can be shown in Figure 5.2.

STEP 1: Define parameter setting of local control of each connected PV system $\{V_{i,cri}, \delta_{i,p}, K_{i,1}, K_{i,2}, V_{i,q}, \delta_{i,q}\}$ or $\{V_{i,p1}, V_{i,p2}, K_{i,1}, K_{i,2}, V_{i,q1}, V_{i,q2}\}$ according to selected type: continuous or piecewise linear local control function.

STEP 2: For each iteration, each member of the set of uncertainty will be selected $z \in \{z1, z2, \dots, z17\}$ until all members of z are selected. Each member will give the different values of load, solar irradiance and ambient temperature.

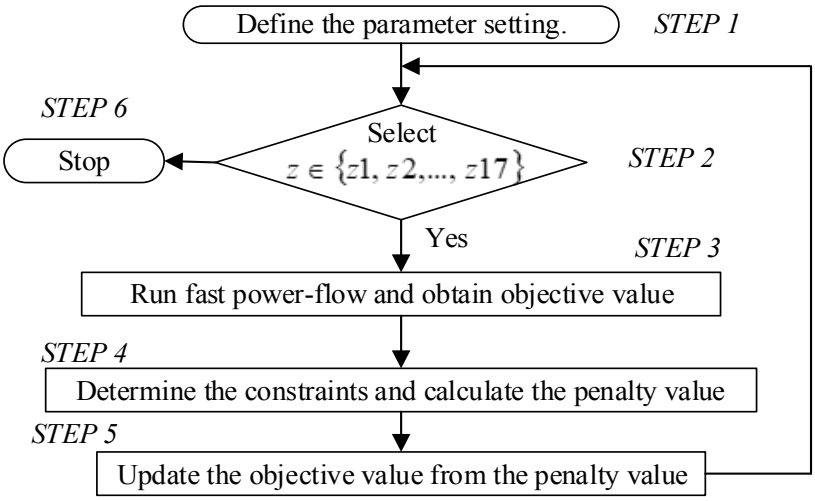

Figure 5.2 The flowchart of the calculation of objective value

STEP 3: From obtained load, solar irradiance and ambient temperature values in the previous step, they will be used in ***The Power Flow Algorithm with Using Local Control Function*** as stated in Subsection 5.1. After that, the results of real and reactive power output from each PV systems, system voltage, system loss, line flow and utilized capacity of MV/LV distribution transformer are obtained. This step objective value (Obj) can be calculated from equation (5.81) if only case $z1$ is selected.

STEP 4: For each selected case $z \in \{z1, z2, \dots, z17\}$, the results from the previous step will be compared to the constraints (5.82)-(5.86) that the equation (5.87) is presented to indicate the constraints qualification. The value $penalty_z$ will be zero if the results from the previous step are within the constraints limit or the value $penalty_z$ will be more than zero if they are vice versa.

$$
\begin{aligned}
penalty_z = {} & K_{p1} \cdot max\left(0, V_{min}^{\sigma} - V_{i,z}^{\sigma}, V_{i,z}^{\sigma} - V_{max}^{\sigma}\right) + \\
& K_{p2} \cdot max\left(0, \left|I_{i-j,z}^{\sigma}\right| - I_{i-j,max}^{\sigma}\right) + \\
& K_{p3} \cdot max\left(0, \left|S_z^{MV/LV}\right| - S_{max}^{MV/LV}\right) + \\
& K_{p4} \cdot max\left(0, VUF_{i,z} - 3\right) \\
& K_{p5} \cdot max\left(0, P_{loss,z} - Loss_{max\ load,\ no\ PV}\right)
\end{aligned}
\tag{5.87}
$$

where K_{p1}, K_{p2},K_{p3}, K_{p4} and K_{p5} are constant values.

STEP 5: Update objective value (Obj), from the value $penalty_z$ which obtains from the previous step, as shown in equation (5.83) after that go to ***STEP 2***.

$$Obj = Obj - penalty_z \tag{5.83}$$

STEP 6: If all members of z in ***STEP 2*** are selected, the iteration terminates and the objective value (Obj), which depends on the parameter setting, is obtained.

PSO optimization does not fit for finding optimal solution from many free variables. Then, this research divides PSO process into two stages. The flow chart of two-stages PSO can be shown in Figure 5.3 and the flow chart of each stage PSO can be shown in Figure 5.4.

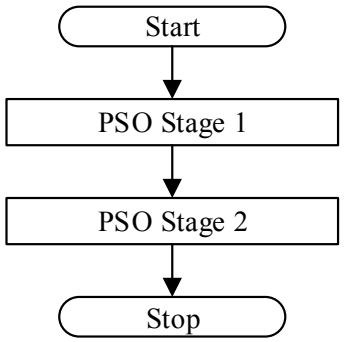

Figure 5.3 The flowchart of 2-stage PSO

1st-STAGE PSO: Define the same parameter adjustment as shown in Tables (5.1) and (5.2) for continuous and piecewise linear local control function. Then, this stage has 6 free variables to find optimal solution.

Table 5.1 The parameters setting of continuous local control function

PV	**Local Control**					
	P(U) Function		**Q(U) Function**			
1st	V_{cri}	δ_p	K_1	K_2	V_q	δ_q
2nd	V_{cri}	δ_p	K_1	K_2	V_q	δ_q
⋮	⋮	⋮	⋮	⋮	⋮	⋮
ith	V_{cri}	δ_p	K_1	K_2	V_q	δ_q
⋮	⋮	⋮	⋮	⋮	⋮	⋮
npv^{th}	V_{cri}	δ_p	K_1	K_2	V_q	δ_q

Table 5.2 The parameters setting of piecewise linear local control function

PV	**Local Control**					
	P(U) Function		**Q(U) Function**			
1st	V_{p1}	V_{p2}	K_1	K_2	V_{q1}	V_{q2}
2nd	V_{p1}	V_{p2}	K_1	K_2	V_{q1}	V_{q2}
⋮	⋮	⋮	⋮	⋮	⋮	⋮
ith	V_{p1}	V_{p2}	K_1	K_2	V_{q1}	V_{q2}
⋮	⋮	⋮	⋮	⋮	⋮	⋮
npv^{th}	V_{p1}	V_{p2}	K_1	K_2	V_{q1}	V_{q2}

2nd-STAGE PSO: This state uses optimal solution from ***1st-STATE PSO*** as initial point. However, the parameter setting of each PV system is not the same or there are $npv \times 6$ free variables if there are npv PV systems. After finishing ***2nd-STAGE PSO***, the optimal parameter setting of each connected PV system will be obtained.

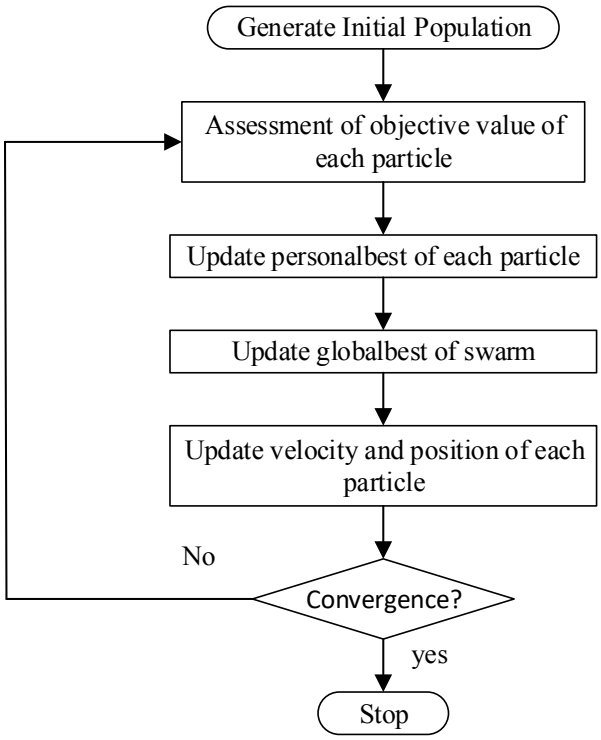

Figure 5.4 The flowchart of each stage PSO

CHAPTER 6

DETAILS OF TEST SYSTEMS

This chapter will address about 2 test systems that are used in this research. The first is a modified 19 node LV distribution system and the second is a modified 29 node LV distribution system. Moreover, load, solar irradiance and ambient temperature data are presented too.

6.1 The Modified 19 Node LV Distribution System

This modified 19 node distribution system [44] as shown in Figure 6.1 is demonstrated in this research and the test system details is composed of:

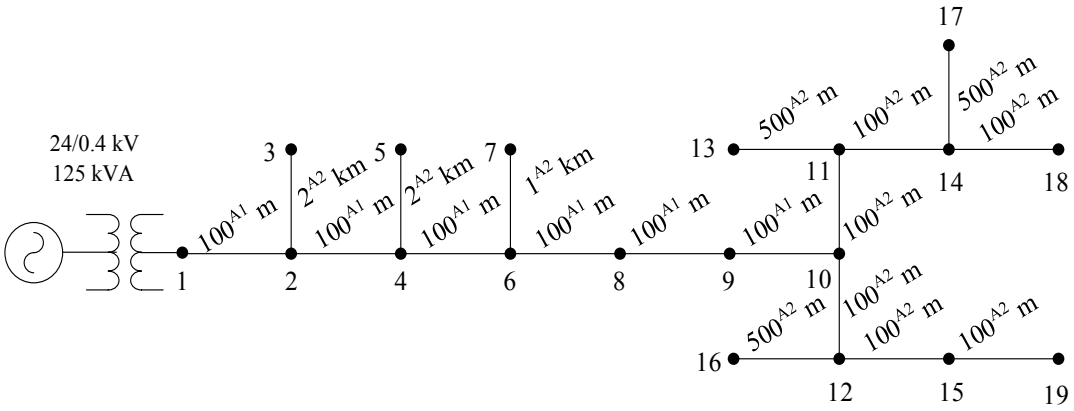

Figure 6.1 The modified 19 node distribution system

- Base voltage is 230 volts, line to neutral.
- Rated transformer is 125 kVA.
- Voltage limit between 0.9-1.1 pu. is complied with the guideline [31].
- Line spacing between phase conductors is 20 cm.
- Utilizing polyethylene insulated weatherproof aluminum conductors and the parameter can be shown in Table 4.5.
- Two types of wiring conductor is applied. Type 1 (represent in Figure 6.1 as “A1”) uses conductor size as 70, 70, 70 and 35 mm^2 for phases A, B, C and neutral respectively. Type 2 (represent in Figure 6.1 as “A2”) uses

conductor size as 35, 35, 35 and 35 mm^2 for phases A, B, C and neutral respectively. The impedance matrix of each type can be shown in Table 6.1.

Table 6.1 The impedance matrix of two type wiring conductors

Type	Impedance (Ω/km)			
	Phase	A	B	C
A1	A	0.5213+j0.5550	0.1721+j0.3204	0.1647+j0.2871
	B	0.1721+j0.3204	0.4970+j0.5887	0.1538+j0.3461
	C	0.1647+j0.2871	0.1538+j0.3461	0.4838+j0.6071
A2	A	0.8439+j0.5765	0.1721+j0.3204	0.1647+j0.2871
	B	0.1721+j0.3204	0.8196+j0.6102	0.1538+j0.3461
	C	0.1647+j0.2871	0.1538+j0.3461	0.8064+j0.6287

- Utilizing polyethylene insulated weatherproof aluminum conductors and the parameter can be shown in Table 4.5.
- Maximum load at each phase of each node can be shown in Table 6.2.

Table 6.2 Maximum load at each phase of each node

Node	Maximum Load					
	Phase A		Phase B		Phase C	
	P (W)	Q (VAr)	P (W)	Q (VAr)	P (W)	Q (VAr)
1	0	0	0	0	0	0
2	2,076	1,002	1,038	504	2,076	1,002
3	2,202	1,068	1,944	942	1,038	504
4	1,296	630	1,134	552	810	390
5	1,296	630	1,038	504	906	438
6	840	408	618	300	582	282
7	1,944	942	1,620	786	1,620	786
8	678	330	1,086	516	1,488	720
9	2,460	1,194	2,982	1,446	2,658	1,284
10	678	330	840	408	516	252
11	1,488	720	1,488	720	2,202	1,068
12	1,944	942	1,620	786	1,620	786
13	876	426	1,068	516	1,296	630
14	618	300	618	300	810	390
15	876	426	972	468	1,392	672
16	1,554	756	2,076	1,002	1,554	756
17	1,296	630	972	468	972	468

Node	Maximum Load					
	Phase A		Phase B		Phase C	
	P (W)	Q (VAr)	P (W)	Q (VAr)	P (W)	Q (VAr)
18	1,068	516	1,068	516	2,202	1,068
19	1,752	846	2,010	972	2,202	1,068

The integration of PV system has only one of PV module as shown in Table 6.3 and the connection points of PV system can be shown in Table 6.4 that the overall capacity is around 127.8 kW or 102.24% of transformer capacity.

Table 6.3 Specifications of Jinko PV modules [45]

Specification at NOCT	Jinko PV Modules
Crystal Structure	Multi-Crystalline Si
P_{MPP} (W)	221
V_{MPP} (V)	33.7
I_{MPP} (A)	6.56
V_{oc} (V)	42.3
I_{oc} (A)	7.16
K_i (A/˚C)	5.3 x 10^{-3}
K_V (V/˚C)	-1.404 x 10^{-1}
N_{OT} (˚C)	45

Table 6.4 The connection point of PV system

PV Name	Node	Type	Phase	Specification of PV Inverter		Number of PV module
				Rated Real Power (W)	Maximum Reactive Power (VAr)	
PV1	5	1-phase	A	4,200	2,100	25
PV2	5	1-phase	B	4,200	2,100	25
PV3	5	1-phase	C	4,200	2,100	25
PV4	6	3-phase	A,B,C	10,000	5,000	58
PV5	7	3-phase	A,B,C	10,000	5,000	58
PV6	8	3-phase	A,B,C	10,000	5,000	58
PV7	10	3-phase	A,B,C	10,000	5,000	58
PV8	11	3-phase	A,B,C	10,000	5,000	58
PV9	12	1-phase	A	4,200	2,100	25

PV Name	Node	Type	Phase	Specification of PV Inverter		Number of PV module
				Rated Real Power (W)	Maximum Reactive Power (VAr)	
PV10	12	1-phase	B	4,200	2,100	25
PV11	12	1-phase	C	4,200	2,100	25
PV12	13	3-phase	A,B,C	10,000	5,000	58
PV13	15	3-phase	A,B,C	10,000	5,000	58
PV14	16	3-phase	A,B,C	10,000	5,000	58
PV15	18	1-phase	A	4,200	2,100	25
PV16	18	1-phase	B	4,200	2,100	25
PV17	18	1-phase	C	4,200	2,100	25
PV18	19	3-phase	A,B,C	10,000	5,000	58

In this modified 19 node distribution system, the voltage profile result can be shown in Figure 6.2 when there is no PV connection and the simulation is tested on maximum load (1 pu.). The result of loss ($Loss_{max\ load,\ no\ PV}$) is 6,547.58 W.

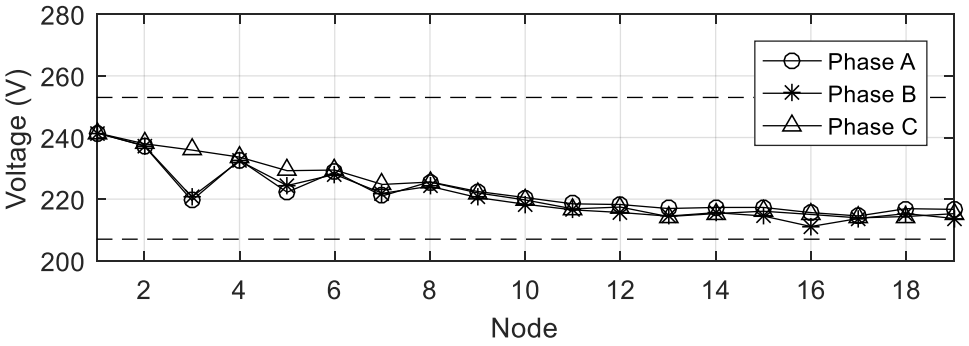

Figure 6.2 The voltage profile result

In this modified 19 node distribution system, the study of the maximum high PV penetration under no local control is addressed in Appendix F.

6.2 The Modified 29 Node LV Distribution System

This modified 29 node distribution system [46] as shown in Figure 6.2 is demonstrated in this research and the test system details is composed of:

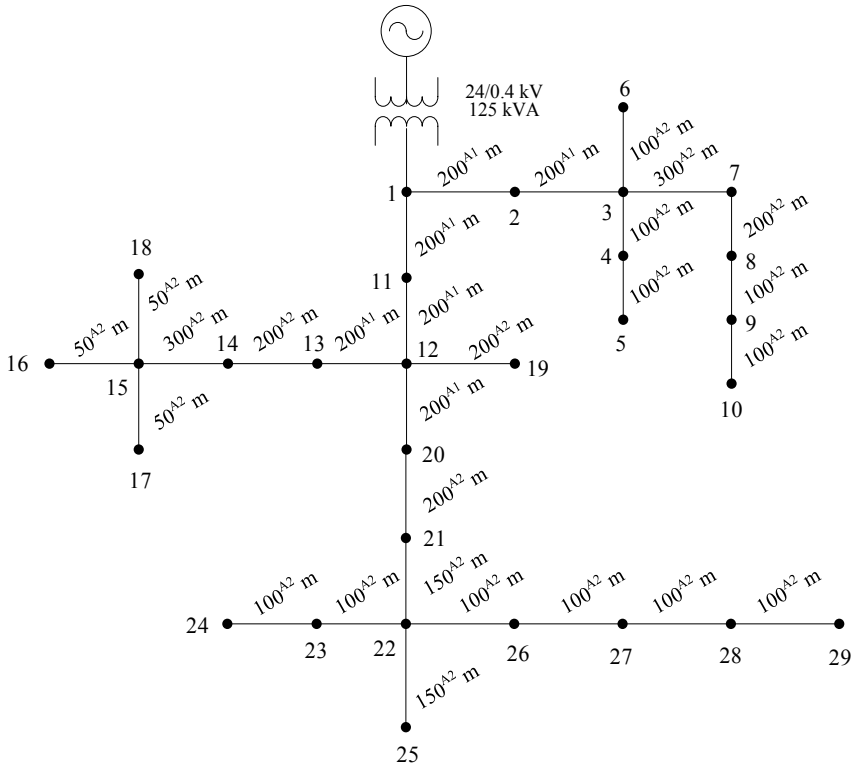

Figure 6.3 The modified 29 node distribution system

- Base voltage is 230 volts, line to neutral.
- Rated transformer is 125 kVA.
- Voltage limit between 0.9-1.1 pu. is complied with the guideline [31].
- Line spacing between phase conductors is 20 cm.
- Utilizing polyethylene insulated weatherproof aluminum conductors and the parameter can be shown in Table 4.5.
- Two types of wiring conductor is applied. Type 1 (represent in Figure 6.1 as "A1") uses conductor size as 70, 70, 70 and 35 mm^2 for phases A, B, C and neutral respectively. Type 2 (represent in Figure 6.1 as "A2") uses conductor size as 35, 35, 35 and 35 mm^2 for phases A, B, C and neutral respectively. The impedance matrix of each type can be shown in Table 6.1.
- Maximum load at each phase of each node can be shown in Table 6.5.

Table 6.5 Maximum load at each phase of each node

Node	Maximum Load (Ω)		
	Phase A	**Phase B**	**Phase C**
1	0	0	0
2	0	0	0
3	0	0	0
4	0	75.36+j24.56	1,371.28+j450.72
5	1,093.44+j359.52	593.2+j194.96	500.24+j164.56
6	0	0	0
7	2,672.96+j878.48	1,657.44+j544.88	2,103.12+j691.44
8	1,359.6+j446.96	1,836.96+j603.6	1,380+j453.6
9	4,350.4+j1,430	4,937.76+j1,622.88	4249.2+j1396.72
10	1,377.12+j452.8	2,343.12+j770.16	3,141.6+j1032.64
11	1880.32+j618.16	873.52+j287.04	0
12	0	0	0
13	783.92+j257.84	1,119.68+j368.24	0
14	613.12+j201.6	1,292.96+j424.88	529.44+j174.08
15	0	0	0
16	1226.32+j403.2	621.6+j204.16	621.6+j204.16
17	1,295.92+j426.16	2,267.68+j745.2	977.6+j321.12
18	621.6+j204.16	986.4+j324.08	899.76+j295.76
19	783.92+j257.84	1,119.68+j368.24	1,466.08+j481.92
20	0	0	0
21	1,570.8+516.08	1,452.08+477.36i	1,680.8+552.32i
22	0	0	0
23	468.64+j154.16	468.64+j154.16	0
24	2,377.68+j781.44	1,139.68+j374.48	0
25	474.48+j155.76	0	2,762+j907.84
26	0	711.44+j233.68	711.44+j233.68
27	1,268.64+j416.88	1,212.16+j398.24	1,429.2+j469.84
28	601.52+j197.84	300.76+j98.92	601.52+j197.84
29	1,185.92+j389.92	1,185.92+j389.92	2,371.84+j779.76

The integration of PV system has only one of PV module as shown in Table 6.3 and the connection points of PV system can be shown in Table 6.6 that the overall capacity is around 125.4 kW or 100.32% of transformer capacity.

Table 6.6 The connection point of PV system

PV Name	Node	Type	Phase	Specification of PV Inverter		Number of PV module
				Rated Real Power (W)	Maximum Reactive Power (VAr)	
PV1	4	3-phase	A,B,C	10,000	5,000	58
PV2	5	1-phase	A	2,000	1,000	12
PV3	5	1-phase	C	2,000	1,000	12
PV4	7	3-phase	A,B,C	7,500	3,750	39
PV5	9	1-phase	A	4,200	2,100	25
PV6	9	1-phase	B	4,200	2,100	25
PV7	9	1-phase	C	4,200	2,100	25
PV8	10	3-phase	A,B,C	10,000	5,000	58
PV9	14	3-phase	A,B,C	7,500	3,750	39
PV10	16	3-phase	A,B,C	10,000	5,000	58
PV11	17	1-phase	A	4,200	2,100	25
PV12	17	1-phase	B	4,200	2,100	25
PV13	17	1-phase	C	4,200	2,100	25
PV14	18	1-phase	C	2,000	1,000	12
PV15	19	1-phase	C	2,000	1,000	12
PV16	21	3-phase	A,B,C	7,500	3,750	39
PV17	23	3-phase	A,B,C	7,500	3,750	39
PV18	24	3-phase	A,B,C	10,000	5,000	58
PV19	25	1-phase	A	2,000	1,000	12
PV20	25	1-phase	C	2,000	1,000	12
PV21	26	1-phase	B	4,200	2,100	25
PV22	27	3-phase	A,B,C	10,000	5,000	58
PV23	28	1-phase	A	2,000	1,000	12
PV24	29	1-phase	C	2,000	1,000	12

In this modified 29 node distribution system, the voltage profile result can be shown in Figure 6.4 when there is no PV connection and the simulation is tested on maximum load (1 pu.). The result of loss ($Loss_{max\ load,\ no\ PV}$) is 7,642.05 W.

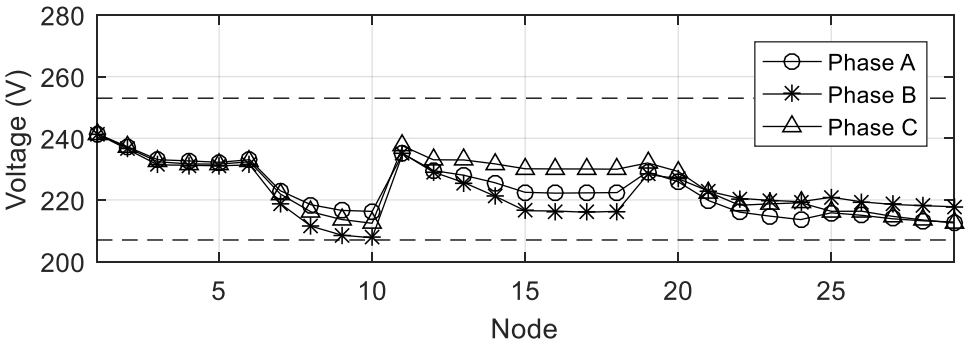

Figure 6.4 The voltage profile result

In this modified 29 node distribution system, the study of the maximum high PV penetration under no local control is addressed in Appendix F.

6.3 Load, Solar Irradiance and Ambient Temperature Data

In this research, the uncertainty analysis unit assumingly uses the collected data at the week 3-9 November 2014 for uncertainty characteristic determination. load, solar irradiance and ambient temperature data every 5 minutes between sun rise period or 6.00-18.00 o'clock along 3-9 November 2014 can be shown in Appendix G or in Figure 6.5 as graph.

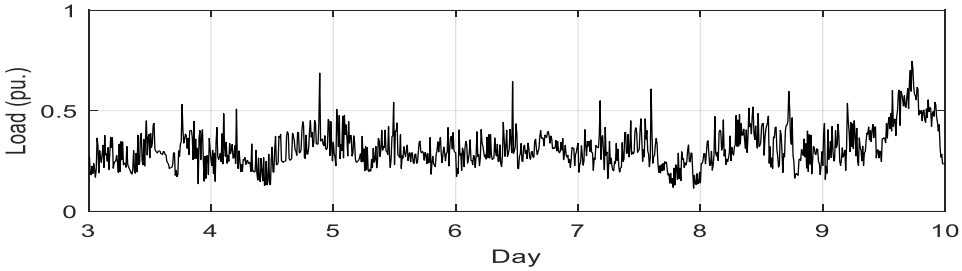

(a) Load phase A

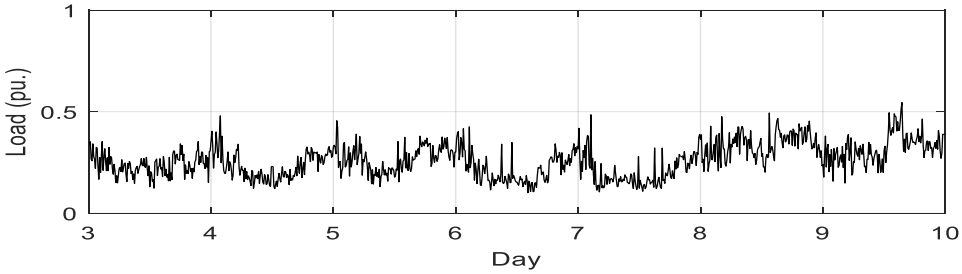

(b) Load phase B

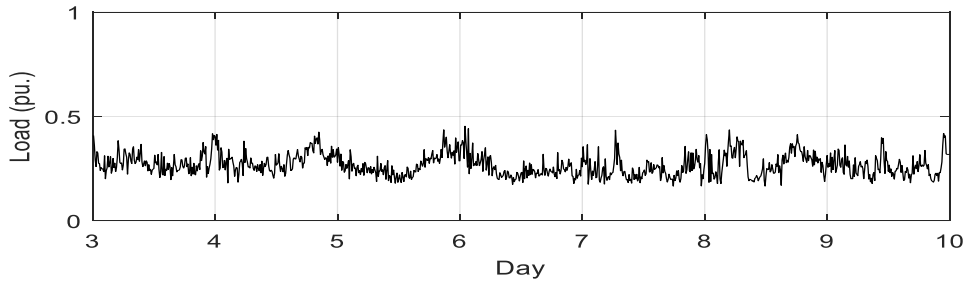

(c) Load phase C

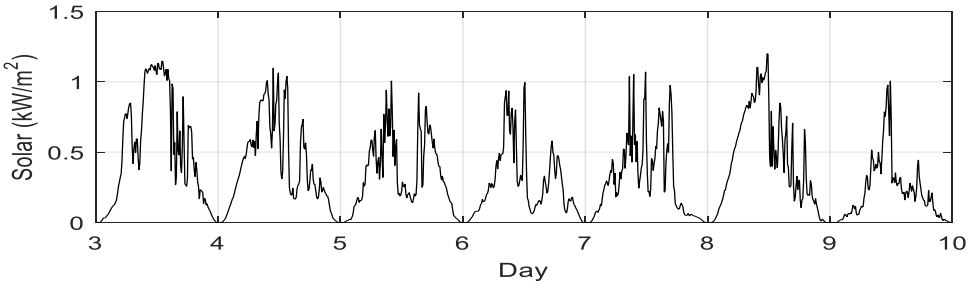

(d) Solar irradiance

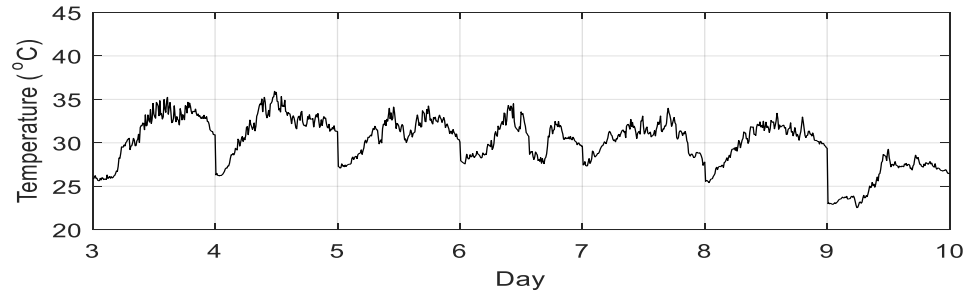

(e) Ambient temperature

Figure 6.5 The collected data in 3-9 November 2014 between 6.00-18.00 o'clock

6.3.1 Uncertainty Determination at the Week 3-9 November 2014

According to the collected data in Figure 6.5 at the week 3-9 November 2014, the normal uncertainty characteristics of load, solar irradiance and ambient temperature are formed as shown in Figure 6.6.

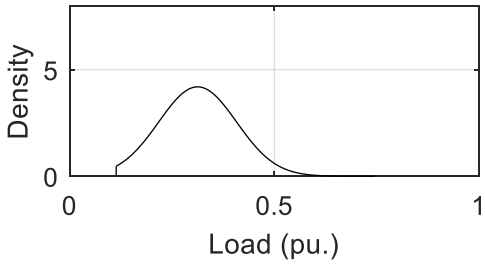

(a) Load phase A

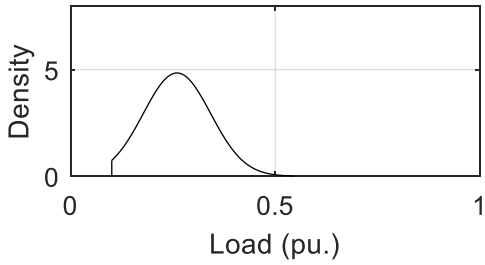

(b) Load phase B

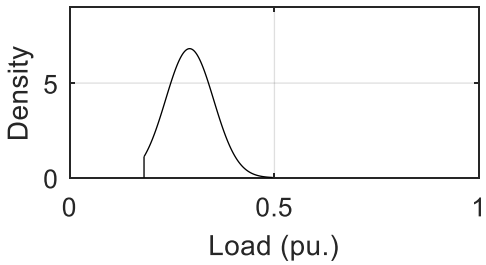

(c) Load phase C

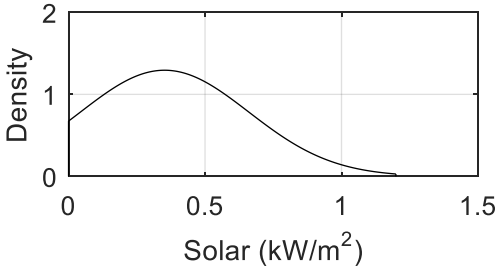

(d) Solar irradiance

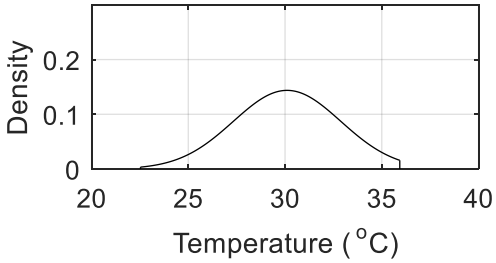

(e) Ambient temperature

Figure 6.6 The normal uncertainty characteristics

According to the uncertainty characteristics in Figure 6.6, the result of the set of uncertainty can be shown in Table 6.7. The minimum solar irradiance will be determined at 0.05 kW/m^2 according to the initial operation of PV inverter [20].

Table 6.7 Set of uncertainty

Case	Load (pu.)			MPP of connected PV system	
	Phase A	**Phase B**	**Phase C**	**Solar (kW/m^2)**	**Temperature (°C)**
z1	0.312398	0.259932	0.2928	0.351894	30.10533
z2	0.745285	0.545107	0.495552	1.19925	22.53
z3	0.745285	0.545107	0.495552	0.05	35.93
z4	0.745285	0.545107	0.181452	1.19925	22.53
z5	0.745285	0.545107	0.181452	0.05	35.93

Case	Load (pu.)			MPP of connected PV system	
	Phase A	Phase B	Phase C	Solar (kW/m^2)	Temperature (^{o}C)
z6	0.745285	0.100666	0.495552	1.19925	22.53
z7	0.745285	0.100666	0.495552	0.05	35.93
z8	0.745285	0.100666	0.181452	1.19925	22.53
z9	0.745285	0.100666	0.181452	0.05	35.93
z10	0.113518	0.545107	0.495552	1.19925	22.53
z11	0.113518	0.545107	0.495552	0.05	35.93
z12	0.113518	0.545107	0.181452	1.19925	22.53
z13	0.113518	0.545107	0.181452	0.05	35.93
z14	0.113518	0.100666	0.495552	1.19925	22.53
z15	0.113518	0.100666	0.495552	0.05	35.93
z16	0.113518	0.100666	0.181452	1.19925	22.53
z17	0.113518	0.100666	0.181452	0.05	35.93

6.3.2 Uncertainty Determination at the Day 3 November 2014

According to the collected data in Figure 6.5 at the day 3 November 2014, the normal uncertainty characteristics of load, solar irradiance and ambient temperature are formed as shown in Figure 6.7.

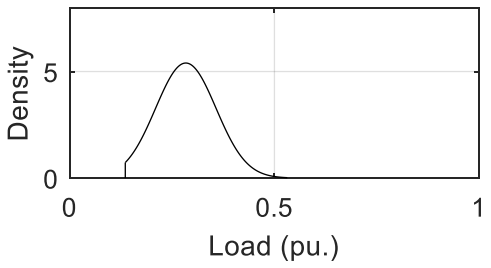

(a) Load phase A

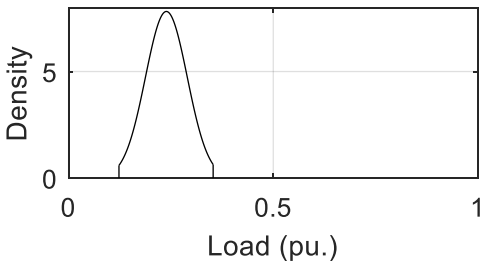

(b) Load phase B

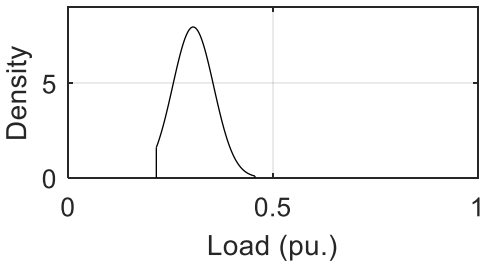

(c) Load phase C

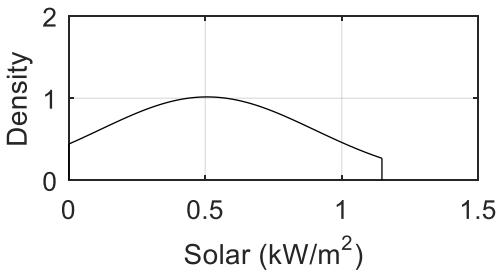

(d) Solar irradiance

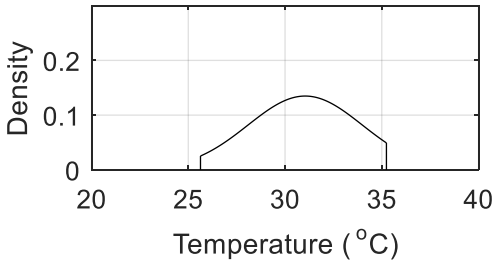

(e) Ambient temperature

Figure 6.7 The normal uncertainty characteristics

According to the uncertainty characteristics in Figure 6.7, the result of the set of uncertainty can be shown in Table 6.8. The minimum solar irradiance will be determined at 0.05 kW/m^2 according to the initial operation of PV inverter [20].

Table 6.8 Set of uncertainty

Case	Load (pu.)			MPP of connected PV system	
	Phase A	Phase B	Phase C	Solar (kW/m^2)	Temperature (^{o}C)
z1	0.283539	0.238877	0.304988	0.506503	31.04063
z2	0.530875	0.353155	0.456019	1.1472	25.63
z3	0.530875	0.353155	0.456019	0.05	35.24
z4	0.530875	0.353155	0.214998	1.1472	25.63
z5	0.530875	0.353155	0.214998	0.05	35.24
z6	0.530875	0.123109	0.456019	1.1472	25.63
z7	0.530875	0.123109	0.456019	0.05	35.24
z8	0.530875	0.123109	0.214998	1.1472	25.63
z9	0.530875	0.123109	0.214998	0.05	35.24
z10	0.135687	0.353155	0.456019	1.1472	25.63
z11	0.135687	0.353155	0.456019	0.05	35.24
z12	0.135687	0.353155	0.214998	1.1472	25.63
z13	0.135687	0.353155	0.214998	0.05	35.24
z14	0.135687	0.123109	0.456019	1.1472	25.63
z15	0.135687	0.123109	0.456019	0.05	35.24
z16	0.135687	0.123109	0.214998	1.1472	25.63
z17	0.135687	0.123109	0.214998	0.05	35.24

6.3.3 Uncertainty Determination at the Day 4 November 2014

According to the collected data in Figure 6.5 at the day 4 November 2014, the normal uncertainty characteristics of load, solar irradiance and ambient temperature are formed as shown in Figure 6.8.

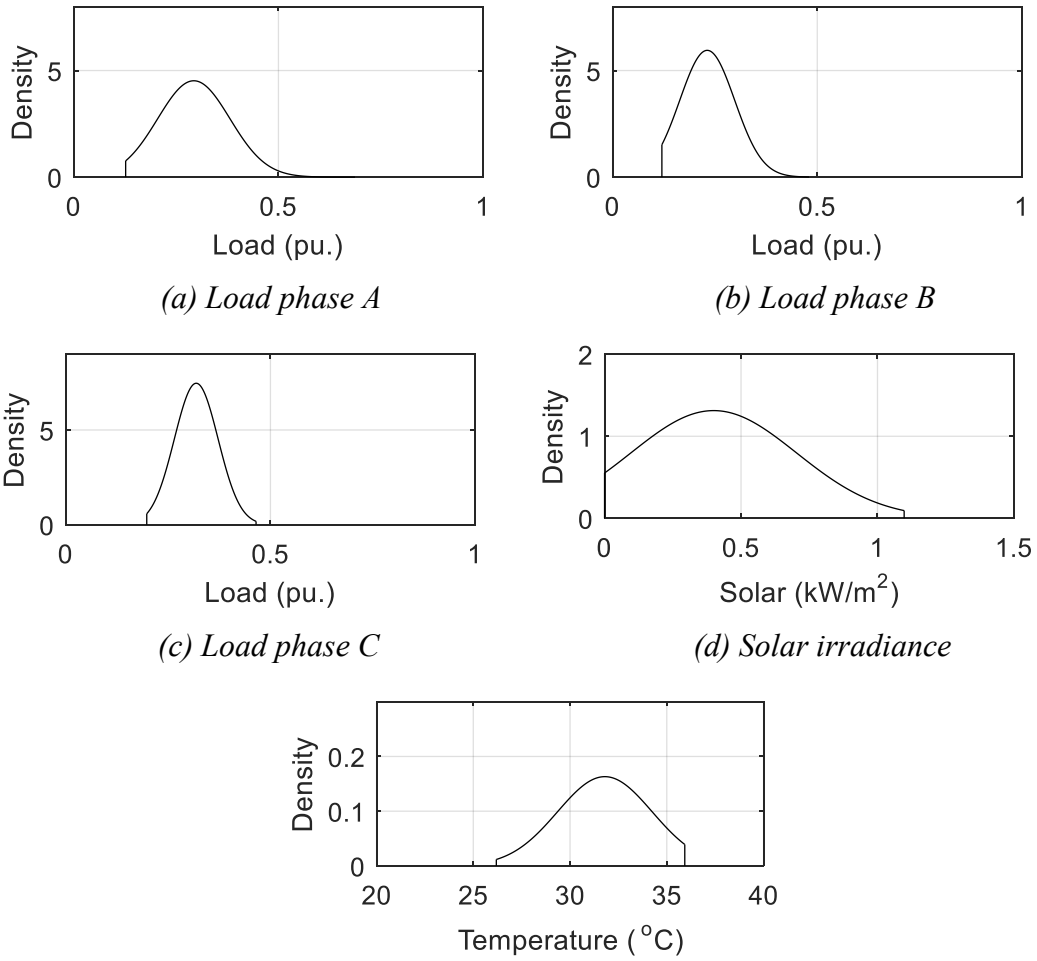

(a) Load phase A

(b) Load phase B

(c) Load phase C

(d) Solar irradiance

(e) Ambient temperature

Figure 6.8 The normal uncertainty characteristics

According to the uncertainty characteristics in Figure 6.8, the result of the set of uncertainty can be shown in Table 6.9. The minimum solar irradiance will be determined at 0.05 kW/m^2 according to the initial operation of PV inverter [20].

Table 6.9 Set of uncertainty

Case	Load (pu.)			MPP of connected PV system	
	Phase A	**Phase B**	**Phase C**	**Solar (kW/m^2)**	**Temperature (^{o}C)**
z1	0.293303	0.231218	0.318742	0.399888	31.79861
z2	0.68703	0.479757	0.464894	1.09764	26.19
z3	0.68703	0.479757	0.464894	0.05	35.93
z4	0.68703	0.479757	0.197892	1.09764	26.19
z5	0.68703	0.479757	0.197892	0.05	35.93
z6	0.68703	0.120469	0.464894	1.09764	26.19
z7	0.68703	0.120469	0.464894	0.05	35.93
z8	0.68703	0.120469	0.197892	1.09764	26.19
z9	0.68703	0.120469	0.197892	0.05	35.93
z10	0.126807	0.479757	0.464894	1.09764	26.19
z11	0.126807	0.479757	0.464894	0.05	35.93
z12	0.126807	0.479757	0.197892	1.09764	26.19
z13	0.126807	0.479757	0.197892	0.05	35.93
z14	0.126807	0.120469	0.464894	1.09764	26.19
z15	0.126807	0.120469	0.464894	0.05	35.93
z16	0.126807	0.120469	0.197892	1.09764	26.19
z17	0.126807	0.120469	0.197892	0.05	35.93

6.3.4 Uncertainty Determination at the Day 5 November 2014

According to the collected data in Figure 6.5 at the day 5 November 2014, the normal uncertainty characteristics of load, solar irradiance and ambient temperature are formed as shown in Figure 6.9.

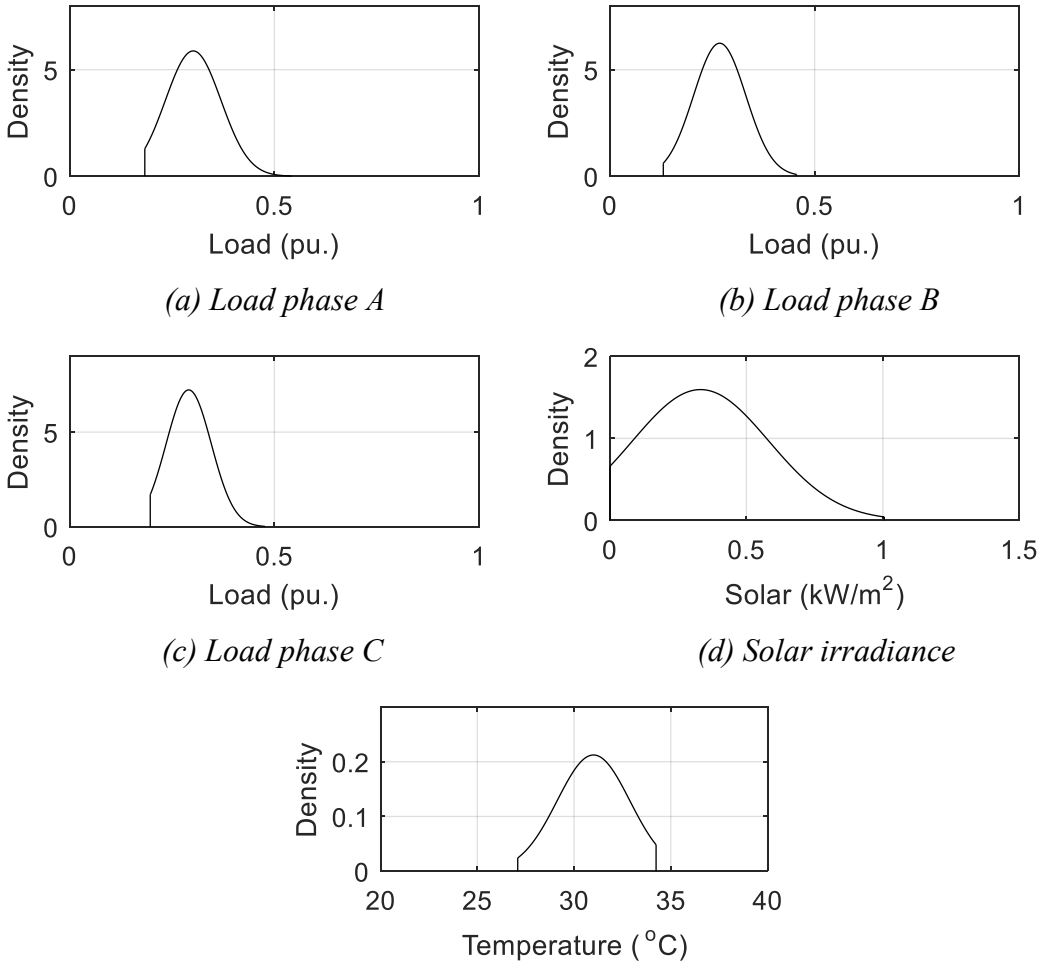

(a) Load phase A *(b) Load phase B*

(c) Load phase C *(d) Solar irradiance*

(e) Ambient temperature

Figure 6.9 The normal uncertainty characteristics

According to the uncertainty characteristics in Figure 6.9, the result of the set of uncertainty can be shown in Table 6.10. The minimum solar irradiance will be determined at 0.05 kW/m^2 according to the initial operation of PV inverter [20].

Table 6.10 Set of uncertainty

Case	Load (pu.)			MPP of connected PV system	
	Phase A	**Phase B**	**Phase C**	**Solar (kW/m^2)**	**Temperature (°C)**
z1	0.301546	0.268058	0.290573	0.331992	31.00528
z2	0.541329	0.455773	0.476513	1.00542	27.09
z3	0.541329	0.455773	0.476513	0.05	34.24
z4	0.541329	0.455773	0.196645	1.00542	27.09

Case	Load (pu.)			MPP of connected PV system	
	Phase A	Phase B	Phase C	Solar (kW/m^2)	Temperature (^{o}C)
z5	0.541329	0.455773	0.196645	0.05	34.24
z6	0.541329	0.13026	0.476513	1.00542	27.09
z7	0.541329	0.13026	0.476513	0.05	34.24
z8	0.541329	0.13026	0.196645	1.00542	27.09
z9	0.541329	0.13026	0.196645	0.05	34.24
z10	0.183361	0.455773	0.476513	1.00542	27.09
z11	0.183361	0.455773	0.476513	0.05	34.24
z12	0.183361	0.455773	0.196645	1.00542	27.09
z13	0.183361	0.455773	0.196645	0.05	34.24
z14	0.183361	0.13026	0.476513	1.00542	27.09
z15	0.183361	0.13026	0.476513	0.05	34.24
z16	0.183361	0.13026	0.196645	1.00542	27.09
z17	0.183361	0.13026	0.196645	0.05	34.24

6.3.5 Uncertainty Determination at the Day 6 November 2014

According to the collected data in Figure 6.5 at the day 6 November 2014, the normal uncertainty characteristics of load, solar irradiance and ambient temperature are formed as shown in Figure 6.10.

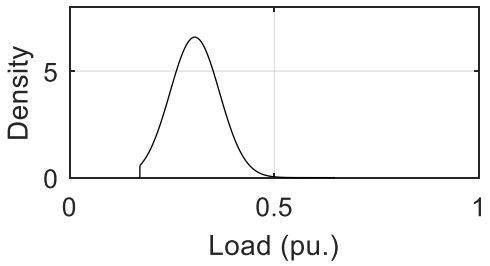

(a) Load phase A

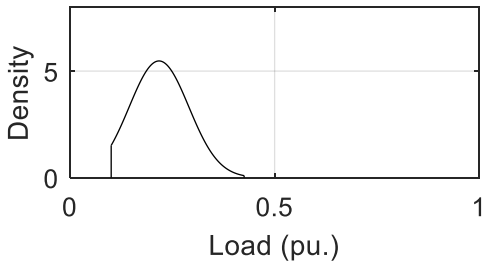

(b) Load phase B

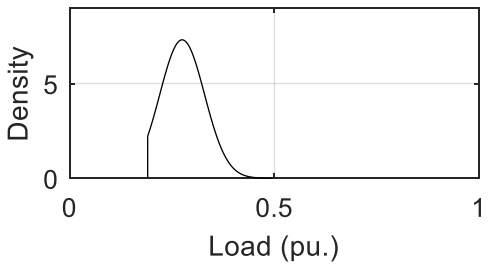

(c) Load phase C

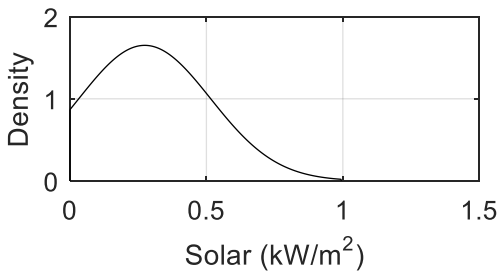

(d) Solar irradiance

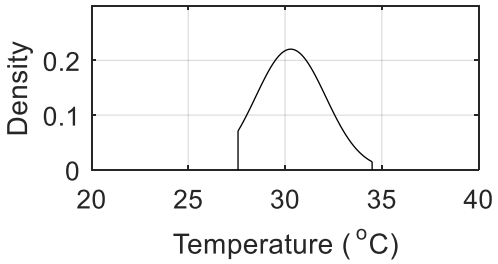

(e) Ambient temperature

Figure 6.10 The normal uncertainty characteristics

According to the uncertainty characteristics in Figure 6.10, the result of the set of uncertainty can be shown in Table 6.11. The minimum solar irradiance will be determined at 0.05 kW/m^2 according to the initial operation of PV inverter [20].

Table 6.11 Set of uncertainty

Case	Load (pu.)			MPP of connected PV system	
	Phase A	**Phase B**	**Phase C**	**Solar (kW/m^2)**	**Temperature (ºC)**
z1	0.30537	0.217527	0.27459	0.273906	30.29354
z2	0.645936	0.425518	0.495552	0.99412	27.57
z3	0.645936	0.425518	0.495552	0.05	34.5
z4	0.645936	0.425518	0.190348	0.99412	27.57
z5	0.645936	0.425518	0.190348	0.05	34.5
z6	0.645936	0.100666	0.495552	0.99412	27.57
z7	0.645936	0.100666	0.495552	0.05	34.5
z8	0.645936	0.100666	0.190348	0.99412	27.57
z9	0.645936	0.100666	0.190348	0.05	34.5
z10	0.171332	0.425518	0.495552	0.99412	27.57
z11	0.171332	0.425518	0.495552	0.05	34.5
z12	0.171332	0.425518	0.190348	0.99412	27.57
z13	0.171332	0.425518	0.190348	0.05	34.5
z14	0.171332	0.100666	0.495552	0.99412	27.57
z15	0.171332	0.100666	0.495552	0.05	34.5
z16	0.171332	0.100666	0.190348	0.99412	27.57
z17	0.171332	0.100666	0.190348	0.05	34.5

6.3.6 Uncertainty Determination at the Day 7 November 2014

According to the collected data in Figure 6.5 at the day 7 November 2014, the normal uncertainty characteristics of load, solar irradiance and ambient temperature are formed as shown in Figure 6.11.

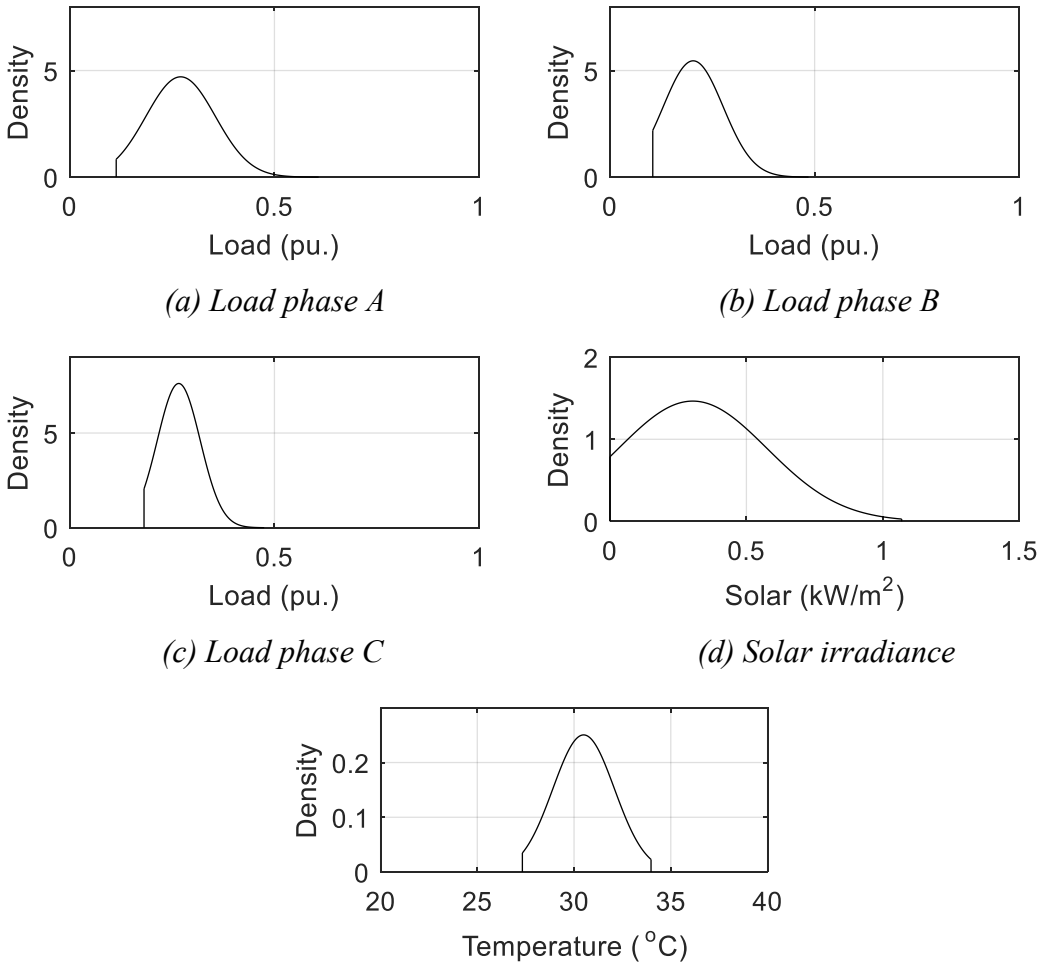

(a) Load phase A

(b) Load phase B

(c) Load phase C

(d) Solar irradiance

(e) Ambient temperature

Figure 6.11 The normal uncertainty characteristics

According to the uncertainty characteristics in Figure 6.11, the result of the set of uncertainty can be shown in Table 6.12. The minimum solar irradiance will be determined at 0.05 kW/m^2 according to the initial operation of PV inverter [20].

Table 6.12 Set of uncertainty

Case	Load (pu.)			MPP of connected PV system	
	Phase A	**Phase B**	**Phase C**	**Solar (kW/m^2)**	**Temperature (^{o}C)**
z1	0.270889	0.203254	0.266264	0.303343	30.49576
z2	0.607929	0.485038	0.47485	1.06902	27.33
z3	0.607929	0.485038	0.47485	0.05	33.98
z4	0.607929	0.485038	0.181452	1.06902	27.33
z5	0.607929	0.485038	0.181452	0.05	33.98
z6	0.607929	0.104544	0.47485	1.06902	27.33
z7	0.607929	0.104544	0.47485	0.05	33.98
z8	0.607929	0.104544	0.181452	1.06902	27.33
z9	0.607929	0.104544	0.181452	0.05	33.98
z10	0.113518	0.485038	0.47485	1.06902	27.33
z11	0.113518	0.485038	0.47485	0.05	33.98
z12	0.113518	0.485038	0.181452	1.06902	27.33
z13	0.113518	0.485038	0.181452	0.05	33.98
z14	0.113518	0.104544	0.47485	1.06902	27.33
z15	0.113518	0.104544	0.47485	0.05	33.98
z16	0.113518	0.104544	0.181452	1.06902	27.33
z17	0.113518	0.104544	0.181452	0.05	33.98

6.3.7 Uncertainty Determination at the Day 8 November 2014

According to the collected data in Figure 6.5 at the day 8 November 2014, the normal uncertainty characteristics of load, solar irradiance and ambient temperature are formed as shown in Figure 6.12.

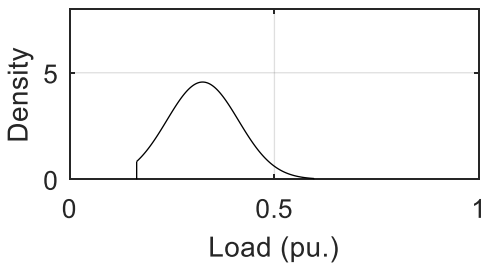

(a) Load phase A

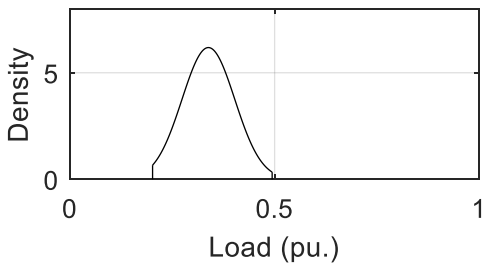

(b) Load phase B

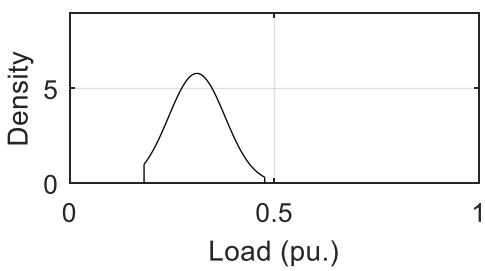

(c) Load phase C

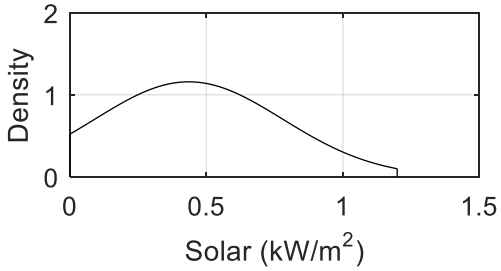

(d) Solar irradiance

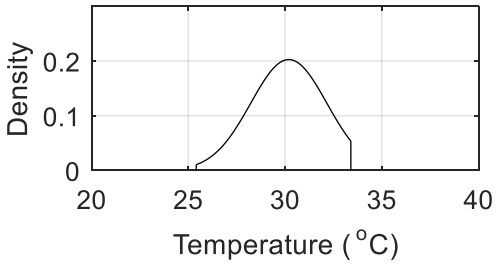

(e) Ambient temperature

Figure 6.12 The normal uncertainty characteristics

According to the uncertainty characteristics in Figure 6.12, the result of the set of uncertainty can be shown in Table 6.13. The minimum solar irradiance will be determined at 0.05 kW/m^2 according to the initial operation of PV inverter [20].

Table 6.13 Set of uncertainty

Case	Load (pu.)			MPP of connected PV system	
	Phase A	**Phase B**	**Phase C**	**Solar (kW/m^2)**	**Temperature (°C)**
z1	0.324574	0.338176	0.310495	0.435371	30.19375
z2	0.596435	0.493949	0.476201	1.19925	25.41
z3	0.596435	0.493949	0.476201	0.05	33.4
z4	0.596435	0.493949	0.181556	1.19925	25.41
z5	0.596435	0.493949	0.181556	0.05	33.4
z6	0.596435	0.201799	0.476201	1.19925	25.41
z7	0.596435	0.201799	0.476201	0.05	33.4
z8	0.596435	0.201799	0.181556	1.19925	25.41
z9	0.596435	0.201799	0.181556	0.05	33.4
z10	0.163492	0.493949	0.476201	1.19925	25.41
z11	0.163492	0.493949	0.476201	0.05	33.4

Case	Load (pu.)			MPP of connected PV system	
	Phase A	Phase B	Phase C	Solar (kW/m^2)	Temperature (^{o}C)
z12	0.163492	0.493949	0.181556	1.19925	25.41
z13	0.163492	0.493949	0.181556	0.05	33.4
z14	0.163492	0.201799	0.476201	1.19925	25.41
z15	0.163492	0.201799	0.476201	0.05	33.4
z16	0.163492	0.201799	0.181556	1.19925	25.41
z17	0.163492	0.201799	0.181556	0.05	33.4

6.3.8 Uncertainty Determination at the Day 9 November 2014

According to the collected data in Figure 6.5 at the day 9 November 2014, the normal uncertainty characteristics of load, solar irradiance and ambient temperature are formed as shown in Figure 6.13.

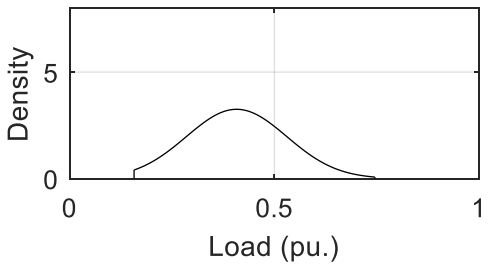

(a) Load phase A

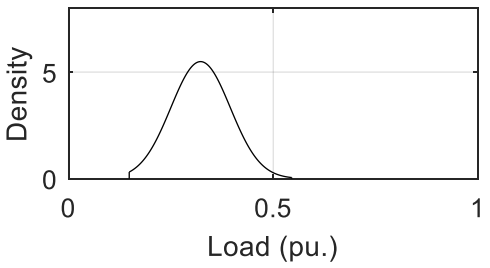

(b) Load phase B

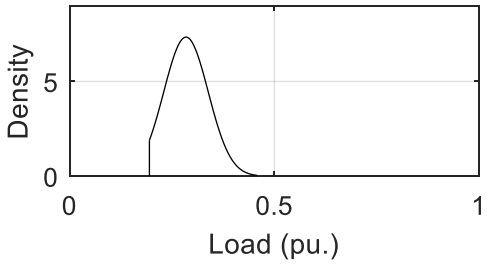

(c) Load phase C

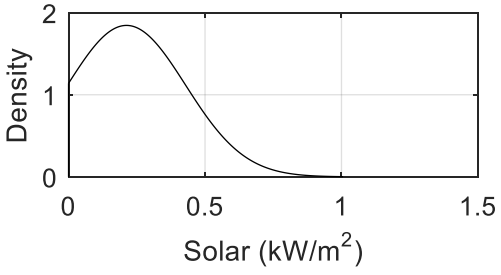

(d) Solar irradiance

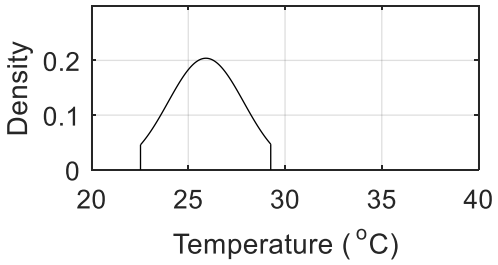

(e) Ambient temperature

Figure 6.13 The normal uncertainty characteristics

According to the uncertainty characteristics in Figure 6.13, the result of the set of uncertainty can be shown in Table 6.14. The minimum solar irradiance will be determined at 0.05 kW/m^2 according to the initial operation of PV inverter [20].

Table 6.14 Set of uncertainty

Case	Load (pu.)			MPP of connected PV system	
	Phase A	**Phase B**	**Phase C**	**Solar (kW/m^2)**	**Temperature (^{o}C)**
z1	0.407567	0.322418	0.283948	0.212253	25.90972
z2	0.745285	0.545107	0.457807	1.00545	22.53
z3	0.745285	0.545107	0.457807	0.05	29.26
z4	0.745285	0.545107	0.194608	1.00545	22.53
z5	0.745285	0.545107	0.194608	0.05	29.26
z6	0.745285	0.148165	0.457807	1.00545	22.53
z7	0.745285	0.148165	0.457807	0.05	29.26
z8	0.745285	0.148165	0.194608	1.00545	22.53
z9	0.745285	0.148165	0.194608	0.05	29.26
z10	0.157131	0.545107	0.457807	1.00545	22.53
z11	0.157131	0.545107	0.457807	0.05	29.26
z12	0.157131	0.545107	0.194608	1.00545	22.53
z13	0.157131	0.545107	0.194608	0.05	29.26
z14	0.157131	0.148165	0.457807	1.00545	22.53
z15	0.157131	0.148165	0.457807	0.05	29.26
z16	0.157131	0.148165	0.194608	1.00545	22.53
z17	0.157131	0.148165	0.194608	0.05	29.26

CHAPTER 7

SIMULATION RESULTS AND DISCUSSION

In this chapter, 2 different LV distribution systems will be demonstrated, i.e. modified 19 and 29 node LV distribution systems. The uncertainty characteristic prediction is assumed to come from at the week 3-9 November 2014. To show the effectiveness of the coordination between central and local control, the simulation results are divided into seven subsections: (7.1) P(U) and Q(U) local control application; (7.2) The same and different parameters setting of local control; (7.3) The continuous and piecewise linear local control application; (7.4) local control adjustment in every one week or one day of continuous local control function; (7.5) local control adjustment in every one week or one day of piecewise linear local control function; (7.6) local control adjustment in the modified 29 node LV distribution system; Monte Carlo simulations.

7.1 P(U) and Q(U) Local Control Application

In this subsection, the comparison between (7.1.1) no local control, (7.1.2) the only P(U) application and (7.1.3) both P(U) and Q(U) application to show the effectiveness of both P(U) and Q(U) application in real power generation enhancement in to LV distribution system. The continuous local control function is selected in this subsection.

7.1.1 No Local Control

In the past, there are many researches, such as [4], that the operation of PV system is considered as unity power factor. According to the set of uncertainty at the week 3-9 November 2014 in Table 6.7, the power flow results can be shown in Figure 7.1 when PV system operates on unity power factor. It can notice that overvoltage and over loss (at 6,547.58 W) is occurred in LV distribution system with high PV penetration.

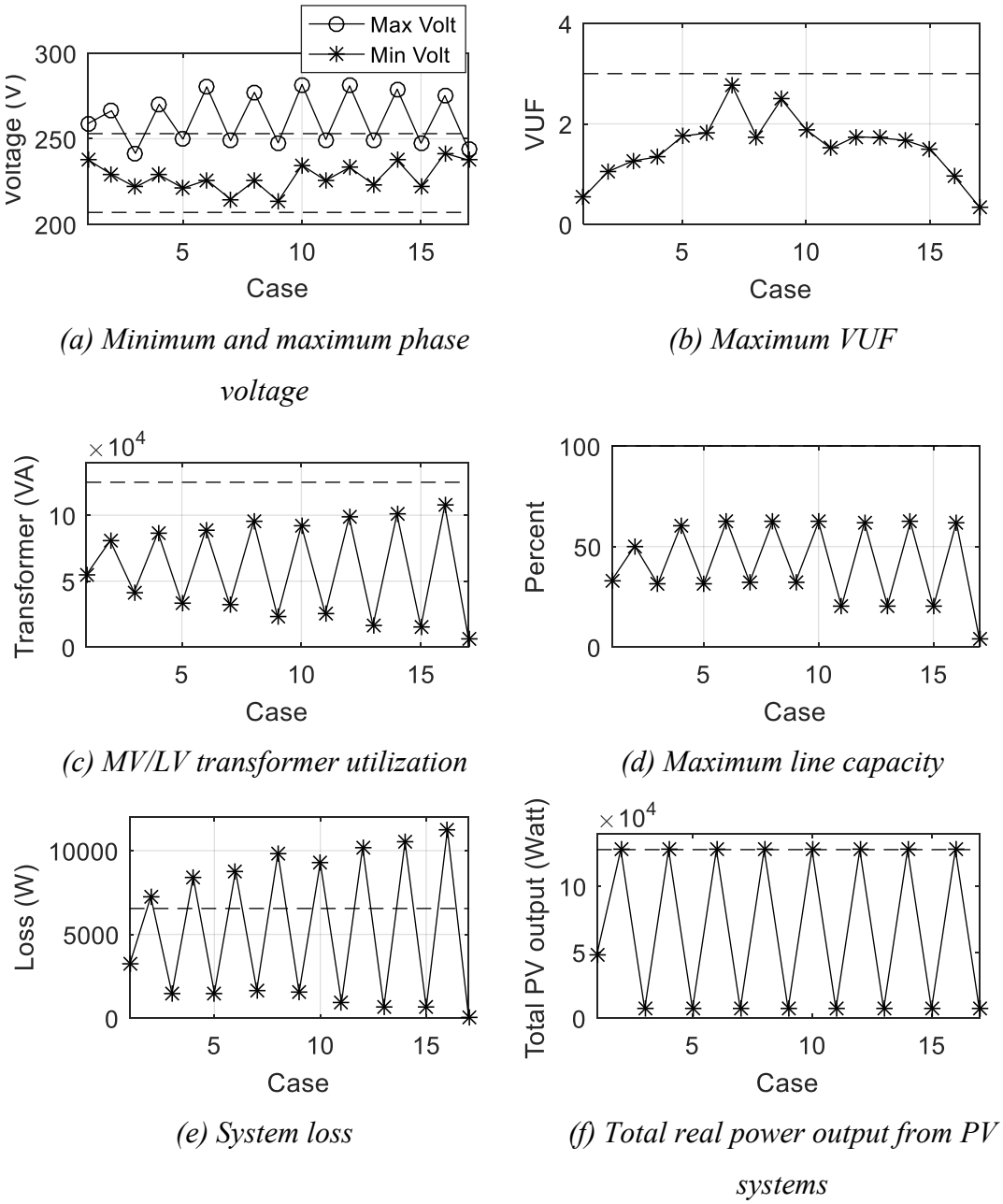

(a) Minimum and maximum phase voltage

(b) Maximum VUF

(c) MV/LV transformer utilization

(d) Maximum line capacity

(e) System loss

(f) Total real power output from PV systems

Figure 7.1 The results of the set of uncertainty

where the minimum voltage is determined from any phase and node according to system voltage result that has the lowest value. The maximum voltage is vice versa. Maximum VUF is determined from any node according to system VUF result that has the highest value. Maximum line capacity is determined from any line of each phase that has the maximum value of $\frac{Line\ Current}{Line\ Capacity} \times 100\%$.

7.1.2 The only P(U) Application

The research [12] considers only local control P(U) function of PV system. The result is that PV system can generate less real power into LV distribution system because only real power output will be limited when voltage at the connection of PV system is increased. According to the set of uncertainty at the week 3-9 November 2014 in Table 6.7, the result of the parameters setting of P(U) function can be shown in Table 7.1. The optimal objective value in equation (5.81) is 33,197.32 W. Considering only the case $z \in \{z1, z2, \dots, z17\}$, the results of minimum and maximum voltage profile, maximum VUF, MV/LV transformer utilization, maximum line capacity and total real power output from PV systems can be shown in Figure 7.2.

Table 7.1 Parameter setting of each connected PV system

PV Name	Parameter Setting					
	V_{cri}	δ_p	K_1	K_2	V_q	δ_q
PV1	1.098	0.011	-	-	-	-
PV2	1.098	0.01	-	-	-	-
PV3	1.099	0.01	-	-	-	-
PV4	1.086	0.01	-	-	-	-
PV5	1.07	0.01	-	-	-	-
PV6	1.133	0.01	-	-	-	-
PV7	1.101	0.01	-	-	-	-
PV8	1.121	0.01	-	-	-	-
PV9	1.087	0.01	-	-	-	-
PV10	1.086	0.01	-	-	-	-
PV11	1.098	0.014	-	-	-	-
PV12	1.056	0.01	-	-	-	-
PV13	1.08	0.01	-	-	-	-
PV14	1.064	0.01	-	-	-	-
PV15	1.089	0.01	-	-	-	-
PV16	1.088	0.01	-	-	-	-
PV17	1.097	0.01	-	-	-	-
PV18	1.059	0.01	-	-	-	-

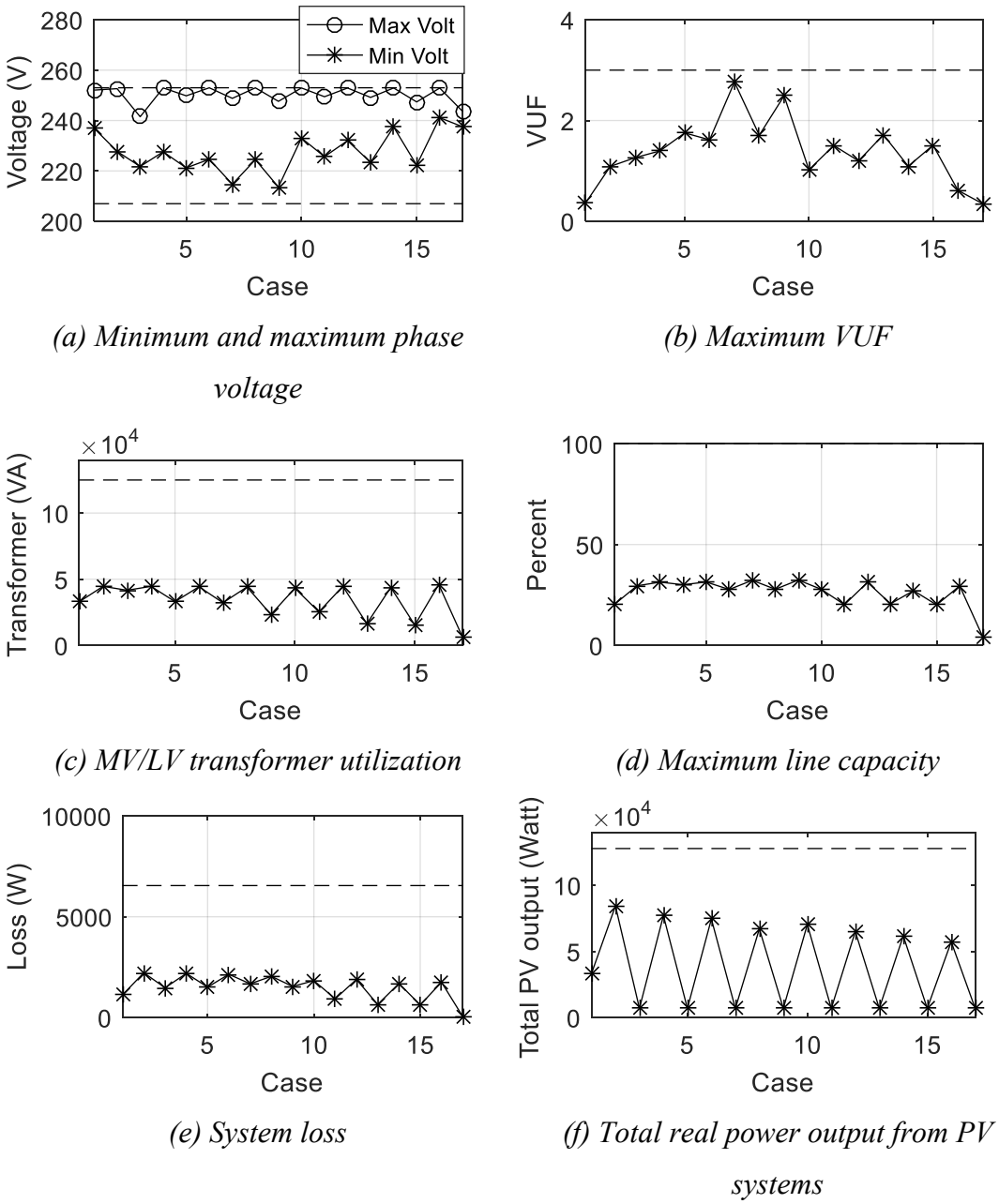

(a) Minimum and maximum phase voltage

(b) Maximum VUF

(c) MV/LV transformer utilization

(d) Maximum line capacity

(e) System loss

(f) Total real power output from PV systems

Figure 7.2 The results of the set of uncertainty

The results according to Figure 7.2 are within the limit. The total real power output from PV systems at maximum value is 84,581.02 W at the case $z2$. It is because the case $z2$ has maximum phase A, B and C loads and, therefore, each connected PV system can generates a lot real power output to LV distribution system before each connected PV system is limited real power output by P(U) function.

7.1.3 Both P(U) and Q(U) Application

In this subsection, the connected PV system will operate on local control on real power adjustment local control as stated in equations (4.3) or (4.4) and reactive power adjustment as stated in equations (4.6) or (4.7). The parameter assessment will be analyzed by central control through 2-stage PSO process. According to the set of uncertainty at the week 3-9 November 2014 in Table 6.7, the optimal objective value in equation (5.81) is 42,643.37 W and the results of optimal parameter setting can be shown in Table 7.2. Considering only the case $z \in \{z1, z2, \ldots, z17\}$, the results of minimum and maximum voltage profile, maximum VUF, MV/LV transformer utilization, maximum line capacity and total real power output from PV systems can be shown in Figure 7.3.

Table 7.2 Parameter setting of each connected PV system

PV Name	Parameter Setting					
	V_{cri}	δ_p	K_1	K_2	V_q	δ_q
PV1	1.094	0.023	0.348	0.605	1	0.017
PV2	1.098	0.011	0.304	0.881	1.001	0.017
PV3	1.102	0.02	0.442	0.951	1.009	0.087
PV4	1.081	0.01	0.225	0.409	1.006	0.07
PV5	1.072	0.013	0.323	1.086	1.018	0.072
PV6	1.126	0.014	0.469	0.925	1.011	0.068
PV7	1.137	0.028	0.597	1.145	1.007	0.048
PV8	1.101	0.021	0.303	0.935	1.009	0.073
PV9	1.082	0.013	0.235	1.161	1.015	0.08
PV10	1.08	0.01	0.85	0.963	1.005	0.077
PV11	1.104	0.016	0.302	0.93	1.015	0.08
PV12	1.071	0.031	0.228	1.028	1.006	0.06
PV13	1.123	0.01	0.417	1.089	1.011	0.063
PV14	1.067	0.022	0.256	0.827	1.007	0.072
PV15	1.076	0.015	0.24	1.018	1.009	0.075
PV16	1.088	0.01	0.315	0.901	1.009	0.083
PV17	1.079	0.014	0.754	1	1.006	0.081
PV18	1.071	0.035	0.426	0.959	1.012	0.078

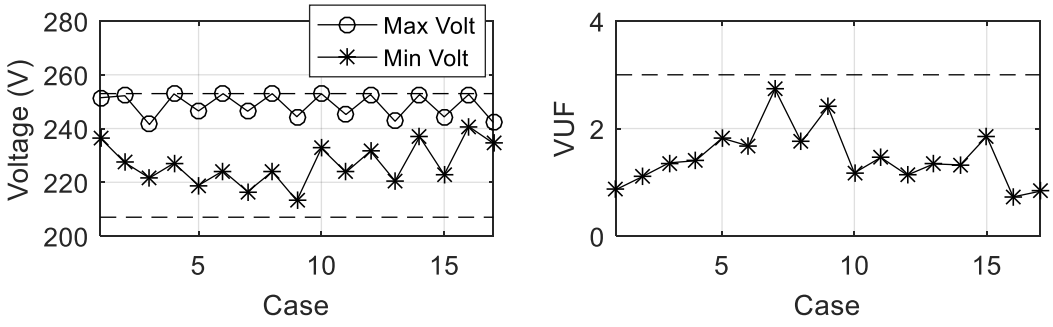

(a) Minimum and maximum phase voltage

(b) Maximum VUF

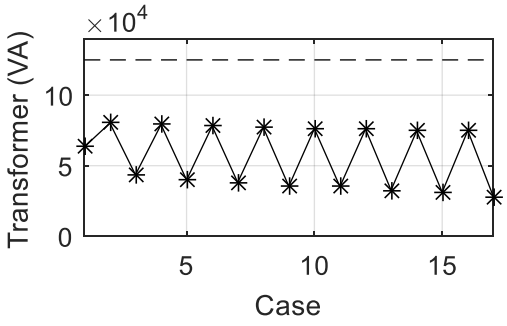

(c) MV/LV transformer utilization

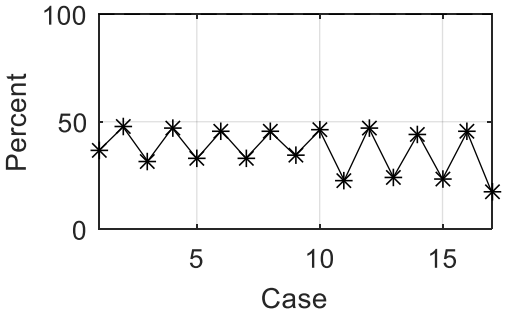

(d) Maximum line capacity

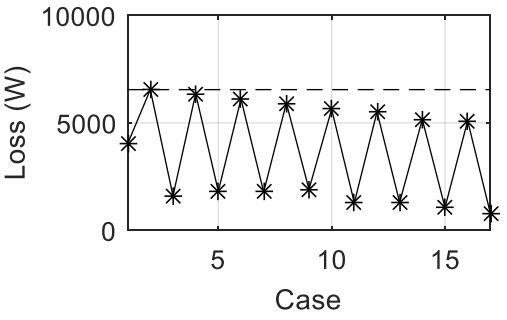

(e) System loss

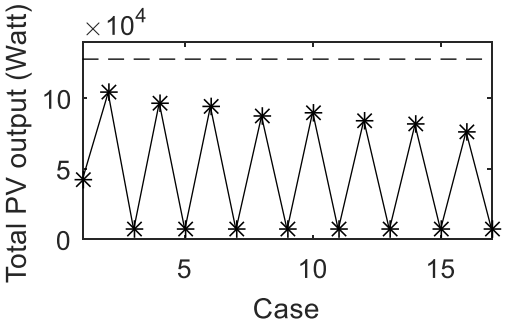

(f) Total real power output from PV systems

Figure 7.3 The results of the set of uncertainty

The results according to Figure 7.1 are within the limit. The total real power output from PV systems at maximum value is 103,937.38 W at the case $z2$. It is because the case $z2$ has maximum phase A, B and C loads and, therefore, each connected PV system can generates a lot real power output to LV distribution system before each connected PV system is limited real power output by P(U) function. Comparing between Subsection 7.1.2 and 7.1.3, the percent different of objective value and

maximum total real power output can be shown in Table 7.3 and it can notice that both P((U) and Q(U) application in Subsection 7.1.3 can apparently generate more real power output into LV distribution system. It is because Q(U) function helps voltage rise support when many PV systems generate real power output into LV distribution system. However, P(U) function also operates to limit real power output for voltage rise support if the operation of Q(U) function is unable to support voltage rise adequately.

Table 7.3 The comparison between only P(U) function and both P(U) and Q(U) functions application

	Only P(U) Function	**Both P(U) and Q(U) Functions**	**Percent Change of Both P(U) and Q(U) Functions**
Objective Value	33,197.32	42,643.37	+28.45%
Maximum total real power output	84,373.67	103,937.38	+23.19%

The comparison of P(U) and Q(U) function of each PV connection from Table 7.2 can be shown as follows.

- Figure 7.4 shows the comparison of PV1-PV3 where PV1 is at phase-A node 5; PV2 is at phase-B node 5; PV3 is at phase-C node 5.
- Figure 7.5 shows the comparison of PV4-PV6 where PV4 is at 3-phase node 6; PV2 is at 3-phase node 7; PV3 is at 3-phase node 8.
- Figure 7.6 shows the comparison of PV7, PV8 and PV12 where PV7 is at 3-phase node 10; PV8 is at 3-phase node 11; PV12 is at 3-phase node 13.
- Figure 7.7 shows the comparison of PV9-PV11 where PV9 is at phase-A node 12; PV10 is at phase-B node 12; PV3 is at phase-C node 12.
- Figure 7.8 shows the comparison of PV13, PV14 and PV18 where PV13 is at 3-phase node 15; PV14 is at 3-phase node 16; PV18 is at 3-phase node 19.
- Figure 7.9 shows the comparison of PV15-PV17 where PV15 is at phase-A node 18; PV16 is at phase-B node 18; PV17 is at phase-C node 18.

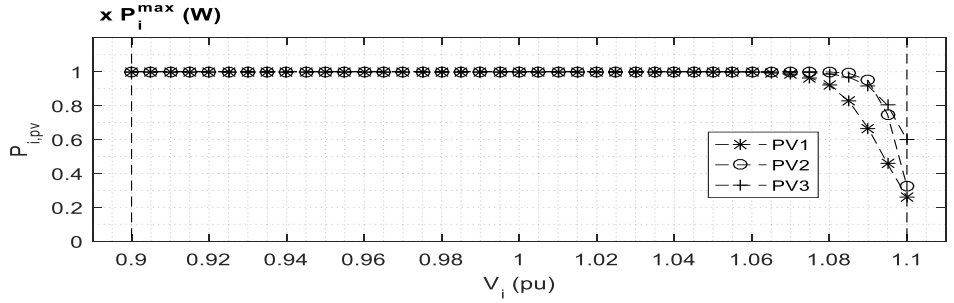

(a) P(U) function

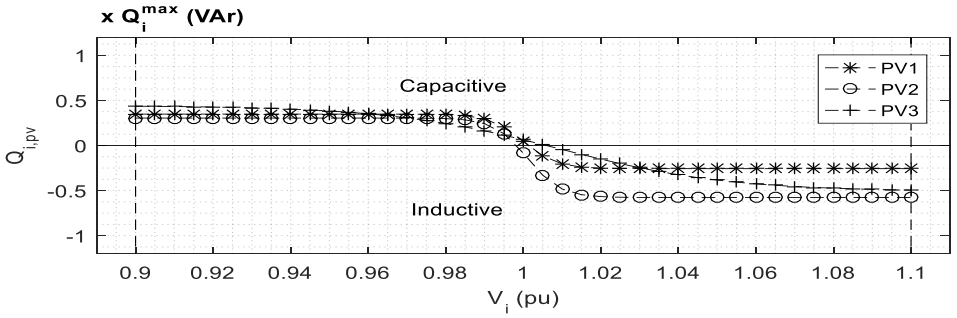

(b) Q(U) function

Figure 7.4 The comparison of PV1-PV3

From Figure 7.4, phase A, B and C loads at the upstream node 5 are not different so much. Then, characteristics of local control are nearly similar.

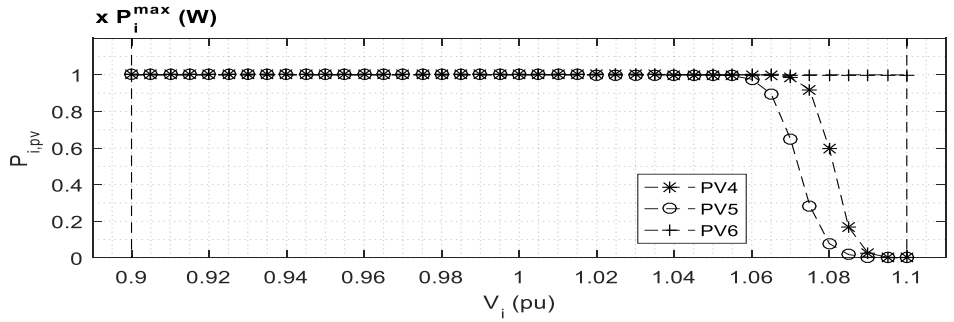

(a) P(U) function

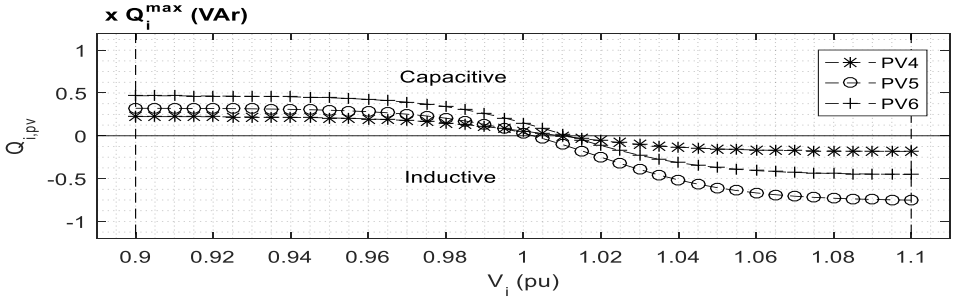

(b) Q(U) function

Figure 7.5 The comparison of PV4-PV6

From Figure 7.5, PV6 has no limitation from P(U) function because this connection point has more load than node 6 at the connection point of PV4 although PV4 and PV6 are close together according to the data in Table 6.2. PV5 is far from transformer around 1.3 km that PV5 connection at node 7 is farther than PV4 (300 m. long) and PV6 (400 m. long) connections. Then, P(U) function of PV5 is more limited than PV4 and PV6. Accordingly, PV5 is set Q(U) function to absorb more reactive power than the others to be capable of more real power injection.

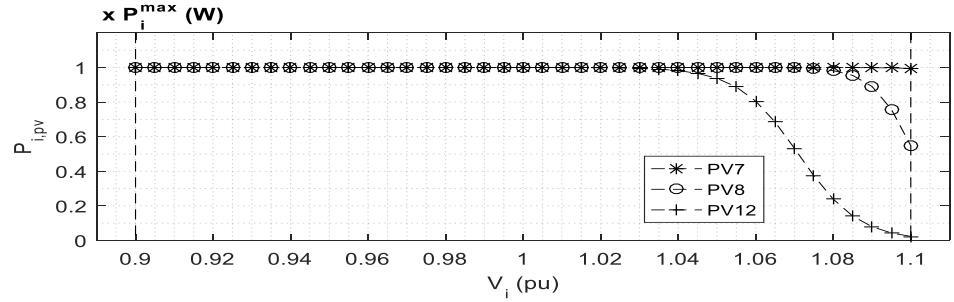

(a) P(U) function

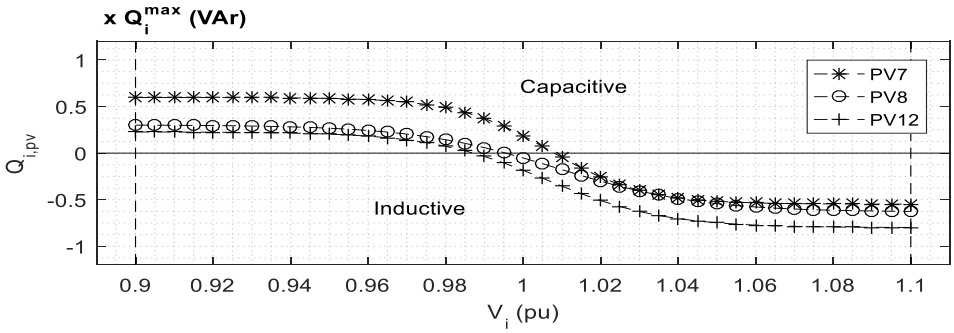

(b) Q(U) function

Figure 7.6 The comparison of PV7, PV8 and PV12

From Figure 7.6, PV7 is near distribution transformer (600 m. long) than the others. Then, $P(U)_{PV7}$ function is set to inject real power more than $P(U)_{PV8}$ function (700 m. long) and $P(U)_{PV12}$ (1.2 km. long). For Q(U) function, the characteristics of PV7, PV8 and PV12 are close.

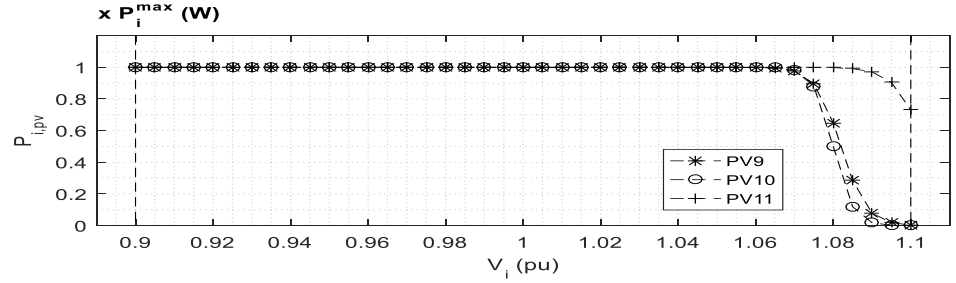

(a) P(U) function

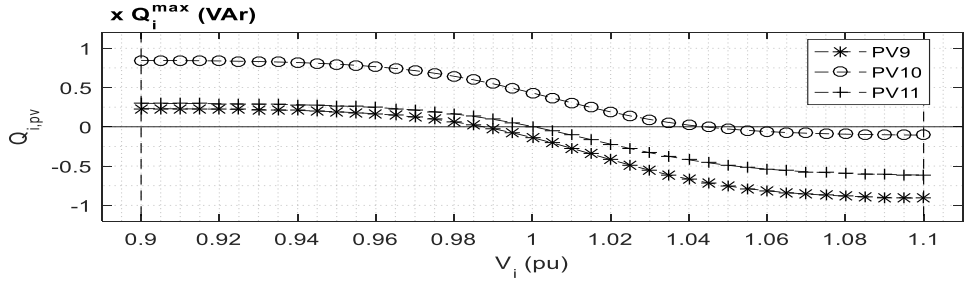

(b) Q(U) function

Figure 7.7 The comparison of PV9, PV10 and PV11

PV9-PV11 connect at the same node but in a different phase. Loads of each phase A, B and C are close according to the data in Table 6.2. From Figure 7.7, The characteristics of both P(U) and Q(U) functions of PV9, PV10 and PV11 are different apparently. Probably, it is because of voltage unbalance effect. If PV10 and PV11 are set to inject more real power, any phase of other nodes may be affected in overvoltage problem.

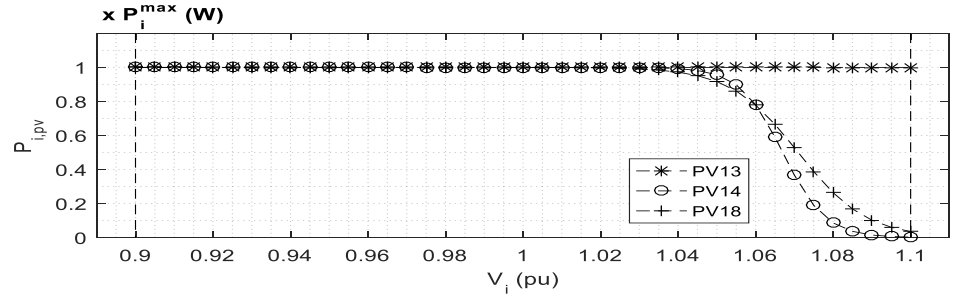

(a) P(U) function

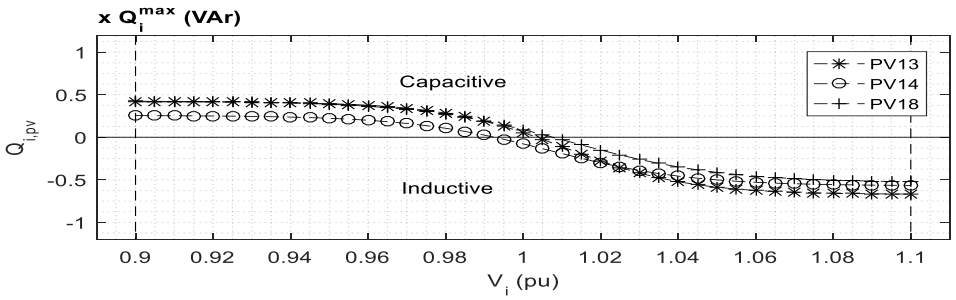

(b) Q(U) function

Figure 7.8 The comparison of PV13, PV14 and PV18

From Figure 7.8, PV13 is nearer distribution transformer (800 m. long) than the others. Then, $P(U)_{PV13}$ function is set to inject real power more than $P(U)_{PV14}$ function (1.2 km. long) and $P(U)_{PV18}$ function (900 m. long). For Q(U) function, the characteristics of PV13, PV14 and PV18 are close.

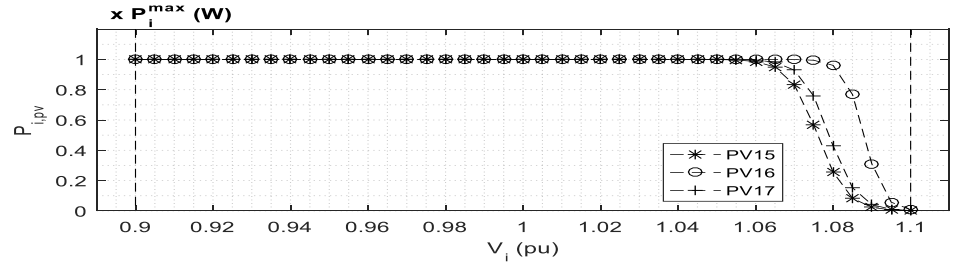

(a) P(U) function

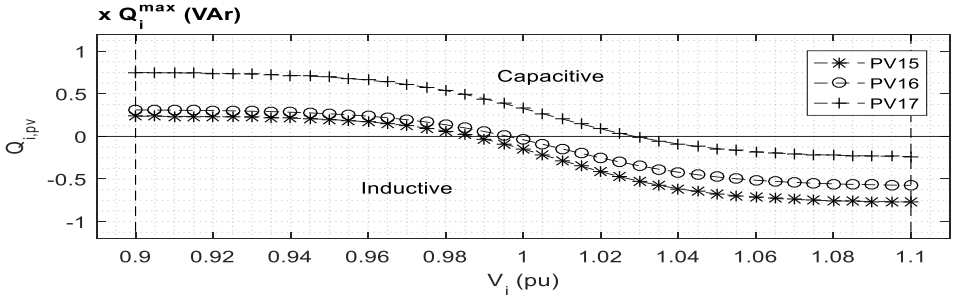

(b) Q(U) function

Figure 7.9 The comparison of PV15, PV16 and PV17

From Figure 7.9, it can notice that the characteristics of P(U) function of PV15, PV16 and PV17 are limited real power output more than P(U) function from PV1-PV3 connections at upstream node. It is due to the ability to inject more real power output at the upstream node than the downstream node. For Q(U) functions of PV15, PV16

and PV17, they are different apparently. Probably, it is because of voltage unbalance effect.

7.2 The Same and Different Parameters Setting of Local Control

According to Subsection 7.1.3, the parameters setting result of each PV system from 2-stage PSO is determined as different setting. However, the same parameters setting result of each PV system will be obtained at the first stage of 2-stage PSO. According to the set of uncertainty at the week 3-9 November 2014 in Table 6.7, the optimal objective value in equation (5.77) is 40,654.36 W when the first stage of 2-stage PSO is terminated. The same parameters setting result $\{V_{i,cri}, \delta_{i,p}, K_{i,1}, K_{i,2}, V_{i,q}, \delta_{i,q}\}$ is {1.066, 0.013, 0.237, 0.882, 1.006, 0.055}. Considering only the case $z \in \{z1, z2, \ldots, z17\}$, the power flow results can be shown in Figure 7.10. The total real power output from PV systems at maximum value is 97,589.40 W at the case $z2$. Comparing between this subsection and Subsection 7.1.3, the percent different of objective value and maximum total real power output can be shown in Table 7.4 and it can notice that the different parameters setting at Subsection 7.1.3 is better because the optimal objective value result is higher and the maximum total real power output from PV systems at the case $z2$ is higher.

Table 7.4 The comparison between the same and different setting of P(U) and Q(U) functions

	The Same Setting	**The Different Setting**	**Percent Change of The Different Setting**
Objective Value	40,654.36	42,643.37	+4.89%
Maximum total real power output	97,589.40	103,937.38	+6.50%

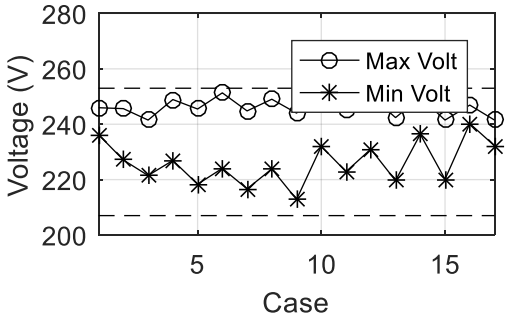

(a) Minimum and maximum phase voltage

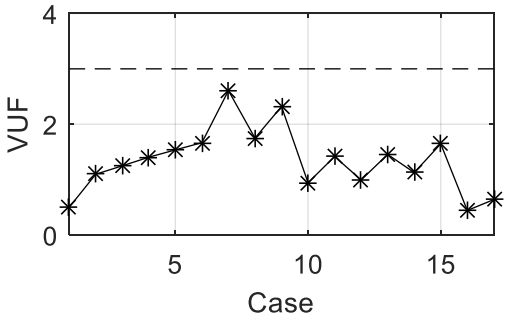

(b) Maximum VUF

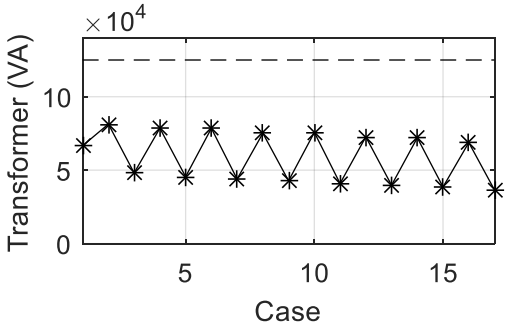

(c) MV/LV transformer utilization

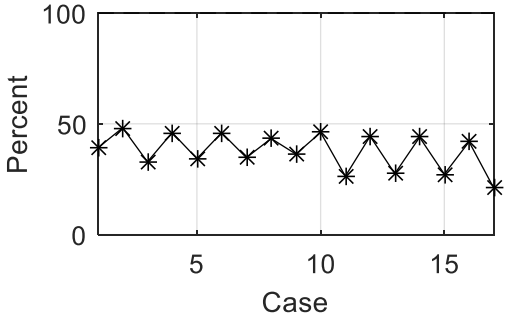

(d) Maximum line capacity

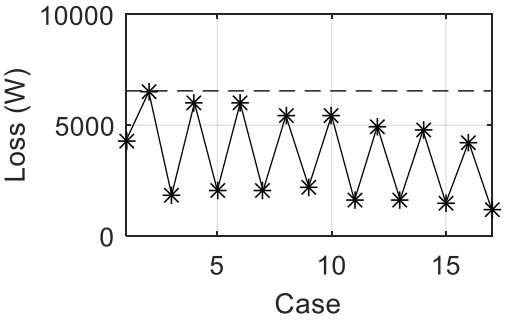

(e) System loss

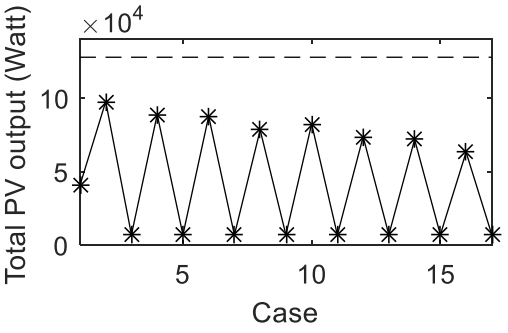

(f) Total real power output from PV systems

Figure 7.10 The results of the set of uncertainty

7.3 The Continuous And Piecewise Linear Local Control Application

In this subsection, the piecewise linear local control function as written in equations (4.8), (4.9), (4.11) and (4.12) will be applied. The parameter assessment will be analyzed by central control through 2-stage PSO process. According to the set of uncertainty at the week 3-9 November 2014 in Table 6.7, the optimal objective value in equation (5.81) is 41,815.83 W and the results of optimal parameter setting can be

shown in Table 7.5. Considering only the case $z \in \{z1, z2, \ldots, z17\}$, the power flow results can be shown in Figure 7.3. The power flow results can be shown in Figure 7.11. The total real power output from PV systems at maximum value is 102,518.32 W at the case $z2$. Comparing between this subsection and Subsection 7.1.3, the percent different of objective value and maximum total real power output can be shown in Table 7.6 and it can notice that the results between this subsection and Subsection 7.1.3 are close. Then, local control application can be chosen any one from continuous or piecewise linear function because of the nearly similar results.

Table 7.5 Parameter setting of each connected PV system

PV Name	Parameter Setting					
	V_{p1}	V_{p2}	K_1	K_2	V_{q1}	V_{q2}
PV1	1.089	1.104	0.552	-0.496	0.904	0.997
PV2	1.089	1.108	0.496	-0.698	0.919	1.039
PV3	1.093	1.11	0.526	-0.557	0.909	1.017
PV4	1.095	1.109	0.544	-0.278	0.901	1.022
PV5	1.063	1.08	0.611	-0.667	0.902	1.007
PV6	1.09	1.105	0.337	-0.392	0.906	0.99
PV7	1.077	1.087	0.435	-0.742	0.9	1.03
PV8	1.095	1.106	0.56	-0.556	0.908	0.987
PV9	1.056	1.092	0.456	-0.627	0.9	0.982
PV10	1.076	1.095	0.379	-0.651	0.91	0.961
PV11	1.055	1.102	0.664	-0.585	0.909	0.997
PV12	1.019	1.099	0.341	-0.605	0.91	1.075
PV13	1.084	1.099	0.707	-0.715	0.91	0.929
PV14	1.057	1.071	0.43	-0.557	0.905	1.1
PV15	1.077	1.088	0.439	-0.49	0.911	1.004
PV16	1.074	1.101	0.458	-0.546	0.909	1.007
PV17	1.087	1.104	0.431	-0.607	0.903	1.093
PV18	1.032	1.088	0.478	-0.726	0.907	1.037

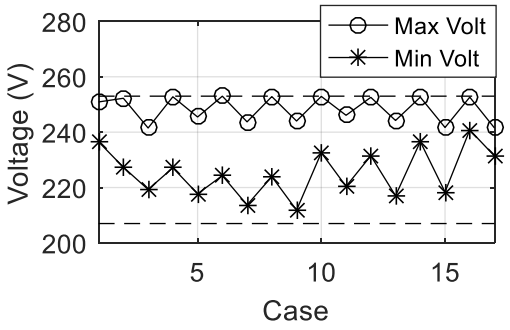

(a) Minimum and maximum phase voltage

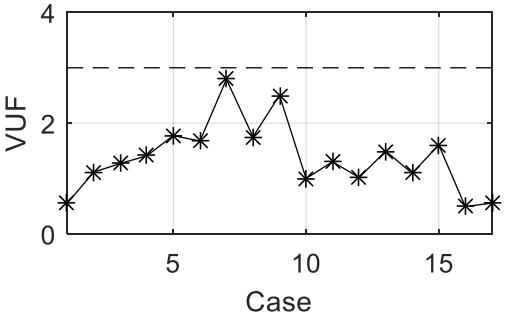

(b) Maximum VUF

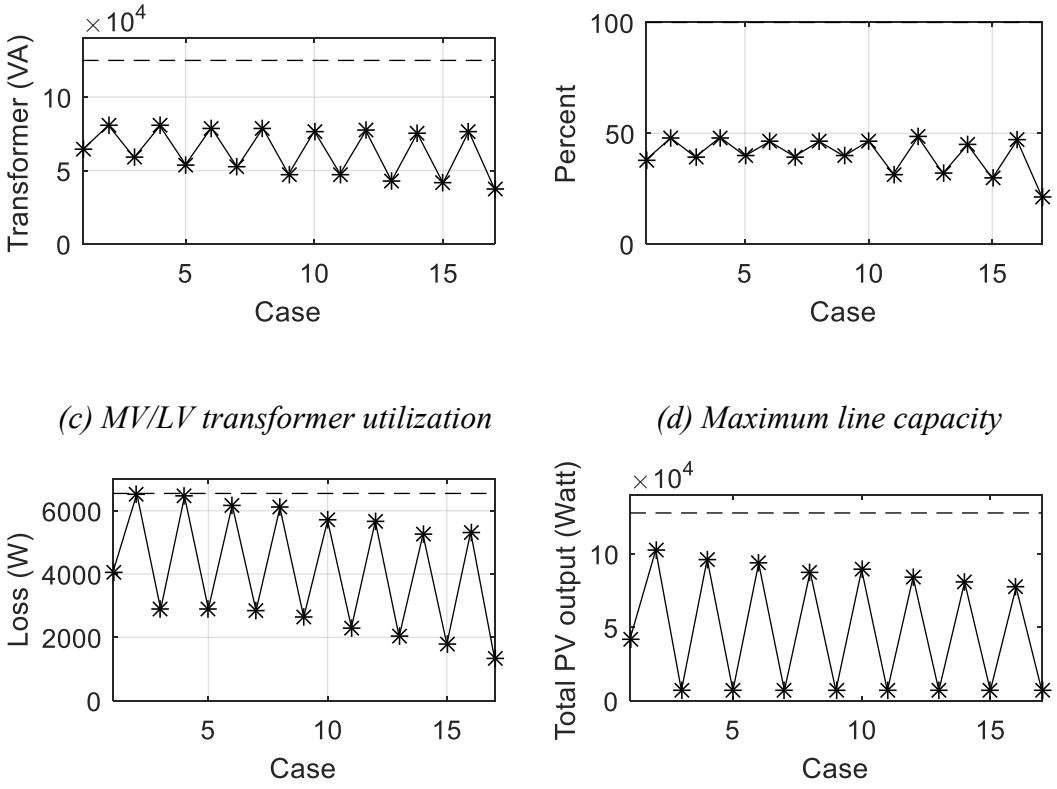

(c) MV/LV transformer utilization

(d) Maximum line capacity

(e) System loss

(f) Total real power output from PV systems

Figure 7.11 The results of the set of uncertainty

Table 7.6 The comparison between the continuous and piecewise linear function application

	Continuous Function	**Piecewise Linear Function**	**Percent Change of Piecewise Linear Function**
Objective Value	42,643.37	41,815.83	-1.94%
Maximum total real power output	103,937.378	102,518.32	-1.37%

7.4 Local Control Adjustment in Every One Week or One Day Of Continuous Local Control Function

In this subsection, the comparison between (7.4.1) adjustment per one week and (7.4.2) adjustment per one day is determined for the suitable operation of coordination between central and local control. The continuous local control function is selected in this subsection.

7.4.1 Adjustment Per One Week

In this subsection, the parameters setting in Table 7.2 is applied. The simulations are divided into 7 parts: (7.4.1.1) at the day 3 November 2014; (7.4.1.2) at the day 4 November 2014; (7.4.1.3) at the day 5 November 2014; (7.4.1.4) at the day 6 November 2014; (7.4.1.5) at the day 7 November 2014; (7.4.1.6) at the day 8 November 2014; (7.4.1.7) at the day 9 November 2014. The objective of this subsection is to determine the simulation results when (1) the set of uncertainty of each day is applied and (2) the parameters setting in Table 7.2 at the week 3-9 November 2014 is applied.

7.4.1.1 At The Day 3 November 2014

According to the set of uncertainty at the day 3 November 2014 in Table 6.8, the calculated objective value in equation (5.81) is 49,472.20 W. Considering the case $z \in \{z1, z2, \ldots, z17\}$, the power flow results can be shown in Figure 7.12 and they are within the limit. The total real power output from PV systems at maximum value is 95,251.06 W at the case $z2$.

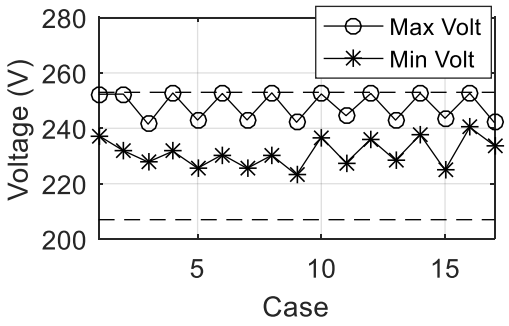

(a) Minimum and maximum phase voltage

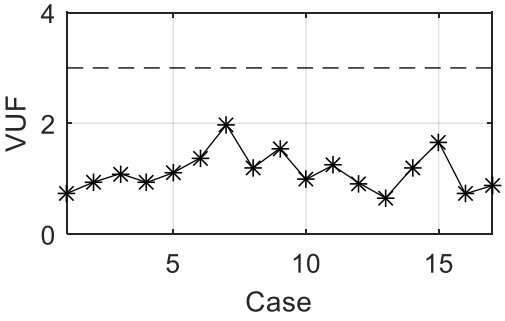

(b) Maximum VUF

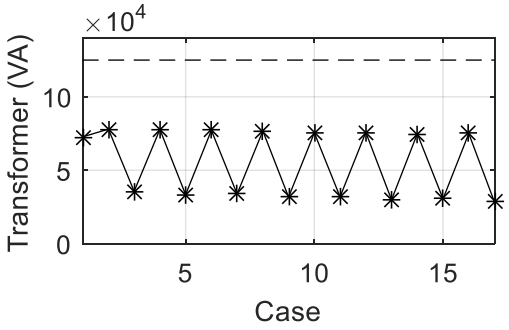

(c) MV/LV transformer utilization

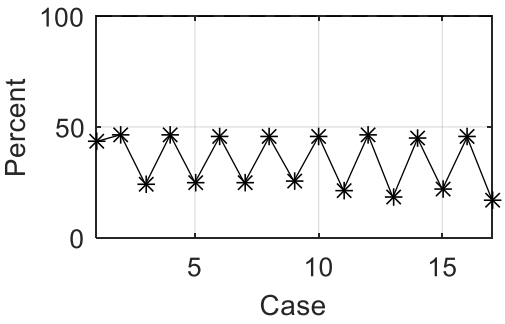

(d) Maximum line capacity

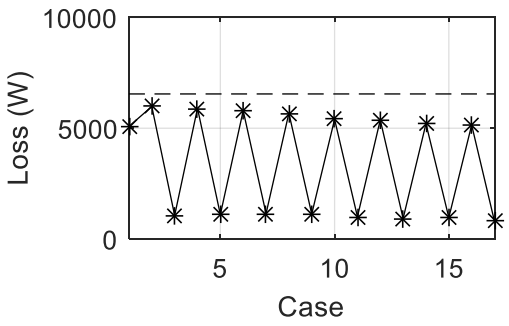

(e) System loss

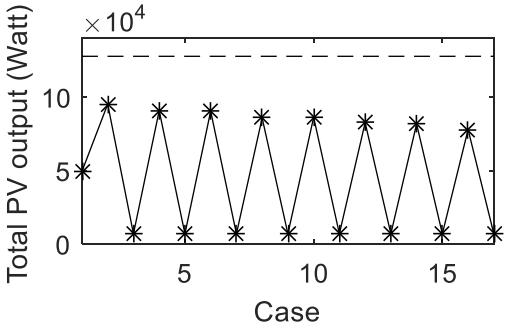

(f) Total real power output from PV systems

Figure 7.12 The results of the set of uncertainty

7.4.1.2 At The Day 4 November 2014

According to the set of uncertainty at the day 4 November 2014 in Table 6.9, the calculated objective value in equation (5.81) is 44,940.84 W. Considering only the case $z \in \{z1, z2, \ldots, z17\}$, the power flow results can be shown in Figure 7.13 and they are within the limit. The total real power output from PV systems at maximum value is 101,056.21 W at the case $z2$.

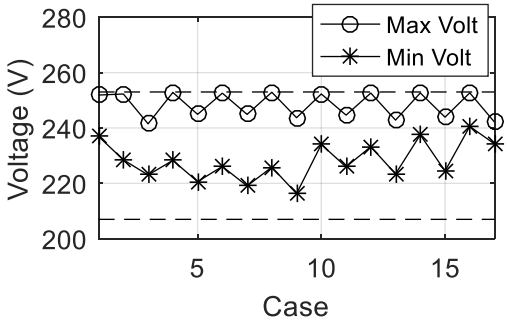

(a) Minimum and maximum phase voltage

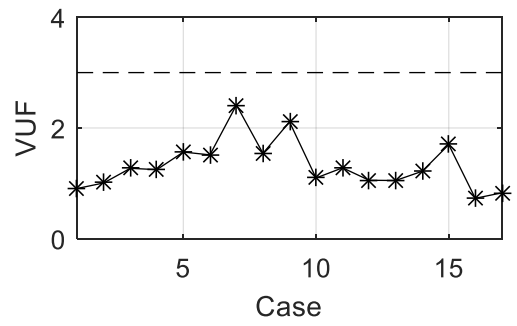

(b) Maximum VUF

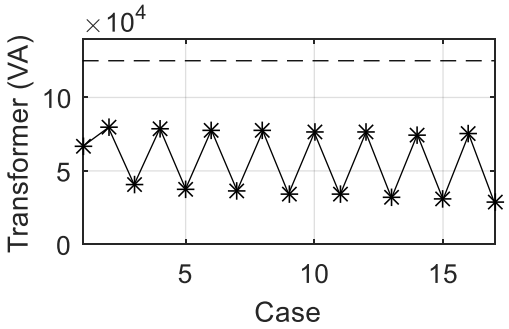

(c) MV/LV transformer utilization

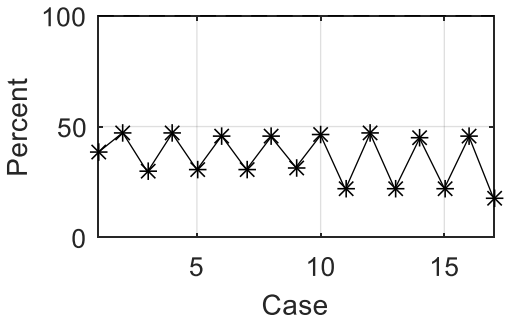

(d) Maximum line capacity

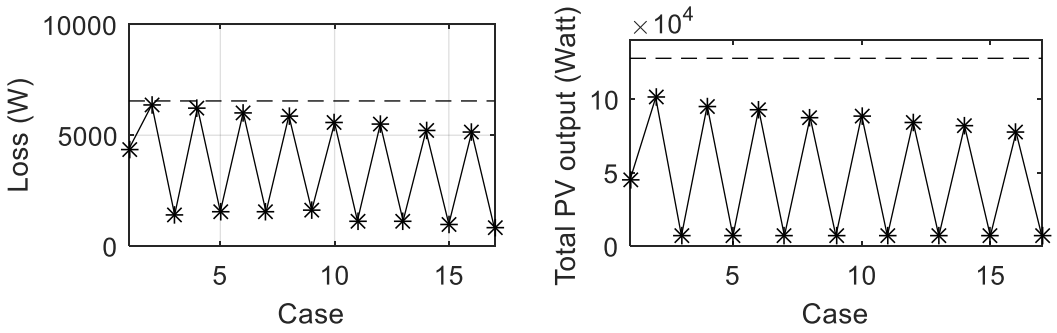

(e) System loss *(f) Total real power output from PV systems*

Figure 7.13 The results of the set of uncertainty

7.4.1.3 At The Day 5 November 2014

According to the set of uncertainty at the day 5 November 2014 in Table 6.10, the calculated objective value in equation (5.81) is 41,080.51 W. Considering only the case $z \in \{z1, z2, \ldots, z17\}$, the power flow results can be shown in Figure 7.14 and they are within the limit. The total real power output from PV systems at maximum value is 97,917.23 W at the case $z2$.

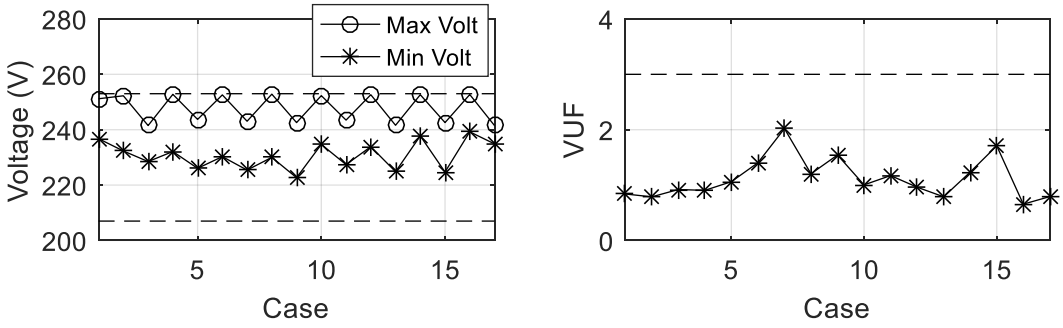

(a) Minimum and maximum phase voltage *(b) Maximum VUF*

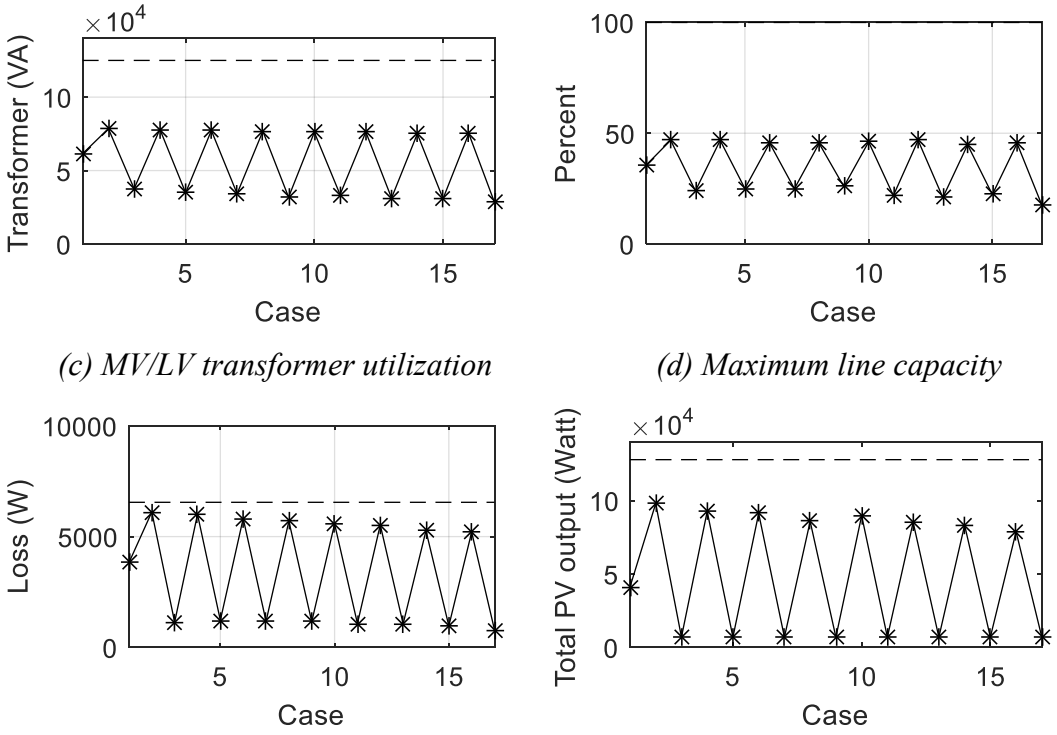

(c) MV/LV transformer utilization

(d) Maximum line capacity

(e) System loss

(f) Total real power output from PV systems

Figure 7.14 The results of the set of uncertainty

7.4.1.4 At The Day 6 November 2014

According to the set of uncertainty at the day 6 November 2014 in Table 6.10, the calculated objective value in equation (5.81) is 35,955.41 W. Considering only the case $z \in \{z1, z2, \ldots, z17\}$, the power flow results can be shown in Figure 7.15 and they are within the limit. The total real power output from PV systems at maximum value is 99,675.54 W at the case $z2$.

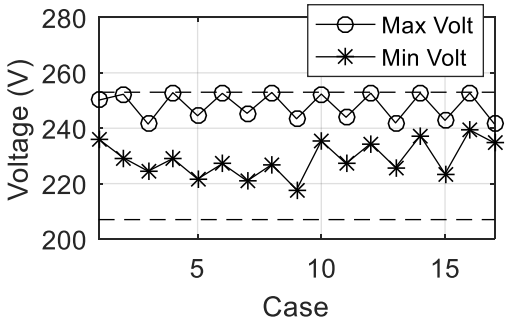

(a) Minimum and maximum phase voltage

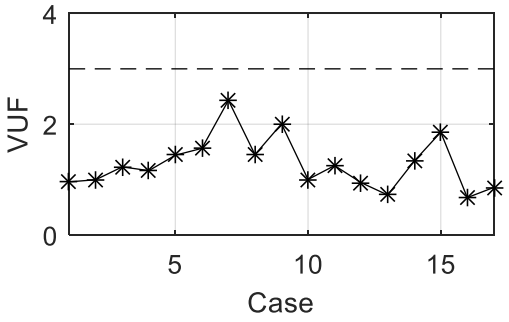

(b) Maximum VUF

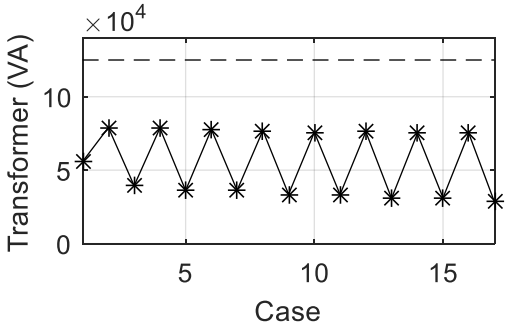

(c) MV/LV transformer utilization

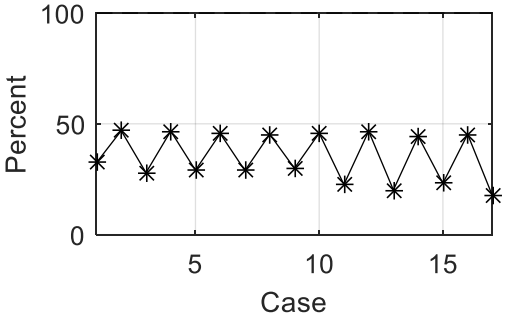

(d) Maximum line capacity

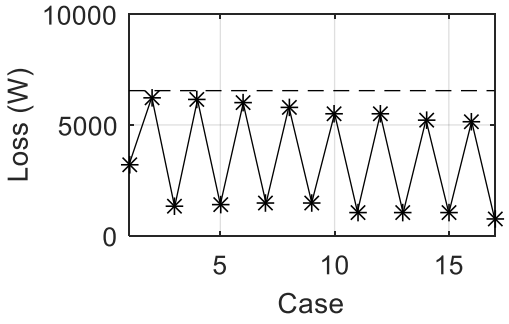

(e) System loss

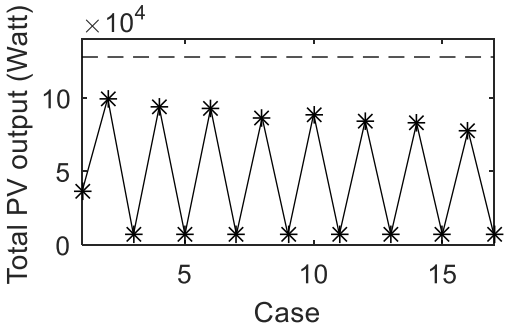

(f) Total real power output from PV systems

Figure 7.15 The results of the set of uncertainty

7.4.1.5 At The Day 7 November 2014

According to the set of uncertainty at the day 7 November 2014 in Table 6.12, the calculated objective value in equation (5.81) is 38,174.22 W. Considering only the case $z \in \{z1, z2, \ldots, z17\}$, the power flow results can be shown in Figure 7.16 and they are within the limit. The total real power output from PV systems at maximum value is 99,870.33 W at the case $z2$.

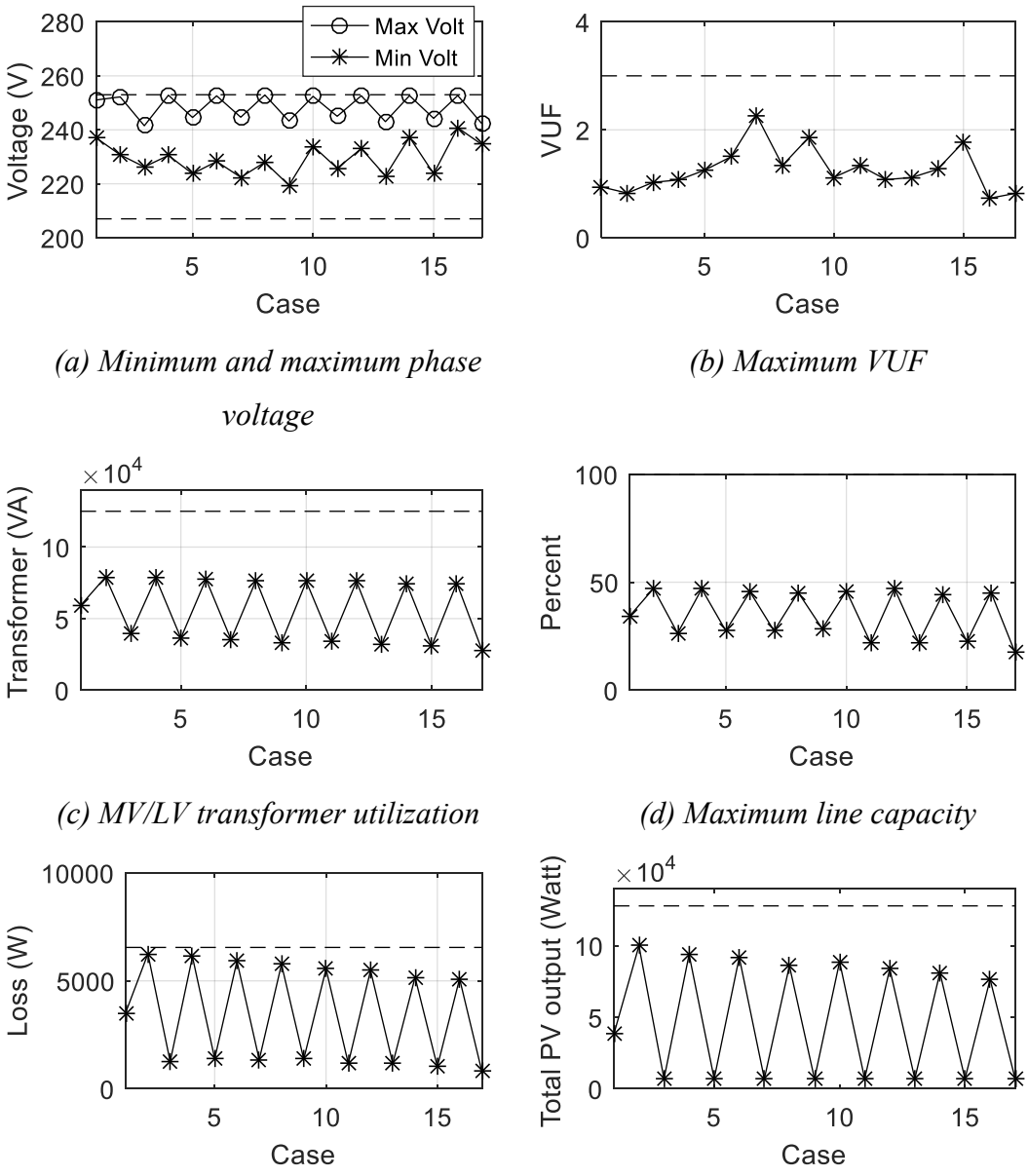

(a) Minimum and maximum phase voltage

(b) Maximum VUF

(c) MV/LV transformer utilization

(d) Maximum line capacity

(e) System loss

(f) Total real power output from PV systems

Figure 7.16 The results of the set of uncertainty

7.4.1.6 At The Day 8 November 2014

According to the set of uncertainty at the day 8 November 2014 in Table 6.13, the calculated objective value in equation (5.81) is 48,299.55 W. Considering only the case $z \in \{z1, z2, \ldots, z17\}$, the power flow results can be shown in Figure 7.17 and they are within the limit. The total real power output from PV systems at maximum value is 99,839.99 W at the case $z2$.

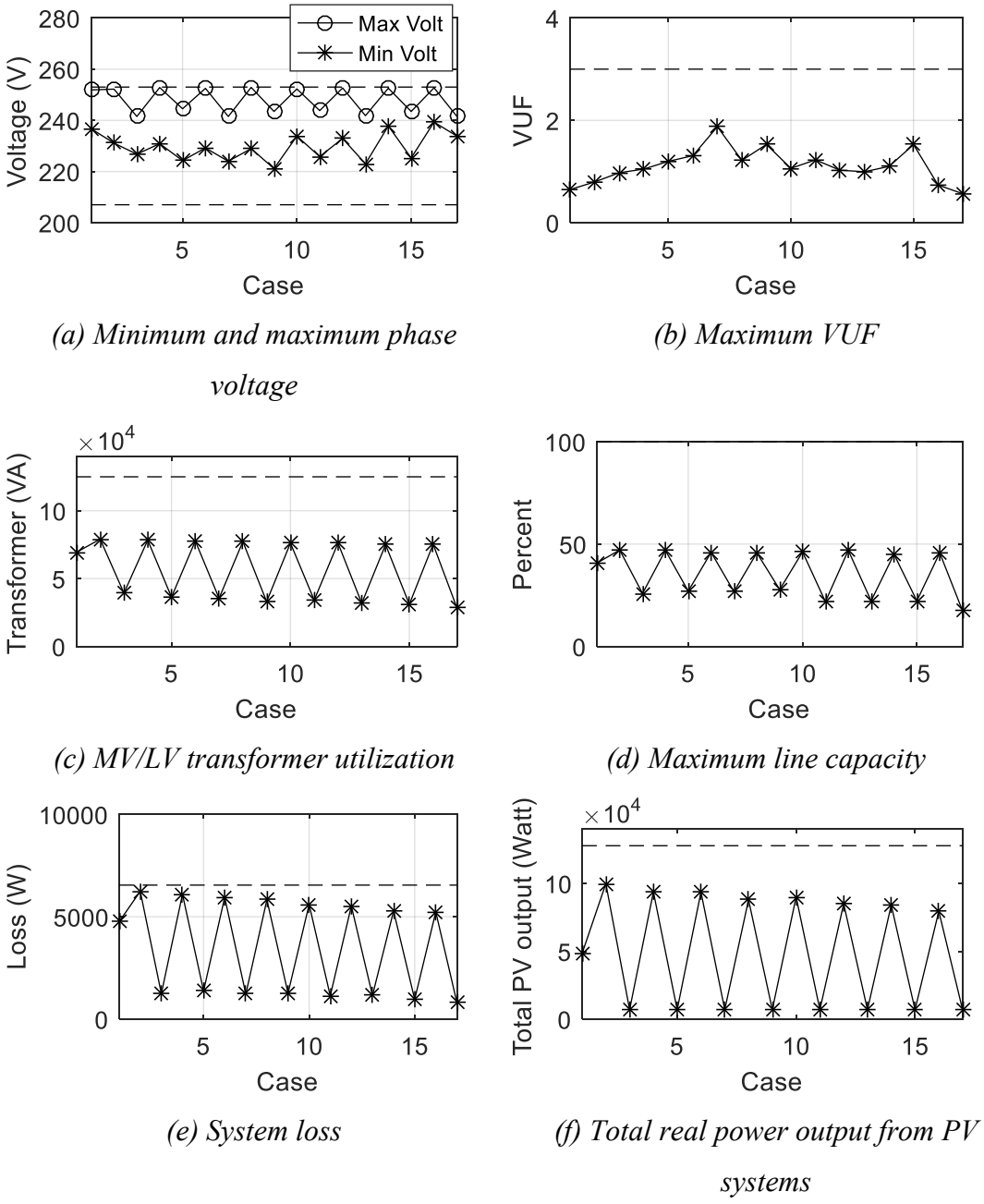

(a) Minimum and maximum phase voltage

(b) Maximum VUF

(c) MV/LV transformer utilization

(d) Maximum line capacity

(e) System loss

(f) Total real power output from PV systems

Figure 7.17 The results of the set of uncertainty

7.4.1.7 At The Day 9 November 2014

According to the set of uncertainty at the day 9 November 2014 in Table 6.14, the calculated objective value in equations (5.81) is 29,586.98 W. Considering only the case $z \in \{z1, z2, \ldots, z17\}$, the power flow results can be shown in Figure 7.18 and they are within the limit. The total real power output from PV systems at maximum value is 103,209.82 W at the case $z2$.

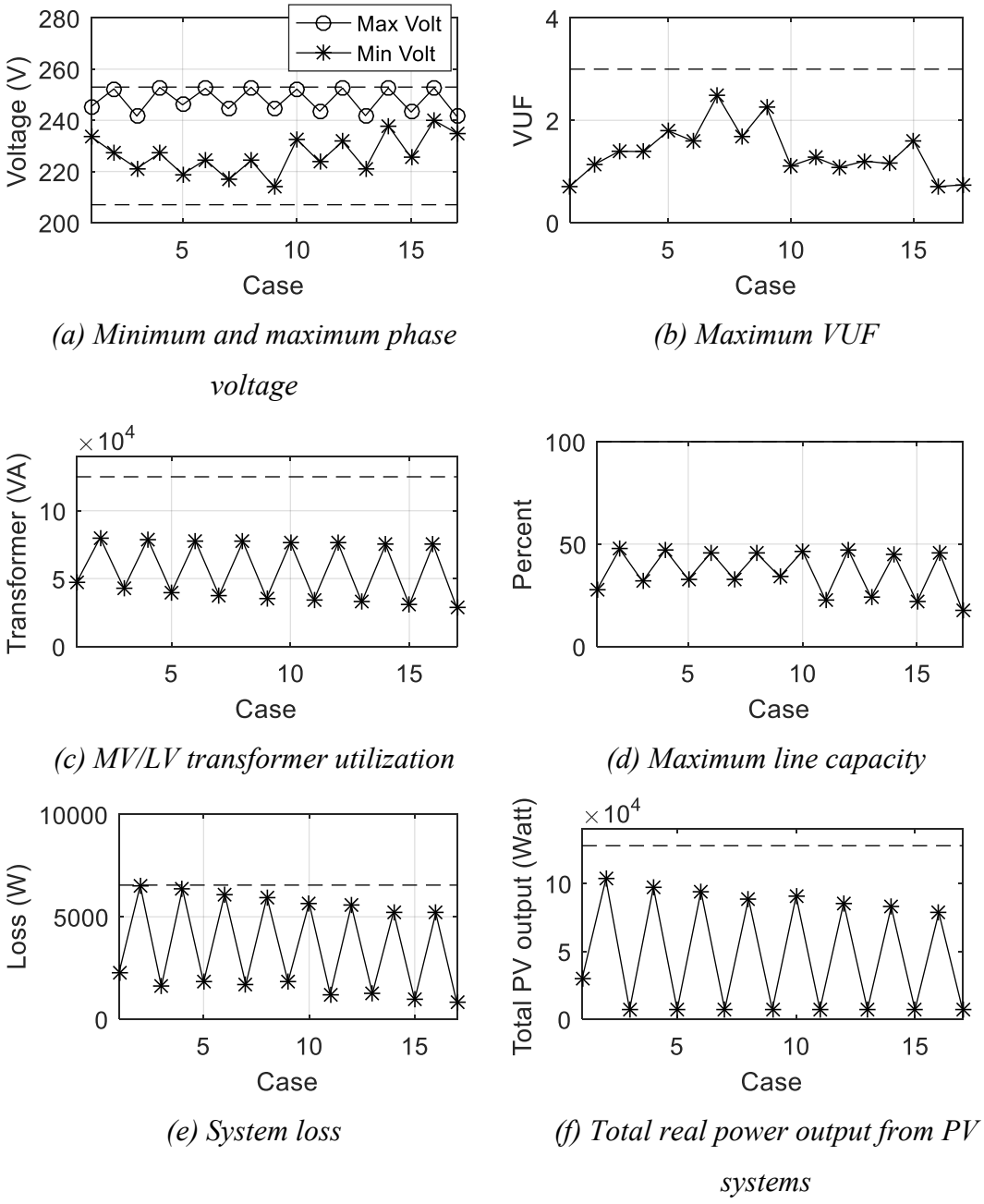

(a) Minimum and maximum phase voltage

(b) Maximum VUF

(c) MV/LV transformer utilization

(d) Maximum line capacity

(e) System loss

(f) Total real power output from PV systems

Figure 7.18 The results of the set of uncertainty

7.4.2 Adjustment Per One Day

In this subsection, the optimal parameters setting will be searched through 2-stage PSO. The set of uncertainty of each day will be applied. The simulation results are divided into seven subsections: (7.4.2.1) at the day 3 November 2014; (7.4.2.2) at the day 4 November 2014; (7.4.2.3) at the day 5 November 2014; (7.4.2.4) at the day 6 November 2014; (7.4.2.5) at the day 7 November 2014; (7.4.2.6) at the day 8 November

2014; (7.4.2.7) at the day 9 November 2014. The results of Subsection 7.4.2 will be compared to subsection 7.4.1.

7.4.2.1 At The Day 3 November 2014

The parameter assessment will be analyzed by central control through 2-stage PSO process. According to the set of uncertainty at the day 3 November 2014 in Table 6.8, the optimal objective value in equation (5.81) is 51,565.54 W and the results of optimal parameter setting can be shown in Table 7.7. Considering only the case $z \in \{z1, z2, \ldots, z17\}$, the power flow results can be shown in Figure 7.19 and they are within the limit. The total real power output from PV systems at maximum value is 98,597.83 W at the case $z2$.

Table 7.7 Parameter setting of each connected PV system

PV Name	Parameter Setting					
	V_{cri}	δ_p	K_1	K_2	V_q	δ_q
PV1	1.1	0.012	0.015	0.804	1.075	0.099
PV2	1.1	0.014	0.012	0.588	1.042	0.099
PV3	1.102	0.016	0.041	0.739	1.042	0.1
PV4	1.119	0.02	0.025	1.025	1.043	0.097
PV5	1.082	0.011	0.018	0.783	1.026	0.1
PV6	1.088	0.011	0.004	0.678	1.029	0.087
PV7	1.105	0.018	0.007	0.775	1.03	0.094
PV8	1.107	0.018	0.015	0.508	1.04	0.097
PV9	1.08	0.013	0.013	0.767	1.039	0.086
PV10	1.086	0.01	0.02	0.689	1.047	0.089
PV11	1.086	0.014	0.013	0.809	1.045	0.098
PV12	1.08	0.019	0.011	0.641	1.035	0.098
PV13	1.083	0.024	0.023	0.632	1.041	0.097
PV14	1.043	0.014	0.012	0.732	1.038	0.1
PV15	1.077	0.017	0.009	0.813	1.033	0.087
PV16	1.072	0.032	0.014	0.896	1.048	0.097
PV17	1.093	0.01	0.015	0.7	1.039	0.1
PV18	1.152	0.017	0.024	0.761	1.035	0.1

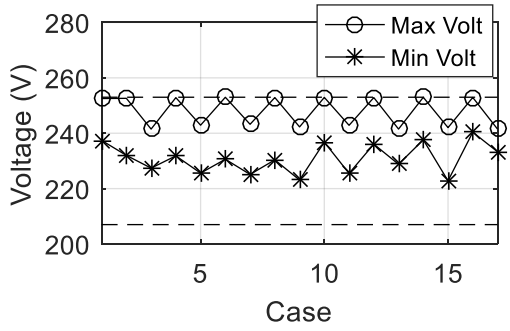

(a) Minimum and maximum phase voltage

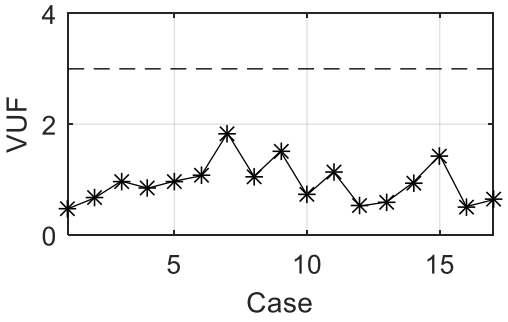

(b) Maximum VUF

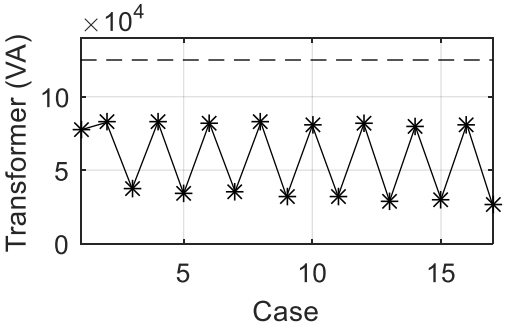

(c) MV/LV transformer utilization

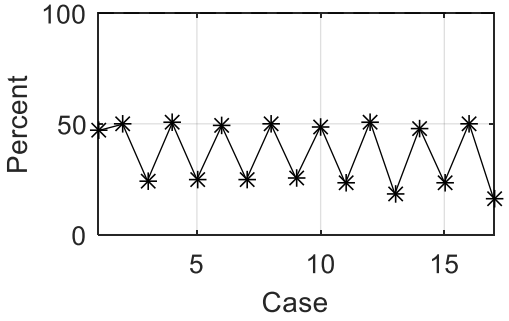

(d) Maximum line capacity

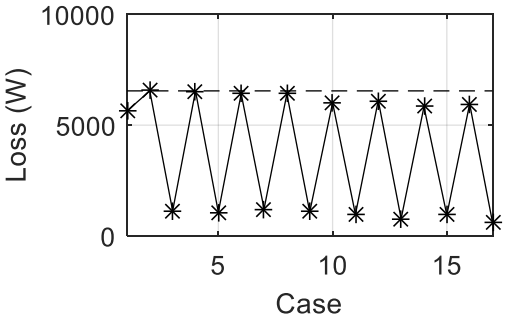

(e) System loss

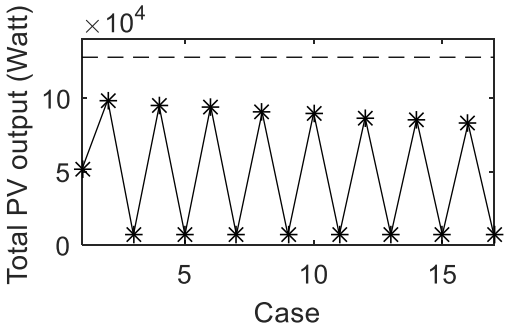

(f) Total real power output from PV systems

Figure 7.19 The results of the set of uncertainty

7.4.2.2 At The Day 4 November 2014

The parameter assessment will be analyzed by central control through 2-stage PSO process. According to the set of uncertainty at the day 4 November 2014 in Table 6.9, the optimal objective value in equation (5.81) is 46,719.23 W and the results of optimal parameter setting can be shown in Table 7.8. Considering only the case $z \in \{z1, z2, \ldots, z17\}$, the power flow results can be shown in Figure 7.20 and they are within

the limit. The total real power output from PV systems at maximum value is 103,531.01 W at the case $z2$.

Table 7.8 Parameter setting of each connected PV system

PV Name	Parameter Setting					
	V_{cri}	δ_p	K_1	K_2	V_q	δ_q
PV1	1.1	0.011	0.019	0.667	1.001	0.017
PV2	1.1	0.011	0	0.616	1	0.032
PV3	1.1	0.01	0.012	0.501	1.007	0.013
PV4	1.092	0.01	0.005	0.727	1.001	0.016
PV5	1.076	0.01	0.003	0.695	1	0.019
PV6	1.139	0.01	0	0.653	1.001	0.013
PV7	1.093	0.01	0.069	0.559	1	0.014
PV8	1.097	0.01	0.003	0.592	1	0.014
PV9	1.086	0.01	0.014	0.338	1	0.01
PV10	1.086	0.01	0.002	0.159	1	0.012
PV11	1.102	0.01	0.008	0.581	1.003	0.015
PV12	1.076	0.01	0	0.592	1	0.01
PV13	1.108	0.01	0.007	0.228	1.001	0.011
PV14	1.075	0.01	0.004	0.635	1.003	0.044
PV15	1.079	0.01	0.003	0.497	1.003	0.011
PV16	1.087	0.01	0.025	0.494	1.001	0.019
PV17	1.102	0.01	0.001	0.62	1	0.011
PV18	1.076	0.01	0	0.534	1.001	0.01

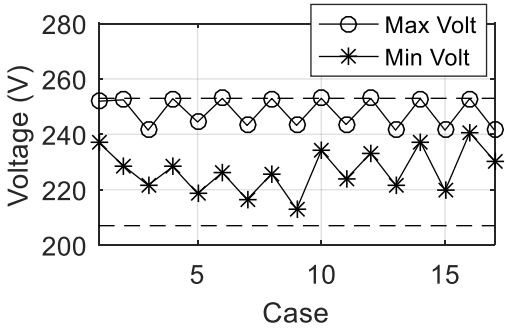

(a) Minimum and maximum phase voltage

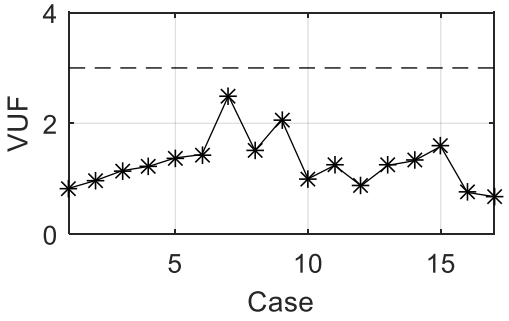

(b) Maximum VUF

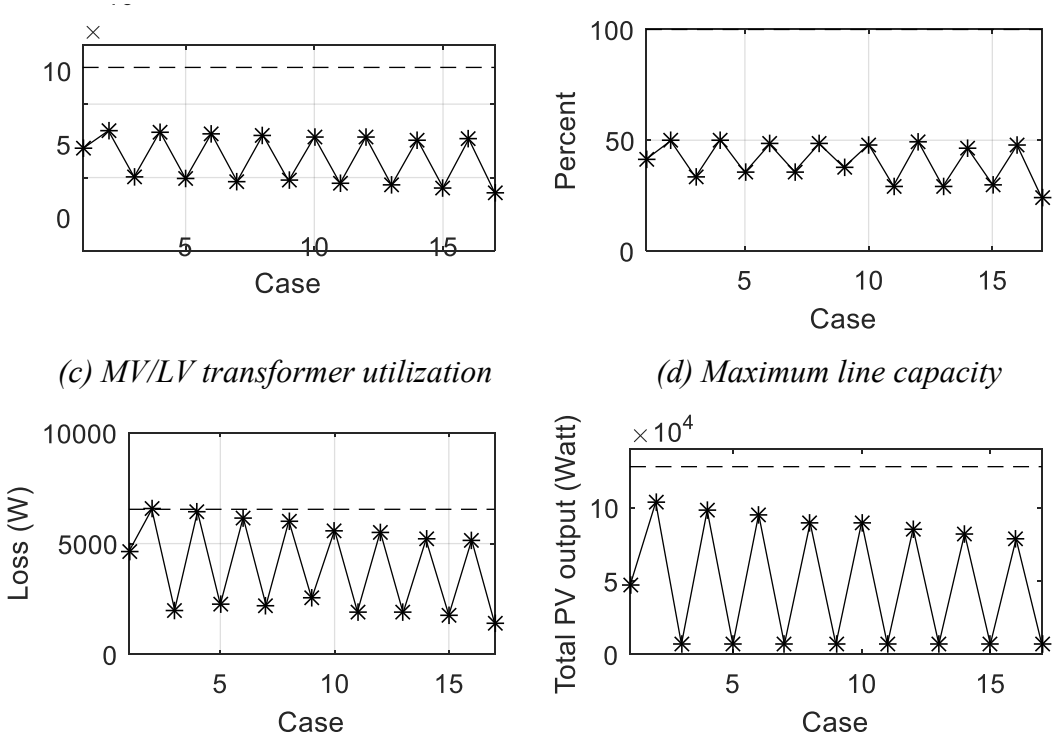

(c) MV/LV transformer utilization *(d) Maximum line capacity*

(e) System loss *(f) Total real power output from PV systems*

Figure 7.20 The results of the set of uncertainty

7.4.2.3 At The Day 5 November 2014

The parameter assessment will be analyzed by central control through 2-stage PSO process. According to the set of uncertainty at the day 5 November 2014 in Table 6.10, the optimal objective value in equation (5.81) is 44,143.82 W and the results of optimal parameter setting can be shown in Table 7.9. Considering only the case $z \in \{z1, z2, \ldots, z17\}$, the power flow can be shown in Figure 7.21 and they are within the limit. The total real power output from PV systems at maximum value is 102,481.48 W at the case $z2$.

Table 7.9 Parameter setting of each connected PV system

PV Name	Parameter Setting					
	V_{cri}	δ_p	K_1	K_2	V_q	δ_q
PV1	1.1	0.01	0.173	0.799	1.001	0.1
PV2	1.1	0.01	0.211	0.925	1.008	0.1
PV3	1.101	0.01	0.286	0.791	1.001	0.1
PV4	1.087	0.01	0.142	0.555	1	0.1

PV Name	Parameter Setting					
	V_{cri}	δ_p	K_1	K_2	V_q	δ_q
PV5	1.081	0.01	0.026	0.826	1.001	0.098
PV6	1.094	0.01	0.16	0.809	1.001	0.1
PV7	1.095	0.01	0.242	0.827	1.001	0.1
PV8	1.118	0.01	0.196	0.731	1.001	0.1
PV9	1.085	0.01	0.173	0.777	1.001	0.1
PV10	1.088	0.01	0.284	0.76	1.001	0.1
PV11	1.109	0.01	0.186	0.76	1.002	0.1
PV12	1.081	0.01	0.17	0.755	1.001	0.1
PV13	1.104	0.01	0.223	0.777	1	0.1
PV14	1.08	0.01	0.197	0.739	1	0.1
PV15	1.079	0.01	0.261	0.845	1.001	0.1
PV16	1.086	0.01	0.187	0.793	1.001	0.1
PV17	1.104	0.01	0.188	0.651	1.002	0.1
PV18	1.081	0.01	0.177	0.636	1	0.1

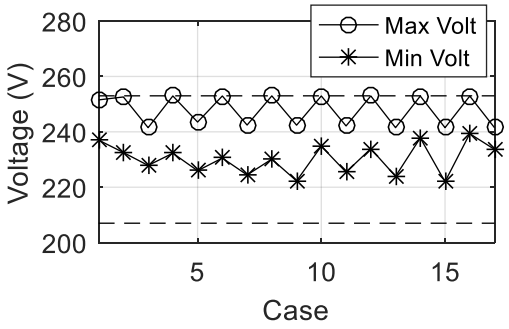

(a) Minimum and maximum phase voltage

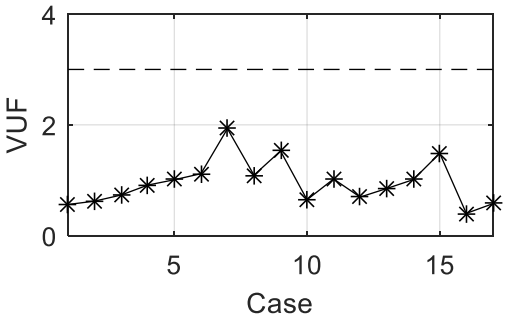

(b) Maximum VUF

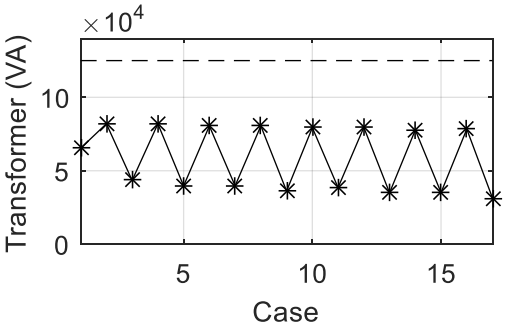

(c) MV/LV transformer utilization

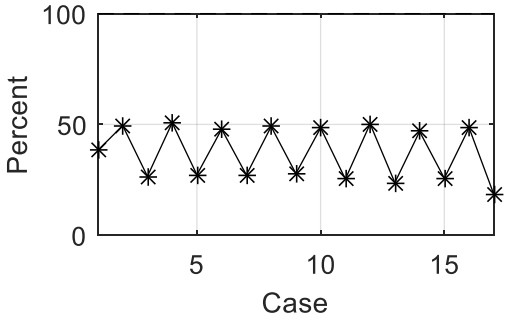

(d) Maximum line capacity

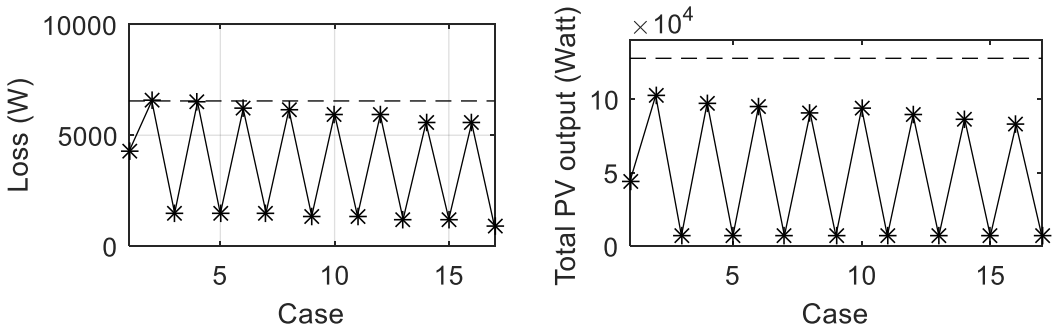

(e) System loss *(f) Total real power output from PV systems*

Figure 7.21 The results of the set of uncertainty

7.4.2.4 At The Day 6 November 2014

The parameter assessment will be analyzed by central control through 2-stage PSO process. According to the set of uncertainty at the day 6 November 2014 in Table 6.11, the optimal objective value in equation (5.81) is 36,814.38 W and the results of optimal parameter setting can be shown in Table 7.10. Considering only the case $z \in \{z1, z2, \ldots, z17\}$, the power flow results can be shown in Figure 7.22 and they are within the limit. The total real power output from PV systems at maximum value is 101,971.62 W at the case $z2$.

Table 7.10 Parameter setting of each connected PV system

PV Name	Parameter Setting					
	V_{cri}	δ_p	K_1	K_2	V_q	δ_q
PV1	1.1	0.012	0.395	1.046	1.021	0.085
PV2	1.1	0.011	0.385	1.062	1.018	0.088
PV3	1.101	0.011	0.382	1.021	1.03	0.083
PV4	1.086	0.011	0.332	1.046	1.02	0.086
PV5	1.075	0.01	0.396	1.034	1.027	0.089
PV6	1.084	0.01	0.372	1.287	1.023	0.084
PV7	1.091	0.011	0.406	1.029	1.024	0.08
PV8	1.111	0.011	0.384	0.965	1.021	0.078
PV9	1.084	0.011	0.396	1.021	1.01	0.078
PV10	1.084	0.011	0.469	1.076	1.019	0.083
PV11	1.102	0.011	0.399	1.052	1.018	0.087
PV12	1.077	0.048	0.369	1.032	1.025	0.097
PV13	1.071	0.014	0.398	0.85	1.019	0.071
PV14	1.077	0.016	0.383	1.158	1.021	0.085
PV15	1.084	0.011	0.35	1.061	1.016	0.081
PV16	1.085	0.011	0.37	1.087	1.023	0.079

PV Name	Parameter Setting					
	V_{cri}	δ_p	K_1	K_2	V_q	δ_q
PV17	1.076	0.011	0.384	1.009	1.025	0.086
PV18	1.125	0.011	0.618	1.048	1.022	0.097

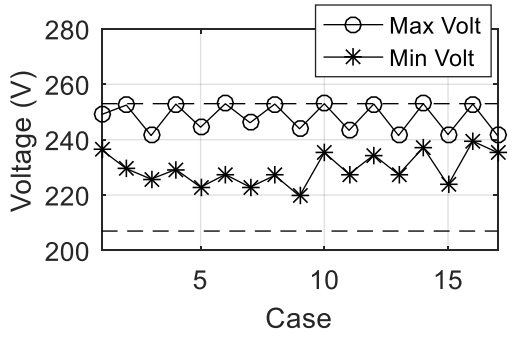

(a) Minimum and maximum phase voltage

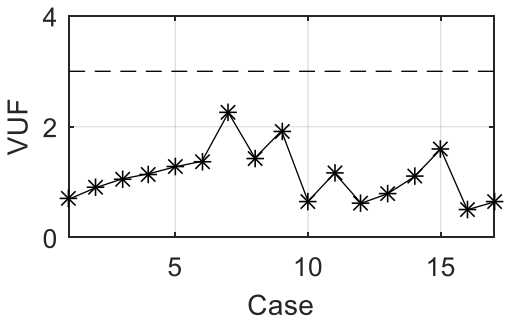

(b) Maximum VUF

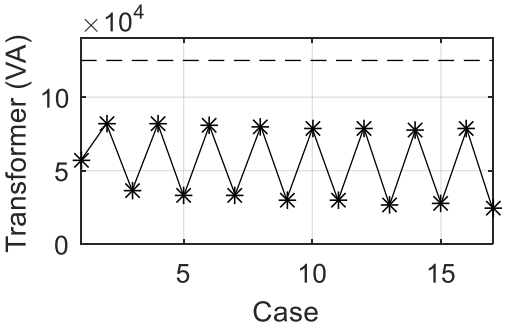

(c) MV/LV transformer utilization

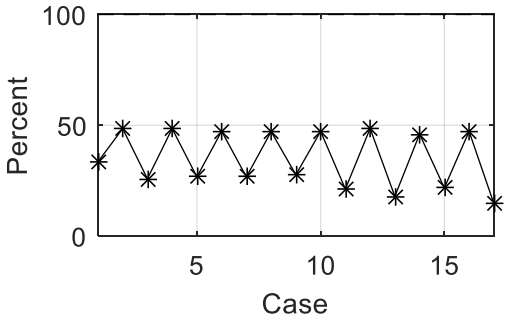

(d) Maximum line capacity

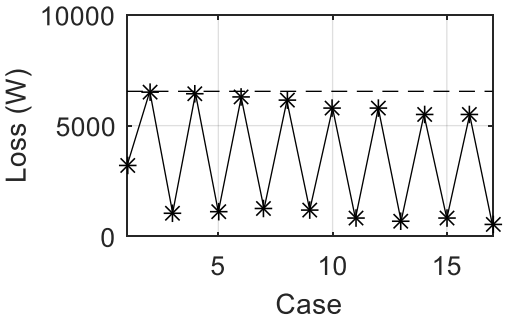

(e) System loss

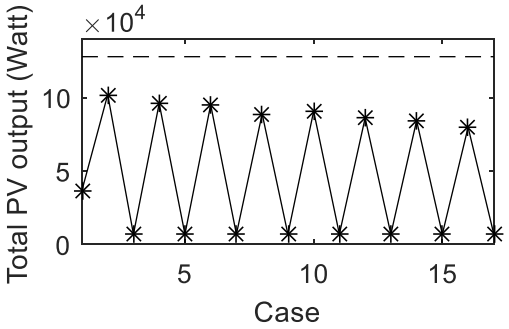

(f) Total real power output from PV systems

Figure 7.22 The results of the set of uncertainty

7.4.2.5 At The Day 7 November 2014

The parameter assessment will be analyzed by central control through 2-stage PSO process. According to the set of uncertainty at the day 7 November 2014 in Table 6.12, the optimal objective value in equation (5.81) is 39,214.69 W and the results of optimal parameter setting can be shown in Table 7.11. Considering only the case $z \in \{z1, z2, \ldots, z17\}$, the power flow results can be shown in Figure 7.23 and they are within the limit. The total real power output from PV systems at maximum value is 102,359.66 W at the case $z2$.

Table 7.11 Parameter setting of each connected PV system

PV Name	Parameter Setting					
	V_{cri}	δ_p	K_1	K_2	V_q	δ_q
PV1	1.1	0.012	0.054	0.908	1.003	0.085
PV2	1.1	0.011	0.019	0.393	1.006	0.091
PV3	1.1	0.01	0.038	0.528	1.006	0.084
PV4	1.092	0.01	0.019	0.957	1	0.1
PV5	1.076	0.011	0.035	0.786	1.003	0.1
PV6	1.089	0.01	0.061	0.712	1.007	0.092
PV7	1.109	0.013	0.036	0.464	1.01	0.1
PV8	1.103	0.011	0.066	0.574	1.003	0.097
PV9	1.084	0.011	0.033	0.679	1.005	0.099
PV10	1.088	0.01	0.057	0.754	1.016	0.08
PV11	1.101	0.011	0.109	0.527	1.007	0.071
PV12	1.072	0.012	0.057	0.769	1.003	0.086
PV13	1.1	0.01	0.047	0.74	1.004	0.1
PV14	1.069	0.032	0	0.209	1.007	0.1
PV15	1.083	0.01	0.015	0.98	1.004	0.1
PV16	1.096	0.011	0.028	0.033	1	0.096
PV17	1.102	0.012	0.064	0.636	1	0.093
PV18	1.074	0.031	0.046	0.633	1.001	0.1

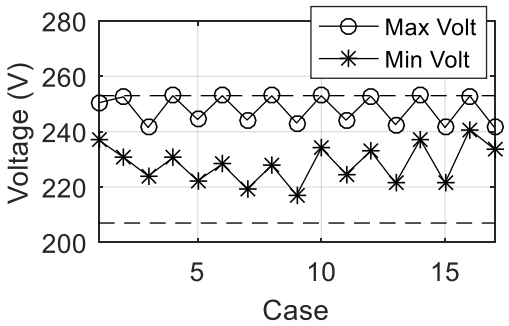

(a) Minimum and maximum phase voltage

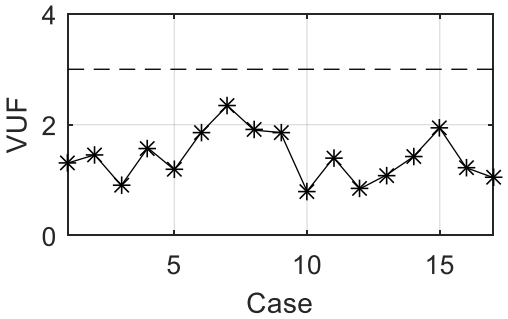

(b) Maximum VUF

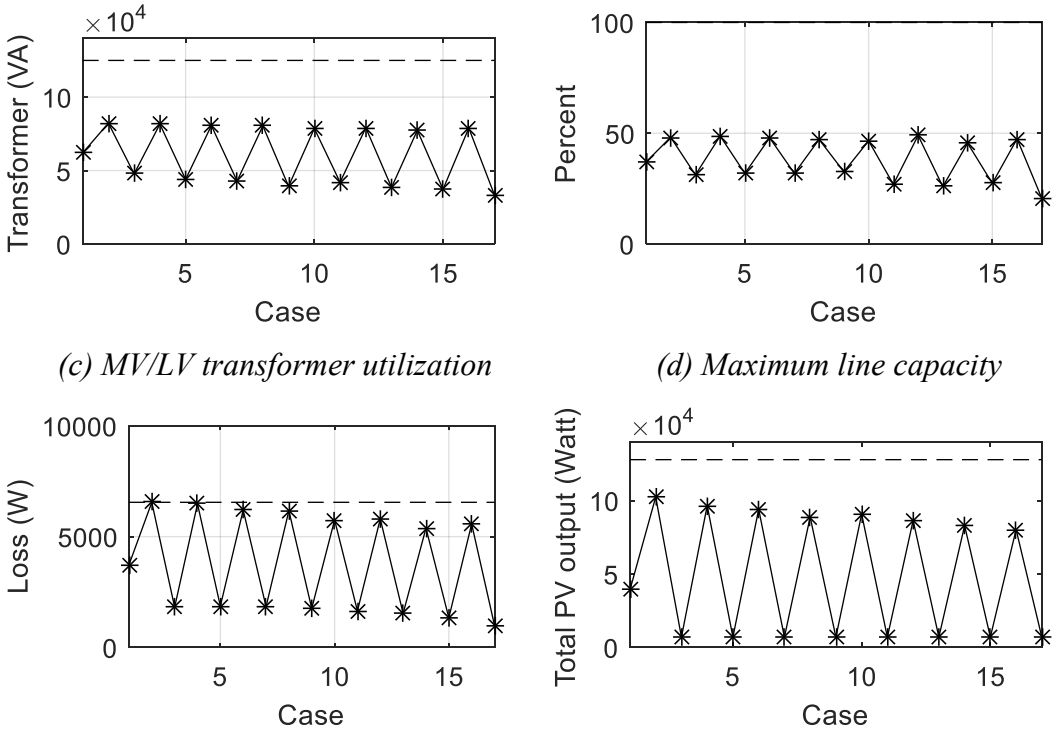

(c) MV/LV transformer utilization *(d) Maximum line capacity*

(e) System loss *(f) Total real power output from PV systems*

Figure 7.23 The results of the set of uncertainty

7.4.2.6 At The Day 8 November 2014

The parameter assessment will be analyzed by central control through 2-stage PSO process. According to the set of uncertainty at the day 8 November 2014 in Table 6.13, the optimal objective value in equation (5.81) is 50,677.69 W and the results of optimal parameter setting can be shown in Table 7.12. Considering only the case $z \in \{z1, z2, \dots, z17\}$, the power flow results can be shown in Figure 7.24 and they are within the limit. The total real power output from PV systems at maximum value is 104,035.63 W at the case $z2$.

Table 7.12 Parameter setting of each connected PV system

PV Name	Parameter Setting					
	V_{cri}	δ_p	K_1	K_2	V_q	δ_q
PV1	1.101	0.014	0.204	0.728	1.043	0.01
PV2	1.099	0.014	0.172	0.613	1.043	0.016
PV3	1.101	0.012	0.106	0.852	1.043	0.014
PV4	1.096	0.013	0.224	0.891	1.058	0.02

PV Name	Parameter Setting					
	V_{cri}	δ_p	K_1	K_2	V_q	δ_q
PV5	1.082	0.01	0.196	0.957	1.036	0.011
PV6	1.107	0.014	0.213	0.97	1.012	0.013
PV7	1.107	0.013	0.089	0.619	1.043	0.017
PV8	1.106	0.01	0.216	0.812	1.082	0.01
PV9	1.082	0.01	0.217	1.152	1.049	0.019
PV10	1.089	0.01	0.251	0.826	1.045	0.016
PV11	1.093	0.016	0.23	0.854	1.038	0.017
PV12	1.074	0.021	0.638	0.739	1.049	0.015
PV13	1.136	0.014	0.133	0.796	1.047	0.015
PV14	1.082	0.028	0.182	0.78	1.042	0.015
PV15	1.075	0.01	0.214	0.844	1.046	0.023
PV16	1.095	0.016	0.549	0.706	1.038	0.015
PV17	1.105	0.014	0.229	0.87	1.027	0.011
PV18	1.083	0.011	0.111	0.803	1.021	0.018

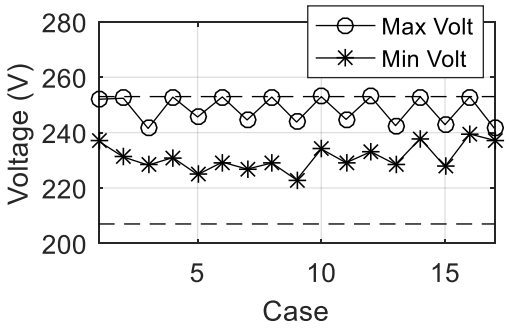

(a) Minimum and maximum phase voltage

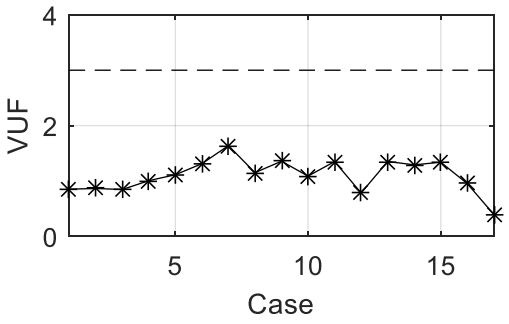

(b) Maximum VUF

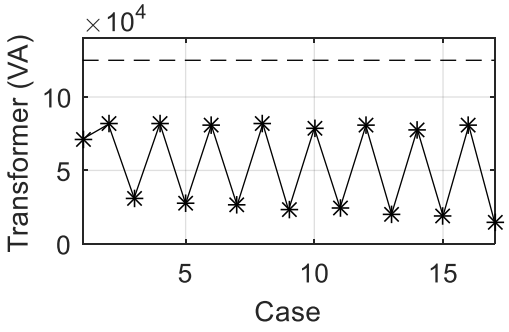

(c) MV/LV transformer utilization

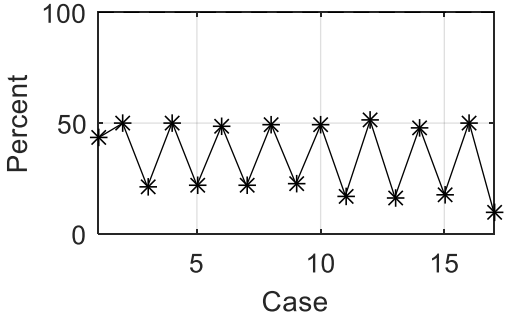

(d) Maximum line capacity

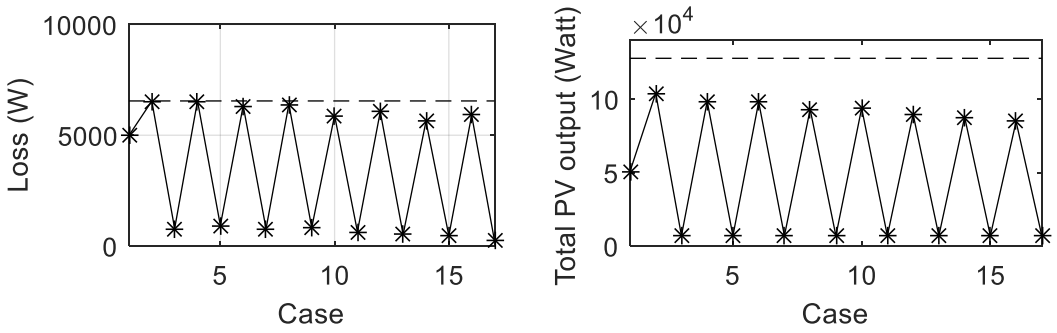

(e) System loss *(f) Total real power output from PV systems*

Figure 7.24 The results of the set of uncertainty

7.4.2.7 At The Day 9 November 2014

The parameter assessment will be analyzed by central control through 2-stage PSO process. According to the set of uncertainty at the day 9 November 2014 in Table 6.14, the optimal objective value in equation (5.81) is 28,240.01 W and the results of optimal parameter setting can be shown in Table 7.13. Considering only the case $z \in \{z1, z2, \ldots, z17\}$, the power flow results can be shown in Figure 7.25 and they are within the limit. The total real power output from PV systems at maximum value is 102,564.62 W at the case $z2$.

Table 7.13 Parameter setting of each connected PV system

PV Name	Parameter Setting					
	V_{cri}	δ_p	K_1	K_2	V_q	δ_q
PV1	1.097	0.024	0.733	1.2	1.017	0.098
PV2	1.105	0.049	0.742	1.658	1.039	0.1
PV3	1.101	0.024	0.621	0.81	1.028	0.1
PV4	1.129	0.032	0.154	0.75	1.008	0.1
PV5	1.081	0.03	0.2	1.114	1.016	0.099
PV6	1.105	0.01	0.258	0.966	1.015	0.079
PV7	1.122	0.031	0.552	1.471	1.01	0.1
PV8	1.115	0.029	0.52	1.21	1.015	0.1
PV9	1.082	0.013	0.338	1.201	1.027	0.098
PV10	1.089	0.013	0.531	1.255	1.014	0.1
PV11	1.09	0.021	0.881	1.258	1	0.078
PV12	1.056	0.039	0.99	1.212	1.057	0.052
PV13	1.103	0.01	0.627	1.397	1.032	0.1
PV14	1.069	0.052	0.67	1.542	1.013	0.065
PV15	1.068	0.024	0.524	1.514	1.031	0.099
PV16	1.107	0.04	0.369	1.354	1.031	0.077
PV17	1.125	0.055	0.616	0.962	1.024	0.099
PV18	1.072	0.055	0.496	1.267	1.02	0.095

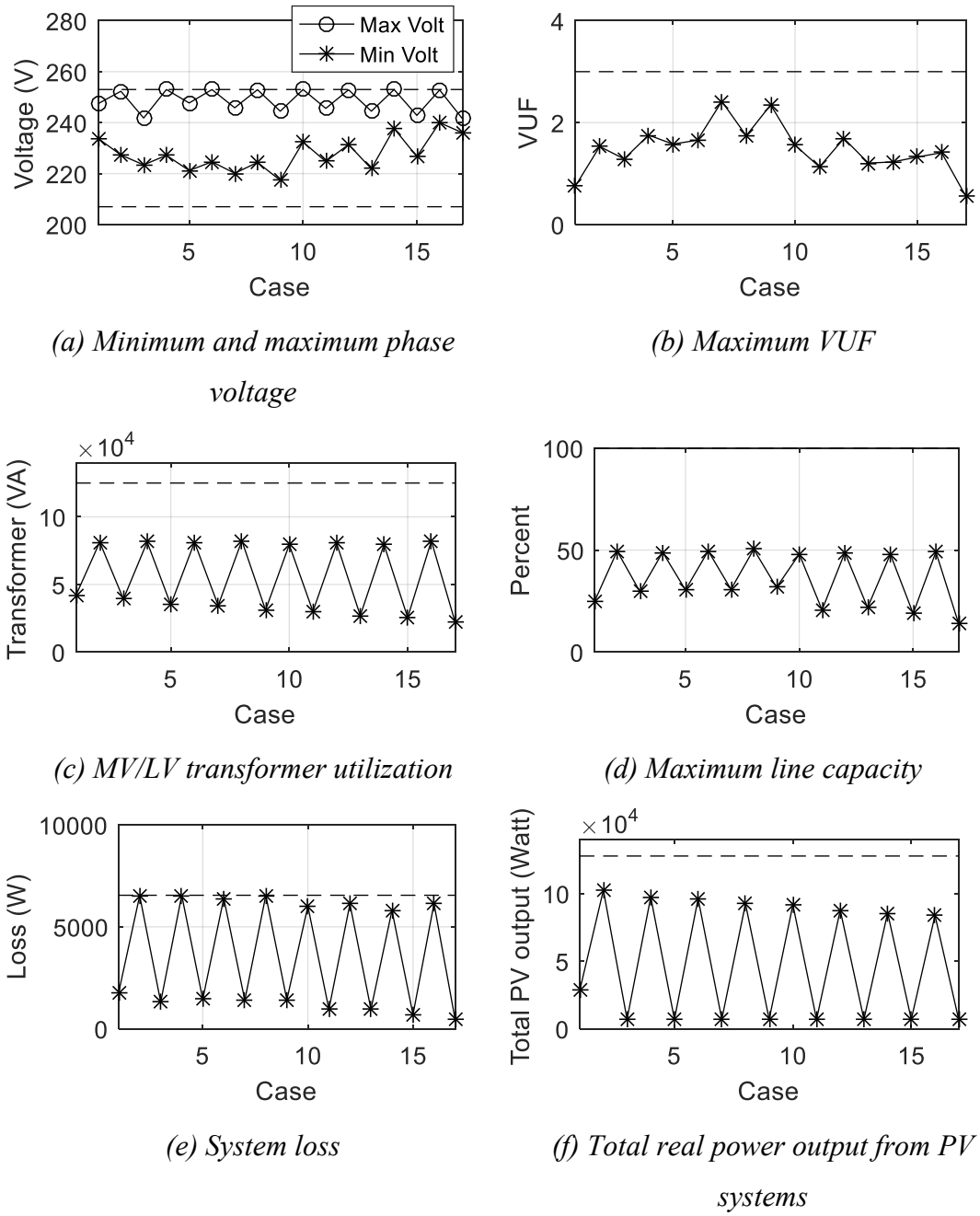

(a) Minimum and maximum phase voltage

(b) Maximum VUF

(c) MV/LV transformer utilization

(d) Maximum line capacity

(e) System loss

(f) Total real power output from PV systems

Figure 7.25 The results of the set of uncertainty

Comparing Subsection 7.4.1 that the parameters of are adjusted in every one week and Subsection 7.4.2 that the parameters are adjusted in every one day, the summary can be shown in Table 7.14. It indicates that adjustment per one day is better than adjustment per one week. According to percent change of adjustment per one day, the objective values are better than around 3.02% and the maximum total real power outputs from PV systems at the case z2 are better than around 2.71%.

Table 7.14 The comparison of the parameters adjustment per one week or one day

Day at Nov 2014	Adjustment per one week		Adjustment per one day		Percent Change of Adjustment per One Day	
	Obj. Value	Max P Output	Obj. Value	Max P Output	Obj. Value	Max P Output
3	49,472.2	95,251.06	51,565.54	98,597.83	+4.23%	+3.51%
4	44,940.84	101,056.21	46,719.23	103,531.01	+3.96%	+2.45%
5	41,080.51	97,917.23	44,143.82	102,481.48	+7.46%	+4.66%
6	35,955.41	99,675.54	36,814.38	101,971.62	+2.39%	+2.30%
7	38,174.22	99,870.33	39,214.69	102,359.66	+2.73%	+2.49%
8	48299.55	99,839.99	50,677.69	104,035.63	+4.92%	+4.20%
9	29586.98	103,209.82	28,240.01	102,564.62	-4.55%	-0.63%
				Mean Change	+3.02%	+2.71%

7.5 Local Control Adjustment in Every One Week or One Day Of Piecewise Linear Local Control Function

In this subsection, the comparison between (7.5.1) adjustment per one week and (7.5.2) adjustment per one day is determined for the suitable operation of coordination between central and local control. The piecewise local control function is selected in this subsection.

7.5.1 Adjustment Per One Week

In this subsection, the parameters setting in Table 7.5 is applied. The simulations are divided into 7 parts: (7.5.1.1) at the day 3 November 2014; (7.5.1.2) at the day 4 November 2014; (7.5.1.3) at the day 5 November 2014; (7.5.1.4) at the day 6 November 2014; (7.5.1.5) at the day 7 November 2014; (7.5.1.6) at the day 8 November 2014; (7.5.1.7) at the day 9 November 2014. The objective of this subsection is to determine the simulation results when (1) the set of uncertainty of each day is applied and (2) the parameters setting in Table 7.5 at the week 3-9 November 2014 is applied.

7.5.1.1 At The Day 3 November 2014

According to the set of uncertainty at the day 3 November 2014 in Table 6.8, the calculated objective value in equation (5.81) is 48,909.94 W. Considering the case $z \in \{z1, z2, \dots, z17\}$, the power flow results can be shown in Figure 7.26 and they are

within the limit. The total real power output from PV systems at maximum value is 94,246.95 W at the case $z2$.

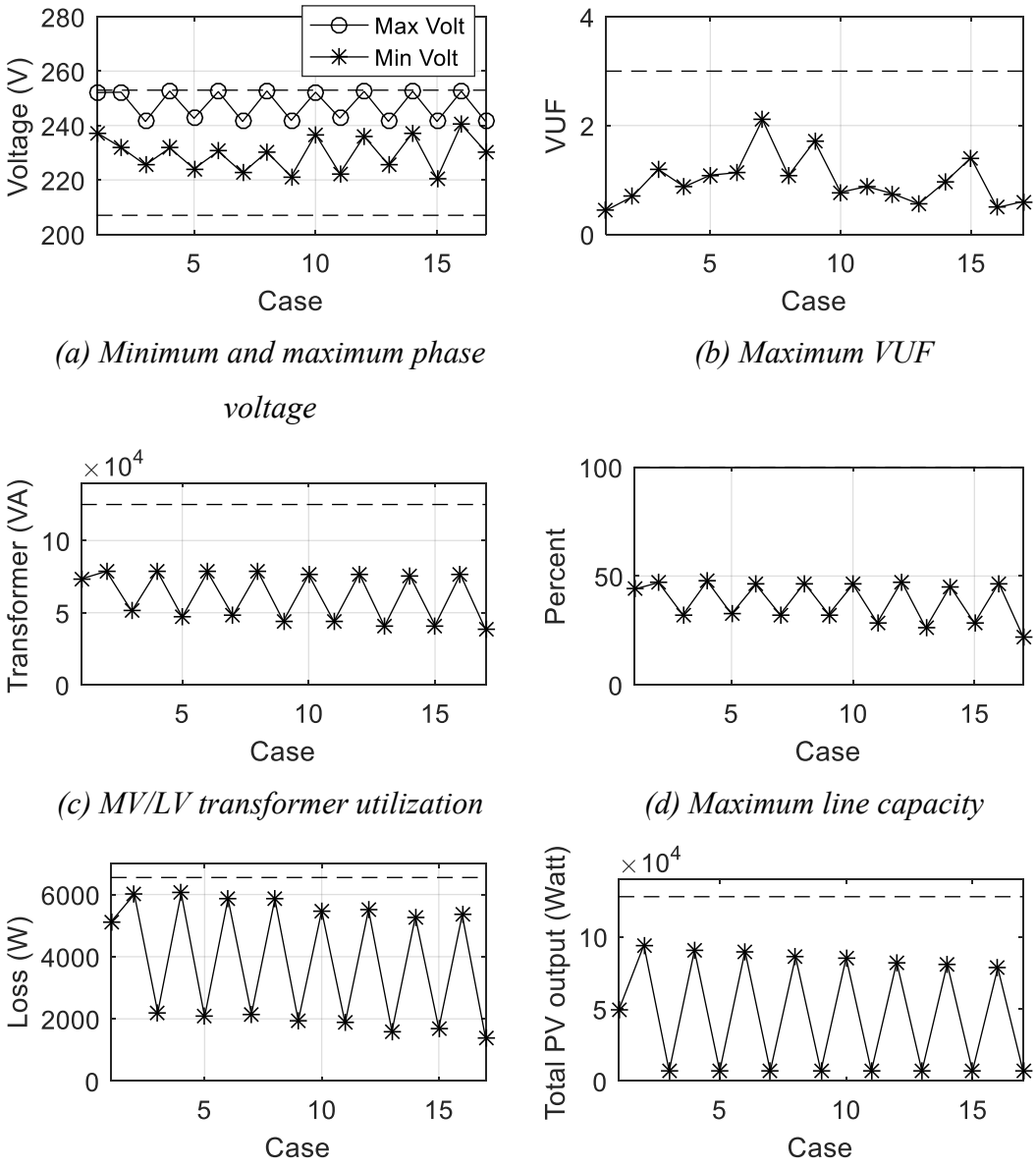

(a) Minimum and maximum phase voltage

(b) Maximum VUF

(c) MV/LV transformer utilization

(d) Maximum line capacity

(e) System loss

(f) Total real power output from PV systems

Figure 7.26 The results of the set of uncertainty

7.5.1.2 At The Day 4 November 2014

According to the set of uncertainty at the day 4 November 2014 in Table 6.9, the calculated objective value in equation (5.81) is 44,159.97 W. Considering the case $z \in \{z1, z2, \ldots, z17\}$, the power flow results can be shown in Figure 7.27 and they are

within the limit. The total real power output from PV systems at maximum value is 99,795.17 W at the case $z2$.

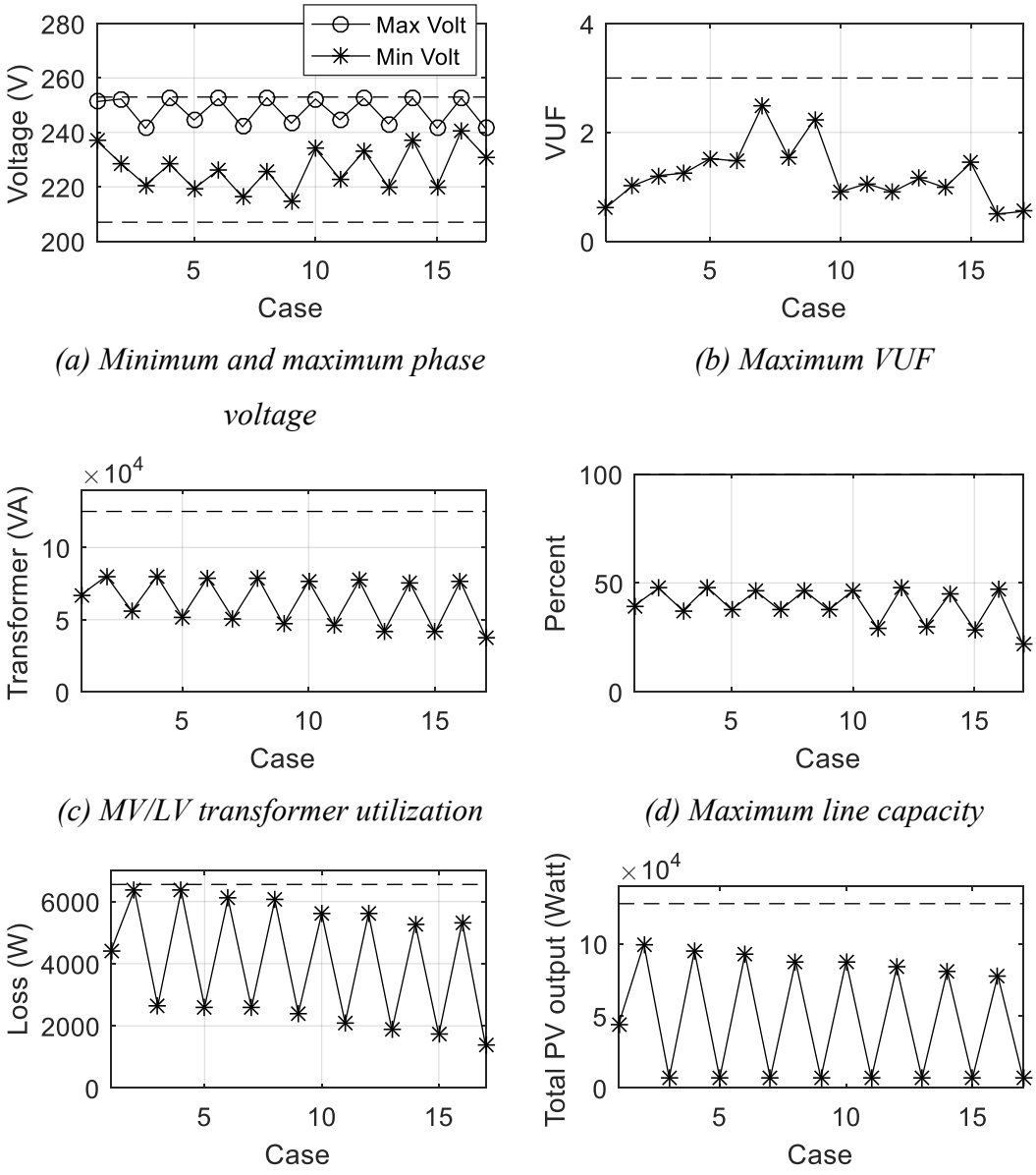

(a) Minimum and maximum phase voltage

(b) Maximum VUF

(c) MV/LV transformer utilization

(d) Maximum line capacity

(e) System loss

(f) Total real power output from PV systems

Figure 7.27 The results of the set of uncertainty

7.5.1.3 At The Day 5 November 2014

According to the set of uncertainty at the day 5 November 2014 in Table 6.10, the calculated objective value in equation (5.81) is 40,287.06 W. Considering the case $z \in \{z1, z2, \ldots, z17\}$, the power flow results can be shown in Figure 7.28 and they are

within the limit. The total real power output from PV systems at maximum value is 96,673.20 W at the case $z2$.

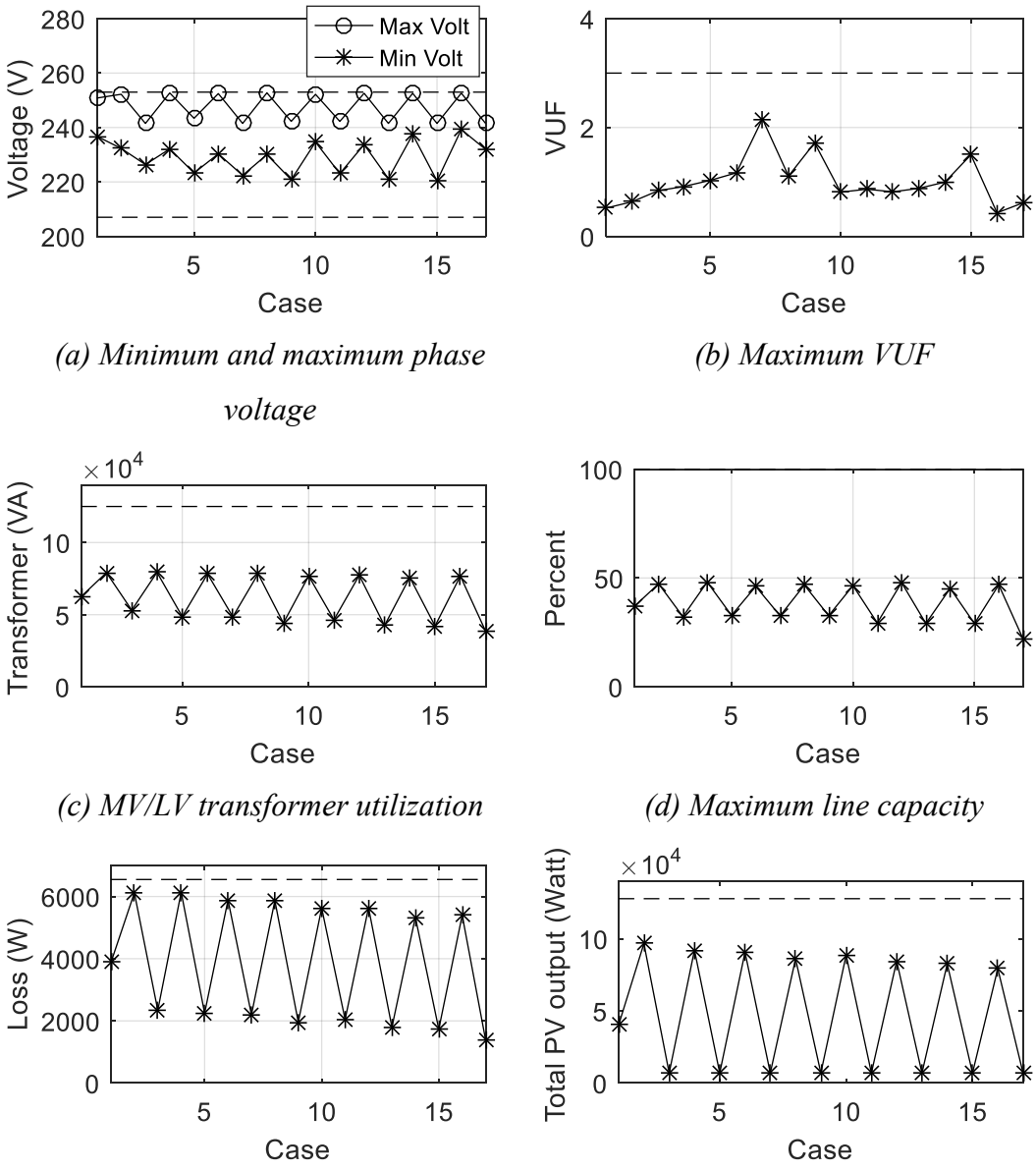

(a) Minimum and maximum phase voltage

(b) Maximum VUF

(c) MV/LV transformer utilization

(d) Maximum line capacity

(e) System loss

(f) Total real power output from PV systems

Figure 7.28 The results of the set of uncertainty

7.5.1.4 At The Day 6 November 2014

According to the set of uncertainty at the day 6 November 2014 in Table 6.11, the calculated objective value in equation (5.81) is 35,170.29 W. Considering the case $z \in \{z1, z2, \ldots, z17\}$, the power flow results can be shown in Figure 7.29 and they are

within the limit. The total real power output from PV systems at maximum value is 98,521.91 W at the case $z2$.

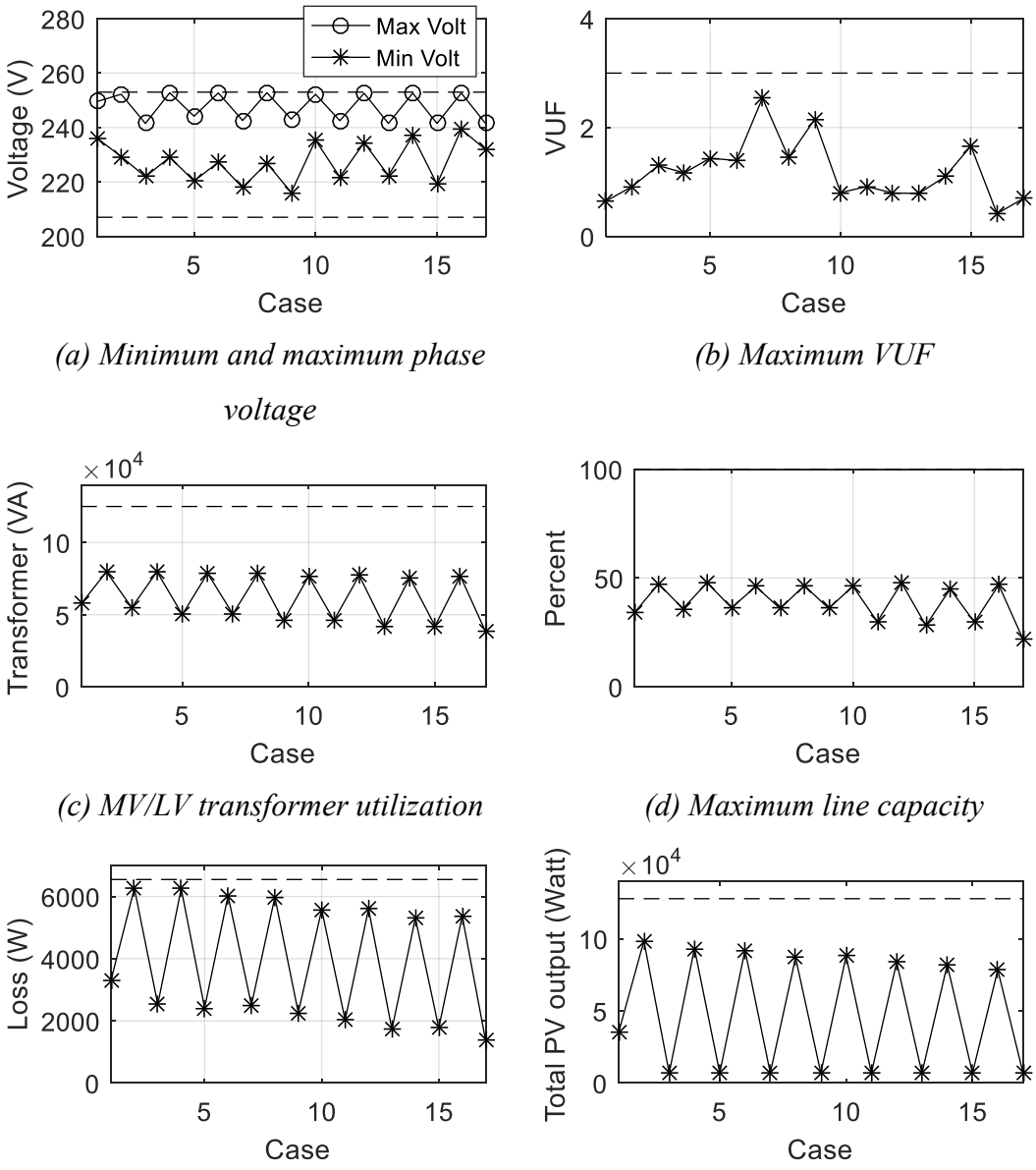

(a) Minimum and maximum phase voltage

(b) Maximum VUF

(c) MV/LV transformer utilization

(d) Maximum line capacity

(e) System loss

(f) Total real power output from PV systems

Figure 7.29 The results of the set of uncertainty

7.5.1.5 At The Day 7 November 2014

According to the set of uncertainty at the day 7 November 2014 in Table 6.12, the calculated objective value in equation (5.81) is 37,402.76 W. Considering the case $z \in \{z1, z2, \ldots, z17\}$, the power flow results can be shown in Figure 7.30 and they are

within the limit. The total real power output from PV systems at maximum value is 98,607.95 W at the case $z2$.

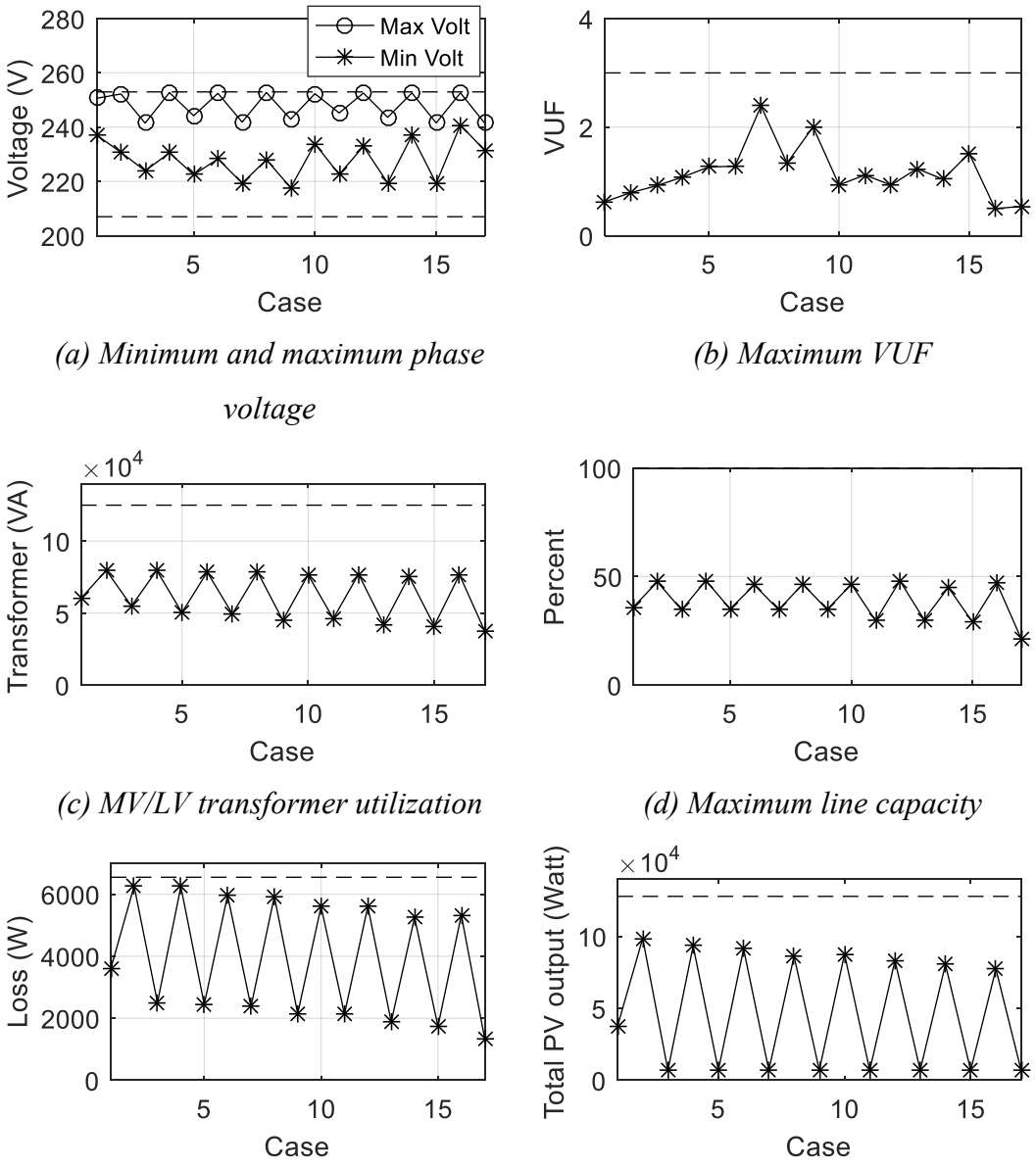

(a) Minimum and maximum phase voltage

(b) Maximum VUF

(c) MV/LV transformer utilization

(d) Maximum line capacity

(e) System loss

(f) Total real power output from PV systems

Figure 7.30 The results of the set of uncertainty

7.5.1.6 At The Day 8 November 2014

According to the set of uncertainty at the day 8 November 2014 in Table 6.13, the calculated objective value in equation (5.81) is 47,478.34 W. Considering the case $z \in \{z1, z2, \ldots, z17\}$, the power flow results can be shown in Figure 7.31 and they are

within the limit. The total real power output from PV systems at maximum value is 98,548.21 W at the case $z2$.

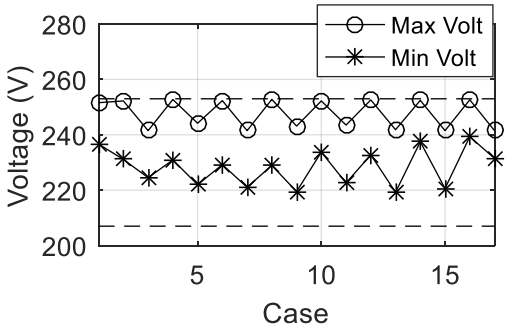

(a) Minimum and maximum phase voltage

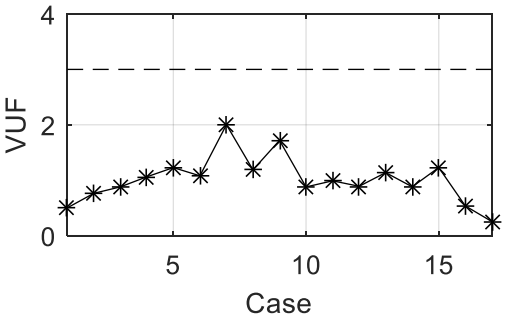

(b) Maximum VUF

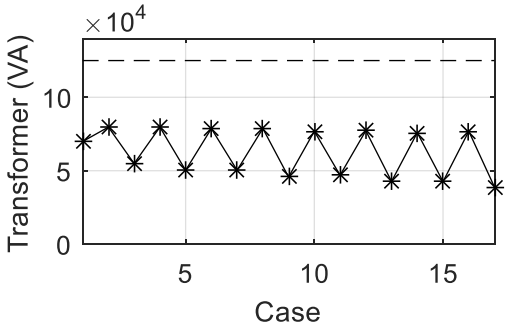

(c) MV/LV transformer utilization

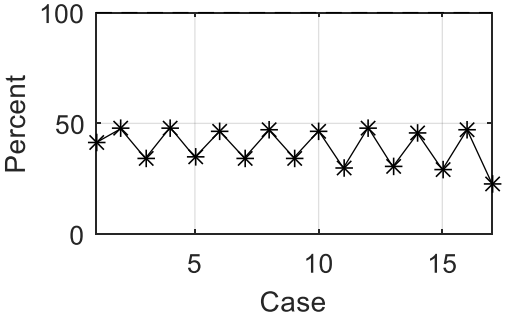

(d) Maximum line capacity

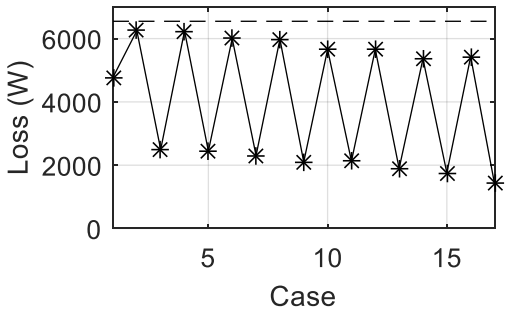

(e) System loss

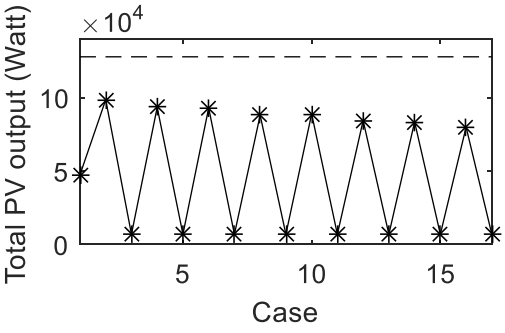

(f) Total real power output from PV systems

Figure 7.31 The results of the set of uncertainty

7.5.1.7 At The Day 9 November 2014

According to the set of uncertainty at the day 9 November 2014 in Table 6.14, the calculated objective value in equation (5.81) is 28,988.39 W. Considering the case $z \in \{z1, z2, \ldots, z17\}$, the power flow results can be shown in Figure 7.32 and they are

within the limit. The total real power output from PV systems at maximum value is 101,836.80 W at the case $z2$.

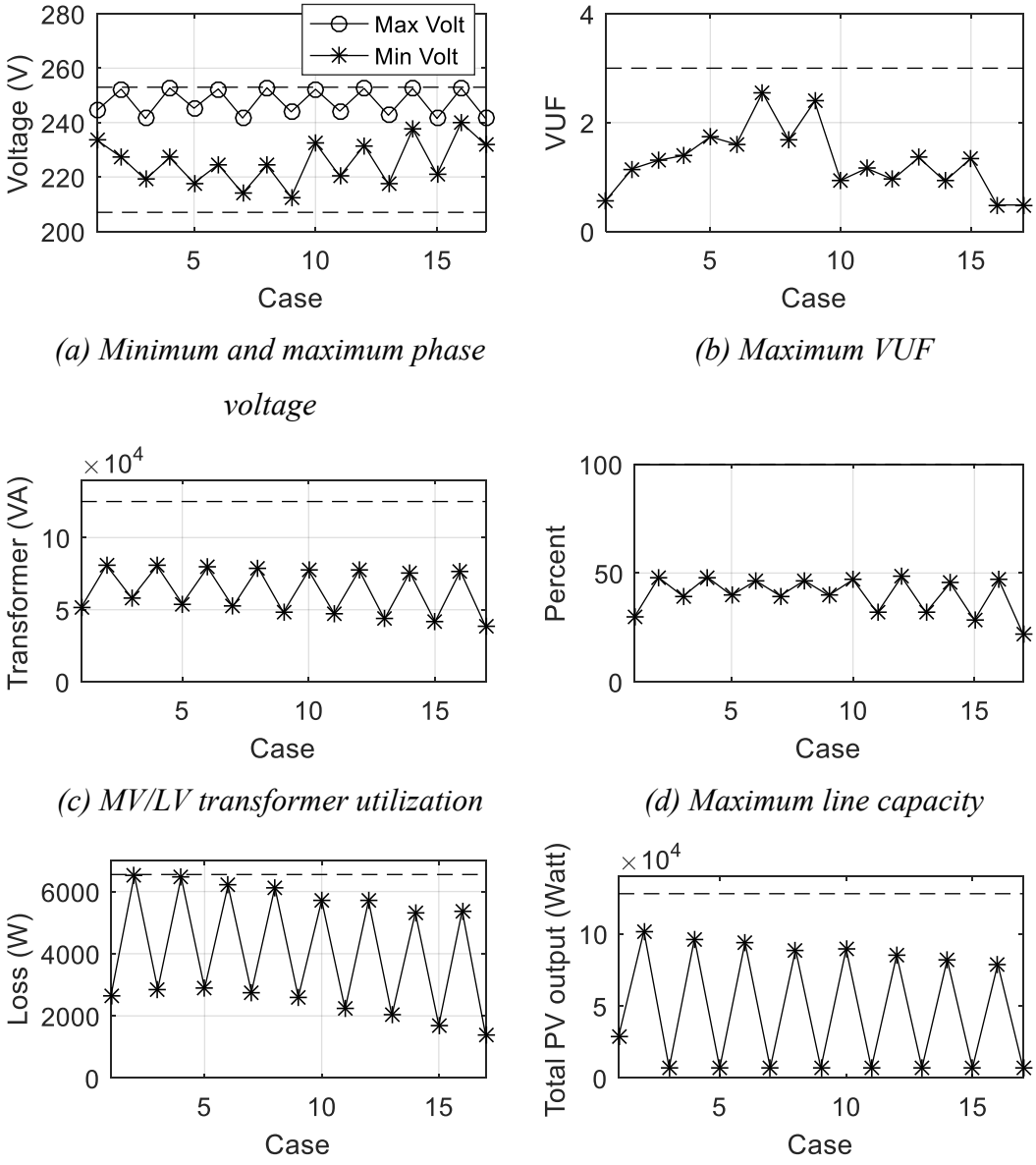

(a) Minimum and maximum phase voltage

(b) Maximum VUF

(c) MV/LV transformer utilization

(d) Maximum line capacity

(e) System loss

(f) Total real power output from PV systems

Figure 7.32 The results of the set of uncertainty

7.5.2 Adjustment Per One Day

In this subsection, the optimal parameters setting will be searched through 2-stage PSO. The set of uncertainty of each day will be applied. The simulation results are divided into seven subsections: (7.5.2.1) at the day 3 November 2014; (7.5.2.2) at

the day 4 November 2014; (7.5.2.3) at the day 5 November 2014; (7.5.2.4) at the day 6 November 2014; (7.5.2.5) at the day 7 November 2014; (7.5.2.6) at the day 8 November 2014; (7.5.2.7) at the day 9 November 2014. The results of Subsection 7.5.2 will be compared to subsection 7.5.1.

7.5.2.1 At The Day 3 November 2014

The parameter assessment will be analyzed by central control through 2-stage PSO process. According to the set of uncertainty at the day 3 November 2014 in Table 6.8, the optimal objective value in equation (5.81) is 52,107.71 W and the results of optimal parameter setting can be shown in Table 7.15. Considering only the case $z \in \{z1, z2, \dots, z17\}$, the power flow results can be shown in Figure 7.33 and they are within the limit. The total real power output from PV systems at maximum value is 99,253.88 W at the case $z2$.

Table 7.15 Parameter setting of each connected PV system

PV Name	Parameter Setting					
	V_{p1}	V_{p2}	K_1	K_2	V_{q1}	V_{q2}
PV1	1.067	1.096	0.98	-0.862	1.02	1.09
PV2	1.093	1.107	0.968	-0.954	0.998	1.075
PV3	1.097	1.107	0.991	-0.89	1.001	1.088
PV4	1.095	1.108	0.974	-0.825	1.004	1.09
PV5	1.074	1.088	0.989	-0.88	1.018	1.089
PV6	1.076	1.097	0.974	-0.832	1.021	1.095
PV7	1.079	1.097	0.973	-0.84	1.002	1.089
PV8	1.094	1.112	0.985	-0.663	1.008	1.089
PV9	1.075	1.092	0.971	-0.834	1.016	1.088
PV10	1.065	1.107	0.986	-0.862	1.052	1.107
PV11	1.077	1.088	0.979	-0.776	1.024	1.11
PV12	1.069	1.09	0.996	-0.867	1.012	1.092
PV13	1.087	1.097	0.987	-0.968	1.018	1.095
PV14	1.071	1.092	0.977	-0.986	0.987	1.098
PV15	1.056	1.089	0.92	-0.846	1.012	1.077
PV16	1.079	1.092	0.973	-0.915	1.025	1.087
PV17	1.075	1.093	0.98	-0.891	1.018	1.084
PV18	1.061	1.1	0.971	-0.885	1.007	1.09

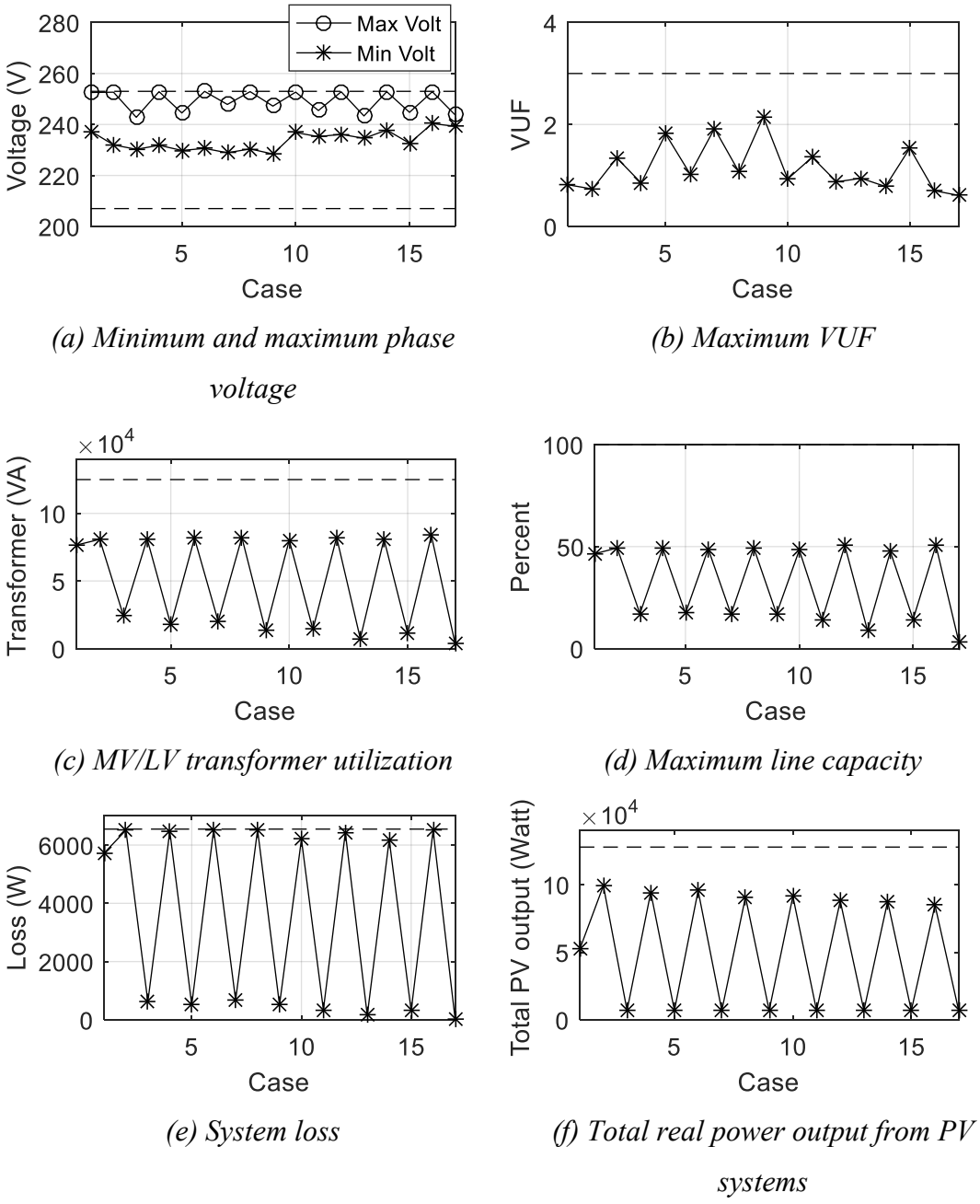

(a) Minimum and maximum phase voltage

(b) Maximum VUF

(c) MV/LV transformer utilization

(d) Maximum line capacity

(e) System loss

(f) Total real power output from PV systems

Figure 7.33 The results of the set of uncertainty

7.5.2.2 At The Day 4 November 2014

The parameter assessment will be analyzed by central control through 2-stage PSO process. According to the set of uncertainty at the day 4 November 2014 in Table 6.9, the optimal objective value in equation (5.81) is 45,218.94 W and the results of optimal parameter setting can be shown in Table 7.16. Considering only the case $z \in \{z1, z2, \ldots, z17\}$, the power flow results can be shown in Figure 7.34 and they are within

the limit. The total real power output from PV systems at maximum value is 101,908.35 W at the case $z2$.

Table 7.16 Parameter setting of each connected PV system

PV Name	Parameter Setting					
	V_{p1}	V_{p2}	K_1	K_2	V_{q1}	V_{q2}
PV1	1.09	1.107	0.112	-0.624	0.974	1.021
PV2	1.093	1.105	0.126	-0.58	0.974	1.037
PV3	1.084	1.106	0.132	-0.575	0.99	1.02
PV4	1.069	1.101	0.164	-0.694	0.988	1.011
PV5	1.068	1.086	0.158	-0.694	1.013	1.026
PV6	1.072	1.084	0.14	-0.665	0.97	1.03
PV7	1.084	1.099	0.305	-0.492	0.927	1.023
PV8	1.087	1.108	0.202	-0.317	0.947	1.008
PV9	1.068	1.09	0.34	-0.561	0.973	1.018
PV10	1.083	1.094	0.146	-0.576	0.972	1.017
PV11	1.09	1.109	0.159	-0.663	0.973	1.013
PV12	1.059	1.09	0.174	-0.63	0.977	1.011
PV13	1.03	1.069	0.132	-0.368	0.955	1.057
PV14	1.06	1.091	0.143	-0.599	0.973	1.044
PV15	1.077	1.088	0.128	-0.594	0.961	1.028
PV16	1.075	1.095	0.149	-0.568	0.998	1.05
PV17	1.071	1.088	0.141	-0.631	0.953	1.04
PV18	1.093	1.109	0.167	-0.595	0.977	1.024

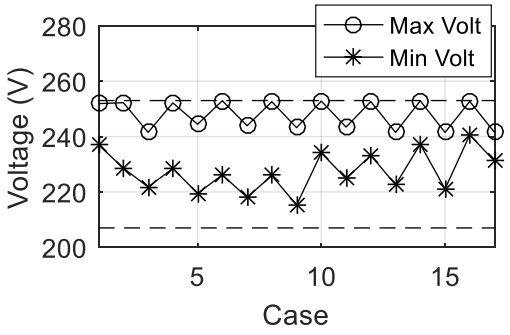

(a) Minimum and maximum phase voltage

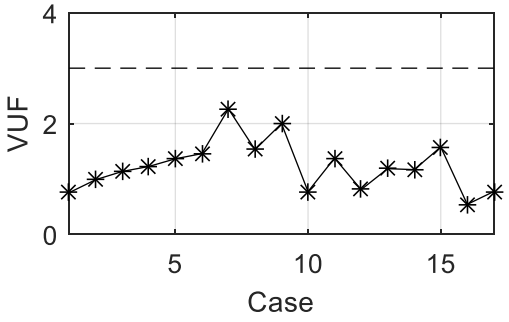

(b) Maximum VUF

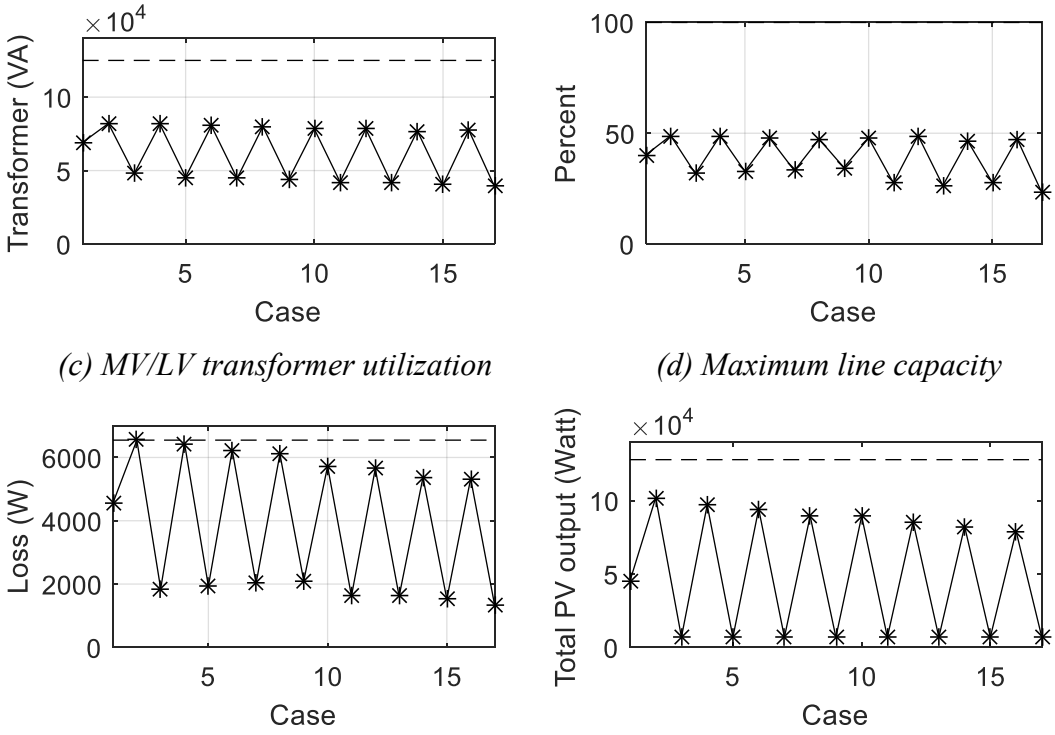

(c) MV/LV transformer utilization *(d) Maximum line capacity*

(e) System loss *(f) Total real power output from PV systems*

Figure 7.34 The results of the set of uncertainty

7.5.2.3 At The Day 5 November 2014

The parameter assessment will be analyzed by central control through 2-stage PSO process. According to the set of uncertainty at the day 5 November 2014 in Table 6.10, the optimal objective value in equation (5.81) is 43,312.98 W and the results of optimal parameter setting can be shown in Table 7.17. Considering only the case $z \in \{z1, z2, \ldots, z17\}$, the power flow results can be shown in Figure 7.35 and they are within the limit. The total real power output from PV systems at maximum value is 102,267.30 W at the case $z2$.

Table 7.17 Parameter setting of each connected PV system

PV Name	Parameter Setting					
	V_{p1}	V_{p2}	K_1	K_2	V_{q1}	V_{q2}
PV1	1.092	1.11	0.061	-0.624	0.938	0.988
PV2	1.094	1.104	0.075	-0.262	0.909	0.932
PV3	1.095	1.105	0.044	-0.608	0.933	0.999
PV4	1.074	1.091	0.024	-0.563	0.937	1

PV Name	Parameter Setting					
	V_{p1}	V_{p2}	K_1	K_2	V_{q1}	V_{q2}
PV5	1.071	1.098	0.036	-0.538	0.918	0.982
PV6	1.078	1.103	0.042	-0.567	0.904	1.001
PV7	1.081	1.093	0.014	-0.579	0.917	1.003
PV8	1.093	1.108	0.044	-0.498	0.919	0.971
PV9	1.082	1.092	0.038	-0.801	0.944	1.001
PV10	1.077	1.089	0.016	-0.541	0.953	0.995
PV11	1.09	1.104	0.026	-0.561	0.925	0.995
PV12	1.064	1.096	0.013	-0.452	0.949	1.001
PV13	1.098	1.11	0.031	-0.585	0.941	0.999
PV14	1.056	1.1	0	-0.511	0.937	0.954
PV15	1.073	1.088	0.048	-0.509	0.905	0.996
PV16	1.083	1.094	0.038	-0.601	0.939	1.009
PV17	1.094	1.104	0.054	-0.229	0.937	1.025
PV18	1.069	1.1	0.035	-0.546	0.93	1.012

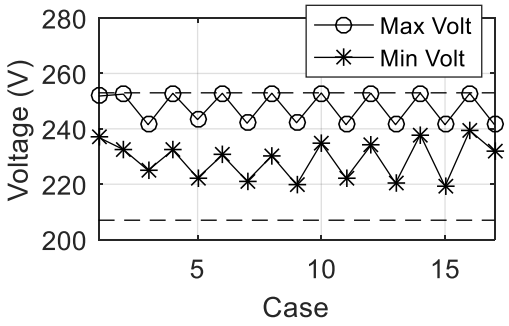

(a) Minimum and maximum phase voltage

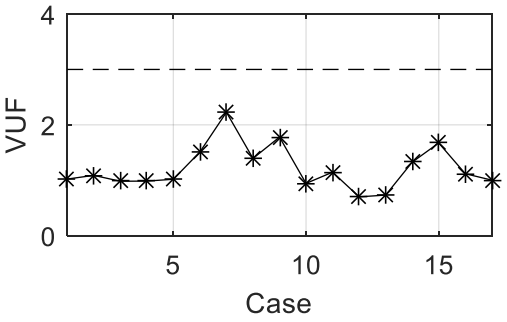

(b) Maximum VUF

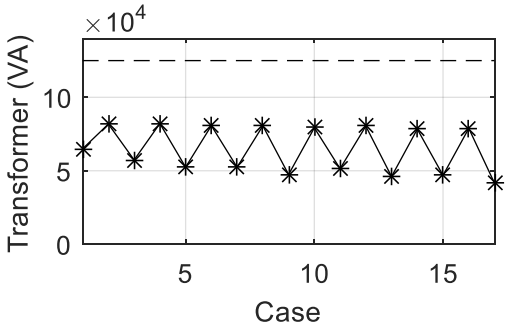

(c) MV/LV transformer utilization

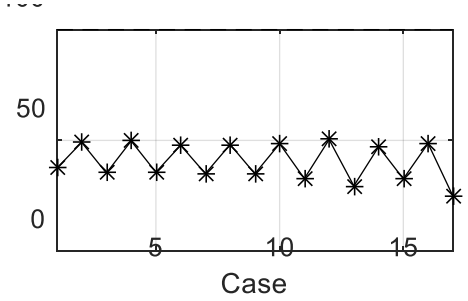

(d) Maximum line capacity

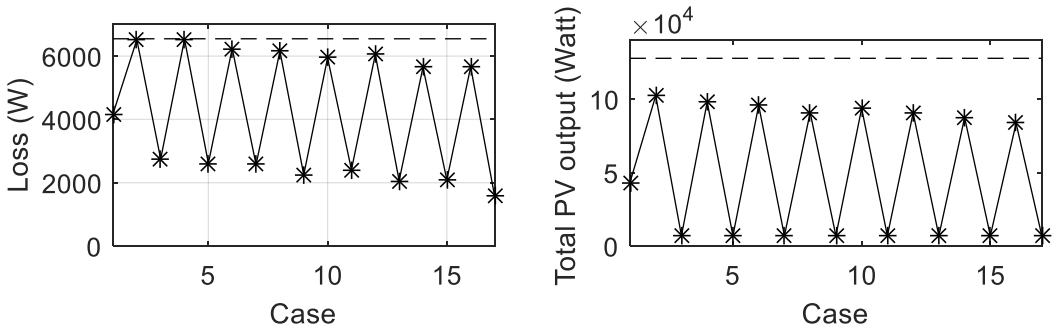

(e) System loss *(f) Total real power output from PV systems*

Figure 7.35 The results of the set of uncertainty

7.5.2.4 At The Day 6 November 2014

The parameter assessment will be analyzed by central control through 2-stage PSO process. According to the set of uncertainty at the day 6 November 2014 in Table 6.11, the optimal objective value in equation (5.81) is 37,396.81 W and the results of optimal parameter setting can be shown in Table 7.18. Considering only the case $z \in \{z1, z2, \ldots, z17\}$, the power flow results can be shown in Figure 7.36 and they are within the limit. The total real power output from PV systems at maximum value is 102,620.89 W at the case $z2$.

Table 7.18 Parameter setting of each connected PV system

PV Name	Parameter Setting					
	V_{p1}	V_{p2}	K_1	K_2	V_{q1}	V_{q2}
PV1	1.09	1.107	0.161	-0.508	0.963	1.021
PV2	1.089	1.103	0.177	-0.588	0.991	1.03
PV3	1.096	1.106	0.207	-0.574	0.96	1.027
PV4	1.072	1.093	0.185	-0.561	0.947	1.037
PV5	1.066	1.093	0.168	-0.542	0.939	1.023
PV6	1.077	1.091	0.022	-0.614	0.959	1.037
PV7	1.095	1.112	0.172	-0.569	0.948	1.044
PV8	1.085	1.095	0.205	-0.598	0.95	1.036
PV9	1.082	1.092	0.189	-0.536	0.954	1.032
PV10	1.08	1.091	0.17	-0.537	0.957	1.014
PV11	1.085	1.096	0.186	-0.609	0.96	1.097
PV12	1.053	1.103	0.276	-0.58	0.931	1.021
PV13	1.071	1.098	0.276	-0.569	0.954	1.026
PV14	1.063	1.093	0.272	-0.551	0.935	1.032
PV15	1.078	1.088	0.16	-0.395	0.956	1.066
PV16	1.081	1.091	0.177	-0.595	0.941	1.019

PV Name	Parameter Setting					
	V_{p1}	V_{p2}	K_1	K_2	V_{q1}	V_{q2}
PV17	1.098	1.112	0.385	-0.524	0.954	1.033
PV18	1.069	1.095	0.152	-0.452	0.955	1.006

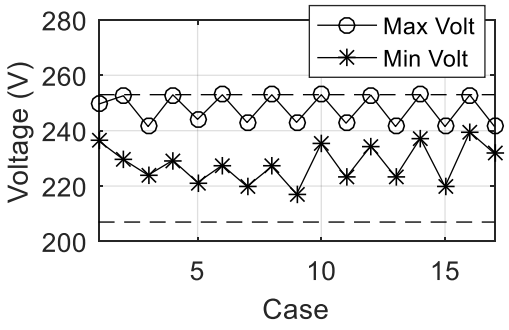

(a) Minimum and maximum phase voltage

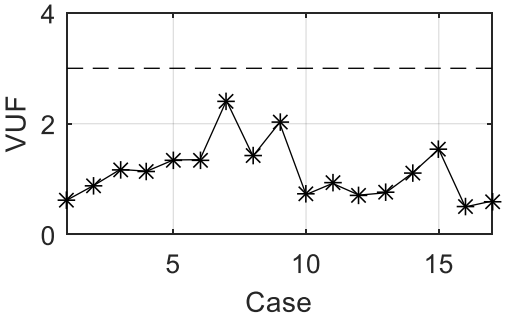

(b) Maximum VUF

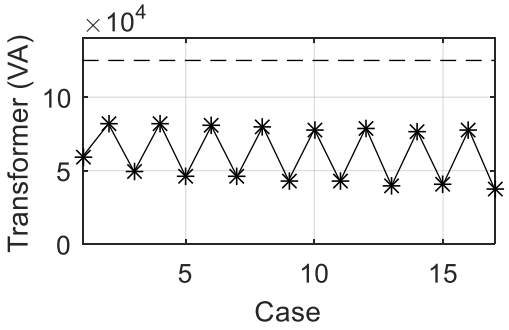

(c) MV/LV transformer utilization

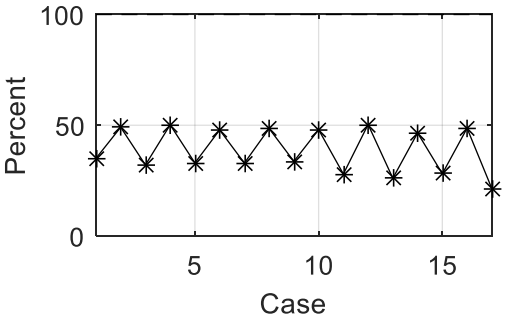

(d) Maximum line capacity

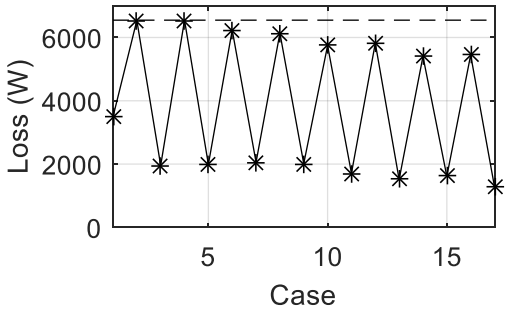

(e) System loss

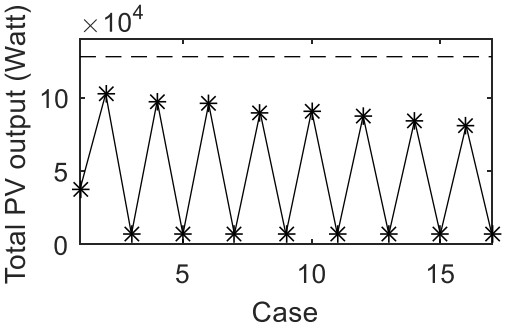

(f) Total real power output from PV systems

Figure 7.36 The results of the set of uncertainty

7.5.2.5 At The Day 7 November 2014

The parameter assessment will be analyzed by central control through 2-stage PSO process. According to the set of uncertainty at the day 7 November 2014 in Table 6.12, the optimal objective value in equation (5.81) is 39,413.84 W and the results of optimal parameter setting can be shown in Table 7.19. Considering only the case $z \in \{z1, z2, \ldots, z17\}$, the power flow results can be shown in Figure 7.37 and they are within the limit. The total real power output from PV systems at maximum value is 102,248.17 W at the case $z2$.

Table 7.19 Parameter setting of each connected PV system

PV Name	Parameter Setting					
	V_{p1}	V_{p2}	K_1	K_2	V_{q1}	V_{q2}
PV1	1.088	1.098	0.667	-0.567	0.924	1.023
PV2	1.093	1.103	0.529	-0.697	0.915	0.984
PV3	1.093	1.108	0.548	-0.636	0.949	1.038
PV4	1.086	1.106	0.527	-0.641	0.906	1.041
PV5	1.058	1.109	0.897	-0.676	0.911	1.11
PV6	1.085	1.11	0.596	-0.304	0.922	1.018
PV7	1.082	1.104	0.499	-0.16	0.942	1.017
PV8	1.1	1.111	0.531	-0.6	0.916	1.029
PV9	1.081	1.091	0.407	-0.89	0.914	0.983
PV10	1.081	1.091	0.421	-0.179	0.918	1.011
PV11	1.089	1.105	0.48	-0.47	0.907	1.039
PV12	1.06	1.094	0.523	-0.499	0.941	1.054
PV13	1.057	1.087	0.515	-0.851	0.926	0.989
PV14	1.06	1.091	0.571	-0.597	0.924	1.01
PV15	1.075	1.087	0.665	-0.476	0.906	1.028
PV16	1.082	1.092	0.437	-0.607	0.918	1.101
PV17	1.093	1.103	0.428	-0.702	0.93	1.024
PV18	1.091	1.103	0.405	-0.667	0.919	1.036

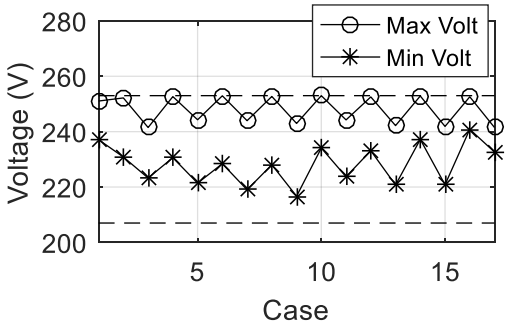

(a) Minimum and maximum phase voltage

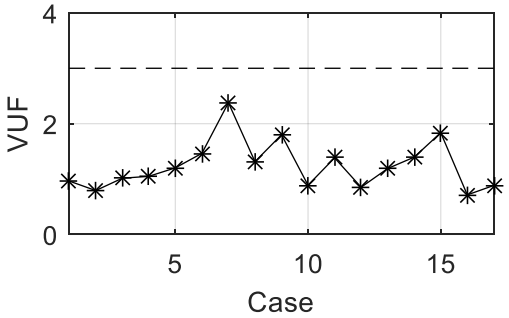

(b) Maximum VUF

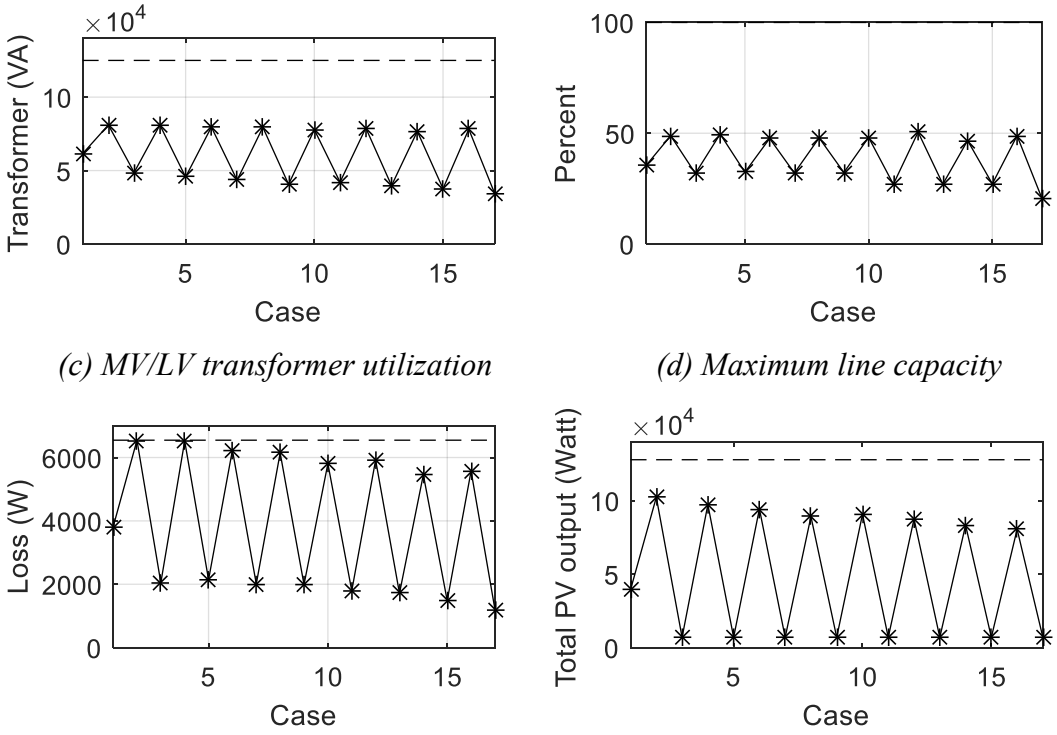

(c) MV/LV transformer utilization *(d) Maximum line capacity*

(e) System loss *(f) Total real power output from PV systems*

Figure 7.37 The results of the set of uncertainty

7.5.2.6 At The Day 8 November 2014

The parameter assessment will be analyzed by central control through 2-stage PSO process. According to the set of uncertainty at the day 8 November 2014 in Table 6.13, the optimal objective value in equation (5.81) is 50,026.80 W and the results of optimal parameter setting can be shown in Table 7.20. Considering only the case $z \in \{z1, z2, \ldots, z17\}$, the power flow results can be shown in Figure 7.38 and they are within the limit. The total real power output from PV systems at maximum value is 103,326.47 W at the case $z2$.

Table 7.20 Parameter setting of each connected PV system

PV Name	Parameter Setting					
	V_{p1}	V_{p2}	K_1	K_2	V_{q1}	V_{q2}
PV1	1.088	1.11	0.743	-0.598	1.017	1.028
PV2	1.067	1.11	0.773	-0.596	0.999	1.06
PV3	1.095	1.105	0.359	-0.425	1.076	1.086
PV4	1.074	1.099	0.894	-0.57	0.944	0.971

PV Name	Parameter Setting					
	V_{p1}	V_{p2}	K_1	K_2	V_{q1}	V_{q2}
PV5	1.072	1.094	0.865	-0.924	0.938	1.001
PV6	1.098	1.11	0.9	-0.52	1.057	1.074
PV7	1.087	1.108	0.782	-0.29	1.06	1.07
PV8	1.089	1.099	0.725	-0.652	0.933	0.991
PV9	1.076	1.093	0.792	-0.911	1.007	1.028
PV10	1.085	1.097	0.768	-0.761	1.085	1.097
PV11	1.084	1.099	0.881	-0.938	0.97	1.029
PV12	1.04	1.1	0.704	-0.666	1.012	1.038
PV13	1.086	1.104	0.833	-0.43	1	1.054
PV14	1.053	1.103	0.805	-0.642	1.029	1.043
PV15	1.087	1.102	0.811	-0.582	0.9	1.04
PV16	1.089	1.107	0.413	-0.076	1.032	1.065
PV17	1.099	1.109	0.784	-0.437	1.033	1.048
PV18	1.047	1.099	0.841	-0.692	1.037	1.055

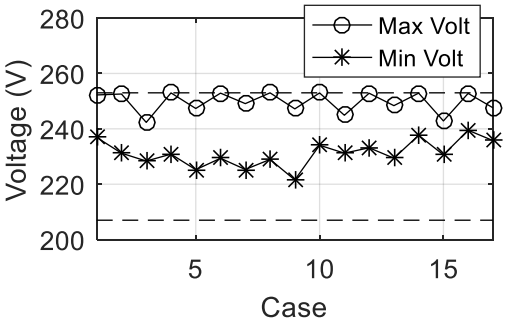

(a) Minimum and maximum phase voltage

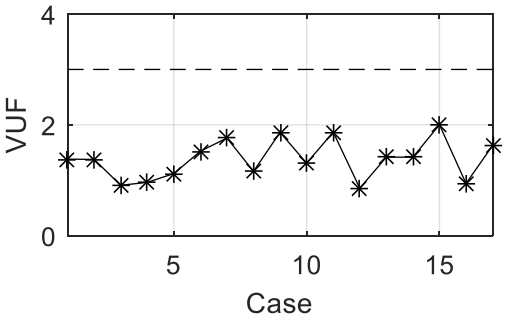

(b) Maximum VUF

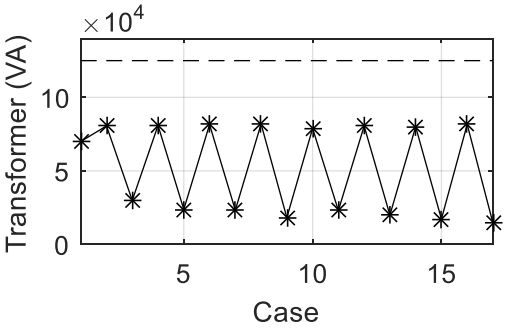

(c) MV/LV transformer utilization

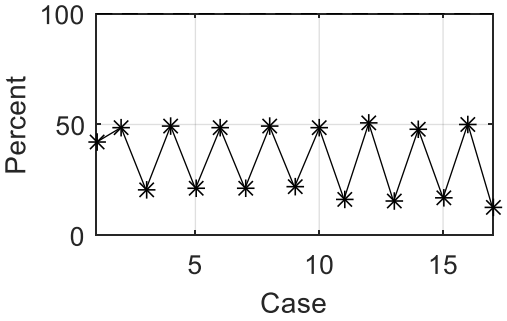

(d) Maximum line capacity

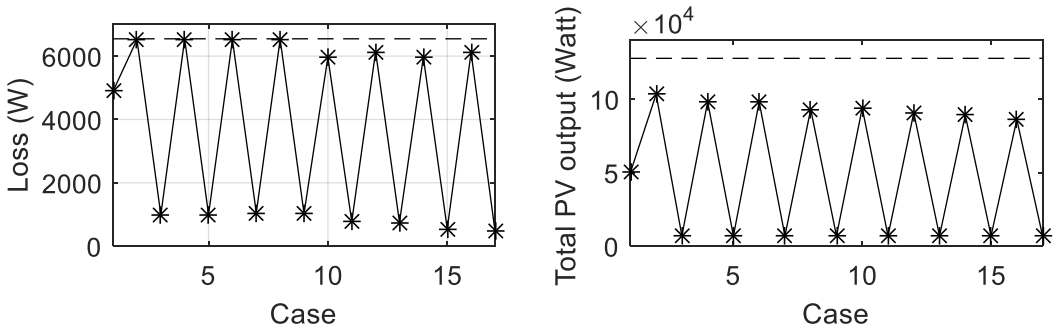

(e) System loss *(f) Total real power output from PV systems*

Figure 7.38 The results of the set of uncertainty

7.5.2.7 At The Day 9 November 2014

The parameter assessment will be analyzed by central control through 2-stage PSO process. According to the set of uncertainty at the day 9 November 2014 in Table 6.14, the optimal objective value in equation (5.81) is 29,809.38 W and the results of optimal parameter setting can be shown in Table 7.21. Considering only the case $z \in \{z1, z2, \dots, z17\}$, the power flow results can be shown in Figure 7.39 and they are within the limit. The total real power output from PV systems at maximum value is 104,640.64 W at the case $z2$.

Table 7.21 Parameter setting of each connected PV system

PV Name	Parameter Setting					
	V_{p1}	V_{p2}	K_1	K_2	V_{q1}	V_{q2}
PV1	1.09	1.105	0.035	-0.586	0.933	1.065
PV2	1.094	1.104	0.051	-0.586	0.935	1.042
PV3	1.094	1.105	0.06	-0.525	0.945	1.042
PV4	1.078	1.107	0.067	-0.37	0.953	1.064
PV5	1.06	1.11	0.023	-0.54	0.955	1.069
PV6	1.096	1.108	0.032	-0.591	0.948	1.069
PV7	1.079	1.099	0.042	-0.515	0.959	1.087
PV8	1.095	1.111	0.038	-0.505	0.986	1.074
PV9	1.062	1.092	0.017	-0.555	0.95	1.099
PV10	1.084	1.094	0.063	-0.504	0.947	1.068
PV11	1.057	1.107	0.067	-0.778	0.972	1.082
PV12	1.056	1.097	0.08	-0.507	0.943	1.067
PV13	1.095	1.115	0.055	-0.619	0.945	1.058
PV14	1.055	1.093	0.072	-0.542	0.941	1.057
PV15	1.066	1.084	0.008	-0.576	0.949	1.062
PV16	1.081	1.091	0.01	-0.451	0.955	1.004

PV Name	Parameter Setting					
	V_{p1}	V_{p2}	K_1	K_2	V_{q1}	V_{q2}
PV17	1.069	1.105	0.082	-0.536	0.949	1.059
PV18	1.058	1.099	0.027	-0.573	0.963	1.067

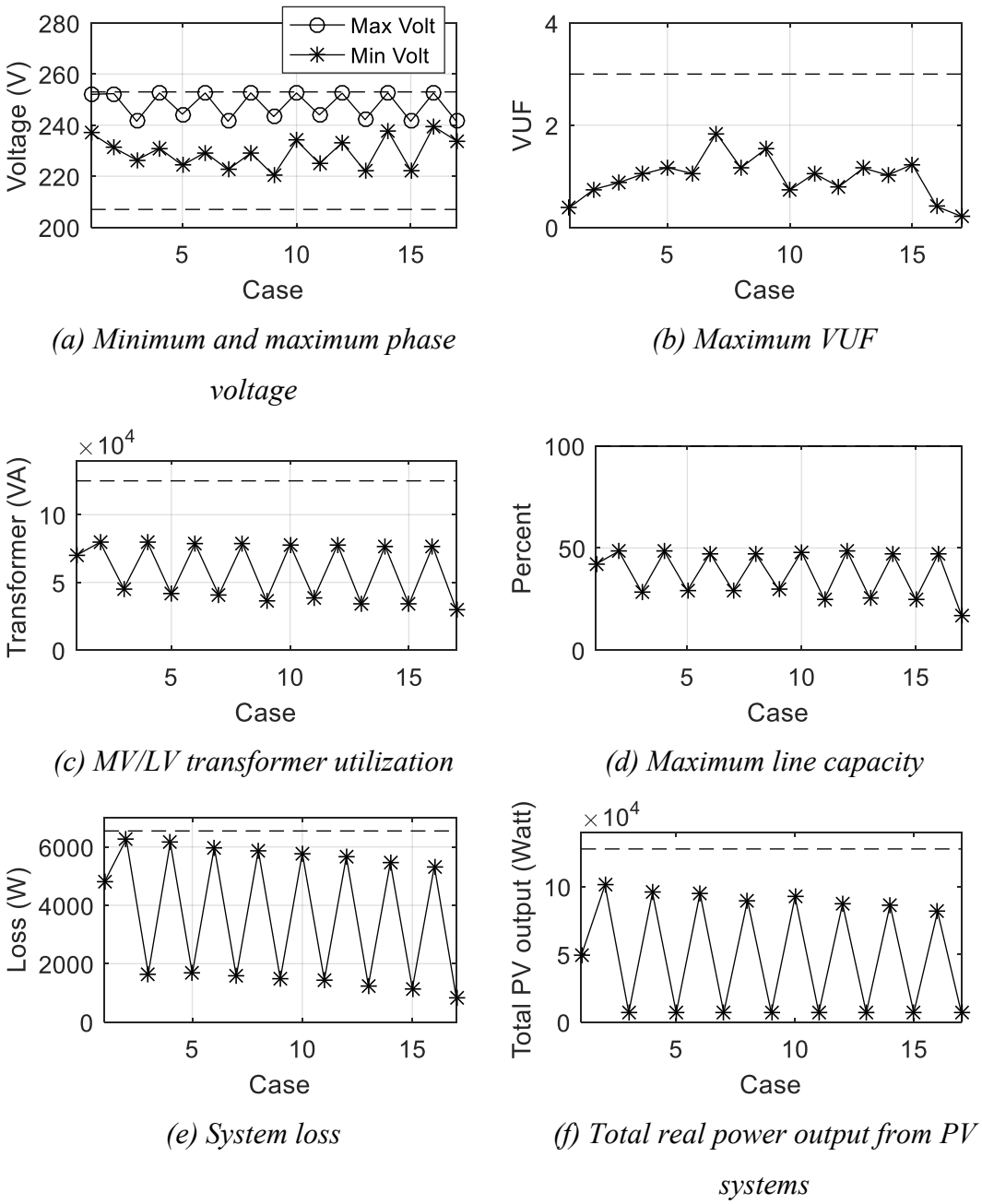

(a) Minimum and maximum phase voltage

(b) Maximum VUF

(c) MV/LV transformer utilization

(d) Maximum line capacity

(e) System loss

(f) Total real power output from PV systems

Figure 7.39 The results of the set of uncertainty

Comparing Subsection 7.5.1 that the parameters of are adjusted in every one week and Subsection 7.5.2 that the parameters are adjusted in every one day, the

summary can be shown in Table 7.22. It indicates that adjustment per one day is better than adjustment per one week. According to percent change of adjustment per one day, the objective values are better than around 5.19% and the maximum total real power outputs from PV systems at the case z2 are better than around 4.10%.

Table 7.22 The comparison of the parameters adjustment per one week or one day

Day at Nov 2014	Adjustment per one week		Adjustment per one day		Percent Change of Adjustment per One Day	
	Obj. Value	Max P Output	Obj. Value	Max P Output	Obj. Value	Max P Output
3	48,909.94	94,246.95	52,107.71	99,253.88	+6.54%	+5.31%
4	44,159.97	99,795.17	45,218.94	101,908.35	+2.40%	+2.12%
5	40,287.06	96,673.2	43,312.98	102,267.3	+7.51%	+5.79%
6	35,170.29	98,521.91	37,396.81	102,620.89	+6.33%	+4.16%
7	37,402.76	98,607.95	39,413.84	102,248.17	+5.38%	+3.69%
8	47,478.34	98,548.21	50,026.8	103,326.47	+5.37%	+4.85%
9	28,988.39	101,836.8	29,809.38	104,640.64	+2.83%	+2.75%
				Mean Change	+5.19%	+4.10%

Comparing the adjustment per one day strategy between Subsection 7.4.2 that local control is applied continuous function and Subsection 7.5.2 that local control is applied piecewise linear function, the percent different of objective value and maximum total real power output can be shown in Table 7.23 and it can notice that the results between Subsection 7.4.2 and Subsection 7.5.2 are close. Then, local control application can be chosen any one from continuous or piecewise linear function because of the nearly similar results.

Table 7.23 The comparison between continuous and piecewise linear local control application

Day at Nov 2014	Continuous Function		Piecewise Linear Function		Percent Change of Piecewise Linear Function	
	Obj. Value	Max P Output	Obj. Value	Max P Output	Obj. Value	Max P Output
3	51,565.54	98,597.83	52,107.71	99,253.88	+1.05%	+0.67%
4	46,719.23	103,531.01	45,218.94	101,908.35	-3.21%	-1.57%
5	44,143.82	102,481.48	43,312.98	102,267.30	-1.88%	-0.21%
6	36,814.38	101,971.62	37,396.81	102,620.89	+1.58%	+0.64%
7	39,214.69	102,359.66	39,413.84	102,248.17	+0.51%	-0.11%

Day at Nov 2014	Continuous Function		Piecewise Linear Function		Percent Change of Piecewise Linear Function	
	Obj. Value	Max P Output	Obj. Value	Max P Output	Obj. Value	Max P Output
8	50,677.69	104,035.63	50,026.80	103,326.47	-1.28%	-0.68%
9	28,240.01	102,564.62	29,809.38	104,640.64	+5.56%	+2.02%
				Mean Change	+0.33%	+0.11%

7.6 Local Control Adjustment in The Modified 29 Node Distribution System

In this subsection, the coordination between central and local control will apply in the modified 29 node distribution system. The simulation results are divided into 2 parts: (7.6.1) the continuous local control function application; (7.6.2) the piecewise linear local control function application.

7.6.1 The Continuous Local Control Function Application

In this subsection, the simulation results are divided into eight subsections: (7.6.1.1) at the week 3-9 November 2014; (7.6.1.2) at the day 3 November 2014; (7.6.1.3) at the day 4 November 2014; (7.6.1.4) at the day 5 November 2014; (7.6.1.5) at the day 6 November 2014; (7.6.1.6) at the day 7 November 2014; (7.6.1.7) at the day 8 November 2014; (7.6.1.8) at the day 9 November 2014. The continuous local control function is selected in this subsection.

7.6.1.1 At The Week 3-9 November 2014

The parameter assessment will be analyzed by central control through 2-stage PSO process. According to the set of uncertainty at the week 3 November 2014 in Table 6.7, the optimal objective value in equation (5.81) is 47,021.54 W and the results of optimal parameter setting can be shown in Table 7.24. Considering only the case $z \in \{z1, z2, \dots, z17\}$, the power flow results can be shown in Figure 7.40 and they are within the limit. The total real power output from PV systems at maximum value is 115,523.26 W at the case $z2$.

Table 7.24 Parameter setting of each connected PV system

PV Name	Parameter Setting					
	V_{cri}	δ_p	K_1	K_2	V_q	δ_q
PV1	1.089	0.01	0.375	1.311	1.035	0.055
PV2	1.106	0.01	0.492	1.188	1.011	0.05

PV Name	Parameter Setting					
	V_{cri}	δ_p	K_1	K_2	V_q	δ_q
PV3	1.09	0.01	0.27	1.22	1.043	0.06
PV4	1.09	0.02	0.43	1.21	1.041	0.063
PV5	1.09	0.01	0.38	1.36	1.03	0.045
PV6	1.09	0.01	0.51	1.24	1.042	0.048
PV7	1.10	0.01	0.89	1.45	1.036	0.061
PV8	1.10	0.01	0.28	1.03	1.022	0.051
PV9	1.12	0.01	0.36	1.00	1.032	0.058
PV10	1.124	0.01	0.407	1.29	1.017	0.07
PV11	1.095	0.01	0.283	0.974	1.036	0.062
PV12	1.097	0.01	0.402	1.23	1.06	0.064
PV13	1.094	0.013	0.374	1.255	1.07	0.011
PV14	1.107	0.01	0.417	1.227	1.04	0.045
PV15	1.087	0.01	0.376	1.235	1.031	0.058
PV16	1.151	0.01	0.389	1.282	1.021	0.069
PV17	1.105	0.01	0.451	1.306	1.03	0.054
PV18	1.077	0.01	0.581	1.388	1.036	0.044
PV19	1.078	0.01	0.317	1.228	1.038	0.043
PV20	1.089	0.01	0.44	1.218	1.01	0.04
PV21	1.086	0.01	0.263	1.222	1.034	0.054
PV22	1.099	0.01	0.409	1.307	1.045	0.05
PV23	1.088	0.01	0.136	1.122	1.035	0.053
PV24	1.082	0.01	0.306	1.131	1.039	0.073

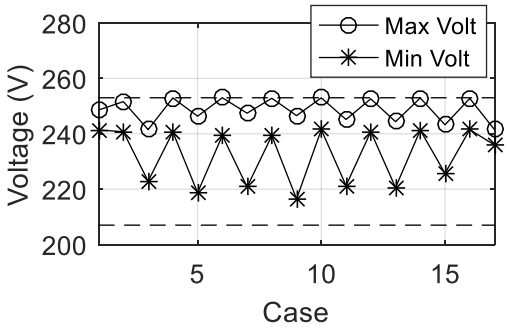

(a) Minimum and maximum phase voltage

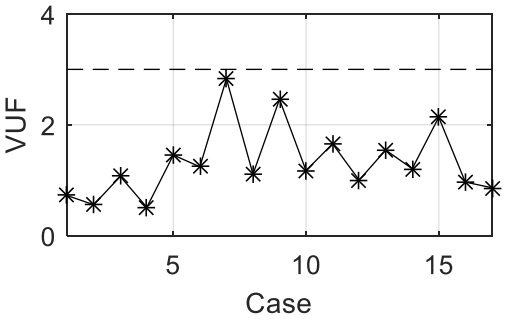

(b) Maximum VUF

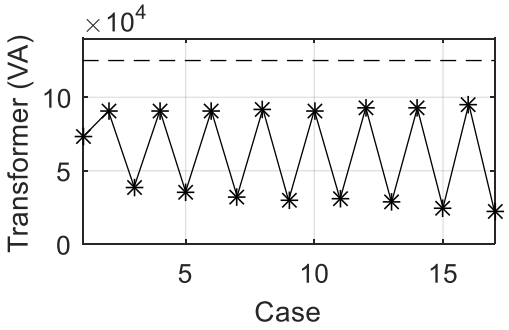

(c) MV/LV transformer utilization

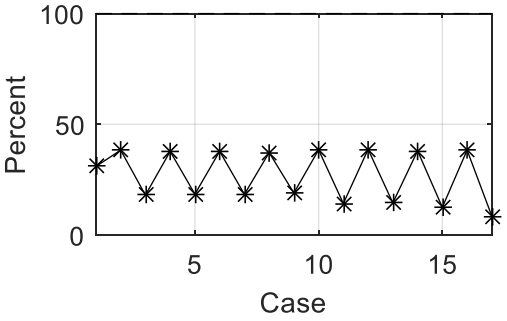

(d) Maximum line capacity

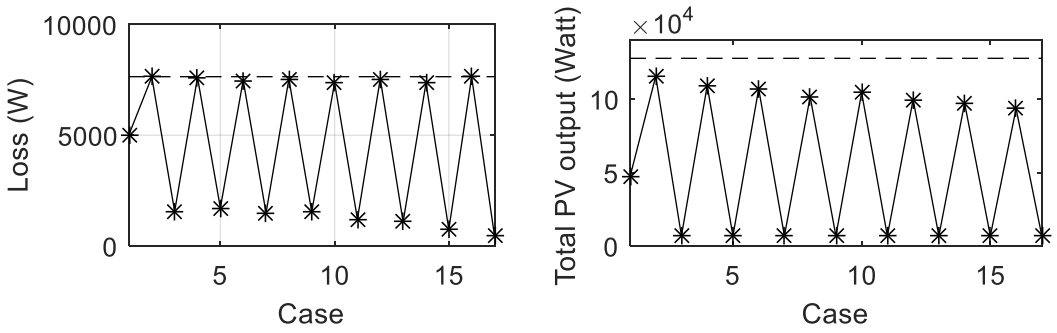

(e) System loss *(f) Total real power output from PV systems*

Figure 7.40 The results of the set of uncertainty

Applying (1) the set of uncertainty of each day and (2) the parameters setting in Table 7.24 at the week 3-9 November 2014, the objective values and the maximum value of total real power output from PV systems at the case $z2$ are shown in Table 7.24. The objective values is negative in days 3-9 because the power flow results are out of limit. Mostly, loss at each day is out of the limit as shown latter in Figures 7.41-7.47. The out of limit is due to the set of uncertainty is not enough considered thoroughly in the modified 29 node distribution system. The solution can be the limit setting in the optimization constraints being less than the truth.

Table 7.25 The results of each day

Day at Nov 2014	Adjustment per One Week	
	Obj. Value	Max P Output
3	-8.2×10^8	110,750.88
4	-2.4×10^8	114,053.61
5	-6.4×10^8	112,284.26
6	-4.4×10^8	113,406.98
7	-3.9×10^8	113,499.34
8	-5.7×10^8	113,477.51
9	-7.1×10^7	115,062.96

The power flow results of the set of uncertainty of each day can be shown as follows:

- At the day 3 November, the power flow results can be shown in Figure 7.41. Losses are out of limit at cases z2, z4, z6, z8, z12 and z16.

- At the day 4 November, the power flow results can be shown in Figure 7.42. Losses are out of limit at cases z2, z4, z8, z12 and z16. Overvoltages occur at cases z4 and z8. Assumingly, overvoltage is neglected because overvoltage is more than the limit slightly about less than 0.5 V.
- At the day 5 November, the power flow results can be shown in Figure 7.43. Losses are out of limit at cases z2, z4, z6, z8, z12 and z16.
- At the day 6 November, the power flow results can be shown in Figure 7.44. Losses are out of limit at cases z2, z4, z8, z12 and z16. Overvoltage occurs at case z4. Assumingly, overvoltage is neglected because overvoltage is more than the limit slightly about less than 0.5 V.
- At the day 7 November, the power flow results can be shown in Figure 7.45. Losses are out of limit at cases z2, z4, z6, z8 and z16. Overvoltage occurs at case z4. Assumingly, overvoltage is neglected because overvoltage is more than the limit slightly about less than 0.5 V.
- At the day 8 November, the power flow results can be shown in Figure 7.46. Losses are out of limit at cases z2, z4, z6, z8 and z16. Overvoltage occurs at cases z4. Assumingly, overvoltage is neglected because overvoltage is more than the limit slightly about less than 0.5 V.
- At the day 9 November, the power flow results can be shown in Figure 7.47. Losses are out of limit at cases z2 and z16. Overvoltages occur at cases z4 and z8. Assumingly, overvoltage is neglected because overvoltage is more than the limit slightly about less than 0.5 V.

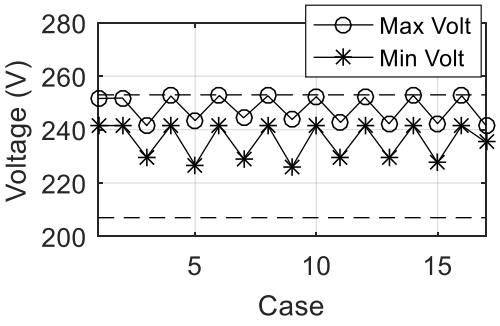

(a) Minimum and maximum phase voltage

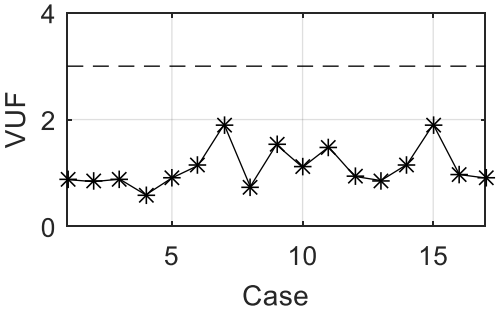

(b) Maximum VUF

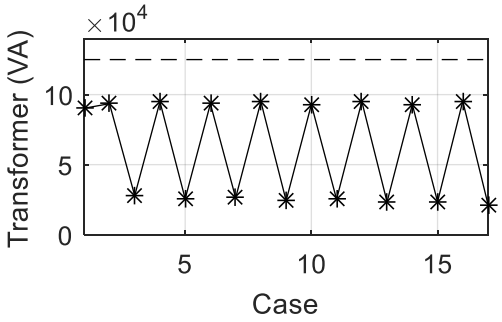

(c) MV/LV transformer utilization

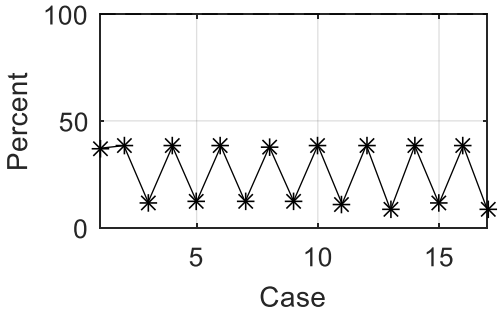

(d) Maximum line capacity

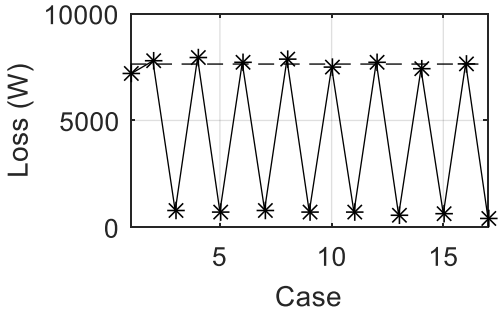

(e) System loss

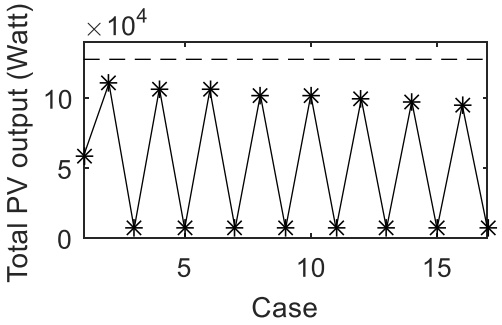

(f) Total real power output from PV systems

Figure 7.41 The results of the set of uncertainty

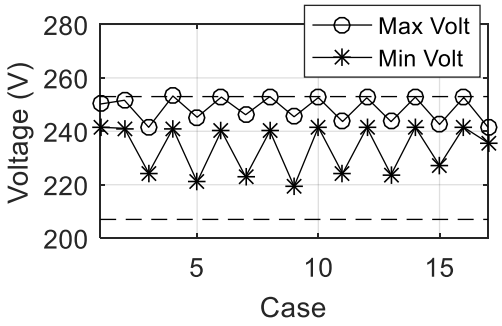

(a) Minimum and maximum phase voltage

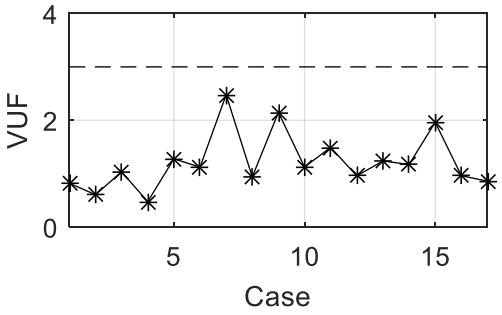

(b) Maximum VUF

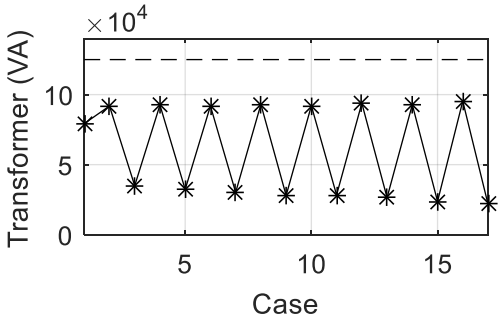

(c) MV/LV transformer utilization

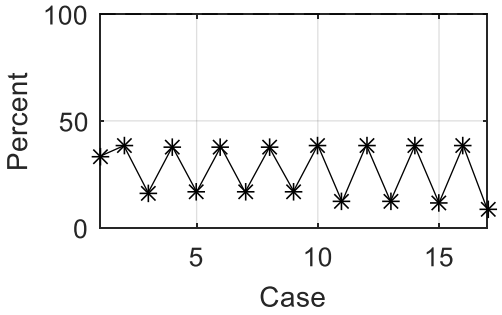

(d) Maximum line capacity

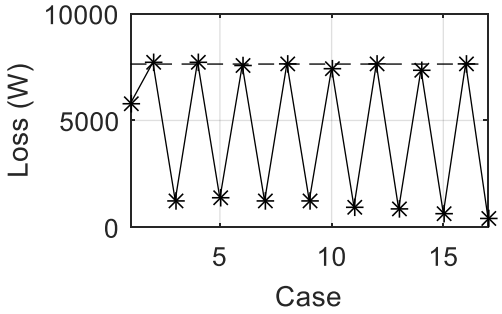

(e) System loss

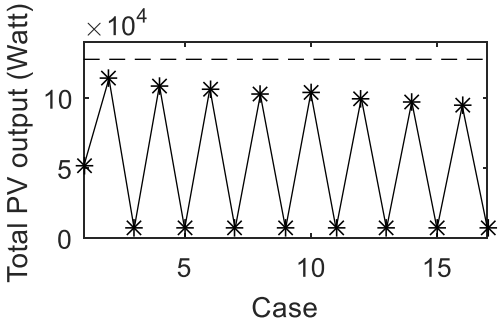

(f) Total real power output from PV systems

Figure 7.42 The results of the set of uncertainty

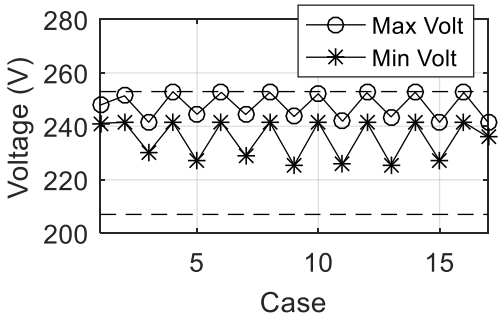

(a) Minimum and maximum phase voltage

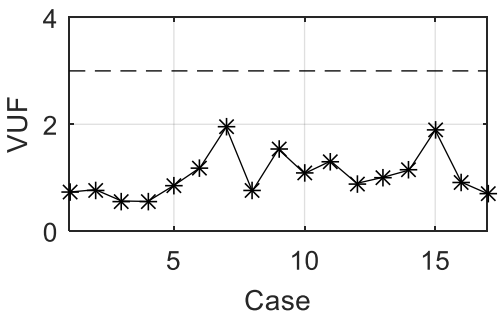

(b) Maximum VUF

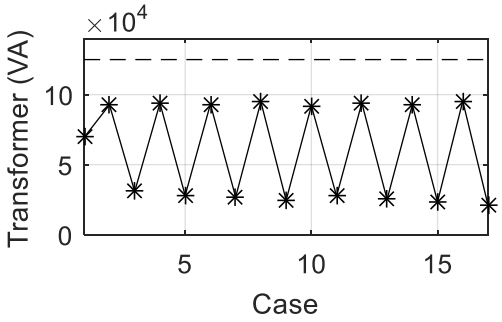

(c) MV/LV transformer utilization

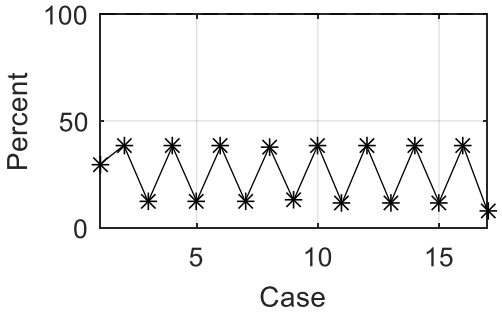

(d) Maximum line capacity

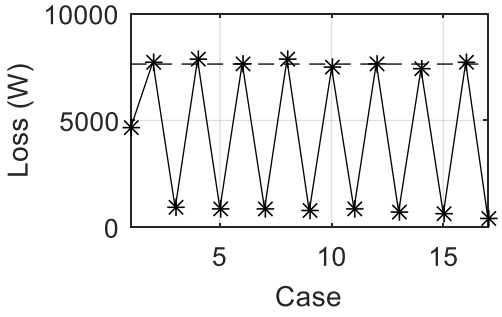

(e) System loss

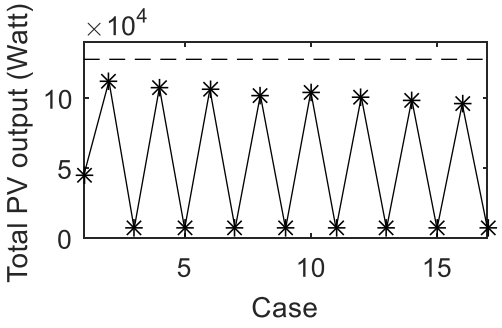

(f) Total real power output from PV systems

Figure 7.43 The results of the set of uncertainty

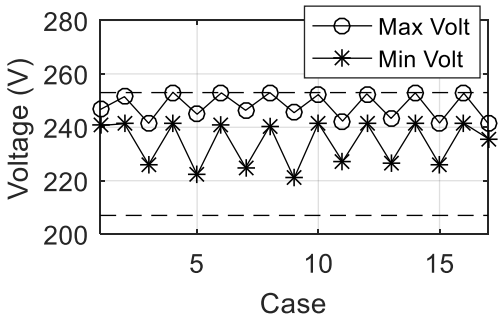

(a) Minimum and maximum phase voltage

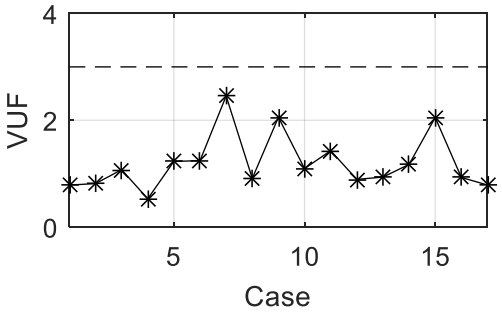

(b) Maximum VUF

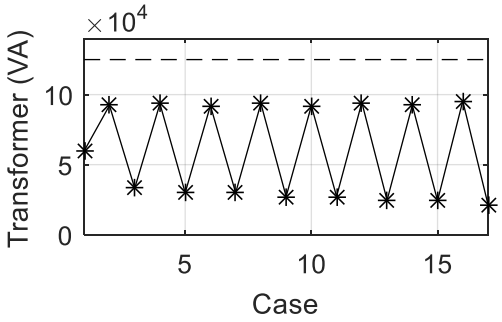

(c) MV/LV transformer utilization

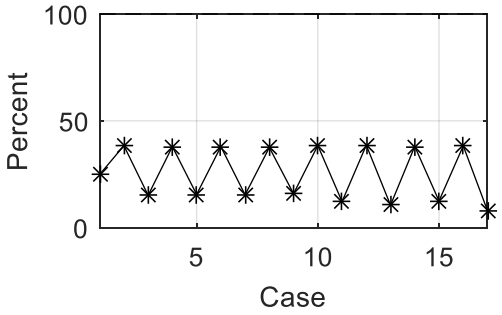

(d) Maximum line capacity

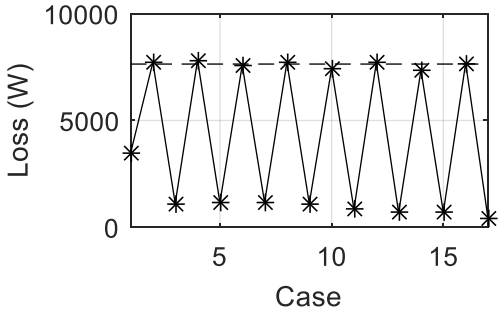

(e) System loss

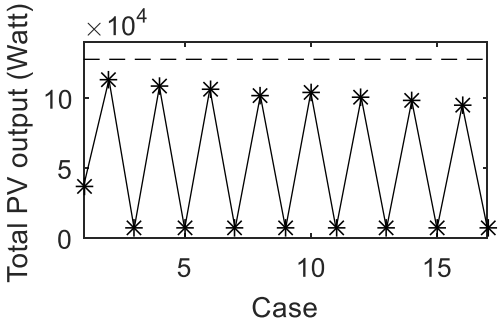

(f) Total real power output from PV systems

Figure 7.44 The results of the set of uncertainty

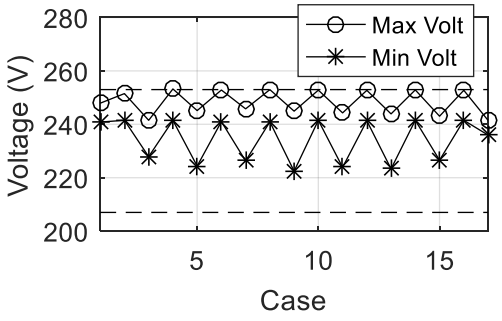

(a) Minimum and maximum phase voltage

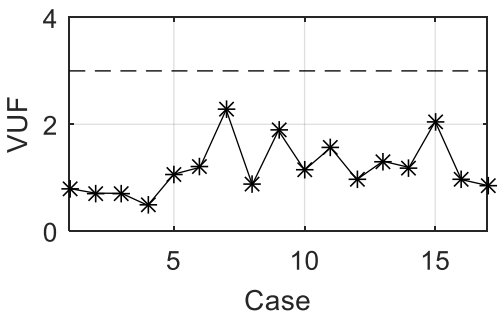

(b) Maximum VUF

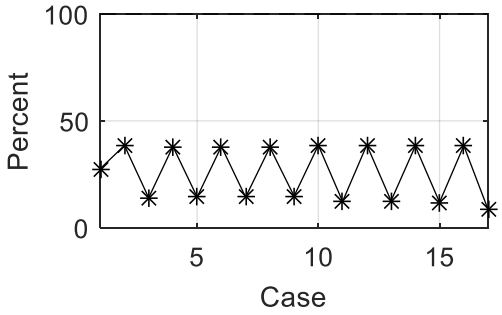

(c) MV/LV transformer utilization

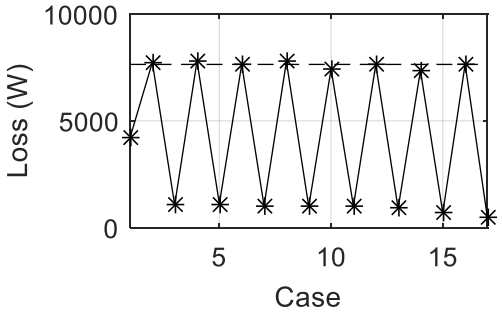

(d) Maximum line capacity

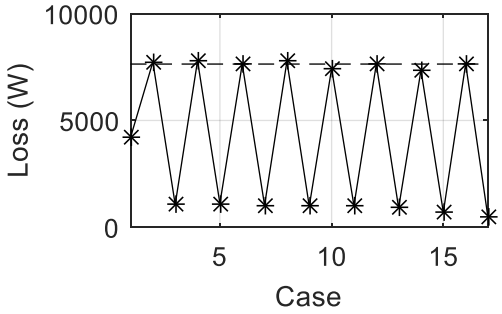

(e) System loss

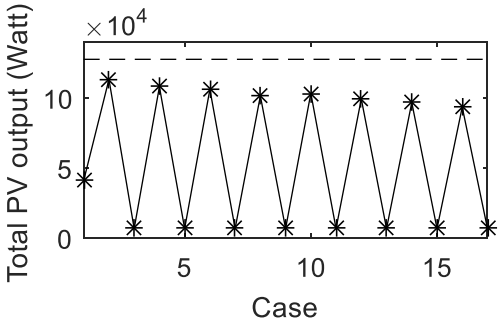

(f) Total real power output from PV systems

Figure 7.45 The results of the set of uncertainty

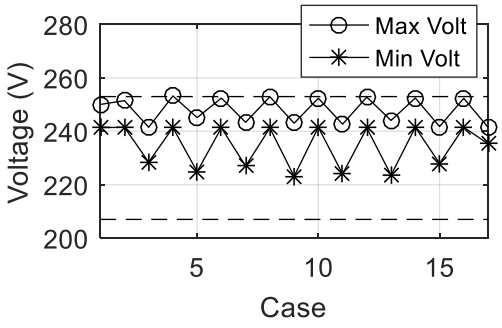

(a) Minimum and maximum phase voltage

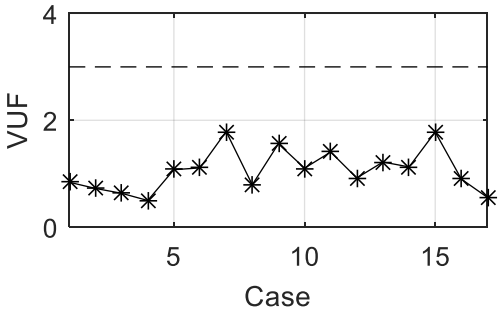

(b) Maximum VUF

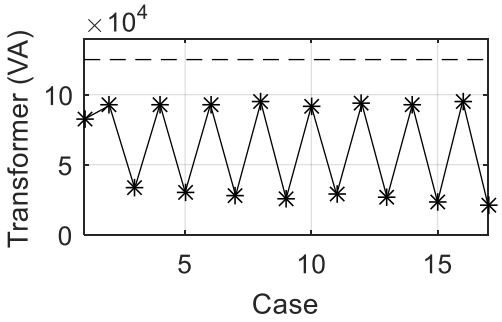

(c) MV/LV transformer utilization

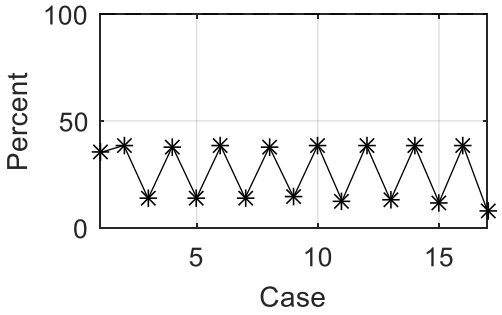

(d) Maximum line capacity

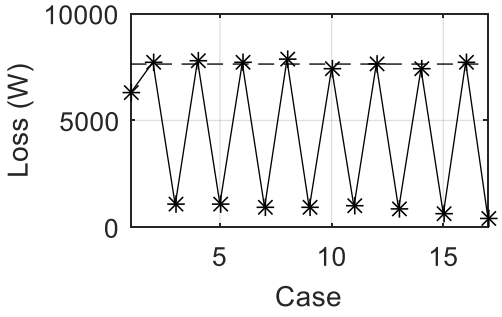

(e) System loss

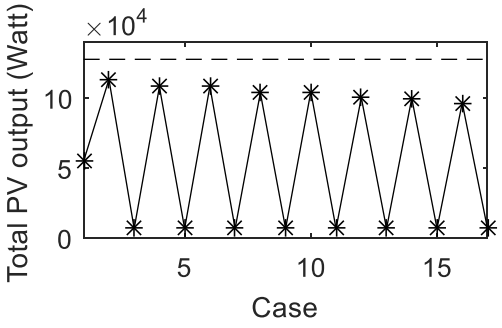

(f) Total real power output from PV systems

Figure 7.46 The results of the set of uncertainty

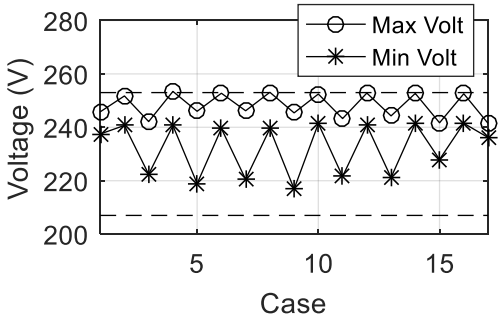

(a) Minimum and maximum phase voltage

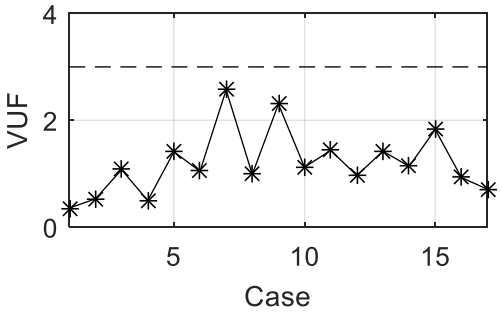

(b) Maximum VUF

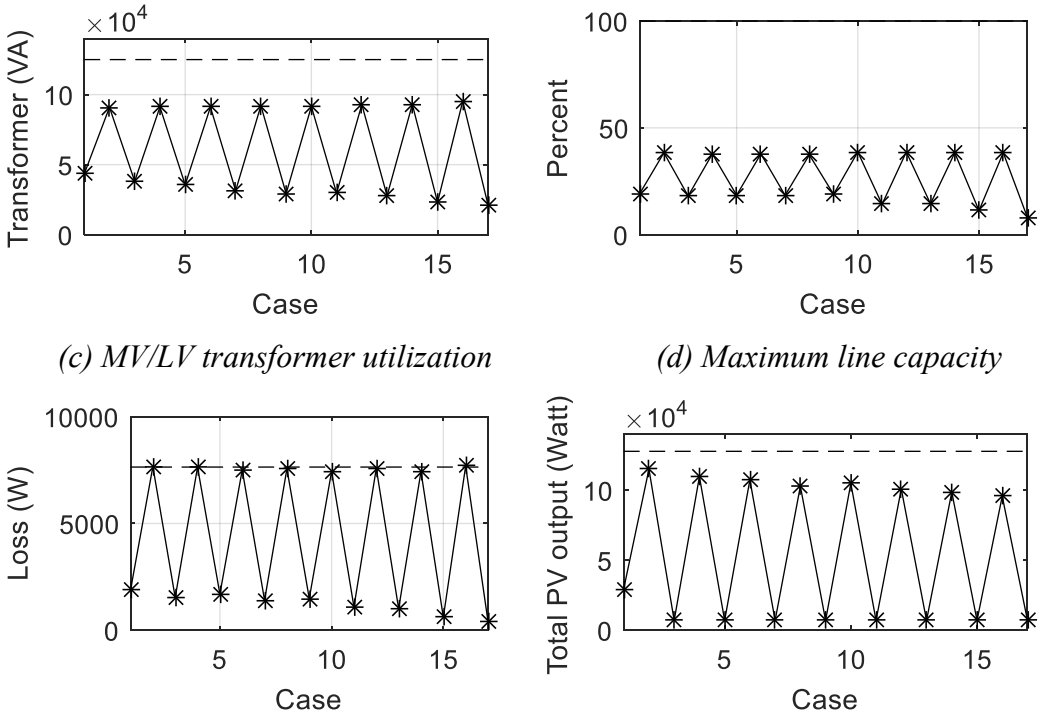

(c) MV/LV transformer utilization

(d) Maximum line capacity

(e) System loss

(f) Total real power output from PV systems

Figure 7.47 The results of the set of uncertainty

7.6.1.2 At The Day 3 November 2014

The parameter assessment will be analyzed by central control through 2-stage PSO process. According to the set of uncertainty at the day 3 November 2014 in Table 6.8, the optimal objective value in equation (5.81) is 58,433.80 W and the results of optimal parameter setting can be shown in Table 7.26. Considering only the case $z \in \{z1, z2, \ldots, z17\}$, the power flow results can be shown in Figure 7.48 and they are within the limit. The total real power output from PV systems at maximum value is 109,474.51 W at the case $z2$.

Table 7.26 Parameter setting of each connected PV system

PV Name	Parameter Setting					
	V_{cri}	δ_p	K_1	K_2	V_q	δ_q
PV1	1.11	0.011	0.3	1.158	1.02	0.053
PV2	1.086	0.015	0.31	1.121	1.02	0.076
PV3	1.08	0.01	0.34	1.07	1.013	0.055
PV4	1.09	0.01	0.37	1.14	1.021	0.059

PV Name	Parameter Setting					
	V_{cri}	δ_p	K_1	K_2	V_q	δ_q
PV5	1.09	0.02	0.34	1.16	1.019	0.055
PV6	1.10	0.02	0.35	1.08	1.025	0.058
PV7	1.09	0.01	0.36	1.13	1.018	0.059
PV8	1.12	0.02	0.34	1.18	1.02	0.055
PV9	1.12	0.02	0.34	1.11	1.013	0.068
PV10	1.099	0.012	0.373	1.086	1.017	0.054
PV11	1.091	0.016	0.259	1.091	1.017	0.063
PV12	1.094	0.01	0.328	1.094	1.018	0.051
PV13	1.096	0.015	0.36	1.148	1.02	0.061
PV14	1.129	0.013	0.327	1.154	1.019	0.062
PV15	1.094	0.016	0.328	1.139	1.018	0.058
PV16	1.093	0.015	0.352	1.229	1.015	0.055
PV17	1.073	0.015	0.32	1.132	1.019	0.03
PV18	1.1	0.016	0.342	1.116	1.021	0.058
PV19	1.081	0.015	0.281	1.111	1.019	0.052
PV20	1.092	0.015	0.316	1.124	1.019	0.059
PV21	1.084	0.016	0.324	1.147	1.018	0.049
PV22	1.099	0.016	0.506	1.198	1.02	0.062
PV23	1.085	0.015	0.313	1.113	1.02	0.051
PV24	1.092	0.014	0.388	1.131	1.022	0.065

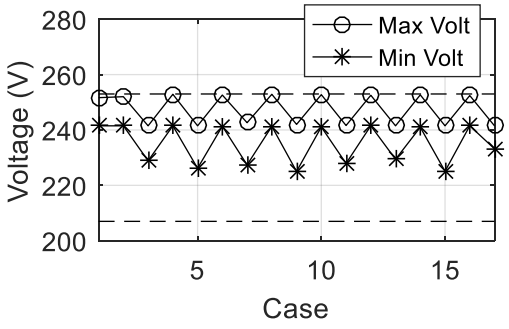

(a) Minimum and maximum phase voltage

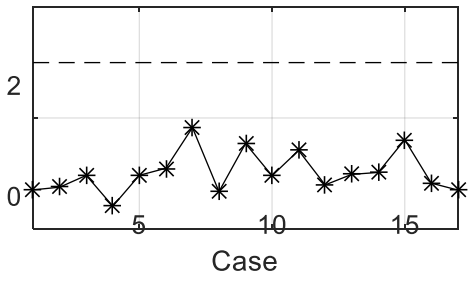

(b) Maximum VUF

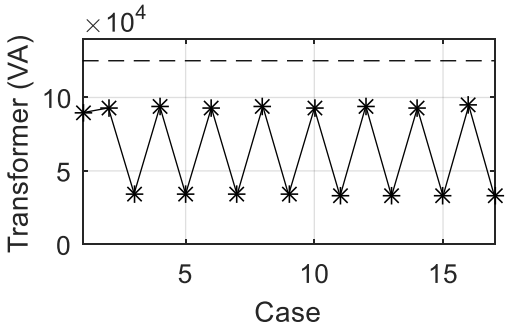

(c) MV/LV transformer utilization

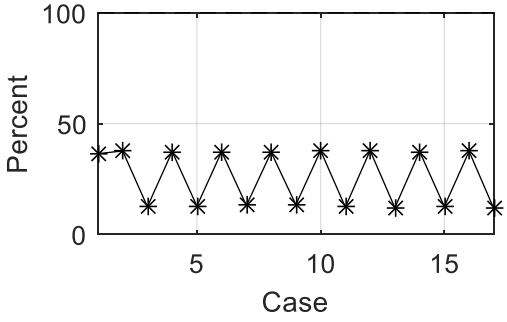

(d) Maximum line capacity

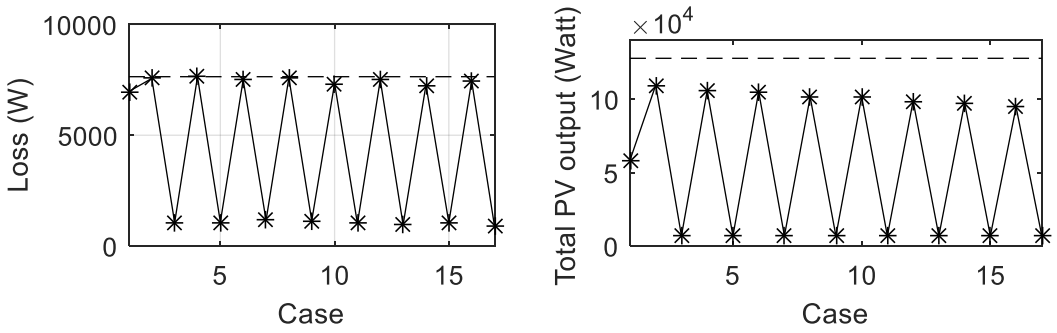

(e) System loss *(f) Total real power output from PV systems*

Figure 7.48 The results of the set of uncertainty

7.6.1.3 At The Day 4 November 2014

The parameter assessment will be analyzed by central control through 2-stage PSO process. According to the set of uncertainty at the day 4 November 2014 in Table 6.9, the optimal objective value in equation (5.81) is 51,862.06 W and the results of optimal parameter setting can be shown in Table 7.27. Considering only the case $z \in \{z1, z2, \ldots, z17\}$, the power flow results can be shown in Figure 7.49 and they are within the limit. The total real power output from PV systems at maximum value is 114,606.26 W at the case $z2$.

Table 7.27 Parameter setting of each connected PV system

PV Name	Parameter Setting					
	V_{cri}	δ_p	K_1	K_2	V_q	δ_q
PV1	1.101	0.012	0.343	1.091	1.018	0.02
PV2	1.091	0.01	0.755	1.097	1.034	0.01
PV3	1.09	0.01	0.21	1.09	1.028	0.01
PV4	1.11	0.01	0.52	1.03	1.025	0.011
PV5	1.09	0.01	0.33	1.04	1.03	0.01
PV6	1.10	0.01	0.54	1.11	1.032	0.01
PV7	1.10	0.01	0.32	0.98	1.031	0.01
PV8	1.11	0.01	0.33	1.07	1.042	0.01
PV9	1.09	0.01	0.27	1.10	1.022	0.01
PV10	1.107	0.01	0.387	1.116	1.026	0.01
PV11	1.093	0.01	0.427	1.073	1.031	0.01
PV12	1.097	0.01	0.353	1.177	1.034	0.01
PV13	1.095	0.01	0.33	1.127	1.013	0.01
PV14	1.113	0.01	0.32	1.093	1.028	0.01
PV15	1.081	0.01	0.346	1.083	1.032	0.01
PV16	1.112	0.016	0.38	1.167	1.024	0.01

PV Name	Parameter Setting					
	V_{cri}	δ_p	K_1	K_2	V_q	δ_q
PV17	1.091	0.01	0.349	1.035	1.037	0.01
PV18	1.081	0.01	0.268	1.267	1.02	0.01
PV19	1.09	0.01	0.277	1.076	1.021	0.01
PV20	1.083	0.01	0.325	1.216	1.019	0.01
PV21	1.091	0.01	0.277	1.016	1.054	0.01
PV22	1.101	0.01	0.324	1.055	1.017	0.01
PV23	1.082	0.01	0.341	1.191	1.03	0.01
PV24	1.087	0.01	0.31	0.606	1.042	0.01

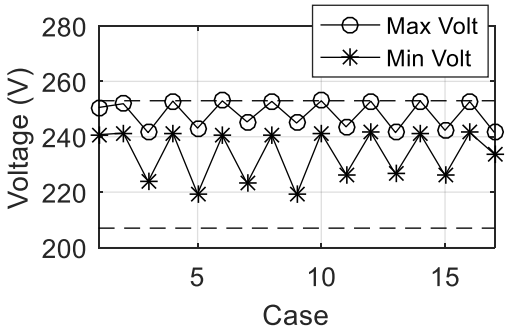

(a) Minimum and maximum phase voltage

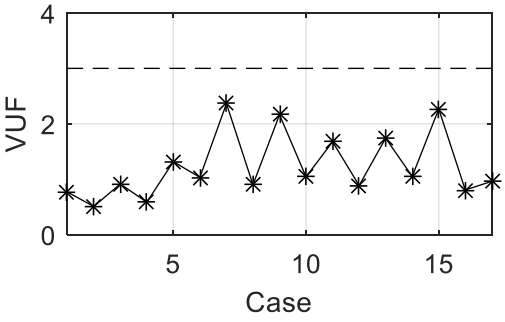

(b) Maximum VUF

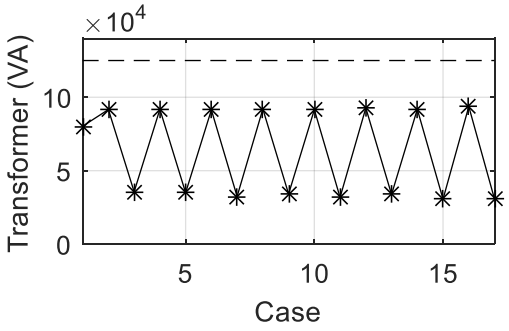

(c) MV/LV transformer utilization

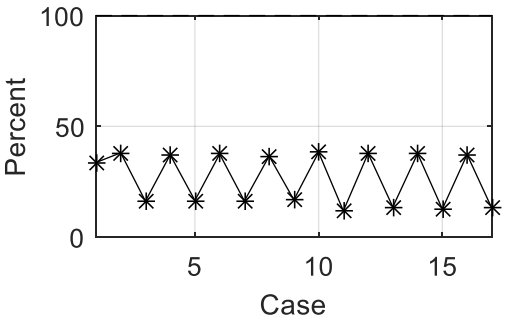

(d) Maximum line capacity

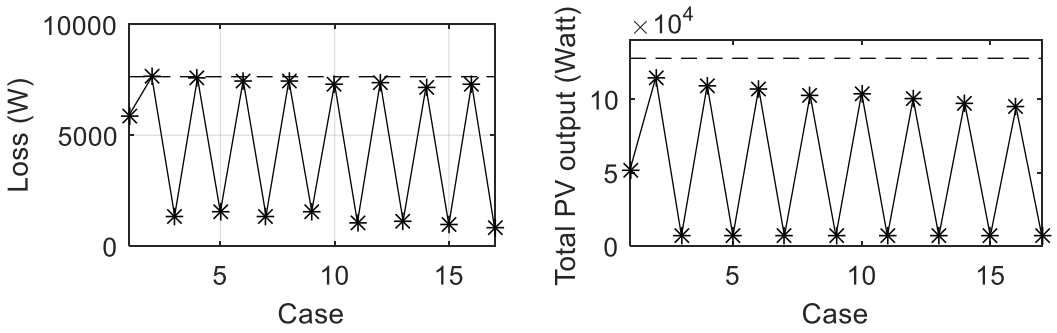

(e) System loss *(f) Total real power output from PV systems*

Figure 7.49 The results of the set of uncertainty

7.6.1.4 At The Day 5 November 2014

The parameter assessment will be analyzed by central control through 2-stage PSO process. According to the set of uncertainty at the day 5 November 2014 in Table 6.10, the optimal objective value in equation (5.81) is 44,890.02 W and the results of optimal parameter setting can be shown in Table 7.28. Considering only the case $z \in \{z1, z2, \ldots, z17\}$, the power flow results can be shown in Figure 7.50 and they are within the limit. The total real power output from PV systems at maximum value is 113,525.61 W at the case $z2$.

Table 7.28 Parameter setting of each connected PV system

PV Name	Parameter Setting					
	V_{cri}	δ_p	K_1	K_2	V_q	δ_q
PV1	1.082	0.01	0.041	0.935	1.044	0.084
PV2	1.102	0.01	0.047	0.946	1.037	0.09
PV3	1.08	0.01	0.04	0.69	1.041	0.088
PV4	1.09	0.01	0.05	0.96	1.043	0.093
PV5	1.09	0.01	0.04	0.93	1.041	0.09
PV6	1.10	0.01	0.04	0.95	1.041	0.079
PV7	1.09	0.02	0.04	0.96	1.03	0.1
PV8	1.11	0.01	0.04	0.95	1.046	0.094
PV9	1.10	0.01	0.05	0.95	1.045	0.1
PV10	1.13	0.01	0.047	0.906	1.038	0.092
PV11	1.099	0.01	0.043	0.884	1.041	0.09
PV12	1.097	0.01	0.056	0.921	1.05	0.1
PV13	1.102	0.01	0.088	0.95	1.045	0.083
PV14	1.094	0.012	0.032	0.912	1.015	0.085
PV15	1.077	0.01	0.056	0.934	1.04	0.093
PV16	1.104	0.01	0.034	0.945	1.045	0.093

PV Name	Parameter Setting					
	V_{cri}	δ_p	K_1	K_2	V_q	δ_q
PV17	1.1	0.01	0.06	0.885	1.038	0.088
PV18	1.088	0.01	0.047	0.948	1.041	0.094
PV19	1.089	0.01	0.059	0.999	1.042	0.095
PV20	1.09	0.01	0.048	0.955	1.044	0.089
PV21	1.088	0.01	0.042	0.976	1.089	0.085
PV22	1.094	0.01	0.051	0.944	1.048	0.091
PV23	1.093	0.01	0.04	0.959	1.044	0.087
PV24	1.09	0.01	0.081	0.945	1.04	0.09

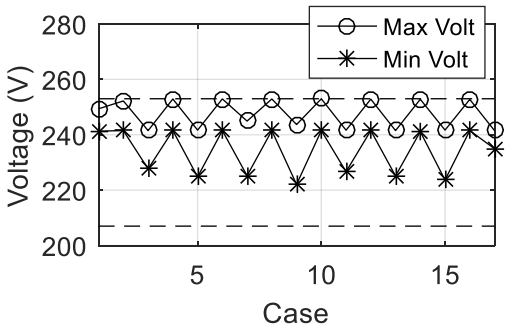

(a) Minimum and maximum phase voltage

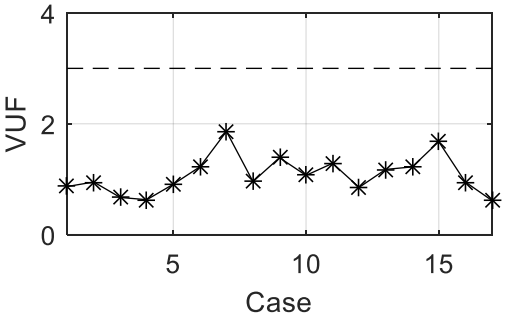

(b) Maximum VUF

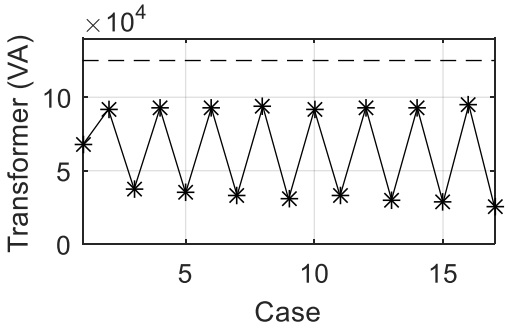

(c) MV/LV transformer utilization

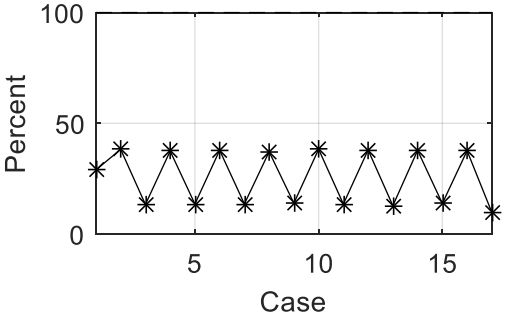

(d) Maximum line capacity

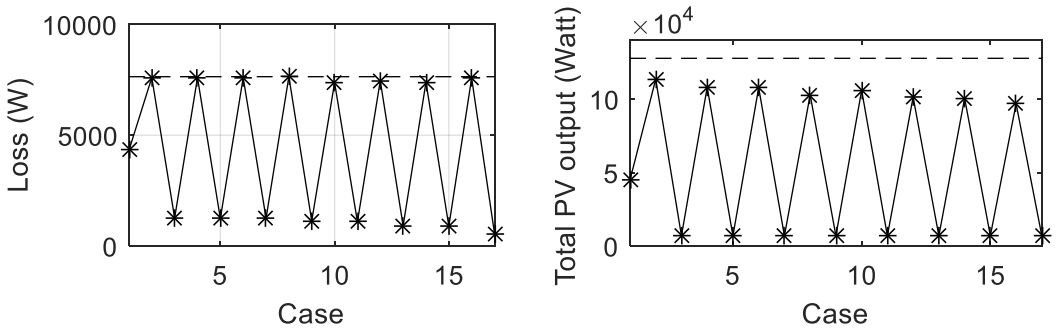

(e) System loss *(f) Total real power output from PV systems*

Figure 7.50 The results of the set of uncertainty

7.6.1.5 At The Day 6 November 2014

The parameter assessment will be analyzed by central control through 2-stage PSO process. According to the set of uncertainty at the day 6 November 2014 in Table 6.11, the optimal objective value in equation (5.81) is 37,443.97 W and the results of optimal parameter setting can be shown in Table 7.29. Considering only the case $z \in \{z1, z2, \ldots, z17\}$, the power flow results can be shown in Figure 7.51 and they are within the limit. The total real power output from PV systems at maximum value is 114,131.95 W at the case $z2$.

Table 7.29 Parameter setting of each connected PV system

PV Name	Parameter Setting					
	V_{cri}	δ_p	K_1	K_2	V_q	δ_q
PV1	1.082	0.01	0.336	1.173	1.002	0.066
PV2	1.088	0.01	0.285	1.155	1.001	0.063
PV3	1.09	0.01	0.38	1.12	1	0.09
PV4	1.10	0.01	0.46	1.10	1.008	0.067
PV5	1.09	0.01	0.32	1.02	1.007	0.071
PV6	1.09	0.01	0.31	1.05	1.008	0.097
PV7	1.10	0.01	0.32	1.13	1.006	0.071
PV8	1.14	0.01	0.34	0.97	1.007	0.078
PV9	1.10	0.01	0.32	0.98	1.003	0.071
PV10	1.107	0.01	0.325	1.049	1.003	0.059
PV11	1.099	0.01	0.308	1.092	1.004	0.059
PV12	1.098	0.01	0.333	1.21	1.015	0.075
PV13	1.097	0.01	0.4	1.048	1.007	0.077
PV14	1.103	0.011	0.319	1.134	1.009	0.079
PV15	1.107	0.01	0.309	1.031	1.011	0.062
PV16	1.095	0.01	0.318	1.054	1.003	0.077

PV Name	Parameter Setting					
	V_{cri}	δ_p	K_1	K_2	V_q	δ_q
PV17	1.095	0.01	0.326	1.184	1.006	0.086
PV18	1.082	0.024	0.268	1.113	1.008	0.075
PV19	1.087	0.01	0.319	1.206	1.004	0.072
PV20	1.083	0.01	0.327	1.084	1.011	0.076
PV21	1.085	0.01	0.291	1.21	1.012	0.093
PV22	1.102	0.01	0.298	1.115	1.008	0.064
PV23	1.088	0.01	0.307	1.097	1.008	0.058
PV24	1.085	0.01	0.416	1.134	1.015	0.081

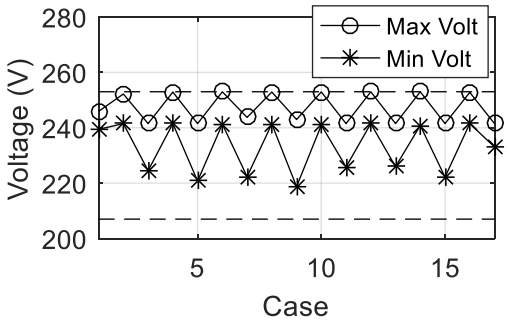

(a) Minimum and maximum phase voltage

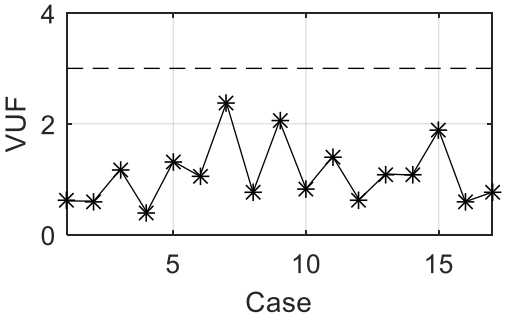

(b) Maximum VUF

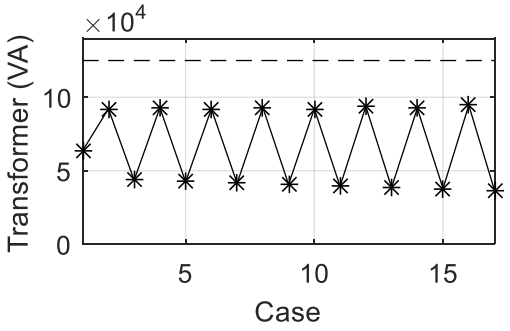

(c) MV/LV transformer utilization

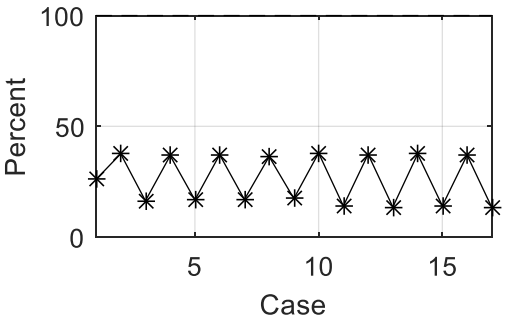

(d) Maximum line capacity

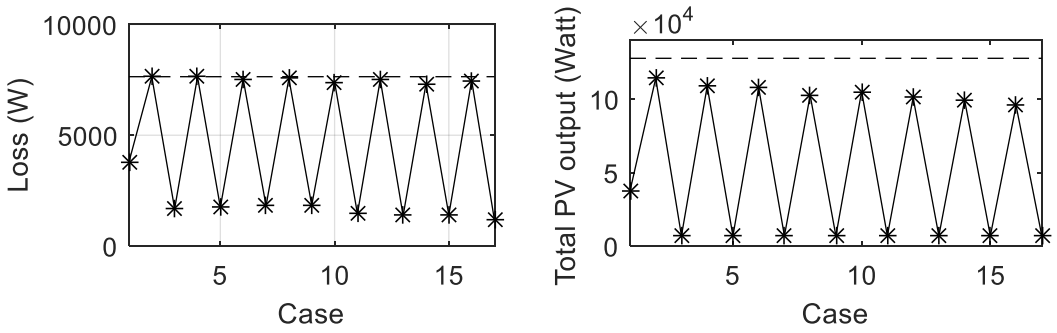

(e) System loss *(f) Total real power output from PV systems*

Figure 7.51 The results of the set of uncertainty

7.6.1.6 At The Day 7 November 2014

The parameter assessment will be analyzed by central control through 2-stage PSO process. According to the set of uncertainty at the day 7 November 2014 in Table 6.12, the optimal objective value in equation (5.81) is 41,338.27 W and the results of optimal parameter setting can be shown in Table 7.30. Considering only the case $z \in \{z1, z2, \ldots, z17\}$, the power flow results can be shown in Figure 7.52 and they are within the limit. The total real power output from PV systems at maximum value is 113,761.11 W at the case $z2$.

Table 7.30 Parameter setting of each connected PV system

PV Name	Parameter Setting					
	V_{cri}	δ_p	K_1	K_2	V_q	δ_q
PV1	1.09	0.01	0.118	0.842	1.018	0.04
PV2	1.096	0.01	0.13	0.894	1.015	0.035
PV3	1.08	0.01	0.13	0.88	1.019	0.039
PV4	1.20	0.01	0.14	1.01	1.023	0.042
PV5	1.09	0.01	0.15	0.92	1.021	0.039
PV6	1.10	0.01	0.14	0.88	1.018	0.032
PV7	1.10	0.01	0.14	1.01	1.017	0.037
PV8	1.12	0.01	0.13	0.80	1.027	0.026
PV9	1.19	0.01	0.22	0.82	1.033	0.047
PV10	1.124	0.01	0.121	0.94	1.025	0.032
PV11	1.098	0.01	0.104	0.935	1.02	0.014
PV12	1.098	0.01	0.042	0.986	1.015	0.052
PV13	1.097	0.01	0.126	0.933	1.015	0.041
PV14	1.105	0.01	0.078	0.853	1.016	0.036
PV15	1.105	0.01	0.117	0.835	1.014	0.037
PV16	1.1	0.01	0.122	0.737	1.008	0.037

PV Name	Parameter Setting					
	V_{cri}	δ_p	K_1	K_2	V_q	δ_q
PV17	1.096	0.01	0.128	0.862	1.022	0.034
PV18	1.08	0.01	0.096	0.862	1.012	0.032
PV19	1.087	0.01	0.097	0.907	1.027	0.026
PV20	1.089	0.01	0.14	0.91	1.013	0.04
PV21	1.089	0.01	0.123	0.872	1.035	0.027
PV22	1.096	0.01	0.17	0.902	1.016	0.037
PV23	1.088	0.01	0.142	1.026	1.016	0.03
PV24	1.086	0.01	0.135	0.921	1.014	0.032

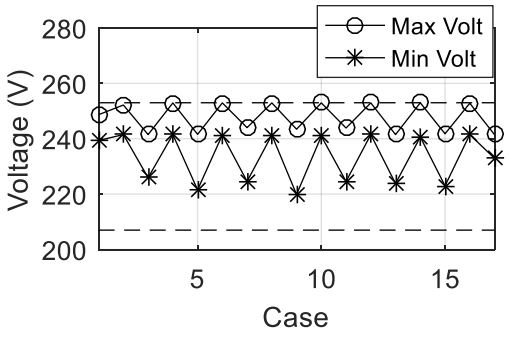

(a) Minimum and maximum phase voltage

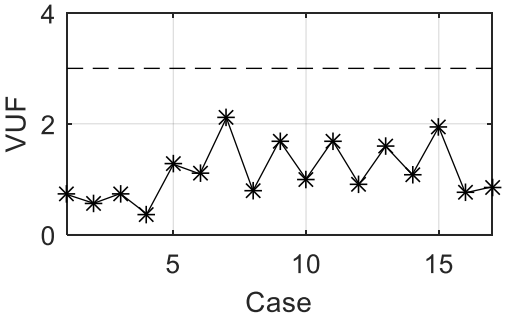

(b) Maximum VUF

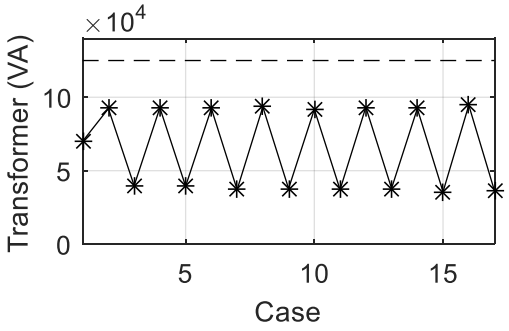

(c) MV/LV transformer utilization

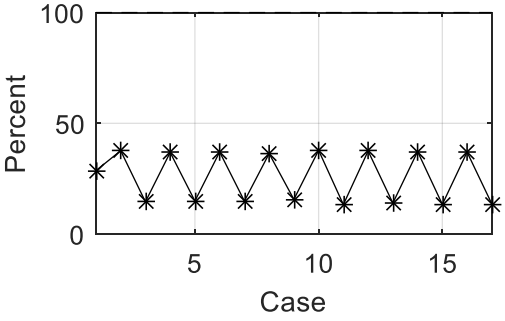

(d) Maximum line capacity

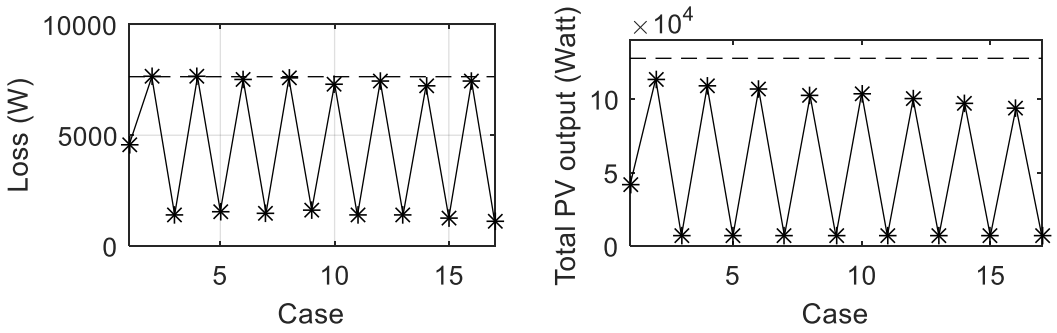

(e) System loss *(f) Total real power output from PV systems*

Figure 7.52 The results of the set of uncertainty

7.6.1.7 At The Day 8 November 2014

The parameter assessment will be analyzed by central control through 2-stage PSO process. According to the set of uncertainty at the day 8 November 2014 in Table 6.13, the optimal objective value in equation (5.81) is 56,218.30 W and the results of optimal parameter setting can be shown in Table 7.31. Considering only the case $z \in \{z1, z2, \ldots, z17\}$, the power flow results can be shown in Figure 7.53 and they are within the limit. The total real power output from PV systems at maximum value is 114,819.12 W at the case $z2$.

Table 7.31 Parameter setting of each connected PV system

PV Name	Parameter Setting					
	V_{cri}	δ_p	K_1	K_2	V_q	δ_q
PV1	1.091	0.01	0.036	0.672	1.023	0.01
PV2	1.106	0.01	0.026	0.768	1.022	0.01
PV3	1.08	0.01	0.01	0.82	1.024	0.01
PV4	1.11	0.01	0.01	0.76	1.028	0.01
PV5	1.09	0.01	0.02	0.69	1.013	0.01
PV6	1.10	0.01	0.02	0.69	1.012	0.01
PV7	1.10	0.01	0.01	0.75	1.015	0.011
PV8	1.11	0.01	0.02	0.61	1.017	0.01
PV9	1.09	0.01	0.00	0.86	1.02	0.01
PV10	1.162	0.01	0.148	0.773	1.022	0.01
PV11	1.097	0.01	0.01	0.738	1.018	0.01
PV12	1.098	0.01	0.034	0.767	1.018	0.01
PV13	1.101	0.01	0	0.892	1.022	0.01
PV14	1.095	0.01	0.009	0.732	1.027	0.01
PV15	1.092	0.01	0.001	0.788	1.02	0.01
PV16	1.095	0.01	0.006	0.813	1.022	0.01

PV Name	Parameter Setting					
	V_{cri}	δ_p	K_1	K_2	V_q	δ_q
PV17	1.108	0.01	0.012	0.711	1.022	0.01
PV18	1.088	0.01	0.006	0.8	1.027	0.01
PV19	1.086	0.01	0.014	0.777	1.022	0.01
PV20	1.097	0.01	0.01	0.802	1.022	0.01
PV21	1.089	0.01	0.053	0.697	1.02	0.01
PV22	1.105	0.01	0.023	0.738	1.019	0.01
PV23	1.089	0.01	0.015	0.795	1.025	0.01
PV24	1.086	0.01	0.018	0.964	1.033	0.01

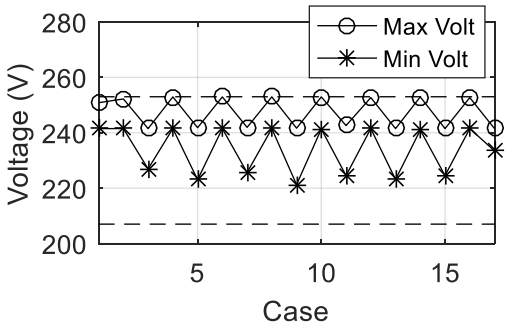

(a) Minimum and maximum phase voltage

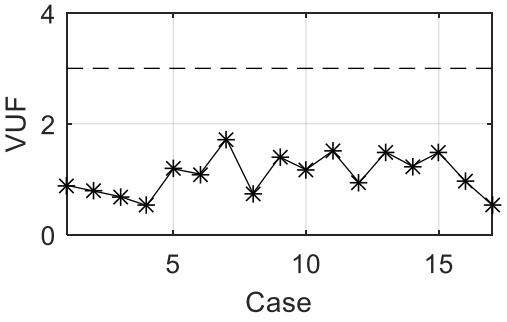

(b) Maximum VUF

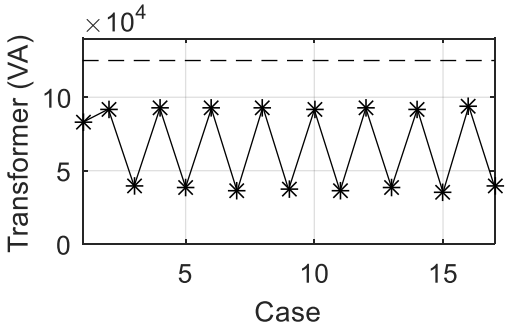

(c) MV/LV transformer utilization

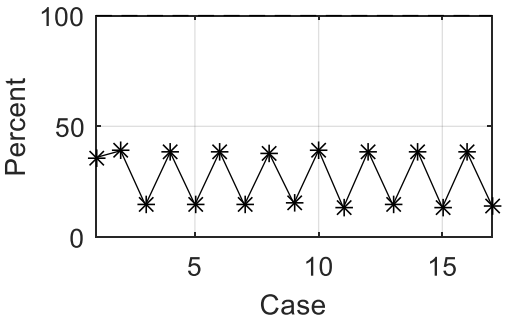

(d) Maximum line capacity

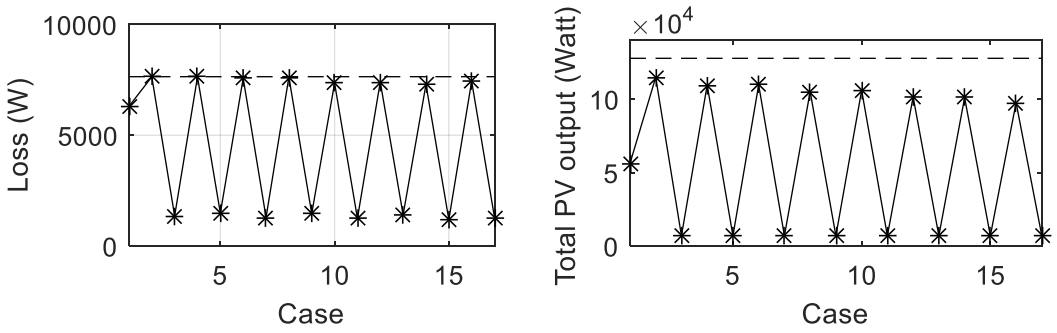

(e) System loss *(f) Total real power output from PV systems*

Figure 7.53 The results of the set of uncertainty

7.6.1.8 At The Day 9 November 2014

The parameter assessment will be analyzed by central control through 2-stage PSO process. According to the set of uncertainty at the day 9 November 2014 in Table 6.14, the optimal objective value in equation (5.81) is 29,558.07 W and the results of optimal parameter setting can be shown in Table 7.32. Considering only the case $z \in \{z1, z2, \ldots, z17\}$, the power flow results can be shown in Figure 7.54 and they are within the limit. The total real power output from PV systems at maximum value is 116,629.84 W at the case $z2$.

Table 7.32 Parameter setting of each connected PV system

PV Name	Parameter Setting					
	V_{cri}	δ_p	K_1	K_2	V_q	δ_q
PV1	1.124	0.018	0.207	1.19	1.07	0.012
PV2	1.095	0.018	0.2	0.994	1.067	0.023
PV3	1.08	0.01	0.19	1.08	1.054	0.033
PV4	1.09	0.01	0.17	1.05	1.057	0.022
PV5	1.08	0.01	0.28	1.13	1.1	0.025
PV6	1.09	0.01	0.20	1.04	1.074	0.027
PV7	1.10	0.02	0.19	1.05	1.046	0.03
PV8	1.12	0.02	0.20	0.50	1.064	0.024
PV9	1.18	0.01	0.15	1.06	1.055	0.028
PV10	1.105	0.012	0.194	1.101	1.059	0.03
PV11	1.097	0.012	0.186	1.071	1.049	0.05
PV12	1.096	0.015	0.417	1.223	1.059	0.027
PV13	1.1	0.014	0.207	0.732	1.005	0.027
PV14	1.095	0.012	0.172	1.15	1.049	0.038
PV15	1.089	0.011	0.203	0.827	1.059	0.036
PV16	1.088	0.011	0.158	1.123	1.063	0.03

PV Name	Parameter Setting					
	V_{cri}	δ_p	K_1	K_2	V_q	δ_q
PV17	1.085	0.013	0.176	1.087	1.037	0.058
PV18	1.093	0.015	0.002	0.998	1.07	0.029
PV19	1.079	0.01	0.179	1.027	1.052	0.034
PV20	1.09	0.013	0.212	1.09	1.052	0.034
PV21	1.086	0.01	0.152	1.117	1.065	0.035
PV22	1.095	0.013	0.144	1.043	1.05	0.034
PV23	1.088	0.01	0.132	1.013	1.061	0.024
PV24	1.093	0.014	0.199	1.03	1.063	0.03

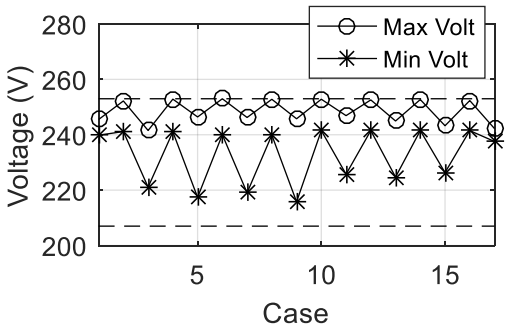

(a) Minimum and maximum phase voltage

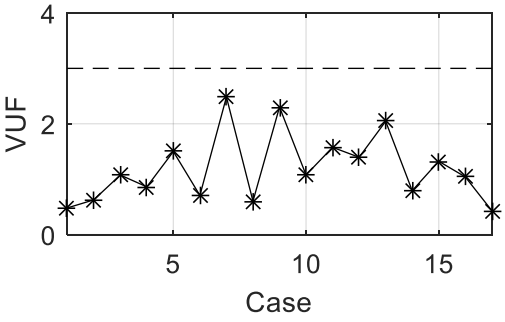

(b) Maximum VUF

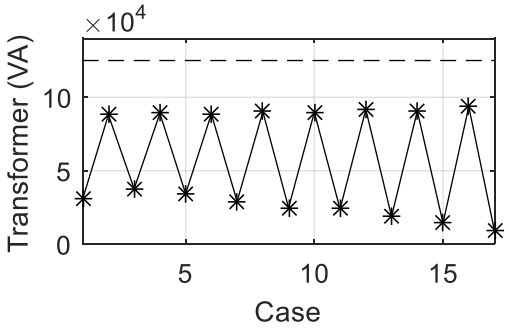

(c) MV/LV transformer utilization

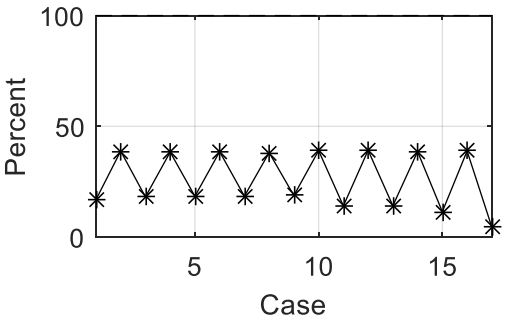

(d) Maximum line capacity

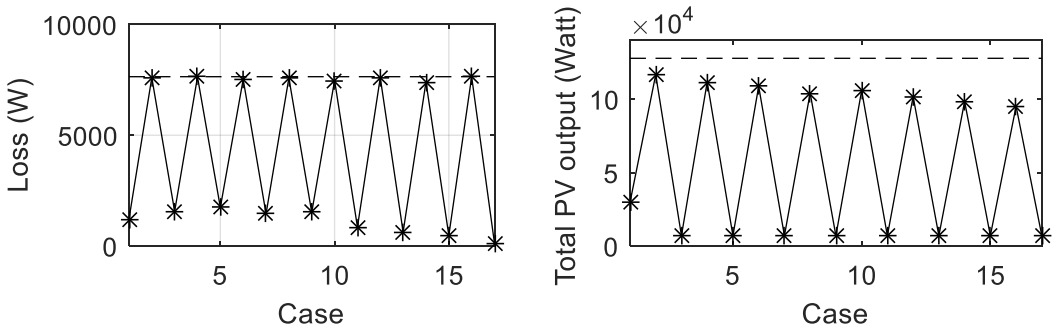

(e) System loss *(f) Total real power output from PV systems*

Figure 7.54 The results of the set of uncertainty

Comparing when the parameters of are adjusted in every one week and when the parameters are adjusted in every one day according to applying the continuous local control function, the summary can be shown in Table 7.33. It indicates that adjustment per one day is better than adjustment per one week because the parameters setting of each day can hold the limit under 17 cases of the set of uncertainty. Note that the objective value is positive because the power flow results are within the limit.

Table 7.33 The comparison between adjustment per one day and one week

Day at Nov 2014	Adjustment per one week		Adjustment per one day		Percent Change of Adjustment per One Day	
	Obj. Value	Max P Output	Obj. Value	Max P Output	Obj. Value	Max P Output
3	-8.2×10^{8}	110,750.88	58,433.80	109,474.51	>100%	-1.15%
4	-2.4×10^{8}	114,053.61	51,862.06	114,606.26	>100%	+0.48%
5	-6.4×10^{8}	112,284.26	44,890.02	113,525.61	>100%	+1.11%
6	-4.4×10^{8}	113,406.98	37,443.97	114,131.95	>100%	+0.64%
7	-3.9×10^{8}	113,499.34	41,338.27	113,761.11	>100%	+0.23%
8	-5.7×10^{8}	113,477.51	56,218.30	114,819.12	>100%	+1.18%
9	-7.1×10^{7}	115,062.96	29,558.07	116,629.84	>100%	+1.36%
				Mean Change	+0.34%	+0.55%

7.6.2 The Piecewise Linear Local Control Function Application

In this subsection, the simulation results are divided into eight subsections: (7.6.2.1) at the week 3-9 November 2014; (7.6.2.2) at the day 3 November 2014; (7.6.2.3) at the day 4 November 2014; (7.6.2.4) at the day 5 November 2014; (7.6.2.5)

at the day 6 November 2014; (7.6.2.6) at the day 7 November 2014; (7.6.2.7) at the day 8 November 2014; (7.6.2.8) at the day 9 November 2014. The piecewise linear local control function is selected in this subsection.

7.6.2.1 At The Week 3-9 November 2014

The parameter assessment will be analyzed by central control through 2-stage PSO process. According to the set of uncertainty at the week 3 November 2014 in Table 6.7, the optimal objective value in equation (5.81) is 47,383.61 W and the results of optimal parameter setting can be shown in Table 7.34. Considering only the case $z \in \{z1, z2, \ldots, z17\}$, the power flow results can be shown in Figure 7.55 and they are within the limit. The total real power output from PV systems at maximum value is 117,434.56 W at the case $z2$.

Table 7.34 Parameter setting of each connected PV system

PV Name	Parameter Setting					
	V_{p1}	V_{p2}	K_1	K_2	V_{q1}	V_{q2}
PV1	1.083	1.093	0.479	-0.884	1.06	1.08
PV2	1.085	1.101	0.504	-0.935	1.067	1.094
PV3	1.073	1.104	0.524	-0.945	1.052	1.088
PV4	1.095	1.107	0.471	-0.826	1.051	1.085
PV5	1.076	1.097	0.547	-0.931	1.057	1.08
PV6	1.076	1.093	0.454	-0.923	1.067	1.088
PV7	1.081	1.101	0.477	-0.901	1.055	1.096
PV8	1.085	1.097	0.513	-0.944	1.044	1.076
PV9	1.078	1.094	0.534	-0.95	1.052	1.072
PV10	1.089	1.1	0.499	-0.949	1.067	1.086
PV11	1.077	1.09	0.515	-0.95	1.065	1.089
PV12	1.087	1.097	0.442	-0.936	1.051	1.084
PV13	1.095	1.106	0.496	-0.895	1.063	1.093
PV14	1.089	1.104	0.511	-0.951	1.052	1.083
PV15	1.077	1.091	0.492	-0.951	1.099	1.112
PV16	1.083	1.104	0.494	-0.965	1.052	1.08
PV17	1.085	1.102	0.385	-0.933	1.051	1.078
PV18	1.079	1.091	0.414	-0.902	1.068	1.078
PV19	1.078	1.09	0.552	-0.957	1.042	1.075
PV20	1.08	1.09	0.582	-0.95	1.05	1.092
PV21	1.077	1.096	0.528	-0.913	1.066	1.094
PV22	1.086	1.096	0.434	-0.936	1.046	1.075
PV23	1.085	1.097	0.432	-0.934	1.041	1.079
PV24	1.08	1.094	0.501	-0.94	1.05	1.077

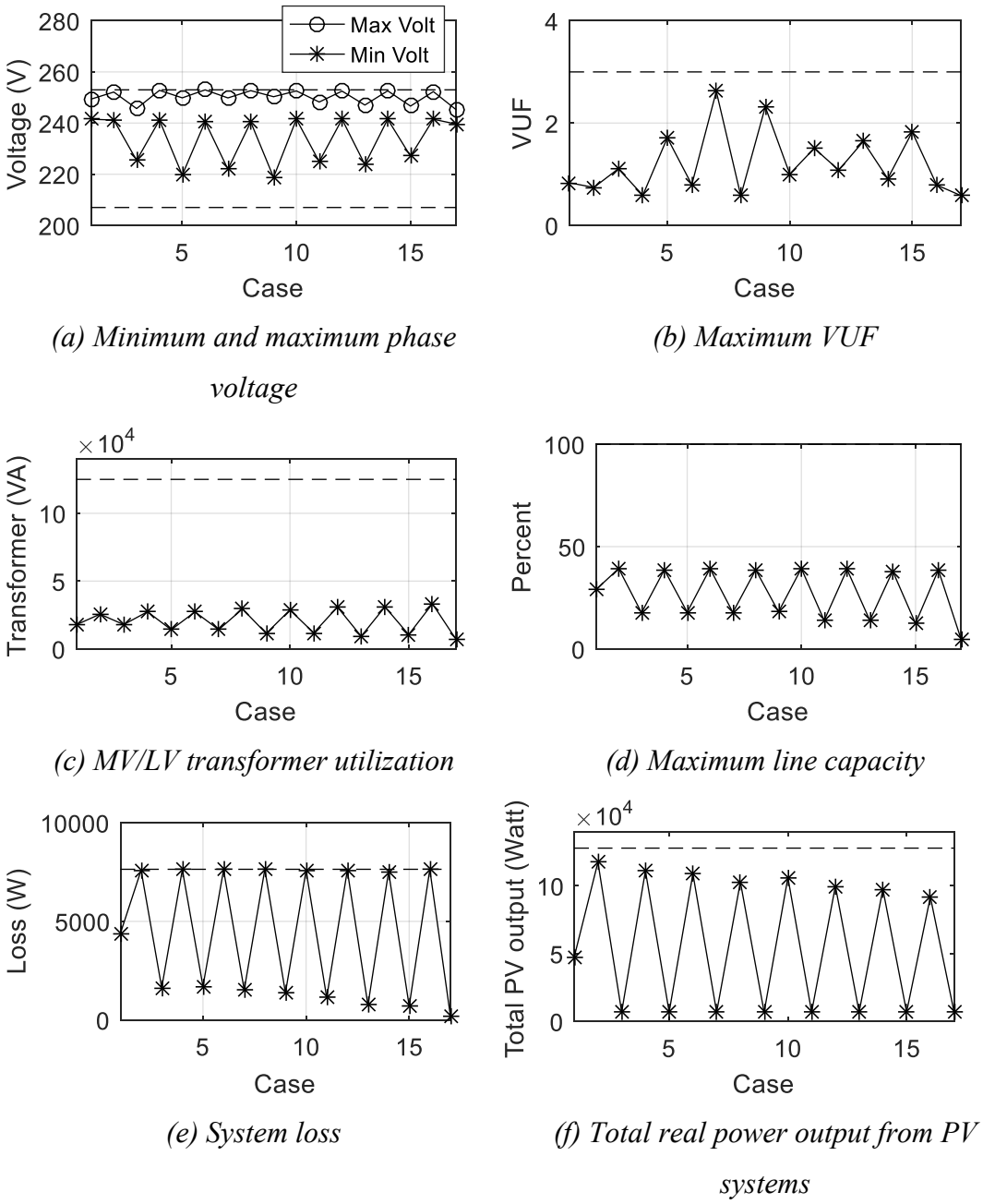

(a) Minimum and maximum phase voltage

(b) Maximum VUF

(c) MV/LV transformer utilization

(d) Maximum line capacity

(e) System loss

(f) Total real power output from PV systems

Figure 7.55 The results of the set of uncertainty

Applying (1) the set of uncertainty of each day and (2) the parameters setting in Table 7.34 at the week 3-9 November 2014, the objective values and the maximum value of total real power output from PV systems at the case $z2$ are shown in Table 7.35. The objective values is negative in days 3-9 because the power flow results are out of limit. Mostly, loss at each day is out of the limit as shown latter in Figures 7.56-7.62. The out of limit is due to the set of uncertainty is not enough considered

thoroughly the uncertainty in the modified 29 node distribution system. The solution can be the limit setting in the optimization constraints being less than the truth.

Table 7.35 The results of each day

Day at Nov 2014	Adjustment per One Week	
	Obj. Value	**Max P Output**
3	-1.2×10^9	111,162.25
4	-5.8×10^8	115,518.28
5	-1.1×10^9	113,433.28
6	-8.5×10^8	114,697.07
7	-8.9×10^8	115,009.99
8	-9.3×10^8	114,925.67
9	-1.4×10^8	116,929.42

- At the day 3 November, the power flow results can be shown in Figure 7.56. Losses are out of limit at cases z2, z4, z6, z8, z10, z12 and z16.
- At the day 4 November, the power flow results can be shown in Figure 7.57. Losses are out of limit at cases z2, z4, z6, z8, z10, z12 and z16.
- At the day 5 November, the power flow results can be shown in Figure 7.58. Losses are out of limit at cases z2, z4, z6, z8, z10, z12 and z16.
- At the day 6 November, the power flow results can be shown in Figure 7.59. Losses are out of limit at cases z2, z4, z6, z8, z10, z12 and z16.
- At the day 7 November, the power flow results can be shown in Figure 7.60. Losses are out of limit at cases z2, z4, z6, z8 and z10.
- At the day 8 November, the power flow results can be shown in Figure 7.61. Losses are out of limit at cases z2, z4, z6, z8, z10, z12 and z16.
- At the day 9 November, the power flow results can be shown in Figure 7.62. Losses are out of limit at cases z6, z8, z10, z14 and z16.

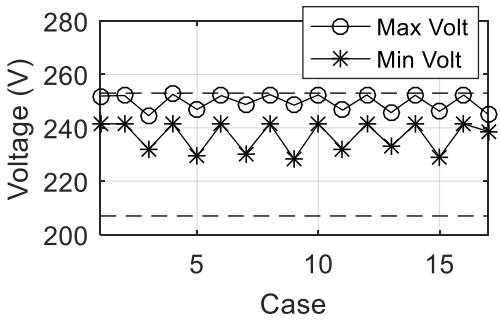

(a) Minimum and maximum phase voltage

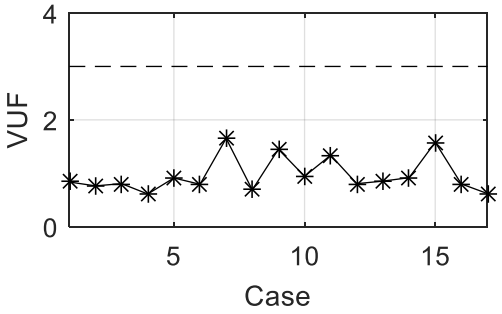

(b) Maximum VUF

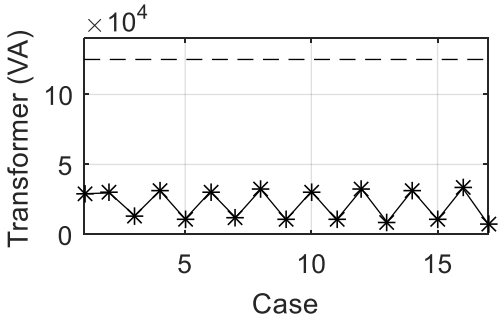

(c) MV/LV transformer utilization

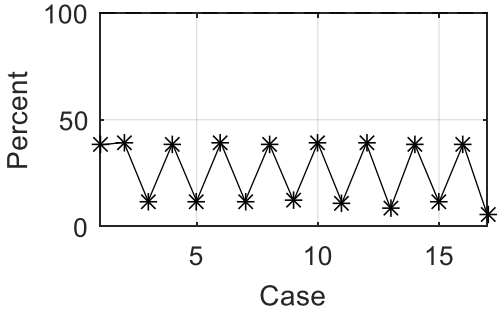

(d) Maximum line capacity

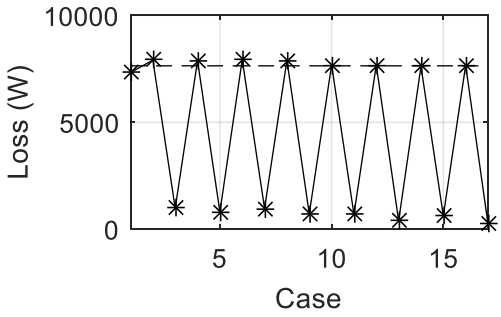

(e) System loss

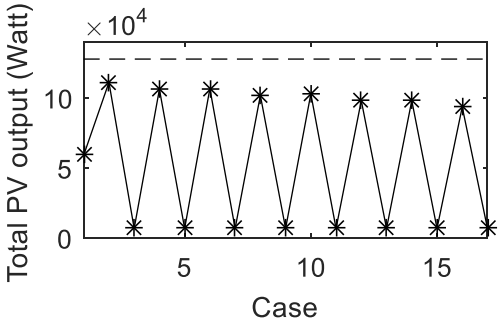

(f) Total real power output from PV systems

Figure 7.56 The results of the set of uncertainty

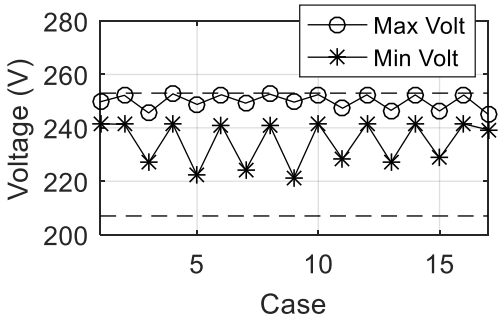

(a) Minimum and maximum phase voltage

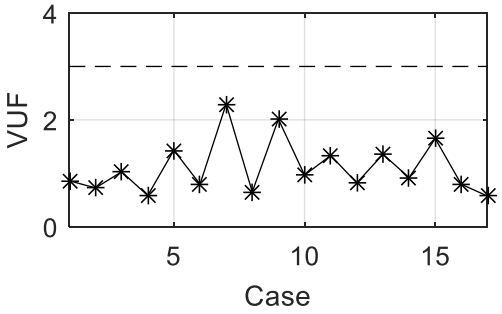

(b) Maximum VUF

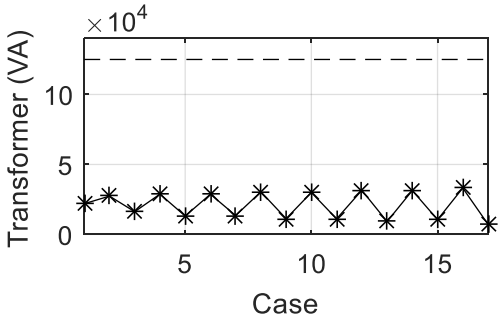

(c) MV/LV transformer utilization

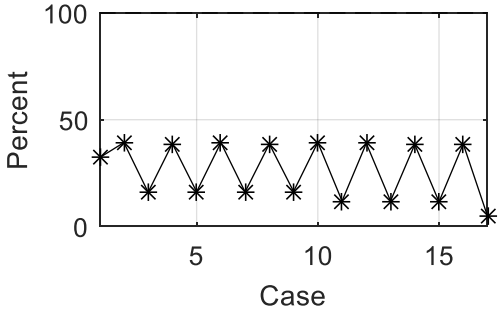

(d) Maximum line capacity

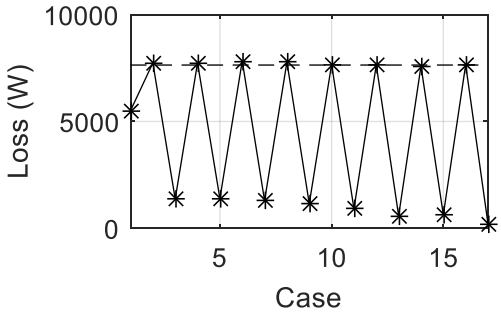

(e) System loss

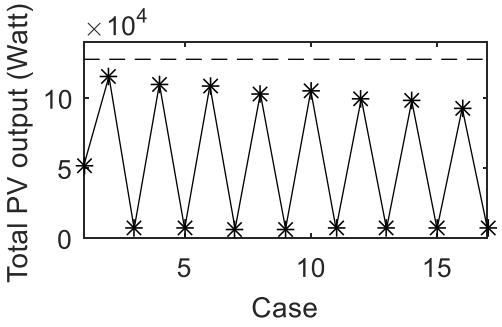

(f) Total real power output from PV systems

Figure 7.57 The results of the set of uncertainty

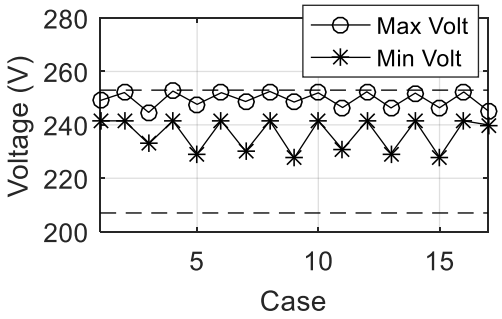

(a) Minimum and maximum phase voltage

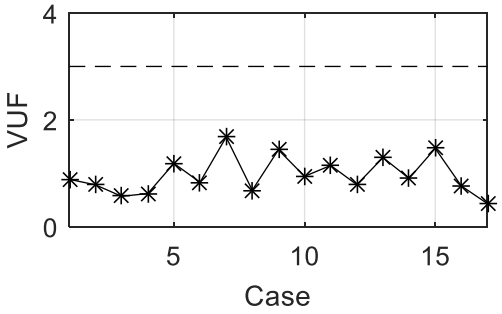

(b) Maximum VUF

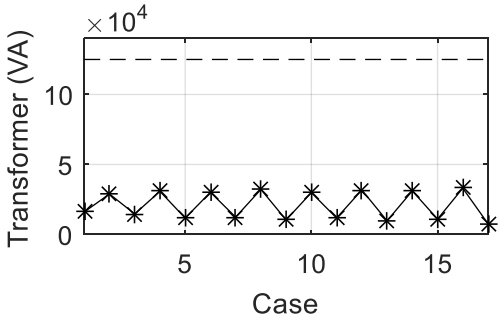

(c) MV/LV transformer utilization

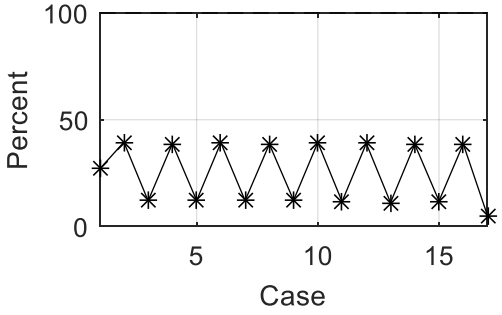

(d) Maximum line capacity

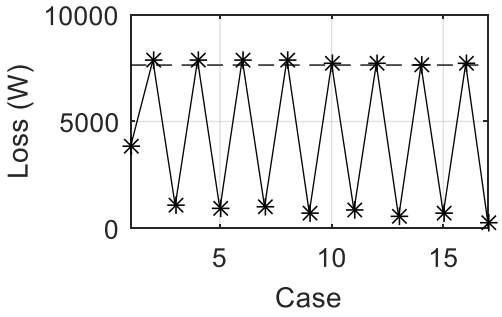

(e) System loss

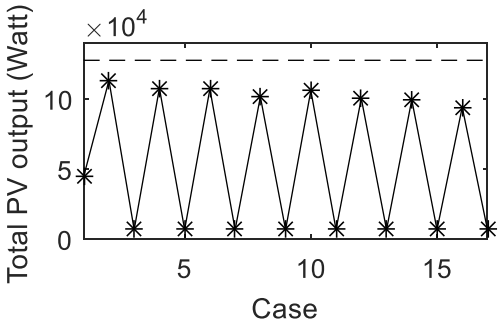

(f) Total real power output from PV systems

Figure 7.58 The results of the set of uncertainty

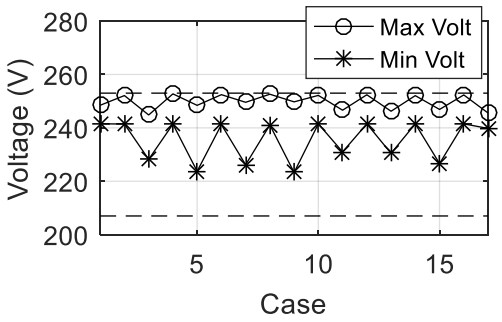

(a) Minimum and maximum phase voltage

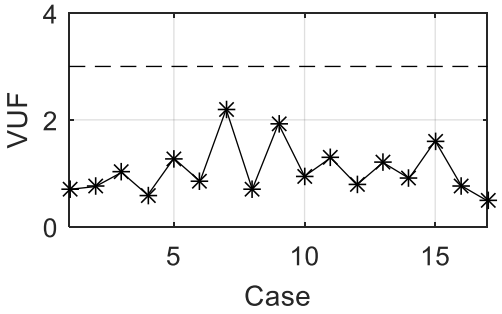

(b) Maximum VUF

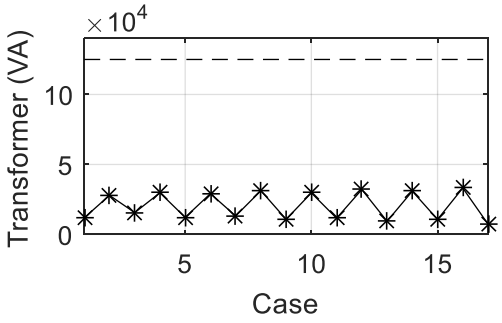

(c) MV/LV transformer utilization

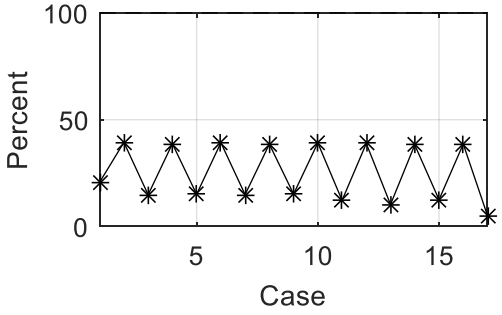

(d) Maximum line capacity

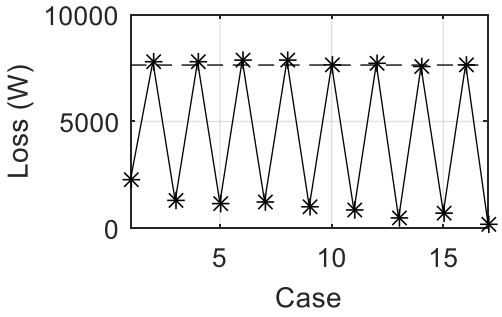

(e) System loss

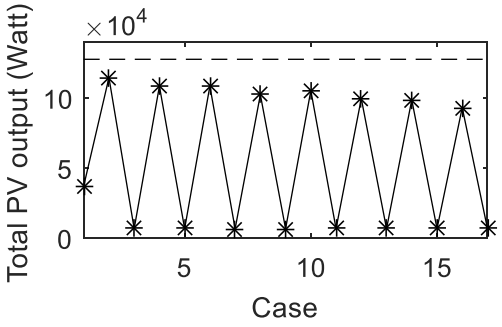

(f) Total real power output from PV systems

Figure 7.59 The results of the set of uncertainty

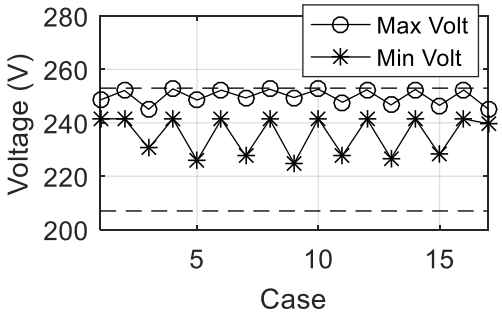

(a) Minimum and maximum phase voltage

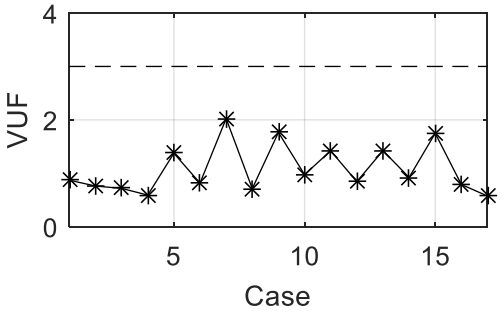

(b) Maximum VUF

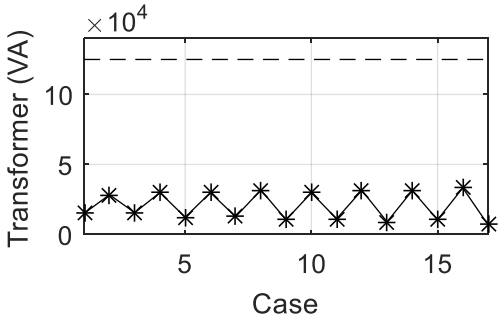

(c) MV/LV transformer utilization

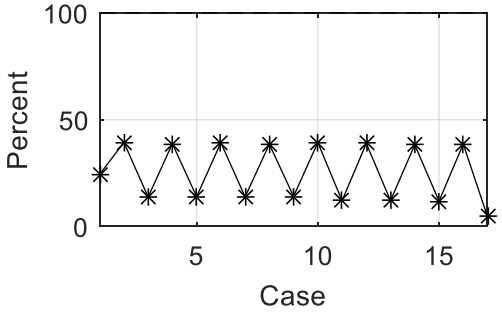

(d) Maximum line capacity

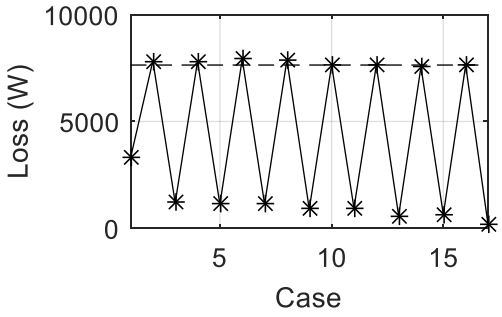

(e) System loss

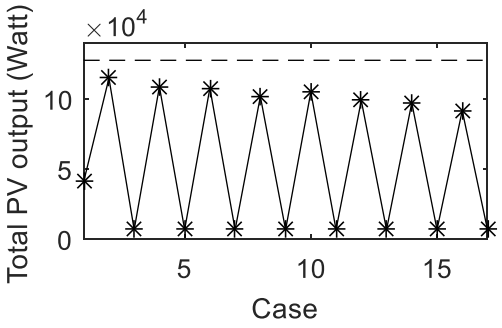

(f) Total real power output from PV systems

Figure 7.60 The results of the set of uncertainty

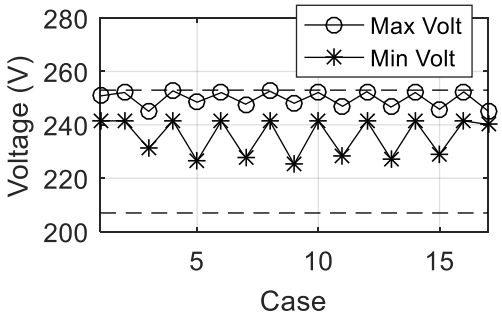

(a) Minimum and maximum phase voltage

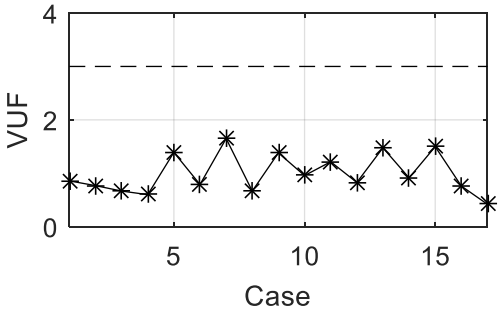

(b) Maximum VUF

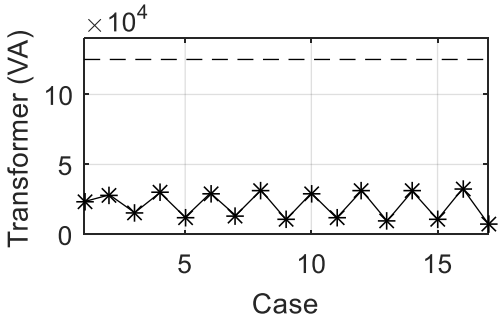

(c) MV/LV transformer utilization

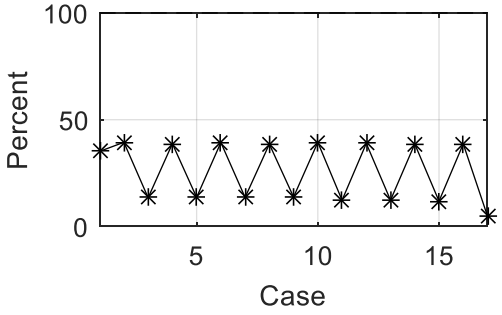

(d) Maximum line capacity

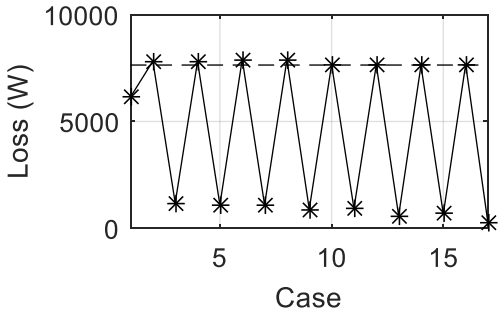

(e) System loss

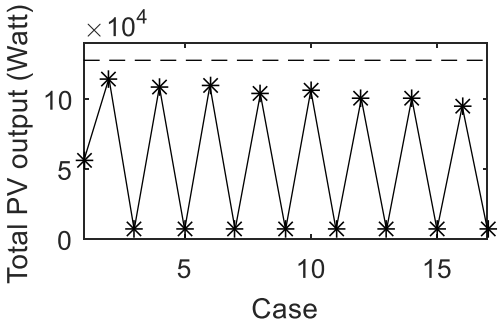

(f) Total real power output from PV systems

Figure 7.61 The results of the set of uncertainty

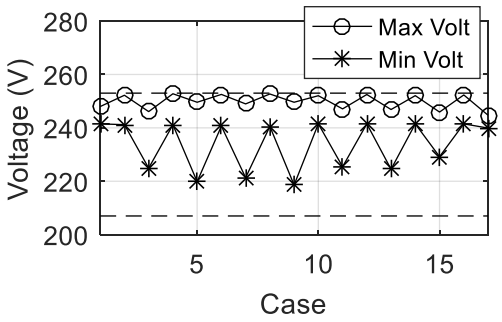

(a) Minimum and maximum phase voltage

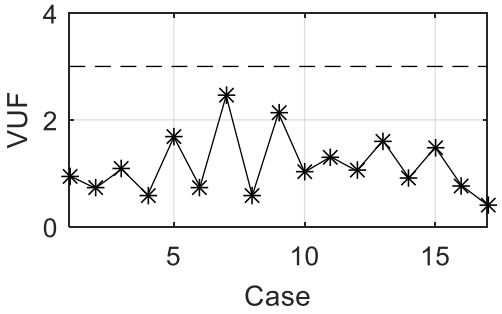

(b) Maximum VUF

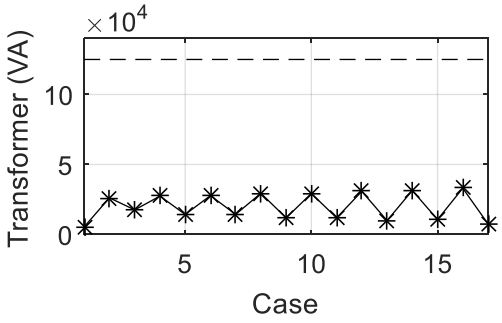

(c) MV/LV transformer utilization

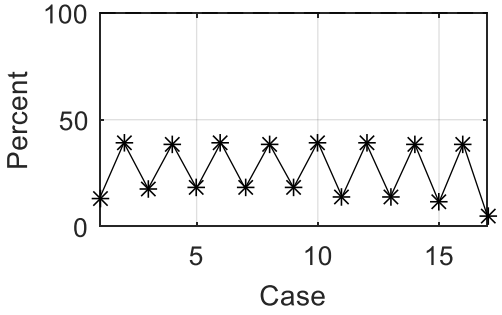

(d) Maximum line capacity

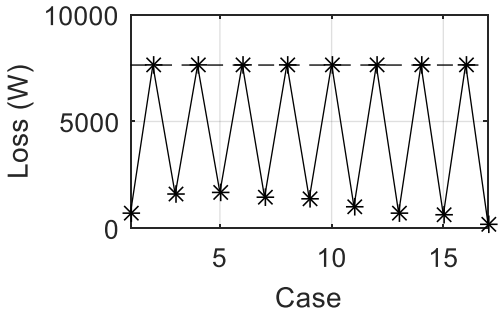

(e) System loss

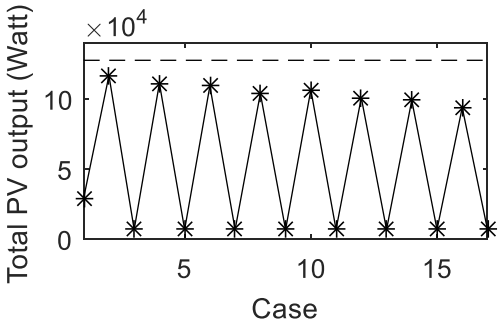

(f) Total real power output from PV systems

Figure 7.62 The results of the set of uncertainty

7.6.2.2 At The Day 3 November 2014

The parameter assessment will be analyzed by central control through 2-stage PSO process. According to the set of uncertainty at the day 3 November 2014 in Table 6.8, the optimal objective value in equation (5.81) is 60,022.07 W and the results of optimal parameter setting can be shown in Table 7.36. Considering only the case $z \in$

$\{z1, z2, \ldots, z17\}$, the power flow results can be shown in Figure 7.63 and they are within the limit. The total real power output from PV systems at maximum value is 112,551.35 W at the case $z2$.

Table 7.36 Parameter setting of each connected PV system

PV Name	Parameter Setting					
	V_{p1}	V_{p2}	K_1	K_2	V_{q1}	V_{q2}
PV1	1.07	1.106	0.253	-0.729	1.022	1.087
PV2	1.086	1.096	0.29	-0.713	1.067	1.077
PV3	1.089	1.102	0.233	-0.669	1.019	1.071
PV4	1.082	1.095	0.285	-0.796	0.986	1.04
PV5	1.083	1.099	0.242	-0.629	0.993	1.036
PV6	1.09	1.101	0.307	-0.718	1.01	1.066
PV7	1.092	1.102	0.262	-0.45	1.022	1.054
PV8	1.095	1.105	0.242	-0.614	0.976	1.054
PV9	1.09	1.102	0.145	-0.615	1.017	1.068
PV10	1.099	1.11	0.299	-0.766	1.025	1.067
PV11	1.092	1.104	0.163	-0.618	1.025	1.058
PV12	1.089	1.104	0.198	-0.767	1.025	1.075
PV13	1.097	1.107	0.207	-0.817	1.081	1.095
PV14	1.09	1.1	0.384	-0.805	1.017	1.072
PV15	1.085	1.101	0.381	-0.818	1.023	1.068
PV16	1.1	1.11	0.287	-0.692	0.986	1.069
PV17	1.096	1.11	0.235	-0.838	1.015	1.032
PV18	1.078	1.1	0.338	-0.755	1.035	1.066
PV19	1.076	1.093	0.695	-0.768	1.035	1.089
PV20	1.099	1.118	0.196	-0.768	1.025	1.051
PV21	1.087	1.097	0.218	-0.74	0.91	1.043
PV22	1.091	1.11	0.211	-0.826	0.997	1.049
PV23	1.089	1.099	0.226	-0.779	1.024	1.062
PV24	1.09	1.1	0.245	-0.525	1.03	1.07

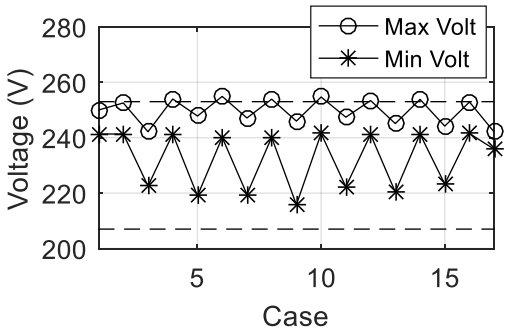

(a) Minimum and maximum phase voltage

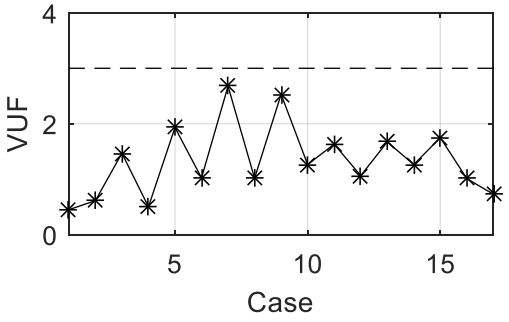

(b) Maximum VUF

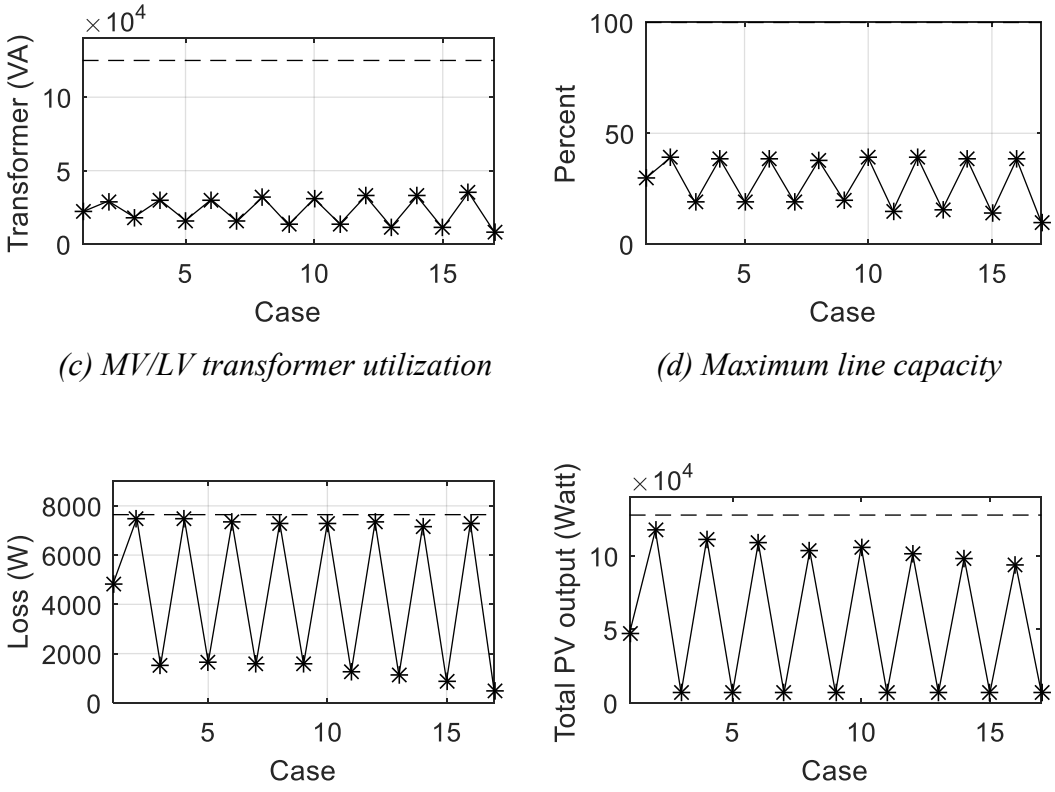

(c) MV/LV transformer utilization *(d) Maximum line capacity*

(e) System loss *(f) Total real power output from PV systems*

Figure 7.63 The results of the set of uncertainty

7.6.2.3 At The Day 4 November 2014

The parameter assessment will be analyzed by central control through 2-stage PSO process. According to the set of uncertainty at the day 4 November 2014 in Table 6.9, the optimal objective value in equation (5.81) is 52,291.58 W and the results of optimal parameter setting can be shown in Table 7.37. Considering only the case $z \in \{z1, z2, \ldots, z17\}$, the power flow results can be shown in Figure 7.64 and they are within the limit. The total real power output from PV systems at maximum value is 116,015.03 W at the case $z2$.

Table 7.37 Parameter setting of each connected PV system

PV Name	Parameter Setting					
	V_{p1}	V_{p2}	K_1	K_2	V_{q1}	V_{q2}
PV1	1.083	1.094	0.155	-0.934	0.979	1.065
PV2	1.083	1.093	0.257	-0.758	1.068	1.079

PV Name	Parameter Setting					
	V_{p1}	V_{p2}	K_1	K_2	V_{q1}	V_{q2}
PV3	1.077	1.087	0.431	-0.841	0.958	1.061
PV4	1.092	1.103	0.352	-0.752	0.97	1.042
PV5	1.086	1.097	0.136	-0.335	0.957	1.104
PV6	1.089	1.1	0.283	-0.576	0.968	1.084
PV7	1.09	1.105	0.264	-0.715	1.021	1.082
PV8	1.099	1.109	0.24	-0.78	0.972	1.068
PV9	1.09	1.105	0.187	-0.773	0.921	1.084
PV10	1.099	1.109	0.562	-0.739	0.971	1.033
PV11	1.09	1.106	0.229	-0.77	0.962	1.081
PV12	1.092	1.103	0.256	-0.742	0.956	1.073
PV13	1.091	1.105	0.282	-0.701	0.981	1.048
PV14	1.094	1.108	0.254	-0.731	0.961	1.075
PV15	1.069	1.096	0.271	-0.893	0.966	1.046
PV16	1.082	1.092	0.275	-0.671	0.955	1.082
PV17	1.096	1.108	0.278	-0.952	0.965	1.065
PV18	1.079	1.098	0.312	-0.85	0.938	1.067
PV19	1.084	1.095	0.51	-0.812	1.002	1.063
PV20	1.084	1.095	0.232	-0.774	0.946	1.102
PV21	1.085	1.096	0.229	-0.931	1.081	1.096
PV22	1.087	1.11	0.178	-0.736	0.975	1.067
PV23	1.086	1.096	0.454	-0.773	0.971	1.082
PV24	1.08	1.097	0.303	-0.743	0.943	1.066

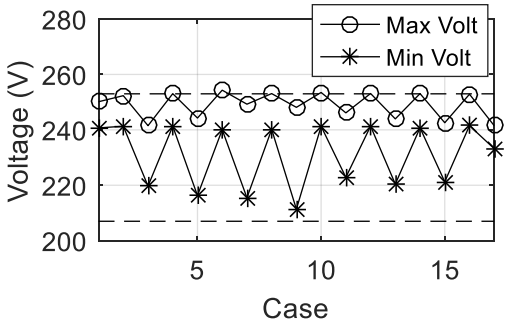

(a) Minimum and maximum phase voltage

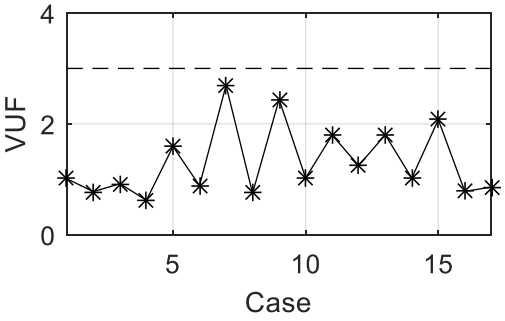

(b) Maximum VUF

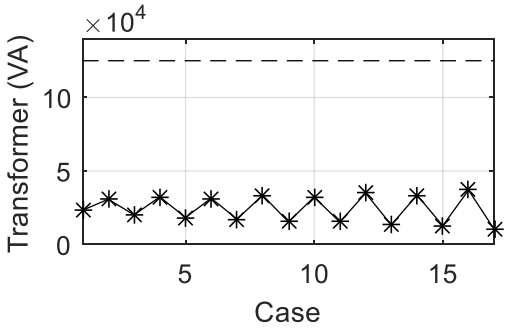

(c) MV/LV transformer utilization

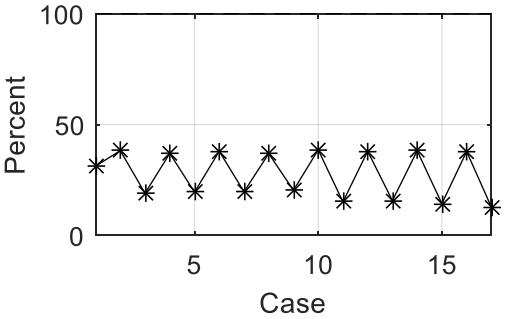

(d) Maximum line capacity

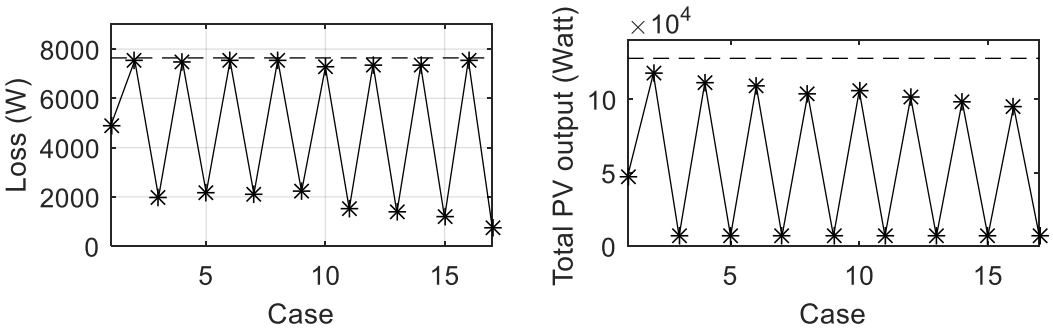

(e) System loss *(f) Total real power output from PV systems*

Figure 7.64 The results of the set of uncertainty

7.6.2.4 At The Day 5 November 2014

The parameter assessment will be analyzed by central control through 2-stage PSO process. According to the set of uncertainty at the day 5 November 2014 in Table 6.10, the optimal objective value in equation (5.81) is 45,003.35 W and the results of optimal parameter setting can be shown in Table 7.38. Considering only the case $z \in \{z1, z2, \dots, z17\}$, the power flow results can be shown in Figure 7.65 and they are within the limit. The total real power output from PV systems at maximum value is 115,153.18 W at the case $z2$.

Table 7.38 Parameter setting of each connected PV system

PV Name	Parameter Setting					
	V_{p1}	V_{p2}	K_1	K_2	V_{q1}	V_{q2}
PV1	1.09	1.104	0.083	-0.767	1.068	1.08
PV2	1.087	1.101	0.032	-0.773	1.076	1.095
PV3	1.076	1.097	0.092	-0.752	1.041	1.089
PV4	1.084	1.095	0.123	-0.902	1.08	1.091
PV5	1.084	1.102	0.1	-0.932	1.052	1.063
PV6	1.089	1.103	0.102	-0.81	1.086	1.096
PV7	1.09	1.102	0.094	-0.764	1.056	1.084
PV8	1.096	1.109	0.14	-0.825	1.051	1.07
PV9	1.083	1.097	0.136	-0.796	1.049	1.085
PV10	1.097	1.107	0.115	-0.839	1.046	1.056
PV11	1.095	1.105	0.16	-0.803	1.076	1.087
PV12	1.093	1.104	0.156	-0.698	1.049	1.082
PV13	1.086	1.11	0.134	-0.816	1.051	1.073
PV14	1.095	1.11	0.1	-0.88	1.052	1.068
PV15	1.084	1.103	0.07	-0.826	1.054	1.077
PV16	1.092	1.107	0.075	-0.708	1.025	1.051

PV Name	Parameter Setting					
	V_{p1}	V_{p2}	K_1	K_2	V_{q1}	V_{q2}
PV17	1.09	1.102	0.228	-0.996	1.06	1.077
PV18	1.083	1.097	0.089	-0.769	0.99	1.082
PV19	1.084	1.096	0.163	-0.661	1.07	1.095
PV20	1.09	1.1	0.079	-0.373	0.959	1.069
PV21	1.087	1.097	0.114	-0.763	1.006	1.042
PV22	1.089	1.102	0.122	-0.838	1.055	1.074
PV23	1.083	1.094	0.111	-0.76	1.056	1.073
PV24	1.086	1.097	0.076	-0.672	1.052	1.073

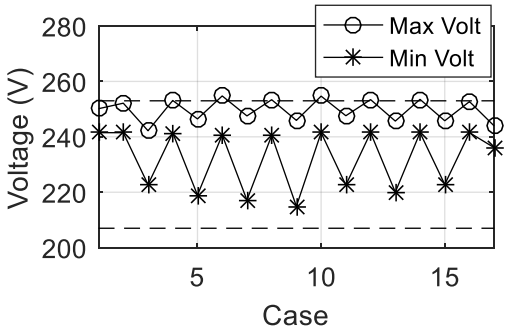

(a) Minimum and maximum phase voltage

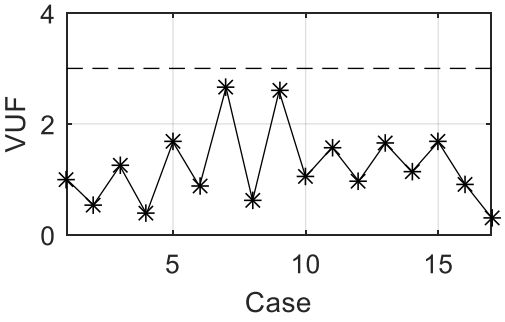

(b) Maximum VUF

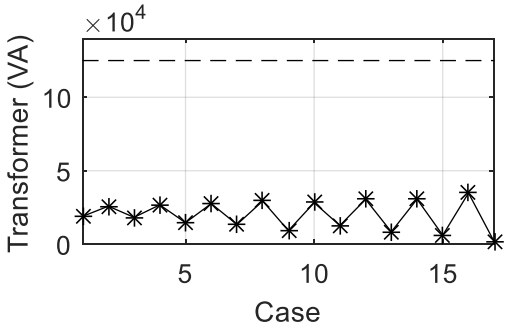

(c) MV/LV transformer utilization

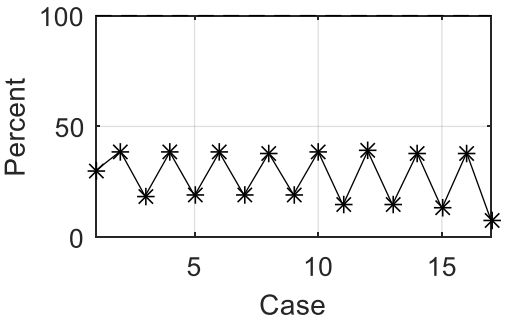

(d) Maximum line capacity

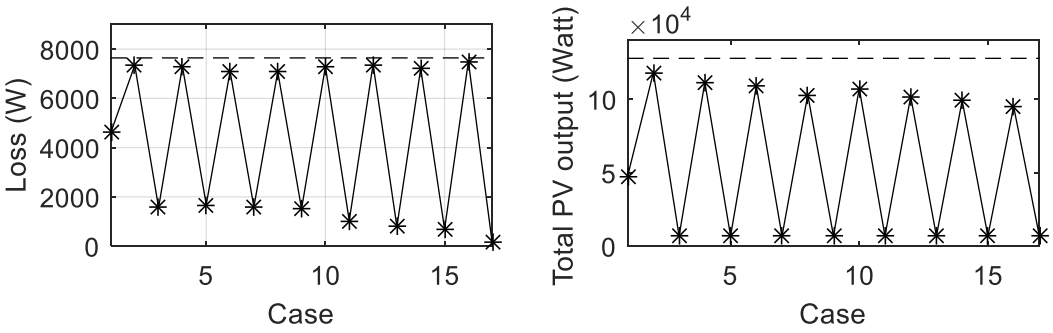

(e) System loss *(f) Total real power output from PV systems*

Figure 7.65 The results of the set of uncertainty

7.6.2.5 At The Day 6 November 2014

The parameter assessment will be analyzed by central control through 2-stage PSO process. According to the set of uncertainty at the day 6 November 2014 in Table 6.11, the optimal objective value in equation (5.81) is 37,522.40 W and the results of optimal parameter setting can be shown in Table 7.39. Considering only the case $z \in \{z1, z2, \dots, z17\}$, the power flow results can be shown in Figure 7.66 and they are within the limit. The total real power output from PV systems at maximum value is 114,352.09 W at the case $z2$.

Table 7.39 Parameter setting of each connected PV system

PV Name	Parameter Setting					
	V_{p1}	V_{p2}	K_1	K_2	V_{q1}	V_{q2}
PV1	1.077	1.1	0.441	-0.8	0.982	0.995
PV2	1.088	1.099	0.678	-0.781	0.944	0.981
PV3	1.086	1.096	0.642	-0.753	0.96	0.975
PV4	1.086	1.096	0.656	-0.768	0.956	1.016
PV5	1.085	1.1	0.528	-0.664	0.956	0.987
PV6	1.088	1.1	0.48	-0.848	0.956	0.978
PV7	1.081	1.1	0.49	-0.766	0.967	0.992
PV8	1.092	1.102	0.557	-0.518	0.937	0.981
PV9	1.086	1.099	0.653	-0.714	0.961	0.98
PV10	1.1	1.111	0.562	-0.755	0.959	0.985
PV11	1.088	1.109	0.521	-0.742	0.94	0.96
PV12	1.092	1.102	0.483	-0.68	0.968	0.982
PV13	1.093	1.105	0.605	-0.819	0.993	1.014
PV14	1.091	1.104	0.747	-0.824	0.96	0.989
PV15	1.078	1.09	0.478	-0.747	0.977	0.99
PV16	1.087	1.102	0.562	-0.555	0.944	1.086

PV Name	Parameter Setting					
	V_{p1}	V_{p2}	K_1	K_2	V_{q1}	V_{q2}
PV17	1.1	1.114	0.54	-0.844	0.958	0.972
PV18	1.071	1.093	0.435	-0.752	1.035	1.071
PV19	1.086	1.097	0.471	-0.92	0.951	0.982
PV20	1.094	1.111	0.539	-0.671	0.915	0.972
PV21	1.08	1.096	0.525	-0.794	0.913	0.975
PV22	1.096	1.112	0.411	-0.873	0.959	0.974
PV23	1.081	1.098	0.794	-0.763	0.947	0.996
PV24	1.093	1.103	0.518	-0.649	0.91	0.973

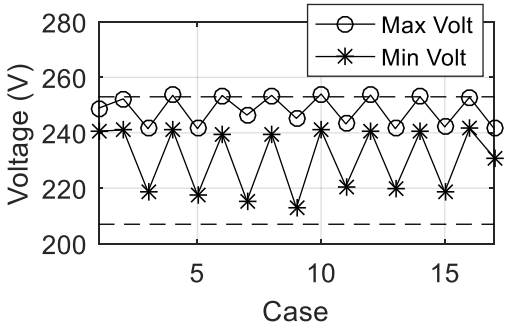

(a) Minimum and maximum phase voltage

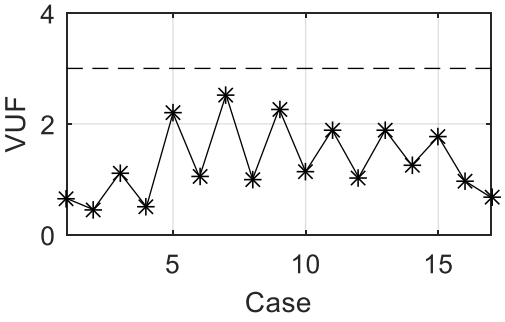

(b) Maximum VUF

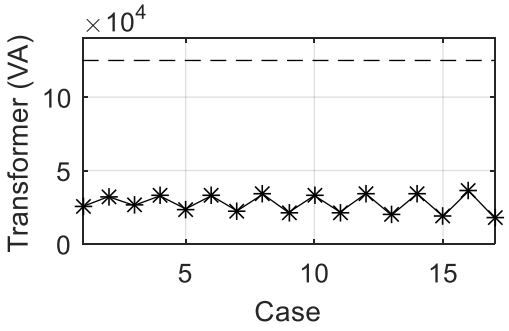

(c) MV/LV transformer utilization

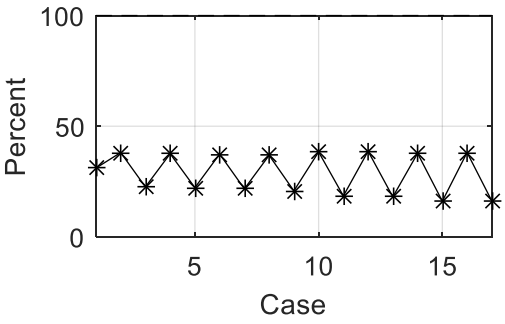

(d) Maximum line capacity

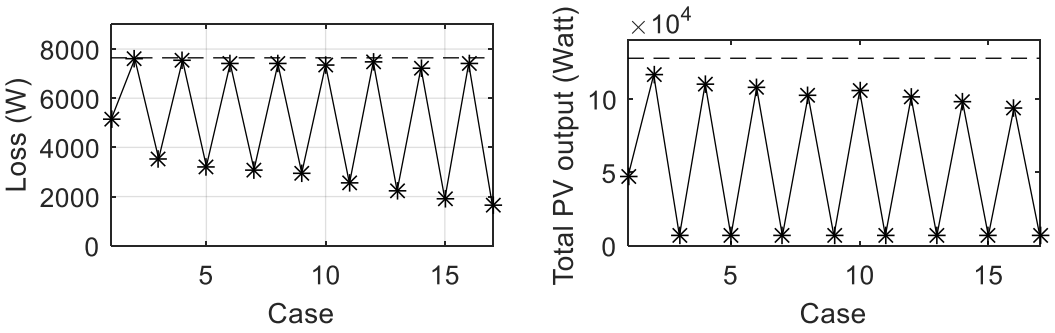

(e) System loss *(f) Total real power output from PV systems*

Figure 7.66 The results of the set of uncertainty

7.6.2.6 At The Day 7 November 2014

The parameter assessment will be analyzed by central control through 2-stage PSO process. According to the set of uncertainty at the day 7 November 2014 in Table 6.12, the optimal objective value in equation (5.81) is 41,431.62 W and the results of optimal parameter setting can be shown in Table 7.40. Considering only the case $z \in \{z1, z2, \ldots, z17\}$, the power flow results can be shown in Figure 7.67 and they are within the limit. The total real power output from PV systems at maximum value is 114,881.27 W at the case $z2$.

Table 7.40 Parameter setting of each connected PV system

PV Name	Parameter Setting					
	V_{p1}	V_{p2}	K_1	K_2	V_{q1}	V_{q2}
PV1	1.083	1.094	0.772	-0.775	0.971	1.092
PV2	1.086	1.098	0.368	-0.879	0.962	1.092
PV3	1.094	1.105	0.373	-0.83	0.956	1.09
PV4	1.094	1.112	0.287	-0.782	0.971	1.094
PV5	1.086	1.097	0.351	-0.792	0.976	1.092
PV6	1.089	1.099	0.342	-0.831	0.964	1.096
PV7	1.093	1.103	0.319	-0.908	0.932	1.097
PV8	1.094	1.105	0.356	-0.814	0.968	1.095
PV9	1.1	1.11	0.326	-0.877	0.969	1.089
PV10	1.1	1.114	0.358	-0.746	0.975	1.089
PV11	1.093	1.103	0.351	-0.89	0.954	1.103
PV12	1.086	1.108	0.389	-0.882	0.946	1.076
PV13	1.096	1.106	0.38	-0.863	0.957	1.091
PV14	1.086	1.103	0.424	-0.819	0.962	1.09
PV15	1.083	1.108	0.299	-0.789	0.962	1.109
PV16	1.092	1.107	0.488	-0.748	0.964	1.091

PV Name	Parameter Setting					
	V_{p1}	V_{p2}	K_1	K_2	V_{q1}	V_{q2}
PV17	1.089	1.104	0.309	-0.866	0.962	1.083
PV18	1.075	1.096	0.328	-0.747	0.964	1.105
PV19	1.08	1.093	0.392	-0.758	0.97	1.096
PV20	1.085	1.098	0.297	-0.792	0.967	1.087
PV21	1.086	1.096	0.344	-0.774	0.941	1.096
PV22	1.087	1.102	0.337	-0.83	0.97	1.085
PV23	1.083	1.095	0.29	-0.999	0.974	1.09
PV24	1.082	1.099	0.35	-0.878	0.954	1.092

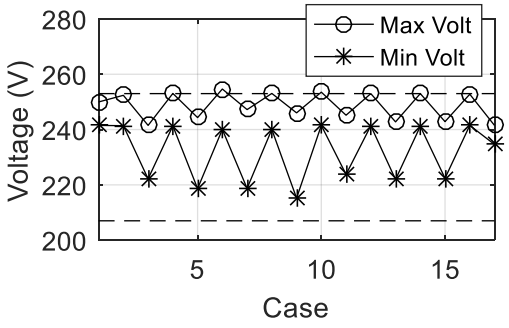

(a) Minimum and maximum phase voltage

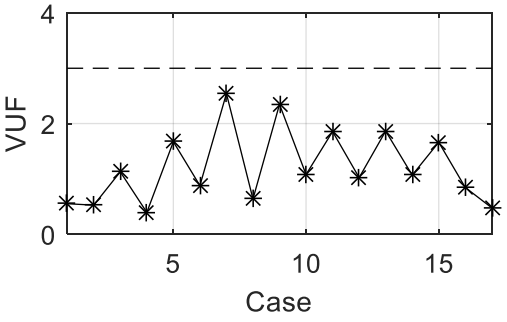

(b) Maximum VUF

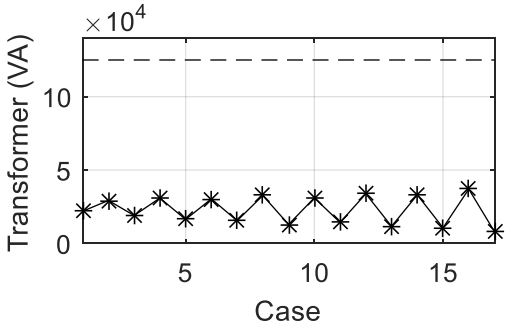

(c) MV/LV transformer utilization

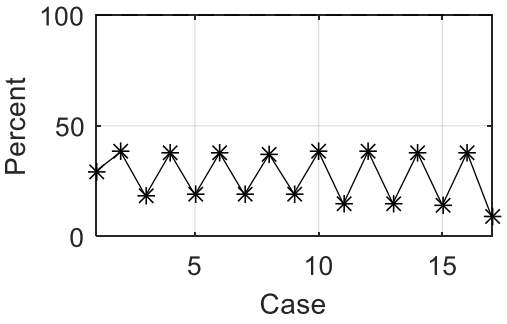

(d) Maximum line capacity

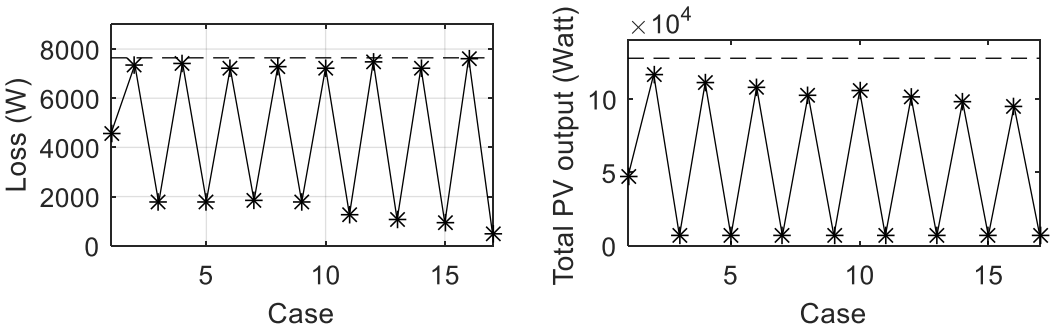

(e) System loss *(f) Total real power output from PV systems*

Figure 7.67 The results of the set of uncertainty

7.6.2.7 At The Day 8 November 2014

The parameter assessment will be analyzed by central control through 2-stage PSO process. According to the set of uncertainty at the day 8 November 2014 in Table 6.13, the optimal objective value in equation (5.81) is 56,674.72 W and the results of optimal parameter setting can be shown in Table 7.41. Considering only the case $z \in \{z1, z2, \ldots, z17\}$, the power flow results can be shown in Figure 7.68 and they are within the limit. The total real power output from PV systems at maximum value is 116,038.12 W at the case $z2$.

Table 7.41 Parameter setting of each connected PV system

PV Name	Parameter Setting					
	V_{p1}	V_{p2}	K_1	K_2	V_{q1}	V_{q2}
PV1	1.076	1.094	0.285	-0.685	1.032	1.075
PV2	1.099	1.109	0.205	-0.776	1.09	1.106
PV3	1.1	1.11	0.182	-0.769	1.034	1.092
PV4	1.089	1.101	0.152	-0.873	1.067	1.097
PV5	1.089	1.099	0.167	-0.777	1.038	1.086
PV6	1.089	1.101	0.188	-0.558	1.089	1.1
PV7	1.093	1.106	0.17	-0.91	1.041	1.069
PV8	1.098	1.11	0.072	-0.716	1.032	1.083
PV9	1.092	1.106	0.207	-0.867	1.009	1.073
PV10	1.098	1.109	0.21	-0.752	0.972	1.027
PV11	1.089	1.11	0.116	-0.816	0.975	1.072
PV12	1.094	1.104	0.176	-0.749	1.04	1.066
PV13	1.093	1.104	0.37	-0.865	1.044	1.08
PV14	1.094	1.104	0.193	-0.75	1.061	1.08
PV15	1.095	1.105	0.205	-0.739	1.021	1.069
PV16	1.09	1.11	0.428	-0.879	1.026	1.08

PV Name	Parameter Setting					
	V_{p1}	V_{p2}	K_1	K_2	V_{q1}	V_{q2}
PV17	1.092	1.103	0.06	-0.672	0.98	1.072
PV18	1.083	1.097	0.179	-0.787	1.044	1.058
PV19	1.068	1.093	0.162	-0.759	1.059	1.071
PV20	1.085	1.099	0.26	-0.626	1.055	1.08
PV21	1.083	1.096	0.121	-0.747	1.039	1.06
PV22	1.093	1.105	0.196	-0.785	1.028	1.087
PV23	1.088	1.098	0.174	-0.978	1.037	1.067
PV24	1.083	1.099	0.105	-0.821	1.051	1.082

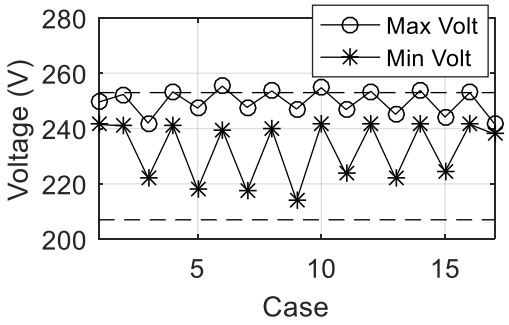

(a) Minimum and maximum phase voltage

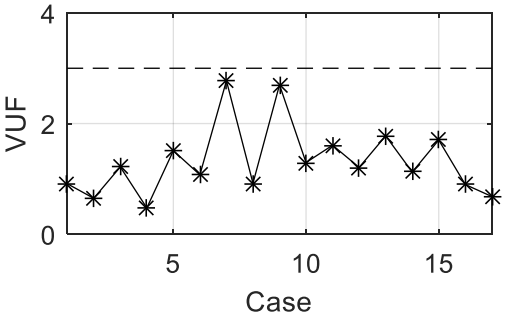

(b) Maximum VUF

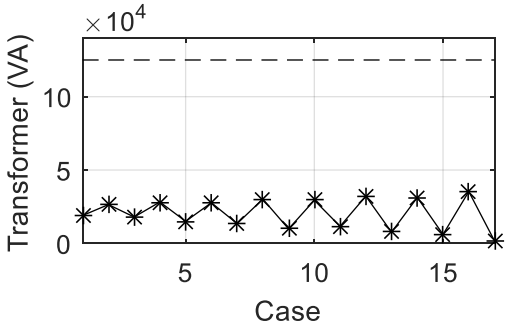

(c) MV/LV transformer utilization

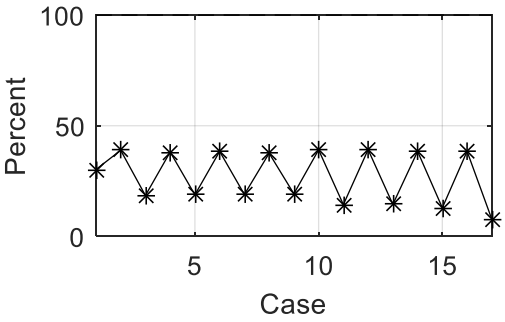

(d) Maximum line capacity

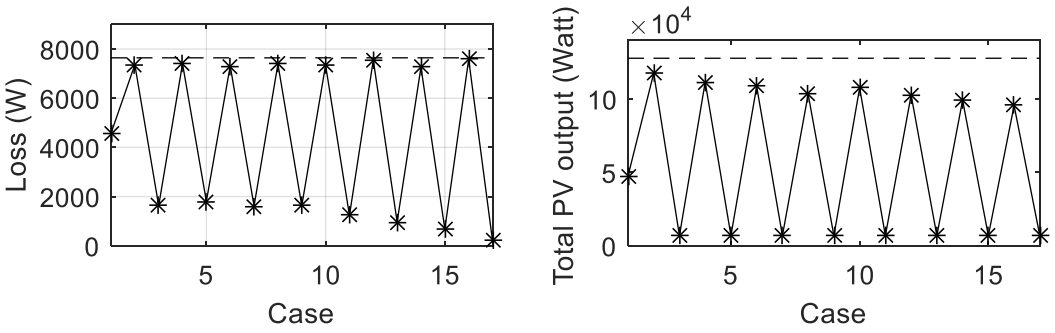

(e) System loss *(f) Total real power output from PV systems*

Figure 7.68 The results of the set of uncertainty

7.6.2.8 At The Day 9 November 2014

The parameter assessment will be analyzed by central control through 2-stage PSO process. According to the set of uncertainty at the day 9 November 2014 in Table 6.14, the optimal objective value in equation (5.81) is 29,559.41 W and the results of optimal parameter setting can be shown in Table 7.42. Considering only the case $z \in \{z1, z2, \ldots, z17\}$, the power flow results can be shown in Figure 7.69 and they are within the limit. The total real power output from PV systems at maximum value is 117,667.88 W at the case $z2$.

Table 7.42 Parameter setting of each connected PV system

PV Name	Parameter Setting					
	V_{p1}	V_{p2}	K_1	K_2	V_{q1}	V_{q2}
PV1	1.086	1.097	0.378	-0.978	1.01	1.089
PV2	1.094	1.107	0.47	-0.91	1.002	1.083
PV3	1.082	1.101	0.511	-0.896	1.005	1.091
PV4	1.098	1.109	0.525	-0.932	1.061	1.093
PV5	1.083	1.098	0.323	-0.952	1.014	1.095
PV6	1.084	1.102	0.512	-0.895	1.013	1.102
PV7	1.083	1.094	0.511	-0.877	1.014	1.087
PV8	1.087	1.097	0.528	-0.914	1.039	1.103
PV9	1.079	1.089	0.507	-0.924	1.011	1.091
PV10	1.091	1.101	0.539	-0.908	1.002	1.096
PV11	1.084	1.096	0.557	-0.916	1.009	1.078
PV12	1.086	1.096	0.535	-0.9	1.002	1.092
PV13	1.086	1.098	0.586	-0.934	1.017	1.058
PV14	1.093	1.109	0.516	-0.849	1.019	1.106
PV15	1.084	1.094	0.535	-0.915	1.009	1.103
PV16	1.087	1.106	0.481	-0.696	1.008	1.082

PV Name	Parameter Setting					
	V_{p1}	V_{p2}	K_1	K_2	V_{q1}	V_{q2}
PV17	1.091	1.101	0.521	-0.834	0.999	1.088
PV18	1.082	1.097	0.579	-0.906	1.004	1.088
PV19	1.08	1.093	0.512	-0.866	1.006	1.074
PV20	1.088	1.098	0.574	-0.932	1.027	1.098
PV21	1.085	1.095	0.597	-0.902	1.008	1.093
PV22	1.091	1.101	0.519	-0.868	1.018	1.08
PV23	1.081	1.096	0.565	-0.928	0.992	1.083
PV24	1.089	1.105	0.519	-0.916	1.007	1.085

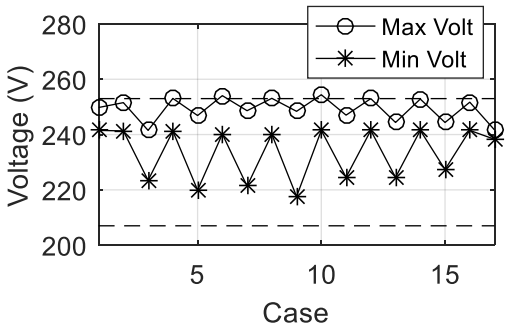

(a) Minimum and maximum phase voltage

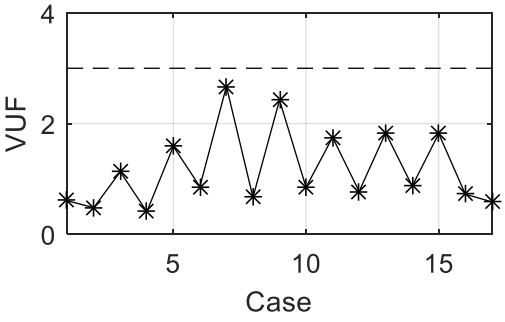

(b) Maximum VUF

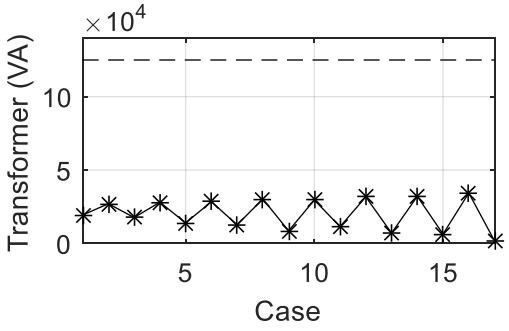

(c) MV/LV transformer utilization

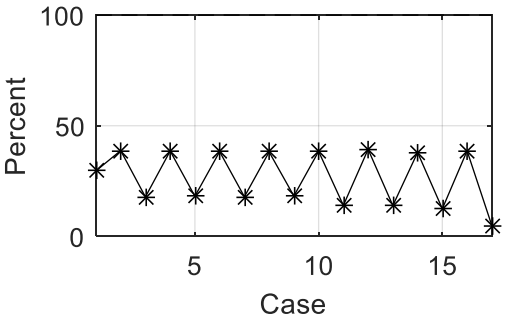

(d) Maximum line capacity

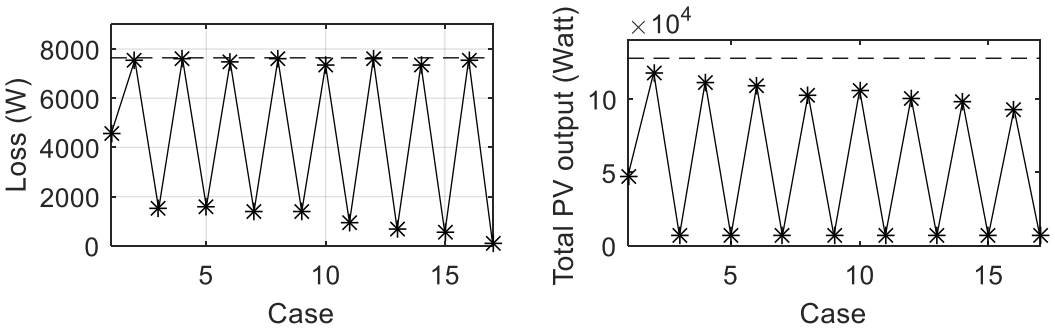

(e) System loss *(f) Total real power output from PV systems*

Figure 7.69 The results of the set of uncertainty

Comparing when the parameters of are adjusted in every one week and when the parameters are adjusted in every one day according to applying the piecewise linear local control function, the summary can be shown in Table 7.43. It indicates that adjustment per one day is better than adjustment per one week because the parameters setting of each day can hold the limit under 17 cases of the set of uncertainty. Note that the objective value is positive because the power flow results are within the limit.

Table 7.43 The comparison between adjustment per one day and one week

Day at Nov 2014	**Adjustment per one week**		**Adjustment per one day**		**Percent Change of Adjustment per One Day**	
	Obj. Value	**Max P Output**	**Obj. Value**	**Max P Output**	**Obj. Value**	**Max P Output**
3	-1.2×10^{9}	111,162.25	60,022.07	112,551.35	>100%	+1.25%
4	-5.8×10^{8}	115,518.28	52,291.58	116,015.03	>100%	+0.43%
5	-1.1×10^{9}	113,433.28	45,003.35	115,153.18	>100%	+1.52%
6	-8.5×10^{8}	114,697.07	37,522.40	114,352.09	>100%	-0.30%
7	-8.9×10^{8}	115,009.99	41,431.62	114,881.27	>100%	-0.11%
8	-9.3×10^{8}	114,925.67	56,674.72	116,038.12	>100%	+0.97%
9	-1.4×10^{8}	116,929.42	29,559.41	117,667.88	>100%	+0.63%
				Mean Change	>100%	+0.63%

Comparing the adjustment per one day strategy between (1) when local control is applied continuous function and (2) when local control is applied piecewise linear function, the percent different of objective value and maximum total real power output can be shown in Table 7.23 and it can notice that the results are close between (1) when

local control is applied continuous function and (2) when local control is applied piecewise linear function. Then, local control application can be chosen any one from continuous or piecewise linear function because of the nearly similar results.

Table 7.44 The comparison between continuous and piecewise linear local control application

Day at Nov 2014	Continuous Function		Piecewise Linear Function		Percent Change of Piecewise Linear Function	
	Obj. Value	Max P Output	Obj. Value	Max P Output	Obj. Value	Max P Output
3	58,433.80	109,474.51	60,022.07	112,551.35	+2.72%	+2.81%
4	51,862.06	114,606.26	52,291.58	116,015.03	+0.83%	+1.23%
5	44,890.02	113,525.61	45,003.35	115,153.18	+0.25%	+1.43%
6	37,443.97	114,131.95	37,522.40	114,352.09	+0.21%	+0.19%
7	41,338.27	113,761.11	41,431.62	114,881.27	+0.23%	+0.98%
8	56,218.30	114,819.12	56,674.72	116,038.12	+0.81%	+1.06%
9	29,558.07	116,629.84	29,559.41	117,667.88	+0.00%	+0.89%
				Mean Change	+0.72%	+1.23%

7.7 Monte Carlo Simulation

The optimization process applies the 17 cases of the set of uncertainty to solve the uncertainty problem. Therefore, the Monte-Carlo simulation is applied with 100,000-times random to prove the sufficiency in applying only the 17 cases of the set of uncertainty. The simulations are divided into 4 parts: (7.7.1) the modified 19 node distribution system with using continuous local control function; (7.7.2) the modified 19 node distribution system with using piecewise linear local control function; (7.7.3) The modified 29 node distribution system with using continuous local control function; (7.7.4) The modified 29 node distribution system with using piecewise linear local control function.

7.7.1 The Modified 19 Node Distribution System With Using Continuous Local Control Function

In this subsection, Monte Carlo simulation applies in eight parts: (7.7.1.1) at the week 3-9 November 2014; (7.7.1.2) at the day 3 November 2014; (7.7.1.3) at the day 4 November 2014; (7.7.1.4) at the day 5 November 2014; (7.7.1.5) at the day 6 November 2014; (7.7.1.6) at the day 7 November 2014; (7.7.1.7) at the day 8 November 2014;

(7.7.1.8) at the day 9 November 2014. The continuous local control function is selected in this subsection.

7.7.1.1 At The Week 3-9 November 2014

In this subsection, the value of load, solar irradiance and ambient temperature will be randomized in 100,000 times, according to the normal uncertainty characteristic of Figure 6.6 at the week 3-9 November 2014. Each random values at a time will be assessed by power flow algorithm. The optimal parameters setting at the week 3-9 November 2014 as shown in Table 7.2 is applied. Then, the power flow results in 100,000 times can be shown in Figure 7.70. The summary from Monte Carlo simulation is shown in Table 7.45. It can notice that mean values from power flow results are within the limit and. Overall results are not more than the limit specified.

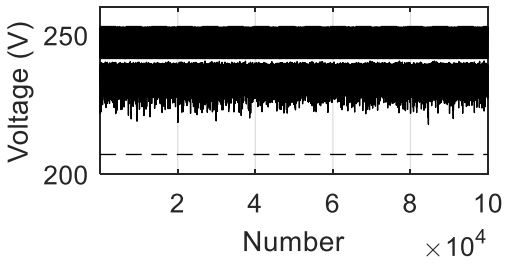

(a) Minimum and maximum phase voltage

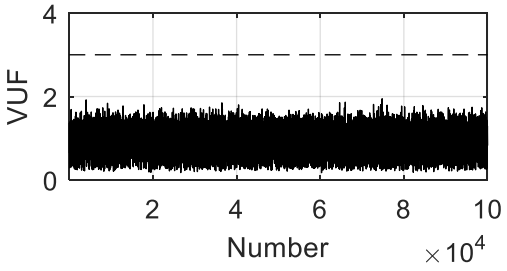

(b) Maximum VUF

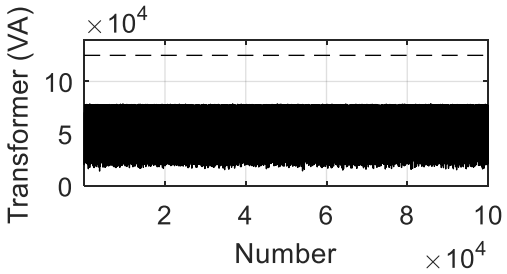

(c) MV/LV transformer utilization

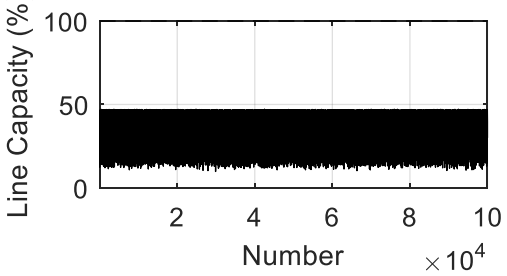

(d) Maximum line capacity

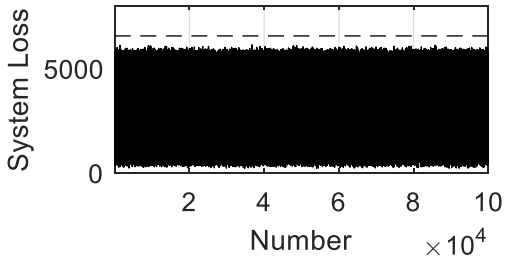

(e) System loss

Figure 7.70 The power flow results from 100,000-times random

Table 7.45 The results of Monte Carlo simulation

Variables	Mean Values from 100,000 times of random	Limit	Over-limit Consideration		
			Probability	Mean of Excess Value	Difference
Min Voltage	249.83 V	253.00 V	0.00%	0.00	0.00
Max Voltage	235.10 V	207.00 V	0.00%	0.00	0.00
Loss	3,890.53 W	6,547.58 W	0.00%	0.00	0.00
Max VUF	0.84	3.00	0.00%	0.00	0.00
Transformer Utilization	61,021.41 VA	125,000.00 VA	0.00%	0.00	0.00
Max Line Capacity	36.47%	100.00%	0.00%	0.00	0.00

where “Mean of Excess Value” is calculated from the excess value that if no excess value from 100,000 times of random, the “Mean of Excess Value” will be zero; “Difference” is calculated from the difference between “Limit” and “Mean of Excess Value”.

7.7.1.2 At The Day 3 November 2014

In this subsection, the value of load, solar irradiance and ambient temperature will be randomized in 100,000 times, according to the normal uncertainty characteristic of Figure 6.7 at the day 3 November 2014. Each random values at a time will be assessed by power flow algorithm. The optimal parameters setting at the day 3 November 2014 as shown in Table 7.7 is applied. Then, the power flow results in 100,000 times can be shown in Figure 7.71. The summary from Monte Carlo simulation is shown in Table 7.46. It can notice that mean values from power flow results are within the limit. The probability of over loss is 0.02%. The mean over loss is 6,570.27 W that is slightly more than the limit around 22.69 W. Other variables have 0% probability to exceed the limits.

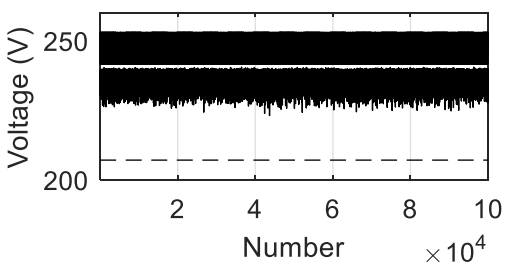

(a) Minimum and maximum phase voltage

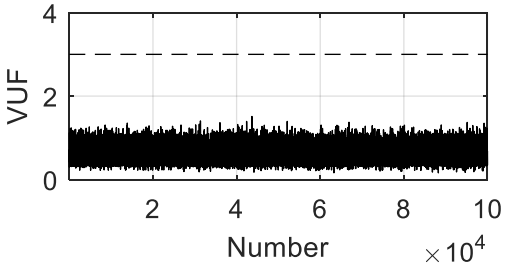

(b) Maximum VUF

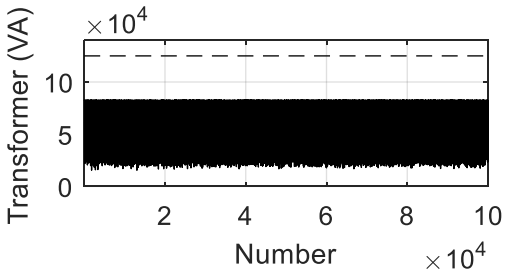

(c) MV/LV transformer utilization

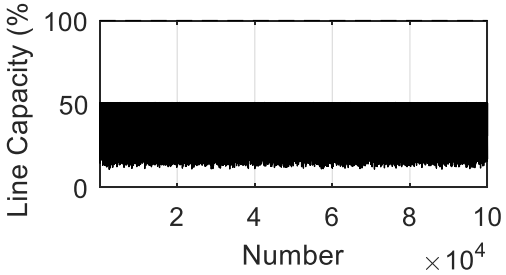

(d) Maximum line capacity

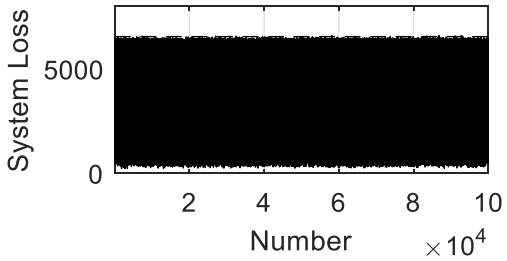

(e) System loss

Figure 7.71 The power flow results from 100,000-times random

Table 7.46 The results of Monte Carlo simulation

Variables	Mean Values from 100,000 times of random	Limit	Over-limit Consideration		
			Probability	Mean of Excess Value	Difference
Min Voltage	250.87 V	253.00 V	0.00%	0.00	0.00
Max Voltage	236.28 V	207.00 V	0.00%	0.00	0.00
Loss	4,707.89 W	6,547.58 W	0.02%	6,570.27 W	22.69 W
Max VUF	0.58	3.00	0.00%	0.00	0.00
Transformer Utilization	68,596.46 VA	125,000.00 VA	0.00%	0.00	0.00
Max Line Capacity	41.54%	100.00%	0.00%	0.00	0.00

7.7.1.3 At The Day 4 November 2014

In this subsection, the value of load, solar irradiance and ambient temperature will be randomized in 100,000 times, according to the normal uncertainty characteristic of Figure 6.8 at the day 4 November 2014. Each random values at a time will be assessed by power flow algorithm. The optimal parameters setting at the day 4 November 2014 as shown in Table 7.8 is applied. Then, the power flow results in 100,000 times can be shown in Figure 7.72. The summary from Monte Carlo simulation is shown in Table 7.47. It can notice that mean values from power flow results are within the limit. Overall results are not more than the limit specified.

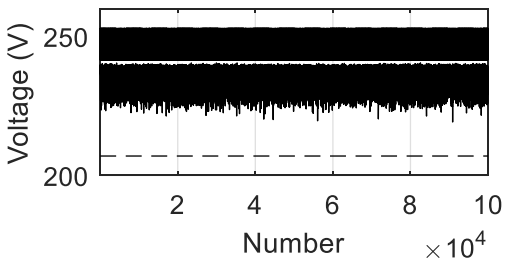

(a) Minimum and maximum phase voltage

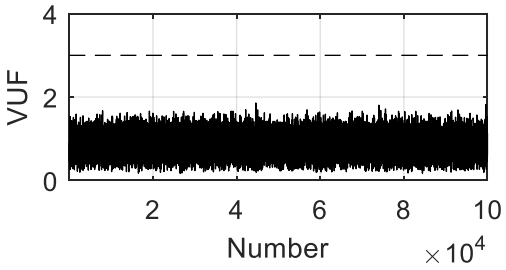

(b) Maximum VUF

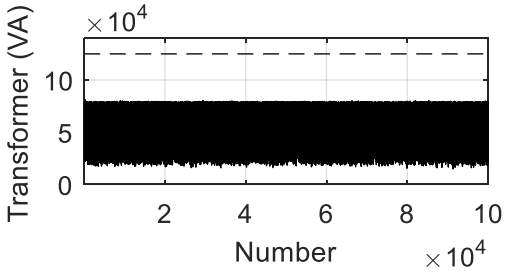

(c) MV/LV transformer utilization

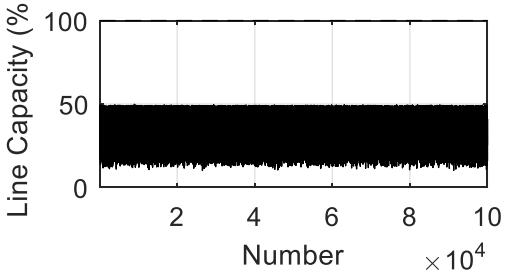

(d) Maximum line capacity

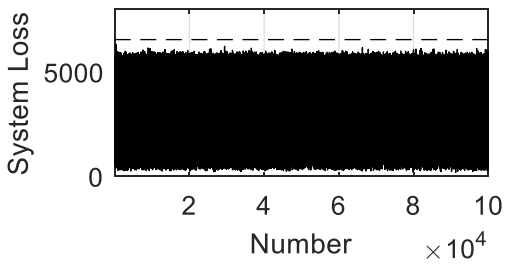

(e) System loss

Figure 7.72 The power flow results from 100,000-times random

Table 7.47 The results of Monte Carlo simulation

Variables	Mean Values from 100,000 times of random	Limit	Over-limit Consideration		
			Probability	Mean of Excess Value	Difference
Min Voltage	250.08 V	253.00 V	0.00%	0.00	0.00
Max Voltage	235.17 V	207.00 V	0.00%	0.00	0.00
Loss	4,240.29 W	6,547.58 W	0.00%	0.00	0.00
Max VUF	0.82	3.00	0.00%	0.00	0.00
Transformer Utilization	65,991.39 VA	125,000.00 VA	0.00%	0.00	0.00
Max Line Capacity	39.81%	100.00%	0.00%	0.00	0.00

7.7.1.4 At The Day 5 November 2014

In this subsection, the value of load, solar irradiance and ambient temperature will be randomized in 100,000 times, according to the normal uncertainty characteristic of Figure 6.9 at the day 5 November 2014. Each random values at a time will be assessed by power flow algorithm. The optimal parameters setting at the day 5 November 2014 as shown in Table 7.9 is applied. Then, the power flow results in 100,000 times can be shown in Figure 7.73. The summary from Monte Carlo simulation is shown in Table 7.48. It can notice that mean values from power flow results are within the limit. Overall results are not more than the limit specified.

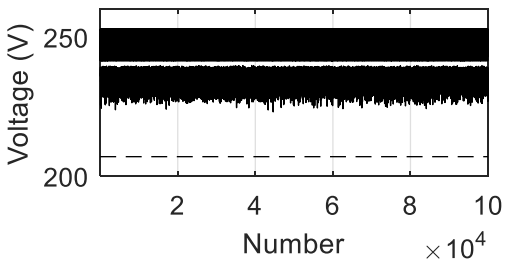

(a) Minimum and maximum phase voltage

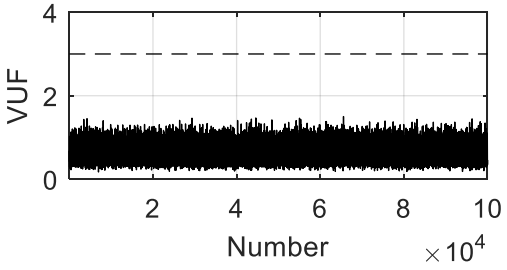

(b) Maximum VUF

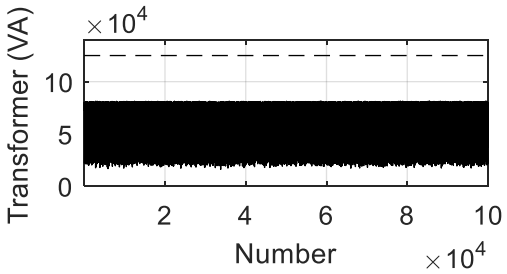

(c) MV/LV transformer utilization

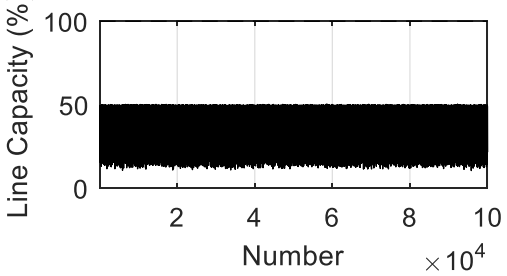

(d) Maximum line capacity

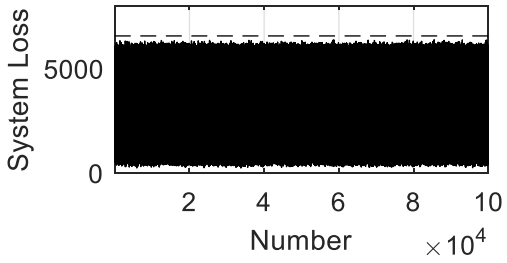

(e) System loss

Figure 7.73 The power flow results from 100,000-times random

Table 7.48 The results of Monte Carlo simulation

Variables	Mean Values from 100,000 times of random	Limit	Over-limit Consideration		
			Probability	Mean of Excess Value	Difference
Min Voltage	249.51 V	253.00 V	0.00%	0.00	0.00
Max Voltage	235.53 V	207.00 V	0.00%	0.00	0.00
Loss	3,964.83 W	6,547.58 W	0.00%	0.00	0.00
Max VUF	0.56	3.00	0.00%	0.00	0.00
Transformer Utilization	62,125.71 VA	125,000.00 VA	0.00%	0.00	0.00
Max Line Capacity	37.16%	100.00%	0.00%	0.00	0.00

7.7.1.5 At The Day 6 November 2014

In this subsection, the value of load, solar irradiance and ambient temperature will be randomized in 100,000 times, according to the normal uncertainty characteristic of Figure 6.10 at the day 6 November 2014. Each random values at a time will be assessed by power flow algorithm. The optimal parameters setting at the day 6 November 2014 as shown in Table 7.10 is applied. Then, the power flow results in 100,000 times can be shown in Figure 7.74. The summary from Monte Carlo simulation is shown in Table 7.49. It can notice that mean values from power flow results are within the limit. Overall results are not more than the limit specified.

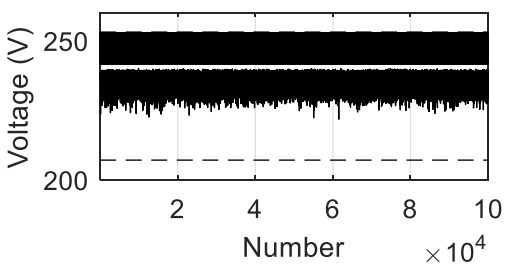

(a) Minimum and maximum phase voltage

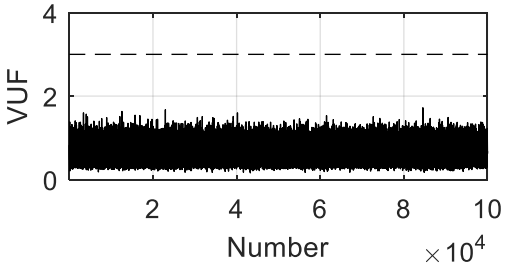

(b) Maximum VUF

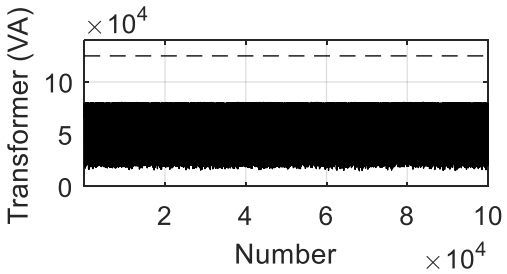

(c) MV/LV transformer utilization

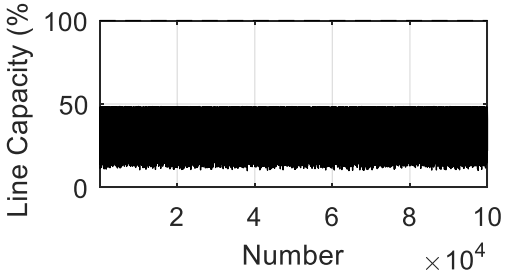

(d) Maximum line capacity

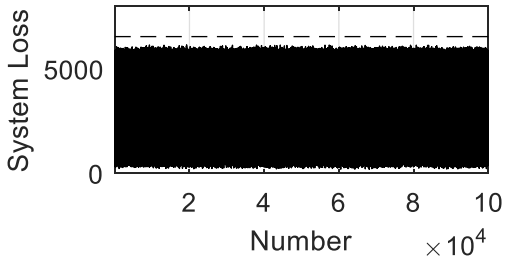

(e) System loss

Figure 7.74 The power flow results from 100,000-times random

Table 7.49 The results of Monte Carlo simulation

Variables	Mean Values from 100,000 times of random	Limit	Over-limit Consideration		
			Probability	Mean of Excess Value	Difference
Min Voltage	248.72 V	253.00 V	0.00%	0.00	0.00
Max Voltage	235.55 V	207.00 V	0.00%	0.00	0.00
Loss	3,400.64 W	6,547.58 W	0.00%	0.00	0.00
Max VUF	0.64	3.00	0.00%	0.00	0.00
Transformer Utilization	56,848.46 VA	125,000.00 VA	0.00%	0.00	0.00
Max Line Capacity	33.85%	100.00%	0.00%	0.00	0.00

7.7.1.6 At The Day 7 November 2014

In this subsection, the value of load, solar irradiance and ambient temperature will be randomized in 100,000 times, according to the normal uncertainty characteristic of Figure 6.11 at the day 7 November 2014. Each random values at a time will be assessed by power flow algorithm. The optimal parameters setting at the day 7 November 2014 as shown in Table 7.11 is applied. Then, the power flow results in 100,000 times can be shown in Figure 7.75. The summary from Monte Carlo simulation is shown in Table 7.50. It can notice that mean values from power flow results are within the limit. Overall results are not more than the limit specified.

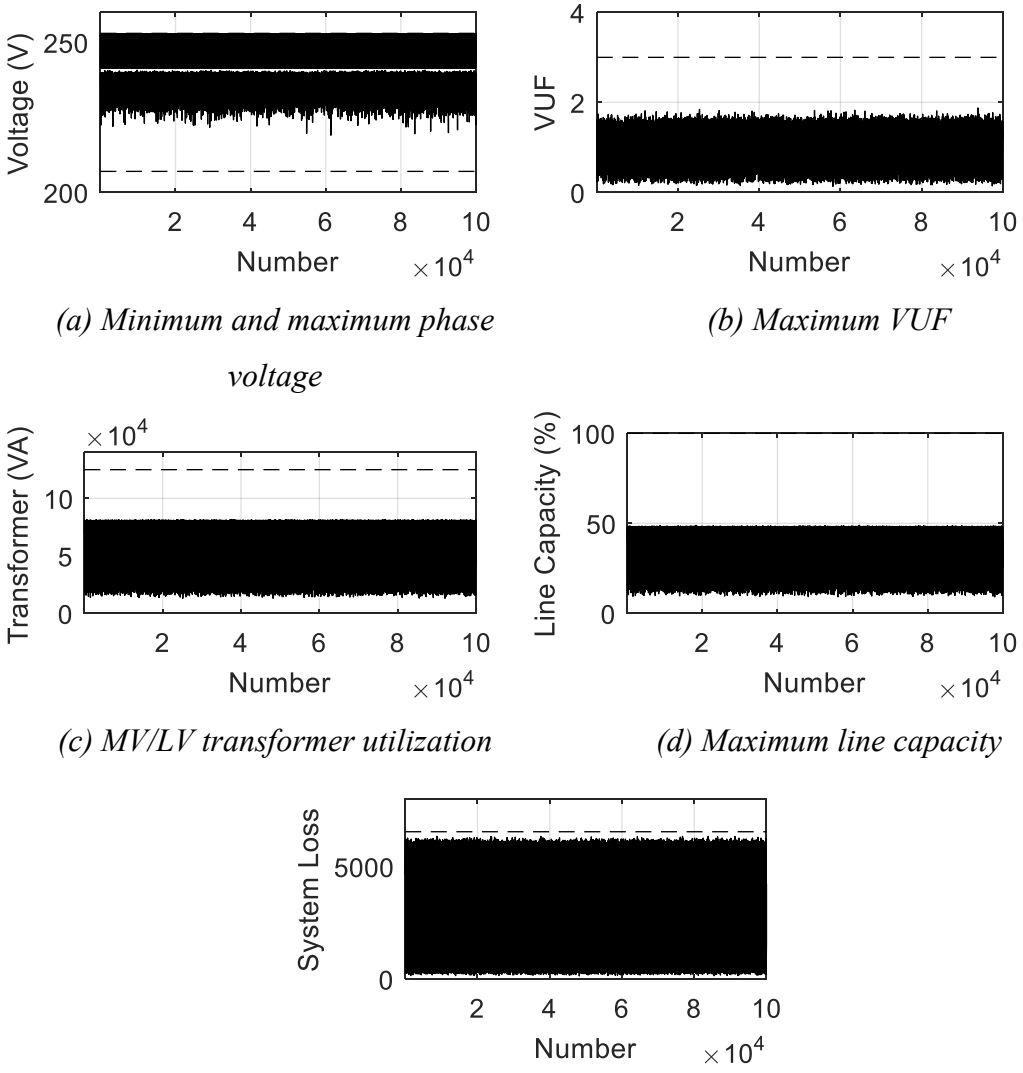

(a) Minimum and maximum phase voltage

(b) Maximum VUF

(c) MV/LV transformer utilization

(d) Maximum line capacity

(e) System loss

Figure 7.75 The power flow results from 100,000-times random

Table 7.50 The results of Monte Carlo simulation

Variables	Mean Values from 100,000 times of random	Limit	Over-limit Consideration		
			Probability	Mean of Excess Value	Difference
Min Voltage	249.31 V	253.00 V	0.00%	0.00	0.00
Max Voltage	235.73 V	207.00 V	0.00%	0.00	0.00
Loss	3,822.44 W	6,547.58 W	0.00%	0.00	0.00
Max VUF	1.23	3.00	0.00%	0.00	0.00
Transformer Utilization	61,599.93 VA	125,000.00 VA	0.00%	0.00	0.00
Max Line Capacity	36.82%	100.00%	0.00%	0.00	0.00

7.7.1.7 At The Day 8 November 2014

In this subsection, the value of load, solar irradiance and ambient temperature will be randomized in 100,000 times, according to the normal uncertainty characteristic of Figure 6.12 at the day 8 November 2014. Each random values at a time will be assessed by power flow algorithm. The optimal parameters setting at the day 8 November 2014 as shown in Table 7.12 is applied. Then, the power flow results in 100,000 times can be shown in Figure 7.76. The summary from Monte Carlo simulation is shown in Table 7.51. It can notice that mean values from power flow results are within the limit. The probability of over loss is 0.01%. The mean over loss is 6,562.24 W that is slightly more than the limit around 14.66 W. Other variables have 0% probability to exceed the limits.

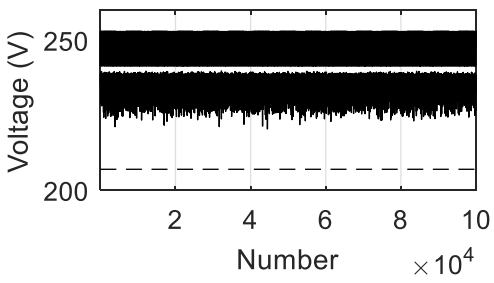

(a) Minimum and maximum phase voltage

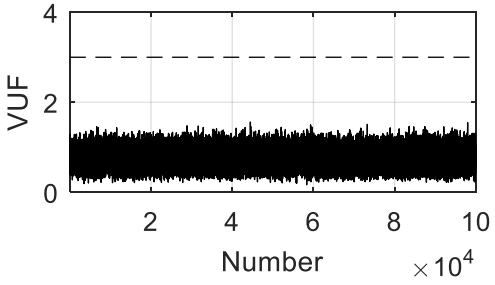

(b) Maximum VUF

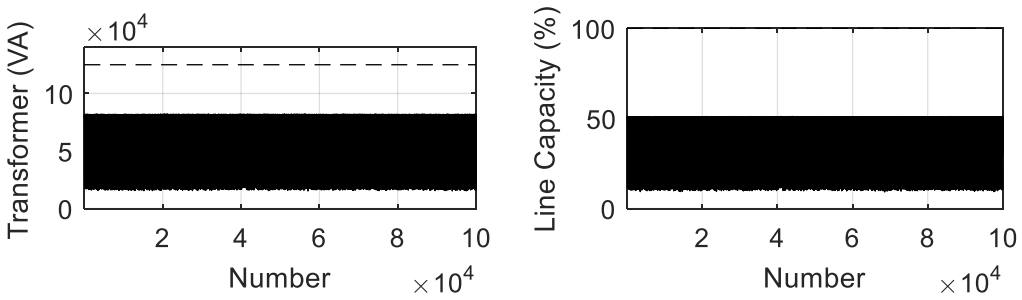

(c) MV/LV transformer utilization *(d) Maximum line capacity*

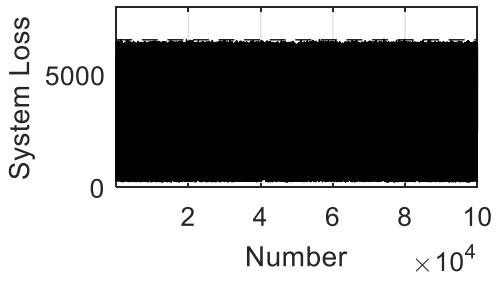

(e) System loss

Figure 7.76 The power flow results from 100,000-times random

Table 7.51 The results of Monte Carlo simulation

Variables	Mean Values from 100,000 times of random	Limit	Over-limit Consideration		
			Probability	Mean of Excess Value	Difference
Min Voltage	250.40 V	253.00 V	0.00%	0.00	0.00
Max Voltage	235.29 V	207.00 V	0.00%	0.00	0.00
Loss	4,426.85 W	6,547.58 W	0.01%	6,562.24 W	14.66 W
Max VUF	0.85	3.00	0.00%	0.00	0.00
Transformer Utilization	64,828.57 VA	125,000.00 VA	0.00%	0.00	0.00
Max Line Capacity	39.88%	100.00%	0.00%	0.00	0.00

7.7.1.8 At The Day 9 November 2014

In this subsection, the value of load, solar irradiance and ambient temperature will be randomized in 100,000 times, according to the normal uncertainty characteristic of Figure 6.13 at the day 9 November 2014. Each random values at a time will be assessed by power flow algorithm. The optimal parameters setting at the day 9 November 2014 as shown in Table 7.13 is applied. Then, the power flow results in 100,000 times can be shown in Figure 7.77. The summary from Monte Carlo simulation is shown in Table 7.52. It can notice that mean values from power flow results are

within the limit. The probability of over loss is 0.13%. The mean over loss is 6,570.90 W that is slightly more than the limit around 23.32 W. Other variables have 0% probability to exceed the limits.

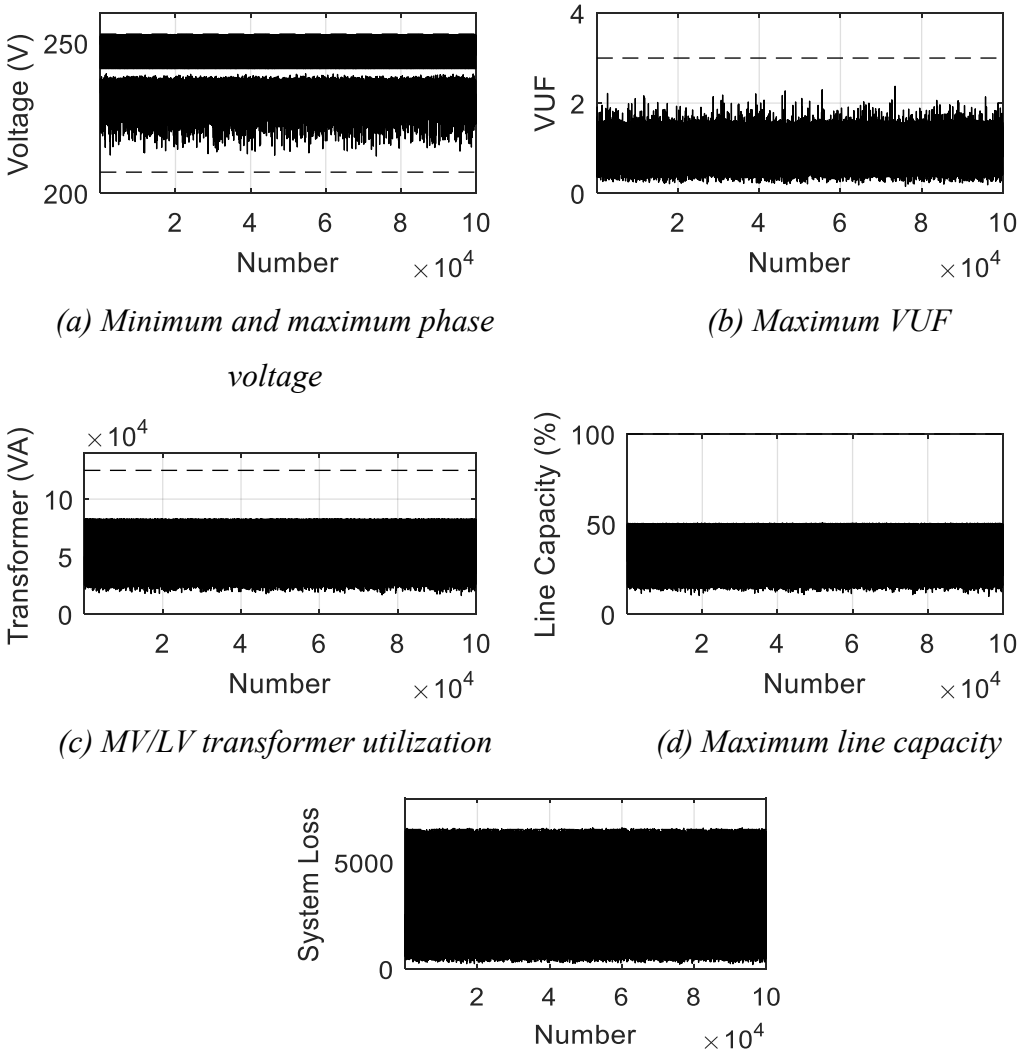

(a) Minimum and maximum phase voltage

(b) Maximum VUF

(c) MV/LV transformer utilization

(d) Maximum line capacity

(e) System loss

Figure 7.77 The power flow results from 100,000-times random

Table 7.52 The results of Monte Carlo simulation

Variables	Mean Values from 100,000 times of random	Limit	Over-limit Consideration		
			Probability	Mean of Excess Value	Difference
Min Voltage	248.13 V	253.00V	0.00%	0.00	0.00
Max Voltage	232.65 V	207.00 V	0.00%	0.00	0.00
Loss	2,762.98 W	6,547.58 W	0.13%	6,570.90 W	23.32 W
Max VUF	1.01	3.00	0.00%	0.00	0.00
Transformer Utilization	50,152.59 VA	125,000.00 VA	0.00%	0.00	0.00
Max Line Capacity	30.83%	100.00%	0.00%	0.00	0.00

From Monte Carlo simulations at the 19 node distribution system with using continuous local control function, it can prove that the determination of only the 17 cases of the set of uncertainty is sufficient to solve the uncertainty problem of load, solar irradiance and ambient temperature. It is because as follows:

- The power flow results of minimum and maximum voltage profile, maximum VUF, MV/LV transformer utilization and maximum line capacity are within the limit. The probabilities have around 100% to hold on those limits under the uncertainty;
- The probability of the loss results have 100% to hold on the limits under the uncertainty in the Day 4, 5, 6, 7 and the Week 3-9 November 2014;
- For the Day 3, 8 and 9 November 2014, the probability of the loss results to exceed the limit is less than 0.2% or the probability of the loss results have around 99.8% to hold on the loss limit under the uncertainty according to the worst case at the day 9 November 2014. Mean over losses are more than the limit about <30 W according to the day 9 November 2014.

However, the results that exceed only a small extent of the loss limit can be resolved by adjusting the loss limit in the optimization problem less than the actual value.

7.7.2 The Modified 19 Node Distribution System With Using Piecewise Linear Local Control Function

In this subsection, Monte Carlo simulation applies in eight parts: (7.7.2.1) at the week 3-9 November 2014; (7.7.2.2) at the day 3 November 2014; (7.7.2.3) at the day 4 November 2014; (7.7.2.4) at the day 5 November 2014; (7.7.2.5) at the day 6 November 2014; (7.7.2.6) at the day 7 November 2014; (7.7.2.7) at the day 8 November 2014; (7.7.2.8) at the day 9 November 2014. The piecewise linear local control function is selected in this subsection.

7.7.2.1 At The Week 3-9 November 2014

In this subsection, the value of load, solar irradiance and ambient temperature will be randomized in 100,000 times, according to the normal uncertainty characteristic of Figure 6.6 at the week 3-9 November 2014. Each random values at a time will be assessed by power flow algorithm. The optimal parameters setting at the week 3-9 November 2014 as shown in Table 7.5 is applied. Then, the power flow results in

100,000 times can be shown in Figure 7.78. The summary from Monte Carlo simulation is shown in Table 7.53. It can notice that mean values from power flow results are within the limit and. Overall results are not more than the limit specified.

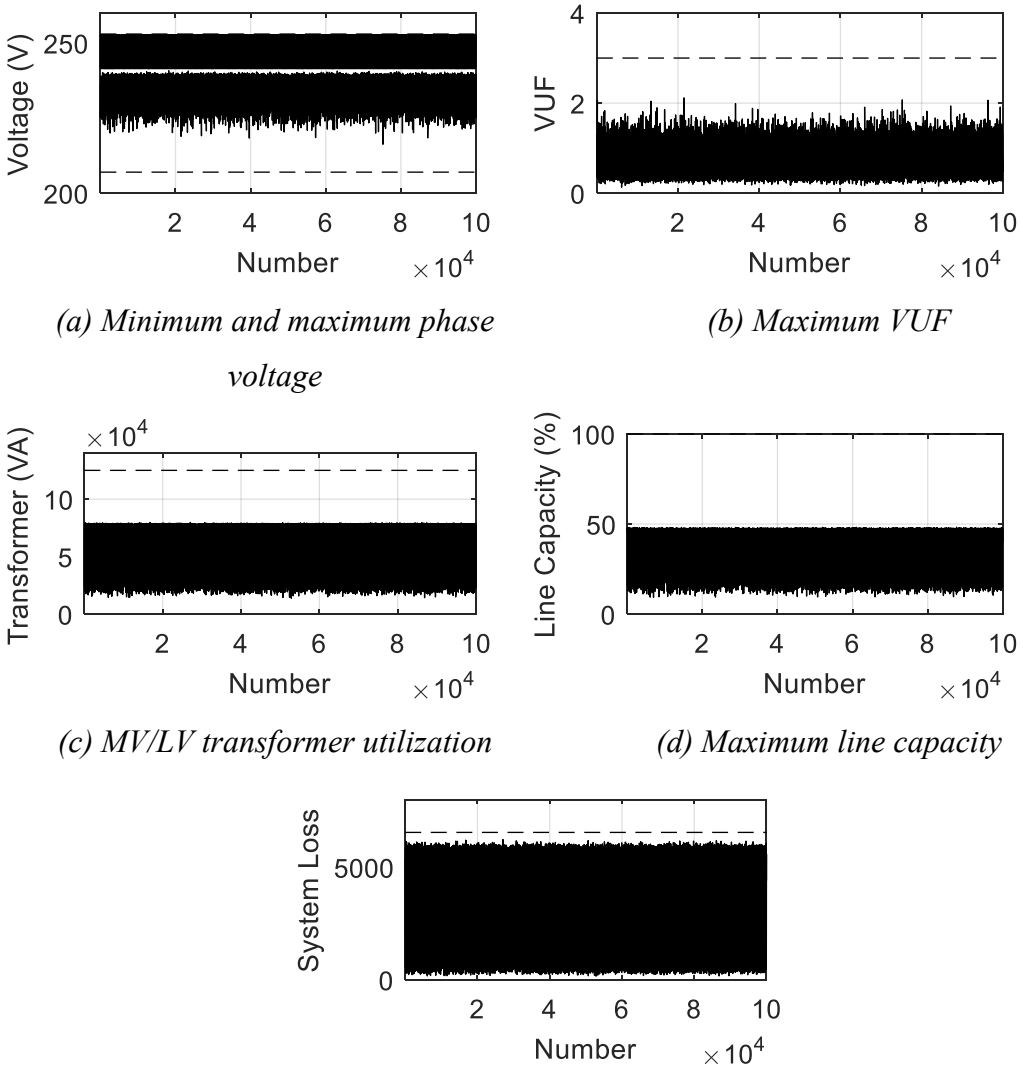

(a) Minimum and maximum phase voltage

(b) Maximum VUF

(c) MV/LV transformer utilization

(d) Maximum line capacity

(e) System loss

Figure 7.78 The power flow results from 100,000-times random

Table 7.53 The results of Monte Carlo simulation

Variables	Mean Values from 100,000 times of random	Limit	Over-limit Consideration		
			Probability	Mean of Excess Value	Difference
Min Voltage	249.54 V	253.00 V	0.00%	0.00	0.00
Max Voltage	234.61 V	207.00 V	0.00%	0.00	0.00
Loss	4,068.95 W	6,547.58 W	0.00%	0.00	0.00
Max VUF	0.63	3.00	0.00%	0.00	0.00
Transformer Utilization	63,498.62 VA	125,000.00 VA	0.00%	0.00	0.00

Variables	Mean Values from 100,000 times of random	Limit	Over-limit Consideration		
			Probability	Mean of Excess Value	Difference
Max Line Capacity	37.98%	100.00%	0.00%	0.00	0.00

7.7.2.2 At The Day 3 November 2014

In this subsection, the value of load, solar irradiance and ambient temperature will be randomized in 100,000 times, according to the normal uncertainty characteristic of Figure 6.7 at the day 3 November 2014. Each random values at a time will be assessed by power flow algorithm. The optimal parameters setting at the day 3 November 2014 as shown in Table 7.15 is applied. Then, the power flow results in 100,000 times can be shown in Figure 7.79. The summary from Monte Carlo simulation is shown in Table 7.54. It can notice that mean values from power flow results are within the limit. The probability of over loss is 1.74%. The mean over loss is 6,556.08 W that is slightly more than the limit around 8.50 W. Other variables have 0% probability to exceed the limits.

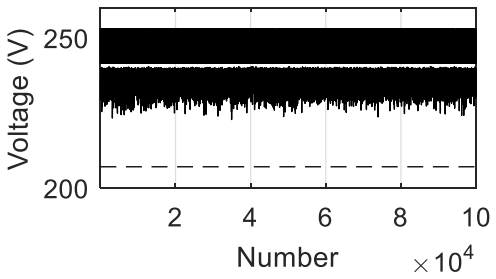

(a) Minimum and maximum phase voltage

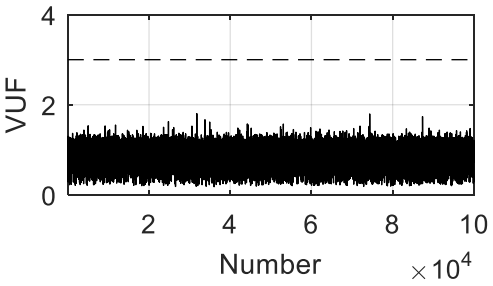

(b) Maximum VUF

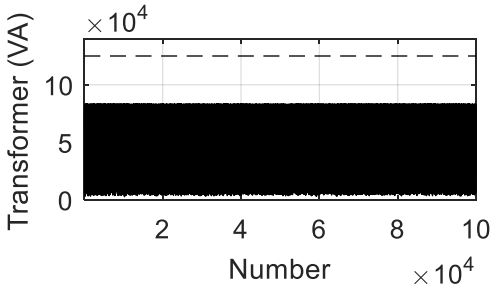

(c) MV/LV transformer utilization

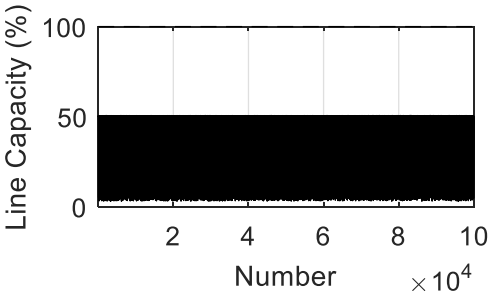

(d) Maximum line capacity

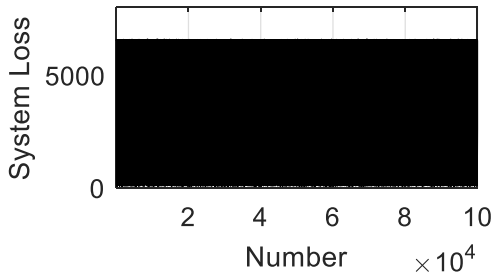

(e) System loss

Figure 7.79 The power flow results from 100,000-times random

Table 7.54 The results of Monte Carlo simulation

Variables	Mean Values from 100,000 times of random	Limit	Over-limit Consideration		
			Probability	Mean of Excess Value	Difference
Min Voltage	250.98 V	253.00 V	0.00%	0.00	0.00
Max Voltage	236.72 V	207.00 V	0.00%	0.00	0.00
Loss	4,670.76 W	6,547.58 W	1.74%	6,556.08 W	8.50 W
Max VUF	0.81	3.00	0.00%	0.00	0.00
Transformer Utilization	65,063.20 VA	125,000.00 VA	0.00%	0.00	0.00
Max Line Capacity	39.72%	100.00%	0.00%	0.00	0.00

7.7.2.3 At The Day 4 November 2014

In this subsection, the value of load, solar irradiance and ambient temperature will be randomized in 100,000 times, according to the normal uncertainty characteristic of Figure 6.8 at the day 4 November 2014. Each random values at a time will be assessed by power flow algorithm. The optimal parameters setting at the day 4 November 2014 as shown in Table 7.16 is applied. Then, the power flow results in 100,000 times can be shown in Figure 7.80. The summary from Monte Carlo simulation is shown in Table 7.55. It can notice that mean values from power flow results are within the limit. Overall results are not more than the limit specified.

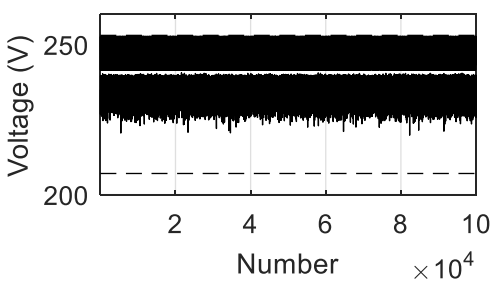

(a) Minimum and maximum phase voltage

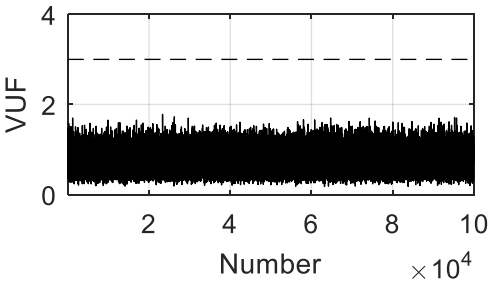

(b) Maximum VUF

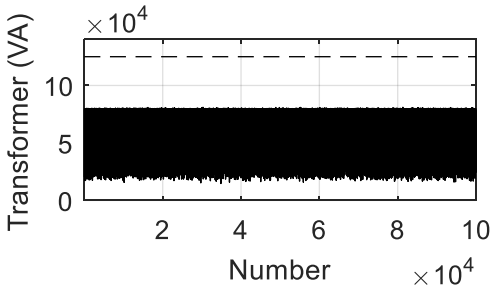

(c) MV/LV transformer utilization

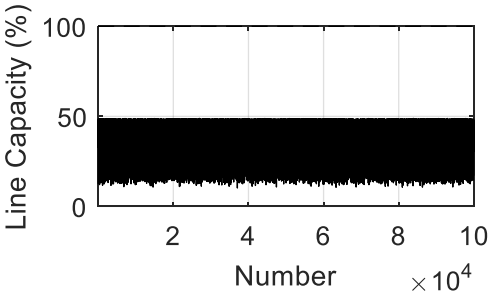

(d) Maximum line capacity

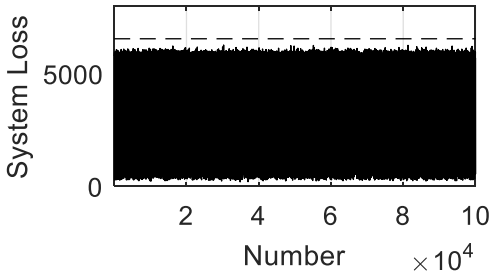

(e) System loss

Figure 7.80 The power flow results from 100,000-times random

Table 7.55 The results of Monte Carlo simulation

Variables	Mean Values from 100,000 times of random	Limit	Over-limit Consideration		
			Probability	Mean of Excess Value	Difference
Min Voltage	249.95 V	253.00 V	0.00	0.00	0.00
Max Voltage	235.12 V	207.00 V	0.00	0.00	0.00
Loss	4,289.15 W	6,547.58 W	0.00	0.00	0.00
Max VUF	0.73	3.00	0.00	0.00	0.00
Transformer Utilization	66,293.99 VA	125,000.00 VA	0.00	0.00	0.00
Max Line Capacity	39.55%	100.00%	0.00	0.00	0.00

7.7.2.4 At The Day 5 November 2014

In this subsection, the value of load, solar irradiance and ambient temperature will be randomized in 100,000 times, according to the normal uncertainty characteristic of Figure 6.9 at the day 5 November 2014. Each random values at a time will be assessed by power flow algorithm. The optimal parameters setting at the day 5 November 2014 as shown in Table 7.17 is applied. Then, the power flow results in 100,000 times can be shown in Figure 7.81. The summary from Monte Carlo simulation is shown in Table 7.56. It can notice that mean values from power flow results are within the limit. Overall results are not more than the limit specified.

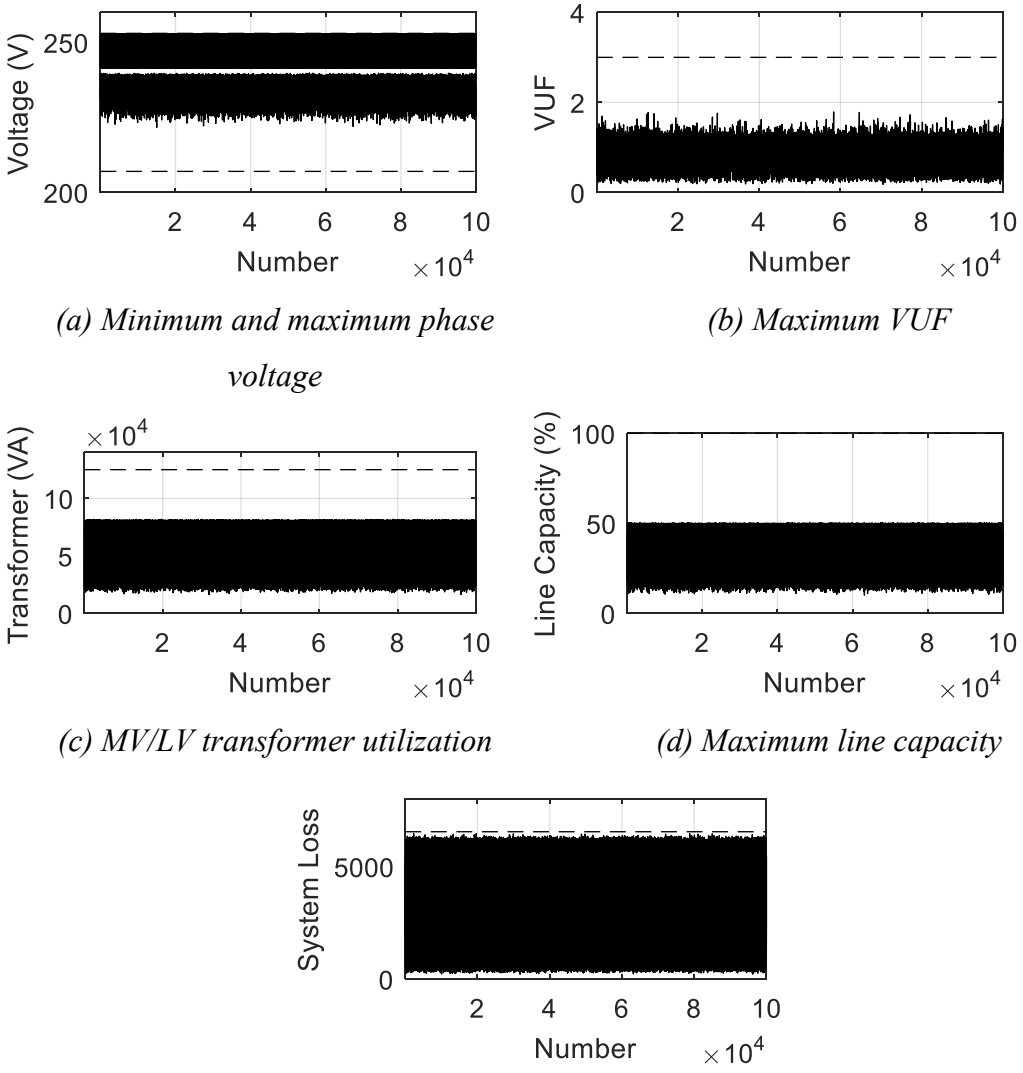

(a) Minimum and maximum phase voltage

(b) Maximum VUF

(c) MV/LV transformer utilization

(d) Maximum line capacity

(e) System loss

Figure 7.81 The power flow results from 100,000-times random

Table 7.56 The results of Monte Carlo simulation

Variables	Mean Values from 100,000 times of random	Limit	Over-limit Consideration		
			Probability	Mean of Excess Value	Difference
Min Voltage	249.64 V	253.00 V	0.00%	0.00	0.00
Max Voltage	235.18 V	207.00 V	0.00%	0.00	0.00
Loss	4,130.50 W	6,547.58 W	0.00%	0.00	0.00
Max VUF	1.01	3.00	0.00%	0.00	0.00
Transformer Utilization	64,042.28 VA	125,000.00 VA	0.00%	0.00	0.00
Max Line Capacity	38.24%	100.00%	0.00%	0.00	0.00

7.7.2.5 At The Day 6 November 2014

In this subsection, the value of load, solar irradiance and ambient temperature will be randomized in 100,000 times, according to the normal uncertainty characteristic of Figure 6.10 at the day 6 November 2014. Each random values at a time will be assessed by power flow algorithm. The optimal parameters setting at the day 6 November 2014 as shown in Table 7.18 is applied. Then, the power flow results in 100,000 times can be shown in Figure 7.82. The summary from Monte Carlo simulation is shown in Table 7.57. It can notice that mean values from power flow results are within the limit. Overall results are not more than the limit specified.

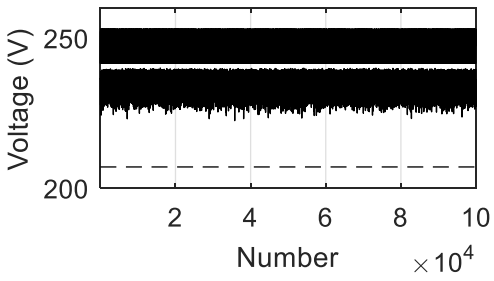

(a) Minimum and maximum phase voltage

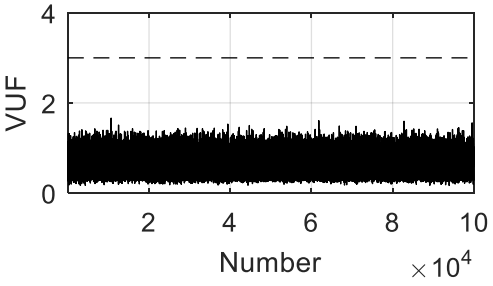

(b) Maximum VUF

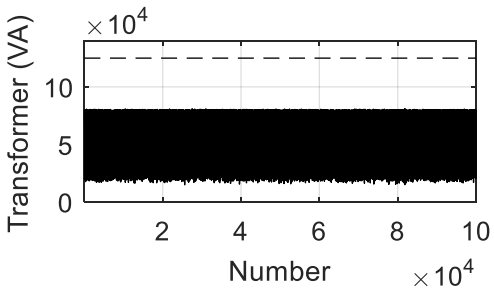

(c) MV/LV transformer utilization

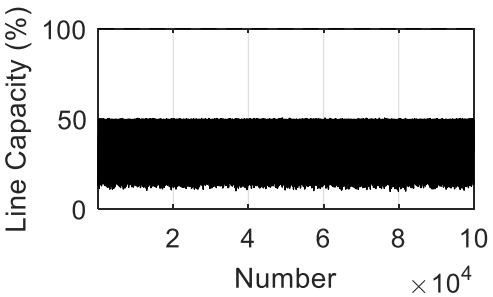

(d) Maximum line capacity

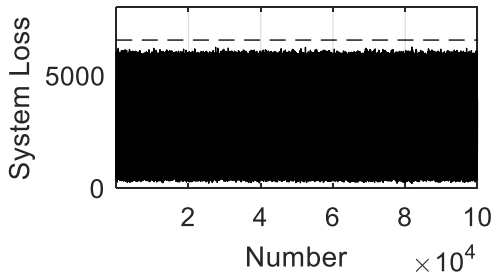

(e) System loss

Figure 7.82 The power flow results from 100,000-times random

Table 7.57 The results of Monte Carlo simulation

Variables	Mean Values from 100,000 times of random	Limit	Over-limit Consideration		
			Probability	Mean of Excess Value	Difference
Min Voltage	248.72 V	253.00 V	0.00%	0.00	0.00
Max Voltage	234.99 V	207.00 V	0.00%	0.00	0.00
Loss	3,685.18 W	6,547.58 W	0.00%	0.00	0.00
Max VUF	0.59	3.00	0.00%	0.00	0.00
Transformer Utilization	60,337.10 VA	125,000.00 VA	0.00%	0.00	0.00
Max Line Capacity	36.05%	100.00%	0.00%	0.00	0.00

7.7.2.6 At The Day 7 November 2014

In this subsection, the value of load, solar irradiance and ambient temperature will be randomized in 100,000 times, according to the normal uncertainty characteristic of Figure 6.11 at the day 7 November 2014. Each random values at a time will be assessed by power flow algorithm. The optimal parameters setting at the day 7 November 2014 as shown in Table 7.19 is applied. Then, the power flow results in 100,000 times can be shown in Figure 7.83. The summary from Monte Carlo simulation is shown in Table 7.58. It can notice that mean values from power flow results are within the limit. Overall results are not more than the limit specified.

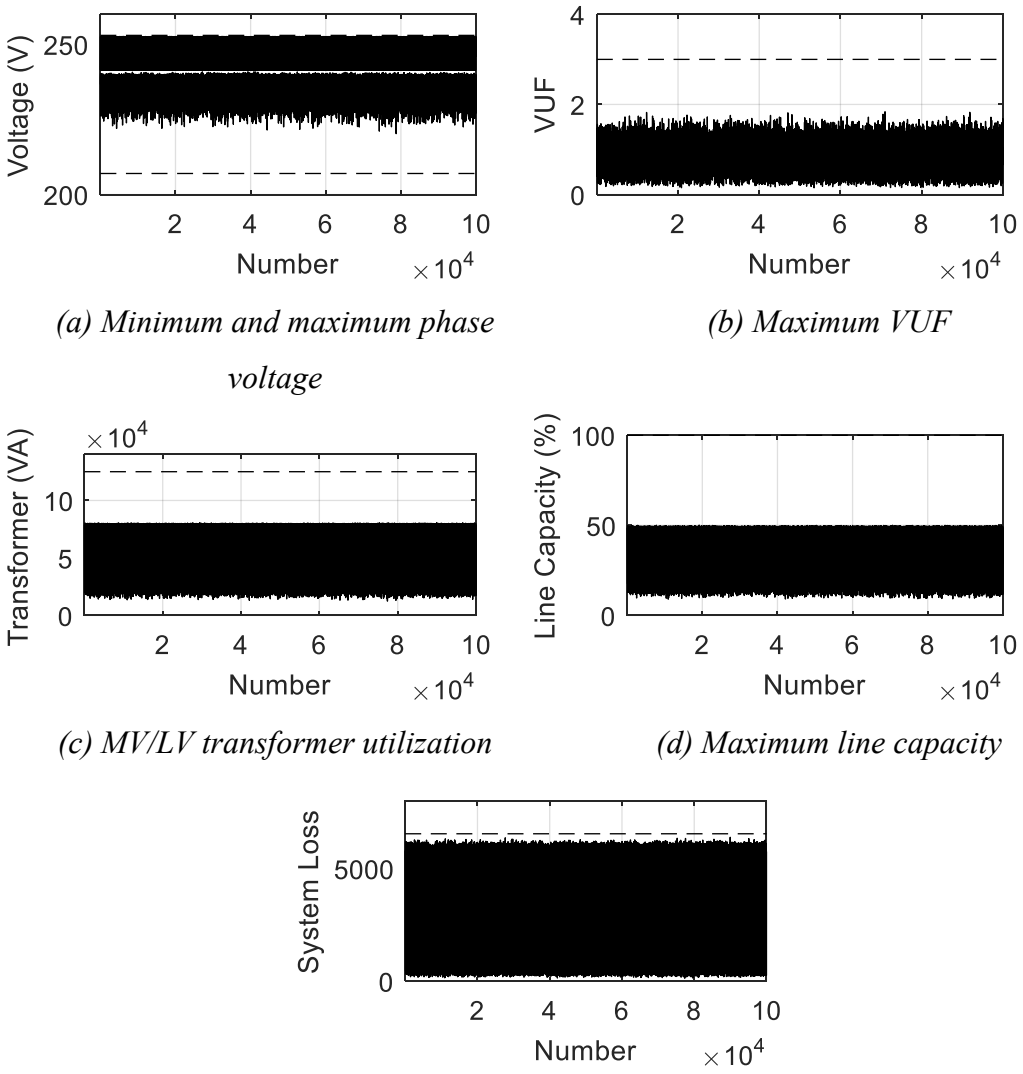

(a) Minimum and maximum phase voltage

(b) Maximum VUF

(c) MV/LV transformer utilization

(d) Maximum line capacity

(e) System loss

Figure 7.83 The power flow results from 100,000-times random

Table 7.58 The results of Monte Carlo simulation

Variables	Mean Values from 100,000 times of random	Limit	Over-limit Consideration		
			Probability	Mean of Excess Value	Difference
Min Voltage	249.16 V	253.00 V	0.00%	0.00	0.00
Max Voltage	235.51 V	207.00 V	0.00%	0.00	0.00
Loss	3,896.38 W	6,547.58 W	0.00%	0.00	0.00
Max VUF	0.86	3.00	0.00%	0.00	0.00
Transformer Utilization	61,285.59 VA	125,000.00 VA	0.00%	0.00	0.00
Max Line Capacity	36.82%	100.00%	0.00%	0.00	0.00

7.7.2.7 At The Day 8 November 2014

In this subsection, the value of load, solar irradiance and ambient temperature will be randomized in 100,000 times, according to the normal uncertainty characteristic of Figure 6.12 at the day 8 November 2014. Each random values at a time will be assessed by power flow algorithm. The optimal parameters setting at the day 8 November 2014 as shown in Table 7.20 is applied. Then, the power flow results in 100,000 times can be shown in Figure 7.84. The summary from Monte Carlo simulation is shown in Table 7.59. It can notice that mean values from power flow results are within the limit. The probability of over loss is 1.05%. The mean over loss is 6,570.01 W that is slightly more than the limit around 22.43 W. Other variables have 0% probability to exceed the limits.

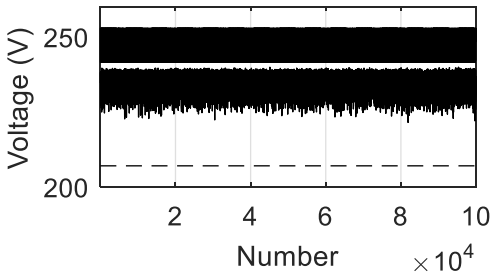

(a) Minimum and maximum phase voltage

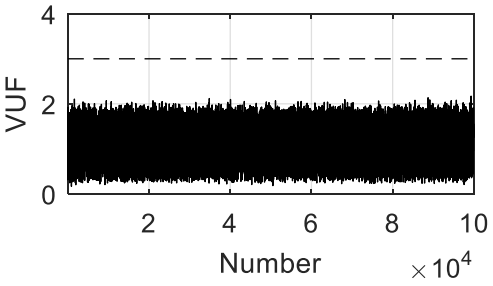

(b) Maximum VUF

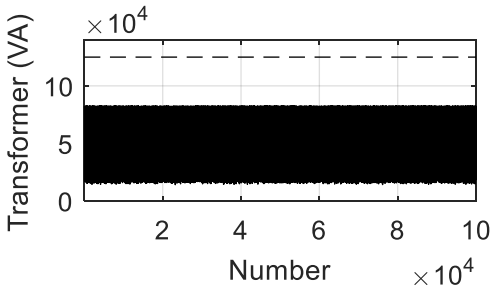

(c) MV/LV transformer utilization

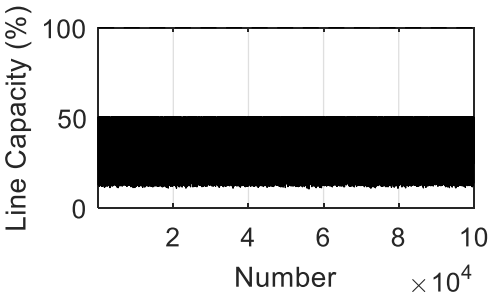

(d) Maximum line capacity

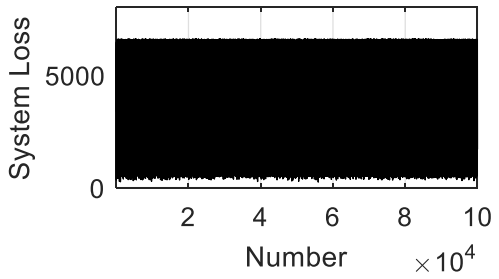

(e) System loss

Figure 7.84 The power flow results from 100,000-times random

Table 7.59 The results of Monte Carlo simulation

Variables	Mean Values from 100,000 times of random	Limit	Over-limit Consideration		
			Probability	Mean of Excess Value	Difference
Min Voltage	251.16 V	253.00 V	0.00%	0.00	0.00
Max Voltage	235.29 V	207.00 V	0.00%	0.00	0.00
Loss	4,427.78 W	6,547.58 W	1.05%	6,570.01 W	22.43 W
Max VUF	1.21	3.00	0.00%	0.00	0.00
Transformer Utilization	63,386.76 VA	125,000.00 VA	0.00%	0.00	0.00
Max Line Capacity	39.20%	100.00%	0.00%	0.00	0.00

7.7.2.8 At The Day 9 November 2014

In this subsection, the value of load, solar irradiance and ambient temperature will be randomized in 100,000 times, according to the normal uncertainty characteristic of Figure 6.13 at the day 9 November 2014. Each random values at a time will be assessed by power flow algorithm. The optimal parameters setting at the day 9 November 2014 as shown in Table 7.21 is applied. Then, the power flow results in 100,000 times can be shown in Figure 7.85. The summary from Monte Carlo simulation is shown in Table 7.60. It can notice that mean values from power flow results are within the limit. Overall results are not more than the limit specified.

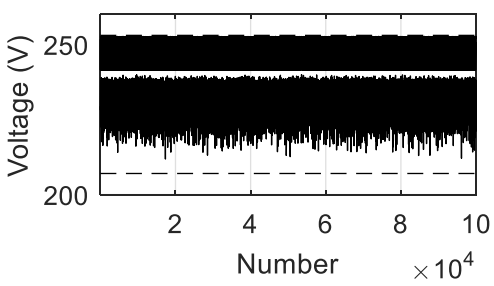

(a) Minimum and maximum phase voltage

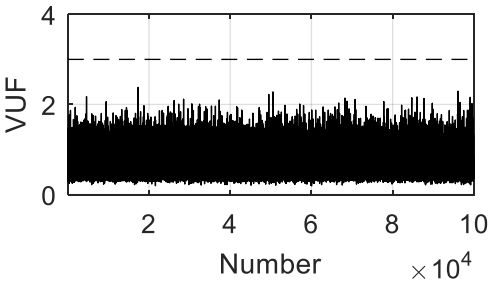

(b) Maximum VUF

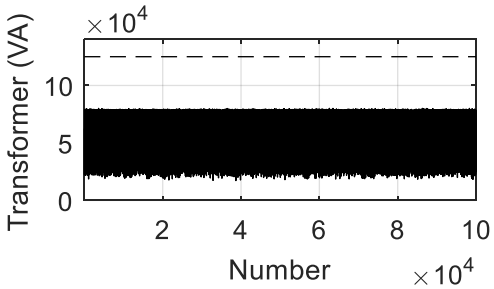

(c) MV/LV transformer utilization

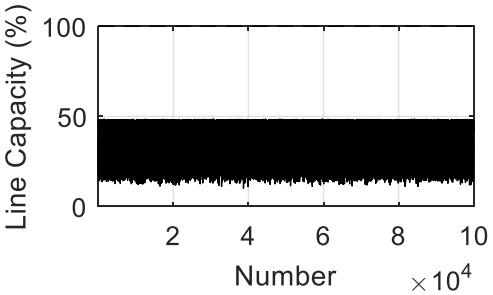

(d) Maximum line capacity

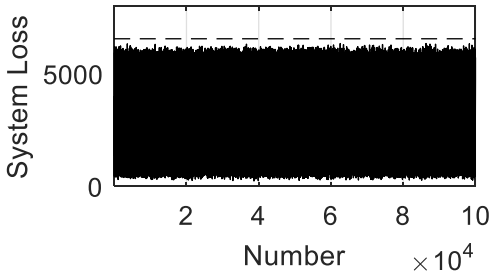

(e) System loss

Figure 7.85 The power flow results from 100,000-times random

Table 7.60 The results of Monte Carlo simulation

Variables	Mean Values from 100,000 times of random	Limit	Over-limit Consideration		
			Probability	Mean of Excess Value	Difference
Min Voltage	247.44 V	253.00 V	0.00	0.00	0.00
Max Voltage	232.41 V	207.00 V	0.00	0.00	0.00
Loss	3,023.57 W	6,547.58 W	0.00	0.00	0.00
Max VUF	0.70	3.00	0.00	0.00	0.00
Transformer Utilization	53,169.41 VA	125,000.00 VA	0.00	0.00	0.00
Max Line Capacity	32.00%	100.00%	0.00	0.00	0.00

From Monte Carlo simulations at the 19 node distribution system with using piecewise linear local control function, it can prove that the determination of only the 17 cases of the set of uncertainty is sufficient to solve the uncertainty problem of load, solar irradiance and ambient temperature. It is because as follows:

- The power flow results of minimum and maximum voltage profile, maximum VUF, MV/LV transformer utilization and maximum line capacity are within the limit. The probabilities have around 100% to hold on those limits under the uncertainty;
- The probability of the loss results have 100% to hold on the limits under the uncertainty in the Day 4, 5, 6, 7, 9 and the Week 3-9 November 2014;
- For the Day 3 and 8 November 2014, the probability of the loss results to exceed the limit is less than 2% or the probability of the loss results have around 98% to hold on the loss limit under the uncertainty according to the worst case at the day 8 November 2014. Mean over losses are more than the limit about <30 W according to the day 8 November 2014.

However, the results that exceed only a small extent of the loss limit can be resolved by adjusting the loss limit in the optimization problem less than the actual value.

7.7.3 The Modified 29 Node Distribution System With Using Continuous Local Control Function

In this subsection, Monte Carlo simulation applies in eight parts: (7.7.3.1) at the week 3-9 November 2014; (7.7.3.2) at the day 3 November 2014; (7.7.3.3) at the day 4 November 2014; (7.7.3.4) at the day 5 November 2014; (7.7.3.5) at the day 6 November 2014; (7.7.3.6) at the day 7 November 2014; (7.7.3.7) at the day 8 November 2014; (7.7.3.8) at the day 9 November 2014. The continuous local control function is selected in this subsection.

7.7.3.1 At The Week 3-9 November 2014

In this subsection, the value of load, solar irradiance and ambient temperature will be randomized in 100,000 times, according to the normal uncertainty characteristic of Figure 6.6 at the week 3-9 November 2014. Each random values at a time will be assessed by power flow algorithm. The optimal parameters setting at the week 3-9 November 2014 as shown in Table 7.24 is applied. Then, the power flow results in

100,000 times can be shown in Figure 7.86. The summary from Monte Carlo simulation is shown in Table 7.61. It can notice that mean values from power flow results are within the limit and. The probability of over loss is 27.38%. The mean over loss is 7,788.69 W that is slightly more than the limit around 146.63 W. Other variables have 0% probability to exceed the limits.

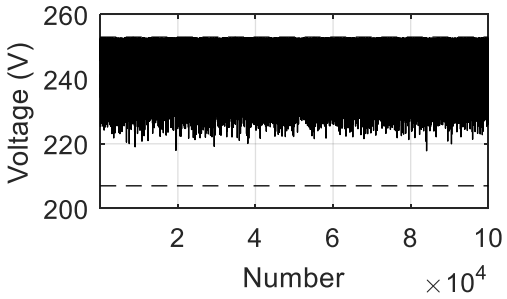

(a) Minimum and maximum phase voltage

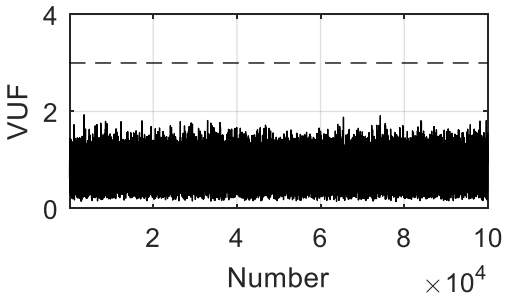

(b) Maximum VUF

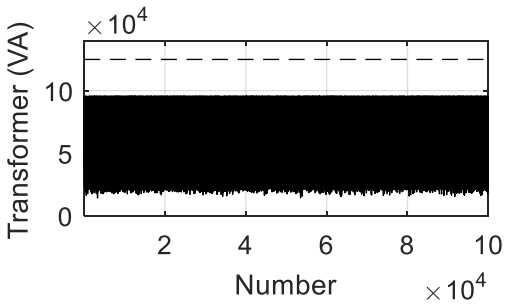

(c) MV/LV transformer utilization

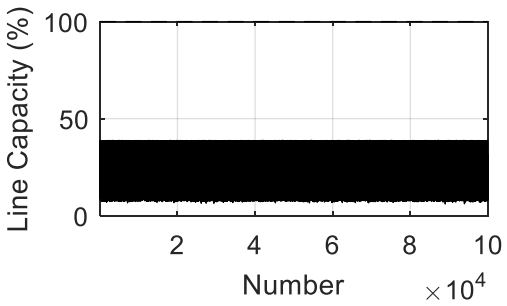

(d) Maximum line capacity

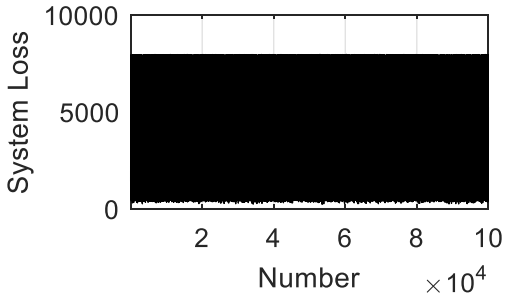

(e) System loss

Figure 7.86 The power flow results from 100,000-times random

Table 7.61 The results of Monte Carlo simulation

Variables	Mean Values from 100,000 times of random	Limit	Over-limit Consideration		
			Probability	Mean of Excess Value	Difference
Min Voltage	248.88 V	253.00 V	0.00%	0.00	0.00
Max Voltage	239.21 V	207.00 V	0.00%	0.00	0.00

Variables	Mean Values from 100,000 times of random	Limit	Over-limit Consideration		
			Probability	Mean of Excess Value	Difference
Loss	4,991.72 W	7,642.05 W	27.38%	7,788.68 W	146.63 W
Max VUF	0.84	3.00	0.00%	0.00	0.00
Transformer Utilization	70,035.73 VA	125,000.00 VA	0.00%	0.00	0.00
Max Line Capacity	28.93%	100.00%	0.00%	0.00	0.00

7.7.3.2 At The Day 3 November 2014

In this subsection, the value of load, solar irradiance and ambient temperature will be randomized in 100,000 times, according to the normal uncertainty characteristic of Figure 6.7 at the day 3 November 2014. Each random values at a time will be assessed by power flow algorithm. The optimal parameters setting at the day 3 November 2014 as shown in Table 7.26 is applied. Then, the power flow results in 100,000 times can be shown in Figure 7.87. The summary from Monte Carlo simulation is shown in Table 7.62. It can notice that mean values from power flow results are within the limit. The probability of over loss is 0.56%. The mean over loss is 7,649.82 W that is slightly more than the limit around 7.76 W. Other variables have 0% probability to exceed the limits.

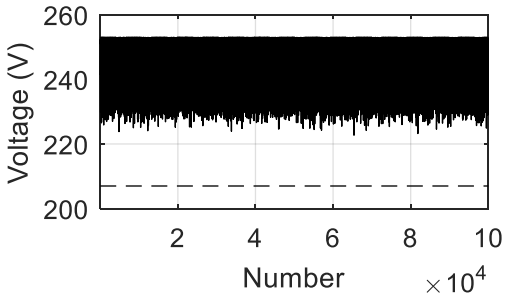

(a) Minimum and maximum phase voltage

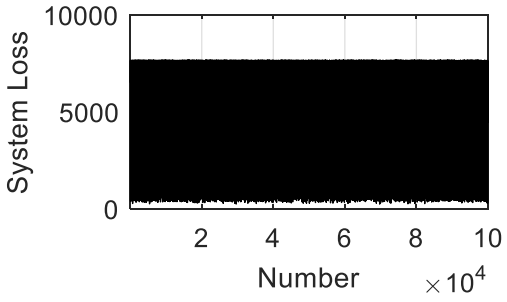

(b) Maximum VUF

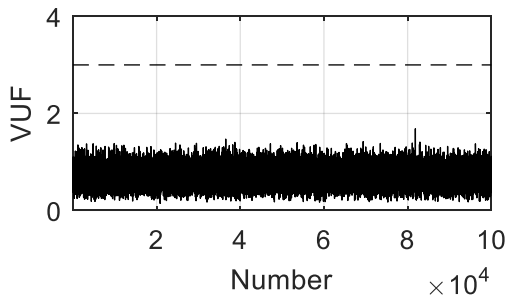

(c) MV/LV transformer utilization

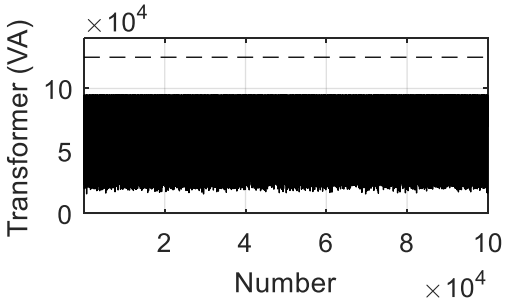

(d) Maximum line capacity

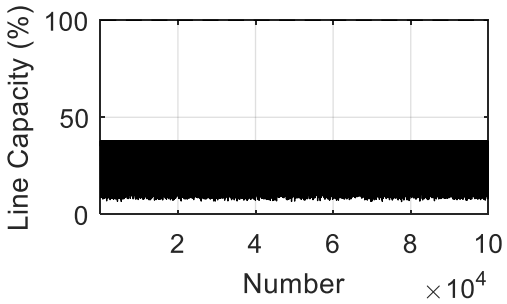

(e) System loss

Figure 7.87 The power flow results from 100,000-times random

Table 7.62 The results of Monte Carlo simulation

Variables	Mean Values from 100,000 times of random	Limit	Over-limit Consideration		
			Probability	Mean of Excess Value	Difference
Min Voltage	249.66 V	253.00 V	0.00%	0.00	0.00
Max Voltage	239.75 V	207.00 V	0.00%	0.00	0.00
Loss	5,810.28 W	7,642.05 W	0.56%	7,649.82 W	7.76 W
Max VUF	0.73	3.00	0.00%	0.00	0.00
Transformer Utilization	79,259.02 VA	125,000.00 VA	0.00%	0.00	0.00
Max Line Capacity	31.86%	100.00%	0.00%	0.00	0.00

7.7.3.3 At The Day 4 November 2014

In this subsection, the value of load, solar irradiance and ambient temperature will be randomized in 100,000 times, according to the normal uncertainty characteristic of Figure 6.8 at the day 4 November 2014. Each random values at a time will be assessed by power flow algorithm. The optimal parameters setting at the day 4 November 2014 as shown in Table 7.27 is applied. Then, the power flow results in 100,000 times can be shown in Figure 7.88. The summary from Monte Carlo simulation is shown in Table 7.63. It can notice that mean values from power flow results are within the limit. The

probability of over loss is 0.43%. The mean over loss is 7,655.33 W that is slightly more than the limit around 13.27 W. Other variables have 0% probability to exceed the limits.

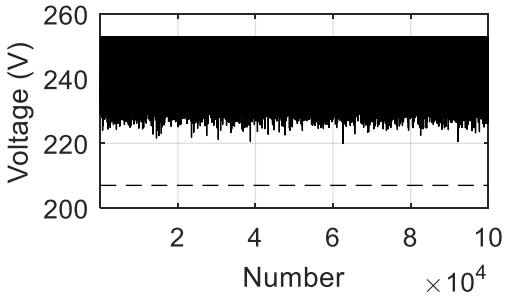

(a) Minimum and maximum phase voltage

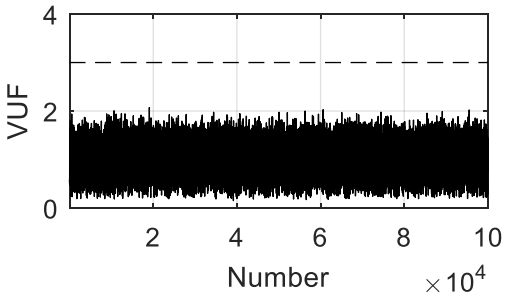

(b) Maximum VUF

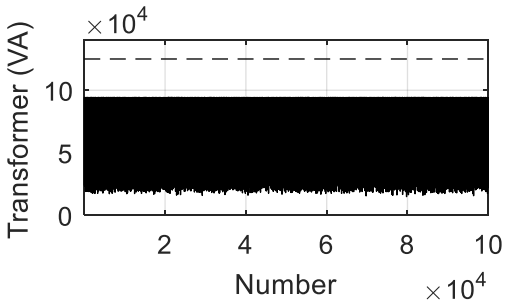

(c) MV/LV transformer utilization

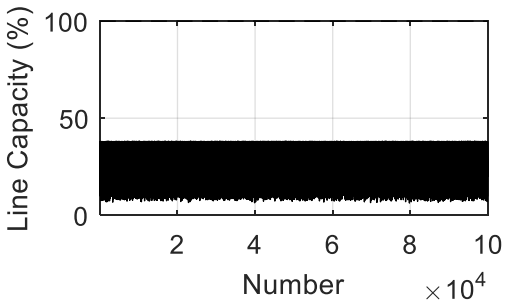

(d) Maximum line capacity

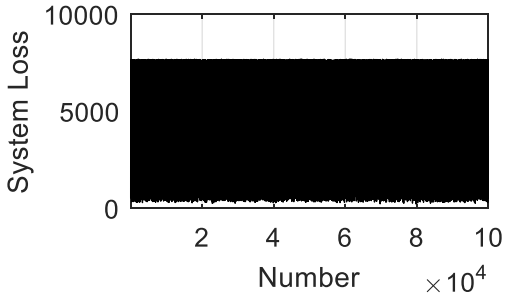

(e) System loss

Figure 7.88 The power flow results from 100,000-times random

Table 7.63 The results of Monte Carlo simulation

Variables	Mean Values from 100,000 times of random	Limit	Over-limit Consideration		
			Probability	Mean of Excess Value	Difference
Min Voltage	248.59 V	253.00 V	0.00%	0.00	0.00
Max Voltage	238.71 V	207.00 V	0.00%	0.00	0.00
Loss	5,069.84 W	7,642.05 W	0.43%	7,655.33 W	13.27 W
Max VUF	0.84	3.00	0.00%	0.00	0.00

Variables	Mean Values from 100,000 times of random	Limit	Over-limit Consideration		
			Probability	Mean of Excess Value	Difference
Transformer Utilization	72,104.55 VA	125,000.00 VA	0.00%	0.00	0.00
Max Line Capacity	29.90%	100.00%	0.00%	0.00	0.00

7.7.3.4 At The Day 5 November 2014

In this subsection, the value of load, solar irradiance and ambient temperature will be randomized in 100,000 times, according to the normal uncertainty characteristic of Figure 6.9 at the day 5 November 2014. Each random values at a time will be assessed by power flow algorithm. The optimal parameters setting at the day 5 November 2014 as shown in Table 7.28 is applied. Then, the power flow results in 100,000 times can be shown in Figure 7.89. The summary from Monte Carlo simulation is shown in Table 7.64. It can notice that mean values from power flow results are within the limit. The probability of over loss is 11.01%. The mean over loss is 7,687.77 W that is slightly more than the limit around 45.72 W. Other variables have 0% probability to exceed the limits.

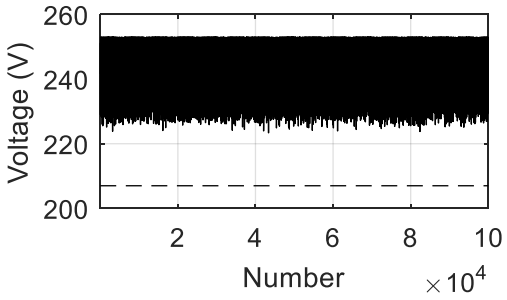

(a) Minimum and maximum phase voltage

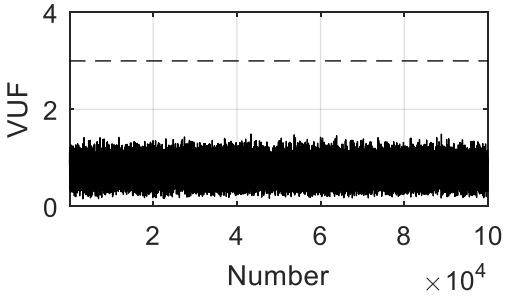

(b) Maximum VUF

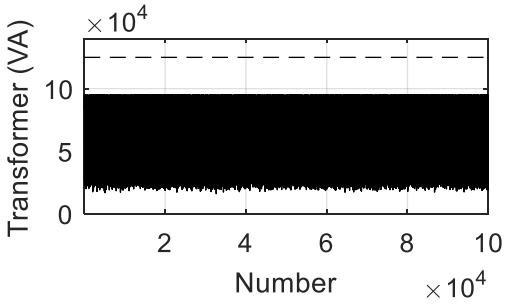

(c) MV/LV transformer utilization

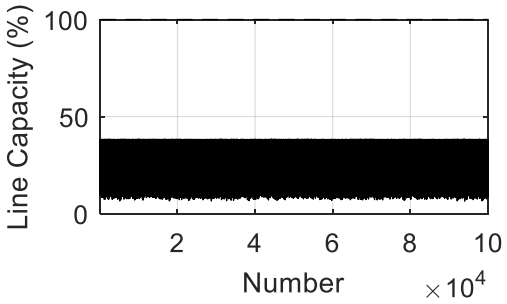

(d) Maximum line capacity

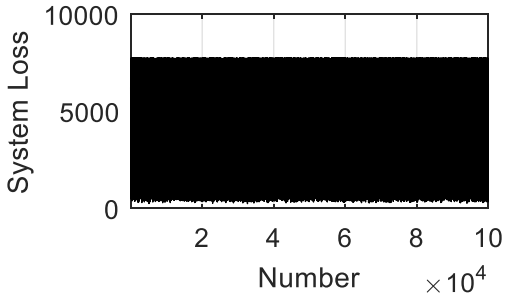

(e) System loss

Figure 7.89 The power flow results from 100,000-times random

Table 7.64 The results of Monte Carlo simulation

Variables	Mean Values from 100,000 times of random	Limit	Over-limit Consideration		
			Probability	Mean of Excess Value	Difference
Min Voltage	248.68 V	253.00 V	0.00%	0.00	0.00
Max Voltage	238.96 V	207.00 V	0.00%	0.00	0.00
Loss	4,501.05 W	7,642.05 W	11.01%	7,687.77 W	45.72 W
Max VUF	0.84	3.00	0.00%	0.00	0.00
Transformer Utilization	66,510.18 VA	125,000.00 VA	0.00%	0.00	0.00
Max Line Capacity	27.70%	100.00%	0.00%	0.00	0.00

7.7.3.5 At The Day 6 November 2014

In this subsection, the value of load, solar irradiance and ambient temperature will be randomized in 100,000 times, according to the normal uncertainty characteristic of Figure 6.10 at the day 6 November 2014. Each random values at a time will be assessed by power flow algorithm. The optimal parameters setting at the day 6 November 2014 as shown in Table 7.29 is applied. Then, the power flow results in 100,000 times can be shown in Figure 7.90. The summary from Monte Carlo simulation is shown in Table 7.65. It can notice that mean values from power flow results are within the limit and. The probability of over loss is 0.89%. The mean over loss is 7,663.60 W that is slightly more than the limit around 21.55 W. Other variables have 0% probability to exceed the limits.

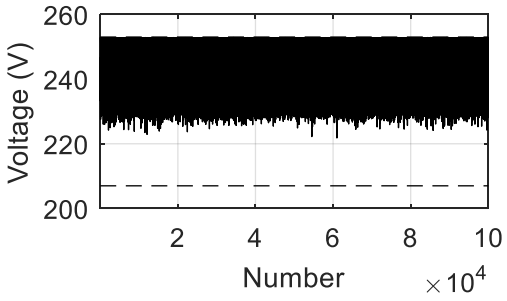

(a) Minimum and maximum phase voltage

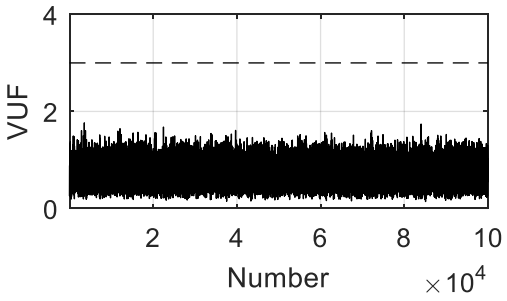

(b) Maximum VUF

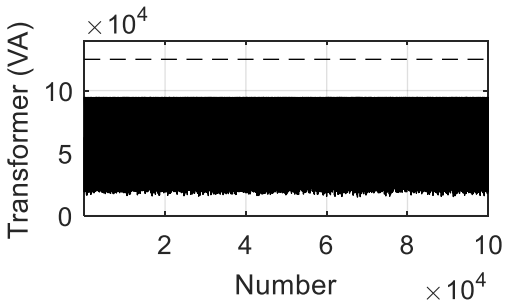

(c) MV/LV transformer utilization

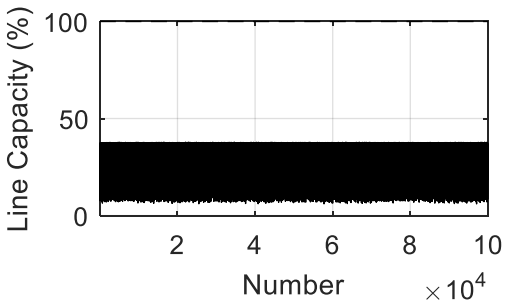

(d) Maximum line capacity

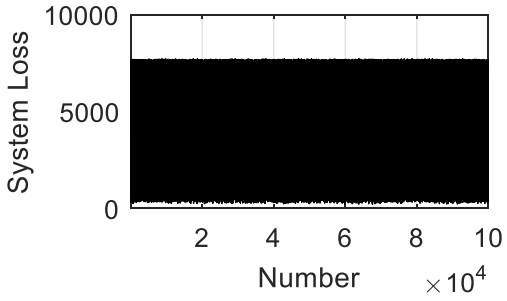

(e) System loss

Figure 7.90 The power flow results from 100,000-times random

Table 7.65 The results of Monte Carlo simulation

Variables	Mean Values from 100,000 times of random	Limit	Over-limit Consideration		
			Probability	Mean of Excess Value	Difference
Min Voltage	247.36 V	253.00 V	0.00%	0.00	0.00
Max Voltage	238.21 V	207.00 V	0.00%	0.00	0.00
Loss	4,394.53 W	7,642.05 W	0.89%	7,663.60 W	21.55 W
Max VUF	0.65	3.00	0.00%	0.00	0.00
Transformer Utilization	66,800.41 VA	125,000.00 VA	0.00%	0.00	0.00
Max Line Capacity	26.86%	100.00%	0.00%	0.00	0.00

7.7.3.6 At The Day 7 November 2014

In this subsection, the value of load, solar irradiance and ambient temperature will be randomized in 100,000 times, according to the normal uncertainty characteristic of Figure 6.11 at the day 7 November 2014. Each random values at a time will be assessed by power flow algorithm. The optimal parameters setting at the day 7 November 2014 as shown in Table 7.30 is applied. Then, the power flow results in 100,000 times can be shown in Figure 7.91. The summary from Monte Carlo simulation is shown in Table 7.66. It can notice that mean values from power flow results are within the limit and. The probability of over loss is 3.59%. The mean over loss is 7,681.22 W that is slightly more than the limit around 39.16 W. Other variables have 0% probability to exceed the limits.

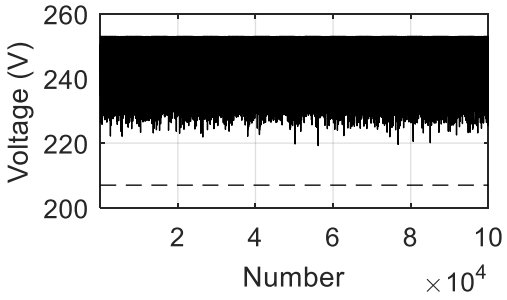

(a) Minimum and maximum phase voltage

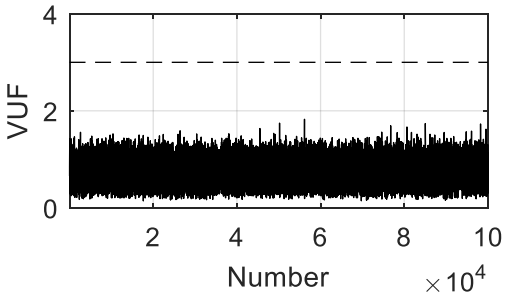

(b) Maximum VUF

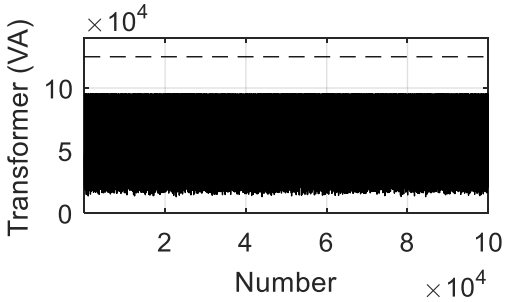

(c) MV/LV transformer utilization

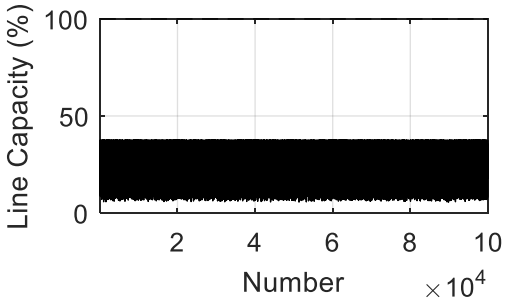

(d) Maximum line capacity

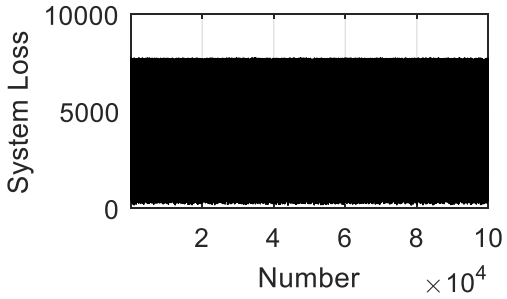

(e) System loss

Figure 7.91 The power flow results from 100,000-times random

Table 7.66 The results of Monte Carlo simulation

Variables	Mean Values from 100,000 times of random	Limit	Over-limit Consideration		
			Probability	Mean of Excess Value	Difference
Min Voltage	247.86 V	253.00 V	0.00%	0.00	0.00
Max Voltage	238.13 V	207.00 V	0.00%	0.00	0.00
Loss	4,614.84 W	7,642.05 W	3.59%	7,681.22 W	39.16 W
Max VUF	0.73	3.00	0.00%	0.00	0.00
Transformer Utilization	68,740.64 VA	125,000.00 VA	0.00%	0.00	0.00
Max Line Capacity	27.74%	100.00%	0.00%	0.00	0.00

7.7.3.7 At The Day 8 November 2014

In this subsection, the value of load, solar irradiance and ambient temperature will be randomized in 100,000 times, according to the normal uncertainty characteristic of Figure 6.12 at the day 8 November 2014. Each random values at a time will be assessed by power flow algorithm. The optimal parameters setting at the day 8 November 2014 as shown in Table 7.31 is applied. Then, the power flow results in 100,000 times can be shown in Figure 7.92. The summary from Monte Carlo simulation is shown in Table 7.67. It can notice that mean values from power flow results are within the limit and. The probability of over loss is 5.58%. The mean over loss is 7,673.75 W that is slightly more than the limit around 31.70 W. Other variables have 0% probability to exceed the limits.

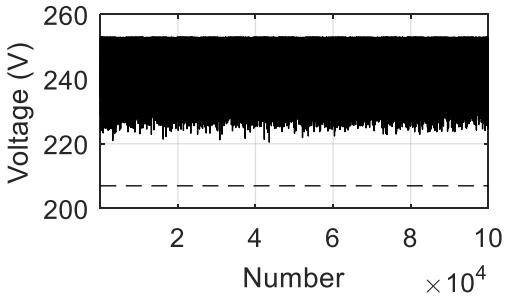

(a) Minimum and maximum phase voltage

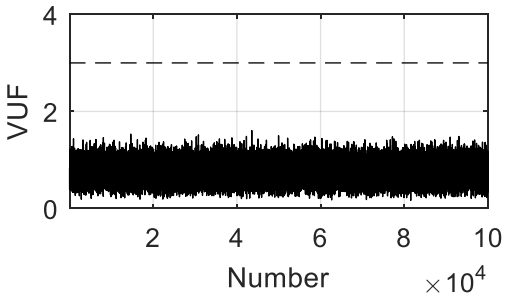

(b) Maximum VUF

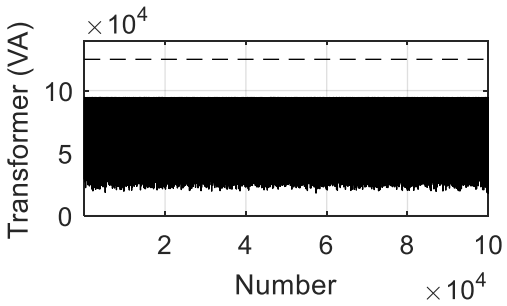

(c) MV/LV transformer utilization

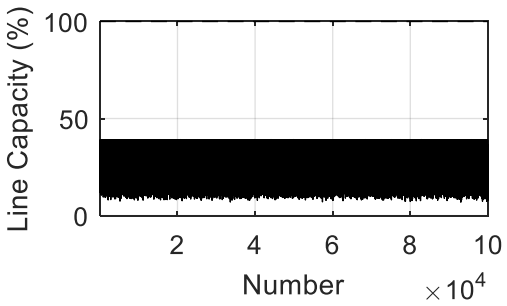

(d) Maximum line capacity

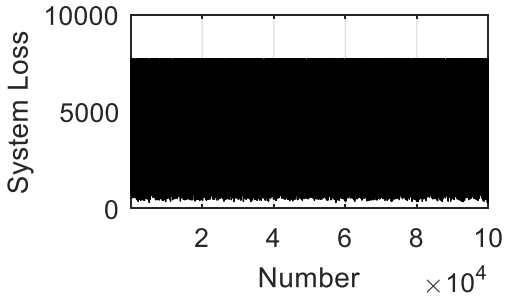

(e) System loss

Figure 7.92 The power flow results from 100,000-times random

Table 7.67 The results of Monte Carlo simulation

Variables	Mean Values from 100,000 times of random	Limit	Over-limit Consideration		
			Probability	Mean of Excess Value	Difference
Min Voltage	249.26 V	253.00 V	0.00%	0.00	0.00
Max Voltage	238.80 V	207.00 V	0.00%	0.00	0.00
Loss	5,661.44 W	7,642.05 W	5.58%	7,673.75 W	31.70 W
Max VUF	0.85	3.00	0.00%	0.00	0.00
Transformer Utilization	77,499.03 VA	125,000.00 VA	0.00%	0.00	0.00
Max Line Capacity	32.42%	100.00%	0.00%	0.00	0.00

7.7.3.8 At The Day 9 November 2014

In this subsection, the value of load, solar irradiance and ambient temperature will be randomized in 100,000 times, according to the normal uncertainty characteristic of Figure 6.13 at the day 9 November 2014. Each random values at a time will be assessed by power flow algorithm. The optimal parameters setting at the day 9 November 2014 as shown in Table 7.32 is applied. Then, the power flow results in 100,000 times can be shown in Figure 7.93. The summary from Monte Carlo simulation is shown in Table 7.68. It can notice that mean values from power flow results are within the limit and. The probability of over loss is 5.59%. The mean over loss is 7,729.12 W that is slightly more than the limit around 87.06 W. Other variables have 0% probability to exceed the limits.

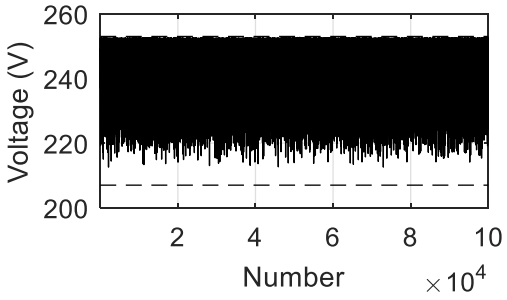

(a) Minimum and maximum phase voltage

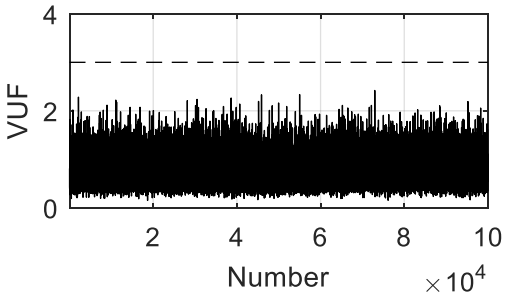

(b) Maximum VUF

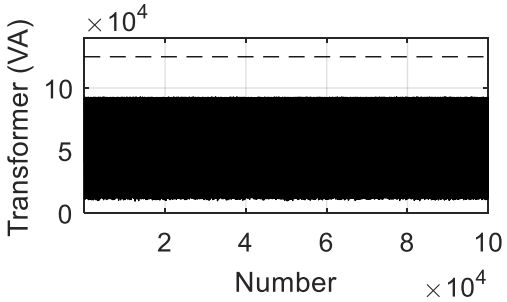

(c) MV/LV transformer utilization

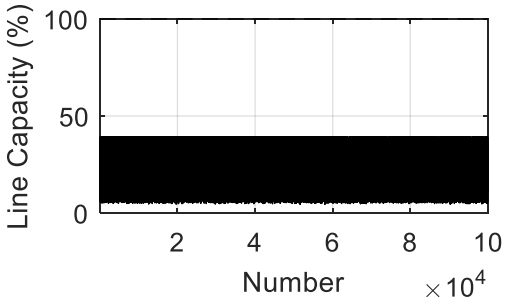

(d) Maximum line capacity

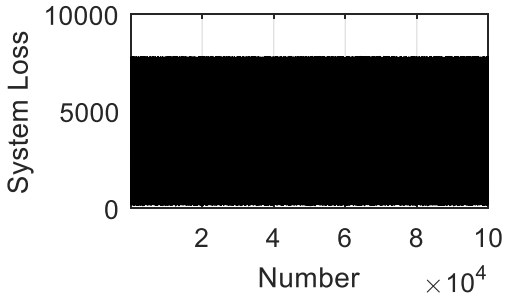

(e) System loss

Figure 7.93 The power flow results from 100,000-times random

Table 7.68 The results of Monte Carlo simulation

Variables	Mean Values from 100,000 times of random	Limit	Over-limit Consideration		
			Probability	Mean of Excess Value	Difference
Min Voltage	247.43 V	253.00 V	0.00%	0.00	0.00
Max Voltage	237.67 V	207.00 V	0.00%	0.00	0.00
Loss	2,973.44 W	7,642.05 W	5.59%	7,729.12 W	87.06 W
Max VUF	0.75	3.00	0.00%	0.00	0.00
Transformer Utilization	47,007.30 VA	125,000.00 VA	0.00%	0.00	0.00
Max Line Capacity	22.26%	100.00%	0.00%	0.00	0.00

From Monte Carlo simulations at the 29 node distribution system with using continuous local control function, it can prove that the determination of only the 17 cases of the set of uncertainty is sufficient to solve the uncertainty problem of load, solar irradiance and ambient temperature. It is because as follows:

- The power flow results of minimum and maximum voltage profile, maximum VUF, MV/LV transformer utilization and maximum line capacity are within those limit. The probabilities have around 100% to hold on the limits under the uncertainty;
- For the Day 3, 4, 5, 7 and 8 November 2014, there is a chance to occur overvoltage. Assumingly, overvoltage is neglected because overvoltage is more than the limit slightly about less than 0.5 V.
- For the Day 3, 4, 5, 6, 7, 8, 9 and the Week 3-9 November 2014, the probability of the loss results to exceed the limit is less than 30% or the probability of the loss results have around 70% to hold on the loss limit under the uncertainty according to the worst case at the week 3-9 November

2014. Mean over losses is more than the limit about <150 W according to the week 3-9 November 2014.

However, the results that exceed only a small extent of the loss limit can be resolved by adjusting the loss limit in the optimization problem less than the actual values.

7.7.4 The Modified 29 Node Distribution System With Using Piecewise Linear Local Control Function

In this subsection, Monte Carlo simulation applies in eight parts: (7.7.4.1) at the week 3-9 November 2014; (7.7.4.2) at the day 3 November 2014; (7.7.4.3) at the day 4 November 2014; (7.7.4.4) at the day 5 November 2014; (7.7.4.5) at the day 6 November 2014; (7.7.4.6) at the day 7 November 2014; (7.7.4.7) at the day 8 November 2014; (7.7.4.8) at the day 9 November 2014. The piecewise linear local control function is selected in this subsection.

7.7.4.1 At The Week 3-9 November 2014

In this subsection, the value of load, solar irradiance and ambient temperature will be randomized in 100,000 times, according to the normal uncertainty characteristic of Figure 6.6 at the week 3-9 November 2014. Each random values at a time will be assessed by power flow algorithm. The optimal parameters setting at the week 3-9 November 2014 as shown in Table 7.34 is applied. Then, the power flow results in 100,000 times can be shown in Figure 7.94. The summary from Monte Carlo simulation is shown in Table 7.69. It can notice that mean values from power flow results are within the limit and. The probability of over loss is 29.60%. The mean over loss is 7,816.74 W that is slightly more than the limit around 174.68 W. Other variables have 0% probability to exceed the limits.

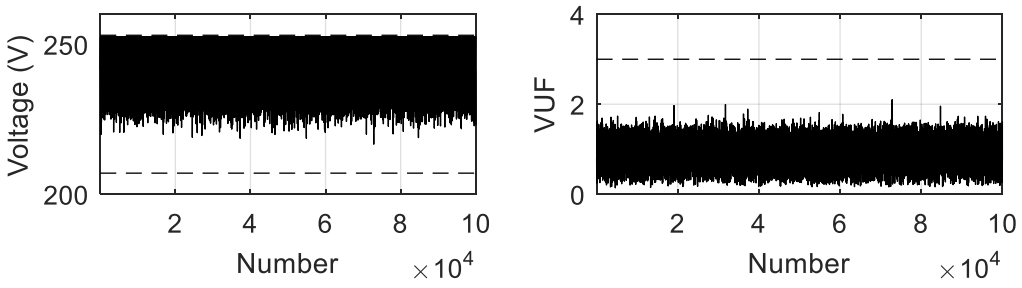

(a) Minimum and maximum phase voltage

(b) Maximum VUF

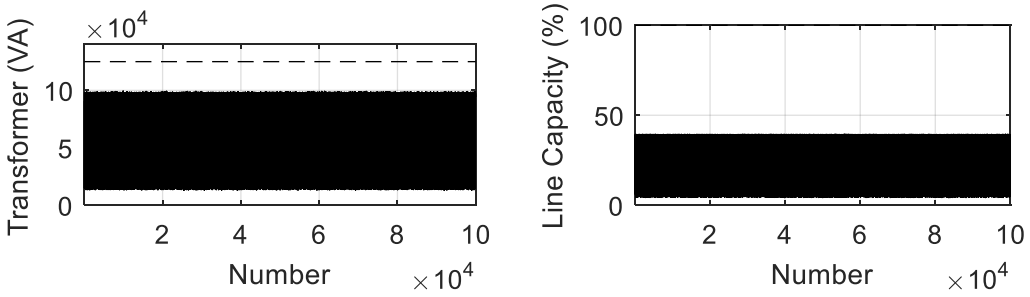

(c) MV/LV transformer utilization *(d) Maximum line capacity*

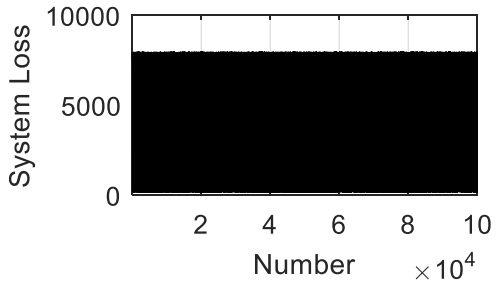

(e) System loss

Figure 7.94 The power flow results from 100,000-times random

Table 7.69 The results of Monte Carlo simulation

Variables	Mean Values from 100,000 times of random	Limit	Over-limit Consideration		
			Probability	Mean of Excess Value	Difference
Min Voltage	249.85 V	253.00 V	0.00%	0.00	0.00
Max Voltage	240.40 V	207.00 V	0.00%	0.00	0.00
Loss	4,642.38 W	7,642.05 W	29.60%	7,816.74 W	174.68 W
Max VUF	0.84	3.00	0.00%	0.00	0.00
Transformer Utilization	60,885.72 VA	125,000.00 VA	0.00%	0.00	0.00
Max Line Capacity	27.51%	100.00%	0.00%	0.00	0.00

7.7.4.2 At The Day 3 November 2014

In this subsection, the value of load, solar irradiance and ambient temperature will be randomized in 100,000 times, according to the normal uncertainty characteristic of Figure 6.7 at the day 3 November 2014. Each random values at a time will be assessed by power flow algorithm. The optimal parameters setting at the day 3 November 2014 as shown in Table 7.36 is applied. Then, the power flow results in 100,000 times can be shown in Figure 7.95. The summary from Monte Carlo simulation is shown in Table

7.70. It can notice that mean values from power flow results are within the limit and. The probability of over loss is 0.22%. The mean over loss is 7,655.99 W that is slightly more than the limit around 13.93 W. Other variables have 0% probability to exceed the limits.

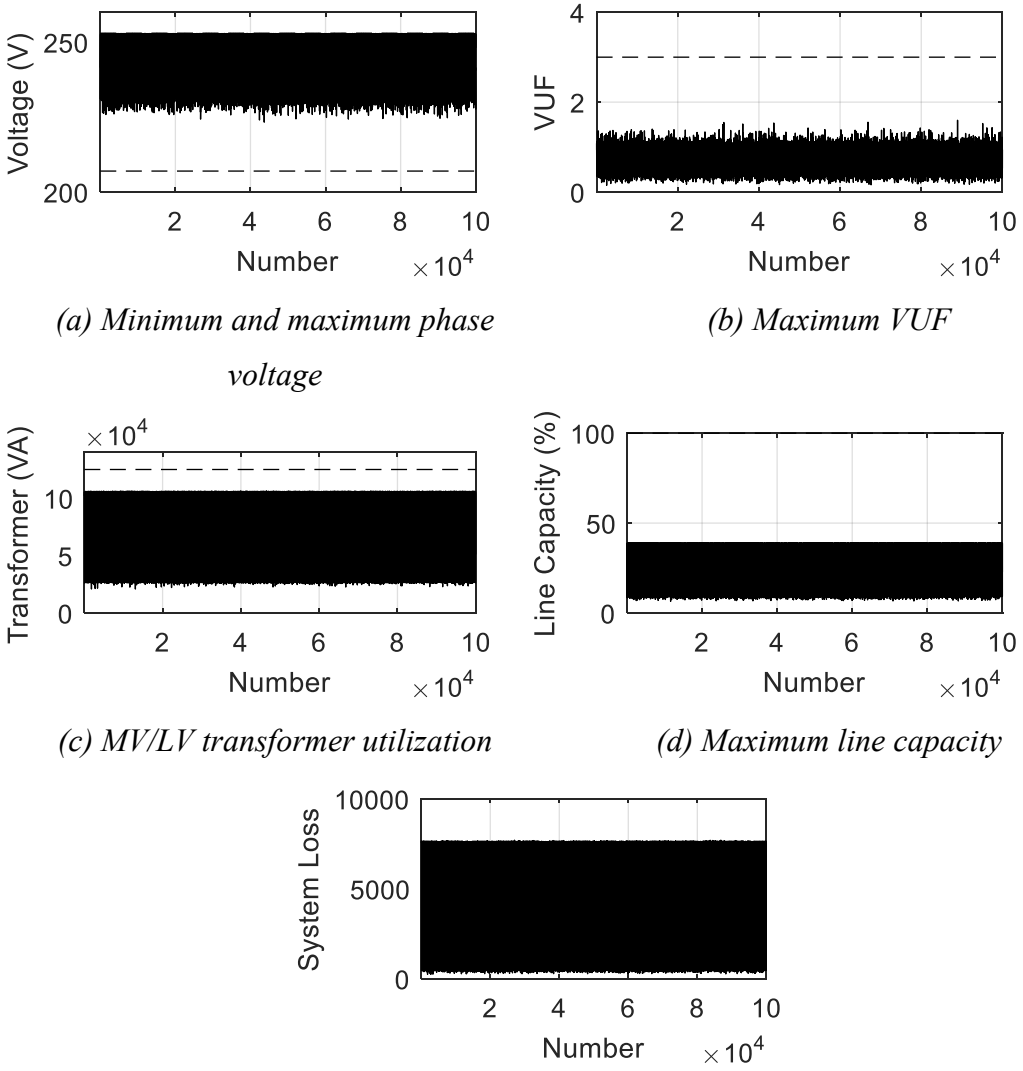

(a) Minimum and maximum phase voltage

(b) Maximum VUF

(c) MV/LV transformer utilization

(d) Maximum line capacity

(e) System loss

Figure 7.95 The power flow results from 100,000-times random

Table 7.70 The results of Monte Carlo simulation

Variables	Mean Values from 100,000 times of random	Limit	Over-limit Consideration		
			Probability	Mean of Excess Value	Difference
Min Voltage	250.51 V	253.00 V	0.00%	0.00	0.00
Max Voltage	240.13 V	207.00 V	0.00%	0.00	0.00
Loss	5,645.15 W	7,642.05 W	0.22%	7, 655.99 W	13.93 W
Max VUF	0.83	3.00	0.00%	0.00	0.00

Variables	Mean Values from 100,000 times of random	Limit	Over-limit Consideration		
			Probability	Mean of Excess Value	Difference
Transformer Utilization	80,977.20 VA	125,000.00 VA	0.00%	0.00	0.00
Max Line Capacity	31.76%	100.00%	0.00%	0.00	0.00

7.7.4.3 At The Day 4 November 2014

In this subsection, the value of load, solar irradiance and ambient temperature will be randomized in 100,000 times, according to the normal uncertainty characteristic of Figure 6.8 at the day 4 November 2014. Each random values at a time will be assessed by power flow algorithm. The optimal parameters setting at the day 4 November 2014 as shown in Table 7.37 is applied. Then, the power flow results in 100,000 times can be shown in Figure 7.96. The summary from Monte Carlo simulation is shown in Table 7.71. It can notice that mean values from power flow results are within the limit and. The probability of over loss is 10.86%. The mean over loss is 7,690.86 W that is slightly more than the limit around 48.81 W. Other variables have 0% probability to exceed the limits.

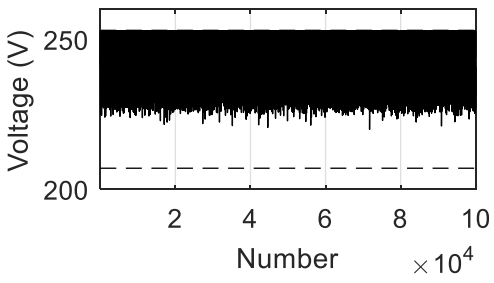

(a) Minimum and maximum phase voltage

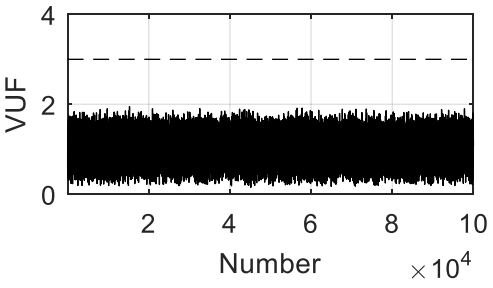

(b) Maximum VUF

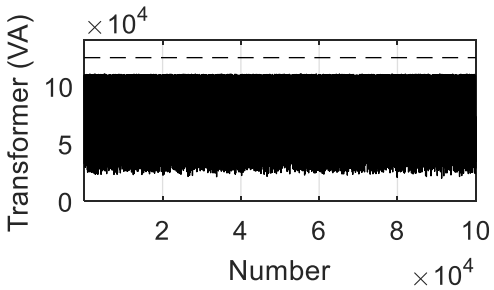

(c) MV/LV transformer utilization

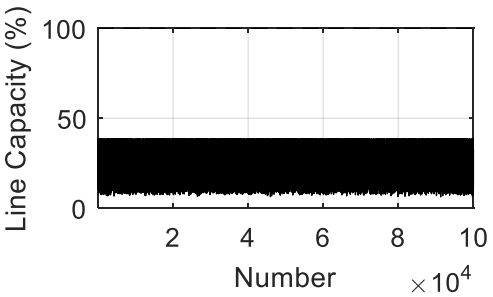

(d) Maximum line capacity

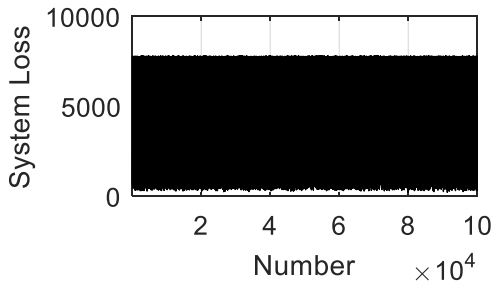

(e) System loss

Figure 7.96 The power flow results from 100,000-times random

Table 7.71 The results of Monte Carlo simulation

Variables	Mean Values from 100,000 times of random	Limit	Over-limit Consideration		
			Probability	Mean of Excess Value	Difference
Min Voltage	249.91 V	253.00 V	0.00%	0.00	0.00
Max Voltage	238.98 V	207.00 V	0.00%	0.00	0.00
Loss	5,225.49 W	7,642.05 W	10.86%	7,690.86 W	48.81 W
Max VUF	0.89	3.00	0.00%	0.00	0.00
Transformer Utilization	78,060.82 VA	125,000.00 VA	0.00%	0.00	0.00
Max Line Capacity	30.59%	100.00%	0.00%	0.00	0.00

7.7.4.4 At The Day 5 November 2014

In this subsection, the value of load, solar irradiance and ambient temperature will be randomized in 100,000 times, according to the normal uncertainty characteristic of Figure 6.9 at the day 5 November 2014. Each random values at a time will be assessed by power flow algorithm. The optimal parameters setting at the day 5 November 2014 as shown in Table 7.38 is applied. Then, the power flow results in 100,000 times can be shown in Figure 7.97. The summary from Monte Carlo simulation is shown in Table 7.72. It can notice that mean values from power flow results are within the limit and. The probability of over loss is 4.31%. The mean over loss is 7,663.65 W that is slightly more than the limit around 21.59 W. Other variables have 0% probability to exceed the limits.

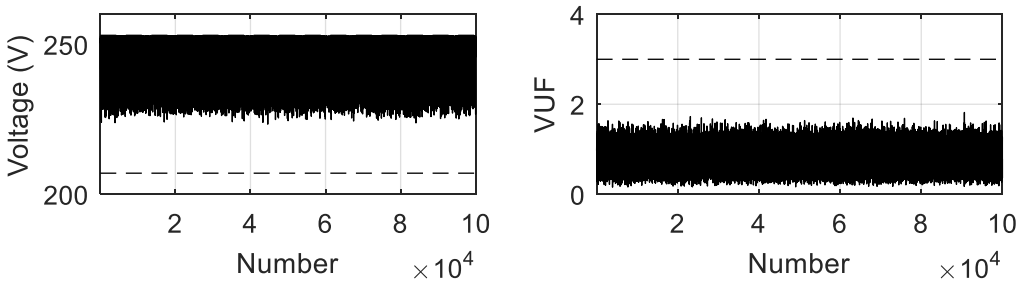

(a) Minimum and maximum phase voltage

(b) Maximum VUF

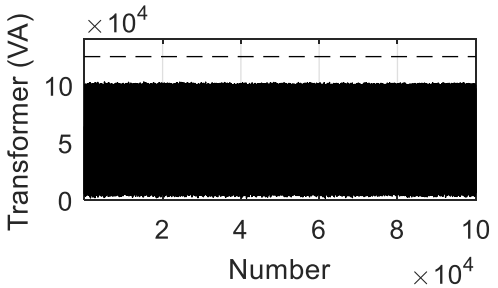

(c) MV/LV transformer utilization

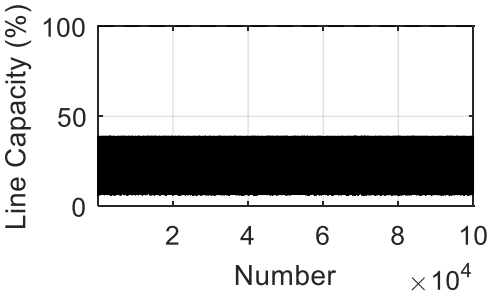

(d) Maximum line capacity

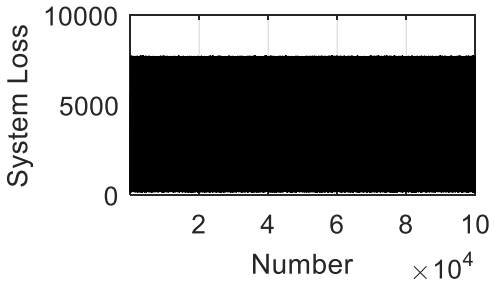

(e) System loss

Figure 7.97 The power flow results from 100,000-times random

Table 7.72 The results of Monte Carlo simulation

Variables	Mean Values from 100,000 times of random	Limit	Over-limit Consideration		
			Probability	Mean of Excess Value	Difference
Min Voltage	249.32 V	253.00 V	0.00%	0.00	0.00
Max Voltage	239.96 V	207.00 V	0.00%	0.00	0.00
Loss	4,276.42 W	7,642.05 W	4.31%	7,663.65 W	21.59 W
Max VUF	0.85	3.00	0.00%	0.00	0.00
Transformer Utilization	56,461.94 VA	125,000.00 VA	0.00%	0.00	0.00
Max Line Capacity	26.85%	100.00%	0.00%	0.00	0.00

7.7.4.5 At The Day 6 November 2014

In this subsection, the value of load, solar irradiance and ambient temperature will be randomized in 100,000 times, according to the normal uncertainty characteristic of Figure 6.10 at the day 6 November 2014. Each random values at a time will be assessed by power flow algorithm. The optimal parameters setting at the day 6 November 2014 as shown in Table 7.39 is applied. Then, the power flow results in 100,000 times can be shown in Figure 7.98. The summary from Monte Carlo simulation is shown in Table 7.73. It can notice that mean values from power flow results are within the limit and. The probability of over loss is 2.92%. The mean over loss is 7,668.07 W that is slightly more than the limit around 26.01 W. Other variables have 0% probability to exceed the limits.

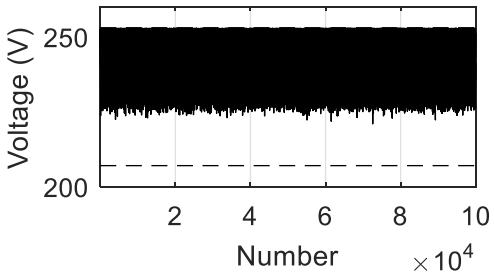

(a) Minimum and maximum phase voltage

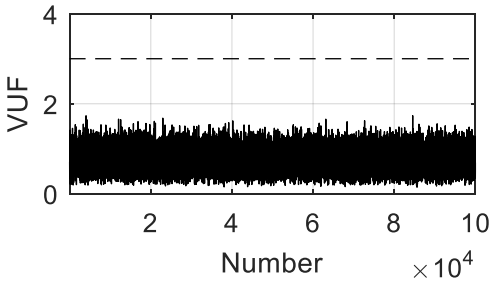

(b) Maximum VUF

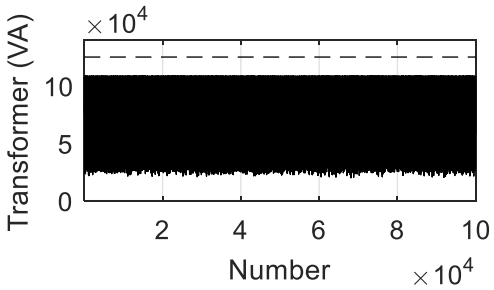

(c) MV/LV transformer utilization

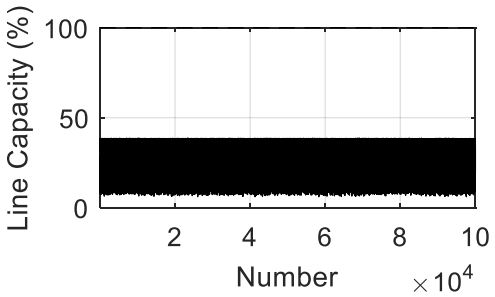

(d) Maximum line capacity

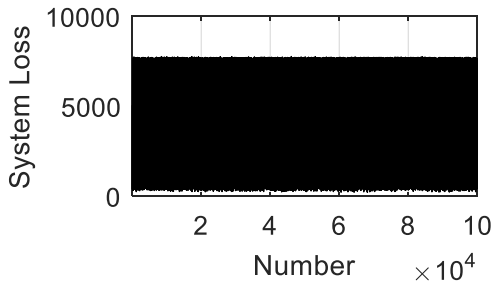

(e) System loss

Figure 7.98 The power flow results from 100,000-times random

Table 7.73 The results of Monte Carlo simulation

Variables	Mean Values from 100,000 times of random	Limit	Over-limit Consideration		
			Probability	Mean of Excess Value	Difference
Min Voltage	247.78 V	253.00 V	0.00%	0.00	0.00
Max Voltage	237.42 V	207.00 V	0.00%	0.00	0.00
Loss	4,524.13 W	7,642.05 W	2.92%	7,668.07 W	26.01 W
Max VUF	0.76	3.00	0.00%	0.00	0.00
Transformer Utilization	75,760.53 VA	125,000.00 VA	0.00%	0.00	0.00
Max Line Capacity	27.73%	100.00%	0.00%	0.00	0.00

7.7.4.6 At The Day 7 November 2014

In this subsection, the value of load, solar irradiance and ambient temperature will be randomized in 100,000 times, according to the normal uncertainty characteristic of Figure 6.11 at the day 7 November 2014. Each random values at a time will be assessed by power flow algorithm. The optimal parameters setting at the day 7 November 2014 as shown in Table 7.40 is applied. Then, the power flow results in 100,000 times can be shown in Figure 7.99. The summary from Monte Carlo simulation is shown in Table 7.74. It can notice that mean values from power flow results are within the limit and. The probability of over loss is 15.62%. The mean over loss is 7,743.72 W that is slightly more than the limit around 101.67 W. Other variables have 0% probability to exceed the limits.

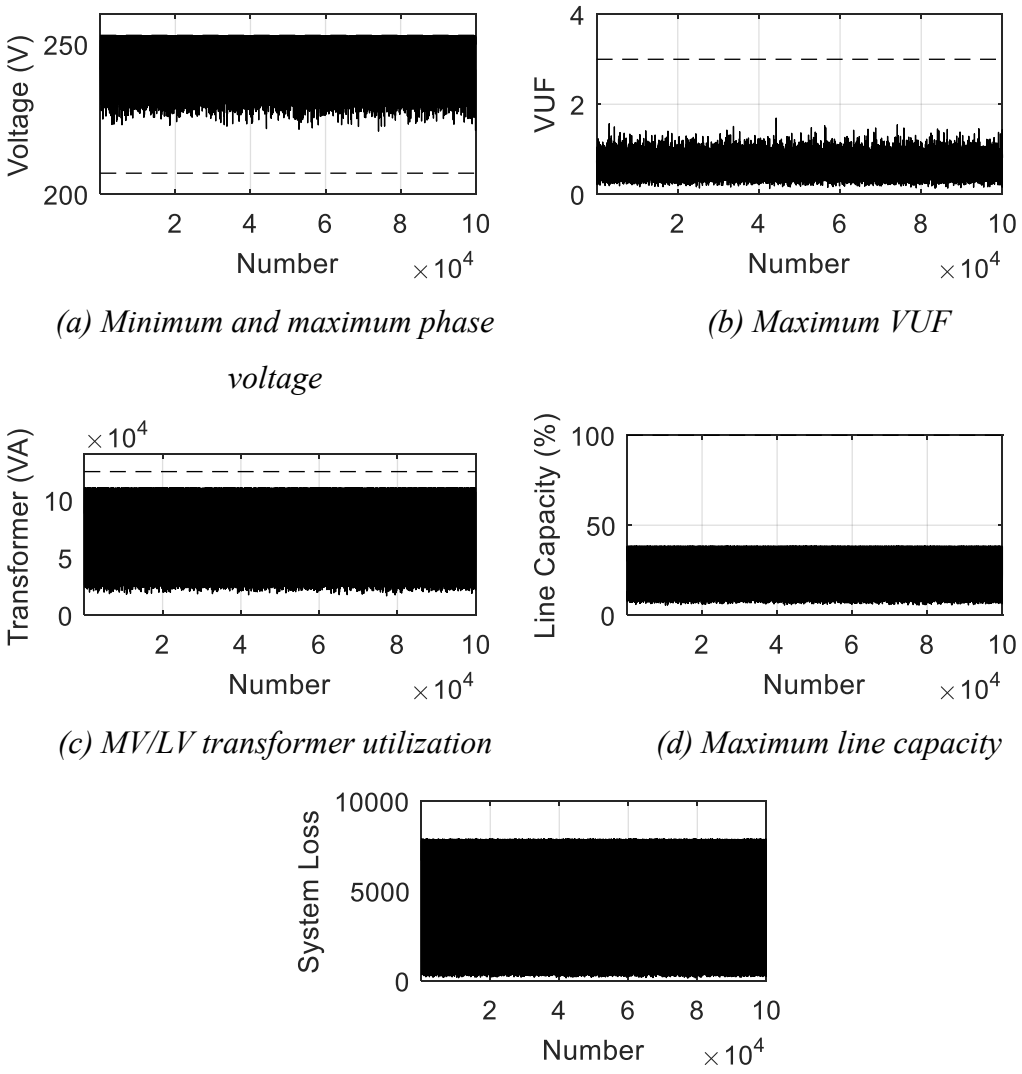

(a) Minimum and maximum phase voltage

(b) Maximum VUF

(c) MV/LV transformer utilization

(d) Maximum line capacity

(e) System loss

Figure 7.99 The power flow results from 100,000-times random

Table 7.74 The results of Monte Carlo simulation

Variables	Mean Values from 100,000 times of random	Limit	Over-limit Consideration		
			Probability	Mean of Excess Value	Difference
Min Voltage	248.81 V	253.00 V	0.00%	0.00	0.00
Max Voltage	239.20 V	207.00 V	0.00%	0.00	0.00
Loss	4,406.84 W	7,642.05 W	15.62%	7,743.72 W	101.67 W
Max VUF	0.69	3.00	0.00%	0.00	0.00
Transformer Utilization	68,056.85 VA	125,000.00 VA	0.00%	0.00	0.00
Max Line Capacity	26.91%	100.00%	0.00%	0.00	0.00

7.7.4.7 At The Day 8 November 2014

In this subsection, the value of load, solar irradiance and ambient temperature will be randomized in 100,000 times, according to the normal uncertainty characteristic of Figure 6.12 at the day 8 November 2014. Each random values at a time will be assessed by power flow algorithm. The optimal parameters setting at the day 8 November 2014 as shown in Table 7.41 is applied. Then, the power flow results in 100,000 times can be shown in Figure 7.100. The summary from Monte Carlo simulation is shown in Table 7.75. It can notice that mean values from power flow results are within the limit and. The probability of over loss is 36.61%. The mean over loss is 7,763.52 W that is slightly more than the limit around 121.46 W. Other variables have 0% probability to exceed the limits.

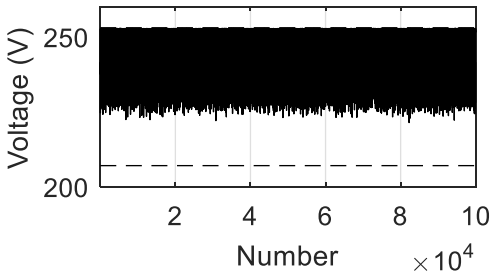

(a) Minimum and maximum phase voltage

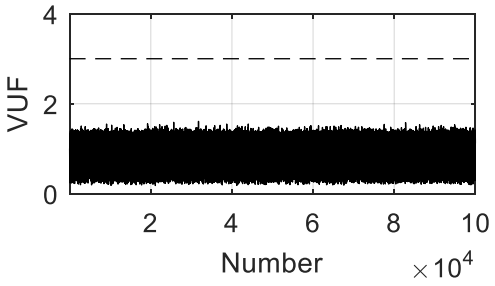

(b) Maximum VUF

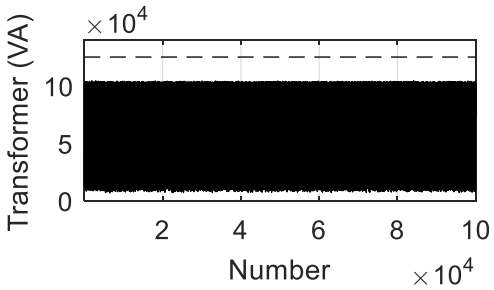

(c) MV/LV transformer utilization

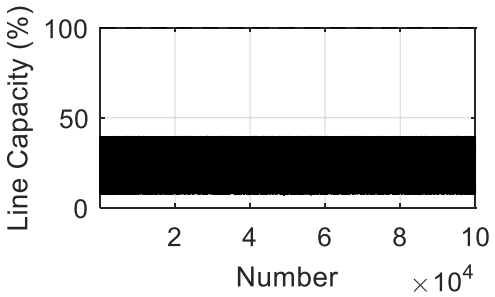

(d) Maximum line capacity

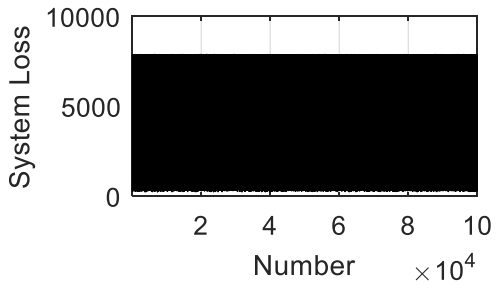

(e) System loss

Figure 7.100 The power flow results from 100,000-times random

Table 7.75 The results of Monte Carlo simulation

Variables	Mean Values from 100,000 times of random	Limit	Over-limit Consideration		
			Probability	Mean of Excess Value	Difference
Min Voltage	250.00 V	253.00 V	0.00%	0.00	0.00
Max Voltage	240.04 V	207.00 V	0.00%	0.00	0.00
Loss	5,333.30 W	7,642.05 W	36.61%	7,763.52 W	121.46 W
Max VUF	0.98	3.00	0.00%	0.00	0.00
Transformer Utilization	69,292.13 VA	125,000.00 VA	0.00%	0.00	0.00
Max Line Capacity	30.80%	100.00%	0.00%	0.00	0.00

7.7.4.8 At The Day 9 November 2014

In this subsection, the value of load, solar irradiance and ambient temperature will be randomized in 100,000 times, according to the normal uncertainty characteristic of Figure 6.13 at the day 9 November 2014. Each random values at a time will be assessed by power flow algorithm. The optimal parameters setting at the day 9 November 2014 as shown in Table 7.42 is applied. Then, the power flow results in 100,000 times can be shown in Figure 7.101. The summary from Monte Carlo simulation is shown in Table 7.76. It can notice that mean values from power flow results are within the limit and. The probability of over loss is 7.22%. The mean over loss is 7,852.06 W that is slightly more than the limit around 210.01 W. Other variables have 0% probability to exceed the limits.

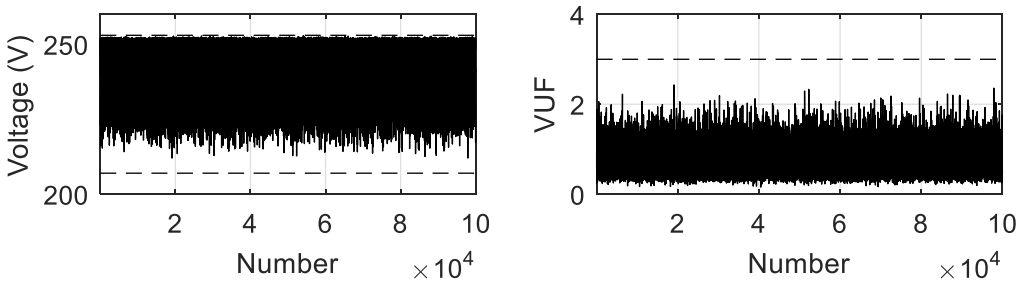

(a) Minimum and maximum phase voltage

(b) Maximum VUF

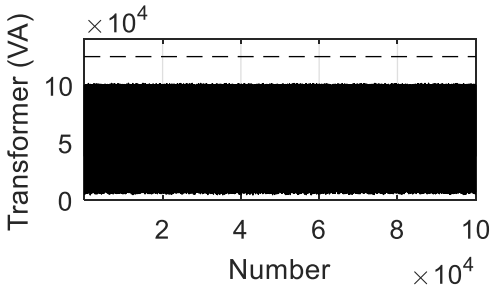

(c) MV/LV transformer utilization

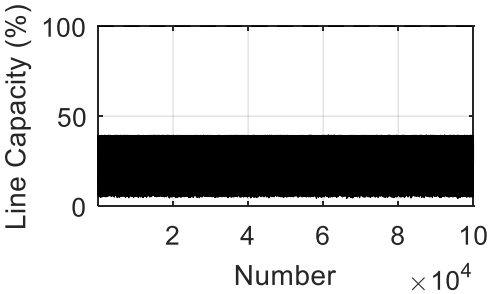

(d) Maximum line capacity

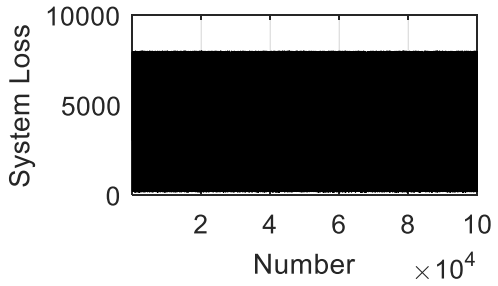

(e) System loss

Figure 7.101 The power flow results from 100,000-times random

Table 7.76 The results of Monte Carlo simulation

Variables	Mean Values from 100,000 times of random	Limit	Over-limit Consideration		
			Probability	Mean of Excess Value	Difference
Min Voltage	247.27 V	253.00 V	0.00%	0.00	0.00
Max Voltage	237.96 V	207.00 V	0.00%	0.00	0.00
Loss	2,947.57 W	7,642.05 W	7.22%	7,852.06 W	210.01 W
Max VUF	0.69	3.00	0.00%	0.00	0.00
Transformer Utilization	41,994.49 VA	125,000.00 VA	0.00%	0.00	0.00
Max Line Capacity	22.08%	100.00%	0.00%	0.00	0.00

From Monte Carlo simulations at the 29 node distribution system with using piecewise linear local control function, it can prove that the determination of only the 17 cases of the set of uncertainty is sufficient to solve the uncertainty problem of load, solar irradiance and ambient temperature. It is because as follows:

- The power flow results of minimum and maximum voltage profile, maximum VUF, MV/LV transformer utilization and maximum line capacity are within those limit. The probabilities have around 100% to hold on the limits under the uncertainty;
- For the Day 3, 4, 5, 6, 7, 8, 9 and the Week 3-9 November 2014, the probability of the loss results to exceed the limit is less than 40% or the probability of the loss results have around 60% to hold on the loss limit under the uncertainty according to the worst case at the day 8 November 2014. Mean over losses is more than the limit about <250 W according to the day 9 November 2014.

However, the results that exceed only a small extent of the loss limit can be resolved by adjusting the loss limit in the optimization problem less than the actual value.

From Monte Carlo simulation, it can notice that when 17 cases of the set of uncertainty is applied in a small system (such as the modified 19 node distribution system), exceeding loss limit can occur rarely. On the other hand, when 17 cases of the set of uncertainty is applied in a larger system (such as the modified 29 node distribution system), exceeding loss limit have more chance to occur. Then, adjusting loss limit in the optimization problem less than the actual value is another way to hold on the loss limit under the uncertainty in larger system.

CHAPTER 8

CONCLUSION

This chapter provides a summary of this dissertation. Then, some suggestions for improvement of this dissertation are also proposed.

8.1 Dissertation Summary

Solar energy is a clean energy and does not cause polluted environment. Then, the technology of generating electricity from solar energy has been developed such as Photovoltaic (PV) system. Currently, PV installation is supported to install in households or at LV distribution system because of the government policies and the cost reduction of PV installation. However, more PV installations in LV distribution system can bring about problems such as the followings:

- Loss of real power generation because of the operation of overvoltage protection of solar power generation systems which are specially on the downstream nodes.
- Voltage unbalance due to the connection of a single-phase PV inverter.

Generally, the aforementioned problems can be resolved by the followings [3-6]:

- Installing an MV/LV transformer with an On-Load Tap Changer (OLTC).
- Installing an energy storage system.
- Changing conductor size of LV feeder to be larger.

To support more PV installation or high PV penetration in LV distribution system, many previous researches [7-13] have studied in controlling PV system instead because it is cheaper than installing OLTC, installing energy storage system, or changing into new larger conductor. Many previous researches [7-13] have proposed 3 different concepts of the control strategies as follows:

- Central control [7, 8, 10].
- Local control [9, 11, 12].
- Coordination between central and local control [13].

This dissertation notices the advantages of the control strategy of coordination between central and local control that has no need of very reliable communication system with central control and, moreover, the parameter setting of local control can be optimally updated to suit at any periods. However, the previous researches [7-13] did not determine the uncertainty of load and solar irradiance which the uncertainty can cause the voltage problem in LV distribution system. Then, the uncertainty is the important topic which is determined in this dissertation.

The optimization process of the coordination between central and local control of this dissertation applies 2-stage PSO to find the optimal parameter setting of local control. The 2-stage PSO is used to solve the disadvantage of ordinary PSO process which is not suitable for solving optimization problem with many free variables. The local control applies P(U) and Q(U) functions to adjust real and reactive power output which are generated by connected PV system when the voltage at the connection point changes. The power flow algorithm applies Newton-Raphson Method with step-length adjustment. Moreover, the 17 cases of the set of uncertainty are presented to take care of the uncertainty of load, solar irradiance and ambient temperature that can be occurred. The resetting of the parameter of local control can be in every day or week. The optimization problem is determined on maximization of total real power output from PV systems on the mean value from the normal uncertainty characteristic. The normal uncertainty characteristic is assessed from the collected data which is consisted of load, solar, and ambient temperature. Note that the mean value has the highest chance to occur according to normal uncertainty characteristic. From the results in Section 7, they can be summarized as follows.

Firstly, the coordination between central and local control strategy can support high PV penetration in LV distribution system. The parameters adjustment can be one day or week.

Secondly, local control should be coordinated between P(U) and Q(U) functions for more injection of real power from connected PV systems. Any continuous or piecewise linear function can be chosen to operate because of the close results.

Thirdly, the different parameters setting of each PV system is better than the same setting according to the comparison between the different and same parameter settings.

Fourthly, the resetting of local control in every day is preferred because of better objective value result than resetting in every week.

Fifthly, Monte-Carlo simulation with 100,000-times random is applied to determine the sufficiency of the determination of only the 17 cases of the set of uncertainty in the optimization problem. It can find as follows:

- In a small system such as the modified 19 node distribution system, the results can hold on the limit effectively. However, exceeding loss limit has about <2% chance.
- In a larger system such as the modified 29 node distribution system, the results have more chance to exceed the loss limit about <40%.
- Other values (the minimum and maximum voltage, VUF, line flow, MV/LV transformer utilization) are absolutely within the limit in small or larger system.

To handle loss within the limit, adjusting limit in the optimization problem less than the actual value is a another solution.

8.2 Recommendation for future research development

Some development and improvement of this dissertation are presented as follows:

- Energy Storage System (ESS) can help support high PV penetration in LV distribution system. Then, the future researches should include ESS installation.
- This dissertation can resets the parameter setting of local control in every day or week. The future researches should reset in faster period by modifying the optimization process to find the faster solution.
- Develop uncertainty analysis in optimization problem to reduce over loss limit probability.

APPENDIX

APPENDIX A

Positive-sequence Current Calculation

The derivation of positive-sequence current calculation in equation (2.6) can be initiated from equation (A.1) to equation (A.7).

$$S^{ABC} = [V^{ABC}]^T \times [I^{ABC}]^* \tag{A.1}$$

$$S^{ABC} = [A_s V^{012}]^T \times [A_s I^{012}]^* \quad ; A_s = \begin{bmatrix} 1 & 1 & 1 \\ 1 & a^2 & a \\ 1 & a & a^2 \end{bmatrix} \tag{A.2}$$

$$S^{ABC} = [V^{012}]^T \times A_s^T \times A_s^* \times [I^{012}]^* \quad ; A_s^T \times A_s^* = 3 \tag{A.3}$$

$$S^{ABC} = 3 \times \begin{bmatrix} V^{ze} \\ V^{po} \\ V^{ne} \end{bmatrix}^T \times \begin{bmatrix} I^{ze} \\ I^{po} \\ I^{ne} \end{bmatrix}^* \tag{A.4}$$

Three phase PV inverter does not generate zero and negative sequence current. Then, $I^{ze} = I^{ne} = 0$.

$$S^{ABC} = 3 \times V^{po} \times [I^{po}]^* \quad ; S^{ABC} = P_{pv} + jQ_{pv} \tag{A.5}$$

$$\frac{1}{3}\left(P_{pv} + jQ_{pv}\right) = (V^{po,r} + jV^{po,m})(I^{po,r} + jI^{po,m})^* \tag{A.6}$$

From (A.6), it can transform into matrix equation (A.7) that is the equation (2.6) for calculating positive-sequence current.

$$\begin{bmatrix} I^{po,r} \\ I^{po,m} \end{bmatrix} = \frac{1}{3} \times \begin{bmatrix} V^{po,r} & V^{po,m} \\ V^{po,m} & -V^{po,r} \end{bmatrix}^{-1} \times \begin{bmatrix} P_{pv} \\ Q_{pv} \end{bmatrix} \tag{A.7}$$

APPENDIX B

Differential Equation of Three-Phase PV system

B.1 Differential Equation by Voltage and Phase Angle

Normally, power output of three-phase PV system can be written into Table B.1.

Table B.1 Power output of three-phase PV system

$P_{i,pv}^{A} + jQ_{i,pv}^{A}$	$= V_i^A \angle \delta_i^A \cdot \left[I_i^{po,r} - jI_i^{po,m}\right]$ $= \left[V_i^A \cos\left(\delta_i^A\right) + jV_i^A \sin\left(\delta_i^A\right)\right] \cdot \left[I_i^{po,r} - jI_i^{po,m}\right]$ $= V_i^A I_i^{po,r} \cos\left(\delta_i^A\right) + V_i^A I_i^{po,m} \sin\left(\delta_i^A\right)$ $+ j\left[V_i^A I_i^{po,r} \sin\left(\delta_i^A\right) - V_i^A I_i^{po,m} \cos\left(\delta_i^A\right)\right]$
$P_{i,pv}^{B} + jQ_{i,pv}^{B}$	$= V_i^B \angle (\delta_i^B + 120°) \cdot \left[I_i^{po,r} - jI_i^{po,m}\right]$ $= [V_i^B \cos(\delta_i^B + 120°) + jV_i^B \sin(\delta_i^B + 120°)] \cdot \left[I_i^{po,r} - jI_i^{po,m}\right]$ $= V_i^B I_i^{po,r} \cos(\delta_i^B + 120°) + V_i^B I_i^{po,m} \sin(\delta_i^B + 120°)$ $+ j\left[V_i^B I_i^{po,r} \sin(\delta_i^B + 120°)\right.$ $\left. - V_i^B I_i^{po,m} \cos(\delta_i^B + 120°)\right]$
$P_{i,pv}^{C} + jQ_{i,pv}^{C}$	$= V_i^C \angle (\delta_i^C - 120°) \cdot \left[I_i^{po,r} - jI_i^{po,m}\right]$ $= \left[V_i^C \cos\left(\delta_i^C - 120°\right) + jV_i^C \sin\left(\delta_i^C - 120°\right)\right] \cdot \left[I_i^{po,r} - jI_i^{po,m}\right]$ $= V_i^C I_i^{po,r} \cos\left(\delta_i^C - 120°\right) + V_i^C I_i^{po,m} \sin\left(\delta_i^C - 120°\right)$ $+ j\left[V_i^C I_i^{po,r} \sin\left(\delta_i^C - 120°\right)\right.$ $\left. - V_i^C I_i^{po,m} \cos\left(\delta_i^C - 120°\right)\right]$

From equation (A.7), $I^{po,r}$ and $I^{po,m}$ can be written into equations (B.1) and (B.2).

$$I_i^{po,r} = \frac{1}{3}\left[\frac{V_i^{po,r} P_{i,pv} + V_i^{po,m} Q_{i,pv}}{V_i^{rm}}\right] \tag{B.1}$$

$$I_i^{po,m} = \frac{1}{3}\left[\frac{V_i^{po,m} P_{i,pv} - V_i^{po,r} Q_{i,pv}}{V_i^{rm}}\right] \tag{B.2}$$

$$V_i^{po,r} = \frac{1}{3}\left[V_i^A \cos\left(\delta_i^A\right) + V_i^B \cos(\delta_i^B + 120^\circ) + V_i^C \cos\left(\delta_i^C - 120^\circ\right)\right] \quad \text{(B.3)}$$

$$V_i^{po,m} = \frac{1}{3}\left[V_i^A \sin\left(\delta_i^A\right) + V_i^B \sin(\delta_i^B + 120^\circ) + V_i^C \sin\left(\delta_i^C - 120^\circ\right)\right] \quad \text{(B.4)}$$

$$\begin{aligned} V_i^{rm} = \frac{1}{9}\Big[&{V_i^A}^2 + {V_i^B}^2 + {V_i^C}^2 + 2V_i^A V_i^B \cos\left(\delta_i^A - \delta_i^B - 120^\circ\right) \\ &+ 2V_i^A V_i^C \cos\left(\delta_i^A - \delta_i^C + 120^\circ\right) \\ &+ 2V_i^B V_i^C \cos\left(\delta_i^B - \delta_i^C + 240^\circ\right)\Big] \end{aligned} \quad \text{(B.5)}$$

The differential of phase-A real power can be written into equations (B.6)-(B.11).

$$\begin{aligned} \frac{\partial P_{i,pv}^A}{\partial V_i^A} = V_i^A &\left[cos\left(\delta_i^A\right)\frac{\partial I_i^{po,r}}{\partial V_i^A} + sin\left(\delta_i^A\right)\frac{\partial I_i^{po,m}}{\partial V_i^A}\right] \\ &+ \left[I_i^{po,r}\cos\left(\delta_i^A\right) + I_i^{po,m}\sin\left(\delta_i^A\right)\right] \end{aligned} \quad \text{(B.6)}$$

$$\frac{\partial P_{i,pv}^A}{\partial V_i^B} = V_i^A \left[cos\left(\delta_i^A\right)\frac{\partial I_i^{po,r}}{\partial V_i^B} + sin\left(\delta_i^A\right)\frac{\partial I_i^{po,m}}{\partial V_i^B}\right] \quad \text{(B.7)}$$

$$\frac{\partial P_{i,pv}^A}{\partial V_i^C} = V_i^A \left[cos\left(\delta_i^A\right)\frac{\partial I_i^{po,r}}{\partial V_i^C} + sin\left(\delta_i^A\right)\frac{\partial I_i^{po,m}}{\partial V_i^C}\right] \quad \text{(B.8)}$$

$$\begin{aligned} \frac{\partial P_{i,pv}^A}{\partial \delta_i^A} = V_i^A &\left[-sin\left(\delta_i^A\right)I_i^{po,r} + cos\left(\delta_i^A\right)\frac{\partial I_i^{po,r}}{\partial \delta_i^A} + cos\left(\delta_i^A\right)I_i^{po,m}\right. \\ &\left. + sin\left(\delta_i^A\right)\frac{\partial I_i^{po,m}}{\partial \delta_i^A}\right] \end{aligned} \quad \text{(B.9)}$$

$$\frac{\partial P_{i,pv}^A}{\partial \delta_i^B} = V_i^A \left[cos\left(\delta_i^A\right)\frac{\partial I_i^{po,r}}{\partial \delta_i^B} + sin\left(\delta_i^A\right)\frac{\partial I_i^{po,m}}{\partial \delta_i^B}\right] \quad \text{(B.10)}$$

$$\frac{\partial P_{i,pv}^A}{\partial \delta_i^C} = V_i^A \left[cos\left(\delta_i^A\right)\frac{\partial I_i^{po,r}}{\partial \delta_i^C} + sin\left(\delta_i^A\right)\frac{\partial I_i^{po,m}}{\partial \delta_i^C}\right] \quad \text{(B.11)}$$

The differential of phase-B real power can be written into equations (B.12)-(B.17).

$$\frac{\partial P_{i,pv}^B}{\partial V_i^A} = V_i^B \left[cos(\delta_i^B + 120°)\frac{\partial I_i^{po,r}}{\partial V_i^A} + sin(\delta_i^B + 120°)\frac{\partial I_i^{po,m}}{\partial V_i^A}\right] \quad \text{(B.12)}$$

$$\begin{aligned} \frac{\partial P_{i,pv}^B}{\partial V_i^B} = V_i^B &\left[cos(\delta_i^B + 120°)\frac{\partial I_i^{po,r}}{\partial V_i^B} + sin(\delta_i^B + 120°)\frac{\partial I_i^{po,m}}{\partial V_i^B}\right] \\ &+ \left[I_i^{po,r}\cos(\delta_i^B + 120°) + I_i^{po,m}\sin(\delta_i^B + 120°)\right] \end{aligned} \quad \text{(B.13)}$$

$$\frac{\partial P_{i,pv}^{B}}{\partial V_i^{C}} = V_i^{B}\left[cos(\delta_i^{B}+120°)\frac{\partial I_i^{po,r}}{\partial V_i^{C}} + sin(\delta_i^{B}+120°)\frac{\partial I_i^{po,m}}{\partial V_i^{C}}\right] \tag{B.14}$$

$$\frac{\partial P_{i,pv}^{B}}{\partial \delta_i^{A}} = V_i^{B}\left[cos(\delta_i^{B}+120°)\frac{\partial I_i^{po,r}}{\partial \delta_i^{A}} + sin(\delta_i^{B}+120°)\frac{\partial I_i^{po,m}}{\partial \delta_i^{A}}\right] \tag{B.15}$$

$$\begin{aligned}\frac{\partial P_{i,pv}^{B}}{\partial \delta_i^{B}} = V_i^{B}\Bigg[&-sin(\delta_i^{B}+120°)I_i^{po,r} + cos(\delta_i^{B}+120°)\frac{\partial I_i^{po,r}}{\partial \delta_i^{B}} \\ &+ cos(\delta_i^{B}+120°)I_i^{po,m} + sin(\delta_i^{B}+120°)\frac{\partial I_i^{po,m}}{\partial \delta_i^{B}}\Bigg]\end{aligned} \tag{B.16}$$

$$\frac{\partial P_{i,pv}^{B}}{\partial \delta_i^{C}} = V_i^{B}\left[cos(\delta_i^{B}+120°)\frac{\partial I_i^{po,r}}{\partial \delta_i^{C}} + sin(\delta_i^{B}+120°)\frac{\partial I_i^{po,m}}{\partial \delta_i^{C}}\right] \tag{B.17}$$

The differential of phase-C real power can be written into equations (B.18)-(B.23).

$$\frac{\partial P_{i,pv}^{C}}{\partial V_i^{A}} = V_i^{C}\left[cos\left(\delta_i^{C}-120°\right)\frac{\partial I_i^{po,r}}{\partial V_i^{A}} + sin\left(\delta_i^{C}-120°\right)\frac{\partial I_i^{po,m}}{\partial V_i^{A}}\right] \tag{B.18}$$

$$\frac{\partial P_{i,pv}^{C}}{\partial V_i^{B}} = V_i^{C}\left[cos\left(\delta_i^{C}-120°\right)\frac{\partial I_i^{po,r}}{\partial V_i^{B}} + sin\left(\delta_i^{C}-120°\right)\frac{\partial I_i^{po,m}}{\partial V_i^{B}}\right] \tag{B.19}$$

$$\begin{aligned}\frac{\partial P_{i,pv}^{C}}{\partial V_i^{C}} = V_i^{C}\Bigg[&cos\left(\delta_i^{C}-120°\right)\frac{\partial I_i^{po,r}}{\partial V_i^{C}} + sin\left(\delta_i^{C}-120°\right)\frac{\partial I_i^{po,m}}{\partial V_i^{C}}\Bigg] \\ &+ \left[I_i^{po,r}\cos\left(\delta_i^{C}-120°\right) + I_i^{po,m}\sin\left(\delta_i^{C}-120°\right)\right]\end{aligned} \tag{B.20}$$

$$\frac{\partial P_{i,pv}^{C}}{\partial \delta_i^{A}} = V_i^{C}\left[cos\left(\delta_i^{C}-120°\right)\frac{\partial I_i^{po,r}}{\partial \delta_i^{A}} + sin\left(\delta_i^{C}-120°\right)\frac{\partial I_i^{po,m}}{\partial \delta_i^{A}}\right] \tag{B.21}$$

$$\frac{\partial P_{i,pv}^{C}}{\partial \delta_i^{B}} = V_i^{C}\left[cos\left(\delta_i^{C}-120°\right)\frac{\partial I_i^{po,r}}{\partial \delta_i^{B}} + sin\left(\delta_i^{C}-120°\right)\frac{\partial I_i^{po,m}}{\partial \delta_i^{B}}\right] \tag{B.22}$$

$$\begin{aligned}\frac{\partial P_{i,pv}^{C}}{\partial \delta_i^{C}} = V_i^{C}\Bigg[&-sin\left(\delta_i^{C}-120°\right)I_i^{po,r} + cos\left(\delta_i^{C}-120°\right)\frac{\partial I_i^{po,r}}{\partial \delta_i^{C}} \\ &+ cos\left(\delta_i^{C}-120°\right)I_i^{po,m} + sin\left(\delta_i^{C}-120°\right)\frac{\partial I_i^{po,m}}{\partial \delta_i^{C}}\Bigg]\end{aligned} \tag{B.23}$$

The differential of phase-A reactive power can be written into equations (B.24)-(B.29).

$$\begin{aligned}\frac{\partial Q_{i,pv}^{A}}{\partial V_i^{A}} = V_i^{A}\Bigg[&sin\left(\delta_i^{A}\right)\frac{\partial I_i^{po,r}}{\partial V_i^{A}} - cos\left(\delta_i^{A}\right)\frac{\partial I_i^{po,m}}{\partial V_i^{A}}\Bigg] \\ &+ \left[I_i^{po,r}\sin\left(\delta_i^{A}\right) - I_i^{po,m}\cos\left(\delta_i^{A}\right)\right]\end{aligned} \tag{B.24}$$

$$\frac{\partial Q_{i,pv}^{A}}{\partial V_i^{B}} = V_i^{A}\left[sin\left(\delta_i^{A}\right)\frac{\partial I_i^{po,r}}{\partial V_i^{B}} - cos\left(\delta_i^{A}\right)\frac{\partial I_i^{po,m}}{\partial V_i^{B}}\right] \tag{B.25}$$

$$\frac{\partial Q_{i,pv}^{A}}{\partial V_i^{C}} = V_i^{A}\left[sin\left(\delta_i^{A}\right)\frac{\partial I_i^{po,r}}{\partial V_i^{C}} - cos\left(\delta_i^{A}\right)\frac{\partial I_i^{po,m}}{\partial V_i^{C}}\right] \tag{B.26}$$

$$\frac{\partial Q_{i,pv}^{A}}{\partial \delta_i^{A}} = V_i^{A}\left[cos\left(\delta_i^{A}\right)I_i^{po,r} + sin\left(\delta_i^{A}\right)\frac{\partial I_i^{po,r}}{\partial \delta_i^{A}} + sin\left(\delta_i^{A}\right)I_i^{po,m} - cos\left(\delta_i^{A}\right)\frac{\partial I_i^{po,m}}{\partial \delta_i^{A}}\right] \tag{B.27}$$

$$\frac{\partial Q_{i,pv}^{A}}{\partial \delta_i^{B}} = V_i^{A}\left[sin\left(\delta_i^{A}\right)\frac{\partial I_i^{po,r}}{\partial \delta_i^{B}} - cos\left(\delta_i^{A}\right)\frac{\partial I_i^{po,m}}{\partial \delta_i^{B}}\right] \tag{B.28}$$

$$\frac{\partial Q_{i,pv}^{A}}{\partial \delta_i^{C}} = V_i^{A}\left[sin\left(\delta_i^{A}\right)\frac{\partial I_i^{po,r}}{\partial \delta_i^{C}} - cos\left(\delta_i^{A}\right)\frac{\partial I_i^{po,m}}{\partial \delta_i^{C}}\right] \tag{B.29}$$

The differential of phase-B reactive power can be written into equations (B.30)-(B.35).

$$\frac{\partial Q_{i,pv}^{B}}{\partial V_i^{A}} = V_i^{B}\left[sin(\delta_i^{B} + 120°)\frac{\partial I_i^{po,r}}{\partial V_i^{A}} - cos(\delta_i^{B} + 120°)\frac{\partial I_i^{po,m}}{\partial V_i^{A}}\right] \tag{B.30}$$

$$\frac{\partial Q_{i,pv}^{B}}{\partial V_i^{B}} = V_i^{B}\left[sin(\delta_i^{B} + 120°)\frac{\partial I_i^{po,r}}{\partial V_i^{B}} - cos(\delta_i^{B} + 120°)\frac{\partial I_i^{po,m}}{\partial V_i^{B}}\right] + \left[I_i^{po,r}\sin(\delta_i^{B} + 120°) - I_i^{po,m}\cos(\delta_i^{B} + 120°)\right] \tag{B.31}$$

$$\frac{\partial Q_{i,pv}^{B}}{\partial V_i^{C}} = V_i^{B}\left[sin(\delta_i^{B} + 120°)\frac{\partial I_i^{po,r}}{\partial V_i^{C}} - cos(\delta_i^{B} + 120°)\frac{\partial I_i^{po,m}}{\partial V_i^{C}}\right] \tag{B.32}$$

$$\frac{\partial Q_{i,pv}^{B}}{\partial \delta_i^{A}} = V_i^{B}\left[sin(\delta_i^{B} + 120°)\frac{\partial I_i^{po,r}}{\partial \delta_i^{A}} - cos(\delta_i^{B} + 120°)\frac{\partial I_i^{po,m}}{\partial \delta_i^{A}}\right] \tag{B.33}$$

$$\frac{\partial Q_{i,pv}^{B}}{\partial \delta_i^{B}} = V_i^{B}\left[cos(\delta_i^{B} + 120°)I_i^{po,r} + sin(\delta_i^{B} + 120°)\frac{\partial I_i^{po,r}}{\partial \delta_i^{B}} + sin(\delta_i^{B} + 120°)I_i^{po,m} - cos(\delta_i^{B} + 120°)\frac{\partial I_i^{po,m}}{\partial \delta_i^{B}}\right] \tag{B.34}$$

$$\frac{\partial Q_{i,pv}^{B}}{\partial \delta_i^{C}} = V_i^{B}\left[sin(\delta_i^{B} + 120°)\frac{\partial I_i^{po,r}}{\partial \delta_i^{C}} - cos(\delta_i^{B} + 120°)\frac{\partial I_i^{po,m}}{\partial \delta_i^{C}}\right] \tag{B.35}$$

The differential of phase-C reactive power can be written into equations (B.36)-(B.41).

$$\frac{\partial Q_{i,pv}^{C}}{\partial V_i^{A}} = V_i^{C}\left[sin\left(\delta_i^{C}-120°\right)\frac{\partial I_i^{po,r}}{\partial V_i^{A}} - cos\left(\delta_i^{C}-120°\right)\frac{\partial I_i^{po,m}}{\partial V_i^{A}}\right] \tag{B.36}$$

$$\frac{\partial Q_{i,pv}^{C}}{\partial V_i^{B}} = V_i^{C}\left[sin\left(\delta_i^{C}-120°\right)\frac{\partial I_i^{po,r}}{\partial V_i^{B}} - cos\left(\delta_i^{C}-120°\right)\frac{\partial I_i^{po,m}}{\partial V_i^{B}}\right] \tag{B.37}$$

$$\begin{aligned}\frac{\partial Q_{i,pv}^{C}}{\partial V_i^{C}} = V_i^{C}&\left[sin\left(\delta_i^{C}-120°\right)\frac{\partial I_i^{po,r}}{\partial V_i^{C}} - cso\left(\delta_i^{C}-120°\right)\frac{\partial I_i^{po,m}}{\partial V_i^{C}}\right]\\ &+\left[I_i^{po,r}\sin\left(\delta_i^{C}-120°\right) - I_i^{po,m}\cos\left(\delta_i^{C}-120°\right)\right]\end{aligned} \tag{B.38}$$

$$\frac{\partial Q_{i,pv}^{C}}{\partial \delta_i^{A}} = V_i^{C}\left[sin\left(\delta_i^{C}-120°\right)\frac{\partial I_i^{po,r}}{\partial \delta_i^{A}} - cos\left(\delta_i^{C}-120°\right)\frac{\partial I_i^{po,m}}{\partial \delta_i^{A}}\right] \tag{B.39}$$

$$\frac{\partial Q_{i,pv}^{C}}{\partial \delta_i^{B}} = V_i^{C}\left[sin\left(\delta_i^{C}-120°\right)\frac{\partial I_i^{po,r}}{\partial \delta_i^{B}} - cos\left(\delta_i^{C}-120°\right)\frac{\partial I_i^{po,m}}{\partial \delta_i^{B}}\right] \tag{B.40}$$

$$\begin{aligned}\frac{\partial Q_{i,pv}^{C}}{\partial \delta_i^{C}} = V_i^{C}&\left[cos\left(\delta_i^{C}-120°\right)I_i^{po,r} + sin\left(\delta_i^{C}-120°\right)\frac{\partial I_i^{po,r}}{\partial \delta_i^{C}}\right.\\ &\left.+ sin\left(\delta_i^{C}-120°\right)I_i^{po,m} - cos\left(\delta_i^{C}-120°\right)\frac{\partial I_i^{po,m}}{\partial \delta_i^{C}}\right]\end{aligned} \tag{B.41}$$

The differential of $I_i^{po,r}$ can be written into equations (B.42)-(B.47).

$$\begin{aligned}&\frac{\partial I_i^{po,r}}{\partial V_i^{A}}\\ &= \frac{V_i^{rm}\left[V_i^{po,r}\frac{\partial P_{i,pv}}{\partial V_i^{A}} + P_{i,pv}\frac{\partial V_i^{po,r}}{\partial V_i^{A}} + V_i^{po,m}\frac{\partial Q_{i,pv}}{\partial V_i^{A}} + Q_{i,pv}\frac{\partial V_i^{po,m}}{\partial V_i^{A}}\right]}{3V_i^{rm^2}}\\ &- \frac{\left[V_i^{po,r}P_{i,pv} + V_i^{po,m}Q_{i,pv}\right]\frac{\partial V_i^{rm}}{\partial V_i^{A}}}{3V_i^{rm^2}}\end{aligned} \tag{B.42}$$

$$\begin{aligned}&\frac{\partial I_i^{po,r}}{\partial V_i^{B}}\\ &= \frac{V_i^{rm}\left[V_i^{po,r}\frac{\partial P_{i,pv}}{\partial V_i^{B}} + P_{i,pv}\frac{\partial V_i^{po,r}}{\partial V_i^{B}} + V_i^{po,m}\frac{\partial Q_{i,pv}}{\partial V_i^{B}} + Q_{i,pv}\frac{\partial V_i^{po,m}}{\partial V_i^{B}}\right]}{3V_i^{rm^2}}\\ &- \frac{\left[V_i^{po,r}P_{i,pv} + V_i^{po,m}Q_{i,pv}\right]\frac{\partial V_i^{rm}}{\partial V_i^{B}}}{3V_i^{rm^2}}\end{aligned} \tag{B.43}$$

$$\frac{\partial I_i^{po,r}}{\partial V_i^C} = \frac{V_i^{rm}\left[V_i^{po,r}\frac{\partial P_{i,pv}}{\partial V_i^C} + P_{i,pv}\frac{\partial V_i^{po,r}}{\partial V_i^C} + V_i^{po,m}\frac{\partial Q_{i,pv}}{\partial V_i^C} + Q_{i,pv}\frac{\partial V_i^{po,m}}{\partial V_i^C}\right]}{3V_i^{rm2}} - \frac{\left[V_i^{po,r}P_{i,pv} + V_i^{po,m}Q_{i,pv}\right]\frac{\partial V_i^{rm}}{\partial V_i^C}}{3V_i^{rm2}} \quad \text{(B.44)}$$

$$\frac{\partial I_i^{po,r}}{\partial \delta_i^A} = \frac{V_i^{rm}\left[P_{i,pv}\frac{\partial V_i^{po,r}}{\partial \delta_i^A} + Q_{i,pv}\frac{\partial V_i^{po,m}}{\partial \delta_i^A}\right] - \left[V_i^{po,r}P_{i,pv} + V_i^{po,m}Q_{i,pv}\right]\frac{\partial V_i^{rm}}{\partial \delta_i^A}}{3V_i^{rm2}} \quad \text{(B.45)}$$

$$\frac{\partial I_i^{po,r}}{\partial \delta_i^B} = \frac{V_i^{rm}\left[P_{i,pv}\frac{\partial V_i^{po,r}}{\partial \delta_i^B} + Q_{i,pv}\frac{\partial V_i^{po,m}}{\partial \delta_i^B}\right] - \left[V_i^{po,r}P_{i,pv} + V_i^{po,m}Q_{i,pv}\right]\frac{\partial V_i^{rm}}{\partial \delta_i^B}}{3V_i^{rm2}} \quad \text{(B.46)}$$

$$\frac{\partial I_i^{po,r}}{\partial \delta_i^C} = \frac{V_i^{rm}\left[P_{i,pv}\frac{\partial V_i^{po,r}}{\partial \delta_i^C} + Q_{i,pv}\frac{\partial V_i^{po,m}}{\partial \delta_i^C}\right] - \left[V_i^{po,r}P_{i,pv} + V_i^{po,m}Q_{i,pv}\right]\frac{\partial V_i^{rm}}{\partial \delta_i^C}}{3V_i^{rm2}} \quad \text{(B.47)}$$

The differential of $I_i^{po,m}$ can be written into equations (B.48)-(B.53).

$$\frac{\partial I_i^{po,m}}{\partial V_i^A} = \frac{V_i^{rm}\left[V_i^{po,m}\frac{\partial P_{i,pv}}{\partial V_i^A} + P_{i,pv}\frac{\partial V_i^{po,m}}{\partial V_i^A} - V_i^{po,r}\frac{\partial Q_{i,pv}}{\partial V_i^A} - Q_{i,pv}\frac{\partial V_i^{po,r}}{\partial V_i^A}\right]}{3V_i^{rm2}} - \frac{\left[V_i^{po,m}P_{i,pv} - V_i^{po,r}Q_{i,pv}\right]\frac{\partial V_i^{rm}}{\partial V_i^A}}{3V_i^{rm2}} \quad \text{(B.48)}$$

$$\frac{\partial I_i^{po,m}}{\partial V_i^B} = \frac{V_i^{rm}\left[V_i^{po,m}\frac{\partial P_{i,pv}}{\partial V_i^B} + P_{i,pv}\frac{\partial V_i^{po,m}}{\partial V_i^B} - V_i^{po,r}\frac{\partial Q_{i,pv}}{\partial V_i^B} - Q_{i,pv}\frac{\partial V_i^{po,r}}{\partial V_i^B}\right]}{3V_i^{rm2}} - \frac{\left[V_i^{po,m}P_{i,pv} - V_i^{po,r}Q_{i,pv}\right]\frac{\partial V_i^{rm}}{\partial V_i^B}}{3V_i^{rm2}} \quad \text{(B.49)}$$

$$\frac{\partial I_i^{po,m}}{\partial V_i^C} = \frac{V_i^{rm}\left[V_i^{po,m}\frac{\partial P_{i,pv}}{\partial V_i^C} + P_{i,pv}\frac{\partial V_i^{po,m}}{\partial V_i^C} - V_i^{po,r}\frac{\partial Q_{i,pv_{pv}}}{\partial V_i^C} - Q_{i,pv}\frac{\partial V_i^{po,r}}{\partial V_i^C}\right]}{3V_i^{rm2}} - \frac{\left[V_i^{po,m}P_{i,pv} - V_i^{po,r}Q_{i,pv}\right]\frac{\partial V_i^{rm}}{\partial V_i^C}}{3V_i^{rm2}} \quad \text{(B.50)}$$

$$\frac{\partial I_i^{po,m}}{\partial \delta_i^A} = \frac{V_i^{rm}\left[P_{i,pv}\frac{\partial V_i^{po,m}}{\partial \delta_i^A} - Q_{i,pv}\frac{\partial V_i^{po,r}}{\partial \delta_i^A}\right] - \left[V_i^{po,m}P_{i,pv} - V_i^{po,r}Q_{i,pv}\right]\frac{\partial V_i^{rm}}{\partial \delta_i^A}}{3V_i^{rm2}} \quad \text{(B.51)}$$

$$\frac{\partial I_i^{po,m}}{\partial \delta_i^B} = \frac{V_i^{rm}\left[P_{i,pv}\frac{\partial V_i^{po,m}}{\partial \delta_i^B} - Q_{i,pv}\frac{\partial V_i^{po,r}}{\partial \delta_i^B}\right] - \left[V_i^{po,m}P_{i,pv} - V_i^{po,r}Q_{i,pv}\right]\frac{\partial V_i^{rm}}{\partial \delta_i^B}}{3V_i^{rm2}} \quad \text{(B.52)}$$

$$\frac{\partial I_i^{po,m}}{\partial \delta_i^C} = \frac{V_i^{rm}\left[P_{i,pv}\frac{\partial V_i^{po,m}}{\partial \delta_i^C} - Q_{i,pv}\frac{\partial V_i^{po,r}}{\partial \delta_i^C}\right] - \left[V_i^{po,m}P_{i,pv} - V_i^{po,r}Q_{i,pv}\right]\frac{\partial V_i^{rm}}{\partial \delta_i^C}}{3V_i^{rm2}} \quad \text{(B.53)}$$

The differential of $V_i^{po,r}$ can be written into equations (B.54)-(B.59).

$$\frac{\partial V_i^{po,r}}{\partial V_i^A} = \frac{\cos\left(\delta_i^A\right)}{3} \quad \text{(B.54)}$$

$$\frac{\partial V_i^{po,r}}{\partial V_i^B} = \frac{\cos(\delta_i^B + 120°)}{3} \tag{B.55}$$

$$\frac{\partial V_i^{po,r}}{\partial V_i^C} = \frac{\cos\left(\delta_i^C - 120°\right)}{3} \tag{B.56}$$

$$\frac{\partial V_i^{po,r}}{\partial \delta_i^A} = \frac{-V_i^A \sin\left(\delta_i^A\right)}{3} \tag{B.57}$$

$$\frac{\partial V_i^{po,r}}{\partial \delta_i^B} = \frac{-V_i^B \sin(\delta_i^B + 120°)}{3} \tag{B.58}$$

$$\frac{\partial V_i^{po,r}}{\partial \delta_i^C} = \frac{-V_i^C \sin\left(\delta_i^C - 120°\right)}{3} \tag{B.59}$$

The differential of $V_i^{po,m}$ can be written into equations (B.60)-(B.65)

$$\frac{\partial V_i^{po,m}}{\partial V_i^A} = \frac{\sin\left(\delta_i^A\right)}{3} \tag{B.60}$$

$$\frac{\partial V_i^{po,m}}{\partial V_i^B} = \frac{\sin(\delta_i^B + 120°)}{3} \tag{B.61}$$

$$\frac{\partial V_i^{po,m}}{\partial V_i^C} = \frac{\sin\left(\delta_i^C - 120°\right)}{3} \tag{B.62}$$

$$\frac{\partial V_i^{po,m}}{\partial \delta_i^A} = \frac{V_i^A \cos\left(\delta_i^A\right)}{3} \tag{B.63}$$

$$\frac{\partial V_i^{po,m}}{\partial \delta_i^B} = \frac{V_i^B \cos(\delta_i^B + 120°)}{3} \tag{B.64}$$

$$\frac{\partial V_i^{po,m}}{\partial \delta_i^C} = \frac{V_i^C \cos\left(\delta_i^C - 120°\right)}{3} \tag{B.65}$$

The differential of V_i^{rm} can be written into equations (B.66)-(B.71).

$$\frac{\partial V_i^{rm}}{\partial V_i^A} = \frac{1}{9}\left[2V_i^A + 2V_i^B \cos\left(\delta_i^A - \delta_i^B - 120°\right) + 2V_i^C \cos\left(\delta_i^A - \delta_i^C + 120°\right)\right] \tag{B.66}$$

$$\frac{\partial V_i^{rm}}{\partial V_i^B} = \frac{1}{9}\left[2V_i^B + 2V_i^A \cos\left(\delta_i^A - \delta_i^B - 120°\right) + 2V_i^C \cos\left(\delta_i^B - \delta_i^C + 240°\right)\right] \tag{B.67}$$

$$\frac{\partial V_i^{rm}}{\partial V^C} = \frac{1}{9}\left[2V_i^C + 2V_i^A\cos\left(\delta_i^A - \delta_i^C + 120°\right) + 2V_i^B\cos\left(\delta_i^B - \delta_i^C + 240°\right)\right] \tag{B.68}$$

$$\frac{\partial V_i^{rm}}{\partial \delta_i^A} = \frac{1}{9}\left[-2V_i^AV_i^B\sin\left(\delta_i^A - \delta_i^B - 120°\right) - 2V_i^AV_i^C\sin\left(\delta_i^A - \delta_i^C + 120°\right)\right] \tag{B.69}$$

$$\frac{\partial V_i^{rm}}{\partial \delta_i^B} = \frac{1}{9}\left[2V_i^AV_i^B\sin\left(\delta_i^A - \delta_i^B - 120°\right) - 2V_i^BV_i^C\sin\left(\delta_i^B - \delta_i^C + 240°\right)\right] \tag{B.70}$$

$$\frac{\partial V_i^{rm}}{\partial \delta_i^C} = \frac{1}{9}\left[2V_i^AV_i^C\sin\left(\delta_i^A - \delta_i^C + 120°\right) + 2V_i^BV_i^C\sin\left(\delta_i^B - \delta_i^C + 240°\right)\right] \tag{B.71}$$

The differential of $P_{i,pv}$ from continuous local control function can be written into equation (B.72).

$$\frac{\partial P_{i,pv}}{\partial V_i^A} = \frac{\partial P_{i,pv}}{\partial V_i^B} = \frac{\partial P_{i,pv}}{\partial V_i^C} = \frac{-4P_i^{max}\cdot exp\left[\frac{\frac{-4}{3}\left(V_i^A + V_i^B + V_i^C - 3\cdot V_{i,cri}\right)}{\delta_{i,p}}\right]}{3\delta_{i,p}\left[1 + exp\left(\frac{\frac{-4}{3}\left(V_i^A + V_i^B + V_i^C - 3\cdot V_{i,cri}\right)}{\delta_{i,p}}\right)\right]^2} \tag{B.72}$$

The differential of $Q_{i,pv}$ from continuous local control function can be written into equation (B.73).

$$\frac{\partial Q_{i,pv}}{\partial V_i^A} = \frac{\partial Q_{i,pv}}{\partial V_i^B} = \frac{\partial Q_{i,pv}}{\partial V^C} = \frac{-4\cdot K_{i,2}\cdot Q_i^{max}\cdot exp\left[\frac{\frac{-4}{3}\left(V_i^A + V_i^B + V_i^C - 3\cdot V_{i,q}\right)}{\delta_{i,q}}\right]}{3\delta_{i,q}\left[1 + exp\left(\frac{\frac{-4}{3}\left(V_i^A + V_i^B + V_i^C - 3\cdot V_{i,q}\right)}{\delta_{i,q}}\right)\right]^2} \tag{B.73}$$

The differential of $P_{i,pv}$ from piecewise linear local control function can be written into equation (B.74).

$$\frac{\partial P_{i,pv}}{\partial |V_i^{\sigma}|} = P_i^{max} \cdot \begin{cases} \dfrac{1}{3 \cdot (V_{i,p1} - V_{i,p2})} & ;\ V_{i,p1} \le |V_i| < V_{i,p2} \\ 0 & ;other \end{cases} \tag{B.74}$$

where $|V_i| = \frac{|V_i^A| + |V_i^B| + |V_i^C|}{3}$.

The differential of $Q_{i,pv}$ from piecewise linear local control function can be written into equation (B.75).

$$\frac{\partial Q_{i,pv}}{\partial |V_i^{\sigma}|} = Q_i^{max} \cdot \begin{cases} \dfrac{K_{i,1} - K_{i,2}}{3 \cdot (V_{i,q1} - V_{i,q2})} & ;\ V_{i,q1} \le |V_i| < V_{i,q2} \\ 0 & ;other \end{cases} \tag{B.75}$$

where $|V_i| = \frac{|V_i^A| + |V_i^B| + |V_i^C|}{3}$.

B.2 Differential Equation by Step-change Value

Normally, power output of three-phase PV system can be written into Table B.2.

Table B.2 Power output of three-phase PV system

$P_{i,pv}^A + jQ_{i,pv}^A$	$= \left[\lvert V_i^A\rvert + w_{V_i^A} \cdot \Delta\lvert V_i^A\rvert\right] I_i^{po,r} \cos\left(\delta_i^A + w_{\delta_i^A} \cdot \Delta\delta_i^A\right)$ $+ \left[\lvert V_i^A\rvert + w_{V_i^A} \cdot \Delta\lvert V_i^A\rvert\right] I_i^{po,m} \sin\left(\delta_i^A + w_{\delta_i^A} \cdot \Delta\delta_i^A\right)$ $+ j\left[\left[\lvert V_i^A\rvert + w_{V_i^A} \cdot \Delta\lvert V_i^A\rvert\right] I_i^{po,r} \sin\left(\delta_i^A + w_{\delta_i^A} \cdot \Delta\delta_i^A\right)\right.$ $\left. - \left[\lvert V_i^A\rvert + w_{V_i^A} \cdot \Delta\lvert V_i^A\rvert\right] I_i^{po,m} \cos\left(\delta_i^A + w_{\delta_i^A} \cdot \Delta\delta_i^A\right)\right]$
$P_{i,pv}^B + jQ_{i,pv}^B$	$= \left[\lvert V_i^B\rvert + w_{V_i^B} \cdot \Delta\lvert V_i^B\rvert\right] I_i^{po,r} \cos\left(\delta_i^B + w_{\delta_i^B} \cdot \Delta\delta_i^B + 120°\right)$ $+ \left[\lvert V_i^B\rvert + w_{V_i^B} \cdot \Delta\lvert V_i^B\rvert\right] I_i^{po,m} \sin\left(\delta_i^B + w_{\delta_i^B} \cdot \Delta\delta_i^B + 120°\right)$ $+ j\left[\left[\lvert V_i^B\rvert + w_{V_i^B} \cdot \Delta\lvert V_i^B\rvert\right] I_i^{po,r} \sin\left(\delta_i^B + w_{\delta_i^B} \cdot \Delta\delta_i^B + 120°\right)\right.$ $\left. - \left[\lvert V_i^B\rvert + w_{V_i^B} \cdot \Delta\lvert V_i^B\rvert\right] I_i^{po,m} \cos\left(\delta_i^B + w_{\delta_i^B} \cdot \Delta\delta_i^B + 120°\right)\right]$
$P_{i,pv}^C + jQ_{i,pv}^C$	$= \left[\lvert V_i^C\rvert + w_{V_i^C} \cdot \Delta\lvert V_i^C\rvert\right] I_i^{po,r} \cos\left(\delta_i^C + w_{\delta_i^C} \cdot \Delta\delta_i^C - 120°\right)$ $+ \left[\lvert V_i^C\rvert + w_{V_i^C} \cdot \Delta\lvert V_i^C\rvert\right] I_i^{po,m} \sin\left(\delta_i^C + w_{\delta_i^C} \cdot \Delta\delta_i^C - 120°\right)$ $+ j\left[\left[\lvert V_i^C\rvert + w_{V_i^C} \cdot \Delta\lvert V_i^C\rvert\right] I_i^{po,r} \sin\left(\delta_i^C + w_{\delta_i^C} \cdot \Delta\delta_i^C - 120°\right)\right.$ $\left. - \left[\lvert V_i^C\rvert + w_{V_i^C} \cdot \Delta\lvert V_i^C\rvert\right] I_i^{po,m} \cos\left(\delta_i^C + w_{\delta_i^C} \cdot \Delta\delta_i^C - 120°\right)\right]$

From equation (A.7), $I^{po,r}$ and $I^{po,m}$ can be written into equations (B.76) and (B.77).

$$I_i^{po,r} = \frac{1}{3}\left[\frac{V_i^{po,r}P_{i,pv} + V_i^{po,m}Q_{i,pv}}{V_i^{rm}}\right] \tag{B.76}$$

$$I_i^{po,m} = \frac{1}{3}\left[\frac{V_i^{po,m}P_{i,pv} - V_i^{po,r}Q_{i,pv}}{V_i^{rm}}\right] \tag{B.77}$$

$$\begin{aligned} V_i^{po,r} = \frac{1}{3}\Big[&\left[\left|V_i^A\right| + w_{V_i^A}\cdot\Delta\left|V_i^A\right|\right]\cos\left(\delta_i^A + w_{\delta_i^A}\cdot\Delta\delta_i^A\right) \\ &+ \left[\left|V_i^B\right| + w_{V_i^B}\cdot\Delta\left|V_i^B\right|\right]\cos\left(\delta_i^B + w_{\delta_i^B}\cdot\Delta\delta_i^B + 120°\right) \\ &+ \left[\left|V_i^C\right| + w_{V_i^C}\cdot\Delta\left|V_i^C\right|\right]\cos\left(\delta_i^C + w_{\delta_i^C}\cdot\Delta\delta_i^C - 120°\right)\Big] \end{aligned} \tag{B.78}$$

$$\begin{aligned} V_i^{po,m} = \frac{1}{3}\Big[&\left[\left|V_i^A\right| + w_{V_i^A}\cdot\Delta\left|V_i^A\right|\right]\sin\left(\delta_i^A + w_{\delta_i^A}\cdot\Delta\delta_i^A\right) \\ &+ \left[\left|V_i^B\right| + w_{V_i^B}\cdot\Delta\left|V_i^B\right|\right]\sin\left(\delta_i^B + w_{\delta_i^B}\cdot\Delta\delta_i^B + 120°\right) \\ &+ \left[\left|V_i^C\right| + w_{V_i^C}\cdot\Delta\left|V_i^C\right|\right]\sin\left(\delta_i^C + w_{\delta_i^C}\cdot\Delta\delta_i^C - 120°\right)\Big] \end{aligned} \tag{B.79}$$

$$\begin{aligned} V_i^{rm} = \frac{1}{9}\Big[&\left[\left|V_i^A\right| + w_{V_i^A}\cdot\Delta\left|V_i^A\right|\right]^2 + \left[\left|V_i^B\right| + w_{V_i^B}\cdot\Delta\left|V_i^B\right|\right]^2 + \left[\left|V_i^C\right| + w_{V_i^C}\cdot\Delta\left|V_i^C\right|\right]^2 \\ &+ 2\left[\left|V_i^A\right| + w_{V_i^A}\cdot\Delta\left|V_i^A\right|\right]\left[\left|V_i^B\right| + w_{V_i^B}\right. \\ &\left.\cdot\Delta\left|V_i^B\right|\right]\cos\left(\delta_i^A + w_{\delta_i^A}\cdot\Delta\delta_i^A - \delta_i^B - w_{\delta_i^B}\cdot\Delta\delta_i^B - 120°\right) \\ &+ 2\left[\left|V_i^A\right| + w_{V_i^A}\cdot\Delta\left|V_i^A\right|\right]\left[\left|V_i^C\right| + w_{V_i^C}\right. \\ &\left.\cdot\Delta\left|V_i^C\right|\right]\cos\left(\delta_i^A + w_{\delta_i^A}\cdot\Delta\delta_i^A - \delta_i^C - w_{\delta_i^C}\cdot\Delta\delta_i^C + 120°\right) \\ &+ 2\left[\left|V_i^B\right| + w_{V_i^B}\cdot\Delta\left|V_i^B\right|\right]\left[\left|V_i^C\right| + w_{V_i^C}\right. \\ &\left.\cdot\Delta\left|V_i^C\right|\right]\cos\left(\delta_i^B + w_{\delta_i^B}\cdot\Delta\delta_i^B - \delta_i^C - w_{\delta_i^C}\cdot\Delta\delta_i^C + 240°\right)\Big] \end{aligned} \tag{B.80}$$

The differential of phase-A real power can be written into equations (B.81)-(B.86).

$$\begin{aligned} \frac{\partial P_{i,pv}^A}{\partial w_{V_i^A}} = \left[\left|V_i^A\right| + w_{V_i^A}\cdot\Delta\left|V_i^A\right|\right]\Bigg[&cos\left(\delta_i^A + w_{\delta_i^A}\cdot\Delta\delta_i^A\right)\frac{\partial I_i^{po,r}}{\partial w_{V_i^A}} \\ &+ sin\left(\delta_i^A + w_{\delta_i^A}\cdot\Delta\delta_i^A\right)\frac{\partial I_i^{po,m}}{\partial w_{V_i^A}}\Bigg] \\ &+ \Delta\left|V_i^A\right|\left[I_i^{po,r}\cos\left(\delta_i^A + w_{\delta_i^A}\cdot\Delta\delta_i^A\right) + I_i^{po,m}\sin\left(\delta_i^A + w_{\delta_i^A}\cdot\Delta\delta_i^A\right)\right] \end{aligned} \tag{B.81}$$

$$\begin{aligned} \frac{\partial P_{i,pv}^A}{\partial w_{V_i^B}} = \left[\left|V_i^A\right| + w_{V_i^A}\cdot\Delta\left|V_i^A\right|\right]\Bigg[&cos\left(\delta_i^A + w_{\delta_i^A}\cdot\Delta\delta_i^A\right)\frac{\partial I_i^{po,r}}{\partial w_{V_i^B}} \\ &+ sin\left(\delta_i^A + w_{\delta_i^A}\cdot\Delta\delta_i^A\right)\frac{\partial I_i^{po,m}}{\partial w_{V_i^B}}\Bigg] \end{aligned} \tag{B.82}$$

$$\frac{\partial P_{i,pv}^{A}}{\partial w_{V_i^C}} = \left[\left|V_i^A\right| + w_{V_i^A}\cdot\Delta\left|V_i^A\right|\right]\left[cos\left(\delta_i^A + w_{\delta_i^A}\cdot\Delta\delta_i^A\right)\frac{\partial I_i^{po,r}}{\partial w_{V_i^C}} + sin\left(\delta_i^A + w_{\delta_i^A}\cdot\Delta\delta_i^A\right)\frac{\partial I_i^{po,m}}{\partial w_{V_i^C}}\right] \tag{B.83}$$

$$\frac{\partial P_{i,pv}^{A}}{\partial w_{\delta_i^A}} = \left[\left|V_i^A\right| + w_{V_i^A}\cdot\Delta\left|V_i^A\right|\right]\left[-\Delta\delta_i^A sin\left(\delta_i^A + w_{\delta_i^A}\cdot\Delta\delta_i^A\right)I_i^{po,r} + cos\left(\delta_i^A + w_{\delta_i^A}\cdot\Delta\delta_i^A\right)\frac{\partial I_i^{po,r}}{\partial w_{\delta_i^A}} + \Delta\delta_i^A cos\left(\delta_i^A + w_{\delta_i^A}\cdot\Delta\delta_i^A\right)I_i^{po,m} + sin\left(\delta_i^A + w_{\delta_i^A}\cdot\Delta\delta_i^A\right)\frac{\partial I_i^{po,m}}{\partial w_{\delta_i^A}}\right] \tag{B.84}$$

$$\frac{\partial P_{i,pv}^{A}}{\partial w_{\delta_i^B}} = \left[\left|V_i^A\right| + w_{V_i^A}\cdot\Delta\left|V_i^A\right|\right]\left[cos\left(\delta_i^A + w_{\delta_i^A}\cdot\Delta\delta_i^A\right)\frac{\partial I_i^{po,r}}{\partial w_{\delta_i^B}} + sin\left(\delta_i^A + w_{\delta_i^A}\cdot\Delta\delta_i^A\right)\frac{\partial I_i^{po,m}}{\partial w_{\delta_i^B}}\right] \tag{B.85}$$

$$\frac{\partial P_{i,pv}^{A}}{\partial w_{\delta_i^C}} = \left[\left|V_i^A\right| + w_{V_i^A}\cdot\Delta\left|V_i^A\right|\right]\left[cos\left(\delta_i^A + w_{\delta_i^A}\cdot\Delta\delta_i^A\right)\frac{\partial I_i^{po,r}}{\partial w_{\delta_i^C}} + sin\left(\delta_i^A + w_{\delta_i^A}\cdot\Delta\delta_i^A\right)\frac{\partial I_i^{po,m}}{\partial w_{\delta_i^C}}\right] \tag{B.86}$$

The differential of phase-B real power can be written into equations (B.87)-(B.92).

$$\frac{\partial P_{i,pv}^{B}}{\partial w_{V_i^A}} = \left[\left|V_i^B\right| + w_{V_i^B}\cdot\Delta\left|V_i^B\right|\right]\left[cos\left(\delta_i^B + w_{\delta_i^B}\cdot\Delta\delta_i^B + 120°\right)\frac{\partial I_i^{po,r}}{\partial w_{V_i^A}} + sin\left(\delta_i^B + w_{\delta_i^B}\cdot\Delta\delta_i^B + 120°\right)\frac{\partial I_i^{po,m}}{\partial w_{V_i^A}}\right] \tag{B.87}$$

$$\frac{\partial P_{i,pv}^{B}}{\partial w_{V_i^B}} = \left[\left|V_i^B\right| + w_{V_i^B}\cdot\Delta\left|V_i^B\right|\right]\left[cos\left(\delta_i^B + w_{\delta_i^B}\cdot\Delta\delta_i^B + 120°\right)\frac{\partial I_i^{po,r}}{\partial w_{V_i^B}} + sin\left(\delta_i^B + w_{\delta_i^B}\cdot\Delta\delta_i^B + 120°\right)\frac{\partial I_i^{po,m}}{\partial w_{V_i^B}}\right] + \Delta\left|V_i^B\right|\left[I_i^{po,r}\cos\left(\delta_i^B + w_{\delta_i^B}\cdot\Delta\delta_i^B + 120°\right) + I_i^{po,m}\sin\left(\delta_i^B + w_{\delta_i^B}\cdot\Delta\delta_i^B + 120°\right)\right] \tag{B.88}$$

$$\frac{\partial P_{i,pv}^{B}}{\partial w_{V_i^C}} = \left[\left|V_i^B\right| + w_{V_i^B}\cdot\Delta\left|V_i^B\right|\right]\left[cos\left(\delta_i^B + w_{\delta_i^B}\cdot\Delta\delta_i^B + 120°\right)\frac{\partial I_i^{po,r}}{\partial w_{V_i^C}} + sin\left(\delta_i^B + w_{\delta_i^B}\cdot\Delta\delta_i^B + 120°\right)\frac{\partial I_i^{po,m}}{\partial w_{V_i^C}}\right] \tag{B.89}$$

$$\frac{\partial P_{i,pv}^{B}}{\partial w_{\delta_i^A}} = \left[|V_i^B| + w_{V_i^B} \cdot \Delta|V_i^B|\right]\left[cos\left(\delta_i^B + w_{\delta_i^B} \cdot \Delta\delta_i^B + 120°\right)\frac{\partial I_i^{po,r}}{\partial w_{\delta_i^A}} + sin\left(\delta_i^B + w_{\delta_i^B} \cdot \Delta\delta_i^B + 120°\right)\frac{\partial I_i^{po,m}}{\partial w_{\delta_i^A}}\right] \tag{B.90}$$

$$\frac{\partial P_{i,pv}^{B}}{\partial w_{\delta_i^B}} = \left[|V_i^B| + w_{V_i^B} \cdot \Delta|V_i^B|\right]\left[-\Delta\delta_i^B sin\left(\delta_i^B + w_{\delta_i^B} \cdot \Delta\delta_i^B + 120°\right) I_i^{po,r} + cos\left(\delta_i^B + w_{\delta_i^B} \cdot \Delta\delta_i^B + 120°\right)\frac{\partial I_i^{po,r}}{\partial w_{\delta_i^B}} + \Delta\delta_i^B cos\left(\delta_i^B + w_{\delta_i^B} \cdot \Delta\delta_i^B + 120°\right) I_i^{po,m} + sin\left(\delta_i^B + w_{\delta_i^B} \cdot \Delta\delta_i^B + 120°\right)\frac{\partial I_i^{po,m}}{\partial w_{\delta_i^B}}\right] \tag{B91}$$

$$\frac{\partial P_{i,pv}^{B}}{\partial w_{\delta_i^C}} = \left[|V_i^B| + w_{V_i^B} \cdot \Delta|V_i^B|\right]\left[cos\left(\delta_i^B + w_{\delta_i^B} \cdot \Delta\delta_i^B + 120°\right)\frac{\partial I_i^{po,r}}{\partial w_{\delta_i^C}} + sin\left(\delta_i^B + w_{\delta_i^B} \cdot \Delta\delta_i^B + 120°\right)\frac{\partial I_i^{po,m}}{\partial w_{\delta_i^C}}\right] \tag{B.92}$$

The differential of phase-C real power can be written into equations (B.93)-(B.98).

$$\frac{\partial P_{i,pv}^{C}}{\partial w_{V_i^A}} = \left[\left|V_i^C\right| + w_{V_i^C} \cdot \Delta\left|V_i^C\right|\right]\left[cos\left(\delta_i^C + w_{\delta_i^C} \cdot \Delta\delta_i^C - 120°\right)\frac{\partial I_i^{po,r}}{\partial w_{V_i^A}} + sin\left(\delta_i^C + w_{\delta_i^C} \cdot \Delta\delta_i^C - 120°\right)\frac{\partial I_i^{po,m}}{\partial w_{V_i^A}}\right] \tag{B.93}$$

$$\frac{\partial P_{i,pv}^{C}}{\partial w_{V_i^B}} = \left[\left|V_i^C\right| + w_{V_i^C} \cdot \Delta\left|V_i^C\right|\right]\left[cos\left(\delta_i^C + w_{\delta_i^C} \cdot \Delta\delta_i^C - 120°\right)\frac{\partial I_i^{po,r}}{\partial w_{V_i^B}} + sin\left(\delta_i^C + w_{\delta_i^C} \cdot \Delta\delta_i^C - 120°\right)\frac{\partial I_i^{po,m}}{\partial w_{V_i^B}}\right] \tag{B.94}$$

$$\frac{\partial P_{i,pv}^{C}}{\partial w_{V_i^C}} = \left[\left|V_i^C\right| + w_{V_i^C} \cdot \Delta\left|V_i^C\right|\right]\left[cos\left(\delta_i^C + w_{\delta_i^C} \cdot \Delta\delta_i^C - 120°\right)\frac{\partial I_i^{po,r}}{\partial w_{V_i^C}} + sin\left(\delta_i^C + w_{\delta_i^C} \cdot \Delta\delta_i^C - 120°\right)\frac{\partial I_i^{po,m}}{\partial w_{V_i^C}}\right] + \Delta\left|V_i^C\right|\left[I_i^{po,r}\cos\left(\delta_i^C + w_{\delta_i^C} \cdot \Delta\delta_i^C - 120°\right) + I_i^{po,m}\sin\left(\delta_i^C + w_{\delta_i^C} \cdot \Delta\delta_i^C - 120°\right)\right] \tag{B.95}$$

$$\frac{\partial P_{i,pv}^{C}}{\partial w_{\delta_i^A}} = \left[\left|V_i^C\right| + w_{V_i^C} \cdot \Delta\left|V_i^C\right|\right]\left[cos\left(\delta_i^C + w_{\delta_i^C} \cdot \Delta\delta_i^C - 120°\right)\frac{\partial I_i^{po,r}}{\partial w_{\delta_i^A}} + sin\left(\delta_i^C + w_{\delta_i^C} \cdot \Delta\delta_i^C - 120°\right)\frac{\partial I_i^{po,m}}{\partial w_{\delta_i^A}}\right] \tag{B.96}$$

$$\frac{\partial P_{i,pv}^{C}}{\partial w_{\delta_i^B}} = \left[\left|V_i^C\right| + w_{V_i^C}\cdot\Delta\left|V_i^C\right|\right]\left[cos\left(\delta_i^C + w_{\delta_i^C}\cdot\Delta\delta_i^C - 120°\right)\frac{\partial I_i^{po,r}}{\partial w_{\delta_i^B}} + sin\left(\delta_i^C + w_{\delta_i^C}\cdot\Delta\delta_i^C - 120°\right)\frac{\partial I_i^{po,m}}{\partial w_{\delta_i^B}}\right] \tag{B.97}$$

$$\begin{aligned}\frac{\partial P_{i,pv}^{C}}{\partial w_{\delta_i^C}} = \left[\left|V_i^C\right| + w_{V_i^C}\cdot\Delta\left|V_i^C\right|\right]\Big[&-\Delta\delta_i^C sin\left(\delta_i^C + w_{\delta_i^C}\cdot\Delta\delta_i^C - 120°\right)I_i^{po,r} \\ &+ cos\left(\delta_i^C + w_{\delta_i^C}\cdot\Delta\delta_i^C - 120°\right)\frac{\partial I_i^{po,r}}{\partial w_{\delta_i^C}} \\ &+ \Delta\delta_i^C cos\left(\delta_i^C + w_{\delta_i^C}\cdot\Delta\delta_i^C - 120°\right)I_i^{po,m} \\ &+ sin\left(\delta_i^C + w_{\delta_i^C}\cdot\Delta\delta_i^C - 120°\right)\frac{\partial I_i^{po,m}}{\partial w_{\delta_i^C}}\Big]\end{aligned} \tag{B.98}$$

The differential of phase-A reactive power can be written into equations (B.99)-(B.104).

$$\begin{aligned}\frac{\partial Q_{i,pv}^{A}}{\partial w_{V_i^A}} = \left[\left|V_i^A\right| + w_{V_i^A}\cdot\Delta\left|V_i^A\right|\right]\Big[&sin\left(\delta_i^A + w_{\delta_i^A}\cdot\Delta\delta_i^A\right)\frac{\partial I_i^{po,r}}{\partial w_{V_i^A}} \\ &- cos\left(\delta_i^A + w_{\delta_i^A}\cdot\Delta\delta_i^A\right)\frac{\partial I_i^{po,m}}{\partial w_{V_i^A}}\Big] \\ &+ \Delta\left|V_i^A\right|\left[I_i^{po,r}\sin\left(\delta_i^A + w_{\delta_i^A}\cdot\Delta\delta_i^A\right) - I_i^{po,m}\cos\left(\delta_i^A + w_{\delta_i^A}\cdot\Delta\delta_i^A\right)\right]\end{aligned} \tag{B.99}$$

$$\frac{\partial Q_{i,pv}^{A}}{\partial w_{V_i^B}} = \left[\left|V_i^A\right| + w_{V_i^A}\cdot\Delta\left|V_i^A\right|\right]\left[sin\left(\delta_i^A + w_{\delta_i^A}\cdot\Delta\delta_i^A\right)\frac{\partial I_i^{po,r}}{\partial w_{V_i^B}} - cos\left(\delta_i^A + w_{\delta_i^A}\cdot\Delta\delta_i^A\right)\frac{\partial I_i^{po,m}}{\partial w_{V_i^B}}\right] \tag{B.100}$$

$$\frac{\partial Q_{i,pv}^{A}}{\partial w_{V_i^C}} = \left[\left|V_i^A\right| + w_{V_i^A}\cdot\Delta\left|V_i^A\right|\right]\left[sin\left(\delta_i^A + w_{\delta_i^A}\cdot\Delta\delta_i^A\right)\frac{\partial I_i^{po,r}}{\partial w_{V_i^C}} - cos\left(\delta_i^A + w_{\delta_i^A}\cdot\Delta\delta_i^A\right)\frac{\partial I_i^{po,m}}{\partial w_{V_i^C}}\right] \tag{B.101}$$

$$\begin{aligned}\frac{\partial Q_{i,pv}^{A}}{\partial w_{\delta_i^A}} = \left[\left|V_i^A\right| + w_{V_i^A}\cdot\Delta\left|V_i^A\right|\right]\Big[&\Delta\delta_i^A cos\left(\delta_i^A + w_{\delta_i^A}\cdot\Delta\delta_i^A\right)I_i^{po,r} \\ &+ sin\left(\delta_i^A + w_{\delta_i^A}\cdot\Delta\delta_i^A\right)\frac{\partial I_i^{po,r}}{\partial w_{\delta_i^A}} + \Delta\delta_i^A sin\left(\delta_i^A + w_{\delta_i^A}\cdot\Delta\delta_i^A\right)I_i^{po,m} \\ &- cos\left(\delta_i^A + w_{\delta_i^A}\cdot\Delta\delta_i^A\right)\frac{\partial I_i^{po,m}}{\partial w_{\delta_i^A}}\Big]\end{aligned} \tag{B.102}$$

$$\frac{\partial Q_{i,pv}^{A}}{\partial w_{\delta_i^B}} = \left[\left|V_i^A\right| + w_{V_i^A}\cdot\Delta\left|V_i^A\right|\right]\left[sin\left(\delta_i^A + w_{\delta_i^A}\cdot\Delta\delta_i^A\right)\frac{\partial I_i^{po,r}}{\partial w_{\delta_i^B}} - cos\left(\delta_i^A + w_{\delta_i^A}\cdot\Delta\delta_i^A\right)\frac{\partial I_i^{po,m}}{\partial w_{\delta_i^B}}\right] \tag{B.103}$$

$$\frac{\partial Q_{i,pv}^{A}}{\partial w_{\delta_i^C}} = \left[\left|V_i^A\right| + w_{V_i^A}\cdot\Delta\left|V_i^A\right|\right]\left[sin\left(\delta_i^A + w_{\delta_i^A}\cdot\Delta\delta_i^A\right)\frac{\partial I_i^{po,r}}{\partial w_{\delta_i^C}} - cos\left(\delta_i^A + w_{\delta_i^A}\cdot\Delta\delta_i^A\right)\frac{\partial I_i^{po,m}}{\partial w_{\delta_i^C}}\right] \tag{B.104}$$

The differential of phase-B reactive power can be written into equations (B.105)-(B.110).

$$\frac{\partial Q_{i,pv}^{B}}{\partial w_{V_i^A}} = \left[\left|V_i^B\right| + w_{V_i^B}\cdot\Delta\left|V_i^B\right|\right]\left[sin\left(\delta_i^B + w_{\delta_i^B}\cdot\Delta\delta_i^B + 120°\right)\frac{\partial I_i^{po,r}}{\partial w_{V_i^A}} - cos\left(\delta_i^B + w_{\delta_i^B}\cdot\Delta\delta_i^B + 120°\right)\frac{\partial I_i^{po,m}}{\partial w_{V_i^A}}\right] \tag{B.105}$$

$$\begin{aligned}\frac{\partial Q_{i,pv}^{B}}{\partial w_{V_i^B}} = {} & \left[\left|V_i^B\right| + w_{V_i^B}\cdot\Delta\left|V_i^B\right|\right]\left[sin\left(\delta_i^B + w_{\delta_i^B}\cdot\Delta\delta_i^B + 120°\right)\frac{\partial I_i^{po,r}}{\partial w_{V_i^B}} - cos\left(\delta_i^B + w_{\delta_i^B}\cdot\Delta\delta_i^B + 120°\right)\frac{\partial I_i^{po,m}}{\partial w_{V_i^B}}\right] \\ & + \Delta\left|V_i^B\right|\left[I_i^{po,r}\sin\left(\delta_i^B + w_{\delta_i^B}\cdot\Delta\delta_i^B + 120°\right) - I_i^{po,m}\cos\left(\delta_i^B + w_{\delta_i^B}\cdot\Delta\delta_i^B + 120°\right)\right]\end{aligned} \tag{B.106}$$

$$\frac{\partial Q_{i,pv}^{B}}{\partial w_{V_i^C}} = \left[\left|V_i^B\right| + w_{V_i^B}\cdot\Delta\left|V_i^B\right|\right]\left[sin\left(\delta_i^B + w_{\delta_i^B}\cdot\Delta\delta_i^B + 120°\right)\frac{\partial I_i^{po,r}}{\partial w_{V_i^C}} - cos\left(\delta_i^B + w_{\delta_i^B}\cdot\Delta\delta_i^B + 120°\right)\frac{\partial I_i^{po,m}}{\partial w_{V_i^C}}\right] \tag{B.107}$$

$$\frac{\partial Q_{i,pv}^{B}}{\partial w_{\delta_i^A}} = \left[\left|V_i^B\right| + w_{V_i^B}\cdot\Delta\left|V_i^B\right|\right]\left[sin\left(\delta_i^B + w_{\delta_i^B}\cdot\Delta\delta_i^B + 120°\right)\frac{\partial I_i^{po,r}}{\partial w_{\delta_i^A}} - cos\left(\delta_i^B + w_{\delta_i^B}\cdot\Delta\delta_i^B + 120°\right)\frac{\partial I_i^{po,m}}{\partial w_{\delta_i^A}}\right] \tag{B.108}$$

$$\begin{aligned}\frac{\partial Q_{i,pv}^{B}}{\partial w_{\delta_i^B}} = {} & \left[\left|V_i^B\right| + w_{V_i^B}\cdot\Delta\left|V_i^B\right|\right]\left[\Delta\delta_i^B cos\left(\delta_i^B + w_{\delta_i^B}\cdot\Delta\delta_i^B + 120°\right)I_i^{po,r}\right. \\ & + sin\left(\delta_i^B + w_{\delta_i^B}\cdot\Delta\delta_i^B + 120°\right)\frac{\partial I_i^{po,r}}{\partial w_{\delta_i^B}} \\ & + \Delta\delta_i^B sin\left(\delta_i^B + w_{\delta_i^B}\cdot\Delta\delta_i^B + 120°\right)I_i^{po,m} \\ & \left. - cos\left(\delta_i^B + w_{\delta_i^B}\cdot\Delta\delta_i^B + 120°\right)\frac{\partial I_i^{po,m}}{\partial w_{\delta_i^B}}\right]\end{aligned} \tag{B.109}$$

$$\frac{\partial Q_{i,pv}^{B}}{\partial w_{\delta_i^C}} = \left[|V_i^B| + w_{V_i^B} \cdot \Delta|V_i^B|\right]\left[sin\left(\delta_i^B + w_{\delta_i^B} \cdot \Delta\delta_i^B + 120°\right)\frac{\partial I_i^{po,r}}{\partial w_{\delta_i^C}} - cos\left(\delta_i^B + w_{\delta_i^B} \cdot \Delta\delta_i^B + 120°\right)\frac{\partial I_i^{po,m}}{\partial w_{\delta_i^C}}\right] \tag{B.110}$$

The differential of phase-C reactive power can be written into equations (B.111)-(B.116).

$$\frac{\partial Q_{i,pv}^{C}}{\partial w_{V_i^A}} = \left[|V_i^C| + w_{V_i^C} \cdot \Delta|V_i^C|\right]\left[sin\left(\delta_i^C + w_{\delta_i^C} \cdot \Delta\delta_i^C - 120°\right)\frac{\partial I_i^{po,r}}{\partial w_{V_i^A}} - cos\left(\delta_i^C + w_{\delta_i^C} \cdot \Delta\delta_i^C - 120°\right)\frac{\partial I_i^{po,m}}{\partial w_{V_i^A}}\right] \tag{B.111}$$

$$\frac{\partial Q_{i,pv}^{C}}{\partial w_{V_i^B}} = \left[|V_i^C| + w_{V_i^C} \cdot \Delta|V_i^C|\right]\left[sin\left(\delta_i^C + w_{\delta_i^C} \cdot \Delta\delta_i^C - 120°\right)\frac{\partial I_i^{po,r}}{\partial w_{V_i^B}} - cos\left(\delta_i^C + w_{\delta_i^C} \cdot \Delta\delta_i^C - 120°\right)\frac{\partial I_i^{po,m}}{\partial w_{V_i^B}}\right] \tag{B.112}$$

$$\frac{\partial Q_{i,pv}^{C}}{\partial w_{V_i^C}} = \left[|V_i^C| + w_{V_i^C} \cdot \Delta|V_i^C|\right]\left[sin\left(\delta_i^C + w_{\delta_i^C} \cdot \Delta\delta_i^C - 120°\right)\frac{\partial I_i^{po,r}}{\partial w_{V_i^C}} - cso\left(\delta_i^C + w_{\delta_i^C} \cdot \Delta\delta_i^C - 120°\right)\frac{\partial I_i^{po,m}}{\partial w_{V_i^C}}\right] + \Delta|V_i^C|\left[I_i^{po,r}\sin\left(\delta_i^C + w_{\delta_i^C} \cdot \Delta\delta_i^C - 120°\right) - I_i^{po,m}\cos\left(\delta_i^C + w_{\delta_i^C} \cdot \Delta\delta_i^C - 120°\right)\right] \tag{B.113}$$

$$\frac{\partial Q_{i,pv}^{C}}{\partial w_{\delta_i^A}} = \left[|V_i^C| + w_{V_i^C} \cdot \Delta|V_i^C|\right]\left[sin\left(\delta_i^C + w_{\delta_i^C} \cdot \Delta\delta_i^C - 120°\right)\frac{\partial I_i^{po,r}}{\partial w_{\delta_i^A}} - cos\left(\delta_i^C + w_{\delta_i^C} \cdot \Delta\delta_i^C - 120°\right)\frac{\partial I_i^{po,m}}{\partial w_{\delta_i^A}}\right] \tag{B.114}$$

$$\frac{\partial Q_{i,pv}^{C}}{\partial w_{\delta_i^B}} = \left[|V_i^C| + w_{V_i^C} \cdot \Delta|V_i^C|\right]\left[sin\left(\delta_i^C + w_{\delta_i^C} \cdot \Delta\delta_i^C - 120°\right)\frac{\partial I_i^{po,r}}{\partial w_{\delta_i^B}} - cos\left(\delta_i^C + w_{\delta_i^C} \cdot \Delta\delta_i^C - 120°\right)\frac{\partial I_i^{po,m}}{\partial w_{\delta_i^B}}\right] \tag{B.115}$$

$$\frac{\partial Q_{i,pv}^{C}}{\partial w_{\delta_i^C}} = \left[|V_i^C| + w_{V_i^C} \cdot \Delta|V_i^C|\right]\left[\Delta\delta_i^C cos\left(\delta_i^C + w_{\delta_i^C} \cdot \Delta\delta_i^C - 120°\right) I_i^{po,r} + sin\left(\delta_i^C + w_{\delta_i^C} \cdot \Delta\delta_i^C - 120°\right)\frac{\partial I_i^{po,r}}{\partial w_{\delta_i^C}} + \Delta\delta_i^C sin\left(\delta_i^C + w_{\delta_i^C} \cdot \Delta\delta_i^C - 120°\right) I_i^{po,m} - cos\left(\delta_i^C + w_{\delta_i^C} \cdot \Delta\delta_i^C - 120°\right)\frac{\partial I_i^{po,m}}{\partial w_{\delta_i^C}}\right] \tag{B.116}$$

The differential of $I_i^{po,r}$ can be written into equations (B.117)-(B.122).

$$\frac{\partial I_i^{po,r}}{\partial w_{V_i^A}} = \frac{V_i^{rm}\left[V_i^{po,r}\frac{\partial P_{i,pv}}{\partial w_{V_i^A}} + P_{i,pv}\frac{\partial V_i^{po,r}}{\partial w_{V_i^A}} + V_i^{po,m}\frac{\partial Q_{i,pv}}{\partial w_{V_i^A}} + Q_{i,pv}\frac{\partial V_i^{po,m}}{\partial w_{V_i^A}}\right]}{3V_i^{rm^2}} - \frac{\left[V_i^{po,r}P_{i,pv} + V_i^{po,m}Q_{i,pv}\right]\frac{\partial V_i^{rm}}{\partial w_{V_i^A}}}{3V_i^{rm^2}} \quad \text{(B.117)}$$

$$\frac{\partial I_i^{po,r}}{\partial w_{V_i^B}} = \frac{V_i^{rm}\left[V_i^{po,r}\frac{\partial P_{i,pv}}{\partial w_{V_i^B}} + P_{i,pv}\frac{\partial V_i^{po,r}}{\partial w_{V_i^B}} + V_i^{po,m}\frac{\partial Q_{i,pv}}{\partial w_{V_i^B}} + Q_{i,pv}\frac{\partial V_i^{po,m}}{\partial w_{V_i^B}}\right]}{3V_i^{rm^2}} - \frac{\left[V_i^{po,r}P_{i,pv} + V_i^{po,m}Q_{i,pv}\right]\frac{\partial V_i^{rm}}{\partial w_{V_i^B}}}{3V_i^{rm^2}} \quad \text{(B.118)}$$

$$\frac{\partial I_i^{po,r}}{\partial w_{V_i^C}} = \frac{V_i^{rm}\left[V_i^{po,r}\frac{\partial P_{i,pv}}{\partial w_{V_i^C}} + P_{i,pv}\frac{\partial V_i^{po,r}}{\partial w_{V_i^C}} + V_i^{po,m}\frac{\partial Q_{i,pv}}{\partial w_{V_i^C}} + Q_{i,pv}\frac{\partial V_i^{po,m}}{\partial w_{V_i^C}}\right]}{3V_i^{rm^2}} - \frac{\left[V_i^{po,r}P_{i,pv} + V_i^{po,m}Q_{i,pv}\right]\frac{\partial V_i^{rm}}{\partial w_{V_i^C}}}{3V_i^{rm^2}} \quad \text{(B.119)}$$

$$\frac{\partial I_i^{po,r}}{\partial w_{\delta_i^A}} = \frac{V_i^{rm}\left[P_{i,pv}\frac{\partial V_i^{po,r}}{\partial w_{\delta_i^A}} + Q_{i,pv}\frac{\partial V_i^{po,m}}{\partial w_{\delta_i^A}}\right] - \left[V_i^{po,r}P_{i,pv} + V_i^{po,m}Q_{i,pv}\right]\frac{\partial V_i^{rm}}{\partial w_{\delta_i^A}}}{3V_i^{rm^2}} \quad \text{(B.120)}$$

$$\frac{\partial I_i^{po,r}}{\partial w_{\delta_i^B}} = \frac{V_i^{rm}\left[P_{i,pv}\frac{\partial V_i^{po,r}}{\partial w_{\delta_i^B}} + Q_{i,pv}\frac{\partial V_i^{po,m}}{\partial w_{\delta_i^B}}\right] - \left[V_i^{po,r}P_{i,pv} + V_i^{po,m}Q_{i,pv}\right]\frac{\partial V_i^{rm}}{\partial w_{\delta_i^B}}}{3V_i^{rm^2}} \quad \text{(B.121)}$$

$$\frac{\partial I_i^{po,r}}{\partial w_{\delta_i^C}} = \frac{V_i^{rm}\left[P_{i,pv}\frac{\partial V_i^{po,r}}{\partial w_{\delta_i^C}} + Q_{i,pv}\frac{\partial V_i^{po,m}}{\partial w_{\delta_i^C}}\right] - \left[V_i^{po,r}P_{i,pv} + V_i^{po,m}Q_{i,pv}\right]\frac{\partial V_i^{rm}}{\partial w_{\delta_i^C}}}{3V_i^{rm2}} \quad \text{(B.122)}$$

The differential of $I_i^{po,m}$ can be written into equations (B.123)-(B.128).

$$\frac{\partial I_i^{po,m}}{\partial w_{V_i^A}} = \frac{V_i^{rm}\left[V_i^{po,m}\frac{\partial P_{i,pv}}{\partial w_{V_i^A}} + P_{i,pv}\frac{\partial V_i^{po,m}}{\partial w_{V_i^A}} - V_i^{po,r}\frac{\partial Q_{i,pv}}{\partial w_{V_i^A}} - Q_{i,pv}\frac{\partial V_i^{po,r}}{\partial w_{V_i^A}}\right]}{3V_i^{rm2}} - \frac{\left[V_i^{po,m}P_{i,pv} - V_i^{po,r}Q_{i,pv}\right]\frac{\partial V_i^{rm}}{\partial w_{V_i^A}}}{3V_i^{rm2}} \quad \text{(B.123)}$$

$$\frac{\partial I_i^{po,m}}{\partial w_{V_i^B}} = \frac{V_i^{rm}\left[V_i^{po,m}\frac{\partial P_{i,pv}}{\partial w_{V_i^B}} + P_{i,pv}\frac{\partial V_i^{po,m}}{\partial w_{V_i^B}} - V_i^{po,r}\frac{\partial Q_{i,pv}}{\partial w_{V_i^B}} - Q_{i,pv}\frac{\partial V_i^{po,r}}{\partial w_{V_i^B}}\right]}{3V_i^{rm2}} - \frac{\left[V_i^{po,m}P_{i,pv} - V_i^{po,r}Q_{i,pv}\right]\frac{\partial V_i^{rm}}{\partial w_{V_i^B}}}{3V_i^{rm2}} \quad \text{(B.124)}$$

$$\frac{\partial I_i^{po,m}}{\partial w_{V_i^C}} = \frac{V_i^{rm}\left[V_i^{po,m}\frac{\partial P_{i,pv}}{\partial w_{V_i^C}} + P_{i,pv}\frac{\partial V_i^{po,m}}{\partial w_{V_i^C}} - V_i^{po,r}\frac{\partial Q_{i,pv}}{\partial w_{V_i^C}} - Q_{i,pv}\frac{\partial V_i^{po,r}}{\partial w_{V_i^C}}\right]}{3V_i^{rm2}} - \frac{\left[V_i^{po,m}P_{i,pv} - V_i^{po,r}Q_{i,pv}\right]\frac{\partial V_i^{rm}}{\partial w_{V_i^C}}}{3V_i^{rm2}} \quad \text{(B.125)}$$

$$\frac{\partial I_i^{po,m}}{\partial w_{\delta_i^A}} = \frac{V_i^{rm}\left[P_{i,pv}\frac{\partial V_i^{po,m}}{\partial w_{\delta_i^A}} - Q_{i,pv}\frac{\partial V_i^{po,r}}{\partial w_{\delta_i^A}}\right] - \left[V_i^{po,m}P_{i,pv} - V_i^{po,r}Q_{i,pv}\right]\frac{\partial V_i^{rm}}{\partial w_{\delta_i^A}}}{3V_i^{rm2}} \quad \text{(B.126)}$$

$$\frac{\partial I_i^{po,m}}{\partial w_{\delta_i^B}} = \frac{V_i^{rm}\left[P_{i,pv}\frac{\partial V_i^{po,m}}{\partial w_{\delta_i^B}} - Q_{i,pv}\frac{\partial V_i^{po,r}}{\partial w_{\delta_i^B}}\right] - \left[V_i^{po,m}P_{i,pv} - V_i^{po,r}Q_{i,pv}\right]\frac{\partial V_i^{rm}}{\partial w_{\delta_i^B}}}{3V_i^{rm2}} \quad \text{(B.127)}$$

$$\frac{\partial I_i^{po,m}}{\partial w_{\delta_i^C}} = \frac{V_i^{rm}\left[P_{i,pv}\frac{\partial V_i^{po,m}}{\partial w_{\delta_i^C}} - Q_{i,pv}\frac{\partial V_i^{po,r}}{\partial w_{\delta_i^C}}\right] - \left[V_i^{po,m}P_{i,pv} - V_i^{po,r}Q_{i,pv}\right]\frac{\partial V_i^{rm}}{\partial w_{\delta_i^C}}}{3V_i^{rm2}} \quad \text{(B.128)}$$

The differential of $V_i^{po,r}$ can be written into equations (B.129)-(B.134).

$$\frac{\partial V^{po,r}}{\partial w_{V_i^A}} = \frac{\Delta\left|V_i^A\right|\cos\left(\delta_i^A + w_{\delta_i^A}\cdot\Delta\delta_i^A\right)}{3} \quad \text{(B.129)}$$

$$\frac{\partial V_i^{po,r}}{\partial w_{V_i^B}} = \frac{\Delta\left|V_i^B\right|\cos\left(\delta_i^B + w_{\delta_i^B}\cdot\Delta\delta_i^B + 120°\right)}{3} \quad \text{(B.130)}$$

$$\frac{\partial V_i^{po,r}}{\partial w_{V_i^C}} = \frac{\Delta\left|V_i^C\right|\cos\left(\delta_i^C + w_{\delta_i^C}\cdot\Delta\delta_i^C - 120°\right)}{3} \quad \text{(B.131)}$$

$$\frac{\partial V_i^{po,r}}{\partial w_{\delta_i^A}} = \frac{-\Delta\delta_i^A\left[\left|V_i^A\right| + w_{V_i^A}\cdot\Delta\left|V_i^A\right|\right]\sin\left(\delta_i^A + w_{\delta_i^A}\cdot\Delta\delta_i^A\right)}{3} \quad \text{(B.132)}$$

$$\frac{\partial V_i^{po,r}}{\partial w_{\delta_i^B}} = \frac{-\Delta\delta_i^B\left[\left|V_i^B\right| + w_{V_i^B}\cdot\Delta\left|V_i^B\right|\right]\sin\left(\delta_i^B + w_{\delta_i^B}\cdot\Delta\delta_i^B + 120°\right)}{3} \quad \text{(B.133)}$$

$$\frac{\partial V_i^{po,r}}{\partial w_{\delta_i^C}} = \frac{-\Delta\delta_i^C\left[\left|V_i^C\right| + w_{V_i^C}\cdot\Delta\left|V_i^C\right|\right]\sin\left(\delta_i^C + w_{\delta_i^C}\cdot\Delta\delta_i^C - 120°\right)}{3} \quad \text{(B.134)}$$

The differential of $V_i^{po,m}$ can be written into equations (B.135)-(B.140)

$$\frac{\partial V_i^{po,m}}{\partial w_{V_i^A}} = \frac{\Delta\left|V_i^A\right| \sin\left(\delta_i^A + w_{\delta_i^A} \cdot \Delta\delta_i^A\right)}{3} \tag{B.135}$$

$$\frac{\partial V_i^{po,m}}{\partial w_{V_i^B}} = \frac{\Delta\left|V_i^B\right| \sin\left(\delta_i^B + w_{\delta_i^B} \cdot \Delta\delta_i^B + 120°\right)}{3} \tag{B.136}$$

$$\frac{\partial V_i^{po,m}}{\partial w_{V_i^C}} = \frac{\Delta\left|V_i^C\right| \sin\left(\delta_i^C + w_{\delta_i^C} \cdot \Delta\delta_i^C - 120°\right)}{3} \tag{B.137}$$

$$\frac{\partial V_i^{po,m}}{\partial w_{\delta_i^A}} = \frac{\Delta\delta_i^A \left[\left|V_i^A\right| + w_{V_i^A} \cdot \Delta\left|V_i^A\right|\right] \cos\left(\delta_i^A + w_{\delta_i^A} \cdot \Delta\delta_i^A\right)}{3} \tag{B.138}$$

$$\frac{\partial V_i^{po,m}}{\partial w_{\delta_i^B}} = \frac{\Delta\delta_i^B \left[\left|V_i^B\right| + w_{V_i^B} \cdot \Delta\left|V_i^B\right|\right] \cos\left(\delta_i^B + w_{\delta_i^B} \cdot \Delta\delta_i^B + 120°\right)}{3} \tag{B.139}$$

$$\frac{\partial V_i^{po,m}}{\partial w_{\delta_i^C}} = \frac{\Delta\delta_i^C \left[\left|V_i^C\right| + w_{V_i^C} \cdot \Delta\left|V_i^C\right|\right] \cos\left(\delta_i^C + w_{\delta_i^C} \cdot \Delta\delta_i^C - 120°\right)}{3} \tag{B.140}$$

The differential of V^{rm} can be written into equations (B.141)-(B.146).

$$\begin{aligned}\frac{\partial V_i^{rm}}{\partial w_{V_i^A}} = \frac{1}{9}\Big[&2\Delta\left|V_i^A\right| \left[\left|V_i^A\right| + w_{V_i^A} \cdot \Delta\left|V_i^A\right|\right] \\ &+ 2\Delta\left|V_i^A\right| \left[\left|V_i^B\right| + w_{V_i^B} \right. \\ &\left. \cdot \Delta\left|V_i^B\right|\right] \cos\left(\delta_i^A + w_{\delta_i^A} \cdot \Delta\delta_i^A - \delta_i^B - w_{\delta_i^B} \cdot \Delta\delta_i^B - 120°\right) \\ &+ 2\Delta\left|V_i^A\right| \left[\left|V_i^C\right| + w_{V_i^C} \cdot \Delta\left|V_i^C\right|\right] \cos\left(\delta_i^A + w_{\delta_i^A} \cdot \Delta\delta_i^A - \delta_i^C - w_{\delta_i^C} \right. \\ &\left. \cdot \Delta\delta_i^C + 120°\right)\Big]\end{aligned} \tag{B.141}$$

$$\begin{aligned}\frac{\partial V_i^{rm}}{\partial w_{V_i^B}} = \frac{1}{9}\Big[&2\Delta|V_i^B| \left[|V_i^B| + w_{V_i^B} \cdot \Delta|V_i^B|\right] \\ &+ 2\Delta|V_i^B| \left[\left|V_i^A\right| + w_{V_i^A} \right. \\ &\left. \cdot \Delta\left|V_i^A\right|\right] \cos\left(\delta_i^A + w_{\delta_i^A} \cdot \Delta\delta_i^A - \delta_i^B - w_{\delta_i^B} \cdot \Delta\delta_i^B - 120°\right) \\ &+ 2\Delta|V_i^B| \left[\left|V_i^C\right| + w_{V_i^C} \cdot \Delta\left|V_i^C\right|\right] \cos\left(\delta_i^B + w_{\delta_i^B} \cdot \Delta\delta_i^B - \delta_i^C - w_{\delta_i^C} \right. \\ &\left. \cdot \Delta\delta_i^C + 240°\right)\Big]\end{aligned} \tag{B.142}$$

$$\frac{\partial V_i^{rm}}{\partial w_{V_i^C}} = \frac{1}{9}\Big[2\Delta\left|V_i^C\right|\left[\left|V_i^C\right| + w_{V_i^C}\cdot\Delta\left|V_i^C\right|\right] + 2\Delta\left|V_i^C\right|\left[\left|V_i^A\right| + w_{V_i^A} \cdot \Delta\left|V_i^A\right|\right]\cos\left(\delta_i^A + w_{\delta_i^A}\cdot\Delta\delta_i^A - \delta_i^C - w_{\delta_i^C}\cdot\Delta\delta_i^C + 120°\right) + 2\Delta\left|V_i^C\right|\left[|V_i^B| + w_{V_i^B}\cdot\Delta|V_i^B|\right]\cos\left(\delta_i^B + w_{\delta_i^B}\cdot\Delta\delta_i^B - \delta_i^C - w_{\delta_i^C} \cdot\Delta\delta_i^C + 240°\right)\Big] \tag{B.143}$$

$$\frac{\partial V_i^{rm}}{\partial w_{\delta_i^A}} = \frac{1}{9}\Big[-2\Delta\delta_i^A\left[\left|V_i^A\right| + w_{V_i^A}\cdot\Delta\left|V_i^A\right|\right]\left[|V_i^B| + w_{V_i^B} \cdot\Delta|V_i^B|\right]\sin\left(\delta_i^A + w_{\delta_i^A}\cdot\Delta\delta_i^A - \delta_i^B - w_{\delta_i^B}\cdot\Delta\delta_i^B - 120°\right) - 2\Delta\delta_i^A\left[\left|V_i^A\right| + w_{V_i^A}\cdot\Delta\left|V_i^A\right|\right]\left[\left|V_i^C\right| + w_{V_i^C}\cdot\Delta\left|V_i^C\right|\right]\sin\left(\delta_i^A + w_{\delta_i^A} \cdot\Delta\delta_i^A - \delta_i^C - w_{\delta_i^C}\cdot\Delta\delta_i^C + 120°\right)\Big] \tag{B.144}$$

$$\frac{\partial V_i^{rm}}{\partial w_{\delta_i^B}} = \frac{1}{9}\Big[2\Delta\delta_i^B\left[\left|V_i^A\right| + w_{V_i^A}\cdot\Delta\left|V_i^A\right|\right]\left[|V_i^B| + w_{V_i^B} \cdot\Delta|V_i^B|\right]\sin\left(\delta_i^A + w_{\delta_i^A}\cdot\Delta\delta_i^A - \delta_i^B - w_{\delta_i^B}\cdot\Delta\delta_i^B - 120°\right) - 2\Delta\delta_i^B\left[|V_i^B| + w_{V_i^B}\cdot\Delta|V_i^B|\right]\left[\left|V_i^C\right| + w_{V_i^C}\cdot\Delta\left|V_i^C\right|\right]\sin\left(\delta_i^B + w_{\delta_i^B} \cdot\Delta\delta_i^B - \delta_i^C - w_{\delta_i^C}\cdot\Delta\delta_i^C + 240°\right)\Big] \tag{B.145}$$

$$\frac{\partial V_i^{rm}}{\partial w_{\delta_i^C}} = \frac{1}{9}\Big[2\Delta\delta_i^C\left[\left|V_i^A\right| + w_{V_i^A}\cdot\Delta\left|V_i^A\right|\right]\left[\left|V_i^C\right| + w_{V_i^C} \cdot\Delta\left|V_i^C\right|\right]\sin\left(\delta_i^A + w_{\delta_i^A}\cdot\Delta\delta_i^A - \delta_i^C - w_{\delta_i^C}\cdot\Delta\delta_i^C + 120°\right) + 2\Delta\delta_i^C\left[|V_i^B| + w_{V_i^B}\cdot\Delta|V_i^B|\right]\left[\left|V_i^C\right| + w_{V_i^C}\cdot\Delta\left|V_i^C\right|\right]\sin\left(\delta_i^B + w_{\delta_i^B} \cdot\Delta\delta_i^B - \delta_i^C - w_{\delta_i^C}\cdot\Delta\delta_i^C + 240°\right)\Big] \tag{B.146}$$

The differential of $P_{i,pv}$ from continuous local control function can be written into equation (B.147)-(B.149).

$$\frac{\partial P_{i,pv}}{\partial w_{V_i^A}} = \Delta\left|V_i^A\right| \cdot P_i^{\Delta ABC} \tag{B.147}$$

$$\frac{\partial P_{i,pv}}{\partial w_{V_i^B}} = \Delta\left|V_i^B\right| \cdot P_i^{\Delta ABC} \tag{B.148}$$

$$\frac{\partial P_{i,pv}}{\partial w_{V_i^C}} = \Delta\left|V_i^C\right| \cdot P_i^{\Delta ABC} \tag{B.149}$$

$$P_i^{\Delta ABC} = \frac{-4P_i^{max} \cdot exp\left[\frac{\frac{-4}{3}\left(V_i^{\Delta ABC} - 3 \cdot V_{i,cri}\right)}{\delta_{i,p}}\right]}{3\delta_{i,p}\left[1 + exp\left(\frac{\frac{-4}{3}\left(V_i^{\Delta ABC} - 3 \cdot V_{i,cri}\right)}{\delta_{i,p}}\right)\right]^2} \tag{B.150}$$

$$V_i^{\Delta ABC} = \left[\left|V_i^A\right| + w_{V_i^A} \cdot \Delta\left|V_i^A\right|\right] + \left[\left|V_i^B\right| + w_{V_i^B} \cdot \Delta\left|V_i^B\right|\right] + \left[\left|V_i^C\right| + w_{V_i^C} \cdot \Delta\left|V_i^C\right|\right] \tag{B.151}$$

The differential of $Q_{i,pv}$ from continuous local control function can be written into equation (B.152)-(B.154).

$$\frac{\partial Q_{i,pv}}{\partial w_{V_i^A}} = \Delta\left|V_i^A\right| \cdot Q_i^{\Delta ABC} \tag{B.152}$$

$$\frac{\partial Q_{i,pv}}{\partial w_{V_i^B}} = \Delta\left|V_i^B\right| \cdot Q_i^{\Delta ABC} \tag{B.153}$$

$$\frac{\partial Q_{i,pv}}{\partial w_{V_i^C}} = \Delta\left|V_i^C\right| \cdot Q_i^{\Delta ABC} \tag{B.154}$$

$$Q_i^{\Delta ABC} = \frac{-4 \cdot K_{i,2} \cdot Q_i^{max} \cdot exp\left[\frac{\frac{-4}{3}\left(V_i^{\Delta ABC} - 3 \cdot V_{i,q}\right)}{\delta_{i,q}}\right]}{3\delta_{i,q}\left[1 + exp\left(\frac{\frac{-4}{3}\left(V_i^{\Delta ABC} - 3 \cdot V_{i,q}\right)}{\delta_{i,q}}\right)\right]^2} \tag{B.155}$$

The differential of $P_{i,pv}$ from piecewise linear local control function can be written into equation (B.156)-(B.158).

$$\frac{\partial P_{i,pv}}{\partial w_{V_i^A}} = \Delta\left|V_i^A\right| \cdot P_i^{\nabla ABC} \tag{B.156}$$

$$\frac{\partial P_{i,pv}}{\partial w_{V_i^B}} = \Delta\left|V_i^B\right| \cdot P_i^{\nabla ABC} \tag{B.157}$$

$$\frac{\partial P_{i,pv}}{\partial w_{V_i^C}} = \Delta\left|V_i^C\right| \cdot P_i^{\nabla ABC} \tag{B.158}$$

$$P_i^{\nabla ABC} = P_i^{max} \cdot \begin{cases} \dfrac{1}{3 \cdot \left(V_{i,p1} - V_{i,p2}\right)} & ;\ V_{i,p1} \le |V_i| < V_{i,p2} \\ 0 & ;\ other \end{cases} \tag{B.159}$$

where $|V_i| = \frac{|V_i^A| + w_{V_i^A} \cdot \Delta|V_i^A| + |V_i^B| + w_{V_i^B} \cdot \Delta|V_i^B| + |V_i^C| + w_{V_i^C} \cdot \Delta|V_i^C|}{3}$.

The differential of $Q_{i,pv}$ from piecewise linear local control function can be written into equation (B.160)-(B.162).

$$\frac{\partial Q_{i,pv}}{\partial w_{V_i^A}} = \Delta\left|V_i^A\right| \cdot Q_i^{\nabla ABC} \tag{B.160}$$

$$\frac{\partial Q_{i,pv}}{\partial w_{V_i^B}} = \Delta\left|V_i^B\right| \cdot Q_i^{\nabla ABC} \tag{B.161}$$

$$\frac{\partial Q_{i,pv}}{\partial w_{V_i^C}} = \Delta\left|V_i^C\right| \cdot Q_i^{\nabla ABC} \tag{B.162}$$

$$Q_i^{\nabla ABC} = Q_i^{max} \cdot \begin{cases} \dfrac{\left(K_{i,1} - K_{i,2}\right)}{3 \cdot \left(V_{i,q1} - V_{i,q2}\right)} & ;\ V_{i,q1} \le |V_i| < V_{i,q2} \\ 0 & ;\ other \end{cases} \tag{B.163}$$

where $|V_i| = \frac{|V_i^A| + w_{V_i^A} \cdot \Delta|V_i^A| + |V_i^B| + w_{V_i^B} \cdot \Delta|V_i^B| + |V_i^C| + w_{V_i^C} \cdot \Delta|V_i^C|}{3}$.

APPENDIX C

The Calculation Example Of The Power Flow Algorithm With Using Local Control Function

The modified 19 node LV distribution system, that is described in Subsection 6.1, is applied. Phase-A, -B and -C loads are 0.3124, 0.2599 and 0.2928 pu. respectively. Solar irradiance is 0.3519 kW/m2. Ambient temperature is 30.10 ºC. The continuous local control function is selected to operate. PV1-PV18 have the same parameters setting: $V_{cri} = 1.062$; $\delta_p = 0.01$; $K_1 = 0.06$; $K_2 = 1.06$; $V_q = 1.021$; $\delta_q = 0.01$. The process of power flow algorithm is as follows.

First: For load buses, where ${P_{i,load}^{\sigma}}^{sch}$ and ${Q_{i,load}^{\sigma}}^{sch}$ are specified, voltage magnitudes and phase angles are set equal to the slack bus values. Initial voltage is 1.05 pu. Initial phase angles (A, B, C) are (0, -2.0944, 2.0944) radians.

Second: For step-change values, ${w_{V_i^{\sigma}}}^{(h0)} = {w_{\delta_i^{\sigma}}}^{(h0)} = 1$.

Third: For load buses, ${P_{i,load}^{\sigma}}^{(k0)}\begin{Bmatrix} V_i^{\sigma(k0)} \\ \delta_i^{\sigma(k0)} \end{Bmatrix}$ and ${Q_{i,load}^{\sigma}}^{(k0)}\begin{Bmatrix} V_i^{\sigma(k0)} \\ \delta_i^{\sigma(k0)} \end{Bmatrix}$ are calculated from equations (5.1), (5.2), (5.16), (5.17), (5.30) and (5.31) as shown Table C.1. ${\Delta P_{i,load}^{\sigma}}^{(k0)}$ and ${\Delta Q_{i,load}^{\sigma}}^{(k0)}$ are calculated from equations (5.40) and (5.41) as shown in Table C.1.

Table C.1 The calculated values

Node		${P_{i,load}^{\sigma}}^{(k0)}$	${Q_{i,load}^{\sigma}}^{(k0)}$	${\Delta P_{i,load}^{\sigma}}^{(k0)}$	${\Delta Q_{i,load}^{\sigma}}^{(k0)}$
2	A	0.00000000	0.00000000	-0.00518831	-0.00250418
	B	0.00000000	0.00000000	-0.00215848	-0.00104805
	C	0.00000000	0.00000000	-0.00486282	-0.00234708
3	A	0.00000000	0.00000000	-0.00550321	-0.00266913
	B	0.00000000	0.00000000	-0.00404247	-0.00195885
	C	0.00000000	0.00000000	-0.00243141	-0.00118057
4	A	0.00000000	0.00000000	-0.00323895	-0.00157449
	B	0.00000000	0.00000000	-0.00235811	-0.00114786
	C	0.00000000	0.00000000	-0.00189734	-0.00091354
5	A	-0.02078118	0.01679984	0.01754223	-0.01837432
	B	-0.02078118	0.01679984	0.01862270	-0.01784788
	C	-0.02078118	0.01679984	0.01865896	-0.01782581
6	A	-0.01601882	0.01333320	0.01391951	-0.01435287
	B	-0.01601882	0.01333320	0.01473372	-0.01395704
	C	-0.01601882	0.01333320	0.01465555	-0.01399376
7	A	-0.01601882	0.01333320	0.01116040	-0.01568744
	B	-0.01601882	0.01333320	0.01265010	-0.01496766
	C	-0.01601882	0.01333320	0.01222414	-0.01517433
8	A	-0.01601882	0.01333320	0.01432437	-0.01415794
	B	-0.01601882	0.01333320	0.01376053	-0.01440620
	C	-0.01601882	0.01333320	0.01253333	-0.01501973
9	A	0.00000000	0.00000000	-0.00614800	-0.00298403

Node		$P_{i,load}^{\sigma}{}^{(k0)}$	$Q_{i,load}^{\sigma}{}^{(k0)}$	$\Delta P_{i,load}^{\sigma}{}^{(k0)}$	$\Delta Q_{i,load}^{\sigma}{}^{(k0)}$
	B	0.00000000	0.00000000	-0.00620095	-0.00300690
	C	0.00000000	0.00000000	-0.00622610	-0.00300764
10	A	-0.01601882	0.01333320	0.01432437	-0.01415794
	B	-0.01601882	0.01333320	0.01427208	-0.01418162
	C	-0.01601882	0.01333320	0.01481014	-0.01392349
11	A	-0.01601882	0.01333320	0.01230003	-0.01513262
	B	-0.01601882	0.01333320	0.01292459	-0.01483041
	C	-0.01601882	0.01333320	0.01086086	-0.01583489
12	A	-0.02078118	0.01679984	0.01592276	-0.01915407
	B	-0.02078118	0.01679984	0.01741245	-0.01843429
	C	-0.02078118	0.01679984	0.01698649	-0.01864096
13	A	-0.01601882	0.01333320	0.01382954	-0.01439786
	B	-0.01601882	0.01333320	0.01379796	-0.01440620
	C	-0.01601882	0.01333320	0.01298307	-0.01480892
14	A	0.00000000	0.00000000	-0.00154450	-0.00074976
	B	0.00000000	0.00000000	-0.00128511	-0.00062384
	C	0.00000000	0.00000000	-0.00189734	-0.00091354
15	A	-0.01601882	0.01333320	0.01382954	-0.01439786
	B	-0.01601882	0.01333320	0.01399759	-0.01430639
	C	-0.01601882	0.01333320	0.01275820	-0.01490730
16	A	-0.01601882	0.01333320	0.01213509	-0.01522259
	B	-0.01601882	0.01333320	0.01170187	-0.01541682
	C	-0.01601882	0.01333320	0.01237873	-0.01510406
17	A	0.00000000	0.00000000	-0.00323895	-0.00157449
	B	0.00000000	0.00000000	-0.00202123	-0.00097319
	C	0.00000000	0.00000000	-0.00227681	-0.00109624
18	A	-0.02078118	0.01679984	0.01811204	-0.01808942
	B	-0.02078118	0.01679984	0.01856031	-0.01787284
	C	-0.02078118	0.01679984	0.01562321	-0.01930152
19	A	-0.01601882	0.01333320	0.01164025	-0.01544752
	B	-0.01601882	0.01333320	0.01183911	-0.01535444
	C	-0.01601882	0.01333320	0.01086086	-0.01583489

Fourth: The elements of the Jacobian matrix (J_1, J_2, J_3 and J_4) are calculated from equations (5.8)-(5.15), (5.18)-(5.29) and (5.32)-(5.39).

Fifth: The linear simultaneous equation (5.7) is solved directly by optimally ordered triangular factorization and Gaussian elimination. The $\Delta\delta_i^{\sigma(k0)}$ and $\Delta\left|V_i^{\sigma(k0)}\right|$ are obtained as shown Table C.2.

Sixth: For load buses, $P_{i,load}^{\sigma}{}^{(h0)}\begin{Bmatrix} V_i^{\sigma(k0)} + w_{V_i^{\sigma}}^{(h0)} \cdot \Delta\left|V_i^{\sigma(k0)}\right| \\ \delta_i^{\sigma(k0)} + w_{\delta_i^{\sigma}}^{(h0)} \cdot \Delta\delta_i^{\sigma(k0)} \end{Bmatrix}$ and $Q_{i,load}^{\sigma}{}^{(h0)}\begin{Bmatrix} V_i^{\sigma(k0)} + w_{V_i^{\sigma}}^{(h0)} \cdot \Delta\left|V_i^{\sigma(k0)}\right| \\ \delta_i^{\sigma(k0)} + w_{\delta_i^{\sigma}}^{(h0)} \cdot \Delta\delta_i^{\sigma(k0)} \end{Bmatrix}$ are calculated from equations (5.44), (5.45), (5.55), (5.56), (5.69) and (5.70) as shown in Table C.2. $\Delta P_{i,load}^{\sigma}{}^{(h0)}$ and $\Delta Q_{i,load}^{\sigma}{}^{(h0)}$ are calculated from equations (5.40) and (5.41) as shown Table C.2.

Table C.2 The calculated values

Node		$\Delta\lvert V_i^{\sigma(k0)}\rvert$	$\Delta\delta_i^{\sigma(k0)}$	$P_{i,load}^{\sigma\ (h0)}$	$Q_{i,load}^{\sigma\ (h0)}$	$\Delta P_{i,load}^{\sigma\ (h0)}$	$\Delta Q_{i,load}^{\sigma\ (h0)}$
2	A	0.00167246	0.01694075	-0.00105929	0.00075997	-0.00412902	-0.00326415
	B	0.00078728	0.01877068	0.00155878	0.00243154	-0.00371726	-0.00347959
	C	-0.00398264	0.01475349	-0.00101911	0.00008281	-0.00384371	-0.00242989
3	A	-0.02121483	0.02304986	-0.00539099	-0.00262203	-0.00011221	-0.00004710
	B	-0.01597663	0.01499544	-0.00399033	-0.00192961	-0.00005214	-0.00002924
	C	-0.00684489	0.01497870	-0.00241399	-0.00116216	-0.00001742	-0.00001841
4	A	0.00540690	0.03952687	0.00155700	0.00290659	-0.00479595	-0.00448108
	B	0.00245237	0.04423819	0.00198843	0.00354084	-0.00434653	-0.00468870
	C	-0.00886207	0.03446042	0.00249636	0.00250723	-0.00439370	-0.00342076
5	A	0.03336391	0.11221838	0.01648899	-0.00193455	-0.01972794	0.00036007
	B	0.02995536	0.11725867	0.01794915	-0.00120597	-0.02010762	0.00015793
	C	0.01447910	0.10237032	0.01288815	-0.00084739	-0.01501036	-0.00017858
6	A	0.00918693	0.05977191	0.00139353	0.00176764	-0.00349285	-0.00278730
	B	0.00414622	0.06752011	0.00200966	0.00250072	-0.00329476	-0.00312456
	C	-0.01365485	0.05213007	0.00146575	0.00157232	-0.00282903	-0.00223288
7	A	0.01795430	0.08902495	-0.00273629	-0.00264436	-0.00212213	0.00029013
	B	0.01382212	0.09783806	-0.00108578	-0.00171597	-0.00228295	0.00008151
	C	-0.00950842	0.07856980	-0.00210379	-0.00155106	-0.00169089	-0.00029007
8	A	0.01226216	0.07641877	0.00078000	0.00084981	-0.00247445	-0.00167455
	B	0.00532103	0.08682277	0.00012925	0.00087628	-0.00238754	-0.00194929
	C	-0.01799862	0.06663219	-0.00163096	-0.00011458	-0.00185453	-0.00157195
9	A	0.01463068	0.09136565	-0.00436932	-0.00140168	-0.00177868	-0.00158234
	B	0.00618602	0.10392775	-0.00461073	-0.00140977	-0.00159021	-0.00159713
	C	-0.02184469	0.07963439	-0.00444799	-0.00187893	-0.00177811	-0.00112871
10	A	0.01691142	0.10258763	0.00003498	0.00015062	-0.00172942	-0.00097535
	B	0.00738504	0.11685918	0.00007062	0.00095756	-0.00181737	-0.00180597
	C	-0.02432861	0.08955923	-0.00060183	-0.00005756	-0.00060685	-0.00053272
11	A	0.02028084	0.11175954	-0.00310288	-0.00190402	-0.00061590	0.00010461
	B	0.01082893	0.12704798	-0.00232660	-0.00126241	-0.00076763	-0.00023480
	C	-0.02383015	0.09840788	-0.00513717	-0.00174167	-0.00002079	-0.00076002
12	A	0.02186633	0.11494475	0.01481679	-0.00239418	-0.01967521	0.00003995
	B	0.01160479	0.13000054	0.00636194	-0.00118841	-0.00973067	-0.00044604
	C	-0.02230407	0.10082368	-0.00257012	-0.00189905	-0.00122457	0.00005793
13	A	0.02785263	0.12579901	0.00005159	-0.00167866	-0.00224087	0.00061400
	B	0.01685637	0.14296452	0.00020310	-0.00130143	-0.00242396	0.00022843
	C	-0.02207448	0.11115633	-0.00159771	-0.00108092	-0.00143804	-0.00039480
14	A	0.02090667	0.11534749	-0.00150054	-0.00068660	-0.00004395	-0.00006315
	B	0.01192316	0.13083164	-0.00124158	-0.00055187	-0.00004352	-0.00007197
	C	-0.02366690	0.10208688	-0.00179724	-0.00082017	-0.00010011	-0.00009337
15	A	0.02448872	0.12058680	-0.00114410	-0.00159021	-0.00104519	0.00052555
	B	0.01373490	0.13638174	-0.00080323	-0.00115303	-0.00121800	0.00017985
	C	-0.02196906	0.10596189	-0.00291006	-0.00115571	-0.00035056	-0.00041838
16	A	0.02795339	0.12973304	-0.00163283	-0.00254699	-0.00225091	0.00065760
	B	0.01520408	0.14566848	-0.00191898	-0.00231564	-0.00239798	0.00023203
	C	-0.02045720	0.11332076	-0.00216862	-0.00141946	-0.00147147	-0.00035139
17	A	0.01745965	0.11583538	-0.00328065	-0.00160269	0.00004170	0.00002820
	B	0.01011828	0.13046612	-0.00203166	-0.00098426	0.00001043	0.00001108
	C	-0.02520695	0.10230072	-0.00223479	-0.00105189	-0.00004202	-0.00004435

Node		$\Delta\lvert V_i^{\sigma(k0)}\rvert$	$\Delta\delta_i^{\sigma(k0)}$	$P_{i,load}^{\sigma\ (h0)}$	$Q_{i,load}^{\sigma\ (h0)}$	$\Delta P_{i,load}^{\sigma\ (h0)}$	$\Delta Q_{i,load}^{\sigma\ (h0)}$
18	A	0.02252138	0.11883702	0.01654545	-0.00200915	-0.01921458	0.00071957
	B	0.01359390	0.13466607	0.01099619	-0.00141595	-0.01321705	0.00034295
	C	-0.02285190	0.10571321	-0.00430173	-0.00331687	-0.00085624	0.00081518
19	A	0.02559296	0.12344526	-0.00317221	-0.00281135	-0.00120637	0.00069704
	B	0.01458364	0.13956936	-0.00277286	-0.00235898	-0.00140685	0.00033775
	C	-0.02194447	0.10852010	-0.00459528	-0.00214245	-0.00056269	-0.00035923

Seventh: The elements of the Jacobian matrix (J_1, J_2, J_3 and J_4) are calculated from equations (5.47)-(5.54), (5.57)-(5.68) and (5.71)-(5.78).

Eighth: The linear simultaneous equation (5.46) is solved directly by optimally ordered triangular factorization and Gaussian elimination. The $\Delta w_{V_i^\sigma}{}^{(h0)}$ and $\Delta w_{\delta_i^\sigma}{}^{(h0)}$ are obtained as shown in Table C.3.

Ninth: The new step-length values $\begin{Bmatrix} w_{V_i^\sigma}^{(h1)} = w_{V_i^\sigma}^{(h0)} + \Delta w_{V_i^\sigma}{}^{(h0)} \\ w_{\delta_i^\sigma}^{(h1)} = w_{\delta_i^\sigma}^{(h0)} + \Delta w_{\delta_i^\sigma}{}^{(h0)} \end{Bmatrix}$ are computed from equations (5.79) and (5.80) as shown in Table C.3.

Table C.3 The calculated values

Node		$\Delta w_{V_i^\sigma}{}^{(h0)}$	$\Delta w_{\delta_i^\sigma}{}^{(h0)}$	$w_{V_i^\sigma}{}^{(h1)}$	$w_{\delta_i^\sigma}{}^{(h1)}$
2	A	-3.36032652	-0.02642235	-2.36032652	0.97357765
	B	-2.50419090	-0.13501303	-1.50419090	0.86498697
	C	-0.04411662	0.13258012	0.95588338	1.13258012
3	A	0.29632616	-0.01216129	1.29632616	0.98783871
	B	0.13777610	-0.17944463	1.13777610	0.82055537
	C	-0.03954849	0.13546324	0.96045151	1.13546324
4	A	-2.33863605	-0.02232056	-1.33863605	0.97767944
	B	-1.69820799	-0.13237305	-0.69820799	0.86762695
	C	-0.09690867	0.13738034	0.90309133	1.13738034
5	A	-2.36076745	-0.02316550	-1.36076745	0.97683450
	B	-2.11905746	-0.34451125	-1.11905746	0.65548875
	C	-0.26435804	-0.02695950	0.73564196	0.97304050
6	A	-1.86339920	-0.01751946	-0.86339920	0.98248054
	B	-1.01362324	-0.10968171	-0.01362324	0.89031829
	C	-0.12492629	0.15339988	0.87507371	1.15339988
7	A	-0.84931341	-0.00159684	0.15068659	0.99840316
	B	-0.16410624	-0.06865747	0.83589376	0.93134253
	C	-0.43291153	0.12604944	0.56708847	1.12604944
8	A	-1.73890128	-0.01712956	-0.73890128	0.98287044
	B	-0.73718668	-0.10475324	0.26281332	0.89524676
	C	-0.15493276	0.16747239	0.84506724	1.16747239
9	A	-1.72831494	-0.01716688	-0.72831494	0.98283312
	B	-0.54638582	-0.10425674	0.45361418	0.89574326
	C	-0.18734310	0.17983860	0.81265690	1.17983860
10	A	-1.66206664	-0.01689394	-0.66206664	0.98310606
	B	-0.38169476	-0.10422139	0.61830524	0.89577861
	C	-0.21604369	0.18697701	0.78395631	1.18697701

Node		$\Delta w_{V_i^\sigma}^{(h0)}$	$\Delta w_{\delta_i^\sigma}^{(h0)}$	$w_{V_i^\sigma}^{(h1)}$	$w_{\delta_i^\sigma}^{(h1)}$
11	A	-1.51911717	-0.01718143	-0.51911717	0.98281857
	B	-0.25206621	-0.10413443	0.74793379	0.89586557
	C	-0.26127794	0.18774238	0.73872206	1.18774238
12	A	-1.38573831	-0.01539558	-0.38573831	0.98460442
	B	-0.17416137	-0.09954601	0.82583863	0.90045399
	C	-0.30401205	0.18669764	0.69598795	1.18669764
13	A	-1.02318073	-0.00839001	-0.02318073	0.99160999
	B	-0.02019153	-0.08747636	0.97980847	0.91252364
	C	-0.40303275	0.18296175	0.59696725	1.18296175
14	A	-1.62739776	-0.02068963	-0.62739776	0.97931037
	B	-0.26742397	-0.11090440	0.73257603	0.88909560
	C	-0.27439412	0.19188499	0.72560588	1.19188499
15	A	-1.20989130	-0.01241195	-0.20989130	0.98758805
	B	-0.09488549	-0.09340851	0.90511451	0.90659149
	C	-0.34811361	0.18342800	0.65188639	1.18342800
16	A	-1.01016304	-0.00780881	-0.01016304	0.99219119
	B	0.01214234	-0.08450666	1.01214234	0.91549334
	C	-0.45240262	0.18112545	0.54759738	1.18112545
17	A	-1.95222259	-0.02058376	-0.95222259	0.97941624
	B	-0.31284718	-0.11124959	0.68715282	0.88875041
	C	-0.25619925	0.19161014	0.74380075	1.19161014
18	A	-1.65230987	-0.02386686	-0.65230987	0.97613314
	B	-0.26855783	-0.11727042	0.73144217	0.88272958
	C	-0.29749272	0.19573832	0.70250728	1.19573832
19	A	-1.14332738	-0.01106838	-0.14332738	0.98893162
	B	-0.06204880	-0.09057420	0.93795120	0.90942580
	C	-0.36939500	0.18199903	0.63060500	1.18199903

Tenth: For load buses, ${P_{i,load}^{\sigma}}^{(h1)} \begin{Bmatrix} V_i^{\sigma(k0)} + w_{V_i^\sigma}^{(h1)} \cdot \Delta\left|V_i^{\sigma(k0)}\right| \\ \delta_i^{\sigma(k0)} + w_{\delta_i^\sigma}^{(h1)} \cdot \Delta\delta_i^{\sigma(k0)} \end{Bmatrix}$ and ${Q_{i,load}^{\sigma}}^{(h1)} \begin{Bmatrix} V_i^{\sigma(k0)} + w_{V_i^\sigma}^{(h1)} \cdot \Delta\left|V_i^{\sigma(k0)}\right| \\ \delta_i^{\sigma(k0)} + w_{\delta_i^\sigma}^{(h1)} \cdot \Delta\delta_i^{\sigma(k0)} \end{Bmatrix}$ are calculated from equations (5.44), (5.45), (5.55), (5.56), (5.69) and (5.70) as shown in Table C.4. ${\Delta P_{i,load}^{\sigma}}^{(h1)}$ and ${\Delta Q_{i,load}^{\sigma}}^{(h1)}$ are calculated from equations (5.40) and (5.41) as shown Table C.4.

Table C.4 The calculated values

Node		${P_{i,load}^{\sigma}}^{(h1)}$	${Q_{i,load}^{\sigma}}^{(h1)}$	${\Delta P_{i,load}^{\sigma}}^{(h1)}$	${\Delta Q_{i,load}^{\sigma}}^{(h1)}$
2	A	-0.00516327	-0.00241395	-0.00002504	-0.00009023
	B	-0.00213766	-0.00090205	-0.00002082	-0.00014600
	C	-0.00486280	-0.00226463	-0.00000002	-0.00008246
3	A	-0.00550242	-0.00266858	-0.00000079	-0.00000055
	B	-0.00404250	-0.00195887	0.00000003	0.00000002
	C	-0.00243133	-0.00118066	-0.00000008	0.00000010
4	A	-0.00309601	-0.00139423	-0.00014294	-0.00018026
	B	-0.00229346	-0.00053076	-0.00006465	-0.00061710

Node		$P_{i,load}^{\sigma\ (h1)}$	$Q_{i,load}^{\sigma\ (h1)}$	$\Delta P_{i,load}^{\sigma\ (h1)}$	$\Delta Q_{i,load}^{\sigma\ (h1)}$
	C	-0.00193196	-0.00075592	0.00003462	-0.00015762
5	A	-0.02283031	-0.01939098	0.01959136	0.01781650
	B	-0.02157382	-0.01625677	0.01941534	0.01520872
	C	-0.00318872	-0.00109415	0.00106651	0.00006818
6	A	-0.00186728	-0.00095434	-0.00023204	-0.00006533
	B	-0.00101704	-0.00059040	-0.00026806	-0.00003344
	C	-0.00110608	-0.00056334	-0.00025719	-0.00009722
7	A	-0.00321329	-0.00234711	-0.00164513	-0.00000713
	B	-0.00174494	-0.00160476	-0.00162378	-0.00002969
	C	-0.00220305	-0.00186981	-0.00159164	0.00002868
8	A	-0.00142627	-0.00077841	-0.00026818	-0.00004632
	B	-0.00194257	-0.00104656	-0.00031572	-0.00002644
	C	-0.00319579	-0.00159035	-0.00028970	-0.00009617
9	A	-0.00613168	-0.00294415	-0.00001632	-0.00003988
	B	-0.00613240	-0.00298630	-0.00006854	-0.00002060
	C	-0.00619294	-0.00291013	-0.00003316	-0.00009751
10	A	-0.00130017	-0.00079834	-0.00039427	-0.00002639
	B	-0.00151812	-0.00091456	-0.00022863	0.00006614
	C	-0.00081254	-0.00069369	-0.00039614	0.00010340
11	A	-0.00282487	-0.00177415	-0.00089392	-0.00002526
	B	-0.00220786	-0.00146827	-0.00088637	-0.00002894
	C	-0.00428040	-0.00250257	-0.00087756	0.00000088
12	A	-0.02026046	-0.00242675	0.01540204	0.00007251
	B	-0.00308676	-0.00161587	-0.00028197	-0.00001859
	C	-0.00382433	-0.00383486	0.00002964	0.00199374
13	A	0.00100274	-0.00104991	-0.00319203	-0.00001474
	B	0.00092383	-0.00099402	-0.00314469	-0.00007898
	C	0.00002826	-0.00155074	-0.00306401	0.00007503
14	A	-0.00154241	-0.00073469	-0.00000209	-0.00001507
	B	-0.00127982	-0.00061423	-0.00000529	-0.00000960
	C	-0.00189226	-0.00090404	-0.00000508	-0.00000950
15	A	-0.00007376	-0.00105423	-0.00211553	-0.00001042
	B	0.00007202	-0.00092697	-0.00209325	-0.00004621
	C	-0.00120806	-0.00161656	-0.00205256	0.00004246
16	A	-0.00094507	-0.00187529	-0.00293866	-0.00001409
	B	-0.00143315	-0.00200976	-0.00288381	-0.00007386
	C	-0.00082296	-0.00184613	-0.00281713	0.00007528
17	A	-0.00323708	-0.00157367	-0.00000187	-0.00000082
	B	-0.00202119	-0.00097295	-0.00000004	-0.00000024
	C	-0.00227701	-0.00109660	0.00000020	0.00000036
18	A	-0.01830172	-0.00144613	0.01563259	0.00015655
	B	-0.00266356	-0.00106331	0.00044270	-0.00000969
	C	-0.00518809	-0.00491261	0.00003013	0.00241093
19	A	-0.00194795	-0.00210911	-0.00243063	-0.00000520
	B	-0.00177713	-0.00196793	-0.00240259	-0.00005331
	C	-0.00280786	-0.00255620	-0.00235010	0.00005452

Eleventh: Determine $max\{|\Delta P_{i,load}^{\sigma\ (h1)}|, |\Delta Q_{i,load}^{\sigma\ (h1)}|\} = 0.0196$ and $max\{|\Delta P_{i,load}^{\sigma\ (h0)}|, |\Delta Q_{i,load}^{\sigma\ (h0)}|\} = 0.0201$. After that, go to the next calculation.

Twelfth: The elements of the Jacobian matrix (J_1, J_2, J_3 and J_4) are calculated from equations (5.47)-(5.54), (5.57)-(5.68) and (5.71)-(5.78).

Thirteenth: The linear simultaneous equation (5.46) is solved directly by optimally ordered triangular factorization and Gaussian elimination. The $\Delta w_{V_i^\sigma}{}^{(h1)}$ and $\Delta w_{\delta_i^\sigma}{}^{(h1)}$ are obtained as shown in Table C.5.

Fourteenth: The new step-length values $\begin{Bmatrix} w_{V_i^\sigma}^{(h2)} = w_{V_i^\sigma}^{(h1)} + \Delta w_{V_i^\sigma}{}^{(h1)} \\ w_{\delta_i^\sigma}^{(h2)} = w_{\delta_i^\sigma}^{(h1)} + \Delta w_{\delta_i^\sigma}{}^{(h1)} \end{Bmatrix}$ are computed from equations (5.79) and (5.80) as shown in Table C.5.

Table C.5 The calculated values

Node		$\Delta w_{V_i^\sigma}{}^{(h1)}$	$\Delta w_{\delta_i^\sigma}{}^{(h1)}$	$w_{V_i^\sigma}{}^{(h2)}$	$w_{\delta_i^\sigma}{}^{(h2)}$
2	A	3.88279211	-0.07040849	1.52246559	0.90316916
	B	-0.76114926	0.28044480	-2.26534016	1.14543177
	C	0.60102123	-0.13924076	1.55690461	0.99333936
3	A	-0.31362002	-0.05379776	0.98270614	0.93404094
	B	0.04121165	0.35347244	1.17898774	1.17402781
	C	0.35473505	-0.13801210	1.31518655	0.99745114
4	A	2.78840565	-0.07896060	1.44976959	0.89871884
	B	-0.44832716	0.27811089	-1.14653514	1.14573784
	C	0.64162409	-0.13614410	1.54471542	1.00123624
5	A	4.34092572	-0.75888286	2.98015827	0.21795164
	B	1.39947427	1.27303706	0.28041680	1.92852581
	C	-0.60226303	0.06237373	0.13337894	1.03541423
6	A	2.03159940	-0.04973986	1.16820020	0.93274068
	B	-0.51046429	0.20973298	-0.52408753	1.10005127
	C	0.55796413	-0.14589492	1.43303784	1.00750496
7	A	0.88603576	-0.04826980	1.03672236	0.95013336
	B	-0.31931199	0.13229820	0.51658178	1.06364073
	C	1.05104617	-0.10808652	1.61813464	1.01796293
8	A	1.83028797	-0.03668829	1.09138669	0.94618215
	B	-0.55201901	0.18634043	-0.28920568	1.08158719
	C	0.52933724	-0.15555850	1.37440448	1.01191388
9	A	1.79546147	-0.02954971	1.06714652	0.95328341
	B	-0.59725183	0.17552165	-0.14363765	1.07126492
	C	0.52587838	-0.16418190	1.33853528	1.01565670
10	A	1.72268819	-0.02628425	1.06062155	0.95682181
	B	-0.57053550	0.16940560	0.04776974	1.06518421
	C	0.53457940	-0.16831915	1.31853571	1.01865786
11	A	1.58264999	-0.02261163	1.06353281	0.96020694
	B	-0.39947451	0.16467462	0.34845928	1.06054019
	C	0.59484101	-0.16756477	1.33356307	1.02017760
12	A	1.43679621	-0.02664569	1.05105790	0.95795873
	B	-0.39116681	0.15948173	0.43467182	1.05993572
	C	0.66214317	-0.16364834	1.35813112	1.02304930
13	A	1.05336226	-0.03028997	1.03018153	0.96132003
	B	-0.39137938	0.13825962	0.58842909	1.05078326
	C	0.74471904	-0.15628332	1.34168629	1.02667843

Node		$\Delta w_{V_i^\sigma}^{(h1)}$	$\Delta w_{\delta_i^\sigma}^{(h1)}$	$w_{V_i^\sigma}^{(h2)}$	$w_{\delta_i^\sigma}^{(h2)}$
14	A	1.71068303	-0.01719090	1.08328527	0.96211946
	B	-0.32637995	0.17094967	0.40619608	1.06004527
	C	0.62246122	-0.17328686	1.34806710	1.01859813
15	A	1.25132803	-0.02891198	1.04143674	0.95867606
	B	-0.37487706	0.14949418	0.53023745	1.05608567
	C	0.70381742	-0.15779871	1.35570381	1.02562929
16	A	1.03437968	-0.03300511	1.02421664	0.95918609
	B	-0.43632204	0.13511824	0.57582030	1.05061158
	C	0.82493984	-0.15253286	1.37253721	1.02859259
17	A	2.05544224	-0.01749177	1.10321965	0.96192447
	B	-0.38609297	0.17164355	0.30105984	1.06039396
	C	0.58683934	-0.17288283	1.33064009	1.01872731
18	A	1.74951954	-0.01220204	1.09720967	0.96393110
	B	-0.25344067	0.17670633	0.47800150	1.05943591
	C	0.66862772	-0.17865428	1.37113500	1.01708404
19	A	1.18135361	-0.03001032	1.03802623	0.95892129
	B	-0.37590287	0.14480662	0.56204834	1.05423241
	C	0.72148565	-0.15517418	1.35209066	1.02682485

Fifteenth: For load buses, ${P_{i,load}^{\sigma}}^{(h2)} \begin{Bmatrix} V_i^{\sigma(k0)} + w_{V_i^\sigma}^{(h2)} \cdot \Delta\left|V_i^{\sigma(k0)}\right| \\ \delta_i^{\sigma(k0)} + w_{\delta_i^\sigma}^{(h2)} \cdot \Delta\delta_i^{\sigma(k0)} \end{Bmatrix}$ and ${Q_{i,load}^{\sigma}}^{(h2)} \begin{Bmatrix} V_i^{\sigma(k0)} + w_{V_i^\sigma}^{(h2)} \cdot \Delta\left|V_i^{\sigma(k0)}\right| \\ \delta_i^{\sigma(k0)} + w_{\delta_i^\sigma}^{(h2)} \cdot \Delta\delta_i^{\sigma(k0)} \end{Bmatrix}$ are calculated from equations (5.44), (5.45), (5.55), (5.56), (5.69) and (5.70) as shown in Table C.6. ${\Delta P_{i,load}^{\sigma}}^{(h2)}$ and ${\Delta Q_{i,load}^{\sigma}}^{(h2)}$ are calculated from equations (5.40) and (5.41) as shown Table C.6.

Table C.6 The calculated values

Node		${P_{i,load}^{\sigma}}^{(h2)}$	${Q_{i,load}^{\sigma}}^{(h2)}$	${\Delta P_{i,load}^{\sigma}}^{(h2)}$	${\Delta Q_{i,load}^{\sigma}}^{(h2)}$
2	A	-0.00498524	-0.00273979	-0.00020307	0.00023560
	B	-0.00170912	-0.00083967	-0.00044936	-0.00020838
	C	-0.00487943	-0.00217097	0.00001660	-0.00017611
3	A	-0.00550299	-0.00266894	-0.00000022	-0.00000019
	B	-0.00404257	-0.00195883	0.00000010	-0.00000002
	C	-0.00243141	-0.00118055	0.00000000	-0.00000002
4	A	-0.00097990	-0.00409130	-0.00225904	0.00251681
	B	0.00044484	0.00114949	-0.00280295	-0.00229735
	C	-0.00208084	-0.00083485	0.00018350	-0.00007869
5	A	0.01958668	0.01838266	-0.02282563	-0.01995715
	B	0.00297121	-0.02275801	-0.00512969	0.02170997
	C	0.00760295	-0.00089692	-0.00972517	-0.00012905
6	A	-0.00211527	-0.00102347	0.00001595	0.00000381
	B	-0.00120032	-0.00061798	-0.00008479	-0.00000586
	C	-0.00134174	-0.00053931	-0.00002154	-0.00012125
7	A	-0.00487149	-0.00233930	0.00001307	-0.00001494
	B	-0.00335621	-0.00163948	-0.00001252	0.00000503

Node		$P_{i,load}^{\sigma\ (h2)}$	$Q_{i,load}^{\sigma\ (h2)}$	$\Delta P_{i,load}^{\sigma\ (h2)}$	$\Delta Q_{i,load}^{\sigma\ (h2)}$
	C	-0.00377361	-0.00183683	-0.00002108	-0.00000429
8	A	-0.00170809	-0.00083449	0.00001364	0.00000975
	B	-0.00217198	-0.00106404	-0.00008632	-0.00000896
	C	-0.00346570	-0.00157314	-0.00001979	-0.00011338
9	A	-0.00615315	-0.00300190	0.00000515	0.00001787
	B	-0.00613162	-0.00299417	-0.00006933	-0.00001273
	C	-0.00621861	-0.00291241	-0.00000748	-0.00009523
10	A	-0.00169922	-0.00078361	0.00000477	-0.00004112
	B	-0.00192770	-0.00097713	0.00018096	0.00012871
	C	-0.00110972	-0.00073085	-0.00009896	0.00014057
11	A	-0.00371790	-0.00176265	-0.00000089	-0.00003676
	B	-0.00305770	-0.00149489	-0.00003653	-0.00000232
	C	-0.00511216	-0.00247421	-0.00004581	-0.00002747
12	A	0.01621436	-0.00243217	-0.02107278	0.00007794
	B	-0.00052920	-0.00158659	-0.00283952	-0.00004787
	C	-0.00378775	-0.01265181	-0.00000694	0.01081068
13	A	-0.00218323	-0.00101846	-0.00000606	-0.00004619
	B	-0.00212808	-0.00108696	-0.00009278	0.00001396
	C	-0.00290950	-0.00146133	-0.00012625	-0.00001438
14	A	-0.00154423	-0.00073187	-0.00000027	-0.00001788
	B	-0.00127923	-0.00061382	-0.00000588	-0.00001002
	C	-0.00189144	-0.00089852	-0.00000590	-0.00001502
15	A	-0.00217144	-0.00102779	-0.00001785	-0.00003686
	B	-0.00194482	-0.00098266	-0.00007641	0.00000948
	C	-0.00316056	-0.00156186	-0.00010006	-0.00001223
16	A	-0.00388442	-0.00184547	0.00000068	-0.00004392
	B	-0.00424017	-0.00209675	-0.00007678	0.00001314
	C	-0.00353096	-0.00175779	-0.00010913	-0.00001306
17	A	-0.00323541	-0.00157098	-0.00000354	-0.00000351
	B	-0.00202255	-0.00097360	0.00000131	0.00000041
	C	-0.00227630	-0.00109604	-0.00000052	-0.00000021
18	A	0.01875872	-0.00223532	-0.02142786	0.00094574
	B	-0.00060458	-0.00101318	-0.00161628	-0.00005982
	C	-0.00516749	-0.01485018	0.00000953	0.01234850
19	A	-0.00435501	-0.00207600	-0.00002357	-0.00003831
	B	-0.00409212	-0.00203352	-0.00008759	0.00001229
	C	-0.00504332	-0.00249011	-0.00011464	-0.00001157

Sixteenth: Determine $max\{|\Delta P_{i,load}^{\sigma\ (h2)}|, |\Delta Q_{i,load}^{\sigma\ (h2)}|\} = 0.0228$ and $max\{|\Delta P_{i,load}^{\sigma\ (h1)}|, |\Delta Q_{i,load}^{\sigma\ (h1)}|\} = 0.0196$. Then, update voltage magnitudes, $|V_i^{\sigma(k1)}| = |V_i^{\sigma(k0)}| + w_{V_i^{\sigma}}{}^{(h1)} \cdot \Delta|V_i^{\sigma(k0)}|$, and phase angles, $\delta_i^{\sigma(k1)} = \delta_i^{\sigma(k0)} + w_{\delta_i^{\sigma}}{}^{(h1)} \cdot \Delta\delta_i^{\sigma(k0)}$, by $w_{V_i^{\sigma}}{}^{(h1)}$ and $w_{\delta_i^{\sigma}}{}^{(h1)}$ at equations (5.42) and (5.43) as shown in Table C.7. After that, renew $w_{V_i^{\sigma}}{}^{(h0)} = w_{\delta_i^{\sigma}}{}^{(h0)} = 0.9$ and go to ***STEP 3*** of the power flow algorithm.

Table C.7 The updated values

Node		$\left\|V_i^{\sigma(k1)}\right\|$	$\delta_i^{\sigma(k1)}$
2	A	1.04605245	0.01649314
	B	1.04881579	-2.07815871
	C	1.04619306	2.11110461
3	A	1.02249866	0.02276954
	B	1.03182218	-2.08209052
	C	1.04342582	2.11140287
4	A	1.04276213	0.03864461
	B	1.04828774	-2.05601286
	C	1.04199674	2.13358970
5	A	1.00459947	0.10961878
	B	1.01647823	-2.01753336
	C	1.06065143	2.19400557
6	A	1.04206801	0.05872474
	B	1.04994352	-2.03428072
	C	1.03805100	2.15452192
7	A	1.05270547	0.08888279
	B	1.06155383	-2.00327436
	C	1.04460789	2.18286858
8	A	1.04093948	0.07510975
	B	1.05139844	-2.01666730
	C	1.03478996	2.17218634
9	A	1.03934425	0.08979719
	B	1.05280607	-2.00130252
	C	1.03224776	2.18835083
10	A	1.03880352	0.10085452
	B	1.05456621	-1.98971515
	C	1.03092744	2.20069985
11	A	1.03947187	0.10983935
	B	1.05809932	-1.98057719
	C	1.03239615	2.21127831
12	A	1.04156532	0.11317511
	B	1.05958369	-1.97733560
	C	1.03447664	2.21404232
13	A	1.04935436	0.12474355
	B	1.06651601	-1.96393660
	C	1.03682226	2.22588879
14	A	1.03688320	0.11296099
	B	1.05873462	-1.97807326
	C	1.03282716	2.21607093
15	A	1.04486003	0.11909008
	B	1.06243166	-1.97075258
	C	1.03567867	2.21979336
16	A	1.04971591	0.12871997
	B	1.06538869	-1.96103658
	C	1.03879769	2.22824114
17	A	1.03337453	0.11345106
	B	1.05695281	-1.97844328
	C	1.03125105	2.21629768
18	A	1.03530908	0.11600076

Node		$\left\|V_i^{\sigma(k1)}\right\|$	$\delta_i^{\sigma(k1)}$
	B	1.05994315	-1.97552138
	C	1.03394637	2.22080043
19	A	1.04633183	0.12207892
	B	1.063678743	-1.967467124
	C	1.036161705	2.222665756

Seventeenth: For load buses, ${P_{i,load}^{\sigma}}^{(k1)}\begin{Bmatrix}V_i^{\sigma(k1)}\\ \delta_i^{\sigma(k1)}\end{Bmatrix}$ and ${Q_{i,load}^{\sigma}}^{(k1)}\begin{Bmatrix}V_i^{\sigma(k1)}\\ \delta_i^{\sigma(k1)}\end{Bmatrix}$ are calculated from equations (5.1), (5.2), (5.16), (5.17), (5.30) and (5.31) as shown Table C.8. ${\Delta P_{i,load}^{\sigma}}^{(k1)}$ and ${\Delta Q_{i,load}^{\sigma}}^{(k1)}$ are calculated from equations (5.40) and (5.41) as shown Table C.8.

Table C.8 The calculated values

Node		${P_{i,load}^{\sigma}}^{(k1)}$	${Q_{i,load}^{\sigma}}^{(k1)}$	${\Delta P_{i,load}^{\sigma}}^{(k1)}$	${\Delta Q_{i,load}^{\sigma}}^{(k1)}$
2	A	-0.00516327	-0.00241395	-0.00002504	-0.00009023
	B	-0.00213766	-0.00090205	-0.00002082	-0.00014600
	C	-0.00486280	-0.00226463	-0.00000002	-0.00008246
3	A	-0.00550242	-0.00266858	-0.00000079	-0.00000055
	B	-0.00404250	-0.00195887	0.00000003	0.00000002
	C	-0.00243133	-0.00118066	-0.00000008	0.00000010
4	A	-0.00309601	-0.00139423	-0.00014294	-0.00018026
	B	-0.00229346	-0.00053076	-0.00006465	-0.00061710
	C	-0.00193196	-0.00075592	0.00003462	-0.00015762
5	A	-0.02283031	-0.01939098	0.01959136	0.01781650
	B	-0.02157382	-0.01625677	0.01941534	0.01520872
	C	-0.00318872	-0.00109415	0.00106651	0.00006818
6	A	-0.00186728	-0.00095434	-0.00023204	-0.00006533
	B	-0.00101704	-0.00059040	-0.00026806	-0.00003344
	C	-0.00110608	-0.00056334	-0.00025719	-0.00009722
7	A	-0.00321329	-0.00234711	-0.00164513	-0.00000713
	B	-0.00174494	-0.00160476	-0.00162378	-0.00002969
	C	-0.00220305	-0.00186981	-0.00159164	0.00002868
8	A	-0.00142627	-0.00077841	-0.00026818	-0.00004632
	B	-0.00194257	-0.00104656	-0.00031572	-0.00002644
	C	-0.00319579	-0.00159035	-0.00028970	-0.00009617
9	A	-0.00613168	-0.00294415	-0.00001632	-0.00003988
	B	-0.00613240	-0.00298630	-0.00006854	-0.00002060
	C	-0.00619294	-0.00291013	-0.00003316	-0.00009751
10	A	-0.00130017	-0.00079834	-0.00039427	-0.00002639
	B	-0.00151812	-0.00091456	-0.00022863	0.00006614
	C	-0.00081254	-0.00069369	-0.00039614	0.00010340
11	A	-0.00282487	-0.00177415	-0.00089392	-0.00002526
	B	-0.00220786	-0.00146827	-0.00088637	-0.00002894
	C	-0.00428040	-0.00250257	-0.00087756	0.00000088
12	A	-0.02026046	-0.00242675	0.01540204	0.00007251
	B	-0.00308676	-0.00161587	-0.00028197	-0.00001859
	C	-0.00382433	-0.00383486	0.00002964	0.00199374
13	A	0.00100274	-0.00104991	-0.00319203	-0.00001474
	B	0.00092383	-0.00099402	-0.00314469	-0.00007898
	C	0.00002826	-0.00155074	-0.00306401	0.00007503

Node		$P_{i,load}^{\sigma\,(k1)}$	$Q_{i,load}^{\sigma\,(k1)}$	$\Delta P_{i,load}^{\sigma\,(k1)}$	$\Delta Q_{i,load}^{\sigma\,(k1)}$
14	A	-0.00154241	-0.00073469	-0.00000209	-0.00001507
	B	-0.00127982	-0.00061423	-0.00000529	-0.00000960
	C	-0.00189226	-0.00090404	-0.00000508	-0.00000950
15	A	-0.00007376	-0.00105423	-0.00211553	-0.00001042
	B	0.00007202	-0.00092697	-0.00209325	-0.00004621
	C	-0.00120806	-0.00161656	-0.00205256	0.00004246
16	A	-0.00094507	-0.00187529	-0.00293866	-0.00001409
	B	-0.00143315	-0.00200976	-0.00288381	-0.00007386
	C	-0.00082296	-0.00184613	-0.00281713	0.00007528
17	A	-0.00323708	-0.00157367	-0.00000187	-0.00000082
	B	-0.00202119	-0.00097295	-0.00000004	-0.00000024
	C	-0.00227701	-0.00109660	0.00000020	0.00000036
18	A	-0.01830172	-0.00144613	0.01563259	0.00015655
	B	-0.00266356	-0.00106331	0.00044270	-0.00000969
	C	-0.00518809	-0.00491261	0.00003013	0.00241093
19	A	-0.00194795	-0.00210911	-0.00243063	-0.00000520
	B	-0.00177713	-0.00196793	-0.00240259	-0.00005331
	C	-0.00280786	-0.00255620	-0.00235010	0.00005452

Eighteenth: The linear simultaneous equation (5.7) is solved directly by optimally ordered triangular factorization and Gaussian elimination. The $\Delta\delta_i^{\sigma(k1)}$ and $\Delta\left|V_i^{\sigma(k1)}\right|$ are obtained as shown Table C.9.

Nineteenth: For load buses, $P_{i,load}^{\sigma\,(h0)}\begin{Bmatrix} V_i^{\sigma(k1)} + w_{V_i^\sigma}^{(h0)} \cdot \Delta\left|V_i^{\sigma(k1)}\right| \\ \delta_i^{\sigma(k1)} + w_{\delta_i^\sigma}^{(h0)} \cdot \Delta\delta_i^{\sigma(k1)} \end{Bmatrix}$ and $Q_{i,load}^{\sigma\,(h0)}\begin{Bmatrix} V_i^{\sigma(k1)} + w_{V_i^\sigma}^{(h0)} \cdot \Delta\left|V_i^{\sigma(k1)}\right| \\ \delta_i^{\sigma(k1)} + w_{\delta_i^\sigma}^{(h0)} \cdot \Delta\delta_i^{\sigma(k1)} \end{Bmatrix}$ are calculated from equations (5.44), (5.45), (5.55), (5.56), (5.69) and (5.70) as shown in Table C.9. $\Delta P_{i,load}^{\sigma\,(h0)}$ and $\Delta Q_{i,load}^{\sigma\,(h0)}$ are calculated from equations (5.40) and (5.41) as shown Table C.9.

Table C.9 The calculated values

Node		$\Delta\left\|V_i^{\sigma(k1)}\right\|$	$\Delta\delta_i^{\sigma(k1)}$	$P_{i,load}^{\sigma\,(h0)}$	$Q_{i,load}^{\sigma\,(h0)}$	$\Delta P_{i,load}^{\sigma\,(h0)}$	$\Delta Q_{i,load}^{\sigma\,(h0)}$
2	A	0.00649382	-0.00119277	-0.00502140	-0.00268582	-0.00016691	0.00018164
	B	-0.00059923	0.00526414	-0.00179235	-0.00086469	-0.00036612	-0.00018336
	C	-0.00239365	-0.00205429	-0.00487634	-0.00219614	0.00001352	-0.00015095
3	A	0.00665339	-0.00124003	-0.00550295	-0.00266892	-0.00000026	-0.00000021
	B	-0.00065842	0.00530047	-0.00404256	-0.00195883	0.00000009	-0.00000002
	C	-0.00242812	-0.00206724	-0.00243140	-0.00118056	-0.00000001	-0.00000001
4	A	0.01507662	-0.00312107	-0.00140624	-0.00359287	-0.00183271	0.00201839
	B	-0.00109946	0.01230312	-0.00009047	0.00077805	-0.00226763	-0.00192592
	C	-0.00568612	-0.00469158	-0.00205518	-0.00083486	0.00015784	-0.00007868
5	A	0.14483027	-0.08516060	0.01727894	0.01603619	-0.02051789	-0.01761068
	B	0.04192176	0.14927464	-0.00231405	-0.02048753	0.00015557	0.01943948
	C	-0.00872022	0.00638522	0.00593754	-0.00092704	-0.00805975	-0.00009893
6	A	0.01866416	-0.00297305	-0.00208939	-0.00101620	-0.00000993	-0.00000347

Node		$\Delta\lvert V_i^{\sigma(k1)}\rvert$	$\Delta\delta_i^{\sigma(k1)}$	$P_{i,load}^{\sigma\ (h0)}$	$Q_{i,load}^{\sigma\ (h0)}$	$\Delta P_{i,load}^{\sigma\ (h0)}$	$\Delta Q_{i,load}^{\sigma\ (h0)}$
	B	-0.00211650	0.01416119	-0.00118995	-0.00061584	-0.00009516	-0.00000800
	C	-0.00761892	-0.00760551	-0.00132046	-0.00055253	-0.00004281	-0.00010803
7	A	0.01590815	-0.00429722	-0.00470455	-0.00234143	-0.00015387	-0.00001280
	B	-0.00441357	0.01294380	-0.00319625	-0.00163556	-0.00017247	0.00000111
	C	-0.00999378	-0.00849234	-0.00361849	-0.00184051	-0.00017620	-0.00000061
8	A	0.02244328	-0.00280367	-0.00167904	-0.00082799	-0.00001541	0.00000325
	B	-0.00293731	0.01617859	-0.00215712	-0.00106323	-0.00010117	-0.00000977
	C	-0.00952734	-0.01036520	-0.00344085	-0.00158497	-0.00004464	-0.00010155
9	A	0.02626883	-0.00269983	-0.00615051	-0.00299443	0.00000251	0.00001040
	B	-0.00369461	0.01824157	-0.00613786	-0.00299460	-0.00006309	-0.00001230
	C	-0.01148765	-0.01307453	-0.00621670	-0.00292062	-0.00000940	-0.00008702
10	A	0.02913310	-0.00269644	-0.00165944	-0.00078906	-0.00003500	-0.00003567
	B	-0.00421343	0.01979660	-0.00187126	-0.00095925	0.00012452	0.00011083
	C	-0.01300557	-0.01507453	-0.00108911	-0.00071473	-0.00011957	0.00012445
11	A	0.03209748	-0.00252707	-0.00363063	-0.00176723	-0.00008816	-0.00003218
	B	-0.00432588	0.02092158	-0.00297785	-0.00149258	-0.00011638	-0.00000463
	C	-0.01417515	-0.01648969	-0.00503488	-0.00247949	-0.00012308	-0.00002219
12	A	0.03141746	-0.00306278	0.01397843	-0.00242906	-0.01883685	0.00007483
	B	-0.00453941	0.02073271	-0.00099567	-0.00159362	-0.00237305	-0.00004084
	C	-0.01476849	-0.01649963	-0.00379176	-0.01027868	-0.00000293	0.00843755
13	A	0.02933891	-0.00381045	-0.00186742	-0.00102582	-0.00032187	-0.00003883
	B	-0.00659724	0.01976622	-0.00183322	-0.00107655	-0.00038765	0.00000355
	C	-0.01643929	-0.01737188	-0.00262894	-0.00147143	-0.00040681	-0.00000429
14	A	0.03576468	-0.00198293	-0.00154407	-0.00073380	-0.00000043	-0.00001595
	B	-0.00389148	0.02236563	-0.00127981	-0.00061476	-0.00000530	-0.00000908
	C	-0.01473173	-0.01769032	-0.00189205	-0.00090040	-0.00000529	-0.00001314
15	A	0.03064342	-0.00348640	-0.00196664	-0.00103379	-0.00022264	-0.00003086
	B	-0.00514890	0.02038828	-0.00175314	-0.00097640	-0.00026810	0.00000322
	C	-0.01546220	-0.01672065	-0.00297729	-0.00156829	-0.00028333	-0.00000580
16	A	0.02891442	-0.00428185	-0.00359199	-0.00185246	-0.00029174	-0.00003693
	B	-0.00663387	0.01968247	-0.00396774	-0.00208698	-0.00034922	0.00000336
	C	-0.01687596	-0.01728514	-0.00327125	-0.00176769	-0.00036884	-0.00000317
17	A	0.03588729	-0.00202617	-0.00323589	-0.00157157	-0.00000305	-0.00000292
	B	-0.00390660	0.02239367	-0.00202229	-0.00097349	0.00000106	0.00000031
	C	-0.01479243	-0.01768604	-0.00227641	-0.00109611	-0.00000040	-0.00000013
18	A	0.03940160	-0.00145005	0.01659939	-0.00214209	-0.01926852	0.00085251
	B	-0.00344525	0.02379635	-0.00094926	-0.00102333	-0.00127160	-0.00004967
	C	-0.01527942	-0.01888612	-0.00516840	-0.01264445	0.00001043	0.01014277
19	A	0.03023433	-0.00370463	-0.00411973	-0.00208279	-0.00025884	-0.00003152
	B	-0.00548203	0.02021057	-0.00387154	-0.00202603	-0.00030817	0.00000479
	C	-0.01583262	-0.01683952	-0.00483297	-0.00249761	-0.00032499	-0.00000407

Twentieth: The elements of the Jacobian matrix (J_1, J_2, J_3 and J_4) are calculated from equations (5.47)-(5.54), (5.57)-(5.68) and (5.71)-(5.78).

Twenty-first: The linear simultaneous equation (5.46) is solved directly by optimally ordered triangular factorization and Gaussian elimination. The $\Delta w_{V_i}^{\sigma\ (h0)}$ and $\Delta w_{\delta_i}^{\sigma\ (h0)}$ are obtained as shown in Table C.10.

Twenty-second: The new step-length values $\begin{Bmatrix} w_{V_i^\sigma}^{(h1)} = w_{V_i^\sigma}^{(h0)} + \Delta w_{V_i^\sigma}{}^{(h0)} \\ w_{\delta_i^\sigma}^{(h1)} = w_{\delta_i^\sigma}^{(h0)} + \Delta w_{\delta_i^\sigma}{}^{(h0)} \end{Bmatrix}$ are computed from equations (5.79) and (5.80) as shown in Table C.10.

Table C.10 The calculated values

Node		$\Delta w_{V_i^\sigma}{}^{(h0)}$	$\Delta w_{\delta_i^\sigma}{}^{(h0)}$	$w_{V_i^\sigma}{}^{(h1)}$	$w_{\delta_i^\sigma}{}^{(h1)}$
2	A	-0.91320023	-0.28872029	-0.01320023	0.61127971
	B	-2.49453181	-0.78845798	-1.59453181	0.11154202
	C	-0.52501585	-0.93091291	0.37498415	-0.03091291
3	A	-0.91491320	-0.31371935	-0.01491320	0.58628065
	B	-2.36762661	-0.78949857	-1.46762661	0.11050143
	C	-0.52869473	-0.93184970	0.37130527	-0.03184970
4	A	-0.91561853	-0.34898437	-0.01561853	0.55101563
	B	-2.94135610	-0.79492082	-2.04135610	0.10507918
	C	-0.53245754	-0.94265918	0.36754246	-0.04265918
5	A	-0.94435744	-0.61274819	-0.04435744	0.28725181
	B	0.46113870	-0.83904978	1.36113870	0.06095022
	C	-1.33029109	2.72732718	-0.43029109	3.62732718
6	A	-0.90385740	-0.22430953	-0.00385740	0.67569047
	B	-1.63053252	-0.80971623	-0.73053252	0.09028377
	C	-0.49044928	-0.80611344	0.40955072	0.09388656
7	A	-1.02556334	-0.32111765	-0.12556334	0.57888235
	B	-0.85073371	-0.86023493	0.04926629	0.03976507
	C	-0.44516958	-0.73686194	0.45483042	0.16313806
8	A	-0.89050944	-0.09596046	0.00949056	0.80403954
	B	-1.22702798	-0.81477954	-0.32702798	0.08522046
	C	-0.46852480	-0.75275165	0.43147520	0.14724835
9	A	-0.88025823	0.02717243	0.01974177	0.92717243
	B	-1.00720182	-0.81698492	-0.10720182	0.08301508
	C	-0.45530279	-0.72348273	0.44469721	0.17651727
10	A	-0.87435576	0.10054464	0.02564424	1.00054464
	B	-0.89467668	-0.81773373	0.00532332	0.08226627
	C	-0.44882845	-0.70905607	0.45117155	0.19094393
11	A	-0.86921101	0.19351617	0.03078899	1.09351617
	B	-0.82567309	-0.81624876	0.07432691	0.08375124
	C	-0.44526215	-0.70434320	0.45473785	0.19565680
12	A	-0.87560215	0.04497353	0.02439785	0.94497353
	B	-0.76217146	-0.81939138	0.13782854	0.08060862
	C	-0.42907428	-0.70644597	0.47092572	0.19355403
13	A	-0.93452180	-0.02756145	-0.03452180	0.87243855
	B	-0.56583535	-0.84863234	0.33416465	0.05136766
	C	-0.41449366	-0.67152406	0.48550634	0.22847594
14	A	-0.85077664	0.45064999	0.04922336	1.35064999
	B	-0.86669768	-0.80705105	0.03330232	0.09294895
	C	-0.45124809	-0.70880840	0.44875191	0.19119160
15	A	-0.89520544	-0.01921791	0.00479456	0.88078209
	B	-0.66606034	-0.82926093	0.23393966	0.07073907
	C	-0.41847476	-0.69601610	0.48152524	0.20398390
16	A	-0.93482281	-0.11078975	-0.03482281	0.78921025

Node		$\Delta w_{V_i^\sigma}^{(h0)}$	$\Delta w_{\delta_i^\sigma}^{(h0)}$	$w_{V_i^\sigma}^{(h1)}$	$w_{\delta_i^\sigma}^{(h1)}$
	B	-0.55570681	-0.84743445	0.34429319	0.05256555
	C	-0.40759765	-0.67853319	0.49240235	0.22146681
17	A	-0.85076536	0.42493470	0.04923464	1.32493470
	B	-0.86665712	-0.80702100	0.03334288	0.09297900
	C	-0.45191209	-0.70893232	0.44808791	0.19106768
18	A	-0.83574213	0.89061806	0.06425787	1.79061806
	B	-0.91882435	-0.79905566	-0.01882435	0.10094434
	C	-0.45686346	-0.71270097	0.44313654	0.18729903
19	A	-0.90595697	-0.04650681	-0.00595697	0.85349319
	B	-0.62429859	-0.83446800	0.27570141	0.06553200
	C	-0.41333481	-0.69068463	0.48666519	0.20931537

Twenty-third: For load buses, ${P_{i,load}^{\sigma}}^{(h1)} \begin{Bmatrix} V_i^{\sigma(k1)} + w_{V_i^\sigma}^{(h1)} \cdot \Delta\left|V_i^{\sigma(k1)}\right| \\ \delta_i^{\sigma(k1)} + w_{\delta_i^\sigma}^{(h1)} \cdot \Delta\delta_i^{\sigma(k1)} \end{Bmatrix}$ and ${Q_{i,load}^{\sigma}}^{(h1)} \begin{Bmatrix} V_i^{\sigma(k1)} + w_{V_i^\sigma}^{(h1)} \cdot \Delta\left|V_i^{\sigma(k1)}\right| \\ \delta_i^{\sigma(k1)} + w_{\delta_i^\sigma}^{(h1)} \cdot \Delta\delta_i^{\sigma(k1)} \end{Bmatrix}$ are calculated from equations (5.44), (5.45), (5.55), (5.56), (5.69) and (5.70) as shown in Table C.11. ${\Delta P_{i,load}^{\sigma}}^{(h1)}$ and ${\Delta Q_{i,load}^{\sigma}}^{(h1)}$ are calculated from equations (5.40) and (5.41) as shown Table C.11.

Table C.11 The calculated values

Node		${P_{i,load}^{\sigma}}^{(h1)}$	${Q_{i,load}^{\sigma}}^{(h1)}$	${\Delta P_{i,load}^{\sigma}}^{(h1)}$	${\Delta Q_{i,load}^{\sigma}}^{(h1)}$
2	A	-0.00510738	-0.00263436	-0.00008093	0.00013018
	B	-0.00183366	-0.00102441	-0.00032482	-0.00002364
	C	-0.00482242	-0.00221898	-0.00004040	-0.00012811
3	A	-0.00550302	-0.00266896	-0.00000019	-0.00000017
	B	-0.00404254	-0.00195883	0.00000007	-0.00000002
	C	-0.00243142	-0.00118056	0.00000001	-0.00000001
4	A	-0.00215761	-0.00338370	-0.00108133	0.00180921
	B	-0.00001491	-0.00114033	-0.00234320	-0.00000753
	C	-0.00167031	-0.00087959	-0.00022703	-0.00003395
5	A	-0.02233084	-0.01626383	0.01909189	0.01468934
	B	0.01102886	-0.00042118	-0.01318734	-0.00062687
	C	0.00982219	-0.00129944	-0.01194440	0.00027347
6	A	-0.00208870	-0.00101033	-0.00001061	-0.00000934
	B	-0.00124264	-0.00061399	-0.00004247	-0.00000985
	C	-0.00133966	-0.00062157	-0.00002361	-0.00003899
7	A	-0.00465947	-0.00234950	-0.00019894	-0.00000474
	B	-0.00317190	-0.00163006	-0.00019682	-0.00000440
	C	-0.00360114	-0.00184335	-0.00019355	0.00000222
8	A	-0.00168120	-0.00081741	-0.00001325	-0.00000732
	B	-0.00221371	-0.00106168	-0.00004458	-0.00001132
	C	-0.00346170	-0.00164959	-0.00002379	-0.00003694
9	A	-0.00614384	-0.00298227	-0.00000416	-0.00000176
	B	-0.00617488	-0.00299389	-0.00002607	-0.00001300
	C	-0.00621982	-0.00297617	-0.00000628	-0.00003147

Node		$P_{i,load}^{\sigma\ (h1)}$	$Q_{i,load}^{\sigma\ (h1)}$	$\Delta P_{i,load}^{\sigma\ (h1)}$	$\Delta Q_{i,load}^{\sigma\ (h1)}$
10	A	-0.00165931	-0.00082707	-0.00003513	0.00000234
	B	-0.00182149	-0.00088182	0.00007475	0.00003340
	C	-0.00116197	-0.00068610	-0.00004671	0.00009582
11	A	-0.00365043	-0.00178323	-0.00006836	-0.00001618
	B	-0.00302331	-0.00149466	-0.00007092	-0.00000255
	C	-0.00508739	-0.00249573	-0.00007058	-0.00000595
12	A	-0.01549246	-0.00237448	0.01063404	0.00002025
	B	-0.00198967	-0.00160019	-0.00137905	-0.00003426
	C	-0.00379929	-0.00586313	0.00000461	0.00402200
13	A	-0.00167270	-0.00105149	-0.00051658	-0.00001316
	B	-0.00170677	-0.00105997	-0.00051409	-0.00001303
	C	-0.00253742	-0.00148122	-0.00049833	0.00000551
14	A	-0.00154406	-0.00074026	-0.00000043	-0.00000949
	B	-0.00128216	-0.00062025	-0.00000295	-0.00000359
	C	-0.00189364	-0.00090629	-0.00000371	-0.00000724
15	A	-0.00194715	-0.00105279	-0.00024213	-0.00001186
	B	-0.00178083	-0.00096759	-0.00024040	-0.00000560
	C	-0.00302636	-0.00157588	-0.00023426	0.00000179
16	A	-0.00335968	-0.00187520	-0.00052406	-0.00001418
	B	-0.00379679	-0.00207043	-0.00052017	-0.00001319
	C	-0.00313425	-0.00177658	-0.00050584	0.00000572
17	A	-0.00323641	-0.00157210	-0.00000254	-0.00000239
	B	-0.00202199	-0.00097338	0.00000076	0.00000020
	C	-0.00227669	-0.00109628	-0.00000013	0.00000003
18	A	-0.01486698	-0.00137574	0.01219785	0.00008616
	B	-0.00082520	-0.00103472	-0.00139566	-0.00003828
	C	-0.00517777	-0.00580463	0.00001980	0.00330295
19	A	-0.00405774	-0.00210139	-0.00032083	-0.00001292
	B	-0.00386272	-0.00201358	-0.00031699	-0.00000765
	C	-0.00484953	-0.00250441	-0.00030843	0.00000272

Twenty-fourth: Determine $max\{|\Delta P_{i,load}^{\sigma\ (h1)}|, |\Delta Q_{i,load}^{\sigma\ (h1)}|\} = 0.0191$ and $max\{|\Delta P_{i,load}^{\sigma\ (h0)}|, |\Delta Q_{i,load}^{\sigma\ (h0)}|\} = 0.0205$. After that, go to the next calculation.

Twenty-fifth: The elements of the Jacobian matrix (J_1, J_2, J_3 and J_4) are calculated from equations (5.47)-(5.54), (5.57)-(5.68) and (5.71)-(5.78).

Twenty-sixth: The linear simultaneous equation (5.46) is solved directly by optimally ordered triangular factorization and Gaussian elimination. The $\Delta w_{V_i^\sigma}^{(h1)}$ and $\Delta w_{\delta_i^\sigma}^{(h1)}$ are obtained as shown in Table C.12.

Twenty-seventh: The new step-length values $\begin{Bmatrix} w_{V_i^\sigma}^{(h2)} = w_{V_i^\sigma}^{(h1)} + \Delta w_{V_i^\sigma}^{(h1)} \\ w_{\delta_i^\sigma}^{(h2)} = w_{\delta_i^\sigma}^{(h1)} + \Delta w_{\delta_i^\sigma}^{(h1)} \end{Bmatrix}$ are computed from equations (5.79) and (5.80) as shown in Table C.12.

Table C.12 The calculated values

Node		$\Delta w_{V_i^g}^{(h1)}$	$\Delta w_{\delta_i^g}^{(h1)}$	$w_{V_i^g}^{(h2)}$	$w_{\delta_i^g}^{(h2)}$
2	A	0.96862606	-0.17154179	0.95542583	0.43973792
	B	2.94596168	0.43655920	1.35142987	0.54810122
	C	0.27617537	1.29808238	0.65115952	1.26716946
3	A	0.97159232	-0.11769522	0.95667912	0.46858544
	B	2.75972695	0.44143771	1.29210034	0.55193914
	C	0.28697854	1.29543089	0.65828380	1.26358119
4	A	0.97328513	-0.06167235	0.95766660	0.48934328
	B	3.60161641	0.44386283	1.56026031	0.54894200
	C	0.29526849	1.32721661	0.66281095	1.28455743
5	A	0.94553129	0.45403911	0.90117385	0.74129092
	B	-1.09170696	0.21274028	0.26943174	0.27369050
	C	1.12523055	-3.57591219	0.69493946	0.05141499
6	A	0.99226586	-0.22020014	0.98840846	0.45549033
	B	2.07239466	0.53637140	1.34186214	0.62665518
	C	0.28231731	1.16813897	0.69186803	1.26202552
7	A	1.13005827	0.04688716	1.00449493	0.62576952
	B	1.10732638	0.56120081	1.15659267	0.60096587
	C	0.30094125	1.07395677	0.75577167	1.23709483
8	A	0.99862121	-0.38611412	1.00811178	0.41792541
	B	1.60406448	0.60388130	1.27703649	0.68910176
	C	0.27933555	1.11085560	0.71081074	1.25810395
9	A	1.00210389	-0.53438404	1.02184566	0.39278840
	B	1.34730902	0.65547151	1.24010720	0.73848659
	C	0.28148291	1.08179534	0.72618012	1.25831261
10	A	1.00413210	-0.60877665	1.02977634	0.39176799
	B	1.21707572	0.68672149	1.22239904	0.76898776
	C	0.28541408	1.06913245	0.73658563	1.26007638
11	A	1.00294882	-0.69991674	1.03373781	0.39359943
	B	1.11829935	0.70605117	1.19262626	0.78980240
	C	0.28979804	1.07914206	0.74453589	1.27479887
12	A	1.01019376	-0.49155469	1.03459161	0.45341884
	B	1.07175738	0.70430333	1.20958592	0.78491196
	C	0.28276630	1.07834510	0.75369202	1.27189913
13	A	1.08002827	-0.27650831	1.04550647	0.59593023
	B	0.77998207	0.72967400	1.11414672	0.78104166
	C	0.29191715	1.03360152	0.77742349	1.26207746
14	A	0.98523446	-1.07145253	1.03445782	0.27919746
	B	1.15543444	0.71738768	1.18873676	0.81033663
	C	0.29283244	1.09887512	0.74158435	1.29006672
15	A	1.03267635	-0.35795008	1.03747091	0.52283201
	B	0.95082786	0.71129618	1.18476752	0.78203524
	C	0.28356118	1.06544271	0.76508641	1.26942661
16	A	1.08161155	-0.18064563	1.04678874	0.60856462
	B	0.78467319	0.72482575	1.12896639	0.77739130
	C	0.28896324	1.03866401	0.78136559	1.26013083
17	A	0.98514537	-1.02940326	1.03438001	0.29553143
	B	1.15342903	0.71757509	1.18677190	0.81055409
	C	0.29420841	1.09881729	0.74229631	1.28988497
18	A	0.97079658	-1.70398698	1.03505445	0.08663107
	B	1.20317493	0.72728665	1.18435058	0.82823098

Node		$\Delta w_{V_i^\sigma}^{(h1)}$	$\Delta w_{\delta_i^\sigma}^{(h1)}$	$w_{V_i^\sigma}^{(h2)}$	$w_{\delta_i^\sigma}^{(h2)}$
	C	0.29604590	1.11631327	0.73918244	1.30361230
19	A	1.04505146	-0.30121204	1.03909449	0.55228115
	B	0.89740236	0.71500714	1.17310377	0.78053914
	C	0.28397036	1.05871515	0.77063555	1.26803053

Twenty-eighth: For load buses, ${P_{i,load}^{\sigma}}^{(h2)} \begin{Bmatrix} V_i^{\sigma(k1)} + w_{V_i^\sigma}^{(h2)} \cdot \Delta\left|V_i^{\sigma(k1)}\right| \\ \delta_i^{\sigma(k1)} + w_{\delta_i^\sigma}^{(h2)} \cdot \Delta\delta_i^{\sigma(k1)} \end{Bmatrix}$ and ${Q_{i,load}^{\sigma}}^{(h2)} \begin{Bmatrix} V_i^{\sigma(k1)} + w_{V_i^\sigma}^{(h2)} \cdot \Delta\left|V_i^{\sigma(k1)}\right| \\ \delta_i^{\sigma(k1)} + w_{\delta_i^\sigma}^{(h2)} \cdot \Delta\delta_i^{\sigma(k1)} \end{Bmatrix}$ are calculated from equations (5.44), (5.45), (5.55), (5.56), (5.69) and (5.70) as shown in Table C.13. ${\Delta P_{i,load}^{\sigma}}^{(h2)}$ and ${\Delta Q_{i,load}^{\sigma}}^{(h2)}$ are calculated from equations (5.40) and (5.41) as shown Table C.13.

Table C.13 The calculated values

Node		${P_{i,load}^{\sigma}}^{(h2)}$	${Q_{i,load}^{\sigma}}^{(h2)}$	${\Delta P_{i,load}^{\sigma}}^{(h2)}$	${\Delta Q_{i,load}^{\sigma}}^{(h2)}$
2	A	-0.00519827	-0.00252599	0.00000996	0.00002181
	B	-0.00200709	-0.00109271	-0.00015139	0.00004466
	C	-0.00479054	-0.00222870	-0.00007228	-0.00011838
3	A	-0.00550301	-0.00266893	-0.00000020	-0.00000020
	B	-0.00404252	-0.00195883	0.00000005	-0.00000002
	C	-0.00243142	-0.00118058	0.00000001	0.00000001
4	A	-0.00276020	-0.00273626	-0.00047875	0.00116177
	B	-0.00178308	-0.00139394	-0.00057503	0.00024608
	C	-0.00182055	-0.00109313	-0.00007679	0.00017960
5	A	0.02050407	0.01889010	-0.02374302	-0.02046459
	B	-0.01934983	-0.00216708	0.01719136	0.00111904
	C	0.00009288	-0.00091996	-0.00221510	-0.00010602
6	A	-0.00208926	-0.00100319	-0.00001005	-0.00001648
	B	-0.00121497	-0.00061850	-0.00007013	-0.00000534
	C	-0.00131068	-0.00059381	-0.00005260	-0.00006675
7	A	-0.00461707	-0.00234618	-0.00024135	-0.00000805
	B	-0.00312793	-0.00163112	-0.00024080	-0.00000333
	C	-0.00355652	-0.00184285	-0.00023816	0.00000173
8	A	-0.00168113	-0.00081177	-0.00001332	-0.00001297
	B	-0.00218560	-0.00106570	-0.00007269	-0.00000730
	C	-0.00343393	-0.00162286	-0.00005156	-0.00006367
9	A	-0.00614357	-0.00297811	-0.00000443	-0.00000592
	B	-0.00615048	-0.00299397	-0.00005046	-0.00001293
	C	-0.00619872	-0.00295039	-0.00002738	-0.00005725
10	A	-0.00162465	-0.00085405	-0.00006979	0.00002932
	B	-0.00184410	-0.00087283	0.00009736	0.00002441
	C	-0.00114607	-0.00073381	-0.00006261	0.00014353
11	A	-0.00364535	-0.00178196	-0.00007344	-0.00001745
	B	-0.00301323	-0.00149844	-0.00008101	0.00000123
	C	-0.00507229	-0.00249455	-0.00008567	-0.00000713
12	A	0.01614575	-0.00244182	-0.02100417	0.00008759

Node		$P_{i,load}^{\sigma\ (h2)}$	$Q_{i,load}^{\sigma\ (h2)}$	$\Delta P_{i,load}^{\sigma\ (h2)}$	$\Delta Q_{i,load}^{\sigma\ (h2)}$
	B	-0.00024198	-0.00156464	-0.00312674	-0.00006981
	C	-0.00381172	-0.00388167	0.00001704	0.00204054
13	A	-0.00162008	-0.00104326	-0.00056921	-0.00002140
	B	-0.00164840	-0.00106253	-0.00057246	-0.00001048
	C	-0.00247651	-0.00147957	-0.00055924	0.00000385
14	A	-0.00154302	-0.00073861	-0.00000148	-0.00001115
	B	-0.00127774	-0.00061810	-0.00000737	-0.00000574
	C	-0.00188585	-0.00090121	-0.00001150	-0.00001233
15	A	-0.00193754	-0.00104638	-0.00025175	-0.00001827
	B	-0.00176722	-0.00097011	-0.00025401	-0.00000308
	C	-0.00300964	-0.00157536	-0.00025098	0.00000127
16	A	-0.00330355	-0.00186658	-0.00058018	-0.00002280
	B	-0.00373605	-0.00207293	-0.00058090	-0.00001069
	C	-0.00307098	-0.00177510	-0.00056911	0.00000425
17	A	-0.00323556	-0.00157124	-0.00000339	-0.00000325
	B	-0.00202199	-0.00097348	0.00000076	0.00000029
	C	-0.00227662	-0.00109648	-0.00000019	0.00000024
18	A	0.01864754	-0.00166213	-0.02131667	0.00037255
	B	0.00022568	-0.00099589	-0.00244654	-0.00007711
	C	-0.00518760	-0.00505591	0.00002963	0.00255422
19	A	-0.00404518	-0.00209378	-0.00033339	-0.00002053
	B	-0.00384579	-0.00201630	-0.00033392	-0.00000493
	C	-0.00482931	-0.00250341	-0.00032866	0.00000173

Twenty-ninth: Determine $max\{|\Delta P_{i,load}^{\sigma\ (h2)}|, |\Delta Q_{i,load}^{\sigma\ (h2)}|\} = 0.0237$ and $max\{|\Delta P_{i,load}^{\sigma\ (h1)}|, |\Delta Q_{i,load}^{\sigma\ (h1)}|\} = 0.0191$. Then, update voltage magnitudes, $|V_i^{\sigma(k2)}| = |V_i^{\sigma(k1)}| + w_{V_i^{\sigma}}{}^{(h1)} \cdot \Delta|V_i^{\sigma(k1)}|$, and phase angles, $\delta_i^{\sigma(k2)} = \delta_i^{\sigma(k1)} + w_{\delta_i^{\sigma}}{}^{(h1)} \cdot \Delta\delta_i^{\sigma(k1)}$, by $w_{V_i^{\sigma}}{}^{(h1)}$ and $w_{V_i^{\sigma}}{}^{(h1)}$ at equations (5.42) and (5.43) as shown in Table C.14. After that, renew $w_{V_i^{\sigma}}{}^{(h0)} = w_{V_i^{\sigma}}{}^{(h0)} = 0.8$ and go to ***STEP 3*** of the power flow algorithm.

Table C.14 The updated values

Node		$\lvert V_i^{\sigma(k2)}\rvert$	$\delta_i^{\sigma(k2)}$
2	A	1.04596673	0.01576402
	B	1.04977129	-2.07757154
	C	1.04529548	2.11116812
3	A	1.02239944	0.02204254
	B	1.03278850	-2.08150481
	C	1.04252425	2.11146871
4	A	1.04252666	0.03692485
	B	1.05053213	-2.05472005
	C	1.03990685	2.13378984
5	A	0.99817517	0.08515624
	B	1.07353956	-2.00843504
	C	1.06440367	2.21716685
6	A	1.04199602	0.05671588
	B	1.05148969	-2.03300219

Node		$\left\|V_i^{\sigma(k2)}\right\|$	$\delta_i^{\sigma(k2)}$
	C	1.03493066	2.15380786
7	A	1.05070799	0.08639521
	B	1.06133639	-2.00275965
	C	1.04006241	2.18148316
8	A	1.04115247	0.07285549
	B	1.05235902	-2.01528856
	C	1.03067915	2.17066008
9	A	1.03986285	0.08729398
	B	1.05320213	-1.99978819
	C	1.02713923	2.18604295
10	A	1.03955061	0.09815662
	B	1.05454378	-1.98808655
	C	1.02505969	2.19782146
11	A	1.04046011	0.10707596
	B	1.05777779	-1.97882498
	C	1.02595017	2.20805199
12	A	1.04233184	0.11028086
	B	1.05895803	-1.97566437
	C	1.02752178	2.21084875
13	A	1.04834152	0.12141917
	B	1.06431145	-1.96292125
	C	1.02884088	2.22191973
14	A	1.03864366	0.11028275
	B	1.05860503	-1.97599440
	C	1.02621627	2.21268869
15	A	1.04500695	0.11601932
	B	1.06122713	-1.96931033
	C	1.02823323	2.21638262
16	A	1.04870903	0.12534069
	B	1.06310469	-1.96000196
	C	1.03048792	2.22441305
17	A	1.03514143	0.11076652
	B	1.05682255	-1.97636114
	C	1.02462274	2.21291845
18	A	1.03784094	0.11340426
	B	1.06000801	-1.97311928
	C	1.02717551	2.21726308
19	A	1.04615172	0.11891704
	B	1.062167339	-1.966142685
	C	1.028456518	2.219140986

Thirtieth: For load buses, $P_{i,load}^{\sigma}{}^{(k2)}\begin{Bmatrix}V_i^{\sigma(k2)}\\ \delta_i^{\sigma(k2)}\end{Bmatrix}$ and $Q_{i,load}^{\sigma}{}^{(k2)}\begin{Bmatrix}V_i^{\sigma(k2)}\\ \delta_i^{\sigma(k2)}\end{Bmatrix}$ are calculated from equations (5.1), (5.2), (5.16), (5.17), (5.30) and (5.31) as shown Table C.15. $\Delta P_i^{\sigma(k2)}$ and $\Delta Q_i^{\sigma(k2)}$ are calculated from equations (5.40) and (5.41) as shown in Table C.15.

Table C.15 The calculated values

Node		$P_{i,load}^{\sigma\ (k2)}$	$Q_{i,load}^{\sigma\ (k2)}$	$\Delta P_{i,load}^{\sigma\ (k2)}$	$\Delta Q_{i,load}^{\sigma\ (k2)}$
2	A	-0.00510738	-0.00263436	-0.00008093	0.00013018
	B	-0.00183366	-0.00102441	-0.00032482	-0.00002364
	C	-0.00482242	-0.00221898	-0.00004040	-0.00012811
3	A	-0.00550302	-0.00266896	-0.00000019	-0.00000017
	B	-0.00404254	-0.00195883	0.00000007	-0.00000002
	C	-0.00243142	-0.00118056	0.00000001	-0.00000001
4	A	-0.00215761	-0.00338370	-0.00108133	0.00180921
	B	-0.00001491	-0.00114033	-0.00234320	-0.00000753
	C	-0.00167031	-0.00087959	-0.00022703	-0.00003395
5	A	-0.02233084	-0.01626383	0.01909189	0.01468934
	B	0.01102886	-0.00042118	-0.01318734	-0.00062687
	C	0.00982219	-0.00129944	-0.01194440	0.00027347
6	A	-0.00208870	-0.00101033	-0.00001061	-0.00000934
	B	-0.00124264	-0.00061399	-0.00004247	-0.00000985
	C	-0.00133966	-0.00062157	-0.00002361	-0.00003899
7	A	-0.00465947	-0.00234950	-0.00019894	-0.00000474
	B	-0.00317190	-0.00163006	-0.00019682	-0.00000440
	C	-0.00360114	-0.00184335	-0.00019355	0.00000222
8	A	-0.00168120	-0.00081741	-0.00001325	-0.00000732
	B	-0.00221371	-0.00106168	-0.00004458	-0.00001132
	C	-0.00346170	-0.00164959	-0.00002379	-0.00003694
9	A	-0.00614384	-0.00298227	-0.00000416	-0.00000176
	B	-0.00617488	-0.00299389	-0.00002607	-0.00001300
	C	-0.00621982	-0.00297617	-0.00000628	-0.00003147
10	A	-0.00165931	-0.00082707	-0.00003513	0.00000234
	B	-0.00182149	-0.00088182	0.00007475	0.00003340
	C	-0.00116197	-0.00068610	-0.00004671	0.00009582
11	A	-0.00365043	-0.00178323	-0.00006836	-0.00001618
	B	-0.00302331	-0.00149466	-0.00007092	-0.00000255
	C	-0.00508739	-0.00249573	-0.00007058	-0.00000595
12	A	-0.01549246	-0.00237448	0.01063404	0.00002025
	B	-0.00198967	-0.00160019	-0.00137905	-0.00003426
	C	-0.00379929	-0.00586313	0.00000461	0.00402200
13	A	-0.00167270	-0.00105149	-0.00051658	-0.00001316
	B	-0.00170677	-0.00105997	-0.00051409	-0.00001303
	C	-0.00253742	-0.00148122	-0.00049833	0.00000551
14	A	-0.00154406	-0.00074026	-0.00000043	-0.00000949
	B	-0.00128216	-0.00062025	-0.00000295	-0.00000359
	C	-0.00189364	-0.00090629	-0.00000371	-0.00000724
15	A	-0.00194715	-0.00105279	-0.00024213	-0.00001186
	B	-0.00178083	-0.00096759	-0.00024040	-0.00000560
	C	-0.00302636	-0.00157588	-0.00023426	0.00000179
16	A	-0.00335968	-0.00187520	-0.00052406	-0.00001418
	B	-0.00379679	-0.00207043	-0.00052017	-0.00001319
	C	-0.00313425	-0.00177658	-0.00050584	0.00000572
17	A	-0.00323641	-0.00157210	-0.00000254	-0.00000239
	B	-0.00202199	-0.00097338	0.00000076	0.00000020
	C	-0.00227669	-0.00109628	-0.00000013	0.00000003
18	A	-0.01486698	-0.00137574	0.01219785	0.00008616
	B	-0.00082520	-0.00103472	-0.00139566	-0.00003828

Node		$P_{i,load}^{\sigma}{}^{(k2)}$	$Q_{i,load}^{\sigma}{}^{(k2)}$	$\Delta P_{i,load}^{\sigma}{}^{(k2)}$	$\Delta Q_{i,load}^{\sigma}{}^{(k2)}$
	C	-0.00517777	-0.00580463	0.00001980	0.00330295
19	A	-0.00405774	-0.00210139	-0.00032083	-0.00001292
	B	-0.00386272	-0.00201358	-0.00031699	-0.00000765
	C	-0.00484953	-0.00250441	-0.00030843	0.00000272

Thirty-first: The linear simultaneous equation (5.7) is solved directly by optimally ordered triangular factorization and Gaussian elimination. The $\Delta\delta_i^{\sigma(k2)}$ and $\Delta\left|V_i^{\sigma(k2)}\right|$ are obtained as shown Table C.16.

Thirty-second: For load buses, $P_{i,load}^{\sigma}{}^{(h0)}\left\{\begin{matrix} V_i^{\sigma(k2)}+w_{V_i^{\sigma}}^{(h0)}\cdot\Delta\left|V_i^{\sigma(k2)}\right| \\ \delta_i^{\sigma(k2)}+w_{\delta_i^{\sigma}}^{(h0)}\cdot\Delta\delta_i^{\sigma(k2)} \end{matrix}\right\}$ and $Q_{i,load}^{\sigma}{}^{(h0)}\left\{\begin{matrix} V_i^{\sigma(k2)}+w_{V_i^{\sigma}}^{(h0)}\cdot\Delta\left|V_i^{\sigma(k2)}\right| \\ \delta_i^{\sigma(k2)}+w_{\delta_i^{\sigma}}^{(h0)}\cdot\Delta\delta_i^{\sigma(k2)} \end{matrix}\right\}$ are calculated from equations (5.44), (5.45), (5.55), (5.56), (5.69) and (5.70) as shown in Table C.16. $\Delta P_{i,load}^{\sigma}{}^{(h0)}$ and $\Delta Q_{i,load}^{\sigma}{}^{(h0)}$ are calculated from equations (5.40) and (5.41) as shown Table C.16.

Table C.16 The calculated values

Node		$\Delta\left\|V_i^{\sigma(k2)}\right\|$	$\Delta\delta_i^{\sigma(k2)}$	$P_{i,load}^{\sigma}{}^{(h0)}$	$Q_{i,load}^{\sigma}{}^{(h0)}$	$\Delta P_{i,load}^{\sigma}{}^{(h0)}$	$\Delta Q_{i,load}^{\sigma}{}^{(h0)}$
2	A	0.00629008	0.00020461	-0.00517847	-0.00254415	-0.00000984	0.00003996
	B	-0.00176532	0.00229811	-0.00199657	-0.00107192	-0.00016190	0.00002388
	C	-0.00066107	-0.00266663	-0.00480848	-0.00224566	-0.00005434	-0.00010142
3	A	0.00646439	0.00014595	-0.00550304	-0.00266897	-0.00000016	-0.00000016
	B	-0.00181707	0.00233983	-0.00404251	-0.00195883	0.00000005	-0.00000002
	C	-0.00069682	-0.00267797	-0.00243142	-0.00118057	0.00000001	0.00000000
4	A	0.01467385	0.00019248	-0.00271993	-0.00267903	-0.00051901	0.00110455
	B	-0.00395984	0.00546090	-0.00152062	-0.00130480	-0.00083748	0.00015694
	C	-0.00167893	-0.00622675	-0.00180322	-0.00102132	-0.00009413	0.00010779
5	A	0.13694156	-0.03866624	0.01567724	0.01497124	-0.01891619	-0.01654573
	B	-0.04576628	0.03175673	-0.01739966	-0.00095543	0.01524118	-0.00009262
	C	-0.00981226	-0.02283298	0.00033292	-0.00101321	-0.00245513	-0.00001276
6	A	0.01851981	0.00065467	-0.00209216	-0.00100737	-0.00000716	-0.00001230
	B	-0.00438622	0.00759566	-0.00123306	-0.00061861	-0.00005204	-0.00000523
	C	-0.00215095	-0.00888429	-0.00132627	-0.00061007	-0.00003701	-0.00005048
7	A	0.01797714	-0.00020148	-0.00467924	-0.00234814	-0.00017918	-0.00000609
	B	-0.00488726	0.00726407	-0.00318955	-0.00163182	-0.00017917	-0.00000263
	C	-0.00300754	-0.00912040	-0.00361764	-0.00184231	-0.00017705	0.00000118
8	A	0.02241234	0.00108254	-0.00168525	-0.00081528	-0.00000920	-0.00000945
	B	-0.00471163	0.00976995	-0.00220474	-0.00106645	-0.00005356	-0.00000655
	C	-0.00266132	-0.01151424	-0.00344965	-0.00163860	-0.00003584	-0.00004792
9	A	0.02632410	0.00144275	-0.00614431	-0.00297986	-0.00000369	-0.00000417
	B	-0.00497778	0.01195683	-0.00616338	-0.00299606	-0.00003756	-0.00001083
	C	-0.00323358	-0.01414396	-0.00620733	-0.00296466	-0.00001877	-0.00004298
10	A	0.02925348	0.00164153	-0.00164675	-0.00084511	-0.00004770	0.00002037
	B	-0.00512806	0.01359475	-0.00182783	-0.00087186	0.00008109	0.00002344
	C	-0.00371197	-0.01611667	-0.00116254	-0.00070246	-0.00004614	0.00011218

Node		$\Delta\lvert V_i^{\sigma(k2)}\rvert$	$\Delta\delta_i^{\sigma(k2)}$	$P_{i,load}^{\sigma\ (h0)}$	$Q_{i,load}^{\sigma\ (h0)}$	$\Delta P_{i,load}^{\sigma\ (h0)}$	$\Delta Q_{i,load}^{\sigma\ (h0)}$
11	A	0.03219213	0.00176874	-0.00367163	-0.00178583	-0.00004716	-0.00001359
	B	-0.00483763	0.01477170	-0.00304125	-0.00149862	-0.00005298	0.00000141
	C	-0.00410793	-0.01779472	-0.00510168	-0.00249635	-0.00005628	-0.00000533
12	A	0.03173772	0.00150553	0.01215869	-0.00242000	-0.01701711	0.00006576
	B	-0.00486515	0.01460212	-0.00097824	-0.00158274	-0.00239048	-0.00005171
	C	-0.00417603	-0.01779229	-0.00380634	-0.00389983	0.00001165	0.00205871
13	A	0.03168685	0.00105362	-0.00181085	-0.00104825	-0.00037844	-0.00001640
	B	-0.00514573	0.01442290	-0.00183717	-0.00106628	-0.00038370	-0.00000672
	C	-0.00479891	-0.01795560	-0.00266087	-0.00147702	-0.00037488	0.00000131
14	A	0.03523660	0.00212461	-0.00154346	-0.00074076	-0.00000104	-0.00000900
	B	-0.00449635	0.01604482	-0.00127980	-0.00061945	-0.00000531	-0.00000438
	C	-0.00431393	-0.01943945	-0.00188924	-0.00090419	-0.00000810	-0.00000935
15	A	0.03164473	0.00124796	-0.00202252	-0.00105075	-0.00016676	-0.00001391
	B	-0.00489572	0.01450210	-0.00185173	-0.00097142	-0.00016951	-0.00000176
	C	-0.00438448	-0.01781489	-0.00309304	-0.00157437	-0.00016758	0.00000028
16	A	0.03127417	0.00077350	-0.00349527	-0.00187193	-0.00038847	-0.00001745
	B	-0.00520542	0.01426636	-0.00392503	-0.00207669	-0.00039192	-0.00000692
	C	-0.00487653	-0.01795345	-0.00325605	-0.00177242	-0.00038404	0.00000156
17	A	0.03535420	0.00208574	-0.00323627	-0.00157194	-0.00000268	-0.00000255
	B	-0.00450598	0.01606914	-0.00202187	-0.00097341	0.00000064	0.00000022
	C	-0.00435206	-0.01943372	-0.00227667	-0.00109640	-0.00000015	0.00000016
18	A	0.03825094	0.00247087	0.01464011	-0.00158893	-0.01730924	0.00029935
	B	-0.00414524	0.01730676	-0.00035066	-0.00101575	-0.00187020	-0.00005725
	C	-0.00452341	-0.02108282	-0.00518062	-0.00475556	0.00002265	0.00225387
19	A	0.03159644	0.00111588	-0.00415610	-0.00209867	-0.00022248	-0.00001564
	B	-0.00491959	0.01445070	-0.00395551	-0.00201818	-0.00022420	-0.00000306
	C	-0.00449600	-0.01782825	-0.00493720	-0.00250207	-0.00022077	0.00000039

Thirty-third: The elements of the Jacobian matrix (J_1, J_2, J_3 and J_4) are calculated from equations (5.47)-(5.54), (5.57)-(5.68) and (5.71)-(5.78).

Thirty-fourth: The linear simultaneous equation (5.46) is solved directly by optimally ordered triangular factorization and Gaussian elimination. The $\Delta w_{V_i^{\sigma}}{}^{(h0)}$ and $\Delta w_{\delta_i^{\sigma}}{}^{(h0)}$ are obtained as shown in Table C.17.

Thirty-fifth: The new step-length values $\begin{Bmatrix} w_{V_i^{\sigma}}^{(h1)} = w_{V_i^{\sigma}}^{(h0)} + \Delta w_{V_i^{\sigma}}{}^{(h0)} \\ w_{\delta_i^{\sigma}}^{(h1)} = w_{\delta_i^{\sigma}}^{(h0)} + \Delta w_{\delta_i^{\sigma}}{}^{(h0)} \end{Bmatrix}$ are computed from equations (5.79) and (5.80) as shown in Table C.17.

Table C.17 The calculated values

Node		$\Delta w_{V_i^{\sigma}}{}^{(h0)}$	$\Delta w_{\delta_i^{\sigma}}{}^{(h0)}$	$w_{V_i^{\sigma}}{}^{(h1)}$	$w_{\delta_i^{\sigma}}{}^{(h1)}$
2	A	-0.65786488	-0.70580099	0.14213512	0.09419901
	B	-0.83802289	-0.44569304	-0.03802289	0.35430696
	C	-0.58402723	-0.53842102	0.21597277	0.26157898
3	A	-0.65875253	-0.71742527	0.14124747	0.08257473
	B	-0.83539992	-0.45038003	-0.03539992	0.34961997
	C	-0.59059293	-0.54113775	0.20940707	0.25886225

Node		$\Delta w_{V_i^{\sigma}}^{(h0)}$	$\Delta w_{\delta_i^{\sigma}}^{(h0)}$	$w_{V_i^{\sigma}}^{(h1)}$	$w_{\delta_i^{\sigma}}^{(h1)}$
4	A	-0.65784017	-0.73254523	0.14215983	0.06745477
	B	-0.85796434	-0.45081988	-0.05796434	0.34918012
	C	-0.58104112	-0.53743327	0.21895888	0.26256673
5	A	-0.81381708	-0.68127777	-0.01381708	0.11872223
	B	-1.41984769	-0.30941150	-0.61984769	0.49058850
	C	-0.13007010	-0.90840256	0.66992990	-0.10840256
6	A	-0.61297923	-0.23423060	0.18702077	0.56576940
	B	-0.74884008	-0.47354146	0.05115992	0.32645854
	C	-0.65294032	-0.48847915	0.14705968	0.31152085
7	A	-0.61920886	-1.66620978	0.18079114	-0.86620978
	B	-0.71972425	-0.47863647	0.08027575	0.32136353
	C	-0.60294646	-0.48794911	0.19705354	0.31205089
8	A	-0.58284766	-0.15279206	0.21715234	0.64720794
	B	-0.66234677	-0.48435448	0.13765323	0.31564552
	C	-0.69247485	-0.46112897	0.10752515	0.33887103
9	A	-0.56134352	-0.10738509	0.23865648	0.69261491
	B	-0.58793784	-0.49010246	0.21206216	0.30989754
	C	-0.71242780	-0.44333136	0.08757220	0.35666864
10	A	-0.54879987	-0.07095326	0.25120013	0.72904674
	B	-0.53739918	-0.49260376	0.26260082	0.30739624
	C	-0.71851565	-0.43338403	0.08148435	0.36661597
11	A	-0.54115559	-0.07168271	0.25884441	0.72831729
	B	-0.50914108	-0.49392341	0.29085892	0.30607659
	C	-0.70722474	-0.43159215	0.09277526	0.36840785
12	A	-0.53889355	0.05442285	0.26110645	0.85442285
	B	-0.48121829	-0.49392852	0.31878171	0.30607148
	C	-0.71963453	-0.42021896	0.08036547	0.37978104
13	A	-0.54323835	0.22219912	0.25676165	1.02219912
	B	-0.49778848	-0.49546591	0.30221152	0.30453409
	C	-0.66556776	-0.43065509	0.13443224	0.36934491
14	A	-0.53438542	-0.12095956	0.26561458	0.67904044
	B	-0.47956665	-0.49451727	0.32043335	0.30548273
	C	-0.70947202	-0.43029664	0.09052798	0.36970336
15	A	-0.53938740	0.17055993	0.26061260	0.97055993
	B	-0.47862607	-0.49438032	0.32137393	0.30561968
	C	-0.70549924	-0.41992667	0.09450076	0.38007333
16	A	-0.54105453	0.58108691	0.25894547	1.38108691
	B	-0.47132282	-0.49554614	0.32867718	0.30445386
	C	-0.67581421	-0.41943291	0.12418579	0.38056709
17	A	-0.53450497	-0.11276343	0.26549503	0.68723657
	B	-0.48002818	-0.49472792	0.31997182	0.30527208
	C	-0.70846557	-0.43045009	0.09153443	0.36954991
18	A	-0.52863491	-0.15569319	0.27136509	0.64430681
	B	-0.44496151	-0.49490860	0.35503849	0.30509140
	C	-0.71090844	-0.42912688	0.08909156	0.37087312
19	A	-0.53968845	0.25076472	0.26031155	1.05076472
	B	-0.47716301	-0.49464733	0.32283699	0.30535267
	C	-0.69846521	-0.41978072	0.10153479	0.38021928

Thirty-sixth: For load buses, ${P_{i,load}^{\sigma}}^{(h1)} \begin{Bmatrix} V_i^{\sigma(k2)} + w_{V_i^{\sigma}}^{(h1)} \cdot \Delta\left|V_i^{\sigma(k2)}\right| \\ \delta_i^{\sigma(k2)} + w_{\delta_i^{\sigma}}^{(h1)} \cdot \Delta\delta_i^{\sigma(k2)} \end{Bmatrix}$ and ${Q_{i,load}^{\sigma}}^{(h1)} \begin{Bmatrix} V_i^{\sigma(k2)} + w_{V_i^{\sigma}}^{(h1)} \cdot \Delta\left|V_i^{\sigma(k2)}\right| \\ \delta_i^{\sigma(k2)} + w_{\delta_i^{\sigma}}^{(h1)} \cdot \Delta\delta_i^{\sigma(k2)} \end{Bmatrix}$ are calculated from equations (5.44), (5.45), (5.55), (5.56), (5.69) and (5.70) as shown in Table C.18. ${\Delta P_{i,load}^{\sigma}}^{(h1)}$ and ${\Delta Q_{i,load}^{\sigma}}^{(h1)}$ are calculated from equations (5.40) and (5.41) as shown Table C.18.

Table C.18 The calculated values

Node		${P_{i,load}^{\sigma}}^{(h1)}$	${Q_{i,load}^{\sigma}}^{(h1)}$	${\Delta P_{i,load}^{\sigma}}^{(h1)}$	${\Delta Q_{i,load}^{\sigma}}^{(h1)}$
2	A	-0.00519424	-0.00251365	0.00000593	0.00000947
	B	-0.00211462	-0.00107285	-0.00004386	0.00002481
	C	-0.00483912	-0.00231392	-0.00002370	-0.00003316
3	A	-0.00550312	-0.00266904	-0.00000009	-0.00000009
	B	-0.00404248	-0.00195884	0.00000002	-0.00000001
	C	-0.00243142	-0.00118057	0.00000000	0.00000000
4	A	-0.00295361	-0.00225161	-0.00028534	0.00067712
	B	-0.00211456	-0.00125579	-0.00024354	0.00010793
	C	-0.00186615	-0.00106375	-0.00003120	0.00015022
5	A	-0.02232867	-0.01747612	0.01908973	0.01590163
	B	0.01943308	-0.00182255	-0.02159155	0.00077450
	C	-0.00196252	-0.00095685	-0.00015969	-0.00006912
6	A	-0.00208981	-0.00102077	-0.00000950	0.00000110
	B	-0.00126685	-0.00061525	-0.00001825	-0.00000859
	C	-0.00135466	-0.00064844	-0.00000862	-0.00001212
7	A	-0.00474779	-0.00235145	-0.00011063	-0.00000278
	B	-0.00326044	-0.00163269	-0.00010829	-0.00000177
	C	-0.00368754	-0.00184233	-0.00010715	0.00000120
8	A	-0.00168363	-0.00082574	-0.00001082	0.00000100
	B	-0.00223923	-0.00106363	-0.00001906	-0.00000937
	C	-0.00347638	-0.00167505	-0.00000911	-0.00001147
9	A	-0.00614363	-0.00298661	-0.00000437	0.00000258
	B	-0.00619141	-0.00299762	-0.00000954	-0.00000928
	C	-0.00622589	-0.00299797	-0.00000021	-0.00000967
10	A	-0.00167821	-0.00082721	-0.00001624	0.00000248
	B	-0.00176193	-0.00085437	0.00001519	0.00000595
	C	-0.00118853	-0.00061564	-0.00002015	0.00002536
11	A	-0.00367795	-0.00179382	-0.00004084	-0.00000559
	B	-0.00305298	-0.00149460	-0.00004125	-0.00000261
	C	-0.00511698	-0.00249938	-0.00004098	-0.00000231
12	A	-0.01160748	-0.00235423	0.00674907	0.00000000
	B	-0.00283661	-0.00162422	-0.00053211	-0.00001024
	C	-0.00379260	-0.00301653	-0.00000209	0.00117540
13	A	-0.00188425	-0.00105926	-0.00030504	-0.00000539
	B	-0.00192158	-0.00106606	-0.00029928	-0.00000694
	C	-0.00274491	-0.00148016	-0.00029084	0.00000445
14	A	-0.00154382	-0.00074756	-0.00000067	-0.00000219
	B	-0.00128360	-0.00062138	-0.00000151	-0.00000246

Node		$P_{i,load}^{\sigma\ (h1)}$	$Q_{i,load}^{\sigma\ (h1)}$	$\Delta P_{i,load}^{\sigma\ (h1)}$	$\Delta Q_{i,load}^{\sigma\ (h1)}$
	C	-0.00189576	-0.00091086	-0.00000158	-0.00000267
15	A	-0.00205345	-0.00105953	-0.00013584	-0.00000513
	B	-0.00188775	-0.00097031	-0.00013348	-0.00000288
	C	-0.00312998	-0.00157560	-0.00013064	0.00000150
16	A	-0.00357693	-0.00188363	-0.00030680	-0.00000575
	B	-0.00401690	-0.00207664	-0.00030006	-0.00000697
	C	-0.00334769	-0.00177550	-0.00029239	0.00000464
17	A	-0.00323797	-0.00157353	-0.00000098	-0.00000096
	B	-0.00202149	-0.00097325	0.00000026	0.00000006
	C	-0.00227677	-0.00109629	-0.00000004	0.00000005
18	A	-0.01081512	-0.00130441	0.00814599	0.00001483
	B	-0.00177568	-0.00105867	-0.00044518	-0.00001433
	C	-0.00515973	-0.00390238	0.00000177	0.00140070
19	A	-0.00419986	-0.00210876	-0.00017871	-0.00000555
	B	-0.00400489	-0.00201736	-0.00017482	-0.00000387
	C	-0.00498724	-0.00250392	-0.00017072	0.00000223

Thirty-seventh: Determine $max\{|\Delta P_{i,load}^{\sigma\ (h1)}|, |\Delta Q_{i,load}^{\sigma\ (h1)}|\} = 0.0216$ and $max\{|\Delta P_{i,load}^{\sigma\ (h0)}|, |\Delta Q_{i,load}^{\sigma\ (h0)}|\} = 0.0189$. Then, update voltage magnitudes, $|V_i^{\sigma(k3)}| = |V_i^{\sigma(k2)}| + w_{V_i}^{\sigma(h0)} \cdot \Delta|V_i^{\sigma(k2)}|$, and phase angles, $\delta_i^{\sigma(k3)} = \delta_i^{\sigma(k2)} + w_{\delta_i}^{\sigma(h0)} \cdot \Delta\delta_i^{\sigma(k2)}$, by $w_{V_i}^{\sigma(h0)}$ and $w_{V_i}^{\sigma(h0)}$ at equations (5.42) and (5.43) as shown in Table C.19. After that, renew $w_{V_i}^{\sigma(h0)} = w_{V_i}^{\sigma(h0)} = 0.7$ and go to ***STEP 3*** of the power flow algorithm.

Table C.19 The updated values

Node		$\lvert V_i^{\sigma(k3)}\rvert$	$\delta_i^{\sigma(k3)}$
2	A	1.05099879	0.01592771
	B	1.04835903	-2.07573305
	C	1.04476663	2.10903481
3	A	1.02757095	0.02215929
	B	1.03133484	-2.07963294
	C	1.04196679	2.10932634
4	A	1.05426574	0.03707884
	B	1.04736426	-2.05035133
	C	1.03856370	2.12880845
5	A	1.10772842	0.05422325
	B	1.03692654	-1.98302966
	C	1.05655386	2.19890046
6	A	1.05681187	0.05723961
	B	1.04798071	-2.02692566
	C	1.03320990	2.14670043
7	A	1.06508970	0.08623402
	B	1.05742658	-1.99694839
	C	1.03765638	2.17418683
8	A	1.05908234	0.07372152
	B	1.04858971	-2.00747260
	C	1.02855009	2.16144869

Node		$\left\|V_i^{\sigma(k3)}\right\|$	$\delta_i^{\sigma(k3)}$
9	A	1.06092212	0.08844818
	B	1.04921991	-1.99022273
	C	1.02455237	2.17472778
10	A	1.06295339	0.09946984
	B	1.05044133	-1.97721075
	C	1.02209011	2.18492812
11	A	1.06621382	0.10849095
	B	1.05390769	-1.96700762
	C	1.02266383	2.19381621
12	A	1.06772201	0.11148528
	B	1.05506591	-1.96398267
	C	1.02418095	2.19661492
13	A	1.07369100	0.12226207
	B	1.06019487	-1.95138294
	C	1.02500175	2.20755525
14	A	1.06683294	0.11198244
	B	1.05500795	-1.96315854
	C	1.02276513	2.19713713
15	A	1.07032274	0.11701769
	B	1.05731055	-1.95770865
	C	1.02472565	2.20213071
16	A	1.07372836	0.12595949
	B	1.05894036	-1.94858887
	C	1.02658670	2.21005029
17	A	1.06342479	0.11243511
	B	1.05321776	-1.96350583
	C	1.02114109	2.19737147
18	A	1.06844169	0.11538096
	B	1.05669182	-1.95927386
	C	1.02355678	2.20039682
19	A	1.07142887	0.11980974
	B	1.05823167	-1.95458213
	C	1.02485972	2.20487838

Thirty-eighth: For load buses, $P_{i,load}^{\sigma}{}^{(k3)}\begin{Bmatrix}V_i^{\sigma(k3)}\\ \delta_i^{\sigma(k3)}\end{Bmatrix}$ and $Q_{i,load}^{\sigma}{}^{(k3)}\begin{Bmatrix}V_i^{\sigma(k3)}\\ \delta_i^{\sigma(k3)}\end{Bmatrix}$ are calculated from equations (5.1), (5.2), (5.16), (5.17), (5.30) and (5.31) as shown Table C.20. $\Delta P_{i,load}^{\sigma}{}^{(k3)}$ and $\Delta Q_{i,load}^{\sigma}{}^{(k3)}$ are calculated from equations (5.40) and (5.41) as shown Table C.20.

Table C.20 The calculated values

Node		$P_{i,load}^{\sigma}{}^{(k3)}$	$Q_{i,load}^{\sigma}{}^{(k3)}$	$\Delta P_{i,load}^{\sigma}{}^{(k3)}$	$\Delta Q_{i,load}^{\sigma}{}^{(k3)}$
2	A	-0.00517847	-0.00254415	-0.00000984	0.00003996
	B	-0.00199657	-0.00107192	-0.00016190	0.00002388
	C	-0.00480848	-0.00224566	-0.00005434	-0.00010142
3	A	-0.00550304	-0.00266897	-0.00000016	-0.00000016
	B	-0.00404251	-0.00195883	0.00000005	-0.00000002
	C	-0.00243142	-0.00118057	0.00000001	0.00000000
4	A	-0.00271993	-0.00267903	-0.00051901	0.00110455

Node		$P_{i,load}^{\sigma\ (k3)}$	$Q_{i,load}^{\sigma\ (k3)}$	$\Delta P_{i,load}^{\sigma\ (k3)}$	$\Delta Q_{i,load}^{\sigma\ (k3)}$
	B	-0.00152062	-0.00130480	-0.00083748	0.00015694
	C	-0.00180322	-0.00102132	-0.00009413	0.00010779
5	A	0.01567724	0.01497124	-0.01891619	-0.01654573
	B	-0.01739966	-0.00095543	0.01524118	-0.00009262
	C	0.00033292	-0.00101321	-0.00245513	-0.00001276
6	A	-0.00209216	-0.00100737	-0.00000716	-0.00001230
	B	-0.00123306	-0.00061861	-0.00005204	-0.00000523
	C	-0.00132627	-0.00061007	-0.00003701	-0.00005048
7	A	-0.00467924	-0.00234814	-0.00017918	-0.00000609
	B	-0.00318955	-0.00163182	-0.00017917	-0.00000263
	C	-0.00361764	-0.00184231	-0.00017705	0.00000118
8	A	-0.00168525	-0.00081528	-0.00000920	-0.00000945
	B	-0.00220474	-0.00106645	-0.00005356	-0.00000655
	C	-0.00344965	-0.00163860	-0.00003584	-0.00004792
9	A	-0.00614431	-0.00297986	-0.00000369	-0.00000417
	B	-0.00616338	-0.00299606	-0.00003756	-0.00001083
	C	-0.00620733	-0.00296466	-0.00001877	-0.00004298
10	A	-0.00164675	-0.00084511	-0.00004770	0.00002037
	B	-0.00182783	-0.00087186	0.00008109	0.00002344
	C	-0.00116254	-0.00070246	-0.00004614	0.00011218
11	A	-0.00367163	-0.00178583	-0.00004716	-0.00001359
	B	-0.00304125	-0.00149862	-0.00005298	0.00000141
	C	-0.00510168	-0.00249635	-0.00005628	-0.00000533
12	A	0.01215869	-0.00242000	-0.01701711	0.00006576
	B	-0.00097824	-0.00158274	-0.00239048	-0.00005171
	C	-0.00380634	-0.00389983	0.00001165	0.00205871
13	A	-0.00181085	-0.00104825	-0.00037844	-0.00001640
	B	-0.00183717	-0.00106628	-0.00038370	-0.00000672
	C	-0.00266087	-0.00147702	-0.00037488	0.00000131
14	A	-0.00154346	-0.00074076	-0.00000104	-0.00000900
	B	-0.00127980	-0.00061945	-0.00000531	-0.00000438
	C	-0.00188924	-0.00090419	-0.00000810	-0.00000935
15	A	-0.00202252	-0.00105075	-0.00016676	-0.00001391
	B	-0.00185173	-0.00097142	-0.00016951	-0.00000176
	C	-0.00309304	-0.00157437	-0.00016758	0.00000028
16	A	-0.00349527	-0.00187193	-0.00038847	-0.00001745
	B	-0.00392503	-0.00207669	-0.00039192	-0.00000692
	C	-0.00325605	-0.00177242	-0.00038404	0.00000156
17	A	-0.00323627	-0.00157194	-0.00000268	-0.00000255
	B	-0.00202187	-0.00097341	0.00000064	0.00000022
	C	-0.00227667	-0.00109640	-0.00000015	0.00000016
18	A	0.01464011	-0.00158893	-0.01730924	0.00029935
	B	-0.00035066	-0.00101575	-0.00187020	-0.00005725
	C	-0.00518062	-0.00475556	0.00002265	0.00225387
19	A	-0.00415610	-0.00209867	-0.00022248	-0.00001564
	B	-0.00395551	-0.00201818	-0.00022420	-0.00000306
	C	-0.00493720	-0.00250207	-0.00022077	0.00000039

Thirty-ninth: The linear simultaneous equation (5.7) is solved directly by optimally ordered triangular factorization and Gaussian elimination. The $\Delta\delta_i^{\sigma(k3)}$ and $\Delta\left|V_i^{\sigma(k3)}\right|$ are obtained as shown Table C.21.

Fortieth: For load buses, ${P_{i,load}^{\sigma}}^{(h0)}\begin{Bmatrix} V_i^{\sigma(k3)} + w_{V_i^{\sigma}}^{(h0)} \cdot \Delta\left|V_i^{\sigma(k3)}\right| \\ \delta_i^{\sigma(k3)} + w_{\delta_i^{\sigma}}^{(h0)} \cdot \Delta\delta_i^{\sigma(k3)} \end{Bmatrix}$ and ${Q_{i,load}^{\sigma}}^{(h0)}\begin{Bmatrix} V_i^{\sigma(k3)} + w_{V_i^{\sigma}}^{(h0)} \cdot \Delta\left|V_i^{\sigma(k3)}\right| \\ \delta_i^{\sigma(k3)} + w_{\delta_i^{\sigma}}^{(h0)} \cdot \Delta\delta_i^{\sigma(k3)} \end{Bmatrix}$ are calculated from equations (5.44), (5.45), (5.55), (5.56), (5.69) and (5.70) as shown in Table C.21. ${\Delta P_{i,load}^{\sigma}}^{(h0)}$ and ${\Delta Q_{i,load}^{\sigma}}^{(h0)}$ are calculated from equations (5.40) and (5.41) as shown Table C.21.

Table C.21 The calculated values

Node		$\Delta\left\|V_i^{\sigma(k3)}\right\|$	$\Delta\delta_i^{\sigma(k3)}$	${P_{i,load}^{\sigma}}^{(h0)}$	${Q_{i,load}^{\sigma}}^{(h0)}$	${\Delta P_{i,load}^{\sigma}}^{(h0)}$	${\Delta Q_{i,load}^{\sigma}}^{(h0)}$
2	A	-0.00413802	-0.00014441	-0.00518827	-0.00252082	-0.00000004	0.00001663
	B	0.00147938	-0.00102425	-0.00208843	-0.00106736	-0.00007005	0.00001931
	C	0.00038608	0.00143577	-0.00483491	-0.00230042	-0.00002791	-0.00004667
3	A	-0.00425843	-0.00010471	-0.00550312	-0.00266904	-0.00000009	-0.00000009
	B	0.00151798	-0.00105381	-0.00404249	-0.00195884	0.00000002	-0.00000001
	C	0.00041154	0.00144915	-0.00243142	-0.00118057	0.00000000	0.00000000
4	A	-0.00965305	-0.00014100	-0.00294179	-0.00223802	-0.00029715	0.00066353
	B	0.00339740	-0.00246188	-0.00198773	-0.00124736	-0.00037038	0.00009950
	C	0.00097553	0.00334646	-0.00185362	-0.00101955	-0.00004372	0.00010601
5	A	-0.11144538	0.02634245	-0.01760117	0.00379753	0.01436223	-0.00537202
	B	0.06498114	-0.00982590	0.01452565	-0.00155047	-0.01668413	0.00050243
	C	0.00127628	0.02074154	-0.00130994	-0.00098807	-0.00081227	-0.00003790
6	A	-0.01135226	-0.00015334	-0.00209218	-0.00101651	-0.00000713	-0.00000316
	B	0.00328458	-0.00359686	-0.00126025	-0.00061804	-0.00002486	-0.00000580
	C	0.00140444	0.00433979	-0.00134764	-0.00063947	-0.00001564	-0.00002109
7	A	-0.01113160	0.00033572	-0.00474679	-0.00235104	-0.00011163	-0.00000319
	B	0.00351748	-0.00347685	-0.00325846	-0.00163271	-0.00011027	-0.00000174
	C	0.00181339	0.00445029	-0.00368566	-0.00184215	-0.00010903	0.00000102
8	A	-0.01306298	-0.00016540	-0.00168595	-0.00082235	-0.00000850	-0.00000238
	B	0.00312073	-0.00473212	-0.00223248	-0.00106640	-0.00002581	-0.00000660
	C	0.00184290	0.00530955	-0.00346986	-0.00166650	-0.00001563	-0.00002003
9	A	-0.01477686	-0.00015493	-0.00614474	-0.00298405	-0.00000325	0.00000003
	B	0.00292663	-0.00586007	-0.00618501	-0.00299910	-0.00001593	-0.00000780
	C	0.00230369	0.00627046	-0.00622036	-0.00299001	-0.00000573	-0.00001763
10	A	-0.01605430	-0.00011647	-0.00167138	-0.00083194	-0.00002306	0.00000721
	B	0.00275581	-0.00669683	-0.00177774	-0.00085824	0.00003099	0.00000982
	C	0.00266711	0.00698471	-0.00118426	-0.00063625	-0.00002442	0.00004597
11	A	-0.01742095	-0.00012679	-0.00368183	-0.00179252	-0.00003696	-0.00000689
	B	0.00246304	-0.00729609	-0.00305544	-0.00149621	-0.00003880	-0.00000100
	C	0.00290523	0.00768006	-0.00511839	-0.00249895	-0.00003957	-0.00000273
12	A	-0.01710325	0.00008193	-0.00876425	-0.00237392	0.00390583	0.00001969
	B	0.00234120	-0.00721240	-0.00240798	-0.00161394	-0.00096074	-0.00002051
	C	0.00300522	0.00747666	-0.00379718	-0.00305682	0.00000249	0.00121570

Node		$\Delta\lvert V_i^{\sigma(k3)}\rvert$	$\Delta\delta_i^{\sigma(k3)}$	$P_{i,load}^{\sigma\ (h0)}$	$Q_{i,load}^{\sigma\ (h0)}$	$\Delta P_{i,load}^{\sigma\ (h0)}$	$\Delta Q_{i,load}^{\sigma\ (h0)}$
13	A	-0.01721351	0.00023411	-0.00190730	-0.00105715	-0.00028199	-0.00000751
	B	0.00256148	-0.00714605	-0.00194094	-0.00106704	-0.00027992	-0.00000596
	C	0.00319400	0.00773267	-0.00276323	-0.00147874	-0.00027252	0.00000303
14	A	-0.01882992	-0.00025699	-0.00154386	-0.00074598	-0.00000064	-0.00000378
	B	0.00215630	-0.00793444	-0.00128278	-0.00062132	-0.00000233	-0.00000252
	C	0.00306061	0.00836473	-0.00189414	-0.00090942	-0.00000321	-0.00000411
15	A	-0.01706877	0.00021285	-0.00206383	-0.00105797	-0.00012546	-0.00000668
	B	0.00234322	-0.00716955	-0.00189647	-0.00097099	-0.00012477	-0.00000219
	C	0.00309325	0.00748095	-0.00313809	-0.00157510	-0.00012253	0.00000101
16	A	-0.01692103	0.00044947	-0.00359826	-0.00188138	-0.00028548	-0.00000801
	B	0.00245343	-0.00706964	-0.00403458	-0.00207759	-0.00028237	-0.00000602
	C	0.00329563	0.00753027	-0.00336440	-0.00177405	-0.00027569	0.00000320
17	A	-0.01889700	-0.00023520	-0.00323766	-0.00157325	-0.00000128	-0.00000124
	B	0.00216300	-0.00794985	-0.00202155	-0.00097328	0.00000032	0.00000010
	C	0.00308328	0.00836525	-0.00227675	-0.00109631	-0.00000006	0.00000007
18	A	-0.02022078	-0.00038470	-0.00818688	-0.00138655	0.00551775	0.00009697
	B	0.00184447	-0.00856527	-0.00144828	-0.00104883	-0.00077258	-0.00002417
	C	0.00321573	0.00904721	-0.00516566	-0.00387988	0.00000769	0.00137820
19	A	-0.01705223	0.00027982	-0.00421280	-0.00210692	-0.00016578	-0.00000739
	B	0.00234745	-0.00714800	-0.00401580	-0.00201810	-0.00016392	-0.00000314
	C	0.00314030	0.00748396	-0.00499745	-0.00250315	-0.00016052	0.00000147

Forty-first: The elements of the Jacobian matrix (J_1, J_2, J_3 and J_4) are calculated from equations (5.47)-(5.54), (5.57)-(5.68) and (5.71)-(5.78).

Forty-second: The linear simultaneous equation (5.46) is solved directly by optimally ordered triangular factorization and Gaussian elimination. The $\Delta w_{V_i^\sigma}{}^{(h0)}$ and $\Delta w_{\delta_i^\sigma}{}^{(h0)}$ are obtained as shown in Table C.22.

Forty-third: The new step-length values $\begin{Bmatrix} w_{V_i^\sigma}^{(h1)} = w_{V_i^\sigma}^{(h0)} + \Delta w_{V_i^\sigma}{}^{(h0)} \\ w_{\delta_i^\sigma}^{(h1)} = w_{\delta_i^\sigma}^{(h0)} + \Delta w_{\delta_i^\sigma}{}^{(h0)} \end{Bmatrix}$ are computed from equations (5.79) and (5.80) as shown in Table C.22.

Table C.22 The calculated values

Node		$\Delta w_{V_i^\sigma}{}^{(h0)}$	$\Delta w_{\delta_i^\sigma}{}^{(h0)}$	$w_{V_i^\sigma}{}^{(h1)}$	$w_{\delta_i^\sigma}{}^{(h1)}$
2	A	-0.38350109	-19.97614659	0.31649891	-19.27614659
	B	-1.78462208	0.09051822	-1.08462208	0.79051822
	C	1.43830854	-1.55363737	2.13830854	-0.85363737
3	A	-0.38524390	-27.33308609	0.31475610	-26.63308609
	B	-1.75489508	0.07948911	-1.05489508	0.77948911
	C	1.31500053	-1.52781574	2.01500053	-0.82781574
4	A	-0.39876087	-47.26466959	0.30123913	-46.56466959
	B	-1.81316154	0.02784136	-1.11316154	0.72784136
	C	1.21624459	-1.57313693	1.91624459	-0.87313693
5	A	-0.53532517	4.35481525	0.16467483	5.05481525
	B	-1.61334535	0.70390964	-0.91334535	1.40390964
	C	4.44228287	-2.91506094	5.14228287	-2.21506094

Node		$\Delta w_{V_i^\sigma}^{(h0)}$	$\Delta w_{\delta_i^\sigma}^{(h0)}$	$w_{V_i^\sigma}^{(h1)}$	$w_{\delta_i^\sigma}^{(h1)}$
6	A	-0.38839126	-41.62586520	0.31160874	-40.92586520
	B	-1.77167972	-0.18153969	-1.07167972	0.51846031
	C	0.63836218	-1.30963076	1.33836218	-0.60963076
7	A	-0.40398230	18.23071547	0.29601770	18.93071547
	B	-1.69007972	-0.22539449	-0.99007972	0.47460551
	C	0.34086414	-1.27490890	1.04086414	-0.57490890
8	A	-0.37824422	-36.94496322	0.32175578	-36.24496322
	B	-1.74398947	-0.28351769	-1.04398947	0.41648231
	C	0.33775758	-1.14755106	1.03775758	-0.44755106
9	A	-0.36921728	-37.67419926	0.33078272	-36.97419926
	B	-1.72281028	-0.34251431	-1.02281028	0.35748569
	C	0.15184308	-1.03627727	0.85184308	-0.33627727
10	A	-0.36347059	-48.28154778	0.33652941	-47.58154778
	B	-1.71491366	-0.37292252	-1.01491366	0.32707748
	C	0.05229183	-0.97375017	0.75229183	-0.27375017
11	A	-0.37097833	-43.40526275	0.32902167	-42.70526275
	B	-1.75149295	-0.40376212	-1.05149295	0.29623788
	C	-0.01958863	-0.93451389	0.68041137	-0.23451389
12	A	-0.34431963	65.66555229	0.35568037	66.36555229
	B	-1.86141969	-0.38052923	-1.16141969	0.31947077
	C	-0.01063337	-0.93579680	0.68936663	-0.23579680
13	A	-0.36543106	22.62696583	0.33456894	23.32696583
	B	-1.76540139	-0.40373839	-1.06540139	0.29626161
	C	-0.11200181	-0.93691493	0.58799819	-0.23691493
14	A	-0.37784709	-21.19998907	0.32215291	-20.49998907
	B	-1.78778263	-0.42797920	-1.08778263	0.27202080
	C	-0.05522400	-0.90159293	0.64477600	-0.20159293
15	A	-0.34383919	24.96778846	0.35616081	25.66778846
	B	-1.87559582	-0.38219071	-1.17559582	0.31780929
	C	-0.03706997	-0.93597763	0.66293003	-0.23597763
16	A	-0.33888473	11.52910265	0.36111527	12.22910265
	B	-1.86277173	-0.38095549	-1.16277173	0.31904451
	C	-0.09805275	-0.93713608	0.60194725	-0.23713608
17	A	-0.37746511	-23.12783814	0.32253489	-22.42783814
	B	-1.78224341	-0.42746263	-1.08224341	0.27253737
	C	-0.05750904	-0.90045790	0.64249096	-0.20045790
18	A	-0.38386476	-14.01348370	0.31613524	-13.31348370
	B	-1.83926998	-0.44840929	-1.13926998	0.25159071
	C	-0.08735918	-0.87405498	0.61264082	-0.17405498
19	A	-0.34343077	18.87014750	0.35656923	19.57014750
	B	-1.88170323	-0.38289470	-1.18170323	0.31710530
	C	-0.05056265	-0.93604020	0.64943735	-0.23604020

Forty-fourth: For load buses, $P_{i,load}^{\sigma}{}^{(h1)}\begin{Bmatrix} V_i^{\sigma(k3)} + w_{V_i^\sigma}^{(h1)} \cdot \Delta\left|V_i^{\sigma(k3)}\right| \\ \delta_i^{\sigma(k3)} + w_{\delta_i^\sigma}^{(h1)} \cdot \Delta\delta_i^{\sigma(k3)} \end{Bmatrix}$ and $Q_{i,load}^{\sigma}{}^{(h1)}\begin{Bmatrix} V_i^{\sigma(k3)} + w_{V_i^\sigma}^{(h1)} \cdot \Delta\left|V_i^{\sigma(k3)}\right| \\ \delta_i^{\sigma(k3)} + w_{\delta_i^\sigma}^{(h1)} \cdot \Delta\delta_i^{\sigma(k3)} \end{Bmatrix}$ are calculated from equations (5.44), (5.45), (5.55), (5.56),

(5.69) and (5.70) as shown in Table C.23. $\Delta P_{i,load}^{\sigma}{}^{(h1)}$ and $\Delta Q_{i,load}^{\sigma}{}^{(h1)}$ are calculated from equations (5.40) and (5.41) as shown Table C.23.

Table C.23 The calculated values

Node		$P_{i,load}^{\sigma}{}^{(h1)}$	$Q_{i,load}^{\sigma}{}^{(h1)}$	$\Delta P_{i,load}^{\sigma}{}^{(h1)}$	$\Delta Q_{i,load}^{\sigma}{}^{(h1)}$
2	A	-0.00515785	-0.00233668	-0.00003047	-0.00016750
	B	-0.00218943	-0.00104174	0.00003095	-0.00000631
	C	-0.00476263	-0.00229678	-0.00010020	-0.00005030
3	A	-0.00550319	-0.00266912	-0.00000002	-0.00000002
	B	-0.00404244	-0.00195883	-0.00000003	-0.00000002
	C	-0.00243140	-0.00118059	-0.00000001	0.00000002
4	A	-0.00208558	0.00036257	-0.00115337	-0.00193706
	B	-0.00266994	-0.00064996	0.00031183	-0.00049790
	C	-0.00106290	-0.00066884	-0.00083444	-0.00024470
5	A	0.01958092	-0.01493413	-0.02281987	0.01335964
	B	-0.02102113	-0.01912634	0.01886266	0.01807829
	C	0.00108014	-0.00098710	-0.00320235	-0.00003887
6	A	-0.00209696	-0.00102002	-0.00000236	0.00000035
	B	-0.00128426	-0.00061695	-0.00000084	-0.00000689
	C	-0.00136506	-0.00065823	0.00000178	-0.00000233
7	A	-0.00485705	-0.00235371	-0.00000136	-0.00000052
	B	-0.00336684	-0.00163382	-0.00000188	-0.00000063
	C	-0.00379295	-0.00184066	-0.00000173	-0.00000047
8	A	-0.00169218	-0.00082471	-0.00000227	-0.00000002
	B	-0.00225747	-0.00106606	-0.00000083	-0.00000694
	C	-0.00348716	-0.00168424	0.00000167	-0.00000228
9	A	-0.00614583	-0.00298438	-0.00000217	0.00000035
	B	-0.00619973	-0.00300124	-0.00000121	-0.00000566
	C	-0.00622740	-0.00300579	0.00000131	-0.00000185
10	A	-0.00168883	-0.00081739	-0.00000562	-0.00000734
	B	-0.00175897	-0.00084114	0.00001223	-0.00000728
	C	-0.00120491	-0.00059682	-0.00000377	0.00000654
11	A	-0.00371769	-0.00179832	-0.00000110	-0.00000109
	B	-0.00309324	-0.00149460	-0.00000100	-0.00000261
	C	-0.00515712	-0.00250053	-0.00000085	-0.00000116
12	A	-0.00018297	-0.00235018	-0.00467545	-0.00000406
	B	-0.00170163	-0.00162652	-0.00166709	-0.00000793
	C	-0.00379041	-0.00184555	-0.00000428	0.00000442
13	A	-0.00218799	-0.00106335	-0.00000129	-0.00000131
	B	-0.00221788	-0.00107304	-0.00000298	0.00000004
	C	-0.00303273	-0.00147481	-0.00000302	-0.00000091
14	A	-0.00154388	-0.00074968	-0.00000062	-0.00000008
	B	-0.00128459	-0.00062149	-0.00000051	-0.00000235
	C	-0.00189735	-0.00091267	0.00000001	-0.00000087
15	A	-0.00218883	-0.00106359	-0.00000046	-0.00000106
	B	-0.00202021	-0.00097303	-0.00000103	-0.00000016
	C	-0.00325934	-0.00157365	-0.00000128	-0.00000044
16	A	-0.00388399	-0.00188827	0.00000025	-0.00000111
	B	-0.00431554	-0.00208367	-0.00000141	0.00000005
	C	-0.00363873	-0.00176993	-0.00000135	-0.00000093

Node		$P_{i,load}^{\sigma\ (h1)}$	$Q_{i,load}^{\sigma\ (h1)}$	$\Delta P_{i,load}^{\sigma\ (h1)}$	$\Delta Q_{i,load}^{\sigma\ (h1)}$
17	A	-0.00323881	-0.00157430	-0.00000013	-0.00000018
	B	-0.00202119	-0.00097320	-0.00000004	0.00000002
	C	-0.00227674	-0.00109628	-0.00000007	0.00000004
18	A	0.00429816	-0.00128939	-0.00696729	-0.00000019
	B	-0.00075348	-0.00106197	-0.00146738	-0.00001103
	C	-0.00515766	-0.00252723	-0.00000030	0.00002554
19	A	-0.00437804	-0.00211316	-0.00000053	-0.00000115
	B	-0.00417835	-0.00202112	-0.00000136	-0.00000011
	C	-0.00515645	-0.00250114	-0.00000151	-0.00000054

Forty-fifth: Determine $max\{|\Delta P_{i,load}^{\sigma\ (h1)}|, |\Delta Q_{i,load}^{\sigma\ (h1)}|\} = 0.0228$ and $max\{|\Delta P_{i,load}^{\sigma\ (h0)}|, |\Delta Q_{i,load}^{\sigma\ (h0)}|\} = 0.0167$. Then, update voltage magnitudes, $|V_i^{\sigma(k4)}| = |V_i^{\sigma(k3)}| + w_{V_i}{}^{\sigma(h0)} \cdot \Delta|V_i^{\sigma(k3)}|$, and phase angles, $\delta_i^{\sigma(k4)} = \delta_i^{\sigma(k3)} + w_{\delta_i}{}^{\sigma(h0)} \cdot \Delta\delta_i^{\sigma(k3)}$, by $w_{V_i}{}^{\sigma(h0)}$ and $w_{V_i}{}^{\sigma(h0)}$ at equations (5.42) and (5.43) as shown in Table C.24. After that, renew $w_{V_i}{}^{\sigma(h0)} = w_{V_i}{}^{\sigma(h0)} = 0.6$ and go to ***STEP 3*** of the power flow algorithm.

Table C.24 The updated values

Node		$\|V_i^{\sigma(k4)}\|$	$\delta_i^{\sigma(k4)}$
2	A	1.04810217	0.01582662
	B	1.04939459	-2.07645003
	C	1.04503689	2.11003985
3	A	1.02459005	0.02208600
	B	1.03239743	-2.08037061
	C	1.04225487	2.11034074
4	A	1.04750861	0.03698013
	B	1.04974244	-2.05207465
	C	1.03924657	2.13115097
5	A	1.02971665	0.07266297
	B	1.08241334	-1.98990779
	C	1.05744725	2.21341954
6	A	1.04886528	0.05713227
	B	1.05027991	-2.02944347
	C	1.03419301	2.14973828
7	A	1.05729758	0.08646902
	B	1.05988881	-1.99938219
	C	1.03892575	2.17730204
8	A	1.04993826	0.07360573
	B	1.05077423	-2.01078508
	C	1.02984012	2.16516537
9	A	1.05057832	0.08833973
	B	1.05126855	-1.99432478
	C	1.02616495	2.17911710
10	A	1.05171538	0.09938831
	B	1.05237040	-1.98189853
	C	1.02395709	2.18981742
11	A	1.05401915	0.10840220

Node		$\left\|V_i^{\sigma(k4)}\right\|$	$\delta_i^{\sigma(k4)}$
	B	1.05563182	-1.97211488
	C	1.02469749	2.19919226
12	A	1.05574974	0.11154263
	B	1.05670475	-1.96903135
	C	1.02628460	2.20184858
13	A	1.06164154	0.12242595
	B	1.06198791	-1.95638517
	C	1.02723755	2.21296812
14	A	1.05365199	0.11180254
	B	1.05651736	-1.96871265
	C	1.02490756	2.20299244
15	A	1.05837460	0.11716669
	B	1.05895080	-1.96272734
	C	1.02689092	2.20736737
16	A	1.06188364	0.12627412
	B	1.06065776	-1.95353762
	C	1.02889364	2.21532148
17	A	1.05019689	0.11227047
	B	1.05473186	-1.96907073
	C	1.02329939	2.20322714
18	A	1.05428715	0.11511167
	B	1.05798295	-1.96526955
	C	1.02580779	2.20672987
19	A	1.05949231	0.12000562
	B	1.05987488	-1.95958573
	C	1.02705793	2.21011715

Forty-sixth: For load buses, ${P_{i,load}^{\sigma}}^{(k4)}\begin{Bmatrix} V_i^{\sigma(k4)} \\ \delta_i^{\sigma(k4)} \end{Bmatrix}$ and ${Q_{i,load}^{\sigma}}^{(k4)}\begin{Bmatrix} V_i^{\sigma(k4)} \\ \delta_i^{\sigma(k4)} \end{Bmatrix}$ are calculated from equations (5.1), (5.2), (5.16), (5.17), (5.30) and (5.31) as shown Table C.25. ${\Delta P_{i,load}^{\sigma}}^{(k4)}$ and ${\Delta Q_{i,load}^{\sigma}}^{(k4)}$ are calculated from equations (5.40) and (5.41) as shown Table C.25.

Table C.25 The calculated values

Node		${P_{i,load}^{\sigma}}^{(k4)}$	${Q_{i,load}^{\sigma}}^{(k4)}$	${\Delta P_{i,load}^{\sigma}}^{(k4)}$	${\Delta Q_{i,load}^{\sigma}}^{(k4)}$
2	A	-0.00518827	-0.00252082	-0.00000004	0.00001663
	B	-0.00208843	-0.00106736	-0.00007005	0.00001931
	C	-0.00483491	-0.00230042	-0.00002791	-0.00004667
3	A	-0.00550312	-0.00266904	-0.00000009	-0.00000009
	B	-0.00404249	-0.00195884	0.00000002	-0.00000001
	C	-0.00243142	-0.00118057	0.00000000	0.00000000
4	A	-0.00294179	-0.00223802	-0.00029715	0.00066353
	B	-0.00198773	-0.00124736	-0.00037038	0.00009950
	C	-0.00185362	-0.00101955	-0.00004372	0.00010601
5	A	-0.01760117	0.00379753	0.01436223	-0.00537202
	B	0.01452565	-0.00155047	-0.01668413	0.00050243
	C	-0.00130994	-0.00098807	-0.00081227	-0.00003790
6	A	-0.00209218	-0.00101651	-0.00000713	-0.00000316
	B	-0.00126025	-0.00061804	-0.00002486	-0.00000580

Node		$P_{i,load}^{\sigma\ (k4)}$	$Q_{i,load}^{\sigma\ (k4)}$	$\Delta P_{i,load}^{\sigma\ (k4)}$	$\Delta Q_{i,load}^{\sigma\ (k4)}$
	C	-0.00134764	-0.00063947	-0.00001564	-0.00002109
7	A	-0.00474679	-0.00235104	-0.00011163	-0.00000319
	B	-0.00325846	-0.00163271	-0.00011027	-0.00000174
	C	-0.00368566	-0.00184215	-0.00010903	0.00000102
8	A	-0.00168595	-0.00082235	-0.00000850	-0.00000238
	B	-0.00223248	-0.00106640	-0.00002581	-0.00000660
	C	-0.00346986	-0.00166650	-0.00001563	-0.00002003
9	A	-0.00614474	-0.00298405	-0.00000325	0.00000003
	B	-0.00618501	-0.00299910	-0.00001593	-0.00000780
	C	-0.00622036	-0.00299001	-0.00000573	-0.00001763
10	A	-0.00167138	-0.00083194	-0.00002306	0.00000721
	B	-0.00177774	-0.00085824	0.00003099	0.00000982
	C	-0.00118426	-0.00063625	-0.00002442	0.00004597
11	A	-0.00368183	-0.00179252	-0.00003696	-0.00000689
	B	-0.00305544	-0.00149621	-0.00003880	-0.00000100
	C	-0.00511839	-0.00249895	-0.00003957	-0.00000273
12	A	-0.00876425	-0.00237392	0.00390583	0.00001969
	B	-0.00240798	-0.00161394	-0.00096074	-0.00002051
	C	-0.00379718	-0.00305682	0.00000249	0.00121570
13	A	-0.00190730	-0.00105715	-0.00028199	-0.00000751
	B	-0.00194094	-0.00106704	-0.00027992	-0.00000596
	C	-0.00276323	-0.00147874	-0.00027252	0.00000303
14	A	-0.00154386	-0.00074598	-0.00000064	-0.00000378
	B	-0.00128278	-0.00062132	-0.00000233	-0.00000252
	C	-0.00189414	-0.00090942	-0.00000321	-0.00000411
15	A	-0.00206383	-0.00105797	-0.00012546	-0.00000668
	B	-0.00189647	-0.00097099	-0.00012477	-0.00000219
	C	-0.00313809	-0.00157510	-0.00012253	0.00000101
16	A	-0.00359826	-0.00188138	-0.00028548	-0.00000801
	B	-0.00403458	-0.00207759	-0.00028237	-0.00000602
	C	-0.00336440	-0.00177405	-0.00027569	0.00000320
17	A	-0.00323766	-0.00157325	-0.00000128	-0.00000124
	B	-0.00202155	-0.00097328	0.00000032	0.00000010
	C	-0.00227675	-0.00109631	-0.00000006	0.00000007
18	A	-0.00818688	-0.00138655	0.00551775	0.00009697
	B	-0.00144828	-0.00104883	-0.00077258	-0.00002417
	C	-0.00516566	-0.00387988	0.00000769	0.00137820
19	A	-0.00421280	-0.00210692	-0.00016578	-0.00000739
	B	-0.00401580	-0.00201810	-0.00016392	-0.00000314
	C	-0.00499745	-0.00250315	-0.00016052	0.00000147

Forty-seventh: The linear simultaneous equation (5.7) is solved directly by optimally ordered triangular factorization and Gaussian elimination. The $\Delta\delta_i^{\sigma(k4)}$ and $\Delta\left|V_i^{\sigma(k4)}\right|$ are obtained as shown Table C.26.

Forty-eighth: For load buses, ${P_{i,load}^{\sigma}}^{(h0)} \begin{Bmatrix} V_i^{\sigma(k4)} + w_{V_i^{\sigma}}^{(h0)} \cdot \Delta\left|V_i^{\sigma(k4)}\right| \\ \delta_i^{\sigma(k4)} + w_{\delta_i^{\sigma}}^{(h0)} \cdot \Delta\delta_i^{\sigma(k4)} \end{Bmatrix}$ and ${Q_{i,load}^{\sigma}}^{(h0)} \begin{Bmatrix} V_i^{\sigma(k4)} + w_{V_i^{\sigma}}^{(h0)} \cdot \Delta\left|V_i^{\sigma(k4)}\right| \\ \delta_i^{\sigma(k4)} + w_{\delta_i^{\sigma}}^{(h0)} \cdot \Delta\delta_i^{\sigma(k4)} \end{Bmatrix}$ are calculated from equations (5.44), (5.45), (5.55), (5.56), (5.69) and (5.70) as shown in Table C.26. ${\Delta P_{i,load}^{\sigma}}^{(h0)}$ and ${\Delta Q_{i,load}^{\sigma}}^{(h0)}$ are calculated from equations (5.40) and (5.41) as shown Table C.26.

Table C.26 The calculated values

Node		$\Delta\left\|V_i^{\sigma(k4)}\right\|$	$\Delta\delta_i^{\sigma(k4)}$	${P_{i,load}^{\sigma}}^{(h0)}$	${Q_{i,load}^{\sigma}}^{(h0)}$	${\Delta P_{i,load}^{\sigma}}^{(h0)}$	${\Delta Q_{i,load}^{\sigma}}^{(h0)}$
2	A	0.00158694	0.00288484	-0.00517735	-0.00245058	-0.00001096	-0.00005360
	B	-0.00264013	-0.00009271	-0.00214163	-0.00105353	-0.00001685	0.00000549
	C	0.00055530	-0.00223067	-0.00481563	-0.00231029	-0.00004719	-0.00003679
3	A	0.00164053	0.00286191	-0.00550316	-0.00266909	-0.00000004	-0.00000004
	B	-0.00266389	-0.00008377	-0.00404247	-0.00195884	0.00000000	-0.00000001
	C	0.00054117	-0.00221404	-0.00243141	-0.00118058	0.00000000	0.00000001
4	A	0.00384926	0.00666445	-0.00271873	-0.00113919	-0.00052022	-0.00043530
	B	-0.00616004	-0.00006854	-0.00232535	-0.00101148	-0.00003276	-0.00013638
	C	0.00118648	-0.00526444	-0.00158159	-0.00086532	-0.00031576	-0.00004821
5	A	0.05965951	0.11471651	0.00849521	-0.00683422	-0.01173416	0.00525974
	B	-0.10483703	-0.00691654	-0.01561215	-0.01282813	0.01345367	0.01178008
	C	0.00566961	-0.06046285	-0.00036946	-0.00100686	-0.00175275	-0.00001911
6	A	0.00440912	0.00638302	-0.00209561	-0.00101853	-0.00000370	-0.00000114
	B	-0.00581922	0.00065297	-0.00127486	-0.00061903	-0.00001025	-0.00000481
	C	0.00089654	-0.00568353	-0.00135766	-0.00065128	-0.00000561	-0.00000927
7	A	0.00449697	0.00612033	-0.00481327	-0.00235277	-0.00004515	-0.00000146
	B	-0.00594482	0.00078366	-0.00332393	-0.00163353	-0.00004479	-0.00000093
	C	0.00061812	-0.00567372	-0.00375044	-0.00184137	-0.00004424	0.00000024
8	A	0.00494100	0.00611082	-0.00169023	-0.00082377	-0.00000422	-0.00000096
	B	-0.00544253	0.00134164	-0.00224767	-0.00106785	-0.00001062	-0.00000515
	C	0.00062245	-0.00609298	-0.00347984	-0.00167770	-0.00000565	-0.00000883
9	A	0.00545587	0.00583684	-0.00614592	-0.00298416	-0.00000208	0.00000014
	B	-0.00504202	0.00200716	-0.00619413	-0.00300174	-0.00000681	-0.00000516
	C	0.00034980	-0.00649794	-0.00622427	-0.00299992	-0.00000182	-0.00000772
10	A	0.00583527	0.00562344	-0.00168320	-0.00082498	-0.00001125	0.00000025
	B	-0.00472598	0.00249740	-0.00176355	-0.00084972	0.00001681	0.00000130
	C	0.00013947	-0.00680136	-0.00119755	-0.00061102	-0.00001113	0.00002074
11	A	0.00646280	0.00550325	-0.00370362	-0.00179627	-0.00001517	-0.00000315
	B	-0.00431399	0.00294588	-0.00307836	-0.00149587	-0.00001587	-0.00000134
	C	-0.00005691	-0.00717713	-0.00514184	-0.00250017	-0.00001612	-0.00000151
12	A	0.00588899	0.00538031	-0.00479959	-0.00236065	-0.00005882	0.00000642
	B	-0.00435795	0.00274453	-0.00228978	-0.00162339	-0.00107895	-0.00001107
	C	-0.00003196	-0.00699663	-0.00379414	-0.00232899	-0.00000055	0.00048787
13	A	0.00629035	0.00529728	-0.00207605	-0.00106118	-0.00011323	-0.00000347
	B	-0.00452205	0.00288514	-0.00210784	-0.00107063	-0.00011302	-0.00000237
	C	-0.00035773	-0.00724485	-0.00292568	-0.00147659	-0.00011007	0.00000088
14	A	0.00711483	0.00544823	-0.00154402	-0.00074822	-0.00000048	-0.00000154
	B	-0.00385500	0.00339578	-0.00128399	-0.00062198	-0.00000112	-0.00000185

Node		$\Delta\lvert V_i^{\sigma(k4)}\rvert$	$\Delta\delta_i^{\sigma(k4)}$	${P_{i,load}^{\sigma}}^{(h0)}$	${Q_{i,load}^{\sigma}}^{(h0)}$	${\Delta P_{i,load}^{\sigma}}^{(h0)}$	${\Delta Q_{i,load}^{\sigma}}^{(h0)}$
	C	-0.00016902	-0.00754158	-0.00189607	-0.00091158	-0.00000128	-0.00000196
15	A	0.00586891	0.00531444	-0.00213895	-0.00106160	-0.00005034	-0.00000305
	B	-0.00439493	0.00274014	-0.00197097	-0.00097225	-0.00005027	-0.00000094
	C	-0.00011467	-0.00700200	-0.00321116	-0.00157434	-0.00004946	0.00000024
16	A	0.00573428	0.00518198	-0.00376964	-0.00188578	-0.00011409	-0.00000360
	B	-0.00457019	0.00269322	-0.00420350	-0.00208123	-0.00011345	-0.00000239
	C	-0.00032315	-0.00705689	-0.00352933	-0.00177180	-0.00011076	0.00000094
17	A	0.00713296	0.00543956	-0.00323838	-0.00157393	-0.00000056	-0.00000056
	B	-0.00385499	0.00339826	-0.00202135	-0.00097323	0.00000011	0.00000005
	C	-0.00017732	-0.00753255	-0.00227676	-0.00109629	-0.00000005	0.00000004
18	A	0.00776205	0.00539096	-0.00264816	-0.00132831	-0.00002097	0.00003873
	B	-0.00339248	0.00384075	-0.00133486	-0.00105935	-0.00088600	-0.00001365
	C	-0.00028092	-0.00790776	-0.00516092	-0.00306214	0.00000296	0.00056046
19	A	0.00585626	0.00528031	-0.00431208	-0.00211094	-0.00006649	-0.00000337
	B	-0.00441720	0.00273693	-0.00411367	-0.00201994	-0.00006605	-0.00000129
	C	-0.00015878	-0.00700528	-0.00509322	-0.00250207	-0.00006474	0.00000039

Forty-ninth: The elements of the Jacobian matrix (J_1, J_2, J_3 and J_4) are calculated from equations (5.47)-(5.54), (5.57)-(5.68) and (5.71)-(5.78).

Fifty-first: The linear simultaneous equation (5.46) is solved directly by optimally ordered triangular factorization and Gaussian elimination. The $\Delta w_{V_i^{\sigma}}{}^{(h0)}$ and $\Delta w_{\delta_i^{\sigma}}{}^{(h0)}$ are obtained as shown in Table C.27.

Fifty-second: The new step-length values $\begin{Bmatrix} w_{V_i^{\sigma}}^{(h1)} = w_{V_i^{\sigma}}^{(h0)} + \Delta w_{V_i^{\sigma}}{}^{(h0)} \\ w_{\delta_i^{\sigma}}^{(h1)} = w_{\delta_i^{\sigma}}^{(h0)} + \Delta w_{\delta_i^{\sigma}}{}^{(h0)} \end{Bmatrix}$ are computed from equations (5.79) and (5.80) as shown in Table C.27.

Table C.27 The calculated values

Node		$\Delta \boldsymbol{w}_{V_i^{\sigma}}{}^{(\boldsymbol{h0})}$	$\Delta \boldsymbol{w}_{\delta_i^{\sigma}}{}^{(\boldsymbol{h0})}$	$\boldsymbol{w}_{V_i^{\sigma}}{}^{(\boldsymbol{h1})}$	$\boldsymbol{w}_{\delta_i^{\sigma}}{}^{(\boldsymbol{h1})}$
2	A	0.22344426	-0.56017859	0.82344426	0.03982141
	B	0.06119173	-28.61644775	0.66119173	-28.01644775
	C	-0.90031302	-0.08186152	-0.30031302	0.51813848
3	A	0.21559401	-0.55838565	0.81559401	0.04161435
	B	0.07437706	-31.57384264	0.67437706	-30.97384264
	C	-0.89281562	-0.07833045	-0.29281562	0.52166955
4	A	0.19194785	-0.56930030	0.79194785	0.03069970
	B	0.03493590	-90.64244989	0.63493590	-90.04244989
	C	-0.97289497	-0.08571540	-0.37289497	0.51428460
5	A	-0.04547275	-0.50686723	0.55452725	0.09313277
	B	-0.21238560	-17.26870340	0.38761440	-16.66870340
	C	-0.92969133	-0.19422698	-0.32969133	0.40577302
6	A	0.14264262	-0.58124160	0.74264262	0.01875840
	B	0.06072191	9.32280739	0.66072191	9.92280739
	C	-1.06369482	-0.04593741	-0.46369482	0.55406259
7	A	0.10450652	-0.59272592	0.70450652	0.00727408
	B	0.03983943	7.66124992	0.63983943	8.26124992

Node		$\Delta w_{V_i^\sigma}^{(h0)}$	$\Delta w_{\delta_i^\sigma}^{(h0)}$	$w_{V_i^\sigma}^{(h1)}$	$w_{\delta_i^\sigma}^{(h1)}$
	C	-1.58150434	-0.04929495	-0.98150434	0.55070505
8	A	0.10959151	-0.59406044	0.70959151	0.00593956
	B	0.09442140	4.45258425	0.69442140	5.05258425
	C	-1.21803460	-0.01001559	-0.61803460	0.58998441
9	A	0.08526435	-0.60859323	0.68526435	-0.00859323
	B	0.13668928	2.92349262	0.73668928	3.52349262
	C	-1.62219589	0.02274019	-1.02219589	0.62274019
10	A	0.07030209	-0.62153758	0.67030209	-0.02153758
	B	0.17356517	2.31999110	0.77356517	2.91999110
	C	-3.08416988	0.04533573	-2.48416988	0.64533573
11	A	0.05276772	-0.63112126	0.65276772	-0.03112126
	B	0.20637767	1.95684018	0.80637767	2.55684018
	C	6.29846601	0.06323527	6.89846601	0.66323527
12	A	0.05197743	-0.63786385	0.65197743	-0.03786385
	B	0.22956346	2.08011877	0.82956346	2.68011877
	C	10.54795625	0.06781111	11.14795625	0.66781111
13	A	0.03382861	-0.65077451	0.63382861	-0.05077451
	B	0.19460996	1.97936644	0.79460996	2.57936644
	C	1.17896421	0.06492397	1.77896421	0.66492397
14	A	0.04375259	-0.63593489	0.64375259	-0.03593489
	B	0.25330522	1.69447471	0.85330522	2.29447471
	C	1.61496935	0.07935808	2.21496935	0.67935808
15	A	0.04569559	-0.64287141	0.64569559	-0.04287141
	B	0.22396861	2.07742200	0.82396861	2.67742200
	C	3.06089770	0.06791060	3.66089770	0.66791060
16	A	0.03093923	-0.65589235	0.63093923	-0.05589235
	B	0.21798820	2.10044578	0.81798820	2.70044578
	C	1.21488348	0.06944812	1.81488348	0.66944812
17	A	0.04344111	-0.63579185	0.64344111	-0.03579185
	B	0.25599839	1.69171532	0.85599839	2.29171532
	C	1.50399982	0.07968081	2.10399982	0.67968081
18	A	0.03633292	-0.64149019	0.63633292	-0.04149019
	B	0.31234982	1.49593488	0.91234982	2.09593488
	C	0.67670670	0.09398857	1.27670670	0.69398857
19	A	0.04236492	-0.64548207	0.64236492	-0.04548207
	B	0.22141842	2.07655904	0.82141842	2.67655904
	C	2.25557958	0.06801747	2.85557958	0.66801747

Fifty-third: For load buses, ${P_{i,load}^{\sigma}}^{(h1)} \begin{Bmatrix} V_i^{\sigma(k4)} + w_{V_i^\sigma}^{(h1)} \cdot \Delta\left|V_i^{\sigma(k4)}\right| \\ \delta_i^{\sigma(k4)} + w_{\delta_i^\sigma}^{(h1)} \cdot \Delta\delta_i^{\sigma(k4)} \end{Bmatrix}$ and ${Q_{i,load}^{\sigma}}^{(h1)} \begin{Bmatrix} V_i^{\sigma(k4)} + w_{V_i^\sigma}^{(h1)} \cdot \Delta\left|V_i^{\sigma(k4)}\right| \\ \delta_i^{\sigma(k4)} + w_{\delta_i^\sigma}^{(h1)} \cdot \Delta\delta_i^{\sigma(k4)} \end{Bmatrix}$ are calculated from equations (5.44), (5.45), (5.55), (5.56), (5.69) and (5.70) as shown in Table C.28. ${\Delta P_{i,load}^{\sigma}}^{(h1)}$ and ${\Delta Q_{i,load}^{\sigma}}^{(h1)}$ are calculated from equations (5.40) and (5.41) as shown Table C.28.

Table C.28 The calculated values

Node		$P_{i,load}^{\sigma}{}^{(h1)}$	$Q_{i,load}^{\sigma}{}^{(h1)}$	$\Delta P_{i,load}^{\sigma}{}^{(h1)}$	$\Delta Q_{i,load}^{\sigma}{}^{(h1)}$
2	A	-0.00512421	-0.00250763	-0.00006410	0.00000345
	B	-0.00207525	-0.00098915	-0.00008323	-0.00005890
	C	-0.00485148	-0.00232308	-0.00001134	-0.00002401
3	A	-0.00550319	-0.00266913	-0.00000002	0.00000000
	B	-0.00404247	-0.00195883	0.00000000	-0.00000002
	C	-0.00243141	-0.00118057	0.00000000	0.00000000
4	A	-0.00245066	-0.00155917	-0.00078828	-0.00001531
	B	-0.00089499	0.00001476	-0.00146312	-0.00116262
	C	-0.00181076	-0.00053208	-0.00008659	-0.00038145
5	A	-0.00487145	-0.00122112	0.00163251	-0.00035337
	B	-0.00030391	-0.02626894	-0.00185456	0.02522089
	C	0.00162214	-0.00135184	-0.00374436	0.00032587
6	A	-0.00209893	-0.00101950	-0.00000039	-0.00000017
	B	-0.00128497	-0.00062366	-0.00000013	-0.00000018
	C	-0.00136272	-0.00066066	-0.00000056	0.00000011
7	A	-0.00485709	-0.00235417	-0.00000132	-0.00000007
	B	-0.00336737	-0.00163458	-0.00000136	0.00000012
	C	-0.00379350	-0.00184104	-0.00000119	-0.00000009
8	A	-0.00169411	-0.00082459	-0.00000034	-0.00000014
	B	-0.00225814	-0.00107294	-0.00000015	-0.00000006
	C	-0.00348492	-0.00168666	-0.00000057	0.00000013
9	A	-0.00614761	-0.00298379	-0.00000039	-0.00000023
	B	-0.00620092	-0.00300665	-0.00000003	-0.00000025
	C	-0.00622559	-0.00300777	-0.00000051	0.00000013
10	A	-0.00169325	-0.00082147	-0.00000120	-0.00000326
	B	-0.00174872	-0.00084588	0.00000197	-0.00000254
	C	-0.00120920	-0.00058999	0.00000052	-0.00000030
11	A	-0.00371859	-0.00179945	-0.00000020	0.00000003
	B	-0.00309398	-0.00149732	-0.00000026	0.00000011
	C	-0.00515776	-0.00250167	-0.00000021	-0.00000001
12	A	-0.00484187	-0.00235187	-0.00001655	-0.00000236
	B	-0.00331432	-0.00163263	-0.00005440	-0.00000183
	C	-0.00379571	-0.00185363	0.00000102	0.00001251
13	A	-0.00218757	-0.00106451	-0.00000172	-0.00000014
	B	-0.00221899	-0.00107327	-0.00000187	0.00000027
	C	-0.00303430	-0.00147563	-0.00000145	-0.00000008
14	A	-0.00154445	-0.00074972	-0.00000005	-0.00000003
	B	-0.00128509	-0.00062385	-0.00000001	0.00000001
	C	-0.00189720	-0.00091359	-0.00000014	0.00000006
15	A	-0.00218859	-0.00106464	-0.00000070	-0.00000002
	B	-0.00202042	-0.00097335	-0.00000081	0.00000017
	C	-0.00326007	-0.00157403	-0.00000055	-0.00000006
16	A	-0.00388155	-0.00188924	-0.00000219	-0.00000015
	B	-0.00431465	-0.00208386	-0.00000231	0.00000024
	C	-0.00363821	-0.00177077	-0.00000187	-0.00000008
17	A	-0.00323890	-0.00157449	-0.00000004	0.00000000
	B	-0.00202122	-0.00097313	-0.00000001	-0.00000005
	C	-0.00227681	-0.00109623	0.00000000	-0.00000001
18	A	-0.00265569	-0.00128807	-0.00001344	-0.00000151
	B	-0.00211363	-0.00107169	-0.00010723	-0.00000131

Node		$P_{i,load}^{\sigma\ (h1)}$	$Q_{i,load}^{\sigma\ (h1)}$	$\Delta P_{i,load}^{\sigma\ (h1)}$	$\Delta Q_{i,load}^{\sigma\ (h1)}$
	C	-0.00515853	-0.00250627	0.00000056	0.00000459
19	A	-0.00437758	-0.00211426	-0.00000099	-0.00000005
	B	-0.00417862	-0.00202139	-0.00000109	0.00000016
	C	-0.00515719	-0.00250160	-0.00000078	-0.00000008

Fifty-fourth: Determine $max\{|\Delta P_{i,load}^{\sigma\ (h1)}|, |\Delta Q_{i,load}^{\sigma\ (h1)}|\} = 0.0252$ and $max\{|\Delta P_{i,load}^{\sigma\ (h0)}|, |\Delta Q_{i,load}^{\sigma\ (h0)}|\} = 0.0135$. Then, update voltage magnitudes, $|V_i^{\sigma(k5)}| = |V_i^{\sigma(k4)}| + w_{V_i}{}^{\sigma(h0)} \cdot \Delta |V_i^{\sigma(k4)}|$, and phase angles, $\delta_i^{\sigma(k5)} = \delta_i^{\sigma(k4)} + w_{\delta_i}{}^{\sigma(h0)} \cdot \Delta\delta_i^{\sigma(k4)}$, by $w_{V_i}{}^{\sigma(h0)}$ and $w_{V_i}{}^{\sigma(h0)}$ at equations (5.42) and (5.43) as shown in Table C.29. After that, renew $w_{V_i}{}^{\sigma(h0)} = w_{V_i}{}^{\sigma(h0)} = 0.5$ and go to ***STEP 3*** of the power flow algorithm.

Table C.29 The updated values

Node		$\|V_i^{\sigma(k5)}\|$	$\delta_i^{\sigma(k5)}$
2	A	1.04905434	0.01755752
	B	1.04781051	-2.07650566
	C	1.04537007	2.10870145
3	A	1.02557437	0.02380315
	B	1.03079909	-2.08042087
	C	1.04257957	2.10901232
4	A	1.04981816	0.04097881
	B	1.04604642	-2.05211578
	C	1.03995846	2.12799230
5	A	1.06551236	0.14149287
	B	1.01951112	-1.99405771
	C	1.06084902	2.17714183
6	A	1.05151075	0.06096209
	B	1.04678838	-2.02905168
	C	1.03473094	2.14632817
7	A	1.05999576	0.09014122
	B	1.05632192	-1.99891199
	C	1.03929662	2.17389781
8	A	1.05290286	0.07727222
	B	1.04750871	-2.00998010
	C	1.03021359	2.16150958
9	A	1.05385184	0.09184183
	B	1.04824333	-1.99312049
	C	1.02637483	2.17521834
10	A	1.05521654	0.10276237
	B	1.04953481	-1.98040009
	C	1.02404077	2.18573660
11	A	1.05789683	0.11170415
	B	1.05304342	-1.97034735
	C	1.02466334	2.19488598
12	A	1.05928313	0.11477082
	B	1.05408998	-1.96738464
	C	1.02626543	2.19765060

Node		$\left\|V_i^{\sigma(k5)}\right\|$	$\delta_i^{\sigma(k5)}$
13	A	1.06541576	0.12560431
	B	1.05927468	-1.95465409
	C	1.02702291	2.20862121
14	A	1.05792089	0.11507148
	B	1.05420436	-1.96667519
	C	1.02480614	2.19846749
15	A	1.06189595	0.12035535
	B	1.05631385	-1.96108326
	C	1.02682212	2.20316617
16	A	1.06532421	0.12938331
	B	1.05791565	-1.95192169
	C	1.02869975	2.21108735
17	A	1.05447667	0.11553421
	B	1.05241887	-1.96703177
	C	1.02319300	2.19870761
18	A	1.05894437	0.11834625
	B	1.05594746	-1.96296510
	C	1.02563924	2.20198522
19	A	1.06300607	0.12317380
	B	1.05722456	-1.95794357
	C	1.02696266	2.20591398

Fifty-fifth: For load buses, $P_{i,load}^{\sigma}{}^{(k5)}\left\{\begin{matrix}V_i^{\sigma(k5)}\\ \delta_i^{\sigma(k5)}\end{matrix}\right\}$ and $Q_{i,load}^{\sigma}{}^{(k5)}\left\{\begin{matrix}V_i^{\sigma(k5)}\\ \delta_i^{\sigma(k5)}\end{matrix}\right\}$ are calculated from equations (5.1), (5.2), (5.16), (5.17), (5.30) and (5.31) as shown Table C.30. $\Delta P_{i,load}^{\sigma}{}^{(k5)}$ and $\Delta Q_{i,load}^{\sigma}{}^{(k5)}$ are calculated from equations (5.40) and (5.41) as shown Table C.30.

Table C.30 The calculated values

Node		$P_{i,load}^{\sigma}{}^{(k5)}$	$Q_{i,load}^{\sigma}{}^{(k5)}$	$\Delta P_{i,load}^{\sigma}{}^{(k5)}$	$\Delta Q_{i,load}^{\sigma}{}^{(k5)}$
2	A	-0.00517735	-0.00245058	-0.00001096	-0.00005360
	B	-0.00214163	-0.00105353	-0.00001685	0.00000549
	C	-0.00481563	-0.00231029	-0.00004719	-0.00003679
3	A	-0.00550316	-0.00266909	-0.00000004	-0.00000004
	B	-0.00404247	-0.00195884	0.00000000	-0.00000001
	C	-0.00243141	-0.00118058	0.00000000	0.00000001
4	A	-0.00271873	-0.00113919	-0.00052022	-0.00043530
	B	-0.00232535	-0.00101148	-0.00003276	-0.00013638
	C	-0.00158159	-0.00086532	-0.00031576	-0.00004821
5	A	0.00849521	-0.00683422	-0.01173416	0.00525974
	B	-0.01561215	-0.01282813	0.01345367	0.01178008
	C	-0.00036946	-0.00100686	-0.00175275	-0.00001911
6	A	-0.00209561	-0.00101853	-0.00000370	-0.00000114
	B	-0.00127486	-0.00061903	-0.00001025	-0.00000481
	C	-0.00135766	-0.00065128	-0.00000561	-0.00000927
7	A	-0.00481327	-0.00235277	-0.00004515	-0.00000146
	B	-0.00332393	-0.00163353	-0.00004479	-0.00000093
	C	-0.00375044	-0.00184137	-0.00004424	0.00000024
8	A	-0.00169023	-0.00082377	-0.00000422	-0.00000096

Node		$P_{i,load}^{\sigma\ (k5)}$	$Q_{i,load}^{\sigma\ (k5)}$	$\Delta P_{i,load}^{\sigma\ (k5)}$	$\Delta Q_{i,load}^{\sigma\ (k5)}$
	B	-0.00224767	-0.00106785	-0.00001062	-0.00000515
	C	-0.00347984	-0.00167770	-0.00000565	-0.00000883
9	A	-0.00614592	-0.00298416	-0.00000208	0.00000014
	B	-0.00619413	-0.00300174	-0.00000681	-0.00000516
	C	-0.00622427	-0.00299992	-0.00000182	-0.00000772
10	A	-0.00168320	-0.00082498	-0.00001125	0.00000025
	B	-0.00176355	-0.00084972	0.00001681	0.00000130
	C	-0.00119755	-0.00061102	-0.00001113	0.00002074
11	A	-0.00370362	-0.00179627	-0.00001517	-0.00000315
	B	-0.00307836	-0.00149587	-0.00001587	-0.00000134
	C	-0.00514184	-0.00250017	-0.00001612	-0.00000151
12	A	-0.00479959	-0.00236065	-0.00005882	0.00000642
	B	-0.00228978	-0.00162339	-0.00107895	-0.00001107
	C	-0.00379414	-0.00232899	-0.00000055	0.00048787
13	A	-0.00207605	-0.00106118	-0.00011323	-0.00000347
	B	-0.00210784	-0.00107063	-0.00011302	-0.00000237
	C	-0.00292568	-0.00147659	-0.00011007	0.00000088
14	A	-0.00154402	-0.00074822	-0.00000048	-0.00000154
	B	-0.00128399	-0.00062198	-0.00000112	-0.00000185
	C	-0.00189607	-0.00091158	-0.00000128	-0.00000196
15	A	-0.00213895	-0.00106160	-0.00005034	-0.00000305
	B	-0.00197097	-0.00097225	-0.00005027	-0.00000094
	C	-0.00321116	-0.00157434	-0.00004946	0.00000024
16	A	-0.00376964	-0.00188578	-0.00011409	-0.00000360
	B	-0.00420350	-0.00208123	-0.00011345	-0.00000239
	C	-0.00352933	-0.00177180	-0.00011076	0.00000094
17	A	-0.00323838	-0.00157393	-0.00000056	-0.00000056
	B	-0.00202135	-0.00097323	0.00000011	0.00000005
	C	-0.00227676	-0.00109629	-0.00000005	0.00000004
18	A	-0.00264816	-0.00132831	-0.00002097	0.00003873
	B	-0.00133486	-0.00105935	-0.00088600	-0.00001365
	C	-0.00516092	-0.00306214	0.00000296	0.00056046
19	A	-0.00431208	-0.00211094	-0.00006649	-0.00000337
	B	-0.00411367	-0.00201994	-0.00006605	-0.00000129
	C	-0.00509322	-0.00250207	-0.00006474	0.00000039

Fifty-sixth: The linear simultaneous equation (5.7) is solved directly by optimally ordered triangular factorization and Gaussian elimination. The $\Delta\delta_i^{\sigma(k5)}$ and $\Delta\left|V_i^{\sigma(k5)}\right|$ are obtained as shown Table C.31.

Fifty-seventh: For load buses, $P_{i,load}^{\sigma\ (h0)}\left\{\begin{matrix} V_i^{\sigma(k5)} + w_{V_i^\sigma}^{(h0)} \cdot \Delta\left|V_i^{\sigma(k5)}\right| \\ \delta_i^{\sigma(k5)} + w_{\delta_i^\sigma}^{(h0)} \cdot \Delta\delta_i^{\sigma(k5)} \end{matrix}\right\}$ and $Q_{i,load}^{\sigma\ (h0)}\left\{\begin{matrix} V_i^{\sigma(k5)} + w_{V_i^\sigma}^{(h0)} \cdot \Delta\left|V_i^{\sigma(k5)}\right| \\ \delta_i^{\sigma(k5)} + w_{\delta_i^\sigma}^{(h0)} \cdot \Delta\delta_i^{\sigma(k5)} \end{matrix}\right\}$ are calculated from equations (5.44), (5.45), (5.55), (5.56),

(5.69) and (5.70) as shown in Table C.31. $\Delta P_{i,load}^{\sigma}{}^{(h0)}$ and $\Delta Q_{i,load}^{\sigma}{}^{(h0)}$ are calculated from equations (5.40) and (5.41) as shown Table C.31.

Table C.31 The calculated values

Node		$\Delta\lvert V_i^{\sigma(k5)}\rvert$	$\Delta\delta_i^{\sigma(k5)}$	$P_{i,load}^{\sigma}{}^{(h0)}$	$Q_{i,load}^{\sigma}{}^{(h0)}$	$\Delta P_{i,load}^{\sigma}{}^{(h0)}$	$\Delta Q_{i,load}^{\sigma}{}^{(h0)}$
2	A	0.00035459	-0.00161603	-0.00516680	-0.00247823	-0.00002151	-0.00002595
	B	-0.00016155	0.00265313	-0.00212924	-0.00103606	-0.00002924	-0.00001199
	C	-0.00049995	0.00018261	-0.00483640	-0.00232269	-0.00002642	-0.00002440
3	A	0.00035369	-0.00159805	-0.00550318	-0.00266911	-0.00000003	-0.00000002
	B	-0.00019813	0.00264483	-0.00404247	-0.00195884	0.00000000	-0.00000001
	C	-0.00048317	0.00017343	-0.00243141	-0.00118057	0.00000000	0.00000000
4	A	0.00073886	-0.00379407	-0.00278111	-0.00135102	-0.00045783	-0.00022347
	B	-0.00021521	0.00621283	-0.00198200	-0.00078264	-0.00037610	-0.00036522
	C	-0.00115432	0.00045124	-0.00172025	-0.00079469	-0.00017709	-0.00011885
5	A	-0.00271288	-0.05814604	0.00219793	-0.00412288	-0.00543688	0.00254839
	B	0.02226588	0.11943974	-0.00842928	-0.01409207	0.00627080	0.01304403
	C	-0.00527098	0.01174352	-0.00036385	-0.00109715	-0.00175836	0.00007118
6	A	0.00062893	-0.00371008	-0.00209737	-0.00101906	-0.00000195	-0.00000061
	B	-0.00035335	0.00608754	-0.00127995	-0.00062139	-0.00000516	-0.00000245
	C	-0.00095365	0.00026109	-0.00136033	-0.00065595	-0.00000295	-0.00000461
7	A	0.00046996	-0.00362768	-0.00483551	-0.00235349	-0.00002291	-0.00000075
	B	-0.00023684	0.00600383	-0.00334598	-0.00163402	-0.00002274	-0.00000043
	C	-0.00097756	0.00027969	-0.00377226	-0.00184122	-0.00002242	0.00000010
8	A	0.00054149	-0.00363019	-0.00169225	-0.00082422	-0.00000219	-0.00000051
	B	-0.00051389	0.00597376	-0.00225294	-0.00107041	-0.00000535	-0.00000259
	C	-0.00075817	0.00006102	-0.00348252	-0.00168214	-0.00000297	-0.00000438
9	A	0.00046519	-0.00355226	-0.00614686	-0.00298404	-0.00000114	0.00000001
	B	-0.00068919	0.00586791	-0.00619753	-0.00300425	-0.00000341	-0.00000264
	C	-0.00056744	-0.00014776	-0.00622506	-0.00300381	-0.00000104	-0.00000383
10	A	0.00041023	-0.00349518	-0.00168853	-0.00082404	-0.00000592	-0.00000069
	B	-0.00082027	0.00579394	-0.00175564	-0.00084844	0.00000889	0.00000002
	C	-0.00043014	-0.00030834	-0.00120324	-0.00060058	-0.00000544	0.00001030
11	A	0.00034103	-0.00347322	-0.00371115	-0.00179785	-0.00000764	-0.00000157
	B	-0.00089031	0.00576463	-0.00308623	-0.00149657	-0.00000800	-0.00000064
	C	-0.00035844	-0.00045385	-0.00514985	-0.00250093	-0.00000811	-0.00000076
12	A	0.00030609	-0.00343190	-0.00482485	-0.00235685	-0.00003357	0.00000262
	B	-0.00100043	0.00570895	-0.00281489	-0.00162846	-0.00055383	-0.00000599
	C	-0.00033707	-0.00047445	-0.00379467	-0.00208815	-0.00000002	0.00024702
13	A	0.00021279	-0.00344733	-0.00213223	-0.00106288	-0.00005706	-0.00000177
	B	-0.00088004	0.00571074	-0.00216388	-0.00107188	-0.00005699	-0.00000112
	C	-0.00042176	-0.00047036	-0.00298034	-0.00147613	-0.00005541	0.00000042
14	A	0.00031129	-0.00346472	-0.00154425	-0.00074898	-0.00000025	-0.00000078
	B	-0.00097649	0.00575406	-0.00128454	-0.00062291	-0.00000056	-0.00000092
	C	-0.00027296	-0.00059849	-0.00189667	-0.00091257	-0.00000068	-0.00000097
15	A	0.00026818	-0.00341650	-0.00216394	-0.00106312	-0.00002535	-0.00000153
	B	-0.00098433	0.00569242	-0.00199589	-0.00097276	-0.00002534	-0.00000043
	C	-0.00035098	-0.00047551	-0.00323575	-0.00157420	-0.00002487	0.00000011
16	A	0.00017741	-0.00339882	-0.00382613	-0.00188755	-0.00005761	-0.00000184
	B	-0.00099625	0.00565696	-0.00425964	-0.00208248	-0.00005732	-0.00000113
	C	-0.00039258	-0.00049009	-0.00358423	-0.00177130	-0.00005586	0.00000045

Node		$\Delta\lvert V_i^{\sigma(k5)}\rvert$	$\Delta\delta_i^{\sigma(k5)}$	$P_{i,load}^{\sigma\ (h0)}$	$Q_{i,load}^{\sigma\ (h0)}$	$\Delta P_{i,load}^{\sigma\ (h0)}$	$\Delta Q_{i,load}^{\sigma\ (h0)}$
17	A	0.00030986	-0.00345843	-0.00323865	-0.00157421	-0.00000029	-0.00000028
	B	-0.00098687	0.00574890	-0.00202129	-0.00097320	0.00000005	0.00000001
	C	-0.00026668	-0.00060020	-0.00227679	-0.00109626	-0.00000003	0.00000002
18	A	0.00028202	-0.00345825	-0.00265528	-0.00130857	-0.00001385	0.00001899
	B	-0.00105964	0.00574550	-0.00174973	-0.00106585	-0.00047113	-0.00000715
	C	-0.00019010	-0.00074324	-0.00515958	-0.00278305	0.00000162	0.00028137
19	A	0.00024810	-0.00340834	-0.00434508	-0.00211261	-0.00003350	-0.00000170
	B	-0.00097805	0.00568340	-0.00414641	-0.00202063	-0.00003330	-0.00000061
	C	-0.00035814	-0.00047648	-0.00512539	-0.00250186	-0.00003257	0.00000018

Fifty-eighth: The elements of the Jacobian matrix (J_1, J_2, J_3 and J_4) are calculated from equations (5.47)-(5.54), (5.57)-(5.68) and (5.71)-(5.78).

Fifty-ninth: The linear simultaneous equation (5.46) is solved directly by optimally ordered triangular factorization and Gaussian elimination. The $\Delta w_{V_i}^{\sigma\ (h0)}$ and $\Delta w_{\delta_i}^{\sigma\ (h0)}$ are obtained as shown in Table C.32.

Sixtieth: The new step-length values $\begin{Bmatrix} w_{V_i}^{\sigma\ (h1)} = w_{V_i}^{\sigma\ (h0)} + \Delta w_{V_i}^{\sigma\ (h0)} \\ w_{\delta_i}^{\sigma\ (h1)} = w_{\delta_i}^{\sigma\ (h0)} + \Delta w_{\delta_i}^{\sigma\ (h0)} \end{Bmatrix}$ are computed from equations (5.79) and (5.80) as shown in Table C.32.

Table C.32 The calculated values

Node		$\Delta \boldsymbol{w}_{V_i}^{\sigma\ (h0)}$	$\Delta \boldsymbol{w}_{\delta_i}^{\sigma\ (h0)}$	$\boldsymbol{w}_{V_i}^{\sigma\ (h1)}$	$\boldsymbol{w}_{\delta_i}^{\sigma\ (h1)}$
2	A	-0.59131977	0.17120279	-0.09131977	0.67120279
	B	-6.33626015	-0.12851383	-5.83626015	0.37148617
	C	0.19351912	2.40081064	0.69351912	2.90081064
3	A	-0.61758153	0.17448312	-0.11758153	0.67448312
	B	-5.26829447	-0.12827269	-4.76829447	0.37172731
	C	0.20585231	2.52923745	0.70585231	3.02923745
4	A	-0.67724610	0.16777613	-0.17724610	0.66777613
	B	-11.00755766	-0.13769494	-10.50755766	0.36230506
	C	0.17540553	2.28936325	0.67540553	2.78936325
5	A	1.53503610	0.22381874	2.03503610	0.72381874
	B	2.02981817	-0.19193282	2.52981817	0.30806718
	C	0.41719279	1.36842025	0.91719279	1.86842025
6	A	-0.69389479	0.13884707	-0.19389479	0.63884707
	B	-5.88616753	-0.17088956	-5.38616753	0.32911044
	C	0.10736916	3.46706358	0.60736916	3.96706358
7	A	-1.19435848	0.14950466	-0.69435848	0.64950466
	B	-8.26603760	-0.19020569	-7.76603760	0.30979431
	C	0.16206989	3.00539289	0.66206989	3.50539289
8	A	-0.66407932	0.10831241	-0.16407932	0.60831241
	B	-3.48941826	-0.20091347	-2.98941826	0.29908653
	C	0.00846819	12.75637934	0.50846819	13.25637934
9	A	-0.59765127	0.07693083	-0.09765127	0.57693083
	B	-2.18219487	-0.22938144	-1.68219487	0.27061856
	C	-0.14952517	-4.39083723	0.35047483	-3.89083723

Node		$\Delta w_{V_i^\sigma}^{(h0)}$	$\Delta w_{\delta_i^\sigma}^{(h0)}$	$w_{V_i^\sigma}^{(h1)}$	$w_{\delta_i^\sigma}^{(h1)}$
10	A	-0.52257634	0.05275623	-0.02257634	0.55275623
	B	-1.56440436	-0.25018335	-1.06440436	0.24981665
	C	-0.35261256	-1.78124201	0.14738744	-1.28124201
11	A	-0.52222427	0.03759520	-0.02222427	0.53759520
	B	-1.20796913	-0.26407609	-0.70796913	0.23592391
	C	-0.52848268	-1.07309513	-0.02848268	-0.57309513
12	A	-0.51448291	0.03547605	-0.01448291	0.53547605
	B	-1.04844908	-0.26674916	-0.54844908	0.23325084
	C	-0.55199697	-0.96406578	-0.05199697	-0.46406578
13	A	-1.11296269	0.04404694	-0.61296269	0.54404694
	B	-1.13226561	-0.27273157	-0.63226561	0.22726843
	C	-0.36262632	-0.95532014	0.13737368	-0.45532014
14	A	-0.41091107	0.02061832	0.08908893	0.52061832
	B	-0.90939259	-0.27492913	-0.40939259	0.22507087
	C	-0.85393792	-0.72721006	-0.35393792	-0.22721006
15	A	-0.63253793	0.03732303	-0.13253793	0.53732303
	B	-1.04539584	-0.26918021	-0.54539584	0.23081979
	C	-0.51292038	-0.94025563	-0.01292038	-0.44025563
16	A	-1.22152426	0.04255555	-0.72152426	0.54255555
	B	-0.97624279	-0.27534993	-0.47624279	0.22465007
	C	-0.37596939	-0.85639084	0.12403061	-0.35639084
17	A	-0.41337904	0.02087923	0.08662096	0.52087923
	B	-0.90262655	-0.27499350	-0.40262655	0.22500650
	C	-0.87248995	-0.72429916	-0.37248995	-0.22429916
18	A	-0.27407630	0.00360910	0.22592370	0.50360910
	B	-0.66012219	-0.28554504	-0.16012219	0.21445496
	C	-1.45558735	-0.51567985	-0.95558735	-0.01567985
19	A	-0.71171987	0.03834379	-0.21171987	0.53834379
	B	-1.04133736	-0.27046880	-0.54133736	0.22953120
	C	-0.49206511	-0.92680134	0.00793489	-0.42680134

Sixty-first: For load buses, $P_{i,load}^{\sigma}{}^{(h1)}\begin{Bmatrix} V_i^{\sigma(k5)} + w_{V_i^\sigma}^{(h1)} \cdot \Delta\left|V_i^{\sigma(k5)}\right| \\ \delta_i^{\sigma(k5)} + w_{\delta_i^\sigma}^{(h1)} \cdot \Delta\delta_i^{\sigma(k5)} \end{Bmatrix}$ and $Q_{i,load}^{\sigma}{}^{(h1)}\begin{Bmatrix} V_i^{\sigma(k5)} + w_{V_i^\sigma}^{(h1)} \cdot \Delta\left|V_i^{\sigma(k5)}\right| \\ \delta_i^{\sigma(k5)} + w_{\delta_i^\sigma}^{(h1)} \cdot \Delta\delta_i^{\sigma(k5)} \end{Bmatrix}$ are calculated from equations (5.44), (5.45), (5.55), (5.56), (5.69) and (5.70) as shown in Table C.33. $\Delta P_{i,load}^{\sigma}{}^{(h1)}$ and $\Delta Q_{i,load}^{\sigma}{}^{(h1)}$ are calculated from equations (5.40) and (5.41) as shown Table C.33.

Table C.33 The calculated values

Node		$P_{i,load}^{\sigma}{}^{(h1)}$	$Q_{i,load}^{\sigma}{}^{(h1)}$	$\Delta P_{i,load}^{\sigma}{}^{(h1)}$	$\Delta Q_{i,load}^{\sigma}{}^{(h1)}$
2	A	-0.00518863	-0.00250504	0.00000032	0.00000086
	B	-0.00215154	-0.00105593	-0.00000694	0.00000789
	C	-0.00485691	-0.00234515	-0.00000591	-0.00000194
3	A	-0.00550321	-0.00266913	0.00000000	0.00000000
	B	-0.00404246	-0.00195885	0.00000000	0.00000000

Node		$P_{i,load}^{\sigma\ (h1)}$	$Q_{i,load}^{\sigma\ (h1)}$	$\Delta P_{i,load}^{\sigma\ (h1)}$	$\Delta Q_{i,load}^{\sigma\ (h1)}$
	C	-0.00243141	-0.00118057	0.00000000	0.00000000
4	A	-0.00324456	-0.00161157	0.00000561	0.00003708
	B	-0.00223100	-0.00137300	-0.00012710	0.00022514
	C	-0.00180279	-0.00091545	-0.00009456	0.00000192
5	A	-0.00417708	-0.00157301	0.00093813	-0.00000148
	B	0.01898891	-0.00677553	-0.02114739	0.00572749
	C	-0.00152947	-0.00102064	-0.00059275	-0.00000533
6	A	-0.00209886	-0.00101911	-0.00000046	-0.00000056
	B	-0.00128542	-0.00062292	0.00000031	-0.00000091
	C	-0.00136308	-0.00066061	-0.00000020	0.00000005
7	A	-0.00485483	-0.00235423	-0.00000359	0.00000000
	B	-0.00336520	-0.00163436	-0.00000353	-0.00000009
	C	-0.00379117	-0.00184114	-0.00000352	0.00000001
8	A	-0.00169412	-0.00082424	-0.00000032	-0.00000049
	B	-0.00225859	-0.00107226	0.00000030	-0.00000074
	C	-0.00348535	-0.00168656	-0.00000014	0.00000003
9	A	-0.00614787	-0.00298360	-0.00000013	-0.00000043
	B	-0.00620128	-0.00300630	0.00000034	-0.00000059
	C	-0.00622610	-0.00300763	0.00000000	-0.00000001
10	A	-0.00169448	-0.00082445	0.00000003	-0.00000028
	B	-0.00174677	-0.00084819	0.00000003	-0.00000023
	C	-0.00120821	-0.00059022	-0.00000047	-0.00000006
11	A	-0.00371856	-0.00179936	-0.00000023	-0.00000006
	B	-0.00309409	-0.00149707	-0.00000014	-0.00000014
	C	-0.00515778	-0.00250169	-0.00000019	0.00000000
12	A	-0.00485483	-0.00235427	-0.00000359	0.00000004
	B	-0.00330667	-0.00163439	-0.00006206	-0.00000006
	C	-0.00379429	-0.00184502	-0.00000040	0.00000390
13	A	-0.00218815	-0.00106466	-0.00000114	0.00000001
	B	-0.00221977	-0.00107297	-0.00000109	-0.00000003
	C	-0.00303463	-0.00147573	-0.00000112	0.00000002
14	A	-0.00154447	-0.00074970	-0.00000003	-0.00000006
	B	-0.00128514	-0.00062372	0.00000003	-0.00000011
	C	-0.00189734	-0.00091353	0.00000000	0.00000000
15	A	-0.00218867	-0.00106466	-0.00000062	0.00000000
	B	-0.00202064	-0.00097317	-0.00000060	-0.00000001
	C	-0.00326001	-0.00157410	-0.00000061	0.00000001
16	A	-0.00388259	-0.00188939	-0.00000114	0.00000000
	B	-0.00431586	-0.00208358	-0.00000109	-0.00000003
	C	-0.00363897	-0.00177087	-0.00000112	0.00000001
17	A	-0.00323894	-0.00157449	0.00000000	0.00000000
	B	-0.00202123	-0.00097319	0.00000000	0.00000000
	C	-0.00227681	-0.00109624	0.00000000	0.00000000
18	A	-0.00266846	-0.00128973	-0.00000067	0.00000015
	B	-0.00217390	-0.00107302	-0.00004696	0.00000002
	C	-0.00515761	-0.00251112	-0.00000035	0.00000944
19	A	-0.00437778	-0.00211431	-0.00000079	0.00000000
	B	-0.00417895	-0.00202122	-0.00000077	-0.00000002
	C	-0.00515719	-0.00250169	-0.00000078	0.00000001

Sixty-second: Determine $max\{|\Delta P_{i,load}^{\sigma}{}^{(h1)}|, |\Delta Q_{i,load}^{\sigma}{}^{(h1)}|\} = 0.0211$ and $max\{|\Delta P_{i,load}^{\sigma}{}^{(h0)}|, |\Delta Q_{i,load}^{\sigma}{}^{(h0)}|\} = 0.0130$. Then, update voltage magnitudes, $|V_i^{\sigma(k6)}| = |V_i^{\sigma(k5)}| + w_{V_i}{}^{\sigma(h0)} \cdot \Delta |V_i^{\sigma(k5)}|$, and phase angles, $\delta_i^{\sigma(k6)} = \delta_i^{\sigma(k5)} + w_{\delta_i}{}^{\sigma(h0)} \cdot \Delta\delta_i^{\sigma(k5)}$, by $w_{V_i}{}^{\sigma(h0)}$ and $w_{V_i}{}^{\sigma(h0)}$ at equations (5.42) and (5.43) as shown in Table C.34. After that, renew $w_{V_i}{}^{\sigma(h0)} = w_{V_i}{}^{\sigma(h0)} = 0.4$ and go to ***STEP 3*** of the power flow algorithm.

Table C.34 The updated values

Node		$\|V_i^{\sigma(k6)}\|$	$\delta_i^{\sigma(k6)}$
2	A	1.04923163	0.01674951
	B	1.04772974	-2.07517909
	C	1.04512009	2.10879275
3	A	1.02575121	0.02300412
	B	1.03070002	-2.07909846
	C	1.04233799	2.10909903
4	A	1.05018759	0.03908177
	B	1.04593882	-2.04900936
	C	1.03938130	2.12821793
5	A	1.06415592	0.11241985
	B	1.03064406	-1.93433784
	C	1.05821352	2.18301359
6	A	1.05182522	0.05910705
	B	1.04661170	-2.02600791
	C	1.03425411	2.14645871
7	A	1.06023075	0.08832738
	B	1.05620350	-1.99591007
	C	1.03880784	2.17403765
8	A	1.05317360	0.07545713
	B	1.04725177	-2.00699321
	C	1.02983451	2.16154010
9	A	1.05408444	0.09006570
	B	1.04789874	-1.99018653
	C	1.02609111	2.17514446
10	A	1.05542166	0.10101478
	B	1.04912468	-1.97750312
	C	1.02382570	2.18558243
11	A	1.05806734	0.10996754
	B	1.05259826	-1.96746504
	C	1.02448412	2.19465906
12	A	1.05943618	0.11305487
	B	1.05358976	-1.96453016
	C	1.02609690	2.19741337
13	A	1.06552215	0.12388065
	B	1.05883466	-1.95179872
	C	1.02681203	2.20838602
14	A	1.05807654	0.11333912
	B	1.05371611	-1.96379816
	C	1.02466966	2.19816825
15	A	1.06203004	0.11864710

Node		$\left\|V_i^{\sigma(k6)}\right\|$	$\delta_i^{\sigma(k6)}$
	B	1.05582168	-1.95823704
	C	1.02664663	2.20292842
16	A	1.06541292	0.12768390
	B	1.05741752	-1.94909321
	C	1.02850346	2.21084230
17	A	1.05463160	0.11380500
	B	1.05192543	-1.96415732
	C	1.02305966	2.19840751
18	A	1.05908538	0.11661713
	B	1.05541764	-1.96009235
	C	1.02554418	2.20161360
19	A	1.06313012	0.12146963
	B	1.05673554	-1.95510187
	C	1.02678359	2.20567574

Sixty-third: For load buses, ${P_{i,load}^{\sigma}}^{(k6)}\begin{Bmatrix}V_i^{\sigma(k6)}\\ \delta_i^{\sigma(k6)}\end{Bmatrix}$ and ${Q_{i,load}^{\sigma}}^{(k6)}\begin{Bmatrix}V_i^{\sigma(k6)}\\ \delta_i^{\sigma(k6)}\end{Bmatrix}$ are calculated from equations (5.1), (5.2), (5.16), (5.17), (5.30) and (5.31) as shown Table C.35. ${\Delta P_{i,load}^{\sigma}}^{(k6)}$ and ${\Delta Q_{i,load}^{\sigma}}^{(k6)}$ are calculated from equations (5.40) and (5.41) as shown Table C.35.

Table C.35 The calculated values

Node		${P_{i,load}^{\sigma}}^{(k6)}$	${Q_{i,load}^{\sigma}}^{(k6)}$	${\Delta P_{i,load}^{\sigma}}^{(k6)}$	${\Delta Q_{i,load}^{\sigma}}^{(k6)}$
2	A	-0.00516680	-0.00247823	-0.00002151	-0.00002595
	B	-0.00212924	-0.00103606	-0.00002924	-0.00001199
	C	-0.00483640	-0.00232269	-0.00002642	-0.00002440
3	A	-0.00550318	-0.00266911	-0.00000003	-0.00000002
	B	-0.00404247	-0.00195884	0.00000000	-0.00000001
	C	-0.00243141	-0.00118057	0.00000000	0.00000000
4	A	-0.00278111	-0.00135102	-0.00045783	-0.00022347
	B	-0.00198200	-0.00078264	-0.00037610	-0.00036522
	C	-0.00172025	-0.00079469	-0.00017709	-0.00011885
5	A	0.00219793	-0.00412288	-0.00543688	0.00254839
	B	-0.00842928	-0.01409207	0.00627080	0.01304403
	C	-0.00036385	-0.00109715	-0.00175836	0.00007118
6	A	-0.00209737	-0.00101906	-0.00000195	-0.00000061
	B	-0.00127995	-0.00062139	-0.00000516	-0.00000245
	C	-0.00136033	-0.00065595	-0.00000295	-0.00000461
7	A	-0.00483551	-0.00235349	-0.00002291	-0.00000075
	B	-0.00334598	-0.00163402	-0.00002274	-0.00000043
	C	-0.00377226	-0.00184122	-0.00002242	0.00000010
8	A	-0.00169225	-0.00082422	-0.00000219	-0.00000051
	B	-0.00225294	-0.00107041	-0.00000535	-0.00000259
	C	-0.00348252	-0.00168214	-0.00000297	-0.00000438
9	A	-0.00614686	-0.00298404	-0.00000114	0.00000001
	B	-0.00619753	-0.00300425	-0.00000341	-0.00000264
	C	-0.00622506	-0.00300381	-0.00000104	-0.00000383
10	A	-0.00168853	-0.00082404	-0.00000592	-0.00000069
	B	-0.00175564	-0.00084844	0.00000889	0.00000002

Node		$P_{i,load}^{\sigma\ (k6)}$	$Q_{i,load}^{\sigma\ (k6)}$	$\Delta P_{i,load}^{\sigma\ (k6)}$	$\Delta Q_{i,load}^{\sigma\ (k6)}$
	C	-0.00120324	-0.00060058	-0.00000544	0.00001030
11	A	-0.00371115	-0.00179785	-0.00000764	-0.00000157
	B	-0.00308623	-0.00149657	-0.00000800	-0.00000064
	C	-0.00514985	-0.00250093	-0.00000811	-0.00000076
12	A	-0.00482485	-0.00235685	-0.00003357	0.00000262
	B	-0.00281489	-0.00162846	-0.00055383	-0.00000599
	C	-0.00379467	-0.00208815	-0.00000002	0.00024702
13	A	-0.00213223	-0.00106288	-0.00005706	-0.00000177
	B	-0.00216388	-0.00107188	-0.00005699	-0.00000112
	C	-0.00298034	-0.00147613	-0.00005541	0.00000042
14	A	-0.00154425	-0.00074898	-0.00000025	-0.00000078
	B	-0.00128454	-0.00062291	-0.00000056	-0.00000092
	C	-0.00189667	-0.00091257	-0.00000068	-0.00000097
15	A	-0.00216394	-0.00106312	-0.00002535	-0.00000153
	B	-0.00199589	-0.00097276	-0.00002534	-0.00000043
	C	-0.00323575	-0.00157420	-0.00002487	0.00000011
16	A	-0.00382613	-0.00188755	-0.00005761	-0.00000184
	B	-0.00425964	-0.00208248	-0.00005732	-0.00000113
	C	-0.00358423	-0.00177130	-0.00005586	0.00000045
17	A	-0.00323865	-0.00157421	-0.00000029	-0.00000028
	B	-0.00202129	-0.00097320	0.00000005	0.00000001
	C	-0.00227679	-0.00109626	-0.00000003	0.00000002
18	A	-0.00265528	-0.00130857	-0.00001385	0.00001899
	B	-0.00174973	-0.00106585	-0.00047113	-0.00000715
	C	-0.00515958	-0.00278305	0.00000162	0.00028137
19	A	-0.00434508	-0.00211261	-0.00003350	-0.00000170
	B	-0.00414641	-0.00202063	-0.00003330	-0.00000061
	C	-0.00512539	-0.00250186	-0.00003257	0.00000018

Sixty-fourth: The linear simultaneous equation (5.7) is solved directly by optimally ordered triangular factorization and Gaussian elimination. The $\Delta\delta_i^{\sigma(k6)}$ and $\Delta\left|V_i^{\sigma(k6)}\right|$ are obtained as shown Table C.36.

Sixty-fifth: For load buses, $P_{i,load}^{\sigma\ (h0)}\begin{Bmatrix} V_i^{\sigma(k6)} + w_{V_i^\sigma}^{(h0)} \cdot \Delta\left|V_i^{\sigma(k6)}\right| \\ \delta_i^{\sigma(k6)} + w_{\delta_i^\sigma}^{(h0)} \cdot \Delta\delta_i^{\sigma(k6)} \end{Bmatrix}$ and $Q_{i,load}^{\sigma\ (h0)}\begin{Bmatrix} V_i^{\sigma(k6)} + w_{V_i^\sigma}^{(h0)} \cdot \Delta\left|V_i^{\sigma(k6)}\right| \\ \delta_i^{\sigma(k6)} + w_{\delta_i^\sigma}^{(h0)} \cdot \Delta\delta_i^{\sigma(k6)} \end{Bmatrix}$ are calculated from equations (5.44), (5.45), (5.55), (5.56), (5.69) and (5.70) as shown in Table C.36. $\Delta P_{i,load}^{\sigma\ (h0)}$ and $\Delta Q_{i,load}^{\sigma\ (h0)}$ are calculated from equations (5.40) and (5.41) as shown Table C.36.

Table C.36 The calculated values

Node		$\Delta\left\|V_i^{\sigma(k6)}\right\|$	$\Delta\delta_i^{\sigma(k6)}$	$P_{i,load}^{\sigma\ (h0)}$	$Q_{i,load}^{\sigma\ (h0)}$	$\Delta P_{i,load}^{\sigma\ (h0)}$	$\Delta Q_{i,load}^{\sigma\ (h0)}$
2	A	-0.00020968	-0.00027667	-0.00517546	-0.00248875	-0.00001285	-0.00001543
	B	0.00102365	-0.00034096	-0.00213983	-0.00104212	-0.00001865	-0.00000593
	C	-0.00009675	0.00043840	-0.00484602	-0.00233214	-0.00001680	-0.00001495

Node		$\Delta\left\|V_i^{\sigma(k6)}\right\|$	$\Delta\delta_i^{\sigma(k6)}$	$P_{i,load}^{\sigma\ (h0)}$	$Q_{i,load}^{\sigma\ (h0)}$	$\Delta P_{i,load}^{\sigma\ (h0)}$	$\Delta Q_{i,load}^{\sigma\ (h0)}$
3	A	-0.00021843	-0.00027883	-0.00550319	-0.00266912	-0.00000002	-0.00000001
	B	0.00104382	-0.00033926	-0.00404247	-0.00195884	0.00000000	-0.00000001
	C	-0.00009946	0.00043864	-0.00243141	-0.00118057	0.00000000	0.00000000
4	A	-0.00050039	-0.00063656	-0.00296520	-0.00144631	-0.00027374	-0.00012817
	B	0.00236890	-0.00085548	-0.00211237	-0.00096481	-0.00024573	-0.00018305
	C	-0.00020247	0.00103306	-0.00177597	-0.00084259	-0.00012138	-0.00007094
5	A	-0.00416437	-0.01301417	-0.00029099	-0.00310328	-0.00294795	0.00152879
	B	0.04519568	-0.02292441	-0.00577422	-0.01104699	0.00361574	0.00999894
	C	-0.00219902	0.01607007	-0.00096499	-0.00106761	-0.00115723	0.00004164
6	A	-0.00043641	-0.00051513	-0.00209808	-0.00101921	-0.00000124	-0.00000046
	B	0.00207990	-0.00104030	-0.00128206	-0.00062222	-0.00000304	-0.00000161
	C	-0.00010239	0.00090520	-0.00136148	-0.00065780	-0.00000180	-0.00000276
7	A	-0.00056130	-0.00054235	-0.00484411	-0.00235378	-0.00001430	-0.00000045
	B	0.00195771	-0.00114196	-0.00335453	-0.00163418	-0.00001419	-0.00000027
	C	-0.00015843	0.00084057	-0.00378069	-0.00184119	-0.00001400	0.00000006
8	A	-0.00035959	-0.00039320	-0.00169308	-0.00082434	-0.00000137	-0.00000039
	B	0.00179318	-0.00120021	-0.00225513	-0.00107133	-0.00000316	-0.00000167
	C	-0.00000642	0.00077846	-0.00348369	-0.00168390	-0.00000180	-0.00000262
9	A	-0.00027802	-0.00027328	-0.00614729	-0.00298397	-0.00000070	-0.00000006
	B	0.00150395	-0.00134599	-0.00619895	-0.00300522	-0.00000199	-0.00000168
	C	0.00008485	0.00064881	-0.00622547	-0.00300534	-0.00000062	-0.00000230
10	A	-0.00021438	-0.00018439	-0.00169090	-0.00082427	-0.00000355	-0.00000046
	B	0.00128323	-0.00144955	-0.00175209	-0.00084839	0.00000534	-0.00000003
	C	0.00015167	0.00054924	-0.00120534	-0.00059645	-0.00000334	0.00000617
11	A	-0.00017809	-0.00013058	-0.00371417	-0.00179847	-0.00000462	-0.00000095
	B	0.00107547	-0.00152230	-0.00308941	-0.00149680	-0.00000482	-0.00000041
	C	0.00018943	0.00048702	-0.00515307	-0.00250123	-0.00000490	-0.00000045
12	A	-0.00015748	-0.00012175	-0.00483770	-0.00235581	-0.00002071	0.00000158
	B	0.00104890	-0.00152286	-0.00302721	-0.00163085	-0.00034151	-0.00000360
	C	0.00018606	0.00045740	-0.00379461	-0.00198997	-0.00000007	0.00014884
13	A	-0.00023683	-0.00015184	-0.00215488	-0.00106359	-0.00003441	-0.00000106
	B	0.00099643	-0.00155750	-0.00218650	-0.00107233	-0.00003436	-0.00000067
	C	0.00015294	0.00044935	-0.00300233	-0.00147597	-0.00003342	0.00000026
14	A	-0.00012791	-0.00007144	-0.00154434	-0.00074928	-0.00000016	-0.00000048
	B	0.00088801	-0.00158196	-0.00128477	-0.00062326	-0.00000033	-0.00000057
	C	0.00023309	0.00043522	-0.00189694	-0.00091296	-0.00000041	-0.00000058
15	A	-0.00016964	-0.00012751	-0.00217398	-0.00106374	-0.00001531	-0.00000092
	B	0.00102901	-0.00153229	-0.00200594	-0.00097293	-0.00001530	-0.00000026
	C	0.00018003	0.00044710	-0.00324560	-0.00157416	-0.00001502	0.00000006
16	A	-0.00021672	-0.00014464	-0.00384899	-0.00188828	-0.00003474	-0.00000110
	B	0.00097258	-0.00155764	-0.00428240	-0.00208293	-0.00003456	-0.00000069
	C	0.00014760	0.00041971	-0.00360640	-0.00177113	-0.00003369	0.00000027
17	A	-0.00012809	-0.00007221	-0.00323877	-0.00157432	-0.00000017	-0.00000017
	B	0.00089078	-0.00158091	-0.00202127	-0.00097319	0.00000003	0.00000001
	C	0.00023268	0.00043472	-0.00227680	-0.00109625	-0.00000002	0.00000001
18	A	-0.00007729	-0.00001248	-0.00266071	-0.00130099	-0.00000842	0.00001141
	B	0.00069949	-0.00164060	-0.00193097	-0.00106871	-0.00028990	-0.00000429
	C	0.00027671	0.00038327	-0.00515888	-0.00267203	0.00000091	0.00017035
19	A	-0.00017658	-0.00013069	-0.00435835	-0.00211329	-0.00002022	-0.00000102
	B	0.00101848	-0.00153718	-0.00415961	-0.00202087	-0.00002010	-0.00000037

Node		$\Delta\left\|V_i^{\sigma(k6)}\right\|$	$\Delta\delta_i^{\sigma(k6)}$	${P_{i,load}^{\sigma}}^{(h0)}$	${Q_{i,load}^{\sigma}}^{(h0)}$	${\Delta P_{i,load}^{\sigma}}^{(h0)}$	${\Delta Q_{i,load}^{\sigma}}^{(h0)}$
	C	0.00017623	0.00044160	-0.00513830	-0.00250179	-0.00001966	0.00000011

Sixty-sixth: The elements of the Jacobian matrix (J_1, J_2, J_3 and J_4) are calculated from equations (5.47)-(5.54), (5.57)-(5.68) and (5.71)-(5.78).

Sixty-seventh: The linear simultaneous equation (5.46) is solved directly by optimally ordered triangular factorization and Gaussian elimination. The $\Delta w_{V_i^{\sigma}}{}^{(h0)}$ and $\Delta w_{\delta_i^{\sigma}}{}^{(h0)}$ are obtained as shown in Table C.37.

Sixty-eighth: The new step-length values $\begin{Bmatrix} w_{V_i^{\sigma}}^{(h1)} = w_{V_i^{\sigma}}^{(h0)} + \Delta w_{V_i^{\sigma}}{}^{(h0)} \\ w_{\delta_i^{\sigma}}^{(h1)} = w_{\delta_i^{\sigma}}^{(h0)} + \Delta w_{\delta_i^{\sigma}}{}^{(h0)} \end{Bmatrix}$ are computed from equations (5.79) and (5.80) as shown in Table C.37.

Table C.37 The calculated values

Node		$\Delta w_{V_i^{\sigma}}{}^{(h0)}$	$\Delta w_{\delta_i^{\sigma}}{}^{(h0)}$	$w_{V_i^{\sigma}}{}^{(h1)}$	$w_{\delta_i^{\sigma}}{}^{(h1)}$
2	A	1.08016010	-0.12326045	1.48016010	0.27673955
	B	0.85998305	2.32261674	1.25998305	2.72261674
	C	-0.16667299	0.78152508	0.23332701	1.18152508
3	A	1.06710694	-0.10389684	1.46710694	0.29610316
	B	0.86560295	2.32520310	1.26560295	2.72520310
	C	-0.10875902	0.78433928	0.29124098	1.18433928
4	A	1.04722878	-0.14133086	1.44722878	0.25866914
	B	0.84617464	2.22118428	1.24617464	2.62118428
	C	-0.27571541	0.77750742	0.12428459	1.17750742
5	A	0.67824225	0.14496067	1.07824225	0.54496067
	B	0.71379122	1.73755914	1.11379122	2.13755914
	C	0.24496279	0.72589723	0.64496279	1.12589723
6	A	1.04142905	-0.34743335	1.44142905	0.05256665
	B	0.85174557	1.96254943	1.25174557	2.36254943
	C	-1.06947121	0.80089193	-0.66947121	1.20089193
7	A	0.95989646	-0.25575121	1.35989646	0.14424879
	B	0.83688501	1.85049996	1.23688501	2.25049996
	C	-0.39071528	0.78794047	0.00928472	1.18794047
8	A	1.05020517	-0.68556051	1.45020517	-0.28556051
	B	0.86152205	1.80268855	1.26152205	2.20268855
	C	-25.02256221	0.83456853	-24.62256221	1.23456853
9	A	1.07437630	-1.31332951	1.47437630	-0.91332951
	B	0.87677143	1.69007501	1.27677143	2.09007501
	C	2.45775895	0.88373870	2.85775895	1.28373870
10	A	1.10936960	-2.30654856	1.50936960	-1.90654856
	B	0.89274561	1.62402201	1.29274561	2.02402201
	C	1.60898552	0.93731927	2.00898552	1.33731927
11	A	1.11033466	-3.56981310	1.51033466	-3.16981310
	B	0.90951154	1.58367754	1.30951154	1.98367754
	C	1.39242894	0.99869288	1.79242894	1.39869288
12	A	1.11571639	-3.85462267	1.51571639	-3.45462267
	B	0.91808738	1.57998588	1.31808738	1.97998588

Node		$\Delta w_{V_i^\sigma}^{(h0)}$	$\Delta w_{\delta_i^\sigma}^{(h0)}$	$w_{V_i^\sigma}^{(h1)}$	$w_{\delta_i^\sigma}^{(h1)}$
	C	1.39415436	1.01381344	1.79415436	1.41381344
13	A	0.96615221	-2.91275123	1.36615221	-2.51275123
	B	0.90711695	1.56068046	1.30711695	1.96068046
	C	1.57728120	1.01187577	1.97728120	1.41187577
14	A	1.18871844	-7.19741132	1.58871844	-6.79741132
	B	0.93719131	1.55516117	1.33719131	1.95516117
	C	1.22934535	1.07393091	1.62934535	1.47393091
15	A	1.06119783	-3.61889502	1.46119783	-3.21889502
	B	0.91527183	1.57320291	1.31527183	1.97320291
	C	1.42374560	1.01639621	1.82374560	1.41639621
16	A	0.95358430	-3.06235408	1.35358430	-2.66235408
	B	0.91717754	1.55723681	1.31717754	1.95723681
	C	1.58555821	1.02895828	1.98555821	1.42895828
17	A	1.18528472	-7.09672965	1.58528472	-6.69672965
	B	0.93871924	1.55503982	1.33871924	1.95503982
	C	1.22569908	1.07455564	1.62569908	1.47455564
18	A	1.37285492	-45.05747691	1.77285492	-44.65747691
	B	0.97925216	1.52937505	1.37925216	1.92937505
	C	1.11934411	1.16975788	1.51934411	1.56975788
19	A	1.03497960	-3.49838681	1.43497960	-3.09838681
	B	0.91408291	1.56967934	1.31408291	1.96967934
	C	1.44186677	1.01795924	1.84186677	1.41795924

Sixty-ninth: For load buses, ${P_{i,load}^{\sigma}}^{(h1)} \begin{Bmatrix} V_i^{\sigma(k6)} + w_{V_i^\sigma}^{(h1)} \cdot \Delta\left|V_i^{\sigma(k6)}\right| \\ \delta_i^{\sigma(k6)} + w_{\delta_i^\sigma}^{(h1)} \cdot \Delta\delta_i^{\sigma(k6)} \end{Bmatrix}$ and ${Q_{i,load}^{\sigma}}^{(h1)} \begin{Bmatrix} V_i^{\sigma(k6)} + w_{V_i^\sigma}^{(h1)} \cdot \Delta\left|V_i^{\sigma(k6)}\right| \\ \delta_i^{\sigma(k6)} + w_{\delta_i^\sigma}^{(h1)} \cdot \Delta\delta_i^{\sigma(k6)} \end{Bmatrix}$ are calculated from equations (5.44), (5.45), (5.55), (5.56), (5.69) and (5.70) as shown in Table C.38. ${\Delta P_{i,load}^{\sigma}}^{(h1)}$ and ${\Delta Q_{i,load}^{\sigma}}^{(h1)}$ are calculated from equations (5.40) and (5.41) as shown Table C.38.

Table C.38 The calculated values

Node		$P_{i,load}^{\sigma(h1)}$	$Q_{i,load}^{\sigma(h1)}$	$\Delta P_{i,load}^{\sigma(h1)}$	$\Delta Q_{i,load}^{\sigma(h1)}$
2	A	-0.00518728	-0.00251046	-0.00000103	0.00000628
	B	-0.00214067	-0.00105863	-0.00001781	0.00001058
	C	-0.00485630	-0.00234298	-0.00000652	-0.00000410
3	A	-0.00550321	-0.00266913	0.00000000	0.00000000
	B	-0.00404246	-0.00195885	0.00000000	0.00000000
	C	-0.00243141	-0.00118057	0.00000000	0.00000000
4	A	-0.00324368	-0.00165710	0.00000473	0.00008261
	B	-0.00208881	-0.00138743	-0.00026930	0.00023957
	C	-0.00180274	-0.00088977	-0.00009460	-0.00002376
5	A	-0.00297238	-0.00149163	-0.00026656	-0.00008286
	B	0.01754928	-0.00058182	-0.01970775	-0.00046622
	C	-0.00218490	-0.00107207	0.00006269	0.00004610
6	A	-0.00209899	-0.00101933	-0.00000033	-0.00000033

Node		$P_{i,load}^{\sigma\ (h1)}$	$Q_{i,load}^{\sigma\ (h1)}$	$\Delta P_{i,load}^{\sigma\ (h1)}$	$\Delta Q_{i,load}^{\sigma\ (h1)}$
	B	-0.00128525	-0.00062327	0.00000014	-0.00000057
	C	-0.00136314	-0.00066058	-0.00000014	0.00000002
7	A	-0.00485509	-0.00235422	-0.00000333	-0.00000001
	B	-0.00336542	-0.00163445	-0.00000331	-0.00000001
	C	-0.00379140	-0.00184113	-0.00000329	0.00000000
8	A	-0.00169423	-0.00082445	-0.00000022	-0.00000029
	B	-0.00225844	-0.00107256	0.00000014	-0.00000044
	C	-0.00348542	-0.00168653	-0.00000007	0.00000000
9	A	-0.00614793	-0.00298377	-0.00000007	-0.00000026
	B	-0.00620116	-0.00300651	0.00000021	-0.00000039
	C	-0.00622616	-0.00300761	0.00000006	-0.00000003
10	A	-0.00169457	-0.00082494	0.00000012	0.00000021
	B	-0.00174644	-0.00084844	-0.00000030	0.00000002
	C	-0.00120826	-0.00059026	-0.00000042	-0.00000002
11	A	-0.00371859	-0.00179938	-0.00000020	-0.00000003
	B	-0.00309407	-0.00149714	-0.00000016	-0.00000007
	C	-0.00515779	-0.00250167	-0.00000017	-0.00000001
12	A	-0.00485403	-0.00235449	-0.00000438	0.00000025
	B	-0.00330885	-0.00163452	-0.00005987	0.00000007
	C	-0.00379432	-0.00184858	-0.00000037	0.00000746
13	A	-0.00218809	-0.00106466	-0.00000120	0.00000001
	B	-0.00221968	-0.00107301	-0.00000118	0.00000001
	C	-0.00303456	-0.00147571	-0.00000119	0.00000000
14	A	-0.00154448	-0.00074972	-0.00000002	-0.00000004
	B	-0.00128513	-0.00062376	0.00000002	-0.00000008
	C	-0.00189735	-0.00091353	0.00000001	-0.00000001
15	A	-0.00218867	-0.00106466	-0.00000062	0.00000001
	B	-0.00202061	-0.00097320	-0.00000062	0.00000002
	C	-0.00326000	-0.00157409	-0.00000062	0.00000000
16	A	-0.00388250	-0.00188939	-0.00000123	0.00000001
	B	-0.00431574	-0.00208362	-0.00000122	0.00000000
	C	-0.00363887	-0.00177085	-0.00000122	0.00000000
17	A	-0.00323894	-0.00157449	0.00000000	0.00000000
	B	-0.00202123	-0.00097318	0.00000000	0.00000000
	C	-0.00227681	-0.00109624	0.00000000	0.00000000
18	A	-0.00266779	-0.00128988	-0.00000134	0.00000030
	B	-0.00217218	-0.00107308	-0.00004868	0.00000008
	C	-0.00515759	-0.00251337	-0.00000037	0.00001169
19	A	-0.00437777	-0.00211432	-0.00000080	0.00000001
	B	-0.00417891	-0.00202125	-0.00000080	0.00000001
	C	-0.00515717	-0.00250168	-0.00000080	0.00000000

Seventieth: Determine $max\{|\Delta P_{i,load}^{\sigma\ (h1)}|, |\Delta Q_{i,load}^{\sigma\ (h1)}|\} = 0.0197$ and $max\{|\Delta P_{i,load}^{\sigma\ (h0)}|, |\Delta Q_{i,load}^{\sigma\ (h0)}|\} = 0.0100$. Then, update voltage magnitudes, $|V_i^{\sigma(k7)}| = |V_i^{\sigma(k6)}| + w_{V_i^{\sigma}}{}^{(h0)} \cdot \Delta|V_i^{\sigma(k6)}|$, and phase angles, $\delta_i^{\sigma(k7)} = \delta_i^{\sigma(k6)} + w_{\delta_i^{\sigma}}{}^{(h0)} \cdot \Delta\delta_i^{\sigma(k6)}$, by $w_{V_i^{\sigma}}{}^{(h0)}$ and $w_{V_i^{\sigma}}{}^{(h0)}$ at equations (5.42) and (5.43) as shown in Table C.39. After that, renew $w_{V_i^{\sigma}}{}^{(h0)} = w_{V_i^{\sigma}}{}^{(h0)} = 0.3$ and go to ***STEP 3*** of the power flow algorithm.

Table C.39 The updated values

Node		$\lvert V_i^{\sigma(k7)} \rvert$	$\delta_i^{\sigma(k7)}$
2	A	1.04914776	0.01663884
	B	1.04813920	-2.07531548
	C	1.04508139	2.10896811
3	A	1.02566384	0.02289259
	B	1.03111755	-2.07923416
	C	1.04229820	2.10927449
4	A	1.04998743	0.03882715
	B	1.04688637	-2.04935155
	C	1.03930031	2.12863115
5	A	1.06249017	0.10721418
	B	1.04872233	-1.94350760
	C	1.05733392	2.18944161
6	A	1.05165066	0.05890099
	B	1.04744367	-2.02642403
	C	1.03421316	2.14682079
7	A	1.06000622	0.08811044
	B	1.05698659	-1.99636686
	C	1.03874447	2.17437388
8	A	1.05302977	0.07529985
	B	1.04796904	-2.00747330
	C	1.02983194	2.16185148
9	A	1.05397323	0.08995639
	B	1.04850032	-1.99072493
	C	1.02612505	2.17540398
10	A	1.05533591	0.10094103
	B	1.04963797	-1.97808294
	C	1.02388637	2.18580212
11	A	1.05799611	0.10991531
	B	1.05302845	-1.96807396
	C	1.02455989	2.19485387
12	A	1.05937318	0.11300617
	B	1.05400932	-1.96513930
	C	1.02617132	2.19759633
13	A	1.06542742	0.12381991
	B	1.05923324	-1.95242172
	C	1.02687321	2.20856576
14	A	1.05802537	0.11331055
	B	1.05407132	-1.96443094
	C	1.02476290	2.19834234
15	A	1.06196218	0.11859609
	B	1.05623329	-1.95884996
	C	1.02671864	2.20310726
16	A	1.06532623	0.12762604
	B	1.05780655	-1.94971626
	C	1.02856250	2.21101019
17	A	1.05458036	0.11377611
	B	1.05228174	-1.96478968
	C	1.02315273	2.19858140
18	A	1.05905447	0.11661213

Node		$\left\|V_i^{\sigma(k7)}\right\|$	$\delta_i^{\sigma(k7)}$
	B	1.05569744	-1.96074859
	C	1.02565487	2.20176691
19	A	1.06305949	0.12141735
	B	1.05714293	-1.95571674
	C	1.02685408	2.20585238

Seventy-First: For load buses, $P_{i,load}^{\sigma}{}^{(k7)}\begin{Bmatrix}V_i^{\sigma(k7)}\\ \delta_i^{\sigma(k7)}\end{Bmatrix}$ and $Q_{i,load}^{\sigma}{}^{(k7)}\begin{Bmatrix}V_i^{\sigma(k7)}\\ \delta_i^{\sigma(k7)}\end{Bmatrix}$ are calculated from equations (5.1), (5.2), (5.16), (5.17), (5.30) and (5.31) as shown Table C.35. $\Delta P_{i,load}^{\sigma}{}^{(k7)}$ and $\Delta Q_{i,load}^{\sigma}{}^{(k7)}$ are calculated from equations (5.40) and (5.41) as shown Table C.40.

Table C.40 The calculated values

Node		$P_{i,load}^{\sigma}{}^{(k7)}$	$Q_{i,load}^{\sigma}{}^{(k7)}$	$\Delta P_{i,load}^{\sigma}{}^{(k7)}$	$\Delta Q_{i,load}^{\sigma}{}^{(k7)}$
2	A	-0.00517546	-0.00248875	-0.00001285	-0.00001543
	B	-0.00213983	-0.00104212	-0.00001865	-0.00000593
	C	-0.00484602	-0.00233214	-0.00001680	-0.00001495
3	A	-0.00550319	-0.00266912	-0.00000002	-0.00000001
	B	-0.00404247	-0.00195884	0.00000000	-0.00000001
	C	-0.00243141	-0.00118057	0.00000000	0.00000000
4	A	-0.00296520	-0.00144631	-0.00027374	-0.00012817
	B	-0.00211237	-0.00096481	-0.00024573	-0.00018305
	C	-0.00177597	-0.00084259	-0.00012138	-0.00007094
5	A	-0.00029099	-0.00310328	-0.00294795	0.00152879
	B	-0.00577422	-0.01104699	0.00361574	0.00999894
	C	-0.00096499	-0.00106761	-0.00115723	0.00004164
6	A	-0.00209808	-0.00101921	-0.00000124	-0.00000046
	B	-0.00128206	-0.00062222	-0.00000304	-0.00000161
	C	-0.00136148	-0.00065780	-0.00000180	-0.00000276
7	A	-0.00484411	-0.00235378	-0.00001430	-0.00000045
	B	-0.00335453	-0.00163418	-0.00001419	-0.00000027
	C	-0.00378069	-0.00184119	-0.00001400	0.00000006
8	A	-0.00169308	-0.00082434	-0.00000137	-0.00000039
	B	-0.00225513	-0.00107133	-0.00000316	-0.00000167
	C	-0.00348369	-0.00168390	-0.00000180	-0.00000262
9	A	-0.00614729	-0.00298397	-0.00000070	-0.00000006
	B	-0.00619895	-0.00300522	-0.00000199	-0.00000168
	C	-0.00622547	-0.00300534	-0.00000062	-0.00000230
10	A	-0.00169090	-0.00082427	-0.00000355	-0.00000046
	B	-0.00175209	-0.00084839	0.00000534	-0.00000003
	C	-0.00120534	-0.00059645	-0.00000334	0.00000617
11	A	-0.00371417	-0.00179847	-0.00000462	-0.00000095
	B	-0.00308941	-0.00149680	-0.00000482	-0.00000041
	C	-0.00515307	-0.00250123	-0.00000490	-0.00000045
12	A	-0.00483770	-0.00235581	-0.00002071	0.00000158
	B	-0.00302721	-0.00163085	-0.00034151	-0.00000360
	C	-0.00379461	-0.00198997	-0.00000007	0.00014884
13	A	-0.00215488	-0.00106359	-0.00003441	-0.00000106
	B	-0.00218650	-0.00107233	-0.00003436	-0.00000067

Node		$P_{i,load}^{\sigma\ (k7)}$	$Q_{i,load}^{\sigma\ (k7)}$	$\Delta P_{i,load}^{\sigma\ (k7)}$	$\Delta Q_{i,load}^{\sigma\ (k7)}$
	C	-0.00300233	-0.00147597	-0.00003342	0.00000026
14	A	-0.00154434	-0.00074928	-0.00000016	-0.00000048
	B	-0.00128477	-0.00062326	-0.00000033	-0.00000057
	C	-0.00189694	-0.00091296	-0.00000041	-0.00000058
15	A	-0.00217398	-0.00106374	-0.00001531	-0.00000092
	B	-0.00200594	-0.00097293	-0.00001530	-0.00000026
	C	-0.00324560	-0.00157416	-0.00001502	0.00000006
16	A	-0.00384899	-0.00188828	-0.00003474	-0.00000110
	B	-0.00428240	-0.00208293	-0.00003456	-0.00000069
	C	-0.00360640	-0.00177113	-0.00003369	0.00000027
17	A	-0.00323877	-0.00157432	-0.00000017	-0.00000017
	B	-0.00202127	-0.00097319	0.00000003	0.00000001
	C	-0.00227680	-0.00109625	-0.00000002	0.00000001
18	A	-0.00266071	-0.00130099	-0.00000842	0.00001141
	B	-0.00193097	-0.00106871	-0.00028990	-0.00000429
	C	-0.00515888	-0.00267203	0.00000091	0.00017035
19	A	-0.00435835	-0.00211329	-0.00002022	-0.00000102
	B	-0.00415961	-0.00202087	-0.00002010	-0.00000037
	C	-0.00513830	-0.00250179	-0.00001966	0.00000011

Seventy-second: The linear simultaneous equation (5.7) is solved directly by optimally ordered triangular factorization and Gaussian elimination. The $\Delta\delta_i^{\sigma(k7)}$ and $\Delta\left|V_i^{\sigma(k7)}\right|$ are obtained as shown Table C.41.

Seventy-third: For load buses, $P_{i,load}^{\sigma\ (h0)}\begin{Bmatrix} V_i^{\sigma(k7)} + w_{V_i^\sigma}^{(h0)} \cdot \Delta\left|V_i^{\sigma(k7)}\right| \\ \delta_i^{\sigma(k7)} + w_{\delta_i^\sigma}^{(h0)} \cdot \Delta\delta_i^{\sigma(k7)} \end{Bmatrix}$ and $Q_{i,load}^{\sigma\ (h0)}\begin{Bmatrix} V_i^{\sigma(k7)} + w_{V_i^\sigma}^{(h0)} \cdot \Delta\left|V_i^{\sigma(k7)}\right| \\ \delta_i^{\sigma(k7)} + w_{\delta_i^\sigma}^{(h0)} \cdot \Delta\delta_i^{\sigma(k7)} \end{Bmatrix}$ are calculated from equations (5.44), (5.45), (5.55), (5.56), (5.69) and (5.70) as shown in Table C.41. $\Delta P_{i,load}^{\sigma\ (h0)}$ and $\Delta Q_{i,load}^{\sigma\ (h0)}$ are calculated from equations (5.40) and (5.41) as shown Table C.41.

Table C.41 The calculated values

Node		$\Delta\left\|V_i^{\sigma(k7)}\right\|$	$\Delta\delta_i^{\sigma(k7)}$	$P_{i,load}^{\sigma\ (h0)}$	$Q_{i,load}^{\sigma\ (h0)}$	$\Delta P_{i,load}^{\sigma\ (h0)}$	$\Delta Q_{i,load}^{\sigma\ (h0)}$
2	A	-0.00022648	0.00003410	-0.00517922	-0.00249395	-0.00000909	-0.00001024
	B	0.00088032	-0.00079193	-0.00214382	-0.00104485	-0.00001466	-0.00000320
	C	0.00001613	0.00034262	-0.00485048	-0.00233625	-0.00001235	-0.00001083
3	A	-0.00023309	0.00002897	-0.00550320	-0.00266912	-0.00000001	-0.00000001
	B	0.00090353	-0.00078885	-0.00404247	-0.00195884	0.00000000	-0.00000001
	C	0.00001082	0.00034404	-0.00243141	-0.00118057	0.00000000	0.00000000
4	A	-0.00052402	0.00008996	-0.00304786	-0.00149218	-0.00019108	-0.00008231
	B	0.00200450	-0.00190017	-0.00216220	-0.00104151	-0.00019591	-0.00010635
	C	0.00005583	0.00080321	-0.00180386	-0.00086184	-0.00009349	-0.00005169
5	A	-0.00282445	-0.00188654	-0.00118832	-0.00263718	-0.00205063	0.00106270
	B	0.03226028	-0.03983251	-0.00115830	-0.00800601	-0.00100017	0.00695796
	C	-0.00053868	0.01166522	-0.00131776	-0.00105909	-0.00080445	0.00003312

Node		$\Delta\left\|V_i^{\sigma(k7)}\right\|$	$\Delta\delta_i^{\sigma(k7)}$	$P_{i,load}^{\sigma\ (h0)}$	$Q_{i,load}^{\sigma\ (h0)}$	$\Delta P_{i,load}^{\sigma\ (h0)}$	$\Delta Q_{i,load}^{\sigma\ (h0)}$
6	A	-0.00045449	0.00017897	-0.00209842	-0.00101932	-0.00000090	-0.00000035
	B	0.00177155	-0.00204163	-0.00128299	-0.00062266	-0.00000212	-0.00000118
	C	0.00010951	0.00072497	-0.00136201	-0.00065863	-0.00000127	-0.00000193
7	A	-0.00053879	0.00013871	-0.00484812	-0.00235392	-0.00001030	-0.00000032
	B	0.00163838	-0.00211320	-0.00335850	-0.00163426	-0.00001022	-0.00000019
	C	0.00006190	0.00066232	-0.00378460	-0.00184117	-0.00001009	0.00000004
8	A	-0.00037765	0.00026956	-0.00169347	-0.00082443	-0.00000098	-0.00000030
	B	0.00154486	-0.00216360	-0.00225609	-0.00107179	-0.00000220	-0.00000121
	C	0.00016065	0.00064967	-0.00348422	-0.00168469	-0.00000127	-0.00000184
9	A	-0.00029870	0.00035890	-0.00614750	-0.00298396	-0.00000050	-0.00000007
	B	0.00131862	-0.00227482	-0.00619957	-0.00300569	-0.00000138	-0.00000121
	C	0.00020853	0.00057338	-0.00622567	-0.00300603	-0.00000043	-0.00000161
10	A	-0.00023782	0.00042531	-0.00169198	-0.00082443	-0.00000247	-0.00000030
	B	0.00114560	-0.00235410	-0.00175046	-0.00084840	0.00000371	-0.00000002
	C	0.00024404	0.00051481	-0.00120631	-0.00059460	-0.00000237	0.00000432
11	A	-0.00019774	0.00046613	-0.00371554	-0.00179875	-0.00000325	-0.00000067
	B	0.00097815	-0.00241083	-0.00309085	-0.00149692	-0.00000339	-0.00000029
	C	0.00026377	0.00048638	-0.00515452	-0.00250136	-0.00000344	-0.00000032
12	A	-0.00017570	0.00046930	-0.00484353	-0.00235536	-0.00001489	0.00000113
	B	0.00096298	-0.00240609	-0.00312467	-0.00163194	-0.00024405	-0.00000252
	C	0.00025940	0.00046372	-0.00379460	-0.00194600	-0.00000008	0.00010487
13	A	-0.00022882	0.00044229	-0.00216509	-0.00106391	-0.00002419	-0.00000074
	B	0.00090388	-0.00243076	-0.00219671	-0.00107253	-0.00002416	-0.00000047
	C	0.00024123	0.00045469	-0.00301225	-0.00147589	-0.00002350	0.00000018
14	A	-0.00015205	0.00051416	-0.00154439	-0.00074942	-0.00000011	-0.00000034
	B	0.00083224	-0.00246020	-0.00128488	-0.00062343	-0.00000023	-0.00000041
	C	0.00028655	0.00046740	-0.00189706	-0.00091313	-0.00000028	-0.00000041
15	A	-0.00018002	0.00046146	-0.00217852	-0.00106401	-0.00001077	-0.00000064
	B	0.00094182	-0.00241060	-0.00201047	-0.00097301	-0.00001076	-0.00000018
	C	0.00025631	0.00045443	-0.00325005	-0.00157414	-0.00001057	0.00000005
16	A	-0.00020666	0.00044293	-0.00385931	-0.00188861	-0.00002443	-0.00000077
	B	0.00089203	-0.00242562	-0.00429266	-0.00208314	-0.00002430	-0.00000048
	C	0.00023403	0.00043186	-0.00361640	-0.00177105	-0.00002369	0.00000019
17	A	-0.00015182	0.00051245	-0.00323882	-0.00157437	-0.00000012	-0.00000012
	B	0.00083619	-0.00245838	-0.00202126	-0.00097319	0.00000002	0.00000000
	C	0.00028519	0.00046714	-0.00227680	-0.00109625	-0.00000001	0.00000001
18	A	-0.00010611	0.00056237	-0.00266312	-0.00129760	-0.00000601	0.00000802
	B	0.00068498	-0.00250909	-0.00201374	-0.00107001	-0.00020712	-0.00000299
	C	0.00030974	0.00044834	-0.00515857	-0.00262199	0.00000061	0.00012031
19	A	-0.00018275	0.00045720	-0.00436435	-0.00211360	-0.00001423	-0.00000071
	B	0.00093097	-0.00241288	-0.00416557	-0.00202098	-0.00001414	-0.00000026
	C	0.00025410	0.00044953	-0.00514413	-0.00250176	-0.00001383	0.00000007

Seventy-fourth: The elements of the Jacobian matrix (J_1, J_2, J_3 and J_4) are calculated from equations (5.47)-(5.54), (5.57)-(5.68) and (5.71)-(5.78).

Seventy-fifth: The linear simultaneous equation (5.46) is solved directly by optimally ordered triangular factorization and Gaussian elimination. The $\Delta w_{V_i^{\sigma}}{}^{(h0)}$ and $\Delta w_{\delta_i^{\sigma}}{}^{(h0)}$ are obtained as shown in Table C.42.

Seventy-sixth: The new step-length values $\begin{Bmatrix} w_{V_i^\sigma}^{(h1)} = w_{V_i^\sigma}^{(h0)} + \Delta w_{V_i^\sigma}{}^{(h0)} \\ w_{\delta_i^\sigma}^{(h1)} = w_{\delta_i^\sigma}^{(h0)} + \Delta w_{\delta_i^\sigma}{}^{(h0)} \end{Bmatrix}$ are computed from equations (5.79) and (5.80) as shown in Table C.42.

Table C.42 The calculated values

Node		$\Delta w_{V_i^\sigma}{}^{(h0)}$	$\Delta w_{\delta_i^\sigma}{}^{(h0)}$	$w_{V_i^\sigma}{}^{(h1)}$	$w_{\delta_i^\sigma}{}^{(h1)}$
2	A	0.54440472	4.49306161	0.84440472	4.79306161
	B	0.22364613	0.94176721	0.52364613	1.24176721
	C	6.22916304	0.20973255	6.52916304	0.50973255
3	A	0.53343490	5.16024837	0.83343490	5.46024837
	B	0.22925975	0.94264586	0.52925975	1.24264586
	C	8.94201905	0.20994611	9.24201905	0.50994611
4	A	0.53002191	4.03430650	0.83002191	4.33430650
	B	0.20645992	0.92216358	0.50645992	1.22216358
	C	4.28259249	0.20436635	4.58259249	0.50436635
5	A	0.55561884	-1.55542374	0.85561884	-1.25542374
	B	0.05362723	0.79953804	0.35362723	1.09953804
	C	-1.51262661	0.18142399	-1.21262661	0.48142399
6	A	0.52375149	2.16492692	0.82375149	2.46492692
	B	0.18241854	0.87390908	0.48241854	1.17390908
	C	2.21719057	0.19648057	2.51719057	0.49648057
7	A	0.45807283	2.63222689	0.75807283	2.93222689
	B	0.15471167	0.84469005	0.45471167	1.14469005
	C	3.73696008	0.17334470	4.03696008	0.47334470
8	A	0.52607788	1.53109062	0.82607788	1.83109062
	B	0.15439905	0.83723047	0.45439905	1.13723047
	C	1.52850059	0.18882429	1.82850059	0.48882429
9	A	0.53577654	1.21924752	0.83577654	1.51924752
	B	0.11864079	0.80713459	0.41864079	1.10713459
	C	1.18565779	0.18003016	1.48565779	0.48003016
10	A	0.55009986	1.07246956	0.85009986	1.37246956
	B	0.08211192	0.78727319	0.38211192	1.08727319
	C	1.01950597	0.17184606	1.31950597	0.47184606
11	A	0.55595336	0.99566922	0.85595336	1.29566922
	B	0.04418252	0.77197312	0.34418252	1.07197312
	C	0.93411192	0.17829411	1.23411192	0.47829411
12	A	0.55969330	1.00120330	0.85969330	1.30120330
	B	0.01906101	0.77432710	0.31906101	1.07432710
	C	0.95527242	0.16283024	1.25527242	0.46283024
13	A	0.51443157	1.01760641	0.81443157	1.31760641
	B	-0.00140718	0.76467258	0.29859282	1.06467258
	C	0.97978552	0.15484638	1.27978552	0.45484638
14	A	0.58843823	0.92700765	0.88843823	1.22700765
	B	0.00777491	0.76041110	0.30777491	1.06041110
	C	0.85572380	0.19264854	1.15572380	0.49264854
15	A	0.54074229	1.00770476	0.84074229	1.30770476
	B	0.00489721	0.77167360	0.30489721	1.07167360
	C	0.96255296	0.15540025	1.26255296	0.45540025
16	A	0.50783866	1.02584631	0.80783866	1.32584631

Node		$\Delta w_{V_i^\sigma}^{(h0)}$	$\Delta w_{\delta_i^\sigma}^{(h0)}$	$w_{V_i^\sigma}^{(h1)}$	$w_{\delta_i^\sigma}^{(h1)}$
	B	-0.02794281	0.76677693	0.27205719	1.06677693
	C	1.00983280	0.13663792	1.30983280	0.43663792
17	A	0.58670314	0.92798139	0.88670314	1.22798139
	B	0.00982513	0.76047572	0.30982513	1.06047572
	C	0.85669995	0.19229898	1.15669995	0.49229898
18	A	0.65069712	0.87012103	0.95069712	1.17012103
	B	-0.04480807	0.74952981	0.25519193	1.04952981
	C	0.78903182	0.20839213	1.08903182	0.50839213
19	A	0.53124556	1.01135028	0.83124556	1.31135028
	B	-0.00263285	0.77033026	0.29736715	1.07033026
	C	0.96743663	0.15132497	1.26743663	0.45132497

Seventy-seventh: For load buses, ${P_{i,load}^{\sigma}}^{(h1)} \begin{Bmatrix} V_i^{\sigma(k7)} + w_{V_i^\sigma}^{(h1)} \cdot \Delta\left|V_i^{\sigma(k7)}\right| \\ \delta_i^{\sigma(k7)} + w_{\delta_i^\sigma}^{(h1)} \cdot \Delta\delta_i^{\sigma(k7)} \end{Bmatrix}$ and ${Q_{i,load}^{\sigma}}^{(h1)} \begin{Bmatrix} V_i^{\sigma(k7)} + w_{V_i^\sigma}^{(h1)} \cdot \Delta\left|V_i^{\sigma(k7)}\right| \\ \delta_i^{\sigma(k7)} + w_{\delta_i^\sigma}^{(h1)} \cdot \Delta\delta_i^{\sigma(k7)} \end{Bmatrix}$ are calculated from equations (5.44), (5.45), (5.55), (5.56), (5.69) and (5.70) as shown in Table C.43. ${\Delta P_{i,load}^{\sigma}}^{(h1)}$ and ${\Delta Q_{i,load}^{\sigma}}^{(h1)}$ are calculated from equations (5.40) and (5.41) as shown Table C.43.

Table C.43 The calculated values

Node		${P_{i,load}^{\sigma}}^{(h1)}$	${Q_{i,load}^{\sigma}}^{(h1)}$	${\Delta P_{i,load}^{\sigma}}^{(h1)}$	${\Delta Q_{i,load}^{\sigma}}^{(h1)}$
2	A	-0.00518582	-0.00250612	-0.00000249	0.00000194
	B	-0.00215017	-0.00104655	-0.00000830	-0.00000150
	C	-0.00486191	-0.00234464	-0.00000092	-0.00000244
3	A	-0.00550321	-0.00266913	0.00000000	0.00000000
	B	-0.00404247	-0.00195885	0.00000000	0.00000000
	C	-0.00243141	-0.00118057	0.00000000	0.00000000
4	A	-0.00321524	-0.00159443	-0.00002371	0.00001995
	B	-0.00223651	-0.00112355	-0.00012159	-0.00002431
	C	-0.00188600	-0.00088743	-0.00001134	-0.00002610
5	A	-0.00310204	-0.00155127	-0.00013690	-0.00002322
	B	-0.00159229	-0.00098290	-0.00056619	-0.00006514
	C	-0.00203851	-0.00106019	-0.00008370	0.00003422
6	A	-0.00209931	-0.00101964	-0.00000001	-0.00000003
	B	-0.00128512	-0.00062379	0.00000002	-0.00000004
	C	-0.00136328	-0.00066055	0.00000000	-0.00000001
7	A	-0.00485828	-0.00235424	-0.00000014	0.00000000
	B	-0.00336858	-0.00163446	-0.00000014	0.00000001
	C	-0.00379455	-0.00184112	-0.00000014	-0.00000001
8	A	-0.00169444	-0.00082471	-0.00000001	-0.00000002
	B	-0.00225830	-0.00107297	0.00000001	-0.00000003
	C	-0.00348549	-0.00168652	0.00000000	-0.00000001
9	A	-0.00614799	-0.00298401	-0.00000001	-0.00000002
	B	-0.00620096	-0.00300686	0.00000002	-0.00000004
	C	-0.00622611	-0.00300763	0.00000001	-0.00000001

Node		$P_{i,load}^{\sigma\ (h1)}$	$Q_{i,load}^{\sigma\ (h1)}$	$\Delta P_{i,load}^{\sigma\ (h1)}$	$\Delta Q_{i,load}^{\sigma\ (h1)}$
10	A	-0.00169448	-0.00082485	0.00000003	0.00000012
	B	-0.00174660	-0.00084845	-0.00000015	0.00000003
	C	-0.00120860	-0.00059026	-0.00000008	-0.00000003
11	A	-0.00371878	-0.00179942	-0.00000001	0.00000000
	B	-0.00309422	-0.00149721	-0.00000001	0.00000000
	C	-0.00515796	-0.00250167	0.00000000	-0.00000001
12	A	-0.00485703	-0.00235433	-0.00000138	0.00000009
	B	-0.00336862	-0.00163452	-0.00000011	0.00000006
	C	-0.00379460	-0.00184773	-0.00000009	0.00000660
13	A	-0.00218927	-0.00106466	-0.00000001	0.00000001
	B	-0.00222084	-0.00107300	-0.00000002	0.00000000
	C	-0.00303573	-0.00147571	-0.00000002	-0.00000001
14	A	-0.00154450	-0.00074975	0.00000000	0.00000000
	B	-0.00128511	-0.00062383	0.00000000	0.00000000
	C	-0.00189734	-0.00091353	0.00000000	0.00000000
15	A	-0.00218928	-0.00106466	-0.00000001	0.00000001
	B	-0.00202121	-0.00097319	-0.00000002	0.00000000
	C	-0.00326061	-0.00157409	-0.00000001	-0.00000001
16	A	-0.00388372	-0.00188940	-0.00000001	0.00000001
	B	-0.00431693	-0.00208362	-0.00000002	0.00000000
	C	-0.00364007	-0.00177085	-0.00000002	-0.00000001
17	A	-0.00323894	-0.00157449	0.00000000	0.00000000
	B	-0.00202123	-0.00097318	0.00000000	0.00000000
	C	-0.00227681	-0.00109624	0.00000000	0.00000000
18	A	-0.00266846	-0.00128964	-0.00000067	0.00000006
	B	-0.00222071	-0.00107303	-0.00000015	0.00000003
	C	-0.00515790	-0.00250878	-0.00000006	0.00000709
19	A	-0.00437856	-0.00211432	-0.00000001	0.00000001
	B	-0.00417969	-0.00202123	-0.00000002	0.00000000
	C	-0.00515795	-0.00250167	-0.00000002	-0.00000001

Seventy-eighth: Determine $max\{|\Delta P_{i,load}^{\sigma\ (h1)}|, |\Delta Q_{i,load}^{\sigma\ (h1)}|\} = 5.6619 \times 10^{-4}$ and $max\{|\Delta P_{i,load}^{\sigma\ (h0)}|, |\Delta Q_{i,load}^{\sigma\ (h0)}|\} = 0.0070$. After that, go to the next calculation.

Seventy-ninth: The elements of the Jacobian matrix (J_1, J_2, J_3 and J_4) are calculated from equations (5.47)-(5.54), (5.57)-(5.68) and (5.71)-(5.78).

Eightieth: The linear simultaneous equation (5.46) is solved directly by optimally ordered triangular factorization and Gaussian elimination. The $\Delta w_{V_i^\sigma}^{(h1)}$ and $\Delta w_{\delta_i^\sigma}^{(h1)}$ are obtained as shown in Table C.44.

Eighty-first: The new step-length values $\begin{Bmatrix} w_{V_i^\sigma}^{(h2)} = w_{V_i^\sigma}^{(h1)} + \Delta w_{V_i^\sigma}^{(h1)} \\ w_{\delta_i^\sigma}^{(h2)} = w_{\delta_i^\sigma}^{(h1)} + \Delta w_{\delta_i^\sigma}^{(h1)} \end{Bmatrix}$ are computed from equations (5.79) and (5.80) as shown in Table C.44.

Table C.44 The calculated values

Node		$\Delta w_{V_i^\sigma}^{(h1)}$	$\Delta w_{\delta_i^\sigma}^{(h1)}$	$w_{V_i^\sigma}^{(h2)}$	$w_{\delta_i^\sigma}^{(h2)}$
2	A	-0.00687095	0.01828699	0.83753377	4.81134861
	B	-0.02085401	-0.00226726	0.50279213	1.23949994
	C	0.08964418	-0.02583202	6.61880721	0.48390053
3	A	-0.00710513	0.02376333	0.82632977	5.48401170
	B	-0.02072570	-0.00222554	0.50853404	1.24042032
	C	0.13920249	-0.02578639	9.38122153	0.48415972
4	A	-0.00705917	0.01585939	0.82296274	4.35016590
	B	-0.02084281	-0.00293785	0.48561711	1.21922573
	C	0.05280486	-0.02595624	4.63539735	0.47841012
5	A	0.01771700	-0.02040964	0.87333584	-1.27583339
	B	-0.00917772	-0.00616005	0.34444951	1.09337799
	C	0.07608971	-0.02341476	-1.13653690	0.45800923
6	A	-0.00749593	0.00099783	0.81625556	2.46592475
	B	-0.02190420	-0.00416684	0.46051434	1.16974224
	C	0.02475130	-0.02878573	2.54194187	0.46769484
7	A	-0.00980945	0.00577625	0.74826338	2.93800314
	B	-0.02257691	-0.00487696	0.43213476	1.13981309
	C	0.05811291	-0.02996606	4.09507299	0.44337865
8	A	-0.00779250	-0.00418717	0.81828538	1.82690345
	B	-0.02320639	-0.00511717	0.43119267	1.13211330
	C	0.01538969	-0.03228238	1.84389027	0.45654191
9	A	-0.00810810	-0.00679228	0.82766845	1.51245524
	B	-0.02491136	-0.00591038	0.39372944	1.10122421
	C	0.01080513	-0.03677612	1.49646292	0.44325404
10	A	-0.00843455	-0.00804138	0.84166531	1.36442818
	B	-0.02664578	-0.00644283	0.35546614	1.08083035
	C	0.00850128	-0.04111980	1.32800725	0.43072626
11	A	-0.00859839	-0.00890724	0.84735497	1.28676198
	B	-0.02834402	-0.00687124	0.31583850	1.06510187
	C	0.00733159	-0.04449165	1.24144351	0.43380246
12	A	-0.00830766	-0.00851556	0.85138564	1.29268774
	B	-0.02933529	-0.00677455	0.28972572	1.06755255
	C	0.00818480	-0.04634458	1.26345721	0.41648565
13	A	-0.00936577	-0.00886955	0.80506580	1.30873686
	B	-0.02988836	-0.00702535	0.26870445	1.05764723
	C	0.00847409	-0.04682388	1.28825961	0.40802250
14	A	-0.00841667	-0.00963749	0.88002157	1.21737015
	B	-0.03018100	-0.00721275	0.27759391	1.05319836
	C	0.00625433	-0.04754520	1.16197813	0.44510334
15	A	-0.00866280	-0.00849118	0.83207949	1.29921359
	B	-0.02978619	-0.00683471	0.27511103	1.06483889
	C	0.00825822	-0.04704944	1.27081118	0.40835081
16	A	-0.00934494	-0.00842786	0.79849372	1.31741845
	B	-0.03094399	-0.00693805	0.24111320	1.05983888
	C	0.00975503	-0.04892958	1.31958783	0.38770834
17	A	-0.00836232	-0.00962355	0.87834082	1.21835785
	B	-0.03011838	-0.00720749	0.27970675	1.05326823
	C	0.00637448	-0.04754552	1.16307443	0.44475346
18	A	-0.00808420	-0.01024798	0.94261292	1.15987305
	B	-0.03282184	-0.00753668	0.22237009	1.04199313

Node		$\Delta w_{V_i^\sigma}^{(h1)}$	$\Delta w_{\delta_i^\sigma}^{(h1)}$	$w_{V_i^\sigma}^{(h2)}$	$w_{\delta_i^\sigma}^{(h2)}$
	C	0.00528630	-0.05087071	1.09431812	0.45752142
19	A	-0.00883586	-0.00847704	0.82240971	1.30287324
	B	-0.03002945	-0.00686463	0.26733770	1.06346563
	C	0.00834796	-0.04743352	1.27578459	0.40389145

Eighty-second: For load buses, ${P_{i,load}^{\sigma}}^{(h2)} \begin{Bmatrix} V_i^{\sigma(k7)} + w_{V_i^\sigma}^{(h2)} \cdot \Delta\left|V_i^{\sigma(k7)}\right| \\ \delta_i^{\sigma(k7)} + w_{\delta_i^\sigma}^{(h2)} \cdot \Delta\delta_i^{\sigma(k7)} \end{Bmatrix}$ and ${Q_{i,load}^{\sigma}}^{(h2)} \begin{Bmatrix} V_i^{\sigma(k7)} + w_{V_i^\sigma}^{(h2)} \cdot \Delta\left|V_i^{\sigma(k7)}\right| \\ \delta_i^{\sigma(k7)} + w_{\delta_i^\sigma}^{(h2)} \cdot \Delta\delta_i^{\sigma(k7)} \end{Bmatrix}$ are calculated from equations (5.44), (5.45), (5.55), (5.56), (5.69) and (5.70) as shown in Table C.45. ${\Delta P_{i,load}^{\sigma}}^{(h2)}$ and ${\Delta Q_{i,load}^{\sigma}}^{(h2)}$ are calculated from equations (5.40) and (5.41) as shown Table C.45.

Table C.45 The calculated values

Node		${P_{i,load}^{\sigma}}^{(h2)}$	${Q_{i,load}^{\sigma}}^{(h2)}$	${\Delta P_{i,load}^{\sigma}}^{(h2)}$	${\Delta Q_{i,load}^{\sigma}}^{(h2)}$
2	A	-0.00518831	-0.00250418	0.00000000	0.00000000
	B	-0.00215848	-0.00104805	0.00000000	0.00000000
	C	-0.00486282	-0.00234708	0.00000000	0.00000000
3	A	-0.00550321	-0.00266913	0.00000000	0.00000000
	B	-0.00404247	-0.00195885	0.00000000	0.00000000
	C	-0.00243141	-0.00118057	0.00000000	0.00000000
4	A	-0.00323895	-0.00157449	0.00000000	0.00000000
	B	-0.00235809	-0.00114788	-0.00000002	0.00000001
	C	-0.00189733	-0.00091353	-0.00000001	-0.00000001
5	A	-0.00323861	-0.00157448	-0.00000034	0.00000000
	B	-0.00214665	-0.00104802	-0.00001183	-0.00000003
	C	-0.00212195	-0.00102597	-0.00000026	0.00000000
6	A	-0.00209932	-0.00101967	0.00000000	0.00000000
	B	-0.00128511	-0.00062384	0.00000000	0.00000000
	C	-0.00136328	-0.00066056	0.00000000	0.00000000
7	A	-0.00485842	-0.00235423	0.00000000	0.00000000
	B	-0.00336872	-0.00163445	0.00000000	0.00000000
	C	-0.00379469	-0.00184113	0.00000000	0.00000000
8	A	-0.00169445	-0.00082473	0.00000000	0.00000000
	B	-0.00225829	-0.00107300	0.00000000	0.00000000
	C	-0.00348549	-0.00168653	0.00000000	0.00000000
9	A	-0.00614800	-0.00298403	0.00000000	0.00000000
	B	-0.00620095	-0.00300690	0.00000000	0.00000000
	C	-0.00622610	-0.00300764	0.00000000	0.00000000
10	A	-0.00169445	-0.00082473	0.00000000	0.00000000
	B	-0.00174675	-0.00084842	0.00000000	0.00000000
	C	-0.00120868	-0.00059028	0.00000000	0.00000000
11	A	-0.00371879	-0.00179941	0.00000000	0.00000000
	B	-0.00309423	-0.00149721	0.00000000	0.00000000
	C	-0.00515796	-0.00250168	0.00000000	0.00000000
12	A	-0.00485842	-0.00235423	0.00000000	0.00000000

Node		$P_{i,load}^{\sigma\ (h2)}$	$Q_{i,load}^{\sigma\ (h2)}$	$\Delta P_{i,load}^{\sigma\ (h2)}$	$\Delta Q_{i,load}^{\sigma\ (h2)}$
	B	-0.00336867	-0.00163445	-0.00000005	0.00000000
	C	-0.00379469	-0.00184113	0.00000000	0.00000000
13	A	-0.00218929	-0.00106465	0.00000000	0.00000000
	B	-0.00222086	-0.00107300	0.00000000	0.00000000
	C	-0.00303575	-0.00147571	0.00000000	0.00000000
14	A	-0.00154450	-0.00074976	0.00000000	0.00000000
	B	-0.00128511	-0.00062384	0.00000000	0.00000000
	C	-0.00189734	-0.00091354	0.00000000	0.00000000
15	A	-0.00218929	-0.00106465	0.00000000	0.00000000
	B	-0.00202123	-0.00097319	0.00000000	0.00000000
	C	-0.00326062	-0.00157409	0.00000000	0.00000000
16	A	-0.00388373	-0.00188938	0.00000000	0.00000000
	B	-0.00431696	-0.00208362	0.00000000	0.00000000
	C	-0.00364009	-0.00177085	0.00000000	0.00000000
17	A	-0.00323895	-0.00157449	0.00000000	0.00000000
	B	-0.00202123	-0.00097319	0.00000000	0.00000000
	C	-0.00227681	-0.00109624	0.00000000	0.00000000
18	A	-0.00266913	-0.00128958	0.00000000	0.00000000
	B	-0.00222081	-0.00107300	-0.00000005	0.00000000
	C	-0.00515796	-0.00250168	0.00000000	0.00000000
19	A	-0.00437857	-0.00211431	0.00000000	0.00000000
	B	-0.00417971	-0.00202123	0.00000000	0.00000000
	C	-0.00515796	-0.00250168	0.00000000	0.00000000

Eighty-third: Determine $max\{|\Delta P_{i,load}^{\sigma\ (h2)}|, |\Delta Q_{i,load}^{\sigma\ (h2)}|\} = 1.1827 \times 10^{-5}$ and $max\{|\Delta P_{i,load}^{\sigma\ (h1)}|, |\Delta Q_{i,load}^{\sigma\ (h1)}|\} = 5.6619 \times 10^{-4}$. It is noticed that $max\{|\Delta P_{i,load}^{\sigma\ (h2)}|, |\Delta Q_{i,load}^{\sigma\ (h2)}|\} < \varepsilon$. Then, the power flow algorithm is terminated and the new voltage magnitudes, $|V_i^{\sigma(k8)}| = |V_i^{\sigma(k7)}| + w_{V_i^{\sigma}}{}^{(h2)} \cdot \Delta|V_i^{\sigma(k7)}|$, and phase angles, $\delta_i^{\sigma(k8)} = \delta_i^{\sigma(k7)} + w_{\delta_i^{\sigma}}{}^{(h2)} \cdot \Delta\delta_i^{\sigma(k7)}$, are computed from equations (5.42) and (5.43) by $w_{V_i^{\sigma}}{}^{(h2)}$ and $w_{\delta_i^{\sigma}}{}^{(h2)}$ as shown in Table C.46.

Table C.46 The updated values

Node		$\lvert V_i^{\sigma(k8)}\rvert$	$\delta_i^{\sigma(k8)}$
2	A	1.04895808	0.01680295
	B	1.04858169	-2.07629713
	C	1.04518815	2.10913386
3	A	1.02547124	0.02305150
	B	1.03157691	-2.08021272
	C	1.04239970	2.10944101
4	A	1.04955620	0.03921859
	B	1.04785951	-2.05166842
	C	1.03955913	2.12901530
5	A	1.06002344	0.10962223
	B	1.05982842	-1.98706107
	C	1.05794625	2.19478265
6	A	1.05127969	0.05934241

Node		$\left\|V_i^{\sigma(k8)}\right\|$	$\delta_i^{\sigma(k8)}$
	B	1.04825921	-2.02881233
	C	1.03449155	2.14715974
7	A	1.05960310	0.08851804
	B	1.05769432	-1.99877561
	C	1.03899801	2.17466743
8	A	1.05272076	0.07579238
	B	1.04863491	-2.00992284
	C	1.03012820	2.16214798
9	A	1.05372602	0.09049928
	B	1.04901925	-1.99323010
	C	1.02643714	2.17565804
10	A	1.05513575	0.10152139
	B	1.05004496	-1.98062740
	C	1.02421048	2.18602378
11	A	1.05782856	0.11051516
	B	1.05333717	-1.97064181
	C	1.02488736	2.19506478
12	A	1.05922360	0.11361288
	B	1.05428810	-1.96770801
	C	1.02649908	2.19778938
13	A	1.06524322	0.12439880
	B	1.05947590	-1.95499267
	C	1.02718400	2.20875120
14	A	1.05789157	0.11393652
	B	1.05430214	-1.96702209
	C	1.02509588	2.19855030
15	A	1.06181240	0.11919568
	B	1.05649217	-1.96141693
	C	1.02704438	2.20329274
16	A	1.06516123	0.12820963
	B	1.05802141	-1.95228710
	C	1.02887134	2.21117754
17	A	1.05444701	0.11440051
	B	1.05251542	-1.96737908
	C	1.02348445	2.19878908
18	A	1.05895444	0.11726445
	B	1.05584957	-1.96336311
	C	1.02599383	2.20197196
19	A	1.06290920	0.12201308
	B	1.05739159	-1.95828283
	C	1.02717828	2.20603387

Eighty-fourth: For cross check, $P_{i,load}^{\sigma}{}^{(k8)}\begin{Bmatrix}V_i^{\sigma(k8)}\\ \delta_i^{\sigma(k8)}\end{Bmatrix}$ and $Q_{i,load}^{\sigma}{}^{(k8)}\begin{Bmatrix}V_i^{\sigma(k8)}\\ \delta_i^{\sigma(k8)}\end{Bmatrix}$ are calculated from equations (5.1), (5.2), (5.16), (5.17), (5.30) and (5.31) as shown Table C.47. $\Delta P_{i,load}^{\sigma}{}^{(k8)}$ and $\Delta Q_{i,load}^{\sigma}{}^{(k8)}$ are calculated from equations (5.38) and (5.39) as shown Table C.47. $max\left\{\left|\Delta P_i^{\sigma(k8)}\right|,\left|\Delta Q_i^{\sigma(k8)}\right|\right\} = 1.1827 \times 10^{-5}$. Then, the power flow algorithm is convergent.

Table C.47 The calculated values

Node		$P_{i,load}^{\sigma\,(k8)}$	$Q_{i,load}^{\sigma\,(k8)}$	$\Delta P_{i,load}^{\sigma\,(k8)}$	$\Delta Q_{i,load}^{\sigma\,(k8)}$
2	A	-0.00517546	-0.00248875	-0.00001285	-0.00001543
	B	-0.00213983	-0.00104212	-0.00001865	-0.00000593
	C	-0.00484602	-0.00233214	-0.00001680	-0.00001495
3	A	-0.00550319	-0.00266912	-0.00000002	-0.00000001
	B	-0.00404247	-0.00195884	0.00000000	-0.00000001
	C	-0.00243141	-0.00118057	0.00000000	0.00000000
4	A	-0.00296520	-0.00144631	-0.00027374	-0.00012817
	B	-0.00211237	-0.00096481	-0.00024573	-0.00018305
	C	-0.00177597	-0.00084259	-0.00012138	-0.00007094
5	A	-0.00029099	-0.00310328	-0.00294795	0.00152879
	B	-0.00577422	-0.01104699	0.00361574	0.00999894
	C	-0.00096499	-0.00106761	-0.00115723	0.00004164
6	A	-0.00209808	-0.00101921	-0.00000124	-0.00000046
	B	-0.00128206	-0.00062222	-0.00000304	-0.00000161
	C	-0.00136148	-0.00065780	-0.00000180	-0.00000276
7	A	-0.00484411	-0.00235378	-0.00001430	-0.00000045
	B	-0.00335453	-0.00163418	-0.00001419	-0.00000027
	C	-0.00378069	-0.00184119	-0.00001400	0.00000006
8	A	-0.00169308	-0.00082434	-0.00000137	-0.00000039
	B	-0.00225513	-0.00107133	-0.00000316	-0.00000167
	C	-0.00348369	-0.00168390	-0.00000180	-0.00000262
9	A	-0.00614729	-0.00298397	-0.00000070	-0.00000006
	B	-0.00619895	-0.00300522	-0.00000199	-0.00000168
	C	-0.00622547	-0.00300534	-0.00000062	-0.00000230
10	A	-0.00169090	-0.00082427	-0.00000355	-0.00000046
	B	-0.00175209	-0.00084839	0.00000534	-0.00000003
	C	-0.00120534	-0.00059645	-0.00000334	0.00000617
11	A	-0.00371417	-0.00179847	-0.00000462	-0.00000095
	B	-0.00308941	-0.00149680	-0.00000482	-0.00000041
	C	-0.00515307	-0.00250123	-0.00000490	-0.00000045
12	A	-0.00483770	-0.00235581	-0.00002071	0.00000158
	B	-0.00302721	-0.00163085	-0.00034151	-0.00000360
	C	-0.00379461	-0.00198997	-0.00000007	0.00014884
13	A	-0.00215488	-0.00106359	-0.00003441	-0.00000106
	B	-0.00218650	-0.00107233	-0.00003436	-0.00000067
	C	-0.00300233	-0.00147597	-0.00003342	0.00000026
14	A	-0.00154434	-0.00074928	-0.00000016	-0.00000048
	B	-0.00128477	-0.00062326	-0.00000033	-0.00000057
	C	-0.00189694	-0.00091296	-0.00000041	-0.00000058
15	A	-0.00217398	-0.00106374	-0.00001531	-0.00000092
	B	-0.00200594	-0.00097293	-0.00001530	-0.00000026
	C	-0.00324560	-0.00157416	-0.00001502	0.00000006
16	A	-0.00384899	-0.00188828	-0.00003474	-0.00000110
	B	-0.00428240	-0.00208293	-0.00003456	-0.00000069
	C	-0.00360640	-0.00177113	-0.00003369	0.00000027
17	A	-0.00323877	-0.00157432	-0.00000017	-0.00000017
	B	-0.00202127	-0.00097319	0.00000003	0.00000001
	C	-0.00227680	-0.00109625	-0.00000002	0.00000001
18	A	-0.00266071	-0.00130099	-0.00000842	0.00001141
	B	-0.00193097	-0.00106871	-0.00028990	-0.00000429

Node		$P_{i,load}^{\sigma\ (k8)}$	$Q_{i,load}^{\sigma\ (k8)}$	$\Delta P_{i,load}^{\sigma\ (k8)}$	$\Delta Q_{i,load}^{\sigma\ (k8)}$
	C	-0.00515888	-0.00267203	0.00000091	0.00017035
19	A	-0.00435835	-0.00211329	-0.00002022	-0.00000102
	B	-0.00415961	-0.00202087	-0.00002010	-0.00000037
	C	-0.00513830	-0.00250179	-0.00001966	0.00000011

APPENDIX D

The Optimization Problem Based On Only Severe Case Consideration Under The Uncertainty

Following the optimization problem based on only severe case consideration under the uncertainty, the optimization problem from equations (5.81)-(5.86) can be transformed to the following:

$$maximize\left[\sum_{i}^{n}\sum_{\sigma\in\{A,B,C\}}P_{i,pv,z16}^{\sigma}\right] \tag{D.1}$$

Subject to:

$$V_{min}^{\sigma} \le V_{i,z16}^{\sigma} \le V_{max}^{\sigma} \tag{D.2}$$

$$\left|I_{i-j,z16}^{\sigma}\right| \le I_{i-j,max}^{\sigma} \tag{D.3}$$

$$\left|S_{z16}^{MV/LV}\right| \le S_{max}^{MV/LV} \tag{D.4}$$

$$VUF_{i,z16} \le 3\%\,;\; VUF_i = \frac{|V_i^{ne}|}{|V_i^{po}|}\times 100\% \tag{D.5}$$

$$P_{loss,z16} \le Loss_{max\ load,\ no\ PV} \tag{D.6}$$

The optimization problem (D.1) and also the constraints (D.2)-(D.6) determine only severe case or case z16. This case z16 is determined on the minimum load and maximum solar irradiance condition. To test this optimization problem (D.1), the configuration is defined as follows:

- Test on the modified 19 node distribution system;
- Determine the set of uncertainty at the week 3-9 November 2014;
- The continuous local control function is selected to operate.

When the 2-stage PSO is applied, the optimal parameters setting can be shown in Table D.1. The objective value from equation (D.1) is 88,412.86 W.

Table D.1 Parameter setting of each connected PV system

PV Name	Parameter Setting					
	V_{cri}	δ_p	K_1	K_2	V_q	δ_q
PV1	1.1	0.01	0.836	1.512	1.034	0.078
PV2	1.1	0.01	0.868	1.55	1.024	0.095
PV3	1.101	0.01	0.819	1.492	1.025	0.096
PV4	1.09	0.01	0.613	0.668	1.017	0.094
PV5	1.096	0.01	0.843	1.499	1.026	0.096
PV6	1.098	0.01	0.926	1.504	1.029	0.091
PV7	1.107	0.01	0.875	1.606	1.022	0.092
PV8	1.11	0.01	0.883	1.528	1.016	0.098
PV9	1.091	0.01	0.785	1.488	1.024	0.092
PV10	1.092	0.01	0.827	1.501	1.027	0.099
PV11	1.098	0.01	0.842	1.517	1.035	0.097
PV12	1.093	0.01	0.866	1.528	1.033	0.096
PV13	1.106	0.01	0.816	1.492	1.023	0.095
PV14	1.095	0.01	0.811	1.512	1.024	0.096
PV15	1.098	0.01	0.835	1.529	1.024	0.1
PV16	1.1	0.01	0.793	1.497	1.024	0.095
PV17	1.106	0.01	0.789	1.488	1.024	0.095
PV18	1.095	0.01	0.878	1.505	1.025	0.092

Apply the parameters setting in Table D.1, the power flow results of total 17 cases of the set of uncertainty can be shown in Figure D.1.

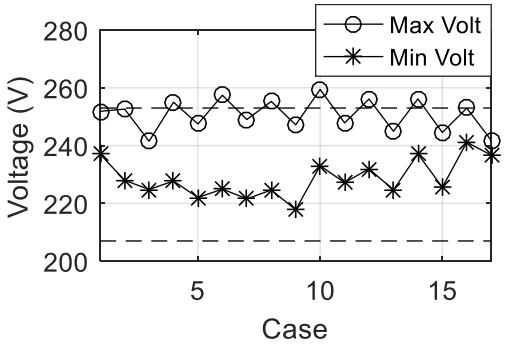

(a) Minimum and maximum phase voltage

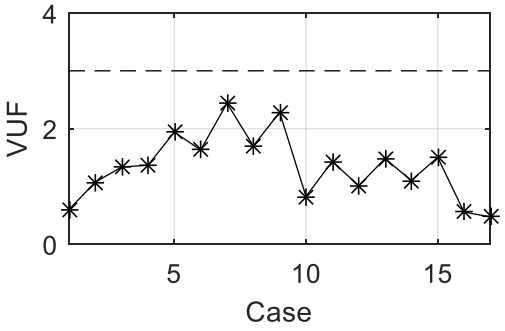

(b) Maximum VUF

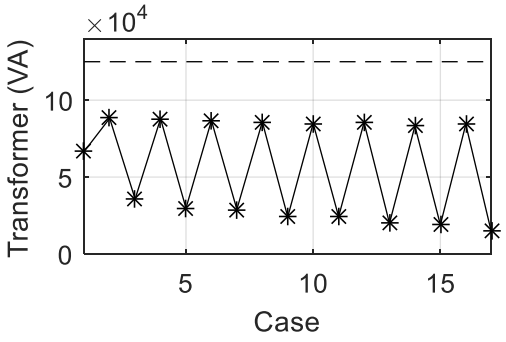

(c) MV/LV transformer utilization

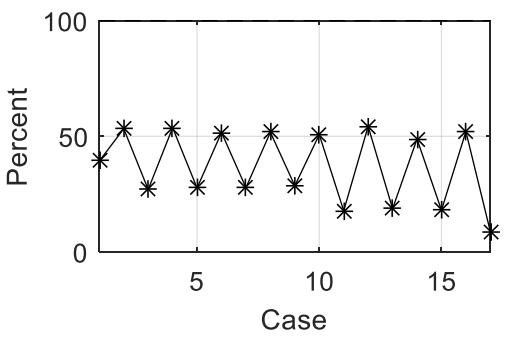

(d) Maximum line capacity

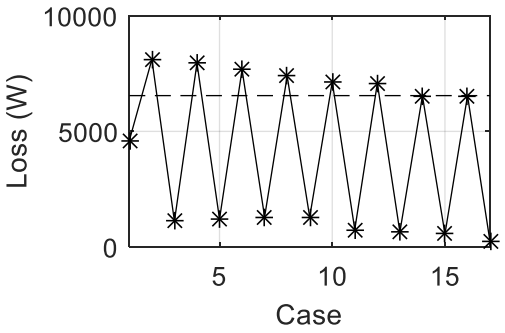

(e) System loss

Figure D.1 The results of the set of uncertainty

From Figure D.1, it can notice that:

- Voltage and loss at the case z16 is within the limit. Surely, it is because only case z16 is determined on optimization problem under the constraint;
- Cases on the minimum solar irradiance condition are within the limit. They are consisted of z3, z5, z7, z9, z11, z13, z15 and z17;
- Case z1 on the mean load and mean solar irradiance condition is luckily within the limit;
- Case z2 on the maximum load and maximum solar irradiance condition is luckily within the voltage limit but out of the maximum loss limit;
- Other cases (z4, z6, z8, z10, z12 and z14) with the maximum solar irradiance condition are out of the voltage and loss limit.

Therefore, it can conclude that the optimization problem based on only severe case consideration under the uncertainty cannot hold on the power flow results within limit under the uncertainty.

APPENDIX E

The Contrast Optimization Problems

In the past proposal, the optimization problem is presented as shown in equation (D.1) to solve the maximization of total real power output from overall PV systems as shown in equation (D.2) and minimization of system loss as shown in equation (D.3) simultaneously. The equation (D.3) can transform to the maximization problem as shown in equation (D.4). When the equations (D.2) and (D.4) are sum together, the equation (D.1) is obtained.

$$maximize\left[\sum_{i}^{n}\sum_{\sigma\in\{A,B,C\}}P_{i,pv,z1}^{\sigma}\right]-P_{loss,z1} \tag{E.1}$$

$$maximize\left[\sum_{i}^{n}\sum_{\sigma\in\{A,B,C\}}P_{i,pv,z1}^{\sigma}\right] \tag{E.2}$$

$$minimize\left[P_{loss,z1}\right] \tag{E.3}$$

$$maximize\left[-P_{loss,z1}\right] \tag{E.4}$$

According to the formulation of optimization problem in equation (D.1), it is incorrect because the equation (D.2) contrasts with the equation (D.3). To express this problem clearly, Multi-Objective Particle Swarm Optimization (MOPSO) [47] will be applied to solve the optimization problems (D.5) and (D.6). For the equation (D.5), it is obtained from the transformed equation (D.2) by changing into the minimization problem. The constraints of equations (D.5) and (D.6) are the system limit as shown in equations (D.7)-(D.10).

$$fob1 = minimize\left[-\sum_{i}^{n}\sum_{\sigma\in\{A,B,C\}}P_{i,pv,z1}^{\sigma}\right] \tag{E.5}$$

$$fob2 = minimize\left[P_{loss,z1}\right] \tag{E.6}$$

$$V_{min}^{\sigma} \le V_{i,z}^{\sigma} \le V_{max}^{\sigma} \tag{E.7}$$

$$\left|I_{i-j,z}^{\sigma}\right| \le I_{i-j,max}^{\sigma} \tag{E.8}$$

$$\left|S_{z}^{M^V/_{LV}}\right| \le S_{max}^{M^V/_{LV}} \tag{E.9}$$

$$VUF_{i,z} \leq 3\%\,;\; VUF_i = \frac{|v_i^{ne}|}{|v_i^{po}|} \times 100\% \qquad \text{(E.10)}$$

where $z \in \{z1, z2, \ldots, z17\}$.

The results from MOPSO can be shown in Figure D.1. It can notice that:

- At the point A of Figure D.1 ($fob1 = -49{,}969.87, fob2 = 5{,}943.88$), it indicates that when $fob1$ is obtained at minimum value but the value of $fob2$ is obtained at non-minimum. Similarly, when the parameter is set to inject more real power output, more loss is occurred.
- At the point B of Figure D.1 ($fob1 = -10{,}581.05, fob2 = 501.70$), it indicates that when $fob2$ is obtained at minimum value but the value of $fob1$ is obtained at non-minimum. Similarly, when the parameter is set to inject less real power output, loss is occurred at the small value.

Then, it can be noticed that the equations (D.2) and (D.3) are conflict together and cannot sum directly, as shown in equation (D.1), to solve both the objectives (D.2) and (D.3).

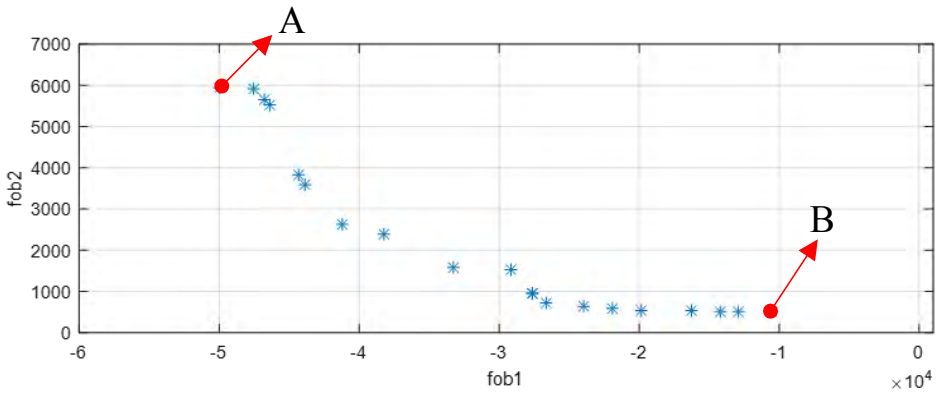

Figure E.1 The results from MOPSO

The results of MOPSO in Figure D.1 is determined on the same parameter setting of continuous local control function of each connected PV system. At the point A, $\{V_{i,cri}, \delta_{i,p}, K_{i,1}, K_{i,2}, V_{i,q}, \delta_{i,q}\}$ is {1.062, 0.01, 0.06, 1.06, 1.021, 0.01}. At the point B, $\{V_{i,cri}, \delta_{i,p}, K_{i,1}, K_{i,2}, V_{i,q}, \delta_{i,q}\}$ is {1.039, 0.01, 0.295, 0.949, 1.053, 0.01}.

APPENDIX F

The Study Of The Maximum High PV Penetration Under No Local Control

In this Appendix, the study is based on the modified 19 and 29 node distribution system. The study will determine only sever case or minimum load condition. According to the set of uncertainty of the week 3-9 November 2014, the minimum load of phase A, B and C are 0.1135, 0.1007 and 0.1815 respectively. Every connected 1-phase PV system is defined to have the same size.

F.1 The Modified 19 Node Distribution System

The study determines in 3 parts as follows.

- Firstly, every load point of each phase has a 1-phase PV system. Increasing size of 1-phase PV systems until the simulation results nearly exceed the limit, the high PV penetration result is 52% of transformer capacity. The size of each 1-phase PV system is around 1.2 kW. The voltage profile of 52% high PV penetration can be shown in Figure F.1.

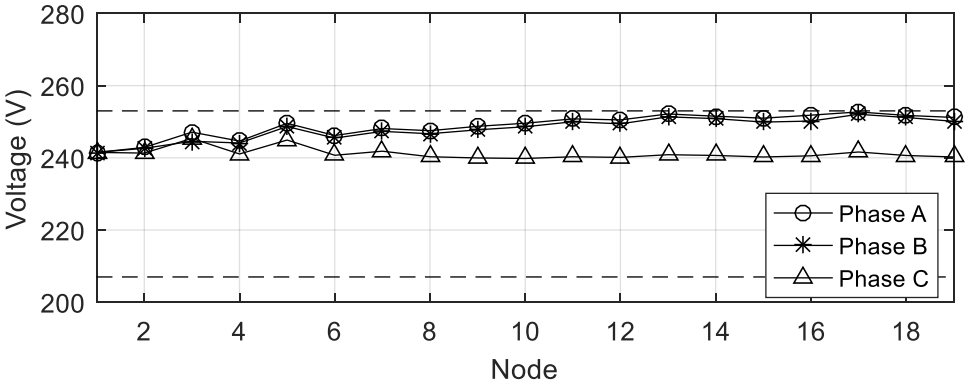

Figure F.1 The voltage profile result

- Secondly, only downstream node 18 and 19 of each phase has 1-phase PV system. Node 18 and 19 are the downstream node of each branch of the modified 19 node distribution system. Increasing size of 1-phase PV systems until the simulation results nearly exceed the limit, the high PV

penetration result is 34% of transformer capacity. The size of each 1-phase PV system is around 7 kW. The voltage profile of 34% high PV penetration can be shown in Figure F.2.

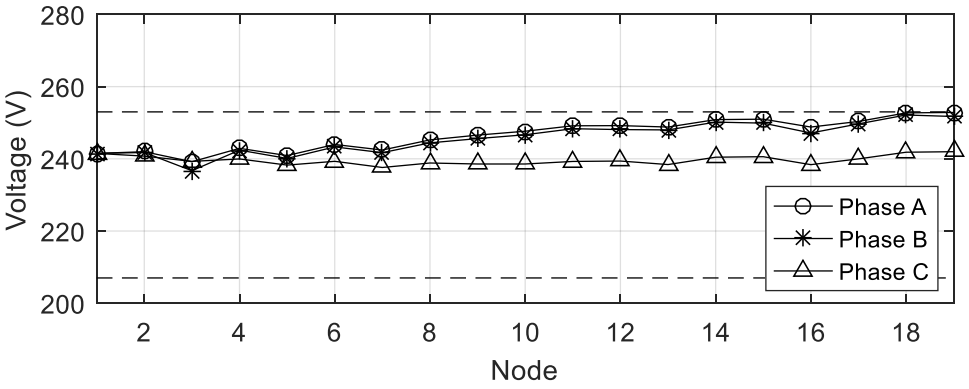

Figure F.2 The voltage profile result

- Finally, only one downstream node 19 of each phase has 1-phase PV system. Increasing size of 1-phase PV systems until the simulation results nearly exceed the limit, the high PV penetration result is 25% of transformer capacity. The size of each 1-phase PV system is around 10 kW. The voltage profile of 25% high PV penetration can be shown in Figure F.3.

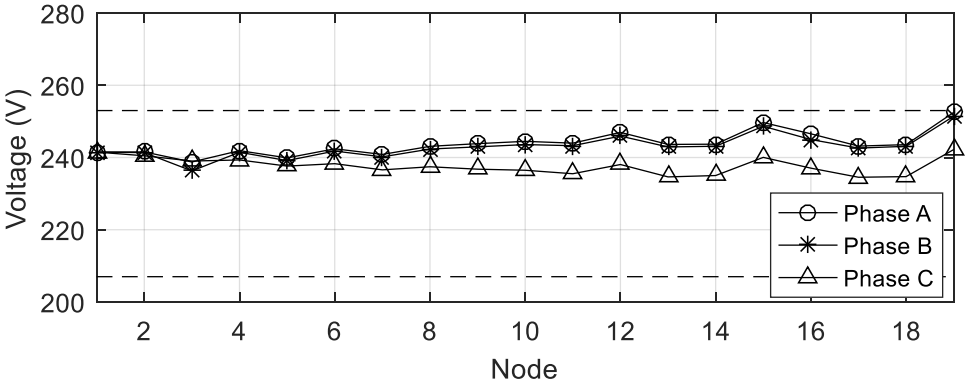

Figure F.3 The voltage profile result

F.2 The Modified 29 Node Distribution System

The study determines in 3 parts as follows.

- Firstly, every load point of each phase has a 1-phase PV system. Increasing size of 1-phase PV systems until the simulation results nearly exceed the limit, the high PV penetration result is 53% of transformer

capacity. The size of each 1-phase PV system is around 1.1 kW. The voltage profile of 53% high PV penetration can be shown in Figure F.1.

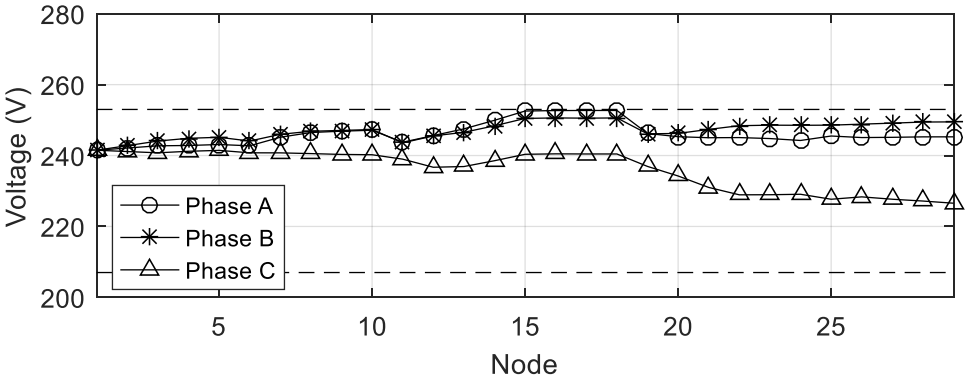

Figure F.4 The voltage profile result

- Secondly, only downstream node 10, 16 and 29 of each phase has 1-phase PV system. There are 3 branches of the modified 29 node distribution system and node 10, 16 and 29 are the downstream node of each branch. Increasing size of 1-phase PV systems until the simulation results nearly exceed the limit, the high PV penetration result is 44% of transformer capacity. The size of each 1-phase PV system is around 6.1 kW. The voltage profile of 44% high PV penetration can be shown in Figure F.5.

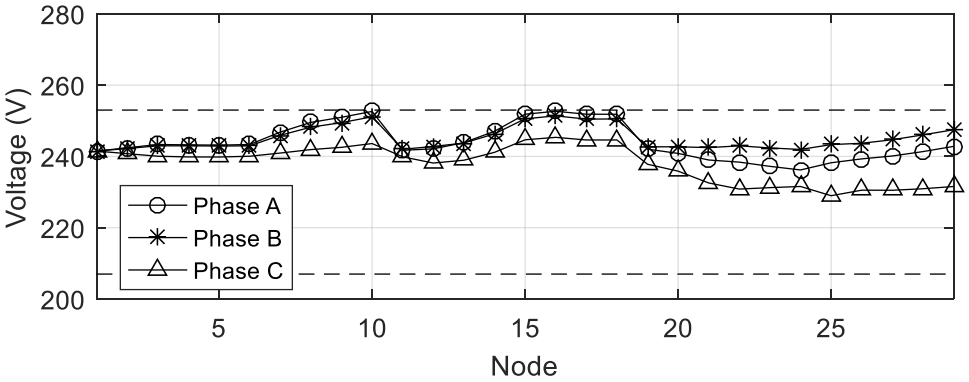

Figure F.5 The voltage profile result

- Finally, only downstream node 29 of each phase has 1-phase PV system. Note that node 29 is the farthest node of the modified 29 node distribution system. Increasing size of 1-phase PV systems until the simulation results nearly exceed the limit, the high PV penetration result is 22% of transformer

capacity. The size of each 1-phase PV system is around 9.1 kW. The voltage profile of 22% high PV penetration can be shown in Figure F.6.

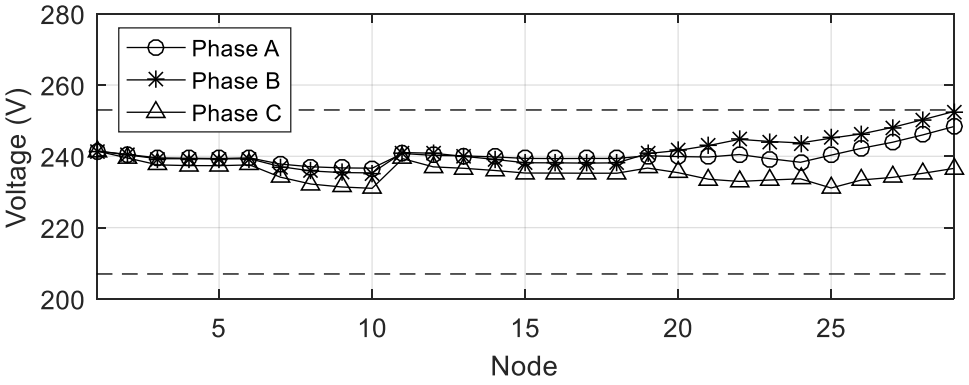

Figure F.6 The voltage profile result

From the high PV penetration results of both Subsection F.1 and F.2 according to no embed local control, it can conclude that:

- Each LV distribution system has a different level of high PV penetration;
- Distributed PV system connection has higher level of high PV penetration than clustered PV system connection.

APPENDIX G

Load, Solar Irradiance and Ambient Temperature Data

The collected data in 3-9 November 2014 between 6.00-18.00 O'clock can be shown in Table 1.

Table G.1 The collected data in 3-9 November 2014 between 6.00-18.00 O'clock

Date	Time	Load (pu.)			Solar (kW/m^2)	Ambient Temp. (^oC)	Date	Time	Load (pu.)			Solar (kW/m^2)	Ambient Temp. (^oC)
		Phase A	Phase B	Phase C					Phase A	Phase B	Phase C		
3 Nov 2014	6:00	0.2696	0.3360	0.4087	0.0000	25.83	7 Nov 2014	6:00	0.1932	0.4186	0.3548	0.0000	27.44
	6:05	0.1829	0.3520	0.3612	0.0000	26.04		6:05	0.2322	0.2689	0.2820	0.0000	27.52
	6:10	0.1801	0.2662	0.2915	0.0000	26.22		6:10	0.2400	0.1664	0.2906	0.0000	27.83
	6:15	0.2229	0.2576	0.2595	0.0000	25.90		6:15	0.3252	0.2562	0.2689	0.0000	27.38
	6:20	0.1867	0.3417	0.3311	0.0006	25.93		6:20	0.2771	0.2044	0.2819	0.0000	27.33
	6:25	0.2367	0.2795	0.3252	0.0054	25.68		6:25	0.2280	0.3091	0.3645	0.0010	27.35
	6:30	0.2101	0.2650	0.2751	0.0122	25.63		6:30	0.2504	0.2743	0.1752	0.0059	27.79
	6:35	0.1683	0.2209	0.2742	0.0210	25.64		6:35	0.4054	0.3345	0.2289	0.0136	28.18
	6:40	0.2082	0.3252	0.2407	0.0306	25.92		6:40	0.3269	0.2154	0.2978	0.0247	27.63
	6:45	0.3633	0.3209	0.2546	0.0317	25.72		6:45	0.2748	0.3514	0.2387	0.0354	27.80
	6:50	0.3235	0.2333	0.2495	0.0319	25.99		6:50	0.3471	0.3824	0.1976	0.0507	28.16
	6:55	0.1895	0.1671	0.2477	0.0374	25.94		6:55	0.3232	0.3797	0.2386	0.0714	29.06
	7:00	0.3007	0.2747	0.2351	0.0461	25.76		7:00	0.3467	0.2356	0.2165	0.0785	28.94
	7:05	0.2613	0.1998	0.3115	0.0524	25.84		7:05	0.2968	0.2215	0.2456	0.0794	28.58
	7:10	0.2419	0.2828	0.2010	0.0605	25.82		7:10	0.3544	0.4850	0.2834	0.0717	28.37
	7:15	0.2854	0.3529	0.2395	0.0715	25.77		7:15	0.2916	0.2132	0.2055	0.0853	28.47
	7:20	0.3278	0.2111	0.2535	0.0818	26.30		7:20	0.2904	0.2710	0.2078	0.1008	28.60
	7:25	0.2164	0.2726	0.3096	0.0945	25.90		7:25	0.2020	0.1890	0.2677	0.1301	28.78
	7:30	0.3771	0.3175	0.2574	0.1052	26.01		7:30	0.2640	0.1416	0.3549	0.1185	28.77
	7:35	0.2782	0.2572	0.2796	0.1142	26.13		7:35	0.2571	0.2543	0.1950	0.1681	28.95
	7:40	0.2871	0.2086	0.3070	0.1206	25.92		7:40	0.3268	0.1427	0.1844	0.2116	29.25
	7:45	0.2476	0.2733	0.2278	0.1257	26.10		7:45	0.3207	0.1132	0.2043	0.2328	29.46
	7:50	0.3163	0.2093	0.2425	0.1357	25.95		7:50	0.3164	0.1361	0.2177	0.2658	29.65
	7:55	0.2068	0.3239	0.2987	0.1518	26.02		7:55	0.3146	0.1384	0.2531	0.2722	29.66
	8:00	0.2927	0.2411	0.2551	0.1750	26.19		8:00	0.3759	0.1045	0.2589	0.2952	29.87
	8:05	0.3680	0.2793	0.2761	0.2169	26.25		8:05	0.5493	0.1502	0.1758	0.2819	30.12
	8:10	0.3166	0.2724	0.2355	0.2608	26.48		8:10	0.2570	0.2445	0.2969	0.2636	30.01
	8:15	0.3653	0.2188	0.2546	0.2889	26.76		8:15	0.3657	0.1245	0.2126	0.2936	29.90
	8:20	0.2131	0.1918	0.3024	0.3211	26.69		8:20	0.3751	0.1359	0.1937	0.3413	30.26
	8:25	0.2369	0.2414	0.3837	0.3440	27.27		8:25	0.2867	0.1241	0.2074	0.3698	30.57
	8:30	0.2480	0.2082	0.3396	0.4390	28.26		8:30	0.2052	0.1314	0.2126	0.3563	31.13
	8:35	0.2480	0.1499	0.2794	0.5934	28.20		8:35	0.4171	0.1932	0.1965	0.4480	31.33
	8:40	0.2775	0.1844	0.2737	0.7183	28.77		8:40	0.2761	0.1843	0.2297	0.4201	31.19
	8:45	0.2467	0.1486	0.2775	0.7428	29.54		8:45	0.2936	0.1421	0.2197	0.2713	30.91
	8:50	0.1922	0.1877	0.2431	0.7714	29.51		8:50	0.1618	0.1811	0.2292	0.3492	30.81
	8:55	0.3338	0.2204	0.2660	0.7725	29.50		8:55	0.2227	0.1757	0.2311	0.1810	30.40
	9:00	0.1953	0.2254	0.3434	0.7390	29.76		9:00	0.3468	0.1466	0.2624	0.2110	30.24
	9:05	0.3458	0.2047	0.3448	0.7789	29.63		9:05	0.2347	0.1675	0.2992	0.1898	30.35
	9:10	0.2542	0.2634	0.3211	0.8225	30.02		9:10	0.2637	0.1716	0.4343	0.2107	30.11
	9:15	0.3446	0.2025	0.3046	0.8435	30.12		9:15	0.2216	0.1664	0.3633	0.2762	30.47
	9:20	0.2295	0.2250	0.2234	0.8491	30.36		9:20	0.2029	0.1536	0.2686	0.3560	30.42
	9:25	0.2392	0.2455	0.2911	0.7681	30.45		9:25	0.2004	0.1763	0.3729	0.3092	30.84
	9:30	0.2382	0.2475	0.3255	0.5364	30.53		9:30	0.2474	0.2362	0.3205	0.3640	30.98
	9:35	0.2178	0.1907	0.3183	0.4190	29.21		9:35	0.2368	0.1986	0.3035	0.3809	30.71
	9:40	0.3219	0.1555	0.2861	0.5230	29.62		9:40	0.3370	0.1622	0.2391	0.5219	31.00
	9:45	0.2331	0.2459	0.2739	0.5722	29.66		9:45	0.2517	0.1303	0.2908	0.5177	31.24
	9:50	0.2201	0.2211	0.3425	0.4978	30.00		9:50	0.3080	0.1315	0.2315	0.3854	31.44
	9:55	0.2106	0.2550	0.3547	0.5947	30.52		9:55	0.2183	0.1693	0.2151	0.4888	31.48
	10:00	0.2008	0.2453	0.2895	0.5930	30.31		10:00	0.1940	0.1576	0.2366	0.6347	31.23
	10:05	0.1887	0.1950	0.2735	0.4601	29.65		10:05	0.2146	0.1803	0.2369	0.5799	31.33
	10:10	0.1839	0.2068	0.2805	0.3752	29.67		10:10	0.2168	0.1538	0.2118	0.5511	30.59
	10:15	0.2089	0.1649	0.3053	0.4234	30.23		10:15	0.3408	0.1550	0.1952	1.0363	31.92
	10:20	0.3013	0.1938	0.2925	0.5871	30.40		10:20	0.2468	0.1679	0.1982	0.4746	32.08
	10:25	0.1987	0.1466	0.3412	0.6576	30.99		10:25	0.2571	0.1608	0.1825	0.6146	32.13
	10:30	0.1886	0.2121	0.2851	0.7757	30.03		10:30	0.3924	0.1892	0.2213	0.4290	31.90
	10:35	0.2881	0.2243	0.3244	0.8628	31.77		10:35	0.3919	0.1770	0.1925	0.6883	31.57
	10:40	0.1946	0.2316	0.3666	0.9780	31.98		10:40	0.2872	0.1781	0.1983	1.0522	32.70
	10:45	0.3782	0.1963	0.2822	1.0743	31.96		10:45	0.2887	0.1501	0.1802	0.5525	31.86
	10:50	0.2313	0.2139	0.2592	1.0918	32.29		10:50	0.3820	0.1506	0.2532	0.6231	32.36
	10:55	0.2355	0.2294	0.2726	1.0784	32.21		10:55	0.2690	0.1444	0.2421	0.4307	31.77
	11:00	0.3681	0.2395	0.2869	1.0606	31.50		11:00	0.3091	0.1581	0.1973	0.5751	31.92
	11:05	0.3872	0.2693	0.2632	1.0814	33.22		11:05	0.4496	0.1937	0.2213	0.3583	31.65
	11:10	0.2503	0.2366	0.2873	1.0927	31.94		11:10	0.2825	0.1871	0.2003	0.2444	31.16
	11:15	0.2294	0.2325	0.2803	1.0837	32.02		11:15	0.2945	0.1444	0.2229	0.2926	30.50
	11:20	0.3567	0.2694	0.2386	1.1174	33.21		11:20	0.2842	0.1210	0.1903	0.3350	31.07
	11:25	0.2241	0.2289	0.2686	1.1219	32.63		11:25	0.2940	0.1992	0.2010	0.3873	31.24
	11:30	0.3650	0.2255	0.2411	1.1050	32.38		11:30	0.3980	0.1613	0.2563	0.4104	31.32
	11:35	0.4493	0.2759	0.2470	1.1054	33.83		11:35	0.4147	0.1353	0.1818	0.5164	31.00

Date	Time	Load (pu.)			Solar (kW/m^2)	Ambient Temp. (^oC)	Date	Time	Load (pu.)			Solar (kW/m^2)	Ambient Temp. (^oC)
		Phase A	Phase B	Phase C					Phase A	Phase B	Phase C		
	11:40	0.2786	0.2194	0.2223	1.0823	32.22		11:40	0.3924	0.1169	0.2101	0.8778	32.52
	11:45	0.3657	0.1841	0.2422	1.1139	32.77		11:45	0.2925	0.1330	0.2007	0.8778	32.52
	11:50	0.3821	0.2338	0.2470	1.0765	34.54		11:50	0.3015	0.2789	0.2298	1.0690	33.08
	11:55	0.2647	0.1295	0.2503	1.0523	33.32		11:55	0.3055	0.1229	0.2343	0.5844	31.82
	12:00	0.3867	0.2044	0.3145	1.1307	33.01		12:00	0.4020	0.1628	0.2436	0.3583	31.02
	12:05	0.3167	0.1983	0.2767	1.1281	32.83		12:05	0.4594	0.1448	0.2170	0.2183	31.22
	12:10	0.3378	0.1572	0.2823	1.0900	34.66		12:10	0.3623	0.1294	0.2246	0.2212	31.66
	12:15	0.4276	0.1663	0.2674	1.0934	34.49		12:15	0.2473	0.1079	0.2911	0.1854	31.83
	12:20	0.4363	0.1231	0.3178	1.0882	34.23		12:20	0.3052	0.1395	0.2813	0.2349	31.13
	12:25	0.3106	0.2525	0.2463	1.1472	33.11		12:25	0.2697	0.1418	0.2841	0.4539	31.01
	12:30	0.2984	0.2593	0.2069	1.1445	34.85		12:30	0.4593	0.1204	0.2332	0.4423	31.12
	12:35	0.2936	0.2672	0.2361	1.0923	33.21		12:35	0.3580	0.1303	0.2349	0.3706	31.24
	12:40	0.2888	0.1854	0.3280	1.0420	33.36		12:40	0.4011	0.1581	0.2780	0.4184	30.68
	12:45	0.2990	0.2277	0.2222	1.0629	32.73		12:45	0.2995	0.1792	0.2271	0.4561	30.78
	12:50	0.2998	0.2305	0.2189	1.0879	32.98		12:50	0.2825	0.1629	0.2331	0.5407	30.85
	12:55	0.2988	0.2687	0.3076	1.0102	34.98		12:55	0.2200	0.1660	0.2692	0.5245	31.01
	13:00	0.2852	0.2170	0.2167	1.0876	33.91		13:00	0.2667	0.1432	0.2458	0.6501	31.40
	13:05	0.2849	0.2246	0.2474	1.0216	33.51		13:05	0.6079	0.1512	0.2505	0.7040	30.79
	13:10	0.2805	0.1801	0.2411	1.0100	34.78		13:10	0.3907	0.1540	0.2533	0.8141	31.53
	13:15	0.2971	0.2799	0.2763	0.7984	35.24		13:15	0.2381	0.1626	0.2681	0.7732	31.86
	13:20	0.2961	0.2505	0.2452	0.3668	33.29		13:20	0.2709	0.1276	0.2659	0.7276	32.40
	13:25	0.2818	0.1842	0.2746	0.9844	34.07		13:25	0.2764	0.3215	0.2529	0.6839	32.11
	13:30	0.2805	0.2174	0.2591	0.9562	34.64		13:30	0.3290	0.1465	0.2597	0.7901	32.40
	13:35	0.2500	0.1773	0.1966	0.4836	33.58		13:35	0.3623	0.1212	0.1920	0.7222	33.09
	13:40	0.2394	0.1910	0.2547	0.5676	32.31		13:40	0.3344	0.1325	0.2096	0.2153	31.39
	13:45	0.2342	0.1591	0.2151	0.2681	32.39		13:45	0.2384	0.1602	0.3028	0.2250	31.27
	13:50	0.2118	0.2758	0.2620	0.3300	32.79		13:50	0.1916	0.1772	0.2288	0.4273	31.61
	13:55	0.2137	0.1589	0.3181	0.7865	34.26		13:55	0.2249	0.1461	0.2646	0.5096	31.58
	14:00	0.2171	0.1986	0.2685	0.5061	33.07		14:00	0.1897	0.1270	0.2369	0.5590	31.95
	14:05	0.2177	0.1647	0.2592	0.4798	32.42		14:05	0.2306	0.1219	0.2272	0.4988	31.92
	14:10	0.2324	0.2891	0.2339	0.6505	33.01		14:10	0.1999	0.3212	0.2017	0.8447	32.24
	14:15	0.2901	0.3071	0.2414	0.4021	32.69		14:15	0.2365	0.1608	0.1852	0.9742	33.34
	14:20	0.2901	0.3071	0.2414	0.3540	32.58		14:20	0.2030	0.1668	0.1993	0.9062	33.98
	14:25	0.1782	0.2423	0.2434	0.5413	32.05		14:25	0.2457	0.1470	0.2236	0.7782	33.46
	14:30	0.2017	0.2855	0.2572	0.8934	33.93		14:30	0.2367	0.1987	0.2079	0.5021	33.17
	14:35	0.1711	0.2916	0.2929	0.5837	33.44		14:35	0.2440	0.1866	0.1978	0.2583	32.67
	14:40	0.1802	0.2638	0.2921	0.2738	32.63		14:40	0.2040	0.1839	0.1995	0.2262	31.90
	14:45	0.3000	0.2627	0.2616	0.2665	33.24		14:45	0.1789	0.2110	0.2002	0.1307	32.19
	14:50	0.2720	0.2593	0.2524	0.2571	32.98		14:50	0.1853	0.2418	0.1660	0.1203	32.59
	14:55	0.3318	0.3417	0.2633	0.3088	32.65		14:55	0.1390	0.2104	0.2180	0.1050	32.92
	15:00	0.3462	0.2884	0.3000	0.6884	34.28		15:00	0.1885	0.1745	0.1921	0.0982	32.32
	15:05	0.5309	0.3340	0.3015	0.6720	34.20		15:05	0.1384	0.1707	0.2040	0.0938	32.13
	15:10	0.4034	0.2587	0.2588	0.6839	33.43		15:10	0.1615	0.2091	0.2391	0.1020	30.62
	15:15	0.3382	0.2909	0.2724	0.6809	34.67		15:15	0.1175	0.1845	0.2158	0.1244	30.42
	15:20	0.3590	0.1666	0.2249	0.6407	34.02		15:20	0.2141	0.1701	0.2409	0.1370	30.59
	15:25	0.3840	0.2382	0.2305	0.4508	34.58		15:25	0.1292	0.2572	0.1989	0.1241	31.23
	15:30	0.3753	0.1962	0.3024	0.4629	34.22		15:30	0.2304	0.2173	0.1847	0.1091	31.39
	15:35	0.3127	0.2109	0.2153	0.3720	33.61		15:35	0.2136	0.2728	0.2030	0.0707	31.36
	15:40	0.3624	0.1952	0.2566	0.3268	33.35		15:40	0.1575	0.2232	0.2644	0.0537	31.16
	15:45	0.2805	0.2542	0.2234	0.4258	33.63		15:45	0.2886	0.2387	0.2309	0.0523	30.84
	15:50	0.3996	0.2385	0.2757	0.3757	33.60		15:50	0.1606	0.2901	0.2357	0.0490	31.15
	15:55	0.4010	0.2042	0.2243	0.2921	33.57		15:55	0.2135	0.2813	0.2877	0.0531	31.02
	16:00	0.4019	0.2203	0.2195	0.2555	33.89		16:00	0.1510	0.2802	0.3569	0.0635	31.31
	16:05	0.3691	0.1718	0.2633	0.1686	33.37		16:05	0.2954	0.2764	0.2271	0.0521	30.94
	16:10	0.2555	0.2218	0.2385	0.2315	33.13		16:10	0.2573	0.2826	0.2443	0.0473	30.22
	16:15	0.4471	0.2033	0.2633	0.2297	33.33		16:15	0.2629	0.2631	0.2952	0.0582	29.99
	16:20	0.2617	0.2520	0.2732	0.2217	33.03		16:20	0.2168	0.3040	0.3307	0.0568	28.82
	16:25	0.3585	0.2616	0.2452	0.2121	33.13		16:25	0.2402	0.2666	0.2392	0.0527	28.62
	16:30	0.2620	0.3043	0.3357	0.1345	32.85		16:30	0.2291	0.2028	0.2338	0.0485	28.47
	16:35	0.3136	0.3078	0.2879	0.1714	32.79		16:35	0.2459	0.1998	0.3256	0.0470	28.69
	16:40	0.1357	0.3532	0.3106	0.1650	33.00		16:40	0.3039	0.2468	0.2403	0.0449	28.71
	16:45	0.3669	0.2391	0.3753	0.1244	32.80		16:45	0.3294	0.2446	0.3251	0.0419	28.54
	16:50	0.4014	0.2790	0.3292	0.1317	33.18		16:50	0.2471	0.2188	0.2478	0.0397	28.30
	16:55	0.2553	0.2495	0.3198	0.1131	32.79		16:55	0.2440	0.2663	0.2607	0.0368	28.32
	17:00	0.3761	0.3020	0.3555	0.0987	32.84		17:00	0.2898	0.2862	0.2911	0.0341	28.46
	17:05	0.4046	0.3011	0.2088	0.0870	33.01		17:05	0.2870	0.2446	0.3426	0.0316	28.86
	17:10	0.2559	0.2436	0.2604	0.0752	32.44		17:10	0.1879	0.2691	0.2937	0.0274	28.91
	17:15	0.1487	0.2442	0.2270	0.0594	32.44		17:15	0.1135	0.3036	0.2807	0.0230	28.81
	17:20	0.2727	0.2199	0.2524	0.0447	32.11		17:20	0.1785	0.3038	0.3126	0.0186	28.82
	17:25	0.1623	0.2849	0.2711	0.0328	31.52		17:25	0.1379	0.2835	0.2530	0.0120	28.86
	17:30	0.2758	0.2268	0.2972	0.0223	31.39		17:30	0.1319	0.2343	0.2740	0.0074	28.72
	17:35	0.2756	0.2743	0.3455	0.0138	31.31		17:35	0.1863	0.2998	0.1667	0.0037	28.48
	17:40	0.1810	0.1515	0.4171	0.0061	31.30		17:40	0.1349	0.2895	0.2203	0.0001	28.16
	17:45	0.3622	0.3041	0.3880	0.0006	30.94		17:45	0.1384	0.3743	0.2009	0.0000	27.41
	17:50	0.3064	0.3057	0.4094	0.0000	30.94		17:50	0.1937	0.3887	0.2443	0.0000	27.67
	17:55	0.2576	0.3510	0.4060	0.0000	30.93		17:55	0.1401	0.3641	0.2757	0.0000	27.79
4 Nov 2014	6:00	0.2255	0.4042	0.3621	0.0000	26.30	8 Nov 2014	6:00	0.2375	0.3861	0.3643	0.0000	25.56
	6:05	0.3033	0.3345	0.4144	0.0000	26.49		6:05	0.2370	0.2492	0.4129	0.0000	25.67
	6:10	0.1860	0.2218	0.3386	0.0000	26.25		6:10	0.2488	0.2665	0.3874	0.0000	25.65
	6:15	0.2891	0.2899	0.3859	0.0000	26.25		6:15	0.2866	0.2056	0.3202	0.0000	25.53
	6:20	0.1479	0.3002	0.2426	0.0025	26.19		6:20	0.2861	0.2855	0.1841	0.0003	25.41
	6:25	0.3401	0.4006	0.2516	0.0088	26.26		6:25	0.2346	0.3368	0.3423	0.0043	25.60
	6:30	0.4161	0.3433	0.3498	0.0144	26.22		6:30	0.2879	0.2796	0.1878	0.0091	25.80
	6:35	0.2717	0.2726	0.3294	0.0216	26.30		6:35	0.3435	0.3463	0.3181	0.0159	25.84
	6:40	0.2563	0.3067	0.2543	0.0325	26.38		6:40	0.3502	0.2061	0.2253	0.0247	25.87
	6:45	0.2685	0.3916	0.2549	0.0487	26.54		6:45	0.2804	0.2432	0.2289	0.0380	26.12
	6:50	0.2870	0.4798	0.2895	0.0644	26.71		6:50	0.2264	0.2615	0.1991	0.0509	26.27
	6:55	0.2456	0.2480	0.2434	0.0794	26.99		6:55	0.2316	0.4289	0.2062	0.0653	26.45
	7:00	0.3849	0.3799	0.2834	0.0984	27.10		7:00	0.2976	0.2654	0.2346	0.0912	27.02

Date	Time	Load (pu.)			Solar (kW/m^2)	Ambient Temp. (^oC)	Date	Time	Load (pu.)			Solar (kW/m^2)	Ambient Temp. (^oC)
		Phase A	Phase B	Phase C					Phase A	Phase B	Phase C		
	7:05	0.2343	0.2659	0.2999	0.1153	27.08		7:05	0.2035	0.2626	0.2149	0.1066	27.19
	7:10	0.4852	0.2094	0.1810	0.1315	27.34		7:10	0.2278	0.3008	0.1782	0.1206	26.91
	7:15	0.3183	0.1970	0.3431	0.1509	27.33		7:15	0.2821	0.3382	0.2817	0.1332	27.19
	7:20	0.2726	0.1953	0.2931	0.1684	27.66		7:20	0.4705	0.2535	0.3404	0.1526	27.27
	7:25	0.3437	0.2219	0.2968	0.1791	28.22		7:25	0.2887	0.3731	0.2012	0.1723	27.29
	7:30	0.2376	0.2553	0.2999	0.2026	28.63		7:30	0.2729	0.3851	0.1779	0.1993	27.24
	7:35	0.2783	0.3019	0.3051	0.2286	28.61		7:35	0.2936	0.2835	0.2283	0.2297	27.42
	7:40	0.2474	0.2089	0.2804	0.2515	28.76		7:40	0.2511	0.2077	0.2637	0.2297	27.42
	7:45	0.3368	0.2532	0.2620	0.2737	28.60		7:45	0.3923	0.3926	0.2981	0.2624	27.17
	7:50	0.2863	0.2435	0.2129	0.2961	28.84		7:50	0.4031	0.2807	0.3389	0.2899	27.75
	7:55	0.3046	0.2121	0.2443	0.3161	29.38		7:55	0.3971	0.2245	0.3109	0.3060	27.78
	8:00	0.3321	0.1628	0.2559	0.3343	29.23		8:00	0.3029	0.4756	0.3249	0.3254	27.99
	8:05	0.2630	0.1877	0.2531	0.3613	29.17		8:05	0.3173	0.3639	0.2610	0.3431	28.27
	8:10	0.2647	0.2869	0.1849	0.3887	30.43		8:10	0.4542	0.3165	0.3275	0.3788	27.95
	8:15	0.3249	0.2496	0.2226	0.4143	30.27		8:15	0.2740	0.3173	0.3855	0.4214	28.32
	8:20	0.2369	0.2724	0.2790	0.4389	29.62		8:20	0.3059	0.2420	0.4356	0.4417	28.58
	8:25	0.5079	0.3156	0.2855	0.4569	30.04		8:25	0.2313	0.2317	0.3562	0.4803	28.32
	8:30	0.2706	0.3084	0.2947	0.4682	30.45		8:30	0.2582	0.2611	0.3595	0.5092	28.89
	8:35	0.2115	0.3403	0.2727	0.4539	30.72		8:35	0.2447	0.3045	0.3013	0.5284	29.25
	8:40	0.2997	0.2285	0.2161	0.4793	30.16		8:40	0.2640	0.3270	0.2994	0.5446	29.28
	8:45	0.2549	0.1871	0.3818	0.5256	30.58		8:45	0.2887	0.3969	0.3367	0.5746	29.27
	8:50	0.1955	0.2119	0.2786	0.5691	30.34		8:50	0.3741	0.2470	0.3520	0.5953	29.42
	8:55	0.2325	0.2315	0.3468	0.5764	30.82		8:55	0.2511	0.3388	0.3016	0.6155	29.14
	9:00	0.1979	0.2108	0.2991	0.5766	31.78		9:00	0.3169	0.3258	0.3434	0.6400	29.48
	9:05	0.2565	0.2124	0.2816	0.5886	31.87		9:05	0.2883	0.3661	0.4022	0.6532	29.04
	9:10	0.2542	0.1549	0.2572	0.5479	30.93		9:10	0.2780	0.3426	0.3822	0.6897	29.58
	9:15	0.2665	0.2222	0.2582	0.5374	31.74		9:15	0.3183	0.3757	0.3799	0.7088	30.27
	9:20	0.2323	0.1694	0.2525	0.5860	32.62		9:20	0.3311	0.3472	0.2607	0.7238	30.05
	9:25	0.2487	0.2049	0.3012	0.5327	32.10		9:25	0.4760	0.3950	0.3821	0.7558	29.43
	9:30	0.2532	0.1647	0.2752	0.5755	31.86		9:30	0.3223	0.3278	0.3662	0.7767	29.90
	9:35	0.2360	0.1841	0.2761	0.4758	31.54		9:35	0.4536	0.4257	0.3629	0.7947	30.31
	9:40	0.2438	0.1741	0.2498	0.6282	31.76		9:40	0.3229	0.4236	0.3862	0.8181	30.52
	9:45	0.2382	0.1579	0.2414	0.7188	32.29		9:45	0.4807	0.2903	0.3018	0.8323	31.26
	9:50	0.1964	0.1354	0.2634	0.5250	31.37		9:50	0.3334	0.3878	0.3137	0.8259	31.14
	9:55	0.3342	0.2105	0.2605	0.7504	31.91		9:55	0.4353	0.4132	0.3163	0.8110	31.14
	10:00	0.1988	0.2066	0.2359	0.8500	33.06		10:00	0.3771	0.4278	0.3358	0.8607	30.45
	10:05	0.2003	0.1220	0.2688	0.8674	33.32		10:05	0.3785	0.4156	0.2657	0.8149	30.51
	10:10	0.1936	0.1472	0.2484	0.8714	33.79		10:10	0.4083	0.3352	0.2097	0.8560	29.94
	10:15	0.1975	0.1865	0.2390	0.8637	34.25		10:15	0.3558	0.3702	0.1914	0.9180	30.16
	10:20	0.3033	0.1732	0.2692	0.8652	34.49		10:20	0.3125	0.3794	0.1988	0.9019	31.22
	10:25	0.1916	0.1887	0.2296	0.9109	34.37		10:25	0.4041	0.3615	0.1964	0.8942	31.85
	10:30	0.1544	0.1695	0.2858	0.9166	35.05		10:30	0.2914	0.2583	0.1950	0.8532	31.82
	10:35	0.2641	0.2065	0.2170	0.9318	33.57		10:35	0.3693	0.3617	0.1892	0.8615	31.81
	10:40	0.1529	0.1464	0.2519	0.9936	34.61		10:40	0.5127	0.3637	0.1915	0.9327	31.82
	10:45	0.1468	0.1891	0.2758	1.0077	35.24		10:45	0.4191	0.3176	0.1851	1.1025	30.97
	10:50	0.2626	0.2171	0.2593	0.9159	34.68		10:50	0.4343	0.4068	0.2034	1.1025	30.97
	10:55	0.1960	0.1911	0.2702	0.8683	33.31		10:55	0.3839	0.3321	0.2061	0.9746	30.84
	11:00	0.1496	0.1525	0.3044	0.6772	32.87		11:00	0.4735	0.2978	0.2169	0.9059	31.80
	11:05	0.2659	0.1433	0.3051	0.6318	33.20		11:05	0.5185	0.2924	0.2086	1.0373	32.14
	11:10	0.1268	0.1908	0.2637	0.5293	33.74		11:10	0.3878	0.2740	0.1912	1.0563	32.05
	11:15	0.1309	0.1799	0.2410	0.6536	33.05		11:15	0.3558	0.2944	0.2020	0.9941	31.96
	11:20	0.2477	0.1413	0.2365	1.0976	34.47		11:20	0.4237	0.2399	0.2106	1.0292	32.41
	11:25	0.1304	0.1443	0.2426	0.6521	34.56		11:25	0.3522	0.2599	0.2146	1.0116	31.82
	11:30	0.1504	0.1898	0.2365	0.7004	34.75		11:30	0.3134	0.3096	0.2302	1.0303	31.98
	11:35	0.2837	0.1639	0.2184	0.8423	35.26		11:35	0.4863	0.3231	0.2487	1.0619	31.74
	11:40	0.1340	0.1367	0.2040	0.8669	35.28		11:40	0.3213	0.3258	0.2970	1.0792	32.49
	11:45	0.1311	0.1310	0.2277	0.9875	35.93		11:45	0.3259	0.3480	0.1937	1.1992	31.41
	11:50	0.2568	0.2283	0.3179	1.0628	35.58		11:50	0.3418	0.3688	0.1661	1.1973	31.76
	11:55	0.3181	0.2312	0.2662	0.7065	35.82		11:55	0.4217	0.2799	0.2145	0.8743	32.38
	12:00	0.1944	0.2286	0.2707	0.5929	34.76		12:00	0.4360	0.2948	0.2502	0.4644	31.77
	12:05	0.1929	0.1328	0.2770	0.3611	34.75		12:05	0.4364	0.2278	0.2453	0.3980	31.92
	12:10	0.3013	0.1205	0.3211	0.3099	33.77		12:10	0.2779	0.2286	0.2450	0.7902	31.70
	12:15	0.3722	0.1424	0.2653	0.3559	33.96		12:15	0.3667	0.2018	0.2786	0.3994	31.19
	12:20	0.2302	0.1588	0.2362	0.6026	33.54		12:20	0.4078	0.2738	0.2334	0.6807	31.60
	12:25	0.2309	0.1313	0.2614	0.9417	35.33		12:25	0.4253	0.2900	0.2398	0.5076	32.58
	12:30	0.2399	0.1694	0.2484	0.8818	34.20		12:30	0.4412	0.2734	0.2688	0.3785	32.42
	12:35	0.3717	0.1968	0.2343	0.9985	34.30		12:35	0.4730	0.2780	0.2486	0.5137	32.35
	12:40	0.3652	0.1693	0.2688	1.0383	34.16		12:40	0.2378	0.4939	0.2272	0.4641	32.41
	12:45	0.3823	0.1533	0.2131	0.9529	34.90		12:45	0.3202	0.2991	0.2277	0.3893	31.61
	12:50	0.2483	0.1953	0.2259	0.5105	33.61		12:50	0.2186	0.3123	0.2328	0.5206	32.03
	12:55	0.2481	0.2289	0.2715	0.2476	33.54		12:55	0.2642	0.3285	0.2723	0.7184	32.52
	13:00	0.2419	0.1811	0.3149	0.2112	33.16		13:00	0.2120	0.3113	0.2605	0.8484	33.40
	13:05	0.2478	0.1775	0.3367	0.1941	33.50		13:05	0.3690	0.2806	0.3170	0.8229	32.78
	13:10	0.2477	0.2072	0.3159	0.1970	33.38		13:10	0.3650	0.2574	0.2301	0.6673	31.56
	13:15	0.2487	0.2022	0.3010	0.2433	33.33		13:15	0.4168	0.3889	0.2634	0.5888	32.06
	13:20	0.3750	0.1749	0.2404	0.1700	32.87		13:20	0.4187	0.4258	0.2446	0.4848	31.82
	13:25	0.3949	0.1908	0.2420	0.1674	32.20		13:25	0.3069	0.4562	0.1697	0.3541	31.85
	13:30	0.3845	0.1827	0.2483	0.1658	32.88		13:30	0.2707	0.4663	0.2913	0.5855	31.94
	13:35	0.2609	0.1400	0.2957	0.1792	33.11		13:35	0.2184	0.4107	0.3145	0.6347	32.01
	13:40	0.2528	0.2157	0.3017	0.2406	32.84		13:40	0.2324	0.4100	0.2720	0.7549	32.03
	13:45	0.2558	0.1611	0.2955	0.2637	32.33		13:45	0.4014	0.3739	0.3052	0.4134	31.69
	13:50	0.2612	0.1700	0.2959	0.2721	31.72		13:50	0.3817	0.3939	0.3248	0.3927	31.77
	13:55	0.3879	0.1632	0.3196	0.2971	31.60		13:55	0.2967	0.3485	0.2777	0.2587	30.95
	14:00	0.3737	0.1870	0.3414	0.5641	32.65		14:00	0.1912	0.3220	0.2903	0.2509	30.97
	14:05	0.3518	0.1801	0.3099	0.6741	33.00		14:05	0.2863	0.3815	0.2804	0.2617	31.51
	14:10	0.3051	0.1999	0.2955	0.6972	33.08		14:10	0.2691	0.3864	0.3039	0.5152	31.65
	14:15	0.2968	0.2260	0.2815	0.7325	32.59		14:15	0.4008	0.3504	0.3527	0.7054	31.68
	14:20	0.2777	0.1838	0.3098	0.5312	33.49		14:20	0.4274	0.3593	0.3696	0.2715	32.30
	14:25	0.3924	0.2818	0.3050	0.5221	33.63		14:25	0.4283	0.3863	0.3237	0.1518	31.23

Date	Time	Load (pu.)			Solar (kW/m^2)	Ambient Temp. (^oC)	Date	Time	Load (pu.)			Solar (kW/m^2)	Ambient Temp. (^oC)
		Phase A	Phase B	Phase C					Phase A	Phase B	Phase C		
	14:30	0.3915	0.2250	0.2523	0.5649	32.44		14:30	0.4498	0.3844	0.3692	0.1739	31.31
	14:35	0.2892	0.1964	0.2762	0.4872	32.09		14:35	0.5964	0.3405	0.3501	0.2560	30.80
	14:40	0.2917	0.2514	0.2760	0.3055	31.96		14:40	0.5129	0.4010	0.3560	0.3282	31.16
	14:45	0.3040	0.2748	0.3501	0.2262	32.04		14:45	0.3701	0.4065	0.3070	0.2342	31.74
	14:50	0.3988	0.1744	0.3413	0.2361	31.89		14:50	0.3325	0.4046	0.3580	0.2973	31.22
	14:55	0.4447	0.2177	0.3518	0.2887	32.24		14:55	0.4647	0.3340	0.3691	0.3011	30.76
	15:00	0.4252	0.2509	0.3120	0.3735	33.01		15:00	0.2779	0.4152	0.4128	0.1594	30.98
	15:05	0.2655	0.1898	0.3526	0.3707	32.72		15:05	0.2464	0.4075	0.3733	0.1061	30.72
	15:10	0.2614	0.2620	0.3485	0.4141	33.23		15:10	0.1635	0.3305	0.3686	0.1575	30.30
	15:15	0.3781	0.3151	0.3749	0.3032	32.72		15:15	0.1835	0.3953	0.3413	0.1699	30.89
	15:20	0.2826	0.3263	0.3713	0.2702	32.73		15:20	0.1872	0.3868	0.3310	0.3031	31.29
	15:25	0.2834	0.2913	0.3716	0.2702	32.73		15:25	0.1802	0.3890	0.3319	0.6625	32.09
	15:30	0.3139	0.3013	0.3355	0.2239	32.80		15:30	0.1777	0.3162	0.3122	0.5741	32.97
	15:35	0.4004	0.2860	0.3247	0.1806	31.82		15:35	0.2558	0.4404	0.2844	0.3205	32.34
	15:40	0.4501	0.2534	0.4061	0.1672	32.42		15:40	0.2592	0.4046	0.3550	0.2032	31.59
	15:45	0.3683	0.3237	0.3708	0.1772	32.95		15:45	0.2518	0.4146	0.3087	0.1930	30.84
	15:50	0.3924	0.3151	0.3931	0.2236	33.24		15:50	0.3071	0.4237	0.2936	0.2003	30.60
	15:55	0.3201	0.2604	0.3976	0.3166	32.96		15:55	0.2926	0.3392	0.2800	0.1928	30.84
	16:00	0.3409	0.3022	0.3675	0.2875	33.37		16:00	0.2771	0.3508	0.3374	0.2966	30.86
	16:05	0.4510	0.2970	0.4252	0.2162	32.50		16:05	0.3589	0.3985	0.2876	0.2717	31.34
	16:10	0.4372	0.2990	0.3890	0.2274	31.78		16:10	0.2691	0.4255	0.3121	0.1858	31.35
	16:15	0.3340	0.2942	0.3173	0.2489	32.03		16:15	0.3355	0.3502	0.3122	0.1624	30.99
	16:20	0.3332	0.3019	0.3347	0.2276	32.65		16:20	0.2138	0.3639	0.3017	0.1493	30.99
	16:25	0.3330	0.2056	0.3428	0.2123	31.98		16:25	0.3987	0.4321	0.2915	0.1301	30.78
	16:30	0.4441	0.2893	0.3168	0.2026	32.67		16:30	0.1958	0.4041	0.2613	0.1682	31.14
	16:35	0.6870	0.2657	0.3054	0.1889	33.01		16:35	0.3805	0.4540	0.3394	0.1325	30.84
	16:40	0.3483	0.2467	0.2934	0.1856	32.81		16:40	0.2331	0.4007	0.2678	0.1063	30.31
	16:45	0.3516	0.2836	0.3023	0.1635	32.86		16:45	0.3783	0.3569	0.3335	0.0803	30.26
	16:50	0.3591	0.2776	0.3006	0.1253	32.21		16:50	0.1846	0.3162	0.2849	0.0466	30.29
	16:55	0.3321	0.2395	0.2644	0.0875	31.80		16:55	0.2484	0.3216	0.3057	0.0242	30.23
	17:00	0.3247	0.2487	0.3108	0.0700	31.70		17:00	0.3222	0.3446	0.2766	0.0107	30.15
	17:05	0.3752	0.2778	0.2847	0.0546	32.14		17:05	0.3160	0.3219	0.2967	0.0131	30.15
	17:10	0.3106	0.2916	0.3216	0.0336	31.33		17:10	0.2837	0.3706	0.2902	0.0240	29.85
	17:15	0.3062	0.2830	0.2760	0.0249	31.58		17:15	0.2816	0.3959	0.2976	0.0163	30.18
	17:20	0.3156	0.2867	0.3576	0.0204	31.48		17:20	0.3104	0.2748	0.2319	0.0098	30.11
	17:25	0.4554	0.3183	0.3045	0.0132	31.76		17:25	0.3070	0.3125	0.2805	0.0051	29.87
	17:30	0.4462	0.3282	0.3409	0.0090	31.58		17:30	0.2455	0.3383	0.2641	0.0000	29.95
	17:35	0.2762	0.2998	0.3044	0.0039	31.96		17:35	0.2369	0.3142	0.2200	0.0000	29.89
	17:40	0.4462	0.3084	0.3084	0.0005	31.39		17:40	0.1815	0.2741	0.1878	0.0000	29.67
	17:45	0.3336	0.2751	0.3166	0.0000	31.32		17:45	0.2285	0.3075	0.2217	0.0000	29.62
	17:50	0.2493	0.2818	0.3440	0.0000	31.35		17:50	0.2953	0.2327	0.2711	0.0000	29.44
	17:55	0.3434	0.3275	0.2803	0.0000	31.29		17:55	0.2263	0.2405	0.3129	0.0000	29.38
5	6:00	0.2865	0.3352	0.3504	0.0000	27.26	9	6:00	0.3819	0.1776	0.2562	0.0000	22.99
Nov	6:05	0.2679	0.3252	0.3162	0.0000	27.22	Nov	6:05	0.4369	0.2835	0.2731	0.0000	23.09
2014	6:10	0.2252	0.2922	0.2618	0.0000	27.09	2014	6:10	0.1571	0.3805	0.2603	0.0000	22.97
	6:15	0.5064	0.4558	0.3199	0.0000	27.13		6:15	0.2206	0.2271	0.3252	0.0000	23.04
	6:20	0.4276	0.4210	0.2419	0.0023	27.58		6:20	0.1882	0.3172	0.2323	0.0000	22.99
	6:25	0.3200	0.2258	0.2844	0.0070	27.32		6:25	0.4049	0.3393	0.3047	0.0000	22.92
	6:30	0.4756	0.2522	0.2805	0.0102	27.38		6:30	0.2572	0.2037	0.2451	0.0004	22.92
	6:35	0.2604	0.2555	0.2323	0.0130	27.24		6:35	0.2803	0.2886	0.2920	0.0009	23.01
	6:40	0.3310	0.1714	0.2389	0.0149	27.45		6:40	0.3474	0.2310	0.3368	0.0026	23.11
	6:45	0.3007	0.2062	0.2698	0.0191	27.27		6:45	0.2659	0.3145	0.2312	0.0083	23.00
	6:50	0.4720	0.2242	0.2512	0.0217	27.40		6:50	0.4212	0.2488	0.2457	0.0143	23.12
	6:55	0.2642	0.3420	0.2667	0.0187	27.47		6:55	0.2989	0.1574	0.2670	0.0170	23.19
	7:00	0.4774	0.3490	0.2885	0.0312	27.52		7:00	0.2484	0.3185	0.3442	0.0204	23.34
	7:05	0.3816	0.2271	0.2002	0.0424	27.54		7:05	0.2621	0.2618	0.3374	0.0186	23.47
	7:10	0.4295	0.2326	0.3403	0.0660	27.53		7:10	0.4008	0.2911	0.2662	0.0214	23.52
	7:15	0.3634	0.2606	0.3062	0.1129	27.63		7:15	0.3151	0.3063	0.2563	0.0359	23.53
	7:20	0.2740	0.2643	0.2375	0.1201	28.21		7:20	0.3310	0.3245	0.2931	0.0546	23.63
	7:25	0.4466	0.3269	0.2705	0.1272	28.37		7:25	0.4327	0.2261	0.3019	0.0583	23.76
	7:30	0.3380	0.1825	0.2758	0.1504	28.07		7:30	0.3680	0.2343	0.2311	0.0483	23.66
	7:35	0.3750	0.2975	0.2502	0.1749	28.26		7:35	0.2458	0.2741	0.2226	0.0403	23.66
	7:40	0.3767	0.2273	0.2535	0.1765	28.44		7:40	0.2268	0.2874	0.3634	0.0595	23.77
	7:45	0.2735	0.2540	0.2151	0.1432	28.44		7:45	0.2561	0.2514	0.2684	0.0637	23.69
	7:50	0.2861	0.3042	0.2573	0.1546	28.18		7:50	0.3149	0.3297	0.2620	0.0593	23.85
	7:55	0.3746	0.3327	0.2666	0.1535	28.63		7:55	0.2684	0.2245	0.3088	0.0669	23.53
	8:00	0.3420	0.2628	0.2296	0.1608	28.76		8:00	0.2800	0.2895	0.2567	0.0631	23.53
	8:05	0.2577	0.3225	0.2403	0.1846	28.76		8:05	0.3030	0.1482	0.2868	0.0878	23.56
	8:10	0.2427	0.3899	0.2211	0.2824	28.87		8:10	0.2020	0.3432	0.2221	0.1212	23.57
	8:15	0.2436	0.2388	0.2503	0.2581	29.19		8:15	0.3178	0.3144	0.2011	0.1157	23.77
	8:20	0.2498	0.2673	0.2335	0.2716	28.67		8:20	0.5368	0.3725	0.2013	0.0964	23.85
	8:25	0.2538	0.2932	0.2740	0.3976	29.08		8:25	0.4493	0.3875	0.2010	0.1122	23.73
	8:30	0.2699	0.3786	0.2178	0.4099	29.41		8:30	0.3948	0.2601	0.2679	0.0632	23.88
	8:35	0.2850	0.2953	0.2804	0.4014	30.10		8:35	0.2960	0.3053	0.2116	0.0517	23.66
	8:40	0.2445	0.3413	0.2747	0.4088	30.31		8:40	0.4417	0.3714	0.3022	0.0582	23.26
	8:45	0.3724	0.1870	0.2524	0.5074	29.98		8:45	0.3215	0.1873	0.2280	0.0582	22.81
	8:50	0.2460	0.2645	0.2296	0.5304	30.22		8:50	0.4341	0.1936	0.2221	0.0889	22.53
	8:55	0.3094	0.2526	0.2544	0.5844	30.65		8:55	0.3102	0.2538	0.2154	0.0998	22.57
	9:00	0.2000	0.2744	0.2540	0.5862	30.60		9:00	0.4499	0.2491	0.2612	0.1155	22.84
	9:05	0.3207	0.3021	0.2295	0.5135	30.76		9:05	0.3862	0.3515	0.2693	0.1086	23.15
	9:10	0.2050	0.2712	0.2599	0.4709	30.89		9:10	0.2741	0.3170	0.2832	0.1140	23.20
	9:15	0.3157	0.2288	0.2241	0.6159	30.78		9:15	0.4123	0.2915	0.2575	0.1745	23.04
	9:20	0.2020	0.1616	0.2455	0.6528	31.29		9:20	0.2534	0.2805	0.2622	0.2044	23.16
	9:25	0.1970	0.2491	0.2309	0.4496	31.65		9:25	0.2274	0.3202	0.2503	0.2806	23.63
	9:30	0.2083	0.2322	0.2568	0.3499	31.52		9:30	0.3643	0.2626	0.2012	0.3345	23.96
	9:35	0.1986	0.2119	0.2432	0.4325	31.91		9:35	0.3201	0.3325	0.2406	0.3210	23.67
	9:40	0.2578	0.1447	0.2301	0.4619	31.68		9:40	0.3024	0.3101	0.2834	0.2381	23.68
	9:45	0.2151	0.2140	0.1879	0.3077	31.49		9:45	0.2497	0.2899	0.2731	0.2303	23.92
	9:50	0.3126	0.1432	0.3096	0.4284	31.49		9:50	0.3234	0.3405	0.2912	0.2644	23.80

Date	Time	Load (pu.)			Solar (kW/m^2)	Ambient Temp. (^oC)	Date	Time	Load (pu.)			Solar (kW/m^2)	Ambient Temp. (^oC)
		Phase A	Phase B	Phase C					Phase A	Phase B	Phase C		
	9:55	0.2431	0.1903	0.2122	0.6627	30.65		9:55	0.2264	0.2929	0.2605	0.3843	24.10
	10:00	0.2539	0.1849	0.2385	0.4633	29.88		10:00	0.2912	0.2280	0.1995	0.5152	24.51
	10:05	0.3224	0.2257	0.2384	0.3206	30.14		10:05	0.2943	0.2327	0.2216	0.4567	25.03
	10:10	0.2150	0.1816	0.2747	0.7690	30.34		10:10	0.3490	0.1994	0.1863	0.4439	24.83
	10:15	0.2477	0.2012	0.2365	0.5669	29.99		10:15	0.3889	0.2666	0.2042	0.3661	24.89
	10:20	0.3627	0.1760	0.2443	0.6844	31.62		10:20	0.3828	0.2642	0.1780	0.3827	25.44
	10:25	0.3510	0.2171	0.2201	0.9411	32.15		10:25	0.4187	0.3498	0.2228	0.4128	25.10
	10:30	0.2716	0.1303	0.2543	0.7384	32.07		10:30	0.3539	0.2904	0.2310	0.3861	25.25
	10:35	0.3097	0.1811	0.2641	0.6129	32.58		10:35	0.4004	0.3390	0.1923	0.4045	24.89
	10:40	0.4023	0.1911	0.1986	0.8077	31.98		10:40	0.3451	0.2890	0.3122	0.4984	25.18
	10:45	0.3030	0.2555	0.2431	0.6146	32.71		10:45	0.4011	0.2764	0.2997	0.4316	25.72
	10:50	0.3200	0.2149	0.2889	0.6761	32.49		10:50	0.4314	0.2362	0.2883	0.4239	26.07
	10:55	0.3159	0.1879	0.1917	1.0054	33.24		10:55	0.3651	0.2697	0.2447	0.3451	25.61
	11:00	0.4033	0.2141	0.2167	0.7873	33.98		11:00	0.4183	0.2863	0.2473	0.4536	26.40
	11:05	0.2982	0.1869	0.2132	0.4686	32.76		11:05	0.4194	0.3038	0.2292	0.5797	26.46
	11:10	0.2970	0.1976	0.1833	0.6559	33.45		11:10	0.2639	0.3111	0.2971	0.6537	26.96
	11:15	0.2819	0.1576	0.2636	0.4056	32.61		11:15	0.3018	0.2830	0.3979	0.7853	27.73
	11:20	0.4209	0.2248	0.2198	0.5391	32.80		11:20	0.3055	0.1983	0.3712	0.7549	27.88
	11:25	0.2826	0.2184	0.2435	0.5888	34.12		11:25	0.2642	0.2903	0.3952	0.8188	28.66
	11:30	0.2169	0.2185	0.2077	0.2781	33.56		11:30	0.2991	0.2581	0.2853	0.9486	28.61
	11:35	0.2574	0.1923	0.1799	0.2004	32.64		11:35	0.2946	0.2014	0.2265	0.9760	28.50
	11:40	0.3709	0.2237	0.2120	0.2070	31.65		11:40	0.2464	0.2239	0.3315	0.7994	28.46
	11:45	0.3731	0.2185	0.2289	0.1879	32.24		11:45	0.3601	0.2676	0.2887	0.6160	27.95
	11:50	0.5413	0.2120	0.1843	0.1955	32.15		11:50	0.3596	0.2003	0.2857	1.0055	28.88
	11:55	0.2306	0.1772	0.2017	0.2227	31.94		11:55	0.3651	0.3077	0.2367	0.7433	29.26
	12:00	0.3984	0.1832	0.2198	0.2868	31.46		12:00	0.3584	0.3303	0.2670	0.2803	28.30
	12:05	0.3983	0.2179	0.1941	0.2566	31.26		12:05	0.3398	0.2488	0.2301	0.3184	27.82
	12:10	0.4389	0.2115	0.1827	0.2534	31.82		12:10	0.4364	0.3000	0.2486	0.3119	27.23
	12:15	0.2776	0.3531	0.2314	0.2720	32.10		12:15	0.3633	0.3356	0.2124	0.2832	27.50
	12:20	0.2758	0.1537	0.2107	0.2059	31.97		12:20	0.4352	0.3974	0.2318	0.3520	27.53
	12:25	0.2662	0.2583	0.1875	0.1745	31.12		12:25	0.4659	0.4950	0.2238	0.2827	27.35
	12:30	0.3805	0.2675	0.2195	0.1968	30.32		12:30	0.4108	0.4087	0.1994	0.2620	27.53
	12:35	0.2117	0.2183	0.2212	0.2004	30.46		12:35	0.4869	0.3836	0.2380	0.2770	27.83
	12:40	0.2747	0.2018	0.2098	0.2113	30.03		12:40	0.3982	0.4084	0.2382	0.2740	27.44
	12:45	0.2635	0.2576	0.2579	0.1834	30.28		12:45	0.6007	0.4213	0.2515	0.3127	27.38
	12:50	0.3203	0.2619	0.2519	0.1624	30.64		12:50	0.4216	0.3949	0.2479	0.3214	27.34
	12:55	0.2889	0.3745	0.2068	0.1441	30.83		12:55	0.4542	0.4898	0.2712	0.2417	27.11
	13:00	0.2708	0.2225	0.2031	0.1411	30.94		13:00	0.4585	0.4772	0.2950	0.2073	27.32
	13:05	0.3055	0.2993	0.2378	0.1697	31.48		13:05	0.3756	0.4752	0.2811	0.2055	27.27
	13:10	0.3288	0.2170	0.1976	0.2033	31.22		13:10	0.4703	0.4044	0.2317	0.2147	27.23
	13:15	0.2510	0.2100	0.2073	0.1872	30.66		13:15	0.5015	0.4506	0.2651	0.1604	27.33
	13:20	0.2825	0.2942	0.2103	0.1989	31.08		13:20	0.5911	0.4073	0.2290	0.2052	27.29
	13:25	0.2906	0.2199	0.2415	0.2989	31.16		13:25	0.6028	0.4070	0.1930	0.2226	27.24
	13:30	0.2450	0.2054	0.2341	0.6672	31.24		13:30	0.4263	0.4529	0.1958	0.2171	27.57
	13:35	0.2879	0.2231	0.2334	0.9204	32.12		13:35	0.5964	0.5108	0.2367	0.1776	27.46
	13:40	0.2906	0.2780	0.2719	0.6933	32.73		13:40	0.5842	0.5451	0.2311	0.2165	27.64
	13:45	0.2412	0.2609	0.2692	0.6688	33.21		13:45	0.5550	0.3892	0.2548	0.2779	27.36
	13:50	0.2370	0.2645	0.2353	0.6442	32.69		13:50	0.5229	0.3050	0.2440	0.2544	27.47
	13:55	0.2826	0.2664	0.2514	0.2503	31.99		13:55	0.5746	0.3653	0.2043	0.2220	27.53
	14:00	0.2845	0.3075	0.2443	0.2653	32.30		14:00	0.5204	0.2991	0.2237	0.2605	27.42
	14:05	0.2375	0.2783	0.2866	0.4730	31.81		14:05	0.5160	0.3921	0.1816	0.2390	27.02
	14:10	0.2403	0.3111	0.2754	0.5487	31.84		14:10	0.5710	0.3949	0.2187	0.2143	27.10
	14:15	0.2914	0.3184	0.2614	0.8024	33.69		14:15	0.6099	0.3194	0.2277	0.1501	26.87
	14:20	0.3428	0.2903	0.2747	0.8253	33.47		14:20	0.5099	0.3145	0.3116	0.1828	27.33
	14:25	0.3487	0.3801	0.3409	0.7131	33.43		14:25	0.6433	0.3345	0.2233	0.2476	27.49
	14:30	0.2943	0.3394	0.2565	0.6356	32.46		14:30	0.7008	0.3538	0.2530	0.4003	28.12
	14:35	0.2893	0.3270	0.2977	0.6282	32.42		14:35	0.5963	0.3957	0.2669	0.4428	28.58
	14:40	0.2968	0.3515	0.2915	0.6929	33.84		14:40	0.7453	0.3662	0.2489	0.3252	28.32
	14:45	0.2875	0.3448	0.2889	0.6798	33.35		14:45	0.7105	0.3478	0.2837	0.2767	28.15
	14:50	0.2532	0.3313	0.3027	0.6280	34.24		14:50	0.6191	0.3510	0.2351	0.2343	28.31
	14:55	0.2919	0.3599	0.2752	0.5744	33.63		14:55	0.5815	0.3470	0.2637	0.1907	27.91
	15:00	0.2830	0.3446	0.3002	0.5292	32.60		15:00	0.5735	0.3376	0.3166	0.1762	27.52
	15:05	0.2353	0.3705	0.2961	0.5931	32.75		15:05	0.5534	0.3621	0.2633	0.1582	27.53
	15:10	0.2870	0.3286	0.3198	0.5292	32.35		15:10	0.6161	0.3759	0.2603	0.1568	27.31
	15:15	0.2393	0.3417	0.3370	0.4915	32.16		15:15	0.6086	0.4161	0.2680	0.1201	27.25
	15:20	0.2438	0.3398	0.2770	0.4882	32.92		15:20	0.4778	0.3520	0.2610	0.1163	27.20
	15:25	0.3665	0.3452	0.3011	0.4686	32.74		15:25	0.5005	0.3798	0.2659	0.1167	27.56
	15:30	0.1834	0.2305	0.2965	0.4189	32.96		15:30	0.4868	0.3458	0.3375	0.1255	27.37
	15:35	0.2355	0.2444	0.3010	0.3973	32.50		15:35	0.5004	0.3731	0.2761	0.2266	27.71
	15:40	0.2728	0.3339	0.3175	0.3973	32.50		15:40	0.4491	0.4643	0.2653	0.1472	27.69
	15:45	0.2353	0.2732	0.2851	0.3298	32.37		15:45	0.4980	0.3353	0.2482	0.1499	27.58
	15:50	0.2278	0.2505	0.2966	0.3030	32.91		15:50	0.5037	0.2737	0.2695	0.1779	27.53
	15:55	0.2204	0.2845	0.2751	0.3279	33.19		15:55	0.4551	0.3084	0.2160	0.2097	27.66
	16:00	0.2809	0.2825	0.2980	0.2902	32.89		16:00	0.4416	0.3101	0.2234	0.1381	27.84
	16:05	0.3006	0.2554	0.3421	0.2893	32.71		16:05	0.5089	0.3508	0.2011	0.0866	27.56
	16:10	0.3449	0.2681	0.3028	0.2676	32.35		16:10	0.4661	0.3566	0.1911	0.0904	27.68
	16:15	0.2939	0.3131	0.3764	0.2583	32.64		16:15	0.5537	0.3083	0.1890	0.0805	27.37
	16:20	0.3355	0.3376	0.4358	0.2347	32.91		16:20	0.4951	0.3544	0.1846	0.0489	27.27
	16:25	0.3670	0.3052	0.3525	0.2041	32.56		16:25	0.5156	0.3512	0.1936	0.0410	27.19
	16:30	0.2890	0.2995	0.3746	0.1846	31.75		16:30	0.5103	0.3188	0.2232	0.0527	27.59
	16:35	0.2405	0.3757	0.4011	0.1660	32.00		16:35	0.4211	0.3230	0.2281	0.0353	27.14
	16:40	0.2815	0.3153	0.3339	0.1481	32.18		16:40	0.4864	0.2738	0.2162	0.0362	26.96
	16:45	0.3192	0.3274	0.3017	0.1406	31.87		16:45	0.4954	0.3183	0.2278	0.0649	27.10
	16:50	0.2895	0.3704	0.3321	0.1348	31.60		16:50	0.4715	0.3272	0.1896	0.0447	27.09
	16:55	0.2496	0.3454	0.3646	0.0929	31.06		16:55	0.5418	0.3486	0.2320	0.0201	27.03
	17:00	0.2855	0.3181	0.3251	0.0537	31.34		17:00	0.5294	0.3190	0.2300	0.0139	26.89
	17:05	0.2935	0.3730	0.3001	0.0425	31.34		17:05	0.4673	0.3586	0.2528	0.0222	26.81
	17:10	0.4157	0.3087	0.3288	0.0384	31.01		17:10	0.4409	0.3149	0.2819	0.0209	26.80
	17:15	0.2241	0.2768	0.3140	0.0301	31.53		17:15	0.3986	0.4075	0.3625	0.0120	26.74

Date	Time	Load (pu.)			Solar (kW/m^2)	Ambient Temp. (^oC)	Date	Time	Load (pu.)			Solar (kW/m^2)	Ambient Temp. (^oC)
		Phase A	Phase B	Phase C					Phase A	Phase B	Phase C		
	17:20	0.3152	0.2605	0.3353	0.0260	31.20		17:20	0.4301	0.3797	0.4187	0.0129	26.81
	17:25	0.3673	0.3105	0.2716	0.0214	31.06		17:25	0.3219	0.3050	0.3986	0.0100	26.80
	17:30	0.3726	0.3129	0.3971	0.0153	30.71		17:30	0.2682	0.2703	0.4071	0.0061	26.91
	17:35	0.3091	0.3087	0.3279	0.0076	31.02		17:35	0.2829	0.2949	0.3205	0.0040	26.87
	17:40	0.3908	0.2879	0.3543	0.0025	30.51		17:40	0.2346	0.3891	0.3180	0.0002	26.65
	17:45	0.3005	0.2270	0.3782	0.0000	30.37		17:45	0.2346	0.3891	0.3180	0.0000	26.48
	17:50	0.2920	0.3010	0.2868	0.0000	30.38		17:50	0.2346	0.3891	0.3180	0.0000	26.50
	17:55	0.2920	0.3010	0.2868	0.0000	30.10		17:55	0.2346	0.3891	0.3180	0.0000	26.42
6 Nov 2014	6:00	0.1713	0.3665	0.3643	0.0000	27.92							
	6:05	0.2116	0.3926	0.3629	0.0000	27.86							
	6:10	0.1870	0.4020	0.3846	0.0000	27.75							
	6:15	0.4041	0.2627	0.3741	0.0000	27.70							
	6:20	0.2781	0.2953	0.2983	0.0006	27.62							
	6:25	0.2881	0.3728	0.4533	0.0046	27.57							
	6:30	0.2020	0.3482	0.3815	0.0096	28.09							
	6:35	0.3138	0.2767	0.3248	0.0160	28.69							
	6:40	0.2974	0.4166	0.2568	0.0241	28.29							
	6:45	0.2198	0.3139	0.4416	0.0320	28.14							
	6:50	0.3163	0.3085	0.2248	0.0398	28.17							
	6:55	0.3473	0.2077	0.3236	0.0517	28.63							
	7:00	0.3303	0.2420	0.2506	0.0639	28.38							
	7:05	0.2385	0.2234	0.2974	0.0735	28.41							
	7:10	0.2602	0.2020	0.3730	0.0789	28.78							
	7:15	0.2911	0.4255	0.2633	0.0796	28.44							
	7:20	0.3547	0.2234	0.2734	0.0789	28.30							
	7:25	0.2516	0.2483	0.2662	0.0790	28.47							
	7:30	0.2523	0.3345	0.2841	0.0874	28.57							
	7:35	0.2304	0.2930	0.2649	0.1041	29.01							
	7:40	0.2773	0.2649	0.3221	0.1281	28.73							
	7:45	0.2715	0.1623	0.2933	0.1336	28.66							
	7:50	0.2170	0.2472	0.2637	0.1636	28.57							
	7:55	0.2714	0.2143	0.2781	0.1480	28.37							
	8:00	0.3950	0.1455	0.2944	0.1490	28.25							
	8:05	0.2717	0.2085	0.3313	0.1553	28.32							
	8:10	0.2817	0.2665	0.2367	0.1785	28.84							
	8:15	0.2257	0.2070	0.2935	0.1991	28.69							
	8:20	0.2650	0.1390	0.3173	0.2070	28.59							
	8:25	0.4058	0.1364	0.3500	0.2279	28.72							
	8:30	0.3394	0.1795	0.2425	0.2792	28.64							
	8:35	0.3231	0.2369	0.2763	0.2705	29.42							
	8:40	0.2957	0.2313	0.3063	0.2488	29.84							
	8:45	0.2687	0.1944	0.2183	0.2759	29.74							
	8:50	0.2796	0.2244	0.3059	0.2680	29.71							
	8:55	0.2585	0.2811	0.3131	0.2455	29.54							
	9:00	0.3680	0.2182	0.2796	0.2600	30.28							
	9:05	0.2647	0.1606	0.2153	0.3084	29.22							
	9:10	0.3807	0.1632	0.2516	0.4007	29.41							
	9:15	0.2636	0.1522	0.2591	0.4391	29.91							
	9:20	0.3808	0.1142	0.2444	0.3809	31.00							
	9:25	0.2821	0.1477	0.2659	0.4519	31.28							
	9:30	0.2565	0.1984	0.2236	0.4914	30.86							
	9:35	0.2611	0.1645	0.2033	0.4401	30.75							
	9:40	0.2638	0.1347	0.1987	0.4819	31.93							
	9:45	0.3644	0.1680	0.1971	0.4865	31.56							
	9:50	0.2932	0.1443	0.2301	0.4865	31.56							
	9:55	0.2737	0.1637	0.2198	0.5310	32.01							
	10:00	0.3332	0.1618	0.2075	0.8526	32.28							
	10:05	0.2462	0.1874	0.2117	0.8943	32.47							
	10:10	0.2463	0.1728	0.2177	0.9368	32.09							
	10:15	0.3299	0.1540	0.2371	0.7624	33.44							
	10:20	0.2381	0.1878	0.2407	0.7601	33.36							
	10:25	0.2206	0.3403	0.1973	0.9340	32.03							
	10:30	0.2726	0.1532	0.2097	0.6550	32.52							
	10:35	0.4419	0.1460	0.2386	0.6273	33.77							
	10:40	0.3618	0.1500	0.2326	0.7789	34.30							
	10:45	0.2723	0.1819	0.2051	0.8127	33.98							
	10:50	0.3224	0.1663	0.2048	0.6821	33.72							
	10:55	0.4033	0.1511	0.2197	0.4233	34.24							
	11:00	0.2714	0.1218	0.2091	0.7070	34.04							
	11:05	0.2880	0.1934	0.1741	0.7998	32.85							
	11:10	0.3079	0.1831	0.2069	0.5443	34.50							
	11:15	0.4072	0.1495	0.1868	0.2938	32.46							
	11:20	0.3458	0.1516	0.1975	0.2564	31.85							
	11:25	0.2902	0.3489	0.1994	0.2637	31.69							
	11:30	0.6459	0.1707	0.2323	0.2980	31.57							
	11:35	0.2867	0.1861	0.2275	0.3352	31.46							
	11:40	0.3010	0.1773	0.2114	0.3087	31.28							
	11:45	0.3167	0.1610	0.1902	0.2977	31.84							
	11:50	0.4345	0.1533	0.2132	0.5605	31.60							
	11:55	0.3846	0.1537	0.2296	0.9591	33.56							
	12:00	0.2126	0.1436	0.2324	0.9941	33.25							
	12:05	0.2102	0.1374	0.1832	0.6321	33.37							
	12:10	0.2714	0.1622	0.2870	0.3468	32.91							
	12:15	0.2844	0.1813	0.2009	0.1731	32.32							
	12:20	0.3363	0.1637	0.2508	0.1563	31.91							
	12:25	0.2491	0.1688	0.2628	0.1131	31.17							
	12:30	0.2461	0.1299	0.2049	0.0940	31.05							
	12:35	0.3213	0.1487	0.2421	0.0697	30.86							
	12:40	0.3287	0.1578	0.2165	0.0643	30.75							

Date	Time	Load (pu.)			Solar (kW/m^2)	Ambient Temp. (^oC)	Date	Time	Load (pu.)			Solar (kW/m^2)	Ambient Temp. (^oC)
		Phase A	Phase B	Phase C					Phase A	Phase B	Phase C		
	12:45	0.2857	0.1413	0.2770	0.0619	28.68							
	12:50	0.3020	0.1851	0.2205	0.0714	28.96							
	12:55	0.2608	0.1603	0.2687	0.0834	28.93							
	13:00	0.3386	0.1007	0.2228	0.1095	29.01							
	13:05	0.3146	0.1586	0.2465	0.1273	28.43							
	13:10	0.2678	0.1385	0.2435	0.1227	28.08							
	13:15	0.2576	0.1067	0.2355	0.1358	28.36							
	13:20	0.2928	0.1490	0.2054	0.1483	28.95							
	13:25	0.2967	0.1518	0.2286	0.1573	28.76							
	13:30	0.2678	0.1054	0.2256	0.1501	28.61							
	13:35	0.2674	0.1070	0.2451	0.1301	27.95							
	13:40	0.3479	0.1496	0.2136	0.1589	28.09							
	13:45	0.3582	0.1501	0.2173	0.2024	27.87							
	13:50	0.3103	0.1273	0.2243	0.2994	28.30							
	13:55	0.2805	0.1876	0.2275	0.3289	27.65							
	14:00	0.2959	0.2251	0.2189	0.2873	28.18							
	14:05	0.3110	0.2218	0.3189	0.2516	27.82							
	14:10	0.3720	0.2216	0.2409	0.2089	27.60							
	14:15	0.4005	0.2369	0.2177	0.2225	28.18							
	14:20	0.3620	0.1892	0.2516	0.2789	28.32							
	14:25	0.3657	0.2003	0.2481	0.3659	28.73							
	14:30	0.3620	0.2038	0.2272	0.4638	29.58							
	14:35	0.3245	0.1627	0.2138	0.5411	30.78							
	14:40	0.3786	0.1518	0.2371	0.5788	30.65							
	14:45	0.3724	0.1660	0.2482	0.5010	31.64							
	14:50	0.3656	0.1869	0.2362	0.4790	31.99							
	14:55	0.3912	0.1491	0.2345	0.3819	31.82							
	15:00	0.3964	0.1604	0.2287	0.3116	31.03							
	15:05	0.3727	0.2601	0.2578	0.3451	31.46							
	15:10	0.3381	0.2678	0.2222	0.4710	31.50							
	15:15	0.3739	0.2779	0.2102	0.4747	32.46							
	15:20	0.3602	0.2769	0.2323	0.4527	32.10							
	15:25	0.3100	0.2511	0.2017	0.4055	32.09							
	15:30	0.3154	0.2511	0.3270	0.3782	31.85							
	15:35	0.3120	0.2665	0.2388	0.3268	32.46							
	15:40	0.3143	0.3418	0.2463	0.2752	31.82							
	15:45	0.3516	0.3094	0.2238	0.2323	32.01							
	15:50	0.2988	0.2508	0.2415	0.1301	31.87							
	15:55	0.3465	0.2817	0.2902	0.0897	31.38							
	16:00	0.2993	0.2742	0.2795	0.0744	31.02							
	16:05	0.2894	0.3002	0.2472	0.0672	30.40							
	16:10	0.2957	0.2849	0.2455	0.0949	30.39							
	16:15	0.3419	0.1887	0.2339	0.1501	30.62							
	16:20	0.3033	0.2980	0.2562	0.1683	30.47							
	16:25	0.3608	0.2159	0.2417	0.1546	30.56							
	16:30	0.2552	0.2365	0.2587	0.1515	30.48							
	16:35	0.2885	0.2024	0.2958	0.1779	30.68							
	16:40	0.3279	0.2624	0.2602	0.1793	30.44							
	16:45	0.2772	0.2506	0.2711	0.1460	30.74							
	16:50	0.2682	0.2398	0.2782	0.1253	30.40							
	16:55	0.2782	0.2605	0.2142	0.1162	30.34							
	17:00	0.2407	0.2892	0.2134	0.1010	30.65							
	17:05	0.2577	0.2335	0.1785	0.0927	30.50							
	17:10	0.2171	0.2702	0.2038	0.0773	30.24							
	17:15	0.2623	0.2508	0.1951	0.0627	30.16							
	17:20	0.3164	0.3081	0.2469	0.0468	30.07							
	17:25	0.3102	0.3148	0.2036	0.0327	29.77							
	17:30	0.3134	0.3424	0.2175	0.0212	29.98							
	17:35	0.2254	0.2822	0.2195	0.0107	29.99							
	17:40	0.2811	0.3228	0.2416	0.0031	29.73							
	17:45	0.2940	0.2993	0.2139	0.0000	29.76							
	17:50	0.3182	0.3297	0.3008	0.0000	29.61							
	17:55	0.3372	0.3161	0.2584	0.0000	29.64							

REFERENCES

[1] U. Büsgen and W. Dürrschmidt, "The expansion of electricity generation from renewable energies in Germany: A review based on the Renewable Energy Sources Act Progress Report 2007 and the new German feed-in legislation," *Energy Policy,* vol. 37, no. 7, pp. 2536-2545, 2009.

[2] T. Sutabutr, "Alternative energy development plan: AEDP 2012-2021," *International journal of renewable energy,* vol. 7, no. 1, pp. 1-10, 2012.

[3] M. Alam, K. Muttaqi, and D. Sutanto, "Mitigation of rooftop solar PV impacts and evening peak support by managing available capacity of distributed energy storage systems," *IEEE Transactions on Power Systems,* vol. 28, no. 4, pp. 3874-3884, 2013.

[4] S. Chaitusaney and A. Yokoyama, "Contribution of distributed generation to voltage regulation under stochastic attribute of renewable energy resources," in *Power System Technology, 2006. PowerCon 2006. International Conference on*, 2006, pp. 1-8: IEEE.

[5] K. Tanaka *et al.*, "Decentralised control of voltage in distribution systems by distributed generators," *IET generation, transmission & distribution,* vol. 4, no. 11, pp. 1251-1260, 2010.

[6] M. Vandenbergh *et al.*, "Prioritisation of technical solutions available for the integration of pv into the distribution grid," *DERlab, Eur. Distrib. Energy Resources Lab. e. V., Kassel, Germany, Tech. Rep. D,* vol. 3, 2013.

[7] E. B. Alzate, Q. Li, and J. Xie, "A novel central voltage-control strategy for smart lv distribution networks," in *International Workshop on Data Analytics for Renewable Energy Integration*, 2015, pp. 16-30: Springer.

[8] E. Dall'Anese, S. V. Dhople, and G. B. Giannakis, "Optimal dispatch of photovoltaic inverters in residential distribution systems," *IEEE Transactions on Sustainable Energy,* vol. 5, no. 2, pp. 487-497, 2014.

[9] T. Stetz, *Autonomous voltage control strategies in distribution grids with photovoltaic systems: technical and economic assessment*. kassel university press GmbH, 2014.

[10] X. Su, M. A. Masoum, and P. J. Wolfs, "Optimal PV inverter reactive power control and real power curtailment to improve performance of unbalanced four-wire LV distribution networks," *IEEE Trans. Sustain. Energy,* vol. 5, no. 3, pp. 967-977, 2014.

[11] R. Tonkoski, L. A. Lopes, and T. H. El-Fouly, "Coordinated active power curtailment of grid connected PV inverters for overvoltage prevention," *IEEE Transactions on Sustainable Energy,* vol. 2, no. 2, pp. 139-147, 2011.

[12] K. Turitsyn, P. Sulc, S. Backhaus, and M. Chertkov, "Options for control of reactive power by distributed photovoltaic generators," *Proceedings of the IEEE,* vol. 99, no. 6, pp. 1063-1073, 2011.

[13] S. Weckx, C. Gonzalez, and J. Driesen, "Combined central and local active and reactive power control of PV inverters," *IEEE Transactions on Sustainable Energy,* vol. 5, no. 3, pp. 776-784, 2014.

[14] I. Altas and A. Sharaf, "A photovoltaic array simulation model for matlab-simulink GUI environment," in *Clean Electrical Power, 2007. ICCEP'07. International Conference on*, 2007, pp. 341-345: IEEE.

[15] D. Dondi, D. Brunelli, L. Benini, P. Pavan, A. Bertacchini, and L. Larcher, "Photovoltaic cell modeling for solar energy powered sensor networks," in *Advances in Sensors and Interface, 2007. IWASI 2007. 2nd International Workshop on*, 2007, pp. 1-6: IEEE.

[16] A. Durgadevi, S. Arulselvi, and S. Natarajan, "Photovoltaic modeling and its characteristics," in *Emerging Trends in Electrical and Computer Technology (ICETECT), 2011 International Conference on*, 2011, pp. 469-475: IEEE.

[17] Z. M. Salameh, B. S. Borowy, and A. R. Amin, "Photovoltaic module-site matching based on the capacity factors," *IEEE transactions on Energy conversion,* vol. 10, no. 2, pp. 326-332, 1995.

[18] MEA Thailand. (2015). *Standard for Interconnecting Distributed Resources with Electric Power Systems*. Available: https://www.mea.or.th/upload/download/file_3c0592dfb9891a50f9de1b68209fadd9.pdf

[19] PEA Thailand. (2016). *Standard for Interconnecting Distributed Resources with Electric Power Systems*. Available: https://www.pea.co.th/Portals/0/Document/connection_code_2016_20170928.pdf

[20] S. Ubertini and U. Desideri, "Performance estimation and experimental measurements of a photovoltaic roof," *Renewable energy,* vol. 28, no. 12, pp. 1833-1850, 2003.

[21] H. Akagi, E. H. Watanabe, and M. Aredes, *Instantaneous power theory and applications to power conditioning*. John Wiley & Sons, 2017.

[22] *Purchase of electricity from solar power and related regulations*. Available: http://www.erc.or.th/ERCWeb2/Upload/Document/part3-Solar-Feb%2024%202015-regulation.pdf

[23] *Solar resource maps and GIS data for 200+ countries*. Available: https://solargis.com/maps-and-gis-data/overview/

[24] *Renewable energy in Germany*. Available: https://en.wikipedia.org/wiki/Renewable_energy_in_Germany

[25] V. Quaschning. (2012). *Role of photovoltaics in the future energy mix : What comes after the current regulations?* Available: https://www.volker-quaschning.de/publis/vortraege/2nd-Inverter-Technology-Forum_Quaschning_2012.pdf

[26] F. Mark, C. Reid, and A. Josef. (2012). *The German Feed-In Tariff: Recent Policy Changes.* Available: https://www.db.com/cr/en/docs/German_FIT_Update_2012.pdf

[27] *JPEA PV OUTLOOK 2030*. Available: http://www.jpea.gr.jp/pdf/t120925.pdf

[28] *Grid Parity – Solar PV Has Caught Up with Japan's Grid Electricity*. Available: https://www.renewable-ei.org/en/column/column_20150730_02.php

[29] R. John and W. Laura. (2014). *Solar Power on the Rise: The Technologies and Policies behind a Booming Energy Sector*. Available: https://www.ucsusa.org/sites/default/files/attach/2014/08/Solar-Power-on-the-Rise.pdf

[30] P. Brad. (2014). *Solar power keeps getting cheaper — but not for the reasons you'd expect*. Available: https://www.vox.com/2014/10/16/6987915/solar-power-cheaper-balance-of-systems-costs

[31] V. V. d. E. E. Informationstechnik, "eV: VDE-AR-N 4105: 2011-08: Power generation systems connected to the low-voltage distribution network Technical minimum requirements for the connection to and parallel operation with low-voltage distribution networks," *English translation of the VDE application rule VDEAR-N-4105*.

[32] T. IEC, "61850–90-7. Communication networks and systems for power utility automation–Part 90–7. Object models for power converters in distributed energy resources (DER) systems," IEC TR 61850–90-7: 20132013.

[33] E. Reiter, K. Ardani, R. Margolis, and R. Edge, *Industry perspectives on advanced inverters for us solar photovoltaic systems: Grid benefits, deployment challenges, and emerging solutions*. National Renewable Energy Laboratory, 2015.

[34] *SMA: Integrated Plant Control and Q on Demand*. Available: https://www.sma.de/en.html

[35] *ABB Solar Inverters: Product Manual*. Available: https://new.abb.com/power-converters-inverters/solar

[36] M. Alam, K. Muttaqi, and D. Sutanto, "An approach for online assessment of rooftop solar PV impacts on low-voltage distribution networks," *IEEE Transactions on Sustainable Energy,* vol. 5, no. 2, pp. 663-672, 2014.

[37] K. A. Joshi and N. M. Pindoriya, "Impact investigation of rooftop Solar PV system: A case study in India," in *Innovative Smart Grid Technologies (ISGT Europe), 2012 3rd IEEE PES International Conference and Exhibition on*, 2012, pp. 1-8: IEEE.

[38] W. H. Kersting, *Distribution system modeling and analysis*. CRC press, 2006.

[39] G. W. Stagg and A. H. El-Abiad, *Computer methods in power system analysis*. McGraw-Hill, 1968.

[40] MEA Thailand, "Physical Characteristics of Weatherproof Aluminum Conductor," 2008.

[41] H. Saadat, *Power System Analysis McGraw-Hill Series in Electrical Computer Engineering*. 1999.

[42] Y. Xu, W. Liu, and J. Gong, "Stable multi-agent-based load shedding algorithm for power systems," *IEEE Transactions on Power Systems,* vol. 26, no. 4, pp. 2006-2014, 2011.

[43] I. Ziari, G. Ledwich, A. Ghosh, and G. Platt, "Integrated distribution systems planning to improve reliability under load growth," *IEEE Transactions on power delivery,* vol. 27, no. 2, pp. 757-765, 2012.

[44] K. Palita, "Impact Assessment of Rooftop PV on Unbalanced Voltage in Low Voltage Distribution Systems," Master Degree, Chulalonhkorn University, 2015.

[45] *Jinko Poly Crystaline PV Module*. Available: https://www.jinkosolar.com/ftp/EN-JKM315P-72(4BB).pdf

[46] L. F. O. Pizzali, "Power Flow Calculation in Distribution Networks with Four-wire Modeling," Master Degree, Estadual Paulista University, 2003.

[47] C. C. Coello and M. S. Lechuga, "MOPSO: A proposal for multiple objective particle swarm optimization," in *Proceedings of the 2002 Congress on Evolutionary Computation. CEC'02 (Cat. No. 02TH8600)*, 2002, vol. 2, pp. 1051-1056: IEEE.

VITA

NAME	Anuwat Chanhome
DATE OF BIRTH	13 February 1987
PLACE OF BIRTH	Kanchanaburi
HOME ADDRESS	60/6 M.4 Plaibang, Bangkruai, Nonthaburi,11130
PUBLICATION	Applying Control Scheme Function of PV Inverter for Minimizing Voltage Fluctuation and Unbalance with Consideration of Maximum PV Generation (IEEJ Trans, 2017)